DOE/EE-0703

2011

annual progress report

Vehicle and Systems Simulation and Testing

U.S. DEPARTMENT OF ENERGY | Energy Efficiency & Renewable Energy

U.S. Department of Energy

Vehicle Technologies Program
1000 Independence Avenue, S.W.
Washington, DC 20585-0121

FY 2011

Annual Progress Report for

Vehicle and Systems Simulation and Testing

Submitted to:
U.S. Department of Energy
Energy Efficiency and Renewable Energy
Vehicle Technologies Program
Vehicle and Systems Simulation and Testing

Lee Slezak, Technology Manager

This report is dedicated to the memory of Jules Routbort (1937-2012).

Jules Routbort, a senior ceramicist at Argonne, passed away on March 1, 2012

Routbort worked in the Thermal Management Group of Argonne's Energy Systems Division where he specialized in transportation, and was highly regarded and respected by many. He worked closely with his sponsors in the Department of Energy Vehicle Technologies Program and was very active with Engineering Conferences International developing small, specialized technical workshops on emerging technological topics.

The loss of Dr Routbort is keenly felt. His integrity, creativity, dedication and sense of humor will be deeply missed.

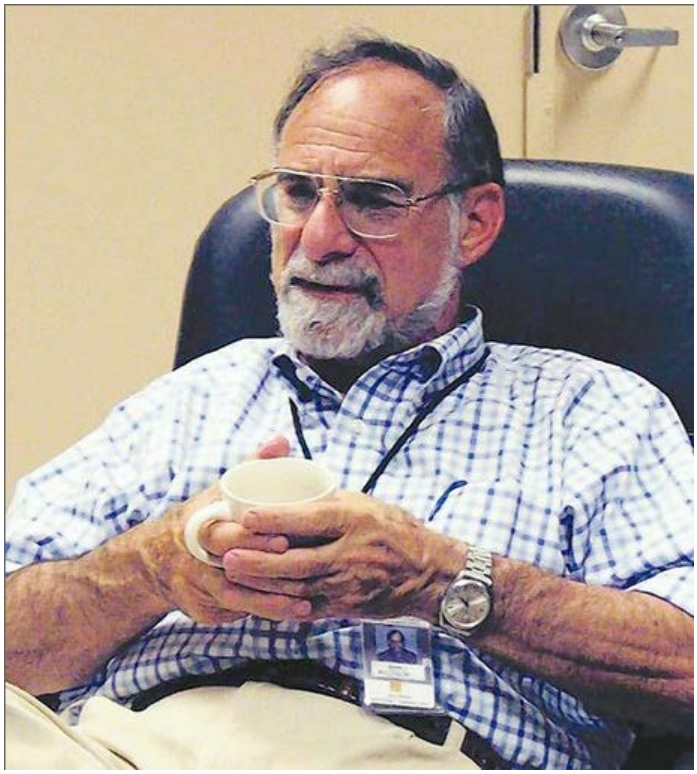

CONTENTS

I. INTRODUCTION

On behalf of the U.S. Department of Energy's Vehicle Technologies Program (VTP), I am pleased to submit the Annual Progress Report for fiscal year 2011 for the Vehicle and Systems Simulation and Testing (VSST) team activities.

Mission

The VSST team's mission is to evaluate the technologies and performance characteristics of advanced automotive powertrain components and subsystems in an integrated vehicle systems context. These evaluations address light-, medium-, and heavy-duty vehicle platforms. This work is directed toward evaluating and verifying the targets of the VTP R&D teams and to providing guidance in establishing roadmaps for achievement of these goals.

Objectives

The prime objective of the VSST team activities is to evaluate VTP targets and associated data that will enable the VTP R&D teams to focus research on specific technology areas. The areas of interest are technologies that will maximize the potential for fuel efficiency improvements, as well as petroleum displacement, and tailpipe emissions reduction. VSST accomplishes this objective through a tight union of computer modeling and simulation, integrated component testing and evaluation, laboratory and field testing of vehicles and systems, vehicle systems optimization, and support for the creation and validation of codes and standards. VSST also supports the VTP goals of fuel consumption reduction by developing and evaluating vehicle system technologies in the area of vehicle ancillary loads reduction.

The integration of computer modeling and simulation, component and systems evaluations, laboratory and field vehicle evaluations, and development and validation of codes and standards for vehicle classes from light-duty to heavy-duty is critical to the success of the VSST team. Information exchange between focus area activities enhances the effectiveness of each activity (illustrated in Figure 1)

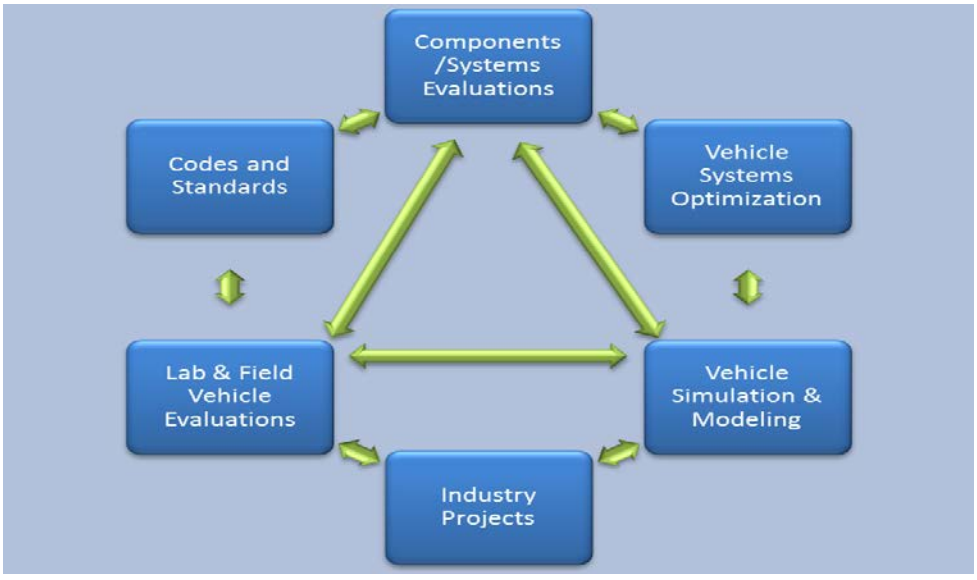

Figure 1 VSST Activities Integration – Arrows represent information flow between activity focus areas that enhances effectiveness of individual activities.

An example of this beneficial data exchange is the increased accuracy of predictive simulation models developed through the Vehicle Simulation & Modeling activity made possible by empirical test data generated through the Lab & Field Vehicle Evaluation activities. Similarly, the credibility and scope of Lab and Field Technology Evaluation studies benefit from real world performance data that is collected from advanced technology vehicles deployed through the Vehicle Electrification Demonstration Projects (under Industry Projects activity.

Major Accomplishments in FY2011:

1) Accumulated data on advanced technology vehicles covering 34 million test miles through the Advanced Vehicle Testing Activity (AVTA). The data was collected from 6,500 electric-drive vehicles (representing 111 models). Data was collected on 5,600 *plug-in* electric vehicles (PEVs) over a combined total of 26 million test miles. The PEV data describes the operational characteristics for 62 models within the Electric Vehicle (EV), Plug-In Hybrid Electric Vehicle (PHEV), and Extended Range Electric Vehicle (EREV) categories.
2) Initiated data collection on thousands of vehicles and Electric Vehicle Supply Equipment (EVSE) units placed into service through the largest deployment of electric-drive vehicles and charging infrastructure ever undertaken in the U.S. Test settings included grid-connected electric drive vehicles (EDVs) in on-road fleets, on the test track, and in the laboratory. Test results show the real-world potentials for various EDV technologies to reduce petroleum consumption. Example projects include: The EV Project, Chrysler Ram PHEV Pickups, ChargePoint America Vehicle Charging Infrastructure, and General Motors Chevrolet Volt Vehicle Demonstration.
3) Development and deployment of the Autonomie vehicle modeling & simulation platform through a Cooperative Research and Development Agreement (CRADA) between Argonne National Laboratory (ANL) and General Motors. This achievement contributes to the VSST objective to accelerate development and introduce advanced technologies with models that are widely adopted by the industry and research communities. The benefits of achieving this objective to the US transportation sector include reducing costs and time-to-market for bringing advanced vehicle technologies to our Nation's roadways. To date, Autonomie has 750 users from 127 organizations/entities, illustrating its impact on the automotive industry.
4) Improved fuel economy estimates for advanced vehicles by adding characteristics of emissions control devices to vehicle simulations. This achievement is significant because emission constraints can have a significant impact on the ability to exploit higher fuel economy of advanced engines and hybrid vehicles. Accurate dynamic after-treatment models are required to accurately simulate the impact of these constraints. This addition (by researchers at Oak Ridge National Laboratory) to integrated system models permits investigation of many configurations and control options for optimizing overall vehicle performance.
5) Began to quantify the potential benefits of combining thermal management systems in electric drive vehicles. The potential benefits include improved range and battery life of PHEVs and EVs, while reducing cost. The project, conducted by the National Renewable Energy Laboratory, simulated a full thermal management system in an EV to include A/C, cabin, power electronics cooling loop, and battery cooling loop.
6) Developed full analytical, computational and experimental understanding of the physics of wireless power charging of stationary PEVs. The knowledge gained will inform SAE standards development and implementation designs that meet industry requirements for efficiency, safety, cost, and vehicle packaging criteria. The project was conducted by Oak Ridge National Laboratory, and performed experimental hardware tests that focused on topics of interoperability, coupling coil compatibility, alignment tolerance, positioning control, and wireless communications.

Approach and Organization of Activities

VSST provides an overarching vehicle systems perspective in support of the technology R&D activities of DOE's VTP and Hydrogen Fuel Cells Technologies Program (HFCTP). VSST uses analytical and empirical tools to model and simulate potential vehicle systems, validate component performance in a systems context, verify and benchmark emerging technologies, and validate computer models. Hardware-in-the-loop testing allows components to be controlled in an emulated vehicle environment. Laboratory testing then provides measurement of progress toward VTP technical goals and eventual validation of DOE-sponsored technologies at the Advanced Powertrain Research Facility for light- and medium-duty vehicles and at the ReFUEL Facility for heavy-duty vehicles. For this sub-program to be successful, extensive collaboration with the technology development activities within the VTP and HFCTP is required for both analysis and testing. Analytical results of this sub-program are used to estimate national benefits and/or impacts of DOE-sponsored technology development, as illustrated in the figure below.

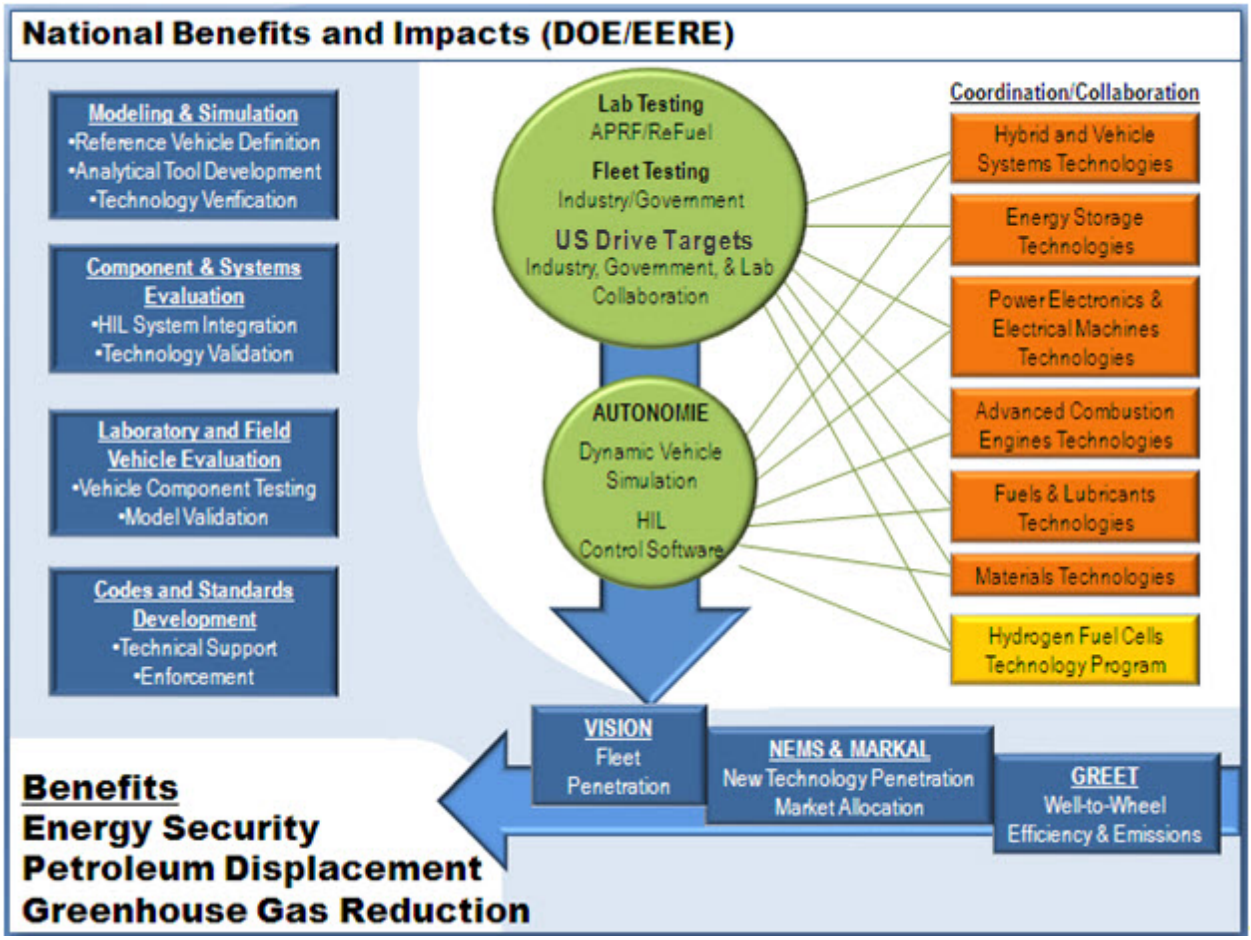

Figure 2 VSST activities providing estimates of national benefits and impacts of advanced technologies.

VSST activities are organized into the six focus areas. A brief description of each Focus Area and its major accomplishment for FY2011are outlined below.

1. *Modeling and Simulation*

   DOE has developed and maintains software tools that support VTP research. VISION, NEMS, MARKAL, and GREET are used to forecast national-level energy, environmental, and economic parameters including oil use, market impacts, and greenhouse gas contributions of new technologies. These forecasts are based on VTP vehicle-level simulations that predict fuel economy and emissions using VSST's Autonomie modeling tool. Autonomie's simulation capabilities allow for accelerated development and introduction of advanced technologies through computer modeling rather than through expensive and time-consuming hardware building. Modeling and laboratory and field testing are closely coordinated to enhance and validate models as well as ensure that laboratory and field test procedures and protocols comprehend the needs of new technologies that may eventually be commercialized.

   Autonomie is a MATLAB-based software environment and framework for automotive control system design, simulation and analysis. This platform enables dynamic analysis of vehicle performance and efficiency to support detailed design, hardware development, and validation. Autonomie was developed under a Cooperative Research and Development Agreement (CRADA) with General Motors and included substantial input from other original equipment manufacturers (OEMs), and replaces its predecessor, the Powertrain Systems Analysis Toolkit (PSAT). One of the primary benefits of Autonomie is its Plug-and-Play foundation which allows integration of models of various degrees of fidelity and abstraction from multiple engineering software environments. This single powerful tool can be used throughout all the phases of Model Based Design of the Vehicle Development Process (VDP).

2. *Component and Systems Evaluation*

   Hardware-in-the-loop (HIL) simulation provides a novel and cost effective approach to isolate and evaluate advanced automotive component and subsystem technologies while maintaining the rest of the system as a control. HIL allows actual hardware components to be tested in the laboratory at a full vehicle level without the extensive cost and lead time of building a complete prototype vehicle. This approach integrates modeling and simulation with hardware in the laboratory to develop and evaluate propulsion subsystems in a full vehicle level context. The propulsion system hardware components: batteries, inverters, electric motors and controllers are further validated in simulated vehicle environments to ensure that they meet the vehicle performance targets established by the government-industry technical teams.

   Through the U.S. DRIVE Vehicle System Analysis Technical Team (VSATT), MATT facilitates interactions between each of the other technical teams by providing a common platform for component integration and testing. Each specific set of technical targets and their impacts on the vehicle and systems can easily be studied using the MATT platform.

   High energy traction battery technology is important to the successful development of plug-in electric vehicles. To support the evaluation of advanced prototype energy storage systems, in FY2011 Idaho National Laboratory (INL), with assistance from Oak Ridge National Laboratory (ORNL) developed and implemented the Electric-Drive Advanced Battery test platform. This test-bed allows advanced battery packs to be evaluated in real-world operating conditions in an on-road vehicle that emulates a variety of electric-drive powertrain architectures.

3. *Laboratory and Field Vehicle Evaluation*

   This section describes the activities related to laboratory validation and fleet testing of advanced propulsion subsystem technologies and advanced vehicles. In laboratory benchmarking, the objective is to extensively test production vehicle and component technology to ensure that VTP-developed technologies represent significant advances over technologies that have been developed by industry. Technology validation involves the testing of DOE-developed

components or subsystems to evaluate the technology in the proper systems context. Validation helps to guide future VTP research and facilitates the setting of performance targets.

To date, over 5,400 Battery Electric Vehicles (BEV), PHEVs, EREVs, HEVs**, Neighborhood Electric Vehicle**s (NEV), fuel cell and hydrogen internal combustion engine vehicles, and propulsion subsystem components have been benchmarked or validated by the VSST team. Combined, they represent more than 100 different electric drive vehicle models. The VSST team has also evaluated the use of more than 5,200 electric vehicle chargers. The results of these evaluations have been used to identify needed areas of improvement for these advanced vehicles and technologies that will help bring them to market faster. They have also been used to identify the most promising new opportunities to achieve greater overall vehicle efficiencies at the lowest possible cost.

The facilities that perform Lab and Field Testing activities include the Advanced Powertrain Research Facility (APRF), Idaho National Laboratory (INL) Transportation Testing Facilities, NREL's ReFuel, and Thermal Test Facilities, and ORNL's Vehicle Systems Integration Lab (VSI).

- The APRF is equipped with-dynamometers (for testing integrated components such as engines, electric motors, and powertrains), and a thermal chamber (for testing BEVs, HEVs and PHEVs in temperatures as low as 20^{o}F, up through 95^{o}F).
- INL's Transportation testing facilities encompass the Advanced Vehicle Testing Activity (for Light Duty Vehicles) Facility, the Heavy Duty Transportation Test Facility, and the Energy Storage Technologies Laboratory. AVTA's capability to securely collect, analyze, and disseminate data from multiple field tests located throughout the US is critical to VSST Lab & Field activities.
- NREL's ReFuel facility is equipped with dynamometers (for testing Medium Duty Vehicles and components). NREL's Thermal Test facilities include capabilities for Light Duty Vehicle cabin thermal studies and Outdoor Heavy Duty Vehicle Cabin studies. NREL also has facilities for testing subsystems (such as ESS and EVSE) and functions such as the VSST data collection and evaluation hub for Medium and Heavy Duty Vehicle Fleet Tests.
- ORNL's facilities for integrated testing include advanced engine technologies (E.g. advanced combustion modes, fuels, thermal energy recovery, emissions after-treatment), advanced power electronics and electric machines (E.g. motor drives, components, power electronics devices, advanced converter topologies), and vehicle testing and evaluation (E.g. chassis and component dynamometers, integrated powertrain stands, test track evaluations, field operational testing).

The Advanced Vehicle Testing Activity (AVTA), working with industry partners, conducts field and fleet testing to accurately measure real-world performance of advanced technology vehicles via a testing regime based on test procedures developed with input from industry and other stakeholders. The performance and capabilities of advanced technologies are benchmarked to support the development of industry and DOE technology targets. The testing results provide data for validating component, subsystem, and vehicle simulation models and hardware-in-the-loop testing. Fleet managers and the public use the test results for advanced technology vehicle acquisition decisions. INL conducts light-duty testing activities. In FY 2011, INL continued its partnership with an industry group led by ECOtality North America. Accelerated reliability testing provides reliable benchmark data of the fuel economy, operations and maintenance requirements, general vehicle performance, engine and

component (such as energy storage system) life, and life-cycle costs. These tests are described below.

Baseline Performance Testing

The objective of baseline performance testing is to provide a highly accurate snapshot of a vehicle's performance in a controlled testing environment. The testing is designed to be highly repeatable. Hence it is conducted on closed tracks and dynamometers, providing comparative testing results that allow "apples-to-apples" comparisons within respective vehicle technology classes. The APRF at ANL is utilized for the dynamometer testing of the vehicles.

Fleet Testing

Fleet testing provides a real-world balance to highly controlled baseline performance testing. Some fleet managers prefer fleet testing results to the more controlled baseline performance or the accelerated reliability testing.

During fleet testing, a vehicle or group of vehicles is operated in normal fleet applications. Operating parameters such as fuel-use, operations and maintenance, costs/expenses, and all vehicle problems are documented. Fleet testing usually lasts one to three years and, depending on the vehicle and energy storage technology, between 5,000 and 12,000 miles are accumulated on each vehicle.

For some vehicle technologies, fleet testing may be the only viable test method. NEVs are a good example. Their manufacturer-recommended charging practices often require up to 10 hours per charge cycle, while they operate at low speeds (<26 mph). This makes it nearly impossible to perform accelerated reliability testing on such vehicles.

Accelerated Reliability Testing

The objective of accelerated reliability testing is to quickly accumulate several years or an entire vehicle-life's worth of mileage on each test vehicle. The tests are generally conducted on public roads and highways, and testing usually lasts for up to 36 months per vehicle. The miles to be accumulated and time required depend heavily on the vehicle technology being tested. For instance, the accelerated reliability testing goal for PHEVs and BEVs is to accumulate 12,000 miles per vehicle in one year while the testing goal for HEVs is to accumulate 160,000 miles per vehicle within three years. This is several times greater than most HEVs will be driven in three years, but it is required to provide meaningful vehicle-life data within a useful time frame. Generally, two vehicles of each model are tested to ensure accuracy. Ideally, a larger sample size would be tested, but funding tradeoffs necessitate only testing two of each model to ensure accuracy.

Depending on the vehicle technology, a vehicle report is completed for each vehicle model for both fleet and accelerated reliability testing. However, because of the significant volume of data collected for the HEVs, fleet testing fact sheets (including accelerated reliability testing) and maintenance sheets are provided for the HEVs.

4. *Codes and Standards Development*

A comprehensive and consistent set of codes and standards addressing grid-connected vehicles and infrastructure is essential for the successful market introduction of electric-drive vehicles. The VTP is active in driving the development of these standards through committee involvement and technical support by the National Laboratories. The VTP also supports activities of the U.S. DRIVE's Grid Interaction Tech Team (GITT), a government/industry partnership aimed at ensuring a smooth transition for vehicle electrification by closing technology gaps that exist in connecting vehicles to the electric grid. In FY2011, GITT worked with Pacific Northwest

National Laboratory (PNNL) and ANL to participate in SAE and NIST standards development for connectivity and communication for grid-connected vehicles.

During FY2011, VSST supported Laboratory staff led and served on committees that develop standards including SAE J1772 for connector standards, SAE J2847 for communication standards, and SAE J2953 for Electric-Vehicle Supply Equipment-Vehicle Compatibility., and SAE J1634 (BEV Test Procedures) revision. Technical support tasks also continued validation of SAE J1711 for PHEV test procedures (as follow-on work to the FY2010 submission), creation of SAE J2907 Motor Rating Standards document, validation of the first power-line communication (physical layer) over pilot-wire G3 communications, development of an SAE J2953/J2931Communication Test Fixture, and investigations to support development of EV Wireless Charging Standard J2954.

The VTP also addressed the codes and standards for grid-connected vehicle charger permitting and installation process, electric drive vehicle components, and sub-metering communication devices for EVSE. Electric vehicles reach beyond national boundaries, so ANL was employed in international cooperative initiatives to adopt international electric drive vehicle standards and promote market penetration of grid-connected vehicles. Many new technologies require adaptations and more careful attention to specific procedures. VSST engineers have contributed to the development of many new standards and protocols which have been presented to a wide audience such as U.S. DRIVE partners, other government agencies, and the European Commission, and are being adopted as industry standard.

Component modeling and simulation also require the use of internationally accepted test procedures and measurement methods. These testing standards must be applicable throughout the industry; therefore it is imperative that component/system interoperability be validated. In FY 2011, ANL provided technical data support and leadership to rewrite SAE J1711, the standard for measuring exhaust emissions and fuel economy for hybrid electric vehicle (HEC), which specifically addressed PHEVs.

Codes and standards were also developed for sanctioned sporting regulations to stimulate rapid vehicle technology development and to educate consumers about the benefits of fuel efficient technologies. The Green Racing Initiative dramatically increased the number of teams using advanced fuels with significant renewable percentages in ALMS racing to include all but two Grand Touring category cars and two Le Mans Prototype cars. Green Racing worked with the American Le Mans Series (ALMS) to strengthen and improve the visibility of the green racing program through the development of scoring protocols to support technology advancement through motorsports competition, promoting market acceptance of advanced vehicle technologies.

5. *Vehicle Systems Optimization*

This focus area involves research and development on a variety of mechanisms to improve the energy efficiency of light, medium, and heavy duty vehicles. Projects in this focus area involve reducing the aerodynamic drag of vehicles, thermal management approaches to increase the engine thermal efficiency and reduce parasitic energy losses, the development of advanced technologies to improve the fuel efficiency of critical engine and driveline components by characterizing the fundamental friction and wear mechanisms, and fast and wireless charging technology development.

Aerodynamic Drag Reduction

The primary goal of this focus area is improving the freight-efficiency of vehicles. Aerodynamic drag reduction, thermal management, and friction and wear are the main focuses of this area. Reduction of aerodynamic drag in Class 8 tractor-trailers can result in a significant improvement

on fuel economy while satisfying regulatory and industry operational constraints. An important part of this effort is to expand and coordinate industry collaborations with DOE and establish buy-in through CRADAs and to accelerate the introduction of proven aerodynamic drag reduction devices into new vehicle offerings.

The primary approach in drag reduction is through the control of the vehicles flow field. This is can be achieved with geometry modifications, integration, and flow conditioning. During 2011 the goal of the research was to develop and design the next generation of aerodynamically integrated tractor-trailer.

Thermal Management

Thermal management of vehicle engines and support systems is a technology area that addresses reduction in energy usage through improvements in engine thermal efficiency and reductions in parasitic energy uses and losses. Fuel consumption is directly related to the thermal efficiency of engines and support systems. New methods to reduce heat related losses are investigated and developed under this program.

FY 2011 Thermal Management R&D focused on exploring:

A) The possibilities of repositioning the class 8 tractor radiator and modifying the frontal area of the tractor to reduce aerodynamic drag.

B) The possibilities of using evaporative cooling under extreme conditions of temperature and engine load.

C) Nucleated boiling in engine coolant for heavy duty trucks. It is well known that boiling heat transfer coefficients are much higher than the convective heat transfer coefficient of the same fluid. This program is designed to measure the heat transfer coefficient and CHF of several possible coolants, compare the results to theories, and transfer the data to industry.

Friction and Wear

Parasitic engine and driveline energy losses arising from boundary friction and viscous losses consume 10 to 15 percent of fuel used in transportation, and thus engines and driveline components are being redesigned to incorporate low-friction technologies to increase fuel efficiency of passenger and heavy-duty vehicles. Research to improve the fuel efficiency and reliability of critical engine and driveline components included:

- Experimentally investigating fundamental friction and wear mechanisms.
- Modeling and validating the impact of friction on components and overall vehicle efficiency.
- Developing advanced low friction technologies (materials, coatings, engineered surfaces, and advanced lubricants)

Fast and Wireless Charging

Electrification of the transportation sector will be enabled by adoption of vehicle charging technologies that minimize costs in terms of time and money while maximizing energy throughput, battery life, safety, and convenience. Developments of systems to safely and efficiently transfer energy to electric-drive vehicles, at high power rates, through both conductive and inductive mechanisms, are being investigated as part of this activity under the Vehicle Systems Optimization focus area.

6. *Industry Awards*

Industry projects for FY2011 include the categories of PHEV Technology Acceleration Demonstration Activities, Transportation Electrification, and SuperTruck. These technology

development and demonstration projects were awarded through DOE's competitive solicitation process and involve resource matching by DOE and industry.

Major projects that were conducted by the national laboratories and industry partners in support of these areas in FY 2011 are described in this report. A summary of the major activities in each area is given first, followed by detailed reports on the approach, accomplishments and future directions for the projects. For further information, please contact the DOE Project Leader named for each project.

Future Directions for VSST

Near-term solutions for reducing the nation's dependence on imported oil, such as PHEVs, will require the development, integration, and control of vehicle components, subsystems, and support systems. These solutions will require exploration of high capacity energy storage and propulsion system combinations to get the most out of hybrid propulsion. Analysis and testing procedures at the national labs will be enhanced to study these advanced powertrains with simulation tools, component/subsystem integration, and hardware-in-the-loop testing. DOE-sponsored hardware developments will be validated at the vehicle level, using a combination of testing and simulation procedures.

In FY 2012, the VSST will continue to expand activities in the area of vehicle simulation and modeling, and laboratory and field testing including further baseline performance testing of conversion and original equipment manufacturer (OEM) electric-drive vehicles. Field and laboratory testing will continue to be integrated with modeling/simulation activities, including validation of simulation models for advanced vehicles tested in the newly-upgraded APRF. Fleet evaluation of plug-in vehicles will continue, with continued emphasis on evaluation fleets of OEM production vehicles. In FY 2008, DOE VT issued a solicitation for the purpose of establishing a PHEV demonstration fleet consisting of large volume manufacturers and OEMs as participants. This program launched in FY 2009, continued in FY 2011, and is scheduled to conclude in FY 2012.

In addition to the HEV and PHEV activities, a full range of simulation and evaluation activities will be conducted on the Battery Electric Vehicles (EV) as they are brought to market by OEMs. Because EVs are dependent on a robust charging infrastructure for their operation and ultimate consumer acceptance, VSST will greatly increase efforts to address issues related to codes and standards for EVs, charging infrastructure, and vehicle/grid integration.

VSST will also be deeply involved in the collection and analysis of data from the American Recovery and Reinvestment Act of 2009 (ARRA) Transportation Electrification Demonstration projects. These eight demonstrations will place more than 12,000 electric drive vehicles and 20,000 recharging stations in service, and VSST will direct the collection and analysis of data from these units. In addition to performance, reliability, and petroleum displacement results, VSST will utilize the data to determine the impact of concentrations of electric dive vehicles on the electricity grid, as well as the changes in operators' driving and recharging patterns as they become more comfortable with this new technology.

Vehicle systems optimization work in the areas of aerodynamics, thermal management, and friction and wear will continue with several new projects in thermal control and friction and wear. The focus of these activities will continue to revolve around cooperative projects with industry partners with the goal of bringing developed technologies to market quickly. New efforts will be supported to conduct evaluations of methods to improve thermal heat transfer efficiencies and reduce parasitic loads with coordination from industry partners. Additionally, activities to develop solutions for wireless power transfer and fast charging of electric-drive vehicles, while evaluating the market barriers and technology impacts for deploying this infrastructure, will ramp up within the Vehicle Systems Optimization area.

In order to develop an accurate vehicle cost model for passenger vehicles, VSST identified market costs for technology combinations for new, emerging, and existing light vehicle fuel economy-improving technologies in FY 2011, which will continue and be validated in FY 2012. VSST technologies for advanced power electronics, energy storage, and combustion engines will continue to be validated as each technology closes in on energy efficiency targets.

Inquiries regarding the VSST activities may be directed to the undersigned.

Lee Slezak
Technology Manager
Vehicle and Systems Simulation and Testing
Vehicle Technologies Program

II. INDUSTRY

PHEV TECHNOLOGY ACCELERATION AND DEPLOYMENT ACTIVITY

II.A. (a) Chrysler Town & Country Mini-Van Plug-In Hybrid Electric Vehicle

Principal Investigator: Abdullah A. Bazzi
Chrysler Group LLC
800 Chrysler Drive
Auburn Hills, MI USA 48326-2757
1-(248) 944-3093; aab5@Chrysler.com

DOE Technology Development Manager: Lee Slezak
1-(202) 586-2335; Lee.Slezak@ee.doe.gov

NETL Project Manager: Adrienne Riggi
(304) 285-5223; Adrienne.Riggi@NETL.DOE.GOV

DOE Award Number: DE-EE0004529
Submitted to: U.S. Department of Energy – National Energy Technology Laboratory

---

II.A.1. Abstract

Objective

- Demonstrate 25 minivans (RT) in diverse geographies and climates, spanning from Michigan, California, and Texas and across a range of drive cycles and consumer usage patterns applicable to the entire NAFTA region
- Run the vehicles for 2 years with relevant data collected to prove the product viability under real-world conditions
- Quantify the benefits to customers and to the nation
- Develop & demonstrate charging capability
- Develop and demonstrate Flex Fuel (E85) capability with PHEV technology.
- Support the creation of "Green" Technology jobs and advance the state of PHEV technology for future production integration
- Develop an understanding of Customer Acceptance & Usage patterns for PHEV technology
- Integration of PHEV technology with Renewable energy generation

Major Accomplishments

Vehicle Build & Test

- Initial build of Demonstration Fleet vehicles
- Development and validation utilized the standard Chrysler Group LLC Vehicle Development Process for a production intent program.
  - Designed and built all development and test vehicles

  - Augmented development process with modified testing procedures to address specific plug in Hybrid Technologies
- Facility Based Testing: hot static cell, hot drive cell, cold static cell, cold drive cell, altitude chamber, engine dynamometer, transmission dynamometer, NHV cell, EMC cell, end of line, emissions test facility; bench Testing: vibration, SOC, thermal, charge / discharge cycling
- Impact Testing: Successfully Completed for FMVSS compliance
- Road trips: development testing and verification: hot trip to 125F, cold trip to -20F, altitude trip to 12,000 ft
- Flex Fuels: Developed PHEV Torque Model to accommodate Flex Fuels (E0 to E85) operations

Future Activities

- Complete Vehicle Builds
- Start Vehicle Deployment
- Complete Participating Dealer Training
- Capture Deployed Fleet Data to support Calibration and Controls development
- Enhance Data Reporting Capabilities
- Customer Interface Server

II.A.2. Technical Discussion.

Introduction

The Chrysler Product Creation Process (CPCP) defines the strategy and method used to execute the development of world class vehicles from concept to market. The Chrysler Town & Country PHEV is following the CPCP process. Fundamental principles include:

- Voice of the Customer – Dictates product decisions
- Timeline Compression – Enables speed to market
- Flexibility – Allows for unique vehicle program characteristics
- Consistency of Execution – Facilitates continuous improvement
- Clear Performance Indicators – Drives accountability
- Interdependencies Identified – Aligns activities across functional areas

Approach

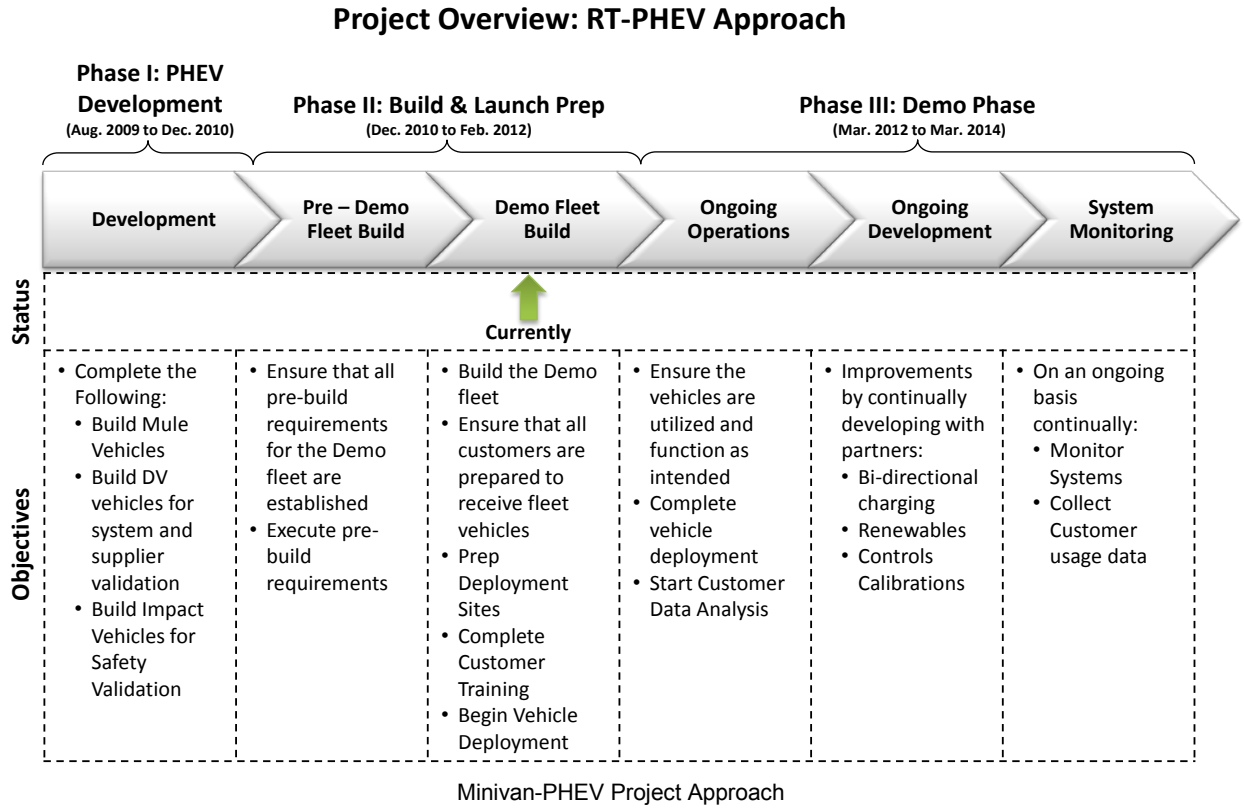

Minivan-PHEV Project Approach

Results

Table 1. RT-PHEV Project Results

	Proposal	RT-PHEV Status	Procedure
RANGE	Equivalent All Electric Range (EAER) of 22 miles	Currently under development. Range is being adversely affected by recently discovered issues. Investigating the following solutions: • Optimizing transmission hardware limits • Investing thermal solutions	California Exhaust Emission Standards And Test Procedures, as amended December 2, 2009
EMISSIONS	BIN 5 / LEVII (Gas & E85)	Gas – Tests are currently under development E85 – New	CFR Title 40: PART 86—CONTROL OF EMISSIONS FROM NEW AND IN-USE HIGHWAY VEHICLES AND ENGINES; Subpart S
FUEL ECONOMY	Charge Depleting City 52 MPG	– Charger Depletion: – City: 55.15 mpg – Hwy: 50.41 mpg – Charger Sustaining: – City: 25.28 mpg – Hwy: 34.5 mpg	SAE J 1711 as published

Conclusions

1. The development process has to be completed
1. The design, procurement, and delivery of all the components have been completed.
2. Build requirements have been defined
3. Completed impact testing

II.A.3. Products

Publications

1. Charge Depleting Control Strategies and Fuel Optimization of Blended-Mode Plug-in Hybrid Electric Vehicles. IEEE Transaction on Vehicular Technology, Vol. 60, No.4, May 2011
2. Analytical Approach for the Power Management of Blended Mode Plug-In Hybrid Electric Vehicles. Accepted by IEEE Transaction on Vehicular Technology
3. A High Efficiency Low Cost Direct Battery Balancing Circuit Using A Multi-Winding Transformer with Reduced Switch Count. IEEE APEC 2012, Orlando, FL, Feb. 5 – 9, 2012
4. Hybrid / Plug-in-Hybrid Technology Overview – Torque Feed forward Control for IPM Motors

Public Presentations

1. Summit on Automotive Electrification. Kokomo, Indiana
2. "Are you plugged in?" Conference. Auburn Hills, Michigan
3. Annual Merit Review. Washington D.C.

Tools & Data

1. Vector Cantech -- Canalyzer equipment utilized for data collection and software development (communication between vehicle controllers)
2. ETAS -- Equipment utilized for software development and drivability / emissions calibration
3. Technical Training Inc. – TTI worked with Chrysler Electrified Powertrain engineers to develop a PHEV dealer technician training course and handbook for the dealerships supporting the DOE fleet vehicles
4. Security Inspection utilized for upgraded infrastructure environment (increased bandwidth requirements and storage requirements) for implementing Microstrategy vehicle logging and data analysis
5. Bright Star Engineering -- Data Recorder Modules (DRM) for each vehicle and monthly cellular access.

Patents

Chrysler IDR No.	Patent Application USPTO Serial No.	Patent Application Title	File Date at USPTO	DOE Program
708551	61 / 536,173	ELECTRIC-DRIVE TRACTABILITY INDICATOR INTEGRATED IN HYBRID ELECTRIC VEHICLE TACHOMETER	19-SEPT-2011	IDR – Ram and Minivan PHEV
708553	13 / 160,561	ADAPTIVE POWERTRAIN CONTROL FOR PLUGIN HYBRID ELECTRIC VEHICLES	15-JUNE-2011	IDR – Ram and Minivan PHEV

PHEV TECHNOLOGY ACCELERATION AND DEPLOYMENT ACTIVITY

II.B. (b) Ford Plug-In Project: Bringing PHEVs to Market

Julie D'Annunzio – Global Electrified Fleet Manager
Ford Motor Company
AEC, MD 44
2400 Village Road
Dearborn, MI 48124
(313) 323-8432; jdannunz@ford.com

DOE Technology Development Manager:Lee Slezak
(202) 586-2335Lee.Slezak@ee.doe.gov

NETL Project Manager John Jason Conley
(304) 285-2023; John.Conley@NETL.DOE.GOV

II.B.1. Abstract

Objective

- OVERALL OBJECTIVE: The Ford Escape Plug-in Hybrid (PHEV) Project was started in October of 2008 with an overall goal of identifying a sustainable pathway toward accelerated, successful mass production of plug-in hybrid vehicles. The project objectives were cascaded via four phases:
  - Phase I: Validate and demonstrate plug-in technology on a new, more fuel efficient engine. *Phase I completed in 2009 CY and included the engineering and development of 11 vehicles.*
  - Phase II: Progress battery/controls closer to production intent and demonstrate bi-directional communication and flex-fuel capability. *Phase II completed in 2010 CY and included engineering, development and delivery of additional 10 PHEVs with E85 flexibility*.
  - Phase III: Demonstrate plug-in technology in fleet operation and perform data analysis. *Phase III completed 1Qtr 2011 and included completion of Ford/INL fleet data correlation and algorithm validation.*
  - Phase IV: Continue vehicle demonstrations from Phase III and demonstrate advanced metering interface. *Phase IV - In progress.*
- FY2011 OBJECTIVE: Phase III was completed in 1st Qtr 2011 with data acquisition, analysis and reporting providing both laboratory and real-world usage data. Remaining FY2011 Phase IV objectives include:
  - Continue demonstration of PHEV fleet and support of public information activities
  - Continue vehicle development and testing; Continue battery and controls development
  - Continue in-field vehicles service and support
  - Continue data acquisition, analysis and reporting

2011 Major Accomplishments

- Over 460,000 fleet miles accumulated with data acquisition systems in place and collecting real-world PHEV usage and performance data. Note: Actual fleet life-time mileage is over 500,000 which includes Ford vehicle development work.
- Over 65 nationwide public outreach activities supported - including auto shows, educational displays and government events.

- SAE J1772 compatible charge port design, development and testing completed to allow vehicle charging using level II 240V EVSE. Level I 120V charging still possible per project requirements. Fleet implementation at 75%. Target completion 1Qtr 2012.
- PHEV-05 upgraded with electric air conditioning, instrument cluster software (unique for electric air conditioning), low voltage charger cooling fans and 57 mph all-electric operation.
- Vehicle operation software continues to be refined based on customer feedback and field operations. PCM calibration revised and installed on PHEV-7 for testing.
- Ford and INL data correlation and algorithm validation completed to support INL Ford Escape PHEV public reporting. INL monthly summary fleet reports now available via AVTA website.
- Electric Power Research Institute (EPRI) conducted field demonstration of Smart Meter communication at utility partner locations. Interface testing work has validated the ability to perform utility charge control direct to vehicle.

Future Activities

- Complete fleet implementation of SAE J1772 compatible charge port design.
- Continued fleet demonstration and ongoing service and support of field vehicles with continued engineering development to drive production vehicle designs.
- Continued collaboration with EPRI, participating utilities, INL and the DOE to support data collection, analysis and reporting on fleet activities.
- Continued communications interface work with EPRI to investigate identified areas of improvement.
- NOTE: Ford Escape PHEV fleet utility demonstration project complete December 2012.

II.B.2. Technical Discussion

Introduction

The Ford Escape PHEV fleet includes 21 advanced research PHEVs deployed to 11 utilities across the US and Canada. Partner utilities include Southern California Edison, Detroit Edison, New York Power Authority, Consolidated Energy, New York State Energy Research & Development Authority, Progress Energy, Southern Company, National Grid, American Electric Power, Pepco Holdings Inc., and Hydro-Quebec. The utility partners utilize the Escape PHEVs in their fleet operations as well as participating in nationwide outreach efforts targeted at education, community and industry/utility events. The Electric Power Research Institute (EPRI) is also a project partner. EPRI coordinates the utility efforts and is leveraging the fleet to conduct vehicle to meter communications interface work.

In June of 2010, the DOE approved a proposal to deploy one Escape PHEV to Ford of China and another to Ford of Europe. In the 2011 CY, these two PHEVs were used to demonstrate Ford electrification technologies to the Chinese and European governments as well as numerous global media and utilities. As shown in Figure 1, the 11 utilities and Ford overseas operations provided a wide geographical area in which to study PHEV technology and operation.

Figure 1. Program Partnership Vehicle Locations

Vehicle data is collected during fleet operations in order to understand what the vehicles are experiencing in the fleet as well as to assess their infield performance. Driving and charging patterns, fuel and electrical consumption, and influencing factors such as ambient temperature and peripheral electrical loads are being assessed and analyzed.

Approach

The Escape PHEVs used in this fleet were based off the production Ford Escape Hybrid (Figure 2). Vehicles were modified to replace the production hybrid high voltage battery with a larger lithium-ion battery capable of propelling the vehicle 40 miles under ideal conditions. The first eleven PHEVs built have 10 kWh batteries; the remaining ten have 11.5 kWh batteries. (Note: Vehicles have minor variations between them resulting from the iterative learning process of implementing improvements learned from the construction of previous vehicles.)

Figure 2. Prototype Escape PHEV

Other upgrades include addition of a 1.4k kW charger, ZigBee module (bi-directional communications), structure and suspension upgrades, charge port and plug, transaxle modifications, flexible fuel (E-85) hardware and software, state of charge displays, PHEV controls strategy and human machine interface controls.

The fleet vehicles were also equipped with data acquisition platforms (DAPs) which collect and transmit vehicle data while driving and charging. The data collection and retrieval process is outlined in Figure 3. This information is collected at a 1Hz frequency and covers a wide range of information about the vehicle and battery pack. The data collected is transmitted through an on-board broadband modem and stored remotely. It is then passed on to be formatted into summary reports available for use by Ford and its utility partners.

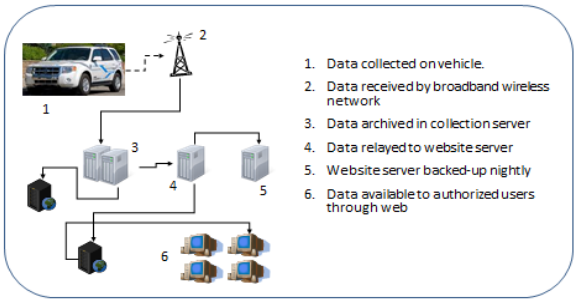

Figure 3. Data Collection System Architecture

Idaho National Laboratories (INL) was directed by the DOE to identify fleet data collection parameters and reporting methods. Ford worked closely with INL to provide the required data, data descriptions and vehicle specific software algorithms. In 2011 CY, the data correlation work was completed and INL began publishing monthly fleet status summary reports on their Advanced Vehicle Testing Activity (AVTA) website.

Results

FLEET USAGE

The data collected during usage of the PHEVs by the utilities has provided an in-depth understanding of what these vehicles are experiencing in the field. To date, data from over 50,000 drive events and 30,000 charge events have been collected and analyzed.

In general, the vehicles are driven roughly every other day, and are driven approximately 56 miles on days they are active. The bulk of the fleet mileage comes from trips less than 40 miles in length. The majority of these trips take place in charge depletion (CD) mode. Charge sustaining (CS) trips account for most of the longer trips, with some trips including a transition from charge depletion to charge sustaining (CD/CS). On a mileage basis, 31% of the distance traveled has been in trips consisting of CS mode only, 34% has been traveled in CD/CS mixed trips and only 26% has been traveled in pure CD trips. Breaking the CD/CS mixed trips apart reveals that the vehicles operate in CS mode over half of the time (58%). A summary of this mileage/mode relationship is shown in Figure 4.

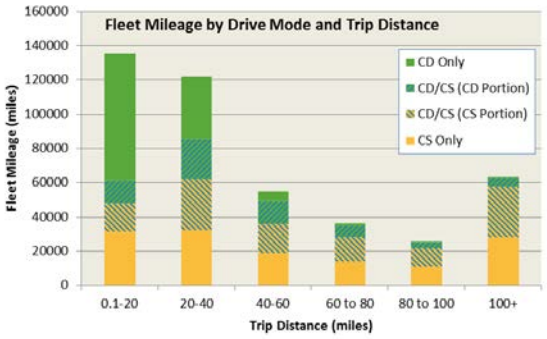

Figure 4. Operation Mode by Trip Distance

Initial design assumptions during the creation and development of this fleet were that the PHEVs would be regularly fully charged overnight. Analysis of the charge event data, however, reveals that the majority of charge events happen during the day and are often interrupted before the vehicles can achieve charge completion. Only 54% of the time does a charge event end with a high voltage battery state of charge (SOC) of >90%, meaning almost half of all charges are interrupted (Figure 5). The fleet average SOC at the end of a charge event is 81%.

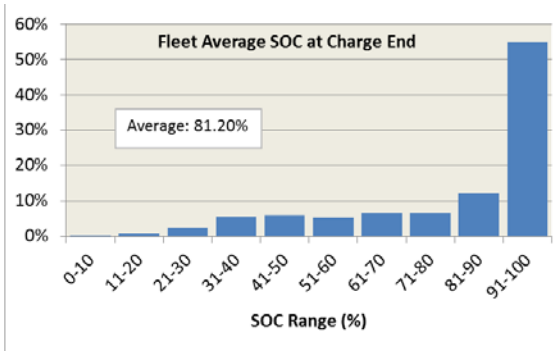

Figure 5. Fleet Average SOC at Charge End

A look at the starting SOC for each drive event further explains the real world charging pattern being experienced by the fleet (Figure 6). Less than 20% of all drive events start with a full state of charge with the average fleet SOC at the start of a drive being about 57%. This charging behavior has a large impact on the fuel economy reported by the fleet and is a key contributor to the limited amount of CD operation being realized.

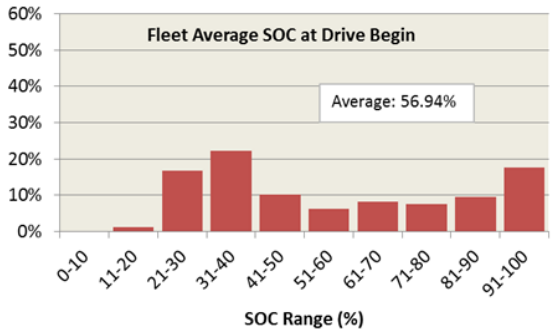

Figure 6. Fleet Average SOC at Charge End

Another key factor which influences the amount of fuel consumed by the fleet is peripheral accessory use. This is particularly noticeable for those accessories powered by the internal combustion engine such as air conditioning (AC). A review of AC-on data and ambient temperature indicates that highest fuel economy is experienced when the ambient temperature is moderate (~60° F) and that it quickly drops off at temperatures over 70°F.

Several technical improvements resulted from this analysis of the data as well as customer feedback. Due to higher energy efficiency, electric AC was initially installed into two vehicles, and was later expanded into a third. Internal testing of a higher electric-only propulsion speed (57 mph vs. 40 mph) was also expanded to three of the vehicles after a positive response from drivers.

Fleet Summary Reports

In 2011 INL began publishing publically available reports entitled the *2010 Ford Escape Advanced Research Vehicle* on their AVTA website. These reports are based on the data collected by the Escape PHEV fleet and include both monthly and annual fleet summary reports.

The monthly publications report the fleet overall gasoline fuel economy for all trips, for those in charge depletion mode, those in charge sustaining mode and those in both modes. The number of trips, trip distance and trip intensity are also reported along with other parameters such as the percentage of miles driven with the internal combustion engine off. Summaries of the plug-in charging events are also available.

The annual fleet summary reports include a graph illustrating the effect of ambient temperature on the fleet realized fuel economy.

The reports are available via the AVTA website: avt.inl.gov/phev.shtml

Communications Interface

(*update provided by John Halliwell, EPRI, 942 Corridor Park Blvd. Knoxville, TN 37932*)

In addition to fleet data collection, the Escape PHEVs in this project have been leveraged to conduct communications interface work. Based on testing conducted, EPRI worked with Pathway Technologies and a collaborating utility to upgrade the ZigBee interface on the vehicle. The ZigBee gateway module firmware was updated to support certificate based authentication based on SE 1.0. The vehicle now supports test and production certificates.

The results of this effort are that the vehicles have demonstrated response to price signals from the advance metering interface (AMI). Due to limitations of the AMI however, the vehicle will not acknowledge a demand response event. The AMI system tested does not allow sending of a negative duty cycle value as required to control the vehicle. SE 1.0 does allow for negative duty cycle values. This issue is being addressed with the AMI system vender and if it can be resolved, additional testing will be carried out in Q1 and Q2 of 2012.

In addition, the vehicle does not have the ability to join multiple meters. One potential way to support joining multiple networks, such as at a work and home location would require that the vehicle user interface be upgraded, allowing the user to select from multiple meter connections. The vehicle system would need to maintain security keys and other information such that the vehicle would reconfigure its settings to match the meter it wants to join. This would require extensive modification of the vehicle human machine interface display and as such, is outside the scope of the current project.

Conclusions

This DOE-sponsored program has:

- Supported the announcement of two mass production PHEV programs in North America and in Europe
- Enabled a nationwide outreach effort including educational, community and industry/utility events

From a Vehicle perspective: The engineering and development conducted for this project has continued to drive production vehicle designs. Analysis of the fleet data, however, has emphasized the contribution of usage patterns on in-field performance. Customer driving and charging patterns are key in matching future vehicle electrification levels in order to achieve maximum fuel economy at a reasonable price. For example, given the infrequency of charges and large percentage of CS operation experienced by this fleet, the battery size of these particular fleet vehicles could be reduced, eliminating weight and cost from the vehicle. Product alternatives (hybrids, PHEVs, all-electric vehicles) which allow consumers to match their personal driving and charging patterns to the most economical level of electrification will achieve greater potential fuel savings than a one-size-fits all approach.

From a Communications perspective: EPRI's interface testing work has validated the ability to perform utility charge control direct to vehicle. Even though the SAE is looking at the use of powerline carrier technology in place of ZigBee and Smart Energy Profiles 2 (SEP2) in place of SE 1.0, there remain issues related to the network security implementation and its impact on establishing communication with the vehicle. These issues are likely to be equally challenging with SEP2 as network joining and authentication requirements remain a concern.

II.B.3. Products

Publications

1. Idaho National Laboratory – 2010 Ford Escape Advance Research Vehicle – *Baseline Performance (PHEV/America) Testing:* avt.inl.gov/phev.shmtl
2. Idaho National Laboratory – 2010 Ford Escape Advance Research Vehicle –

Summary Results to date: avt.inl.gov/phev.shmtl

3. Idaho National Laboratory – 2010 Ford Escape Advance Research Vehicle – *2010 Summary Results*: avt.inl.gov/phev.shmtl
4. Idaho National Laboratory – 2010 Ford Escape Advance Research Vehicle – *2011 Summary Results*: avt.inl.gov/phev.shmtl
5. Idaho National Laboratory – 2010 Ford Escape Advance Research Vehicle – Monthly Summary Results for September 2011, October 2911, November 2011, December 2011 (for additional monthly summary results see library) avt.inl.gov/phev.shmtl
6. Idaho National Laboratory – 2010 Ford Escape Advance Research Vehicle – *Ford PHEV Report Notes:* avt.inl.gov/phev.shmtl
7. Paper Accepted and Under Development for EVS-26 – Carlson, R., D'Annunzio, J., Fortin, C., Shirk, M. "*Ford Escape PHEV On-Road Results from US DOE's Technology Acceleration and Deployment Activity*". EVS 26, Los Angeles, California, 2012

PHEV TECHNOLOGY ACCELERATION AND DEPLOYMENT ACTIVITY

II.C. (c) Development of Production-Intent Plug-In Hybrid Vehicle, using Advanced Lithium-Ion Battery Packs with Deployment to a Demonstration Fleet– DE-FC26-08NT04386

Principal Investigator: Mr. Greg Cesiel
General Motors
30001 Van Dyke Ave
Warren, MI 48090
M/C: 480-210-240
(586) 575-3670; greg.cesiel@gm.com

DOE Technology Development Manager: Lee Slezak
(202) 586-2335; lee-slezak@ee.doe.gov

NETL Project Manager: Jason Conley
(304) 904-7590; E-mail: john.conley@netl.doe.gov

II.C.1. Abstract

Objective

- Overall Objectives
  - The primary goal of the project is to develop the first commercially available, OEM-produced plug-in hybrid electric vehicle (PHEV). The performance of the PHEV is expected to double the uel economy of the conventional hybrid version of the same vehicle. This vehicle program, which incorporates advanced lithium-ion battery packs and features an E85-capable FlexFuel engine, seeks to develop, fully integrate, and validate the plug-in specific systems and controls by using GM's Global Vehicle Development Process (GVDP) for production vehicles. The Engineering Development related activities include two physical builds that produced 29 mule vehicles and 29 integration vehicles for internal deployment at GM. Future planned work includes engineering tasks for the development of a new thermal management design for a second generation battery module.
- FY2011 Objectives
  - The PHEV Vehicle Development team ran development on the new compact cross-over architecture. This new architecture incorporates both current hybrid designs and enhanced hybrid components and systems. The vehicle packaging and component designs completed numerous design iterations aimed at enhancing the performance of production intent vehicles.

Major Accomplishments

- Mule vehicle builds completed
- Integration vehicle builds initiated
- Virtual on-site review with Department of Energy completed in May
- Hot and cold weather development completed
- Powertrain cooling and warm-up development completed
- Drivability enhancements

Future Activities

Phase III of the proposed project captures the first half or Alpha phase of the Engineering tasks for the development of a new thermal management design for a second generation battery module. Engineering Development is a structured process for meeting requirements by selecting, modifying, and optimizing through analyses, demonstrations, inspections, and/or tests. The new thermal management design for the battery module is targeted for introduction with GM's second generation battery. This new design will incorporate reduced complexity, thus allowing for a more cost efficient design. Thermal management of batteries is essential to propulsion system performance. Effective thermal management ensures the maintenance of proper operating temperatures thus increasing range, reliability and durability.

II.C.2. Technical Discussion

Introduction – Engineering Development of Year 1 Mule Vehicles

The first phase of the project captures the first half of the Engineering tasks for the development of key plug-in technologies. This involves the development of components and subsystems required for a PHEV and fully integrate them in a production vehicle.

Approach – Engineering Development of Year 1 Mule Vehicles

This development includes Charge Depletion Development, Lithium-Ion Battery Development, Battery System Integration, Charger Development, Powertrain Systems Integration, and Vehicle Integration.

Results – Engineering Development of Year 1 Mule Vehicles

The PHEV vehicle development team coordinated the above mentioned development testing working towards final designs. At the end of the Mule Vehicle phase, the vehicle packaging and component designs were nearly production intent.

Conclusions – Vehicle and Powertrain Development

All development was completed to the extent required to meet all required Vehicle Technical Specifications (VTS) requirements. This type of development testing will ensure that the vehicle will meet all Federal Motor Vehicle Safety Standards (MVSS).

Introduction – Engineering Development of Year 2 Integration Vehicles

The second phase of the project captures the second half of the Engineering tasks for the development of key plug-in technologies. This involves the development of components and subsystems required for a PHEV and fully integrate them in a production vehicle.

Approach – Engineering Development of Year 2 Integration Vehicles

This development includes Charge Depletion Development, Lithium-Ion Battery Development, Battery System Integration, Charger Development, Powertrain Systems Integration, and Vehicle Integration.

Results – Engineering Development of Year 2 Integration Vehicles

The PHEV vehicle development team coordinated the above mentioned development testing working towards final designs. At the end of the Integration Vehicle phase, the vehicle packaging and component designs are intended to be production intent.

Conclusions – Vehicle and Powertrain Development

All development was completed to the extent required to meet all required Vehicle Technical Specifications (VTS) requirements. This type of development testing will ensure that the vehicle will meet all Federal Motor Vehicle Safety Standards (MVSS).

II.C.3. Products

Publications

1. Plug-In Charging Symposium (San Jose, CA) - July 22nd, 2008
2. California Air Resources Board (CARB) vehicle demonstration (Milford, MI) – Sept 9, 2008
3. EPA vehicle demonstration (Milford, MI) - Oct 30, 2008
4. Hollywood Goes Green Event: - Dec 8, 2008
5. North American International Auto Show (NAIAS) - Jan, 2009

Patents

To date, the project team has generated 31 subject inventions generated. Ten patent applications have been filed. As the contents of these patent applications are not yet subject to public disclosure, GM respectfully refrains from further disclosure regarding these inventions. GM looks forward to sharing the contents of the patent applications once they are publicly available

Tools & Data

N/A

TRANSPORTATION ELECTRIFICATION

II.D. (a) Interstate Electrification Improvement Project DE-FOA-0000028

Principal Investigator: Jon Gustafson
Cascade Sierra Solutions
4750 Village Plaza Loop
Eugene, OR 97401
jgustafson@cascadesierrasolutions.org

DOE Technology Development Manager: Lee Slezak
lee.slezak@ee.doe.gov

NETL Project Manager: Jason Conley
john.conley@NETL.DOE.GOV

II.D.1. Abstract

This demonstration project will accelerate the reduction of petroleum consumption and associated emissions and greenhouse gases by (1) implementing transportation electrification infrastructure at fifty (50) sites along major interstate corridors and (2) providing a 20% rebate incentive for battery operated and/or shore power enabled idle reduction equipment on medium and heavy-duty trucks. Both Truck Stop Electrification (TSE) connections and grid appropriate equipment rebate promotions will be implemented at the travel centers. The project adopted the market title "Shorepower Truck Electrification Project" (STEP) in March, 2011.

Objectives

Overall Objectives

- Identify, finalize selection, and secure contracts to build (50) TSE sites.
- Design and produce build plans for each TSE site.
- Develop the marketing plan for and introduce the rebate program to the trucking industry.
- Successfully complete the implementation of the fifty (50) TSE sites.
- Mark each site opening with an event. Some adjacent sites may hold concurrent events.
- Successfully distribute all rebates by September, 2012.
- Complete final reporting requirements on time.
- Responsibly manage Department of Energy funding to accomplish goals of the program.

Short-term Outcomes:

- The installation and implementation of new, reliable, fuel efficient equipment to support battery operation where feasible and instantly increase fuel economy, maximizing an older trucks environmental performance.
- Job creation will be tracked and documented through money.

Medium-term Outcomes:

- Reduce the nation's dependence on petroleum based fuels (9,450,000 gals in 4 years)
- Reduction in significant amounts of pollution

- Improve respiratory health of surrounding communities, especially children, the elderly, the poor and minorities who are disproportionately affected by diesel pollution.
- Reduce heart disease, respiratory disease, asthma attacks, premature deaths, lost productivity and health costs resulting from diesel pollution.

Long-term Outcomes:

- Promoting the use and acceptance of vehicle electrification as a viable alternative to more costly fuel burning choices.

FY2011 Objectives

- Complete definitization requirements set in place as a result of DCAA audits.
- Identify fifty site locations.
- Launch rebate operations on up to 5,000 truck projects.
- Set up marketing systems to promote the utilization of grid power to rebated trucks and other fleets that can be recruited to the grid.
- Initiate the data collection system at installed sites.
- Formulate a data analysis régime to analyze utilization at the end of the project.

Major Accomplishments in 2011

- ***Completed all DOE Definitization and Administration Requirements***
  - Established job costing and project tracking systems in CSS finance and accounting department for all personnel and operations supporting the DOE grant project.
  - Processed all quarterly reports for Q1 through Q4 on a timely basis.
  - Process all ARRA reports required by the DOE grant contract.
  - Processed and submitted all management reports to NETL.
- ***Contractual relationships between grant recipient and contractors completed by March, 2011.*** Shorepower and CSS negotiated four separate contracts to formalize the partnership to supply pedestals, locate and design sites, operate sites and wind up the contract at end of project. Administrative systems for project control established by mid-summer. Full implementation of construction management and control launched late summer, 2011.
- ***National competitive solicitation completed for electrical general contractor to complete fifty (50) sites using competitive bid processes prescribed for procurement of construction services using Federal funds***. The electrical contractor selected is EC Company. The first Shorepower STEP site was completed less than 3 months from the start date, on or around June 1, 2011. Processes put in place to solicit participation with MBE and DBE. Local subcontractor notification processes completed to encourage local subcontracting of electrical and underground work. Contracts include all Federal contract award and wage compliance reporting requirements.
- ***NEPA reviews and approvals received from DOE on 117 prospective site locations***. Additional sites submitted as backups to the top fifty sites accepted for pre-engineering and schematic design.
- ***Twenty-five sites completed or in various stages of construction by year end.*** Three sites completed and accepted. Five (5) additional locations in construction with an additional 17 sites in preconstruction, permitting and schematic review, for a total of 25 sites at the end of the 2011 reporting period. EC Company has performed well and is taking the lead on site engineering and planning activities at each site. EC is responsible for the final design, permitting and coordinating installation of the utilities. Overall, the project has negotiated and secured site agreements with 67 truck stops/host sites on time (Sept 1 milestone) - 50 chosen and 17 alternates spread across 31 states along major interstates; including the largest truck stop chain in the world. Map: http://g.co/maps/5ukja
- ***Redesigned eTRU plug-in capabilities to accommodate users of grid for trailer refrigeration***. Although included in the original DOE approved budget, CSS requested that Shorepower submit a proposal for the eTRU connections and portable AC units. In discussions with Carrier and other

industry professionals, CSS and Shorepower found that most TRUs with the electric standby option are moving towards the more efficient 480 volt AC power. Therefore, the project will focus on providing infrastructure that meets these future needs within the bounds of the initial infrastructure budget.

- ***Equipment Supplier Agreements negotiated with thirty (30) manufacturers of rebate qualified lines of equipment***. Requests for Proposals (RFP) were elicited from manufacturers of U.S. EPA SmartWay verified technologies that incorporated electric standby options. RFPs were also elicited from truck and trailer refrigeration system manufacturers that incorporated electric standby options that could significantly reduce engine idling necessary to maintain load temperatures in transit. The equipment categories and the number of approved manufacturers and equipment models are indicated as follows:

Equipment Category	No. Manufacturers	No. Models
Auxiliary Power Units	9	14
Battery A/C Systems	12	25
Thermal Storage Systems	1	2
Evaporative Coolers	1	2
Trailer TRU & E-hybrid TRU	2	5
Straight Truck Refrig Systems	2	2
Truck Cold Plate Systems	3	5

- ***A rebate application database developed with an automated database integration to provide electronic data processing by CSS Tech Advisors***. Applications are reviewed, assigned, monitored, approved, identified as completed for DOE reimbursement through a secure CSS internal database access capability. Status reports are generated by CSS management to review project rebate status by equipment categories, transportation corridors, completion dates, or by month as well as customized extracts.

- ***Processed 2,359 rebate applications to reach 50% of project goal valued at $3,088,716.79***. with an additional 150 currently being reviewed for approval. The equipment funding allocation for the two main categories of approved rebates are 75% Idle Reduction Technologies and 25% Refrigeration Technologies. These rebates represent a total grant fund allocation of $5.98 Million. Approximately 2500 individual rebates remain and will be processed in 2012. The corridor, or route, assignments of the rebated vehicles has been somewhat evenly distributed throughout the nation with the exception of the Central Routes which has about 4 times that of the other routes. This is to be expected giving the nature of Long Haul/Over-the-Road Trucking in America.

West Coast:	302
Central Routes	1315
East Coast	267
Southern Routes	260
Northern Routes	215
Total All Rebates:	2359

- ***A rebate marketing program established to recruit the best qualified equipment owners into the TSE program***. Initial marketing of the STEP Rebates during 2011 was accomplished by leveraging relationships with the eligible equipment manufacturers and their distribution channels. CSS Marketing attended the Mid-American Truck Show (MATS) in March and visited with all eligible equipment manufacturers in attendance. Upon receipt of an acceptable Proposal and subsequent approval, equipment models were added to the eligible equipment listing web page and a "Vendor Packet" of materials were distributed to the equipment manufacturer. The Vendor Packet provided copies of all documents associated with the rebate program, instructions for dealers and installers for facilitating rebate applications and marketing materials to help the dealerships market the STEP rebate project. Many equipment manufacturers repurposed the marketing materials with their monikers to enhance the

credibility of the program through their distribution channels. This effort was sufficient to jump start the rebate program and push several equipment categories to near full subscription by the end of 2011. CSS Marketing will reach out again to the equipment manufacturers in Q1 of 2012 to ensure full allocation of all rebates by mid-2012.

- ***A Fleet and Owner-Operator Program Marketing Program launched to provide national publicity to the DOE grant project***. Surveys were initiated with major fleets from the FleetOwner top 500 Private Fleet List (early 2011) and with smaller refrigerated van fleets (late 2011) to gauge participation at the STEP truck stops. E-mail communications and press releases to transportation industry media publications were launched periodically throughout the year to keep the project in the public eye. The marketing to fleets is planned to begin in earnest during Q1 of 2012 with TSE benefits education and incentives to use the truck stop electrified parking as additional truck stops come on line.
- ***A STEP Project Website created to host all marketing and project management details***. www.the-step-project.org Website development was contracted to Ricochet Partners in Portland, OR. The content was developed mutually by Shorepower Technologies (SPT) and CSS. Upon completion of the initial website design, the site maintenance was turned over to SPT and CSS. Various pages on the CSS website were developed and maintained throughout 2011 referencing STEP project related activities. These included news releases and rebate application info on Home Page, updates to Product Showcase, Grant Opportunities, On-Line Rebate Application, STEP program description pages and the current rebate eligible equipment listing page.
- ***Idle reduction data collection and emission reductions research surveyed and settled into a data analysis concept***. Initial research was performed throughout 2011 to evaluate reliable sources of electrical grid utilization data that can tie to fuel savings from the various equipment categories. Data sources that could be included in the industry study include but are not limited to SPT pedestal transaction data, telematics used by the fleets, vehicle ECM data and driver logs, records obtained from on-going fleet benchmark tests and blind utilization data from guest (non-rebated) vehicles at the SPT pedestals or obtained from other TSE manufacturer's transaction databases. Emissions reduction calculation strategies were also investigated in advance of adding that capability to the STEP Rebate applications database where rebated vehicle profiles were captured from on-line rebate applications.
- ***Truck Stop Grand Opening Event Planning launched with the completion of the first three sites and has now been programmed for the majority of the remaining 47 locations***. The CSS Marketing Dept. in Eugene provided support for the Grand Openings throughout 2011 in advance of the initial truck stop roll outs. This included but was not limited to design and production of the 10x10 STEP Event canopy, podium stand, sound system, various marketing documents for on-site distribution, review and assist with signage production, review and assist with ad designs for OverDrive and Transporte Latino magazines and communicating with eligible equipment manufacturers and regional dealers to attend the Grand Opening events.
- ***Promotional TSE connector kits procured and made ready for distribution at TSE sites to promote and recruit truckers to the TSE sites***. To conveniently access shore power, the cab should have a plug inlet that is included with the connector kit. 1,300 connector kits are available through the STEP rebate project but require a different rebate and installation process compared to the other rebated equipment categories. A Request for Proposal was presented to 12 manufacturers. Two suppliers who had previous experience producing connector kits for trucks were approved. A separate on-line application form and process has been developed and initial orders for connector kits have been issued to each of the two approved connector kit manufacturers. Rebates will be processed beginning in Q1 of 2012. Because 1,300 connector kits represent a small percentage of the market need, all rebates are anticipated to be allocated by the end of Q3 in 2012.
- ***TSE industry group organized and named National Idle Reduction Technologies Association (NIRTA) to promote truck stop utilization of grid power by all levels of the trucking industry***. Its founders include all major suppliers of grid friendly equipment with associate memberships from on-board equipment suppliers and the truck stop operators. First operation of NIRTA occurred in November, 2011. It will be publically announced in Q2 2012. DOE has an advisory function out of Argonne National Laboratory where the Idle Reduction Office operates to promote fuel efficiency in freight movement. Recognizing that the industry and the STEP project were best served by coordinating the efforts of the five main TSE equipment infrastructure manufacturers to educate the

public and provide electrified truck parking nationally, CSS helped coordinate the companies and create the National Idle Reduction Technology Association (NIRTA).

- ***SPT completed integration of the STEP database Integration and Vehicle ID System***. All TSE manufacturers' transaction databases only track financial data to a company or individual today. To tie grid utilization to rebated equipment, this project requires each electric use session to be tied to the vehicle, not the operator. This required both the development of a Vehicle ID number system and modifications to the SPT transaction Kiosk software and database. CSS can now receive data field extracts from the SPT transaction database sufficient to allow electrical use to be tied to rebated idle reduction equipment allowing calculations to be made for fuel savings and utilization behavior changes over time. Extracted data includes: transaction date, time, site location, charge point identity, type of power connection used, length of session, cost to user, KWH used, Vehicle ID, Payee name and payment type. Vehicle ID cards have been ordered with delivery in January 2012. Vehicle IDs with instructions for use will be mailed to all rebated vehicle owners beginning in Q1 of 2012. Provisions have been made with the vehicle ID system to include other data sets such as other SPT customers without rebates, CSS Fleet Members without rebates, non-rebated vehicles from rebated fleets and other TSE supplier customers.
- ***Grand opening events held in Lincoln, Nebraska, Baker City, Oregon and Wendover, Utah***. The overall success of the grand openings has been excellent and stakeholder relationships have been built. The leveraging of existing partners. Clean Cites Coalitions, clean diesel collaboratives, and Trucking Associations in Nebraska and Utah will be integral to the long term success of TSE. Each of these two states has multiple TSE sites in the STEP project.
- ***Industry engagement and DOE project marketing launched with radio broadcasts and webinars in Nov and well attended by target market customers and thru articles in Transportation Topics and Transportation Latino***. This industry engagement process is lively and is cost effective and will offer a continued means to communication to the fleets. The first webinar was well attended and demonstrates an ability to grow awareness of the status of the project. Vendor sales of the TSE related technologies have spiked significantly, especially in APU and refrigeration technologies of the Shorepower capable APU and Trailer Refrigeration Units (TRU). The STEP website serves as an information clearinghouse for all target audiences. www.the-step-project.org Using a public relationship contractor the project has been featured in no fewer than 70 mentions or feature articles in major trade publications, magazines, and blogs. Achieved awareness for STEP, CSS, Shorepower and their respective roles in Truck Stop Electrification. . http://www.truckpr.com/ and http://www.truckpr.com/shorepower-technologies/ and launched in social media campuses: http://www.facebook.com/shorepowertechnologies

Future Activities

- Complete remaining TSE sites by end of summer 2012. All fifty sites are scheduled for completion before September, 2012.
- Hold grand opening events at all sites. Four openings to be multi-day events featuring vendor fairs with equipment displays of the on-board equipment. Approximately 20 openings to feature full gatherings of industry and public officials with full press coverage. The remaining grand openings to have local officials and trucking company participation.
- Complete rebate commitments and installations by late-summer 2012. Deploy connector kits as incentives to 1,300 truckers coming into the project.
- Launch marketing to all rebated truckers to promote the adoption of TSE as a key strategy to eliminate idling.
- Begin data collection on truck utilization as trucks become equipped along routes hosting TSE sites. Have all trucks in the rebate project on the data collection network by September, 2012.
- Begin tracking utilization data by selected data sorts and begin to study patterns of utilization by year end.
- Review all rebated vehicles to see where there is no utilization and make contact with vehicle owners to launch grid utilization

II.D.2. Technical Discussion

- See STEP website - an information clearinghouse for all target audiences. www.the-step-project.org
- See awareness promotion products for STEP, CSS, Shorepower and their respective roles in Truck Stop Electrification. http://www.truckpr.com/ and http://www.truckpr.com/shorepower-technologies/
- Launched and managed social media campaigns:

  http://www.facebook.com/shorepowertechnologies

  http://www.facebook.com/CascadeSierraSolutions

  https://twitter.com/CascadeSierra

  http://www.youtube.com/user/CascadeSierra
- See education and awareness campaigns via email and blog with above average open and click rates. http://www.the-step-project.org/program-progress/blog/
- See map of all existing and future TSE locations.

Patents

None

Publications

None

II.E. (b) RAM 1500 Plug-In Hybrid Electric Vehicle

Principal Investigator: Abdullah A. Bazzi
Chrysler Group LLC
800 Chrysler Drive
Auburn Hills, MI USA 48326-2757
1-(248) 944-3093; aab5@Chrysler.com

DOE Technology Development Manager: Lee Zlezak
1-(202) 586-2335; Lee.Slezak@ee.doe.gov

NETL Project Manager: John Jason Conley
(304) 285-2023; John.Conley@NETL.DOE.GOV

DOE Award Number: DE-EE0002720
Submitted to: U.S. Department of Energy – National Energy Technology Laboratory

II.E.1. Abstract

Objective

- Demonstrate 140 pickup trucks in diverse geographies and climates, spanning from New York to Arizona & California to Massachusetts, and across a range of drive cycles and consumer usage patterns applicable to the entire NAFTA region
- Verify plug-in charging mode performance based on charger and battery model
- Verify AC power generation mode
- Prove product viability in "real-world" conditions
- Develop bi-directional (communication and power) charger interface
- Support the creation of "Green" Technology jobs and advance the state of PHEV technology for future production integration
- Develop an understanding of Customer Acceptance & Usage patterns for PHEV technology
- Quantify the benefits to customers and to the nation

Major Accomplishments

Vehicle Build & Test

- Built a 140 demonstration fleet vehicles
- Deployed 105 vehicles to the demonstration partners
- Development and validation utilized the standard Chrysler Group LLC Vehicle Development Process for a production intent program.
  - Designed and built all development and test vehicles
  - Augmented development process with modified testing procedures to address specific plug in Hybrid Technologies
- Facility Based Testing: hot static cell, hot drive cell, cold static cell, cold drive cell, altitude chamber, engine dynamometer, transmission dynamometer, NHV cell, EMC cell, end of line, emissions test facility; bench Testing: vibration, SOC, thermal, charge / discharge cycling
- Impact Testing: Successfully Completed for FMVSS compliance

- Road trips: development testing and verification: hot trip to 125F, cold trip to -20F, altitude trip to 12,000 ft
- Durability testing: powertrain, high mileage, two charge cycles per day

Future Activities

- Complete Vehicle Deployments
- Continue to Capture Deployed Fleet Data to support Calibration and Controls development
- Enhance Data Reporting Capabilities
- Finalize Smart Grid & Reverse Powerflow
- Customer Interface Server

II.E.2. Technical Discussion

Introduction

The Chrysler Product Creation Process (CPCP) defines the strategy and method used to execute the development of world class vehicles from concept to market. The RAM 1500 PHEV is following the CPCP process. Fundamental principles include:

- Voice of the Customer – Dictates product decisions
- Timeline Compression – Enables speed to market
- Flexibility – Allows for unique vehicle program characteristics
- Consistency of Execution – Facilitates continuous improvement
- Clear Performance Indicators – Drives accountability
- Interdependencies Identified – Aligns activities across functional areas

Approach

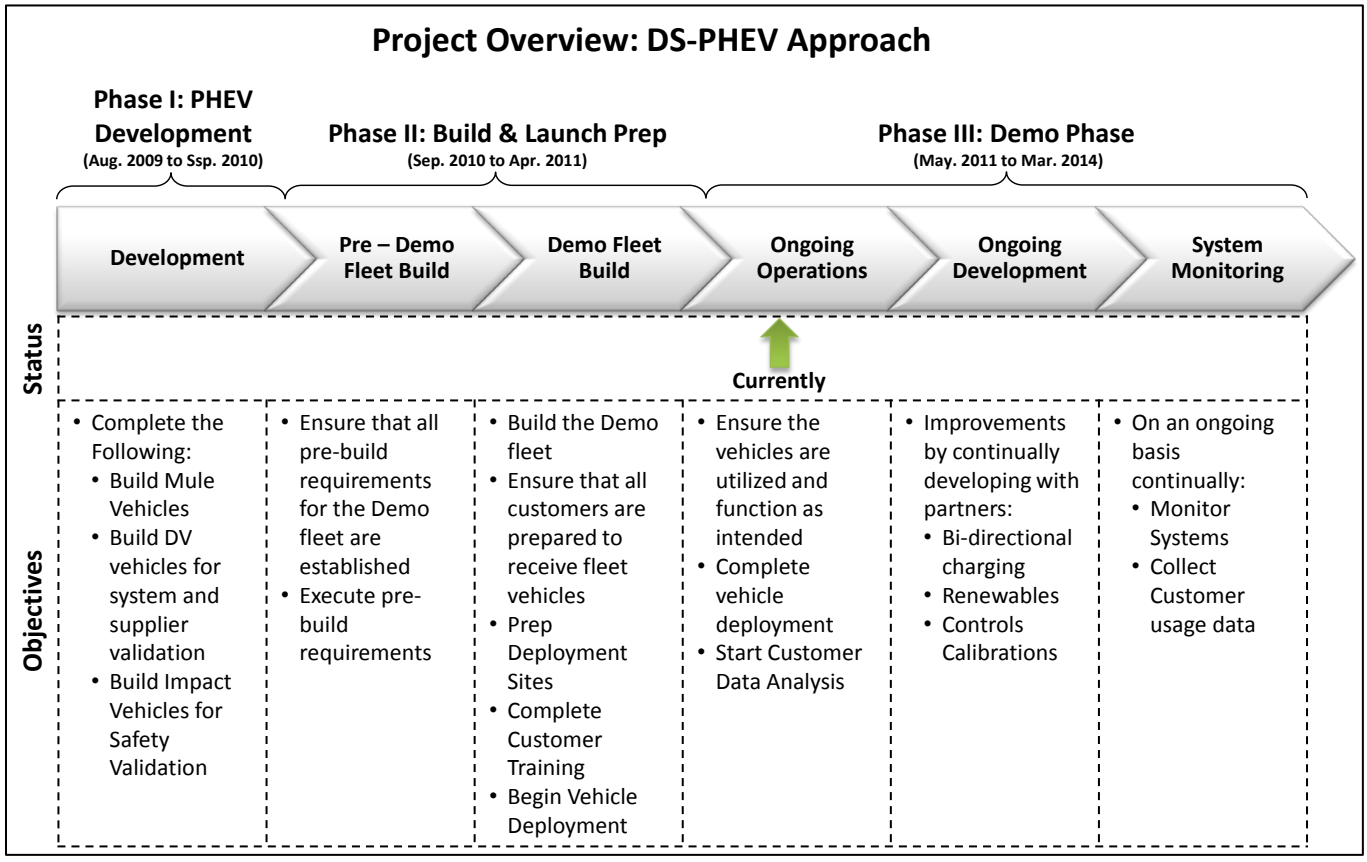

Figure 1. DS-PHEV Project Approach

Results

Federal Test Procedure Results

Table 1. DS-PHEV Federal Test Procedure Results

<table>
<tr><th></th><th>Proposal</th><th>DS-PHEV Status</th><th>Procedure</th></tr>
<tr><td>RANGE</td><td>Equivalent All Electric Range (EAER) of 20 miles</td><td>20+ miles EAER achieved</td><td>California Exhaust Emission Standards And Test Procedures, as amended December 2, 2009</td></tr>
<tr><td>EMISSIONS</td><td>ATPZEV Compliance</td><td>
<table>
<tr><th>Test</th><th>Test Mode</th><th>Standard</th><th>Results</th></tr>
<tr><td>FTP City</td><td>CD & CS</td><td>SULEV</td><td>Passed ✓</td></tr>
<tr><td>US06</td><td>CS</td><td>SULEV</td><td>Passed ✓</td></tr>
<tr><td>SC03</td><td>CS</td><td>SULEV</td><td>Passed ✓</td></tr>
<tr><td>Highway</td><td>CS</td><td>SULEV</td><td>Passed ✓</td></tr>
<tr><td>50 F City</td><td>CS</td><td>SULEV</td><td>Passed ✓</td></tr>
<tr><td>20 F Cold</td><td>CS</td><td>SULEV</td><td>Passed ✓</td></tr>
<tr><td>Evaporative</td><td>CS</td><td>PZEV</td><td>Passed ✓</td></tr>
<tr><td>Purge Volume</td><td>CS</td><td>PZEV</td><td>Passed ✓</td></tr>
</table>
</td><td>California Exhaust Emission Standards And Test Procedures, as amended December 2, 2009</td></tr>
<tr><td>FUEL ECONOMY</td><td>Charge Depleting City 32 MPG</td><td>– Charge Depletion:
– City: 37.4mpg
– Hwy: 32.5 mpg</td><td>SAE J 1711 as published</td></tr>
</table>

Real World Results

Table 2. DS-PHEV Real-World Results Observed from Vehicles at Partner Locations

	DS-PHEV Status	Background
FUEL ECONOMY & Mileage Accumulation (Real World)	– Charge Depletion: Accumulated Miles – 48,300 – City: 22 mpg – Hwy: 26 mpg – Charge Depletion / Charge Sustaining: Accumulated Miles – 18,683(CD) / 32,992(CS) – City: 19 mpg – Hwy: 21 mpg – Charge Sustaining: Accumulated Miles – 119,047 – City: 16 mpg – Hwy: 19 mpg	• Data taken from 100 partner vehicles deployed throughout the United States • Total mileage : 218,902 • Vehicle fuel economy is based on customer usage and may not be representative of maximum potential fuel economy

Conclusions

Chrysler is actively tracking vehicles, and collecting vehicle usage and technical data. Vehicle Usage Agreements have been finalized and vehicles have been delivered to the following locations:

- City of Yuma, Arizona – 10 vehicles
- Sacramento Municipal Utility District (SMUD) in California – 14 vehicles
- City of San Francisco in California – 14 vehicles
- Duke Energy in Charlotte North Carolina – 10 vehicles
- Central Hudson in Albany, New York – 3 vehicles.
- National Grid placed vehicles in New York, Massachusetts & Rhode Island – 6 Vehicles
- Massachusetts Bay Transit Authority (MBTA) – 10 Vehicles
- City of Auburn Hills, Michigan – 4 Vehicles
- EPRI (North Carolina and California) – 2 Vehicles
- CenterPoint, Houston, Texas – 5 Vehicles
- Argonne National Lab (DOE) – 1 Vehicle
- NV Energy, Las Vegas and Reno , Nevada – 5 Vehicles
- DTE, Detroit, Michigan – 10 Vehicles (9 delivered; remaining 1 is being tested for Reverse Power Flow with both DTE and NextEnergy)
- NYPD, New York – 5 Vehicles
- TriState, Colorado – 6 Vehicles

The remaining Demonstration Partner Vehicle Usage Agreements are in process for the Idaho National Laboratory and Department of Defense (Air Force Bases in Los Angeles and Fort Carson in Colorado).

II.E.3. Products

Publications

1. Charge Depleting Control Strategies and Fuel Optimization of Blended-Mode Plug-in Hybrid Electric Vehicles. IEEE Transaction on Vehicular Technology, Vol. 60, No.4, May 2011
2. Analytical Approach for the Power Management of Blended Mode Plug-In Hybrid Electric Vehicles. Accepted by IEEE Transaction on Vehicular Technology
3. A High Efficiency Low Cost Direct Battery Balancing Circuit Using A Multi-Winding Transformer with Reduced Switch Count. IEEE APEC 2012, Orlando, FL, Feb. 5 – 9, 2012
4. Hybrid / Plug-in-Hybrid Technology Overview – Torque Feed forward Control for IPM Motors

Public Presentations

1. Summit on Automotive Electrification. Kokomo, Indiana
2. “Are you plugged in?” Conference. Auburn Hills, Michigan
3. Annual Merit Review. Washington, D.C.

Patents

Chrysler IDR No.	Patent Application USPTO Serial No.	Patent Application Title	File Date at USPTO	DOE Program
708376	12 / 844,872	REMOTE CONTROL SYSTEM FOR A HYBRID VEHICLE	28-JULY-2010	IDR – Ram PHEV
708551	61 / 536,173	ELECTRIC-DRIVE TRACTABILITY INDICATOR INTEGRATED IN HYBRID ELECTRIC VEHICLE TACHOMETER	19-SEPT-2011	IDR – Ram and Minivan PHEV
708553	13 / 160,561	ADAPTIVE POWERTRAIN CONTROL FOR PLUGIN HYBRID ELECTRIC VEHICLES	15-JUNE-2011	IDR – Ram and Minivan PHEV

Tools & Data

1. Vector Cantech – Canalyzer equipment utilized for data collection and software development (communication between vehicle controllers)
2. ETAS – Equipment utilized for software development and drivability / emissions calibration
3. Technical Training Inc. – TTI worked with Chrysler Electrified Powertrain engineers to develop a PHEV dealer technician training course and handbook for the dealerships supporting the DOE fleet vehicles
4. Security Inspection utilized for upgraded infrastructure environment (increased bandwidth requirements and storage requirements) for implementing Microstrategy vehicle logging and data analysis
5. Bright Star Engineering -- Data Recorder Modules (DRM) for each vehicle and monthly cellular access

II.F. (c) ChargePoint America

Principal Investigator: Richard Lowenthal
Coulomb Technologies, Inc.
1692 Dell Avenue
Campbell, CA 95008
(408) 841-4501; Richard.Lowenthal@coulombtech.com

DOE Technology Development Manager: Lee Slezak
(202) 586-8055; Lee.Slezak@ee.doe.gov

NETL Project Manager: John Jason Conley
(304) 285-2023; John.Conley@NETL.DOE.GOV

II.F.1. Abstract

Objective

- CHARGEPOINT AMERICA will demonstrate the viability, economic and environmental benefits of an electric vehicle charging infrastructure. With the arrival of electric vehicles (EVs) and plug in electric vehicles (PHEVs) late 2010, there is a substantial lack of infrastructure to support these vehicles. CHARGEPOINT AMERICA will deploy a charging infrastructure in ten (10) metropolitan regions in coordination with vehicle deliveries targeting those same regions by our OEM partners: General Motors, Ford and smart USA. The metropolitan regions include Austin/San Antonio (TX), Bellevue/Richmond (WA), Boston (MA), Southern Michigan, Los Angeles (CA), New York (NY), Orlando/Tampa (FL), Sacramento (CA), San Francisco/San Jose (CA) and Washington (DC). CHARGEPOINT AMERICA will install more than 4000 Level 2 (220v) SAE J1772™ compliant, UL Listed networked charging stations in home, public and commercial locations to support approximately 2400 program vehicles. Coulomb's ChargePoint® Network will collect data to analyze how individuals, businesses and local governments are using their vehicles. Understanding driver charging behavior patterns will provide the DOE with critical information as EV adoption increases in the United States. Deployment of the charging station infrastructure has begun in July 2010.
- The project will provide public and private Level 2 charging stations from which data will be collected and forwarded to INL for compilation and analysis. The project will leverage other company efforts and infrastructure. The project is also working with the local press to expand awareness and receptivity. The first phase of the program, which began in June 2010, involved the deployment of the charging stations. Phase 2 will have a two-year duration, during which time data will be collected concerning the times of highest charging, charging rates, and load on the grid.

Major Accomplishments

- Residential and public station allocations in the 10 regions of the program are well underway and we are extremely pleased with the progress of the program. We have fully allocated our supply of stations and are no longer accepting applications for free public charging stations. More and more EVs in our program are becoming available (such as those from Ford) and home stations will be provided to qualified vehicle owners.
- ChargePoint America program is progressing as per the plan to deploy over 4000 charging stations.
  - Public committed - 100%
  - Public shipped - Over 85%
  - Private Committed - 100%
- Public stations are fully assigned.
  - Boston region (City of Boston, MBTA, National Grid, City of Cambridge etc.)

  - New York region (Edison Parking, GMC Parking, Icon Parking, NYPD, NY DOT, Stony Brook University, Rutgers, LaGuardia/Kennedy Airports)
  - DC/Baltimore Region (DC DOT, City of Baltimore, University of Maryland, VA Tech, Verizon)
  - Detroit region (Detroit, Dearborn, Flint, Consumers Energy, Michigan State, Whirlpool, Compuware, GM, UAW, Mercedes, Kohl's)
  - Orlando/Tampa region (OUC, Orlando, Tampa, Marriot, Best Western, UCF, USF, AAA)
  - Austin/San Antonio region (Walmart, HEB, Kohl's ERCOT, Port of San Antonio, Wyndham, Dell Children's Hospital,)
  - Bellevue/Redmond region (City of Redmond, City of Bellevue, Tacoma, Valley Medical etc.)
  - Los Angeles region (Irvine Company, UCLA, CSF, CSLA, Cities of Orange, Burbank, Anaheim, Venture, Riverside)
  - Sacramento region (UC Davis, County of Sacramento, USAA etc.)
  - San Francisco region (City of San Francisco, City of San Jose, City of Oakland, SFO Airport, Facebook, SunPower, Bloom Energy, Stanford University, County of Marin)
- All charging stations data is regularly forwarded to Idaho National Labs for analysis and summary. INL released first report on ChargePoint America Program in November 2011. The report provides information on charging units installed per state, charging sessions, charging unit utilization, charging unit usage by type, and electricity consumed.
- We stopped accepting applications for the public program and have reached out to all customers who have applied and communicated to potential customers that they will be placed on a wait list. The ChargePoint America web site was updated with this information.
- Coulomb marketing and public relations held unveiling events in several CPA regions and some of the events were in Detroit, Orlando, New York City, Los Angeles, San Francisco, San Jose and Bellevue.
- Volt Promotion – In March, CPA home station application information (brochures) sent to every Chevrolet dealer in the US selected for Volt sales.
- In April 2011, CTI expanded the CPA program into one new US city: (Boston, MA) and extended its existing metropolitan areas to include: Baltimore, Md., Tampa, Fla., Santa Barbara, Calif., San Antonio, TX, and Santa Cruz, California.
- Coulomb partnered with BMW for the Boston release of ActiveE all-electric vehicle. Drivers of BMW, ActiveE can easily and conveniently fuel their electric vehicle (EV) at any ChargePoint-enabled electric vehicle charging station in the US as well as access ChargePoint Network and mobile phone applications
- CTI has released mobile apps for smart phones including iPhone, Android and Blackberry. The app provides electric vehicle drivers the ability to locate and check occupancy status and make reservations for a charging station. The ChargePoint apps continue to be the industry's first and only mobile apps that give EV drivers real-time charging station status, reservations, smart phone payments, location information and navigation.

Future Activities

CTI is planning to complete installations of residential and public charging stations in 2012 and after installations are complete we will continue with data collection and reporting until the end of the program.

- Public charging stations deployment will be completed in 2012

- Residential program deployment will be completed in 2012
  - GM Volt has been the primary electric vehicle for the residential program and it will continue into 2012
  - Planning to bring Nissan LEAF into the CPA program in 2012 and initially target Austin/San Antonio and Sacramento regions and later to other CPA regions.
  - Planning to bring Fisker Karma into the CPA program in 2012 and targeting all 10 CPA regions.
  - Ford Focus will also be targeted in all CPA regions.
  - Some of the residential charging stations will be targeted towards Multi Dwelling Units.
- Continue to coordinate completion of installations and receipt of Davis Bacon paper work.
- Data collection and reporting will continue and data will be uploaded to INL on a regular basis.
- INL will continue to provide CPA reports.

II.F.2. Technical Discussion

CTI developed and released two new products CT2025 and CT2021 in 2011. We specifically developed CT2025 for this program. We worked with DC DOT to develop CT2025 product that has integrated cord management.

The CT2021 dual charging stations provide two 7.2 kW (208/240 V @ 30 A) Level II charging ports and are designed for public outdoor applications for the North American marketplace. Charging is delivered via standard SAE J1772™ connectors attached to self retracting cords. The product CT2021 is shown in Figure 1. Detailed CTI product information can be found at

http://www.coulombtech.com/products.php
http://www.coulombtech.com/products-chargepoint-stations.php

Detailed customer list can be found at http://www.coulombtech.com/customers.php

Below is a map of all the publicly available charging stations.

Below are links to press releases, media coverage, events, and photo gallery.

http://www.coulombtech.com/news-press-releases-2011.php

http://www.coulombtech.com/news-media-coverage.php

http://www.coulombtech.com/news-video-coverage-openings.php

http://www.coulombtech.com/news-video-coverage-reports.php

http://www.coulombtech.com/news-video-coverage-customers.php

http://www.coulombtech.com/news-video-coverage-demos.php

http://www.coulombtech.com/news-products-photos.php

http://www.coulombtech.com/news-products-photos-installation.php


ChargePoint
1
2

II.F.3. Products

CTI products CT-2025 and CT-2021 were developed to enhance safety and eliminate energy theft, drivers access and energize the station using a ChargePoint card or contactless credit card. The station's highly visible display guides drivers with instructive messages and can be used to display custom advertisement or greetings for drivers.

Detailed information about the ChargePoint America program can be found at http://chargepointamerica.com/

To apply for a charging station, information can be found at http://chargepointamerica.com/search-zip-code.php

Publications

Patents

In 2011 CTI filed for 15 patents and 1 was issued and 14 are pending.

II.G. (d) Electric Drive Vehicle Demonstration & Vehicle Infrastructure Evaluation (DE-EE-00002194)

Principal Investigator: Donald Karner
ECOtality North America
430 S. 2nd Avenue
Phoenix, AZ 85003-2418
(602) 345-9000; dkarner@ecotality.com

DOE Manager, Vehicle Systems
Vehicle Technologies Program: Lee Slezak
(202) 586-2335; Lee.Slezak@ee.doe.gov

NETL Project Manager: John J. Conley
(304) 285-2023; John.Conley@NETL.DOE.GOV

II.G.1. Abstract

Objective

- Overall Objectives
  - The objective of the Electric Drive Vehicle Demonstration and Vehicle Infrastructure Evaluation is to use production electric vehicles (EVs) to develop, implement, and study techniques for optimizing the effectiveness of infrastructure supporting widespread EV deployment. It will utilize the deployment of these production plug-in EVs for the purpose of evaluating and/or optimizing (1) vehicle use, (2) charge infrastructure utilization, (3) charging interface with smart grid operations, and (4) charge infrastructure sustainability models.
  - This project (DE-EE0002194) is scheduled to collect and evaluate data from vehicles and charging infrastructure through April 2013. It was awarded to Electric Transportation Engineering Corporation (now doing business as ECOtality North America, referred to in this document as ECOtality) at the end of September 2009.
- FY2011 Objectives
  - Deploy approximately 8,000 Level 2 electric vehicle supply equipment (EVSE).
  - Deploy approximately 5,000 Level 2 EVSE and DC fast chargers in non-residential locations in order to characterize charging infrastructure and vehicle use in diverse topographic and climatic conditions.

Major Accomplishments

- 3,123 Level 2 Residential EVSE installed
- 493 Level 2 Commercial EVSE installed (publicly accessible, fleet, workplace)
- 1 DC Fast Chargers (DCFC) installed
- Data collected from 2,822 vehicles and 2,990 EVSE
- Documented 6.2 million test miles and 178,000 charging events
- Networked location maps available via mobile apps
- “Over the Air” software updates
  - Future Activities
- Deploy up to 5,177 additional Level 2 Residential EVSEs
- Deploy up to 4,731 additional Level 2 Commercial EVSEs and DCFCs

- Continue accumulating both vehicle and EVSE use data
- Access fee administration for open access to EVSE network
- Media sales from deployed EVSE

II.G.2. Technical Discussion

Introduction

The EV Project is an American Recovery and Reinvestment Act (ARRA) funded Department of Energy (DOE) project for deploying and testing plug-in electric vehicle (PEV) recharging infrastructure. Led by ECOtality, it is the largest deployment and testing of EVSE and fast chargers ever attempted. Approximately 13,000 Level 2 EVSE and DCFCs, along with approximately 8,000 Nissan Leafs and Chevrolet Volts are being deployed in the major population areas of:

- Phoenix and Tucson, Arizona
- San Diego, San Francisco and Los Angeles, California
- Portland, Eugene, Salem and Corvallis, Oregon
- Seattle, Washington
- Nashville, Knoxville, Chattanooga, and Memphis, Tennessee
- Dallas, Fort Worth and Houston, Texas
- Washington, D.C.

The project intent is to deploy Level 2 EVSE in the residents of each Leaf or Volt purchaser in the project areas, deploy Level 2 EVSE and DCFCs in public locations in order to characterize charging infrastructure and vehicle use in diverse topographic and climatic conditions, evaluate the effectiveness of public versus private charge infrastructure, and conduct trials of various revenue systems for public charge infrastructures.

Approach

The locations for commercial and public charging infrastructure were initially determined through a series of stakeholder reviews that involved organizations such as local government, electric utilities, local employers, large retailers, and other stakeholders with potential interest in deploying charge infrastructure. Level 2 EVSE and DCFCs are being installed using a Certified Contractor Network (CCN). Novel charge infrastructure and vehicle use demonstrations will be undertaken to evaluate solar charging, subscription public charging, vehicle rental, and transportation corridor development.

Data is being collected from both vehicles and the charge infrastructure. Data is then sent to the DOEs Idaho National Laboratory (INL). Data is being analyzed by INL, as well as by university participants and industry experts to evaluate the effectiveness of deployed infrastructure, develop lessons learned, and suggest methods for improving infrastructure effectiveness. These methods for improving effectiveness will be implemented and their effects monitored and evaluated.

Data collected and information developed will be disseminated on a periodic basis to participants, stakeholders, and the DOE. Task reports will be prepared to document methods, metrics, results, and lessons learned from implementation and operation.

Results

As FY2011 ended, data had been collected from 2,801 Nissan Leaf battery electric vehicles (BEV) (Figure 1), 21 Chevrolet Volt extended range electric vehicles (EREV), and 2,990 ECOtality EVSE that were being operated (Figure 2) in six states. A total of 6.2 million test miles and 178,000 charging events have been documented on the Project Overview Report for the EV Project to date (http://avt.inel.gov/pdf/EVProj/EVProjOverviewQ32011.pdf).

For the Nissan Leafs, there is a complete elimination of in-vehicle use of petroleum for transportation. Because the Volt is an EREV, the fuel use is reported in three modes: 1) overall operations, 2) EV mode operations, and 3)

extended range mode operations (ERM) when the gasoline engine is running.

Using the July through September 2011 summary report for 110 Volts and 208,000 miles, the vehicle averaged 369 AC watt-hours (Wh) per mile with no gasoline used. This operation totaled 50.3% of all 208,000 miles. In ERM operations, the vehicle averaged 37.2 mpg with no electricity used. Overall, the Volts averaged 74.8 mpg and 185 AC Wh per mile. It should be noted that the reports only contain numbers of EV Project vehicles and charging infrastructure that have provided data to the INL at the end of FY 2011. Actual deployment numbers are higher.

The EV Project's Nissan Leaf summary report: http://avt.inel.gov/pdf/EVProj/EVProjNissanLeafQ32011.pdf) provides national and regional Leaf usage statistics for each reporting quarter, and this data includes the national vehicle usage data seen in Table 1. Additional data for each region can be found in the above referenced PDF.

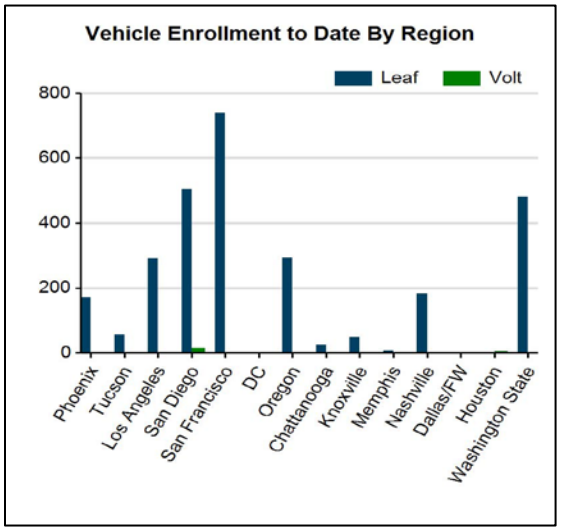

Figure 1. Number of EV Project Vehicles Providing Data and Deployment by Major Cities as of the End of FY 2011

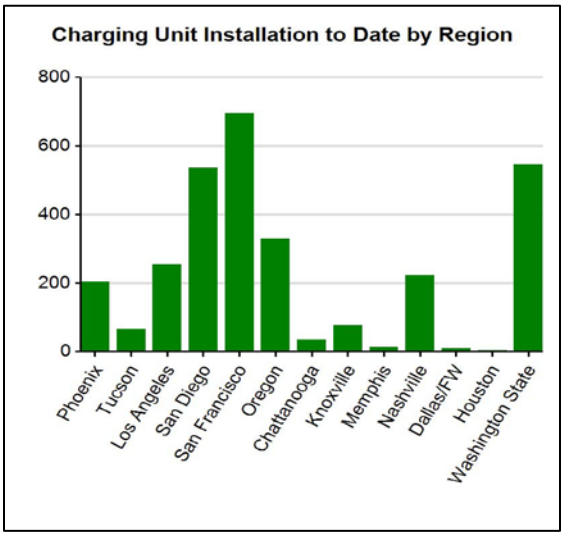

Figure 2. Number of EV Project EVSE Deployed and Providing Data by Major Cities as of the End of FY 2011

Figures 3 and 4 document the Nissan Leaf battery state of charge (SOC) before and after charging events. It will be interesting to see if SOC before-charging changes as operators become more familiar with the vehicles and if SOC at end-of-charging changes as drivers use public charging, including fast chargers for shorter periods of time.

Table 1. EV Project Nissan Leaf BEV Usage Data for the July 2011 to September 2011 Quarter.

Number vehicles	2,394
Total miles	3,718,272
Average miles per trip	6.9
Average miles driven per day when driven	30.8
Average number trips between charge events	4.3
Ave miles driven between charge events	30.1
Ave number of charges per day when driven	1.0
Number of at home charging events	98,891
Number away from home charging events	19,219
Unknown charging event locations	5,485

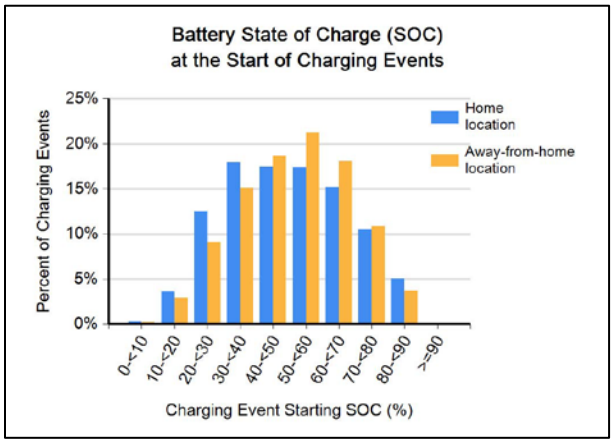

Figure 3. EV Project Nissan Leaf Battery SOC at Start of Charging Events

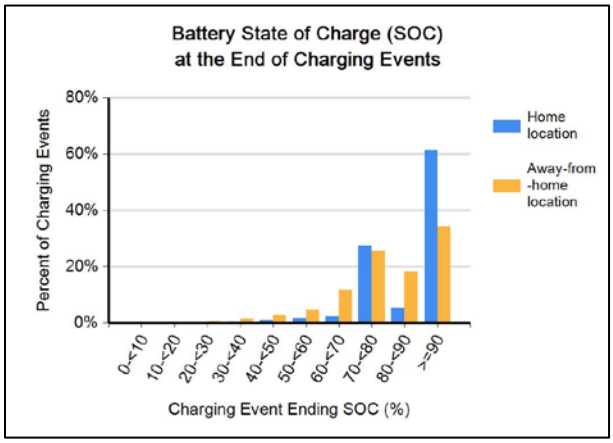

Figure 4. EV Project Nissan Leaf Battery SOC at End of Charging Events

The July–September 2011 quarterly Infrastructure Summary report documents infrastructure utilization nationally and regionally for residential Level 2 EVSE and publicly available Level 2 EVSE. As additional units are installed, this report will also include DCFC data as well as private access, nonresidential Level 2 EVSE.

See: http://avt.inel.gov/pdf/EVProj/EVProjInfrastructureQ32011.pdf for the July through September 2011 report.

Figure 5 highlights the percent of all national Level 2 EVSE charging units in 15-minute increments with an EV Project vehicle connected during week days. Figure 6 is the charging profile in AC MW for all Level 2 EVSE in the EV Project. Note the heavy use of post-midnight charging.

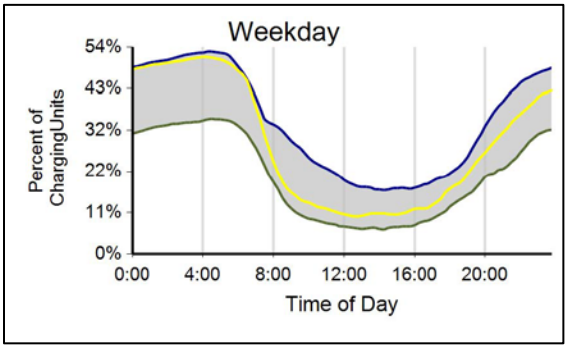

Figure 5. EV Project Percent of All National Level 2 EVSE with a Vehicle Connected During Weekdays (Data is in 15-minute increments for any time in the reporting quarter.)

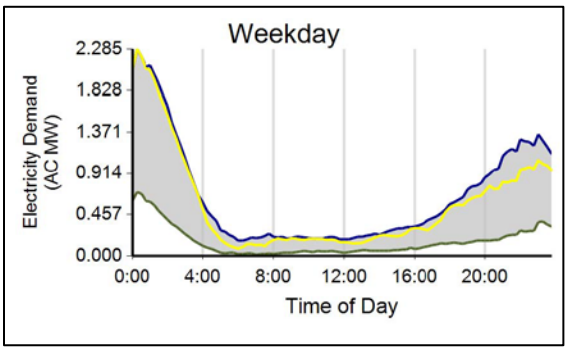

Figure 6. EV Project Charging Profile Based on National Energy Demand for Weekdays (Data is in 15-minute increments for any time in the reporting quarter.)

Figure 7 documents the length of time vehicles are connected to residential EVSE. The two sets of peaks suggest short opportunity charging for less than one or two hours, and overnight charging for 10 to 14 hours. Figure 8 shows the same set of vehicles drawing power for much shorter periods of time than when they were connected as shown in Figure 7. Figure 9 matches Figure 8, as would be expected as the distribution of energy consumed would have a similar profile to the length of time the vehicles draw power.

Figure 10 is the charging profile for public access Level 2 EVSE as measured by the number of vehicles connected as a percent. Figure 11 documents a similar work day peak profile when vehicles are connected and start drawing power about 8 a.m. Note that the EVSE

at Oak Ridge National Laboratories (ORNL) heavily influences these profiles.

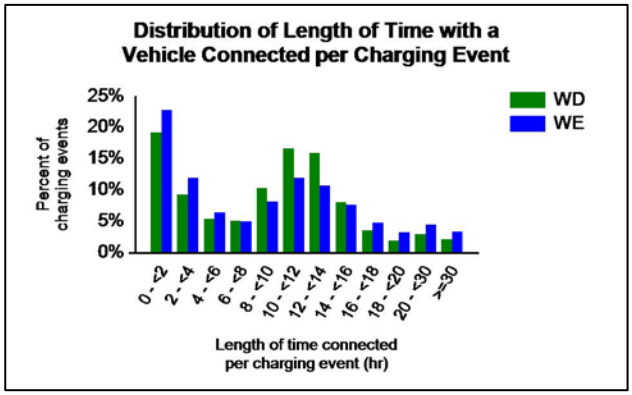

Figure 7. EV Project Distribution of Length of Time with a Vehicle Connected per Charging Unit for Residential Level 2 EVSE

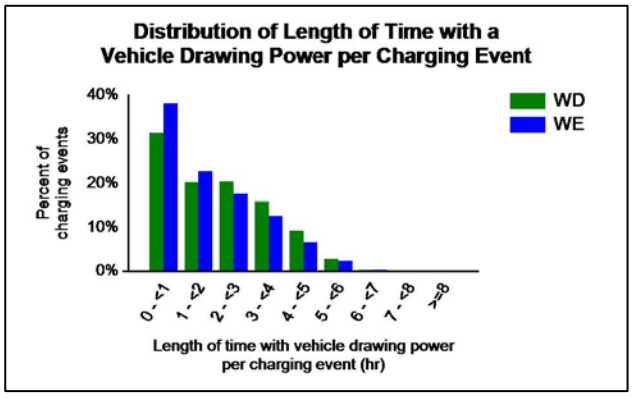

Figure 8. EV Project Distribution of Length with a Vehicle Drawing Power per Charging Event for Residential Level 2 EVSE

The EV Project will continue accumulating both vehicle and EVSE data, with the first fast chargers coming on line as FY 2011 ended. As FY 2011 ended, more than one-half a million miles of data was being collected weekly.

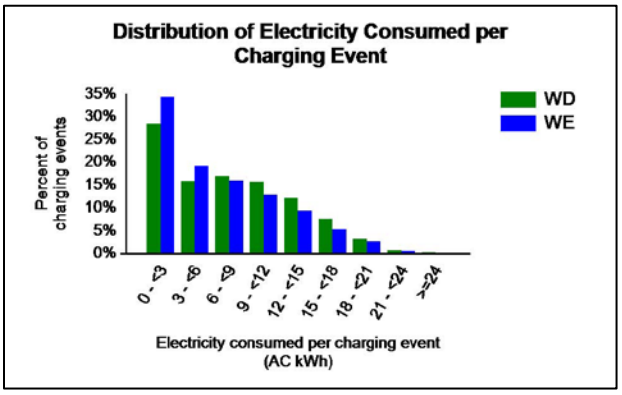

Figure 9. EV Project Distribution of Electricity Consumed per Charging Event for Residential Level 2 EVSE

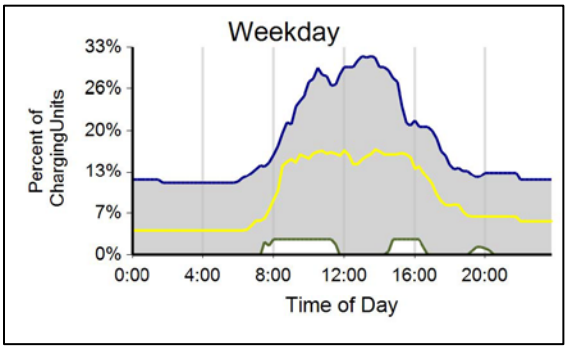

Figure 10. EV Project Percent of All Publicly Available Level 2 EVSE with a Vehicle Connected During Weekdays (Data is in 15-minute increments for any time in the reporting quarter.)

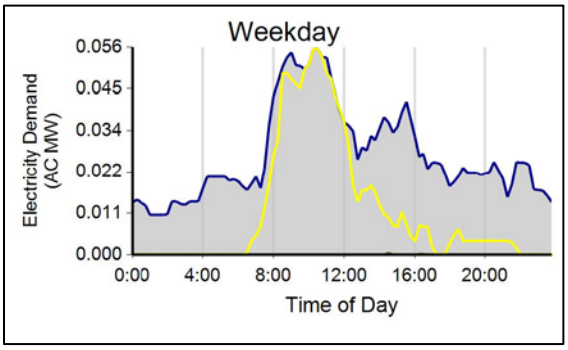

Figure 11. EV Project Publicly Available Level 2 EVSE Charging Profile Based on Energy Demand for Weekdays (Data is in 15-minute increments for any time in the reporting quarter.)

Conclusions

- Vehicle deployment is market driven, as is commercial market enthusiasm and support, and vehicle deliveries are fewer than original equipment manufacturers (OEMs) forecasted.

- Data collection and transmission are continuously undergoing improvement in reliability and content.

II.G.3. Products

Publications

EV Project Quarterly Reports

1. EV Project EVSE and Vehicle Usage Report: 2nd Quarter 2011
2. EV Project EVSE and Vehicle Usage Report: 3rd Quarter 2011

Electric Vehicle Charging Infrastructure Deployment Guidelines

1. Electric Vehicle Charging Infrastructure Deployment Guidelines for the Central Puget Sound Area
2. Electric Vehicle Charging Infrastructure Deployment Guidelines for the Oregon I-5 Metro Areas of Portland, Salem, Corvallis and Eugene
3. Electric Vehicle Charging Infrastructure Deployment Guidelines for the Greater Tucson Area
4. Electric Vehicle Charging Infrastructure Deployment Guidelines for the State of Tennessee
5. Electric Vehicle Charging Infrastructure Deployment Guidelines for the Greater San Diego Area
6. Electric Vehicle Charging Infrastructure Deployment Guidelines for the Greater Phoenix Area

Long-Range EV Charging Infrastructure Plans

1. Long-Range EV Charging Infrastructure Plan for Arizona
2. Long-Range EV Charging Infrastructure Plan for Greater San Diego
3. Long-Range EV Charging Infrastructure Plan for Western Oregon
4. Long-Range EV Charging Infrastructure Plan for Tennessee

EV Project Lessons Learned Reports

1. EV Project: Accessibility at Public EV Charging Locations
2. Lessons Learned - EV Project: First Responder Training

Presentations

1. Technologies required to fully integrate electric vehicles and the smart grid

II.H. (e) [Recovery Act – Strategy to Accelerate U.S. Transition to Electric Vehicles – DE-EE0002628]

Principal Investigator: Greg Cesiel
General Motors
30001 Van Dyke Avenue
Warren, MI 48090
(586) 575-3670; greg.cesiel@gm.com

DOE Technology Development Manager: Lee Slezak
(202) 586-2335; lee.slezak@ee.doe.gov

NETL Project Manager: Jason Conley
(304) 904-7590; John.Conley@NETL.DOE.GOV

II.H.1. Abstract

Objective

- Overall Objectives
  - The objective of this project is to develop Extended Range Electric Vehicles (EREV) advanced propulsion technology and demonstrate a fleet of EREVs to gather data on vehicle performance and infrastructure to understand the impacts on commercialization while also creating or retaining a significant number of jobs in the United States. This objective will be achieved by developing and demonstrating EREVs in real world conditions with customers in several diverse locations across the United States and installing, testing and demonstrating charging infrastructure.
- FY2011 Objectives
  - In 2011, we completed the development of the Chevrolet Volt and placed the vehicle in the hands of consumers in diverse locations across the United States. The project demonstration leverages the unique OnStar telematics platform, standard on all Chevrolet Volts, to capture the operating experience that will lead to better understand of customer usage. The project includes utility partners that have installed and are demonstrating and testing charging infrastructure located in home, workplace and public locations to understand installation issues, customer usage and interaction with the electric grid. In 2011, we delivered all of the Chevrolet Volts to the electric utility company participants and initiated the demonstration portion of this project.

Major Accomplishments

- Final internal evaluation of 219 Chevrolet Volts completed in the first quarter
- Distribution of 140 Volts to electric utility customers completed
- Customer usage of demonstration fleet initiated
- Vehicle data report content finalized with Idaho National Lab
- Regular data delivery to Idaho National lab initiated
- First quarterly reports published by Idaho National Lab
- 325 charging stations installed
- OnStar smart charging demonstrations initiated

Future Activities

- Continue smart Charging OnStar demonstrations to exhibit capabilities with various utilities
- Initiate PLC smart charging demonstrations

- Initiate battery to grid demonstration
- Fast Charging demonstration
- Continue to collect data from demonstration vehicles across the United States

II.H.2. Technical Discussion

Introduction – Smart Charging

The capability to identify and manage electric vehicle charging loads through OnStar and Power Line Communications (PLC) will be developed and demonstrated. This technology will support managing interaction with the electric grid using the current grid infrastructure.

Approach – Smart Charging

OnStar's task is to design, develop and implement smart charging to interface with utility systems.

The PLC portion will design, develop and implement the interface that enables communication between a smart meter and the vehicle.

Results – Smart Charging

Utility control of the Volt was successfully demonstrated by Duke Energy, a program partner. Duke was able to actively control the Volts charging status and rate table using OnStar's smart grid connectivity and infrastructure.

Benches were built in order to develop and demonstrate the PLC portion. Bench 1 is the Proof of Concept bench incorporating Smart Energy Profile (SEP) 1.0 messaging. Bench 2 is the operation bench with utility communications to a vehicle simulation. Bench 3 will consist of utility communications to a functional electric vehicle.

Introduction – Fast Charging

Charging an EV battery in less than 30 minutes provides additional opportunities for the customer to fuel with electricity and increase petroleum displacement. Fast charging shall support development of standard electrical and communication interfaces between the EV and the charger and increase the understanding of the vehicle and grid impacts of fast charging.

Approach – Fast Charging

This approach starts with the development of a standard DC connection interface and communication standard for fast charging; this includes integration of this into a vehicle. From here, the demonstration period will be utilized to collect and analyze data to study grid impacts, vehicle impact, thermal management, charging profiles, user ergonomics and efficiency.

Results – Fast Charging

The fast charge development team completed tasks for internal development as well as standards feedback and development. The fast charge station development work has been initiated to switch to the Home Plug Green PHY interface over the control pilot line to begin using the proposed standard for DC charging communication. The connector durability testing is ongoing.

Introduction – Battery to Grid

The increased demand for stationary energy storage on the electric grid to enable renewable energy sources and reduce infrastructure stress through load management is an opportunity to extend the usage of automotive batteries. This task will study the technical challenges of automotive battery reuse for grid storage and demonstrate this application.

Approach – Battery to Grid

This task studies the stationary energy storage requirements and compares them to battery capabilities following vehicle use. In order to demonstrate battery to grid functionality, a grid-tied bidirectional power converter with a battery pack will be utilized. Communication requirements for grid to storage systems shall be developed to provide dispatched power capability. A demonstration period will collect

and analyze data to study the grid and battery impacts of bidirectional power flow.

Results – Battery to Grid

Battery to grid functionality is understood and the current focus is on the demonstration phase. This phase will ensure proper understanding of the grid to battery impact of bidirectional power flow by collecting and analyzing data.

II.H.3. Products

Publications

Idaho National Laboratory website; listed under "General Motors Chevrolet Volt Vehicle Demonstration" – aggregated data report http://avt.inel.gov/evproject.shtml

Patents

To date, this demonstration program has not generated any subject inventions or made any related patent filings.

Tools & Data

Driving and charging data will be transferred from the vehicles via the OnStar telematics to the OnStar lab. OnStar personnel will receive the data and process it appropriately for transfer to Idaho National Labs. The following data will be collected by OnStar and transferred to Idaho National Lab:

All trips combined:

- Overall fuel economy
- Total number of trips
- Total distance traveled
- Average ambient temperature
- Vehicle maintenance records

Trips in charge depletion mode:

- Fuel economy
- Number of trips
- Percent of trips city/highway
- Distance traveled
- Average trip aggressiveness (scale of 0-10)
- Percent of total distance traveled

Trips in both charge depletion and charge sustaining mode:

- Fuel economy
- Number of trips
- Percent of trips city/highway
- Distance traveled
- Average trip aggressiveness (scale of 0-10)
- Percent of total distance traveled

II.I. (f) Smith Electric Vehicles Medium Duty Electric Vehicle Demonstration Project (EE0002614)

Principal Investigator: Robin J.D.Mackie, Chief Technology Officer
Smith Electric Vehicles U.S. Corp.
12200 N.W. Ambassador Drive, Suite 326
Kansas City, MO 64163
(816) 243-1611 ; robin.mackie@smithelectric.com

DOE Technology Development Manager: Lee Slezak
(202) 586-2335; lee.slezak@ee.doe.gov

NETL Project Manager: John J. Conley
(304) 285-2023; John.Conley@NETL.DOE.GOV

II.I.1. Abstract

Objective

- The objective of the SEV-US Demonstration Project is to obtain performance information from an All Electric Vehicle (AEV) fleet to accelerate production, reduce costs, enhance the technology, and procure early acceptance of AEV's in the US commercial vehicle marketplace.
- Smith will demonstrate at least 500 electric vehicles based on the Newton medium duty platform. The vehicles will be placed in locations including California, Missouri, Ohio, Michigan, Washington, DC, New York, and Texas. A Generation II Newton platform will be developed during the project utilizing the performance data collected. The development of this platform will enable the Company to reduce cost, expand the vehicle range from class 4 through 7, and additional improvements will be made in powertrain and battery technology. It is intended that the base vehicle platform be applied to both shuttle bus and step-through van applications.

FY2011 Objectives

- Deploy to customers approximately 50% of the 500+ vehicle fleet.
- Launch Smith Link providing data to:
  (1) NREL
  (2) Smith service
  (3) Smith engineering
  (4) Selected Smith customers.
- Sales & Marketing:
  (1) Expand the market boundaries to support the overall fulfillment of the DOE objectives through the introduction of additional launch partners,
  (2) Continue to establish the Smith brand as the pre-eminent supplier of Zero Emission Electric Commercial Vehicles,
  (3) Establish the process for user feedback in line with DOE requirements.
- Operationally:
  (1) Expansion of the Smith assembly facility to match demand,
  (2) Continued recruitment and training of assembly staff,
  (3) Expansion of the service team and resources to meet customer deployment plans,
  (4) Launch of Gen 2 Newton platform incorporating Smith Power, Smith Drive and Smith Link.

(5) Supply Chain:

(6) Develop suitable supply chain to support engineering activities, production requirements for Gen 2 systems, cost down activity and meet "Buy America" criteria.

- Engineering :
  (1) Expansion of the U.S. based technical team,
  (2) Reorganization and integration of the UK and US technical teams into a single global technical resource;
  (3) Delivery of Smith Power- Smith's in house battery strategy,
  (4) Delivery of Smith Drive- Smith's in house driveline strategy,
  (5) Integration of Smith Power, Smith drive and Smith Link onto the Newton platform.
- Quality-
  (1) Establish and imbed quality systems within the newly formed US operation in preparation for ISO audit in early 2012,
- Finance and Administration:
  (1) Continued development and maturation of internal administrative processes from an initial start-up position that support the outcomes and recommendations for improvement from various audits undertaken by DOE, GSA, DCAA and Smith financial auditors Deloitte & Touche.
  (2) Comply with all project reporting requirements for the DOE and ARRA.
- Corporate:
  (1) Acquisition and integration of Smith UK.
  (2) Fund raising to support ongoing development and company growth.

Major Accomplishments

- Deployed to customers 246 vehicles under the Participation Program through calendar 2011.
- Placed in service Smith Link and commenced transfer of data to NREL. Provided internal access to vehicle data through Smith Link system to the Smith service and engineering teams. In collaboration with key customers a Smith Link portal was developed providing access by the customer to relevant vehicle data in support of fleet operations.
- Sales & Marketing:
  (1) Expanded customer base from our initial six launch us partners to the "Table of 20" expanding the range of vehicle applications and addressable markets e.g. step-through van and shuttle bus.
- Operations:
  (1) Expanded assembly to 2 production lines.
  (2) Recruited an additional 33 employees within engineering, service, production and administration.
  (3) Achieved Job 1 Gen 2 Newton in November 2011.
- Supply Chain:
  (1) Purchasing and manufacturing costs have been reduced 5%.
  (2) Established new supply chain to support engineering and operations in delivery of the Gen 2 platform.
- Engineering:
  (1) Delivered by October 2011 fully integrated Newton platform incorporating Smith Drive and Smith Power.
  (2) Completed re-organization and integration of US and UK technical teams.
- Quality:
  (1) Completed the implementation of ISO standards across the US operations in preparation for the independent audit in 2012.

- Finance and Administration:
  (1) Successfully adopted all recommendations made during prior audits and further elevated the controls and processes in line with the Company's aspirations for a public listing of the Company.
  (2) Complied with all reporting requirements, including the Annual Merit Review.
- Corporate:
  (1) Maintained fund raising activities in line with corporate goals.
  (2) Submitted Form S-1 Registration Statement to the SEC on November 10, 2011.

Future Activities

- Secure customer participation for the balance of the demonstration fleet.
- Deploy the remainder of the 500+ vehicle fleet under the Grant participation program within the project timescale.
- Continuously develop Smith Power, Smith Drive and Smith Link, enhancing reliability, efficiency and reducing cost.
- Maintain supplier development and cost down activities to reduce overall vehicle cost by a targeted incremental 23%, improving market competitiveness with traditional ICE commercial vehicles.
- Expand Smith Link to support the requirements of the demonstration fleet for the full duration of the project, ensuring the timely delivery of data to NREL.

II.I.2. Technical Discussion

Introduction

Smith's overall technical objectives are to leverage the 80 years of knowledge and experience of its UK subsidiary within the electric vehicle market in Europe, and apply it to the North American marketplace. This activity can be broken down into two main phases:

Phase1:
The homologation of the European Newton Gen 1 platform to US Department of Transportation standards to support immediate production during 2010-2011.

Phase 2:
The development of a Smith proprietary driveline, battery and telemetry systems under the technical sub-brands of Smith Power, Smith Drive and Smith Link.

The Gen 1 driveline and battery systems were developed in conjunction with vendor system providers with the final vehicle integration being carried out by Smith. By using this approach Smith limited its ability to influence both cost and development, suffering from early quality issues.

It was decided that the experience gained through the use of these system providers that Smith should develop its own powertrain, battery and telemetry systems, thus enabling greater control over the specification, test and validation of the new system to improve quality and reduce warranty issues.

This approach also enables the Company to buy at the component level and reduce overall systems costs in line with its goals.

Smith Drive-

System objectives over Gen1-

- More efficient drive motor- 150kw permanent magnet.
- Drive motor and controller to be compatible with electric gearbox development.
- Higher speeds- 65 mph.
- Improved grade ability.
- Fully integrated drive controller including auxiliary inverters for power assisted steering and brakes.
- Drive motor and controller compatible with cooling system.

Smith Power-

System objectives over Gen1-

In-house development of the Smith battery management system (BMS) with the following capabilities-

- Management of different cell chemistries,
- Support a modular approach to battery pack sizing,
- Active thermal management.

Modular approach to the mechanical and electrical integration of cells allowing battery pack sizes from 40 kwh to 120 kwh.

On-vehicle modular charging strategy to support differing battery pack configurations.

Smith Link-

System objectives-

- Development of the telemetry unit for vehicular use, interfacing with Smith Drive and Smith Power systems,
- Real time collection of over 1200 data points per second per vehicle,
- Secure transmission of the data to in-house server arrays for post-processing,
- The development of portals to create appropriate access to vehicular data for use by the following internal and external customers-
  1. Smith service
  2. Smith engineering
  3. Department of Energy agent NREL
  4. Customers.

II.I.3. Products

Existing products- See Attachment A for full set of descriptions and specifications.

Top left – cargo van
Top right– utility truck with lift
Bottom left – refrigerated van (cold plate)
Bottom right – military transport vehicle

Above – Stake bed truck

Above – cargo van

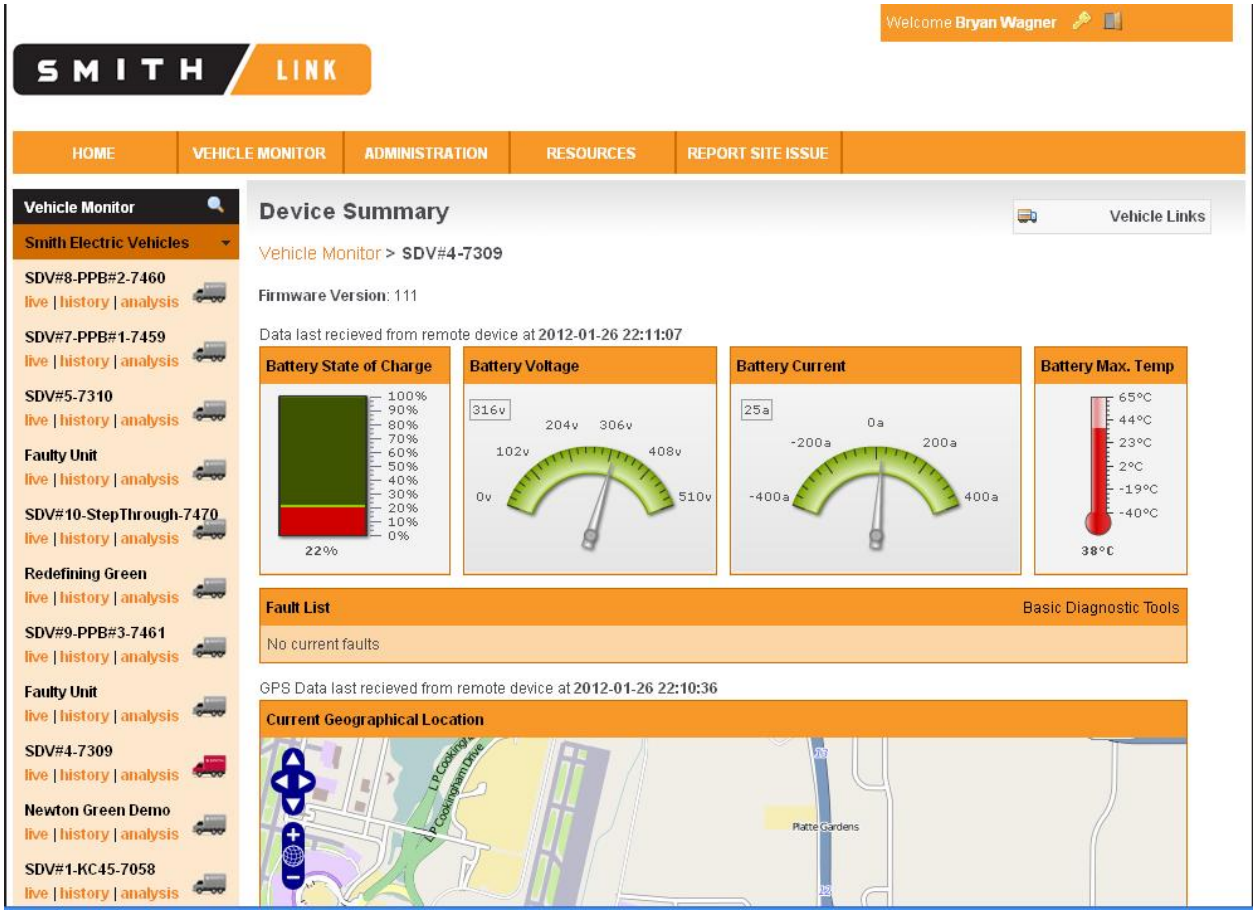

Above – Smith Link

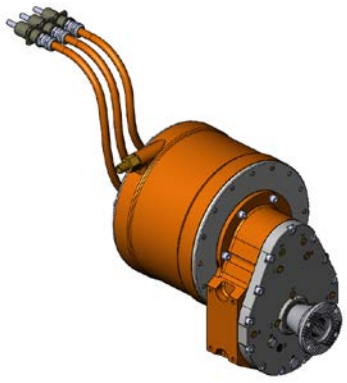

Left- Smith Drive motor

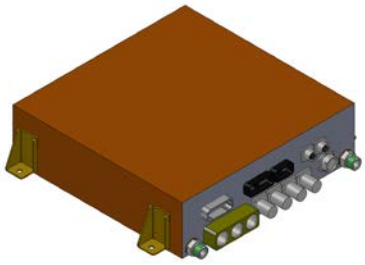

Left- Smith Drive motor controller

Left- Smith Gen 2 cab.chassis

Products still in final development/prototype stages.

Above- step-through van

Above- shuttle bus

Publications

None.

Patents

None.

Tools & Data

None.

II.J. (g) Plug-In Hybrid Electric Medium Duty Commercial Fleet Demonstration and Evaluation

Principal Investigator: Matt Miyasato
South Coast Air Quality Management District
21865 Copley Drive
Diamond Bar, CA 91765
(909) 396-3249; mmiyasato@aqmd.gov

DOE Technology Development Manager: Lee Slezak
(202) 586-2335; lee.slezak@ee.doe.gov

NETL Project Manager: Jason Conley
(304) 285-2023; John.Conley@netl.doe.gov

II.J.1. Abstract

Objective

This program will develop and deploy a fleet of medium-duty plug-in hybrid vehicles that will provide improved fuel economy and reduced emissions by grid connecting a portion of the vehicle's use-profile. These vehicles will be fully-integrated with production plug-in hybrid systems for medium-duty trucks and shuttle buses. A demonstration fleet of approximately 250 vehicles will be deployed for nationwide testing in daily fleet use. This deployment will also include the development and installation of 'smart' charging infrastructure.

These program objectives will be met through the following activities:

- Develop a production-ready plug-in hybrid electric vehicle system with a high capacity Li Ion battery system for Class 4 to 7 trucks and shuttle buses (14,050 lbs – 33,000 lbs Gross Vehicle Weight)
- Establish production at a 'ship-through' facility for commercial assembly and installation of the PHEV systems.
- Develop production-ready 'smart charging' capability for vehicle and the supporting charging infrastructure for these vehicles.
- Evaluate technical feasibility and build substantial customer familiarity and interest in a nationwide fleet test and demonstration program.
- Launch system into commercial ship-through production by 2013 with goal of building enough demand for high volume line production in 2015.
- Use project results for system development to optimize performance and reduce costs.

Major Accomplishments

The relevant work during the last half of FY2011 was generally focused on restructuring the program. The restructured program resulted in a broader coverage of vehicle platforms that would be enabled by three plug-in hybrid systems developed between Azure Dynamics and Odyne Systems. The systems that will be developed by these respective organizations include a:

- Class 4 gasoline PHEV that is compatible with Ford's E450 platform for shuttle bus applications by Azure;
- Class 5 diesel PHEV that is compatible with Ford's F550 platform for bucket truck applications by Azure; and
- Class 6 and 7 PHEV's that are focused on work truck applications such as bucket trucks and digger derricks by Odyne.

Future Activities

The major milestones left to complete the program include:

- Complete validation testing of the Azure E450 PHEV drive system
- Finalize the design and calibration of the Odyne Class 6/7 PHEV drive system
- Complete the validation testing of the Odyne Class 6/7 PHEV drive system
- Finalize the design and calibration of the Azure F550 PHEV drive system
- Complete the validation testing of the Azure F550 PHEV drive system
- Build and deploy a nationwide fleet of approximately 250 medium-duty PHEV's built on the Azure and Odyne drive systems
- Install the requisite charging infrastructure to support the vehicle fleet
- Conduct a two year evaluation of the nationwide fleet

II.J.2. Technical Discussion

Introduction

The program was originally structured to develop, deploy, and demonstrate a 378 vehicle fleet of medium-duty plug-in hybrid electric vehicles. Eaton Corporation was the slated technology developer that was responsible for the development and integration of the vast majority of the PHEV systems that would be deployed as part of the original project. However, on March 22, 2011, Eaton advised that their development timeline would need to be significantly extended and eluded that much of the development work necessary for the successful deployment of the 378 vehicle demonstration fleet would not result in a salable commercial product. Given that the program was facing significant delays and continued efforts did not appear to be driving towards a commercial product, the project team was afforded the opportunity to restructure the program to yield a commercially intent PHEV product.

The project team worked closely with the DOE to restructure the program in a way that would meet the original objectives of the Recovery Act solicitation. The fruits of these efforts resulted in the program being restructured to develop three plug-in hybrid drive systems that would be deployed on an ever broader range of vehicles than was originally planned. The original project was limited to Class 4-5 applications; whereas, the restructured program would develop three discrete plug-in hybrid drive systems that would cover vehicles ranging from Class 4 through 7, with all systems being production intent. A consequence of the restructured program was a downward revision in the total number of vehicles that would be deployed, with the new fleet size targeting approximately 250 vehicles.

The broader coverage of vehicle platforms would be enabled by three plug-in hybrid systems that would be developed between Azure Dynamics and Odyne Systems. The systems that will be developed by these respective organizations include a Class 4 gasoline PHEV that is compatible with Ford's E450 platform, for shuttle bus applications by Azure; Class 5 diesel PHEV that is compatible with Ford's F550 platform, for bucket truck applications by Azure; and Class 6 and 7 PHEV's that are focused on work truck applications, such as bucket trucks and digger derricks by Odyne.

Approach

The Odyne PHEV system is a PTO-driven architecture. The stock powertrain is augmented by a 60 kW electric motor that interfaces with the vehicle's drive system through the PTO. This enables the electric machine to wholly operate the PTO at the worksite, as well as supplement or displace the use of the primary drive engine for traction operation. A schematic of the system architecture is shown in Figure 1.

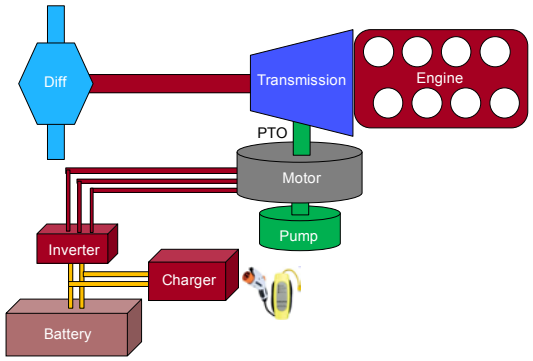

Figure 1. Odyne PHEV drive system architecture

The Azure PHEV drive systems for the E450 and F550 applications will both be based on a post-transmission architecture. An electric motor will reside downstream of the transmission to provide tractive power and enable regenerative braking. The Front End Accessory Drive (FEAD) will be modified to incorporate an electric motor and clutched main pulley to allow for the engine accessories to be driven independent of the IC engine. The electrification of the engine accessories is an integral part of enabling the vehicle to operate with the IC engine shut off. A large energy battery pack will also be used to displacement liquid fuel consumption during traction events as well as jobsite use of the hydraulic devices.

The deployment of these systems will occur between the third quarter of 2012 through the third quarter of 2013. The Azure E450 and Odyne Class 6/7 systems would be the first to be fielded, with product on the road in mid-to late-2012. The deployment of the Azure F550 vehicles will follow shortly thereafter and should be placed in normal fleet service in mid-to late-2013.

Conclusions

The program will commercialize three plug-in hybrid vehicle products, which will provide coverage across the Class 4 – 7 vehicle markets. Azure Dynamics would target the lighter weight class vehicles by developing plug-in hybrid systems for Ford's E450 and F550 platforms and Odyne would cover the heavier Class 6/7 vehicles for nearly any vehicle equipped with an Allison transmission. Targeting the Class 4 – 7 vehicle segment will provide the opportunity to meaningfully impact fossil fuel consumption through the deployment of a relatively small fleet deployment, due to the higher per capita fuel usage associated with these vehicles when compared to light-duty vehicles. Each of the three vehicle technologies will provide reductions in fossil fuel consumption and emission of air pollutants through the electrification of a portion of each vehicle's daily drive cycle, with the work truck applications additionally benefiting from the electrification of their jobsite operation.

II.K. (h) Recovery Act-Commercial Electric Vehicle (EV) Development and Manufacturing Program

Principal Investigator; Darren Gosbee
Workhorse Sales Corp.
922 S State Rte 32
Union City IN 473909153
(331) 332-6942; Darren.gosbee@navistar.com

DOE Technology Development Manager: Lee Slezak
Lee.slezak@ee.doe.gov

NETL Project Manager; John Conley
(304) 285-2023; John.conley@NETLdoe.gov

II.K.1. Abstract

Objective

- The objective of this project is to manufacture and distribute zero tailpipe emission, light/ medium duty commercial electric vehicles (EV) in the United States. The Recipient shall develop and demonstrate at least 950 EVs (which may range from Class 2c through Class 5 trucks) in the U.S. market. Specific objectives of this project include demonstrating the applicability of EV technology for commercial transportation applications, demonstrating reliability in geographically and climatically diverse locations, demonstrating a reduction in carbon emissions and use of fossil fuels and addressing the needs of the customers while enhancing the EV attributes to achieve mass market penetration in the future.
- The Recipient is applying its affiliates' in-house engineering, product development, manufacturing, marketing and distribution expertise to prepare the vehicles for market introduction. This preparation requires, among other activities, ensuring full compliance with Federal Motor Vehicle Safety Standards (FMVSS) and tailoring the functionality of the vehicle to customer requirements. The Recipient shall demonstrate in-service functionality and accelerate the adoption of electric vehicles. This market introduction will provide substantial fuel savings, reduced dependence on petroleum-based fuels and displace greenhouse gas and other tailpipe emissions in United States.

- FY2011 Objectives: 1) Launch MY2011 upgraded eStar. 2) Charter and commence development of next generation Electric Vehicle (EV) Generation 2 product on existing Navistar platform.

Major Accomplishments

- Passed the 100th unit shipped milestone this year.
- Completed the upgrade and integration into the vehicle this year inclusive of;
  - Battery pack upgrade
  - On board charger localization and upgrade
  - Electric motor drive upgrade
  - Enhanced heater output
  - Improved vehicle reliability
- Future Activities
- Current generation 1 eStar will continue to be produced and sold as market demand dictates

- Charter approved; Development efforts underway for generation 2 EV. Will be integrated into existing Workhorse W-62i platform with improved power electric systems; motor, inverter, battery pack, charger, electric accessories, and controls.

II.K.2. Technical Discussion

HEATER SYSTEM

Approach

Incorporated a 5Kw heater in order to improve cab heating, air flow, and defrost performance. Functionality of the heater allows for the mode options of fresh or recirculation air effects. The heater is supplied power from the vehicle's main battery to heat the PTC elements

Figure 1. 5kW Heater

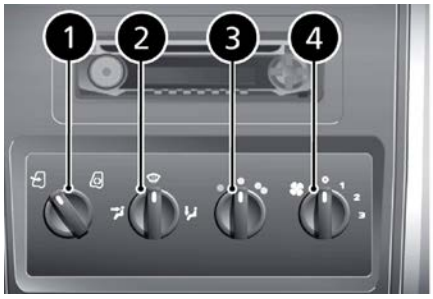

Heater Control Panel
1. Fresh air/recirculation control.
2. Air distribution control.
3. Temperature control.
4. Blower fan speed control.

Figure 2. 5kW Heater Control Head

Results

Enhanced heating, air flow, and defrost performance in comparison to the previous 2kW version.

Conclusions

Based on supplier test report DP080-6 dated 6/9/2011, the 5kW heater showed acceptable overall interior cab temperature, air flow, and defrost improvements, based on customer requirements.

AIR CONDITIONING SYSTEM

Approach

As a customer desired feature, specific climatic conditions were established to cool the interior cab based on a moderate temperature with a high humidity environment. The testing conditions were established to be 90°F at 82% RH with 1000W/m² solar loading. Integral system charging was incorporated for the 4 deep cycle batteries which does not compromise overall vehicle run time.

Figure 3. Air Conditioning System

Figure 4. Battery Box Internal Components (compressor batteries & charger)

Results

System performance allowed for an average interior cab temperature reduction of 10 degrees in 20 minutes.

Conclusions

Based on supplier test report TR#10-0063 dated 10/21/2010, the system showed acceptable overall reduction in interior cab temperature based on customer requirements

FRP RESS (RECHARGEABLE ENERGY STORAGE SYSTEM)

Introduction

As part of the continuous improvement of the Navistar eStar, a design change of the RESS has been implemented that reduces the weight, implements additional diagnostics and integrates with a new J1772 charger.

Approach

The packaging of the RESS was modified to change from a steel enclosure to a Fiber-Reinforced Plastic (FRP) enclosure. Support of the ensuing FRP enclosure (and RESS modules) is accomplished through a steel frame which is then affixed to the vehicle chassis in the same locations as the previous steel enclcolsure.

In addition to the packaging, the supplier implemented hardware and software changes that:

- improved overall EMC performance.
- provided additional diagnostics to service and support the RESS more effectively.
- provides an interface with a separate water-cooled J1772 vehicle charger.

Finally, the RESS external interface was modified to allow the use of an external charger.

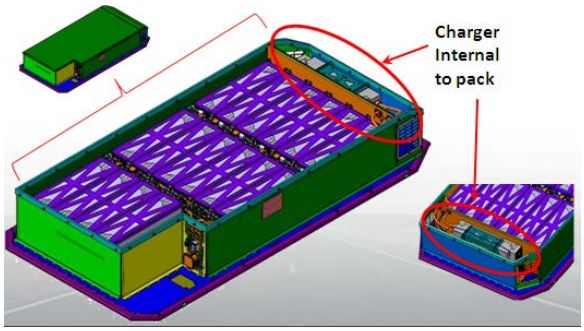

Figure 5. RESS and charger prior to modicifcation

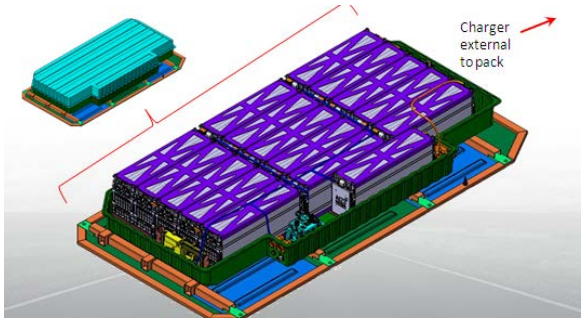

Figure 6. RESS post modification

Results

Supplier validation was completed and approved. Updated RESS was integrated and validated in the eStar vehicle.

Weight savings of 400lbs. was achieved.

Conclusions

Based on Supplier Validation Test Report TR 000120 dated 6/22/2011, the system demonstrated acceptable performance.

ELECTRIC MOTOR/DRIVE UPGRADE

Introduction

As part of the continuous improvement of the Navistar eStar, a design change of the Motor/Drive has been implemented to increase the performance envelope such that it can operate down to -20C. Furthermore, the ancillary supply controls and hardware were modified to be able to operate the enhnaced 5kW heater.

Figure 7. Motor / Inverter Assembly

Approach

1. Modified internal motor case machining to relieve stator to case stress concentration at -20deg C
2. Updated Inverter micro-controller board with below new/changed features:
   a. Low temperature controls including different thermistor for -20deg C operation
   b. New microprocessor crystal
   c. New temperature measurement thermistor and associated software to measure to lower temperature range
3. Modified ancillary controls calibration to enable additional output for 5kW heater.

Results/Conclusions

Vehicle operation tested and validated at -20C – Navistar Test report # 10-29923.

5kW Heater integration and performance validated on the vehicle. Navistar Test report # 11-34417 and 11-33515.

II.K.3. Products

Publications

http://www.estar-ev.com/

Patents

N/A

Tools & Data

N/A

Schedule for Electric Vehicle (EV) Generation II

Time		FY 2011			FY 2012													FY 2013												FY 2014			
Start	Phase/Milestones/Activity	A	S	O	N	D	J	F	M	A	M	J	J	A	S	O	N	D	J	F	M	A	M	J	J	A	S	O	Q1	Q2	Q3	Q4
9/12/2011	CA Gate																															
	Styling Theme Approval																															
11/30/2011	RA Gate																															
2/6/2012	PA Gate																															
2/20/2012	Production Design & Release																															
6/11/2012	VESO (Virtual)																															
12/20/2012	Field Test (Reliability Growth)																															
5/7/2012	Long Lead Production Tooling																															
7/9/2012	Non-Saleable Pilot Build (CV/DV/SV/Cert)																															
8/20/2012	Test & Validation (DVP)																															
11/14/2012	DV Gate																															
2/4/2013	FESO																															
10/1/2012	Saleable Pilot Builds (PV/Q/VC)																															
12/19/2012	LR Gate																															
3/18/2013	Ramp Build (Job 1 thru OKTS)																															
5/20/2013	OK to Ship Phase 1																															
9/16/2013	Ramp Build (Job 1 thru OKTS)																															
11/20/2013	OK to Ship Phase 2																															

SUPERTRUCK

II.L. (a) Technology and System Level Demonstration of Highly Efficient and Clean, Diesel Powered Class 8 Trucks

Principal Investigator: David Koeberlein
Cummins, Inc.
P.O. Box 3005
Mail Code 50197
Columbus, IN 47201
(812) 377-5285; david.e.koeberlein@cummins.com

DOE Technology Development Manager: Roland Gravel
(202) 586-9263; roland.gravel@hq.doe.gov

NETL Project Manager Ralph Nine
(304) 285-2017; ralph.nine@netl.doe.gov

II.L.1. Abstract

Objective

- Objective 1: Engine system demonstration of 50% or greater brake thermal efficiency in a test cell at an operating condition indicative of a vehicle traveling at 65 mph.
- Objective 2:

  a: Tractor-trailer vehicle demonstration of 50% or greater freight efficiency improvement over a defined drive cycle utilizing the engine developed in Objective 1.

  b: Tractor-trailer vehicle demonstration of 68% or greater freight efficiency improvement over a defined 24 hour duty cycle (above drive cycle + extended idle) representative of real world, line haul applications.
- Objective 3: Technology scoping and demonstration of a 55% brake thermal efficiency engine system. Engine tests, component technologies, and model/analysis will be developed to a sufficient level to validate 55% brake thermal efficiency.

FY2011 Objectives

- • Investigate contributing component designs and technologies to achieving brake thermal efficiency and freight efficiency targets.
- • Design a vehicle inclusive of waste heat recovery and road load management for early system development.
- • Complete design and analysis of advanced transmission and engine; begin procurement.
- • Complete design and analysis of vehicle aerodynamic and weight reductions; begin procurement.

Major Accomplishments

- Achieved engine efficiency, which when waste heat recovery benefits are added in, results in >48% brake thermal efficiency.
- Completed design and analysis for a higher cylinder pressure capability, low pump parasitic engine.
- Baseline vehicle freight efficiency testing completed over defined, repeatable drive cycle route.
- Completed design and analysis of tractor-trailer baseline aerodynamics and developed new concepts to attain >14% freight efficiency improvement. Began hardware fabrication.

- Completed design study of tractor-trailer weight reduction opportunities resulting in >3% freight efficiency improvement.
- Completed design for advanced heavy duty transmission.
- A Solid Oxide Fuel Cell idle management system was designed into the truck chassis and electrical systems. The driver communication interface has been interlaced within the vehicle network and truck display systems.

FY2012 Activities

- Complete demonstration of 50% thermal efficient engine.
- Complete the truck & trailer build; development testing to achieve the 50% freight efficiency demonstration.

II.L.2. Technical Discussion

Introduction

Cummins Inc. is engaged in developing and demonstrating advanced diesel engine technologies to significantly improve the engine thermal efficiency while meeting US EPA 2010 emissions. Peterbilt Motors is engaged in the design and manufacturing of heavy duty class 8 trucks.

Together, Cummins and Peterbilt provide a comprehensive approach to achievement of a 68% or greater increase in vehicle freight efficiency over a 24 hour operating cycle. The integrated vehicle demonstration includes a highly efficient and clean diesel engine with 50% or greater brake thermal efficiency including advanced waste heat recovery, aerodynamic Peterbilt tractor-trailer combination, reduced rolling resistance tire technology, advanced transmission, and an efficient solid oxide fuel cell APU for idle management. In order to maximize fuel efficiency, each aspect associated with the energy consumption of a Class 8 tractor/trailer vehicle will be addressed through the development and integration of advanced technologies.

In addition, Cummins will scope and demonstrate evolutionary and innovative technologies for a 55% BTE engine system.

Approach

Cummins and Peterbilt's approach to these program objectives is a vehicle system's level approach, with analysis, followed by verification. Emphasis is placed on modeling and simulation results that lead to attractive feasible solutions to include in the vehicle design. Vehicle simulation modeling is used to evaluate freight efficiency improvement technologies and CFD analysis is used for aerodynamic design evaluations. Technologies are evaluated individually along with combination effects resulting in our path to target measure of program status and for setting program direction.

Data, experience, and information gained throughout the research exercise will be applied wherever possible to the final commercial products. We continue to follow this cost-effective, analysis-led approach both in research agreements with the Department of Energy as well as in commercial product development. We believe this common approach to research effectively shares risks and results.

Results

A vehicle power train system analysis was used to outline a path to target for the freight efficiency improvement. The path to target study involved an analysis of the various power train component changes, including both hardware and control algorithms, and their freight efficiency impact. This analysis was conducted using PSAT (Powertrain System Analysis Toolkit) with the application of map based models for the various sub-components. Figure 1 shows the path to target roadmap for both the drive cycle 50% improvement and 68% improvement on the 24hr cycle. Path to target

analysis is an on-going effort that seeks to increase accuracy and fidelity of expected vehicle performance as new component data is verified.

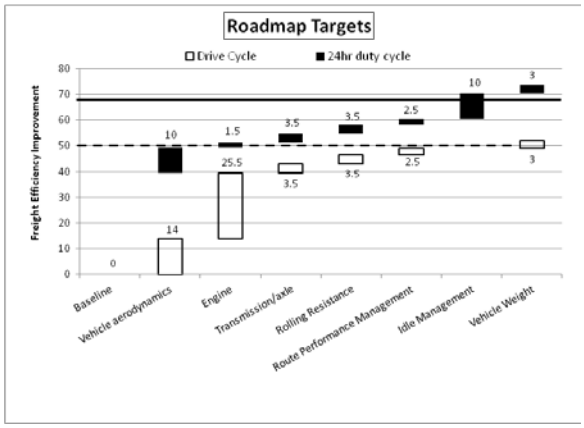

Figure 1. Freight Efficiency Roadmap Targets

The baseline truck fuel economy and freight efficiency testing was completed. The drive cycle route is 311 miles in length, with approximately 550feet of elevation change over the route course and 8 controlled stop/starts are included. The round trip route starts northwest of Fort Worth, Texas, on a northwest route toward Vernon, Texas.

A comparison study of the baseline vehicle fuel economy test results over the SuperTruck test route was found to be within 2.5% of the simulated value. This 2.5% difference between measured and simulation is considered very good, given the various sources of uncertainty associated with driver behavior modeling, aftertreatment thermal management and route simulation accuracy.

An EGR engine architecture combined with high efficiency SCR aftertreatment and waste heat recovery has been selected for our 50% brake thermal efficiency engine and vehicle demonstrations. Maturation of the specific engine components and their specifications is on-going work.

An exhaust waste heat recovery technology will be utilized on the demonstration vehicle. This system uses a refrigerant working fluid combined with a turbine expander. This waste heat recovery system has a uniquely designed vehicle cooling system module with sized components for drive cycle efficiency gains. Figure 2 shows cooling module analysis results that aid its design iterations.

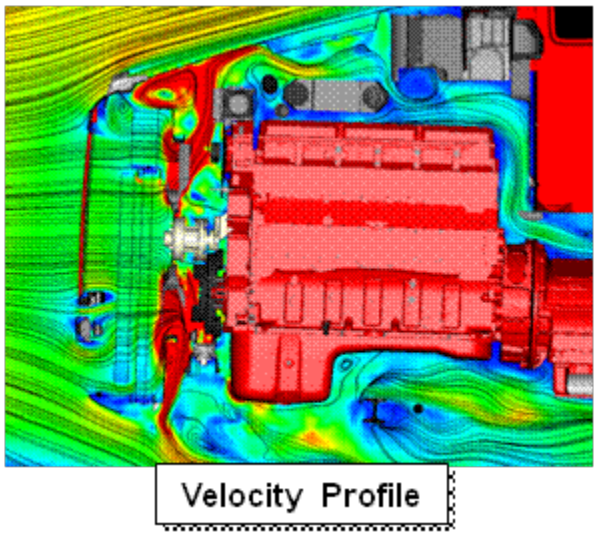

Figure 2. Cooling module analysis velocity profile

An aerodynamic drag improvement over the baseline tractor/trailer combination of 40% has been shown with a full tractor/trailer aerodynamic CFD analysis. Procurement of these first generation aerodynamic devices is underway. Decision analysis considers aerodynamic device mass, performance and complexity, as the program transitions from concept to demonstration design and hardware.

Conclusions

The SuperTruck Engine and Vehicle System Level Demonstration of Highly Efficient and Clean, Diesel Powered Class 8 Truck program has successfully completed the first year of the four year program. The following conclusions have come from the first year:

- Vehicle power train system analysis shows path to achievement of program freight efficiency goals.
- Baseline truck freight efficiency test results are within 2.5% of analytical predictions.
- EGR engine architecture with high efficiency SCR aftertreatment and WHR has been selected.

- Analysis results show a 40% aerodynamic drag improvement over the baseline tractor/trailer combination.

II.L.3. Product/Publications

Journal Publications:

1. Lyle Kocher, Ed Koeberlein, Dan Van Alstine, Karla Stricker, and Gregory M. Shaver, Physically-Based Volumetric Efficiency Model for Diesel Engines Utilizing Variable Intake Valve Actuation, Accepted (August 2011), to appear in: International Journal of Engine Research

Conference Papers and Presentations:

1. Lyle Kocher, Ed Koeberlein, Karla Stricker, Daniel Van Alstine, and Gregory M. Shaver, Control-Oriented Modeling of Diesel Engine Gas Exchange, 2011 American Control Conference.
2. Ed Koeberlein, Lyle Kocher, Daniel Van Alstine, Karla Stricker, and Gregory M. Shaver, Physics-based Control-Oriented Modeling of Exhaust Gas Enthalpy for Engines Utilizing Variable Valve Actuation, 2011 Dynamic Systems and Control Conference.
3. Karla Stricker, Lyle Kocher, Ed Koeberlein, Daniel Van Alstine, and Gregory M. Shaver, Turbocharger Map Reduction for Control-Oriented Modeling, 2011 Dynamics Systems and Control Conference.
4. Lyle Kocher, Ed Koeberlein, Daniel Van Alstine, Karla Stricker, and Gregory M. Shaver, Physically-Based Volumetric Efficiency Model for Diesel Engines Utilizing Variable Intake Valve Actuation, 2011 Dynamics Systems and Control Conference.
5. David Koeberlein, Cummins SuperTruck Program, Technology Demonstration of Highly Efficient Clean, Diesel Powered Class 8 Trucks, 2011 DEER conference.

Patents

None

Tools & Data

None

II.M. (b) Systems Level Technology Development and Integration for Efficient Class 8 Trucks

Principal Investigator: Derek Rotz (Vehicle)
Daimler Trucks North America LLC
Mailcode POC-AE
4747 North Channel Avenue
Portland, OR 97217
(503)746-6303; Derek.Rotz@Daimler.com

Principal Investigator: Kevin Sisken (Engine)
Detroit Diesel Corporation
HPC A-08
13400 Outer Drive West
Detroit, MI 48239-4001
(313) 592-5815; Kevin.Sisken@Daimler.com

DOE Technology Development Manager:Roland Gravel
(301) 938-3347; roland.gravel@ee.doe.gov

NETL Project Manager: Carl Maronde
(412) 386-6402 ; Carl.Maronde@netl.doe.gov

II.M.1. Abstract

Objective

- Overall Objectives
  - Demonstration of a 50% total increase in vehicle freight efficiency measured in ton-miles per gallon (at least 20% improvement through the development of a heavy-duty diesel engine)
  - Development of a heavy-duty diesel engine capable of achieving 50% brake thermal efficiency on a dynamometer under a load representative of road load
  - Identify key pathways through modeling and analysis to achieving a 55% brake thermal efficient heavy-duty diesel engine
- FY2011 Objectives
  - Comprehensively analyze efficiency potential across all vehicle systems to define major system specification and down-select technologies
  - Evaluate and select concepts for aerodynamics, hybrid and powertrain configuration based on theoretical analysis and simulation

Major Accomplishments

- Phase 1: Baseline Evaluation
  - Completed drive cycle tests with the baseline vehicle configuration
  - Developed roadmap of vehicle efficiency metrics needed to achieve 50% vehicle freight efficiency, based on vehicle-level efficiency simulation and analysis
  - Developed roadmap for 50% engine thermal efficiency at road load
- Phase 2: Concept Creation and Theoretical Analysis
  - Conducted basic shape analysis for tractor aerodynamics using computational fluid dynamics simulation and scale model tests

- Developed two concepts for vehicle cooling based on system cooling requirements and conducted thermodynamics analysis
- Conducted engine, powertrain and drivetrain analysis to select engine rating, transmission/axle gear ratios and configuration.
- Selected hybrid electric powertrain architecture and sized major components through simulation
- Designed and analyzed load-optimized chassis frame. Fabricated and tested lightweight frame rails.
- Designed and analyzed power steering and air systems with reduced power consumption.
- Developed and tested torque management and eco driver application for improving driving behavior with respect to efficiency.

Future Activities

- Phase 3: Preliminary System Prototypes
  - Build and test prototype vehicle and engine systems for empirical measurement of efficiency improvement.
- Phase 4: Target System Optimization
  - Optimize vehicle systems to reach efficiency targets including SuperTruck integration
- Phase 5: SuperTruck Buildup
  - Build and test final SuperTruck vehicle to demonstrate 50% vehicle freight efficiency

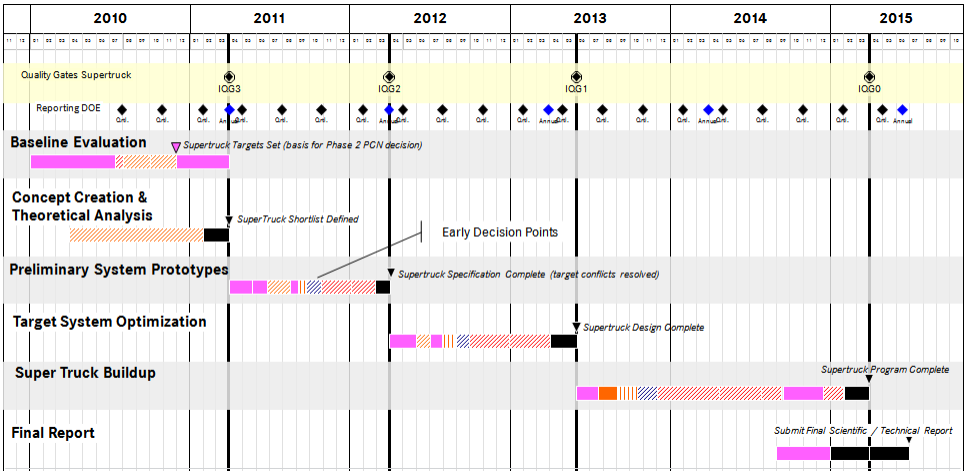

Figure 1. SuperTruck Project Schedule

II.M.2. Technical Discussion

Introduction

SuperTruck is a 5 year research and development program with a focus on improving diesel engine and vehicle efficiencies. The objective is to develop and demonstrate a class 8, long haul tractor-trailer which achieves a 50% vehicle freight efficiency improvement (measured in ton-miles per gallon) over a best-in-class 2009 baseline vehicle. The engine for the SuperTruck program will deliver 50% brake thermal efficiency.

Approach

In FY2011, SuperTruck entered the second phase of the program. The approach used in Phase 2 of the program has primarily centered on system analysis through the use of modeling and simulation, bench testing and on-road vehicle tests. Vehicle efficiency simulation software, Autonomie, was used for determining

the optimal engine, powertrain and drivetrain specification, including engine rating, transmission/axle gear ratio sets, driveline efficiencies and rolling resistance. External aerodynamics and vehicle cooling systems have been analyzed through the use of 1 dimensional thermodynamics and 3 dimensional fluid dynamic modeling in addition to the use of scale model wind tunnel testing. Finite element analysis software has been used in the design of load optimized chassis design with lightweight materials with subsequent testing both in bench tests and on vehicle.

The approach for the engine development in Phase 2 consisted of both testing and engine simulations to evaluate various technology pathways. Separate models for waste heat recovery and aftertreatment systems were used to size and optimize components for procurement. Some of the parasitic reduction measures were tested on component dynamometer.

Results

To date the SuperTruck program is on track towards reaching the 50% freight efficiency target. A roadmap of vehicle systems and their performance targets exists which cascade to the system level. Progress on each vehicle system has been gauged and numerous systems have been specified based on the analysis conducted to date (see Figure 1). Work continues toward the specification of the remaining systems, followed by the buildup and testing of system prototypes.

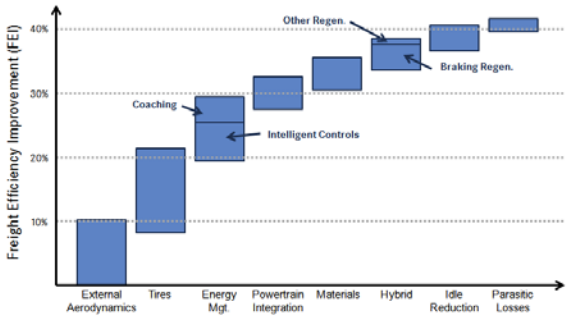

Figure 2. Vehicle Technologies Roadmap

Engine, powertrain and drivetrain analysis was conducted to determine the optimal specification to meet the efficiency targets while maintaining comparable driving performance. Various hybrid configurations were qualitatively evaluated to determine the preferred architecture which balances the desired functionality, performance and weight. Load optimized chassis designs were investigated to minimize the material and weight requirements and to determine the applicability of lighter weight materials. Basic shape analysis continues, using scale model wind tunnels and computational fluid dynamics simulation to determine an optimal aerodynamic shape that minimizes the drag force, while accommodating adequate cooling systems and providing an adequate envelope for vehicle packaging. Two idle reduction solutions are also under consideration that provides adequate climate control in summer and winter modes. The vehicle parasitic loads were analyzed and modeled to determine the baseline power consumption and to develop system models for power reduction.

Conclusions

The analysis provides a technology path that when implemented and tested will demonstrate the overall 50% freight efficiency target and 50% engine brake thermal efficiency. The SuperTruck Program is on track towards reaching that goal and the vehicle specification is scheduled to be defined at the end of phase 2 in Q1, 2012. Similarly, engine sub-system specifications are being defined and components procured to be tested at system level prior to the overall integration of technologies for meeting the overall goal of 50% brake thermal efficiency.

II.M.3. Products

Publications

1. Sisken, Kevin: "Super Truck Program: Engine Project Review Recovery Act –Class 8 Truck Freight Efficiency Improvement Project", Project ID:ACE058, DoE Annual Merit Review, May 12, 2011
2. Rotz, Derek: "Super Truck Program: Vehicle Project Review Recovery Act –

Class 8 Truck Freight Efficiency Improvement Project", Project ID ARRAVT080, DoE Annual Merit Review, May 12, 2011

3. Singh, Sandeep: "Exhaust Heat Driven Rankine Cycle for a Heavy Duty Diesel Engine", Project ID:ACE058, DOE DEER Conference, October 5th, 2011.
4. Sisken, Kevin: "Super Truck -- 50% Improvement In Class 8 Freight Efficiency", Project ID:ACE058, DOE DEER Conference, October 5th, 2011.

Patents

None

Tools & Data

II.N. (c) (Navistar 2011 DOE Supertruck Annual Report for Vehicle Systems)

Dennis Jadin (Principal Investigator)
Director, Advanced Vehicle Technologies
Navistar, Inc.
2601 Navistar Drive
Lisle IL 60532
(331) 332-6889; dennis.jadin@navistar.com

Chief Engineer, Advanced Vehicle Integration and Validation: Dale Oehlerking
Navistar, Inc.
2601 Navistar Drive
Lisle IL 60532
(331) 332-6552; dale.oehlerking@navistar.com

DOE Technology Development Manager: Dave L. Anderson
(202) 287-5688; david.anderson@ee.doe.gov

NETL Project Manager: Ralph Nine
(304) 285-2017; ralph.nine@netl.doe.gov

Primary Partners:
Alcoa, ATDynamics, Meritor, Michelin, Wabash National, Argonne National Lab, and Lawrence Livermore National Lab

---

II.N.1. Abstract

Overall Objectives

- Demonstrate a 50% improvement in overall freight efficiency on a heavy-duty Class 8 tractor-trailer measured in ton-miles per gallon.

Fiscal Year 2011 Objectives

- Create detailed models for use in simulation
  - Conventional ProStar tractor/trailer
  - Meritor dual-mode hybrid drive
  - Lithium-ion batteries
  - Conventional and electrified accessories
- Develop powertrain control algorithms
- Compare freight efficiency between conventional and hybrid Prostar using model-in-the-loop simulation for various drive cycles
- Compare simulated vehicle performance to Navistar requirements
- Build and test a prototype ProStar tractor with dual-mode hybrid drive and electrified accessories

Accomplishments

- Navistar partnered with Argonne National Laboratory and built detailed Autonomie models of a ProStar Class 8 tractor with both a conventional 9-speed transmission and a dual-mode hybrid drive. Electrified accessories were included.

- Powertrain control algorithms were developed, both in Autonomie and Simulink
- Simulations predicted freight efficiency improvements from 7 to 22 percent depending on drive cycle
- Analysis showed that most – but not all – vehicle performance requirements will be met by the dual-mode hybrid drive system
- A dual-mode hybrid powertrain development vehicle was constructed and tested on test tracks and public roads.

Future Directions

- Build a second powertrain development vehicle by Q2 of 2012, including incremental upgrades
  - Turbo-compounding
  - Upgraded hybrid drive unit
  - Upgraded battery cooling system
  - Low rolling resistance tires
  - Simple aerodynamic improvements
  - Other
- Design and procure significantly smaller and lighter hybrid drive units
- Upgrade both vehicle with new drive units
- Run performance and fuel economy tests to document impact of these changes

II.N.2. Technical Discussion

Introduction

A dual-mode electric hybrid powertrain is being developed for SuperTruck. The powertrain consists of a Navistar MaxxForce13 diesel engine, a Meritor dual-mode drive unit, electrically-driven accessories, lithium-ion batteries, and a cooling system.

Two Navistar ProStar class-8 semi-tractors were purchased to serve as development platforms for the hybrid powertrain. At the time of this writing, one vehicle has been converted to hybrid and the other is in process.

Approach

Class 8 vehicle performance requirements shall be gathered. Analysis will be done on various powertrain alternatives to determine its basic performance requirements can be met. Once a suitable concept has been selected, detailed models will be developed to gain insight into the potential for fuel economy improvement. Powertrain specifications will be adjusted based on lessons learned in the analysis phase.

Hybrid powertrains will be constructed and installed Navistar ProStar tractors. These tractors will be used to develop powertrain controls and to obtain real-world fuel economy and performance data, and to learn new lessons to be applied to future designs.

Results

Hybrid Powertrain Simulation

An analysis of several concepts indicated that a dual-mode hybrid concept had the best chance of meeting the goals of this project. In this concept, the hybrid drive unit works in series/EV mode at low and moderate vehicle speeds. Once higher speeds are reached, the system switches to parallel mode.

The use of series/EV mode at low and moderate speeds enables the deletion of clutch and conventional transmission, thereby saving packaging space, weight and cost. At higher speeds, the need for a multitude of gear ratios diminishes, and the more efficient parallel mode can be made to work with only two ratios. A schematic of the dual-mode concept can be seen in Figure 1.

Detailed vehicle-level plant models of the hybrid powertrain and conventional powertrain were constructed in the Autonomie simulation environment. Powertrain control algorithms were developed and the models were run in accordance to these algorithms. This is known as "model-in-the-loop" simulation.

The conventional and hybrid models were run on a variety of drive cycles shown in Figure 2. Fuel consumption and freight efficiency were calculated for every case. The results were compared. The result of that calculation can be seen in Figure 3.

Navistar has basic performance requirements for Class 8 vehicles, mostly focused on performance on grades. A series of calculations was performed to determine wheel torque as a function of road speed. Know this and making assumptions about vehicle mass, it is possible to predict vehicle performance on grades.

In addition to uphill performance requirements, Navistar has downhill performance requirements as well. A fully-loaded Class 8 vehicle cannot rely on the vehicle brakes alone when descending a long grade. The powertrain must be designed in such a way that it absorbs a significant portion of the burden when controlling speed on downhill grades. Normally, this requires the addition of an engine brake or retarder. In the case of the dual-mode hybrid, significant retardation can be accomplished with the regenerative braking feature that most hybrid powertrains demonstrate. However, this is possible only if the battery is able accept energy from the drive unit. If the battery happens to be at 100% charge level, regenerative braking is not possible. In order to assure that regenerative braking is possible on long downhill grades, a means to bleed off excess battery energy is required. This can be accomplished by adding an energy-dissipating resistor or by using the engine-mounted generator to spin the engine and consume electrical energy.

Predicted performance characteristics are compared to Navistar guidelines in Figure 4.

Hybrid Powertrain Development

Based on the positive indicators obtained during the analysis and modeling activities, the construction of two vehicles was commissioned. The first of these vehicles has been in operation since July of 2011. It has been in development at various test tracks, including the Navistar test track in Fort Wayne, Indiana, the Ohio Transportation Research Center, and Romeo Proving Grounds in Michigan. It has also been legally operated on public roads in Illinois, Colorado, Indiana, and Michigan.

The first hybrid development vehicle can be seen in Figure 5.

A second hybrid development vehicle is currently under construction. One of the most important differences in this vehicle will be the addition of turbo-compounding. Turbo-compounding recovers energy from the exhaust system that would normally be lost to the atmosphere. Turbo-compounding is a perfect complement to hybrid-electric technology because it is most effective when hybridization delivers the least benefit, i.e. steady-state operation. Also, some means of delivering the turbo-compound energy to the driveshaft is required. A hybrid-electric vehicle, with its high-voltage electric motor, is already situated to make use of the electrical energy supplied by the turbo-compounder.

See Figure 6 for a schematic of turbo-compounding and hybridization.

Conclusions

- Analysis and simulation indicates that electric hybrid technology can make significant contributions to the overall program goal of 50%
- A class 8 vehicle with dual-mode hybrid drive can meet Navistar performance requirements with some exceptions
- Turbo-compounding is an excellent addition to a vehicle with an electric-hybrid drivetrain

- On-track and on-road testing of the dual-mode drive unit will serve to accelerate the maturation of the design

II.N.3. Products

FY 2011 Publications/Presentations

1. Annual Merit Review and Peer Evaluation, Vehicle Technologies Programs, USDOE, May 12, 2011, Washington, D.C.
2. Commercial Vehicle Innovation Summit (CVIS), Automotive World, September 27, 2011, Washington, D.C.

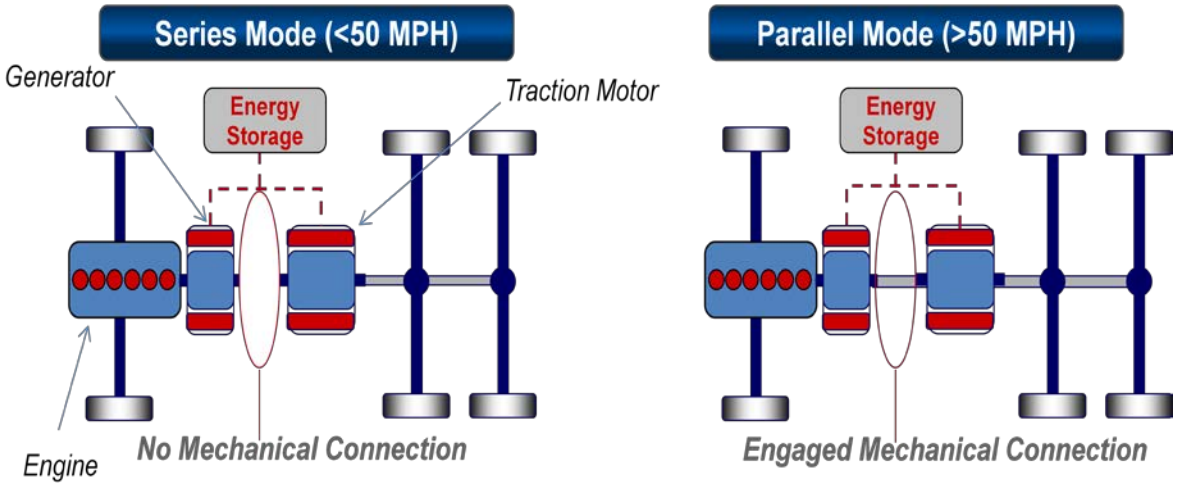

Figure 1. Dual-Mode Hybrid Drive Concept

HHDDT65	Heavy Heavy-Duty Truck 65 mph	Representative of highway operation. Largely steady-state. 65 mph cruise speed.
HHDDT Cruise	Heavy Heavy-Duty Truck, Cruise Mode	Slightly slower highway cycle. Includes more transients than HHDDT Cruise
HHDDT High Speed	Heavy Heavy-Duty Truck	A short cycle accelerating up to 65 mph and back down
HHDDT Transient	Heavy Heavy-Duty Truck, Transient Mode	Highly-transient series of accels/decels
HD-UDDS Truck	Heavy-Duty Urban Dynamometer Driving Schedule	Highly-transient cycle representative of urban driving

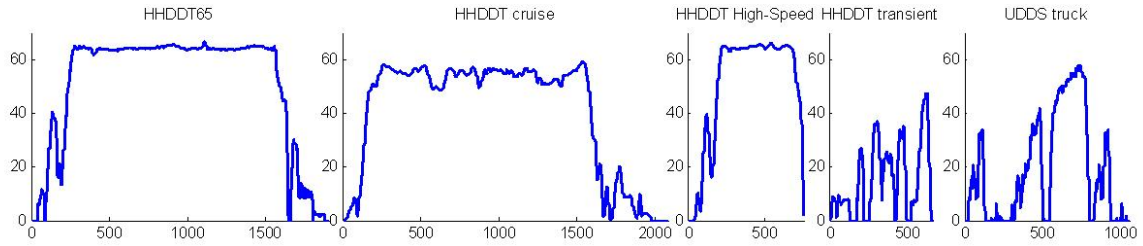

Figure 2. Drive Cycles Used in Analysis

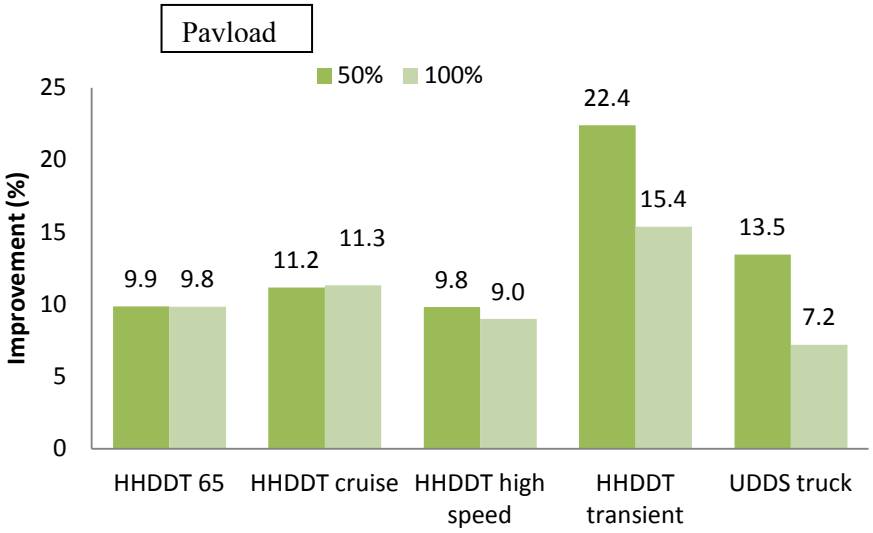

Figure 3. Predicted Freight Efficiency Improvements

Requirement	Goal	Prediction	Comment
Startability	15% at 80k lbs	17%	Series mode
Road Speed	Maintain cruise speed in top gear, 80k lbs, 1% grade	75 mph	Parallel mode, high gear
Gradeability	50 mph, 3% grade, 80k lbs	53 mph	Parallel mode, low gear
Gradeability	20 mph, 7% grade, 80k lbs	16 mph	Series mode, continuous power rating
Powertrain Braking	Hold 30 mph without using service brakes	---	The goal is achievable as long as some means of bleeding off electrical energy is provided (not available at this time)

Figure 4. Performance Predictions

Figure 5. Hybrid Development Vehicle (Foreground)

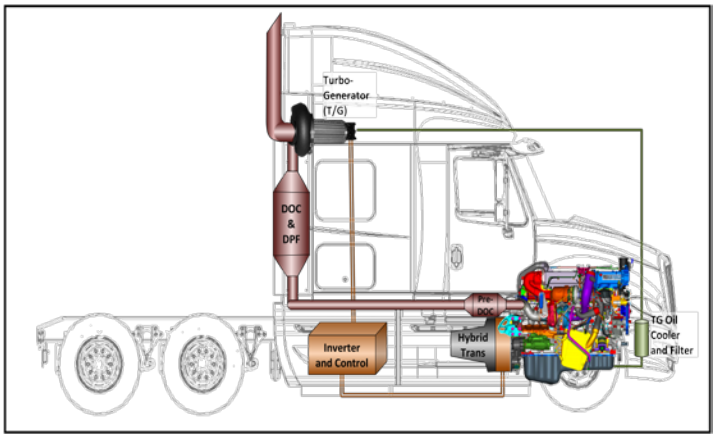

Figure 6. Turbo-Compounding Applied to Hybrid Powertrain

II.O. (d) Volvo Energy Efficient Vehicle

Principal Investigator: Pascal Amar
Volvo Technology of America
7825 National Service Road
Mail Stop: AP1/3-41
Greensboro, NC 27409
pascal.amar@volvo.com

DOE Technology Development Manager: Roland Gravel

NETL Project Manager: Ralph Nine

II.O.1. Abstract

Objective

- Overall objectives
  - Reduce friction and parasitic losses to improve overall fuel efficiency
  - Reduce fuel use during long haul driving cycle
  - Reduce fuel use during 'hotel mode'
  - Reduce curb weight of complete vehicle
  - Optimize energy usage in the complete vehicle
  - Demonstrate benefits of e.g. driver coaching systems
- FY2011 Objectives
  - Establish baseline vehicle configuration
  - Develop detailed plan for technologies selection and development

Major Accomplishments

- Early tests with redesigned prototype high performance pistons show an improvement of 2% in thermal efficiency
- The Waste Heat Recovery (WHR) system configuration and layout selected is expected to provide close to 10kW at cruise conditions and close to 25kW at full load condition.
- Second Generation WHR system components with improved control and reliability have been defined and procurement initiated
- Converting the traditional tractor to a new proprietary suspension design, along with a new axle configuration saved approximately 600 lbs compared with the baseline tractor configuration.
- We completed a study on a sleeper cab using mixed materials, and identified the concept of choice as well as a prototype supplier. We expect to reduce cab weight by 16 to 18% compared with the MY2009 tractor.
- We configured and ordered a light-weight trailer, which is expected to weigh approximately 3,000lbs less than the baseline trailer at delivery. This trailer will be used to demonstrate innovative lighting and aerodynamic technologies.

- An advanced system of three aerodynamic attachments to reduce the aerodynamic drag of the trailer has been designed to improve upon the performance of existing products that have demonstrated fuel savings over 7%.
- Thermal testing and evaluation of the baseline cab was completed.

  Installed new proprietary suspension which should reduce tire wear by 5-15%

Future Activities

- Evaluate the new combustion system together with waste heat recovery components in a multi-cylinder engine dynamometer
- Install improved driveline in a chassis for on-road testing and verification
- Install first prototype lighting system in a light weight trailer for on-road testing and verification
- Correlate CFD model of complete vehicle with full scale vehicle test results for aerodynamic drag evaluation and improvements
- Analyze results from Hotel Load consumption to determine power requirement for auxiliary power unit
- Evaluate further light-weight components, e.g. driveshaft, wheels, etc
- Complete low-energy consumption retrofit for interior and exterior lighting of the cab
- Investigate potential of Long Combination Vehicles in improving freight efficiency

II.O.2. Technical Discussion

Introduction

The first step towards achieving higher transport efficiency is to ensure that as much energy as possible is extracted from the fuel burned. We will therefore explore various solutions to increasing the efficiency of the combustion process, recover energy which would otherwise be rejected in the form of heat, and reduce friction losses in the overall driveline to maximize the amount of energy which actually contributes to moving freight.

Such changes to the driveline will impact packaging and heat rejection. Therefore the installation, cooling and venting concepts need to be modified to provide optimum vehicle efficiency.

Weight reduction of the tractor and trailer directly benefit the freight efficiency of a long-haul truck. New materials will be evaluated to provide maximum weight reduction without sacrificing structural integrity, safety, durability or ergonomics.

Earlier studies have shown that auxiliary devices account for 5–7% of the total fuel consumption. The Volvo SuperTruck team is designing a complete energy-balancing system to optimize the trade-off between mission performance and energy consumption. A new high-efficiency lighting system will help reduce electrical consumption of the complete truck. The reduced power requirements will also enable redesign of some components for lighter weight and/or lower air resistance.

Aerodynamic drag force accounts for the major part of the tractive load of a vehicle-trailer moving at highway speeds, and is a key target for optimizing the complete vehicle efficiency. The project team will investigate ways to optimize the tractor design with regard to shape and contour to reduce aerodynamic drag and provide a smooth interface to the trailer. Freight Wing's latest advancements in aerodynamic trailer fairings and skirts shown in Figure 1 provide a solid foundation for continued development to achieve the goals of the SuperTruck program.

Figure 1. Freight Wing's advanced aerodynamic system to reduce the drag of the trailer, which is expected to yield fuel savings over 7% compared with the baseline.

Field data shows that some long haul fleets idle as much as 40% of vehicle operating time. In order to address the efficiency of long-haul trucks under their complete operating cycle it is crucial for long-haul applications to address energy use during idling time.

Approach

There are a large number of possible Waste Heat Recovery (WHR) system configurations. A detailed comparison of the possibilities concluded that a system layout comprised of an EGR cooler in parallel with an exhaust stack heat exchanger was best suited for this application. With the selected parallel layout, the Rankine WHR system can be used for EGR cooling in place of a standard coolant based EGR cooler. After consideration of factors related to layout of the chosen system, stability, freezing point, material compatibility, lubrication, environmental impact and legal aspects, ethanol was selected as the working fluid generating torque through the use of a piston expander.

Cooling the additional WHR components is a challenge, therefore packaging and installation studies are on-going to identify possible interferences between the new driveline and the chassis. We are investigating new ways to collect air flow and/or improve the cooling capacity of the existing cooling package. Prototype low temperature radiators were selected and ordered.

Studies have begun to identify new structure and materials for a lighter cab, for example new sleeper cabinets with an anticipated weight reduction of up to 20% over the current package. The new sleeper cab concept under evaluation is expected to be approximately 15% lighter than its baseline.

The SuperTruck demonstrator will be equipped with state-of-the art low friction tires which the team will select from existing suppliers and industry partners. The team will further reduce the rolling resistance of the complete vehicle by optimizing synthetic lubes for axles and transmission, as well as to using improved bearings for axles and wheel ends.

In order to reduce energy usage during idling, the team will develop an energy management system that efficiently shuts down the main engine after parking, and identify the most efficient energy source / storage system to power typical Hotel Mode loads. Volvo will also introduce energy saving materials, like insulation materials and reflective coating, to minimize power requirements when the truck is parked while creating a more comfortable climate for the driver. This study also includes alternative solutions for energy storage.

Complete vehicle model CFD simulations will provide insight into the areas of the vehicle shape that will provide the biggest gain in overall vehicle aerodynamics. The impact of aerodynamic trailer component geometry will be optimized and verified through simulations and analysis to provide the best benefit for the complete vehicle. Freight Wing will then produce prototypes for bench and/or full size testing to validate improvements as well as identify possible operational issues.

In order to reduce driver impact on the efficiency of the complete vehicle, the Volvo team plans on implementing advanced driver assistance solutions for powertrain, and controls optimized for best fuel economy and safety based on preview information (e-Horizon).

Telematics will also be investigated as a mean to improve freight efficiency.

Complete Vehicle Simulation

The SuperTruck concept involves development in multiple components that affect the performance and operation of the truck. These are interrelated and can affect the performance of each other. Hence it is important to understand the overall impact of the development of each component. It is also important to direct the development efforts towards target high impact area. The Volvo team uses its complete vehicle simulation capabilities to address this and to identify an overall optimal design.

The complete vehicle simulation platform used consists of models of the truck concept, which consist of the sub-models for the vehicle, driver and the road and environment. Each of these sub-models is further built from its component models in a modular form.

While many component models were available at the start of the project, the SuperTruck will be using many new technologies for which models need to be developed. Substantial progress has been made in this area and most of the new models will be available during the next reporting period.

The complete vehicle model for the baseline truck is currently being used to determine the target areas for improvement and to characterize the performance of the baseline truck, and to compare the performance of the baseline truck model with road test to verify the level of accuracy of the simulation platform.

Results

Early tests with prototype high performance pistons show an improvement of 2% in engine thermal efficiency with a slight decrease in soot with other pollutant emission levels remaining unchanged. Simulations predict that the Waste Heat Recovery system configuration and layout selected should provide close to 10kW at cruise conditions and close to 25kW at full load condition.

The Hotel and parasitic load reduction effort started with a comprehensive assessment of the cab thermal insulation. We completed testing and evaluation and calculated the current R-value of the baseline cab. A plan was then laid out to improve the cab by increasing the R-value of its insulation by over 60% for the SuperTruck demonstrator.

Volvo and Freight Wing are developing a CFD model of the complete vehicle. This will be used to establish the direction and areas of focus for the aerodynamic improvements to implement and validate on the first concept vehicle. The team also completed baseline idle fuel consumption tests.

The auxiliary components identified with the largest potential for reduced parasitic energy consumption are the steering pumps, fan drives, steering gear and compressors. These will be further investigated in the following reporting period.

Conclusions

During the first months of the Volvo SuperTruck project, the team put a clear plan into action to significantly improve the energy efficiency of the complete vehicle, and ultimately the freight efficiency of highway transports. All areas of the vehicle were considered to identify the biggest short-term impact, as well as select candidate technologies with the greatest potential for use in long-haul trucks.

This short reporting period focused on refining our technology development plans, securing resources and initiating development activities, as well as on defining and evaluating the baseline truck which will serve as a reference for all improvements deployed in this project. The next reporting period will see the start of component tests as well as further refinement of the SuperTruck concept using our Global Simulation Platform.

III. LABORATORY AND FIELD TESTING (LIGHT DUTY)

III.A. Level 1 Benchmarking of Advanced Technology Vehicles

Principal Investigator: Henning Lohse-Busch, Ph.D
Argonne National Laboratory
9700 South Cass Avenue
Bldg 361, Office B-217
Argonne, IL 60439
(630) 252-9615; hlb@anl.gov

DOE Program Manager: Lee Slezak
(202) 586-2335; Lee.Slezak@ee.doe.gov

III.A.1. Abstract

Objectives

- Provide independent evaluation of advanced automotive technology by benchmarking high-efficiency vehicles as part of the U.S. Department of Energy's (DOE's) mission of laboratory and field evaluations of hybrid. plug-in hybrid, and other electric vehicles.
- Establish the state-of-the-art automotive technology baseline for powertrain systems and components through data from testing and analysis.
- Disseminate vehicle and component testing data to partners of the DOE, such as national laboratories, the U.S. Council for Automotive Research, OEMs, and suppliers. Provide data to support codes and standards development. Support model development and validation with test data.

Approach

- Use advanced and unique facilities with extensive instrumentation expertise. The Advanced Powertrain Research Facility at Argonne includes a 4WD and 2WD chassis dynamometer with a wide range of equipment and a focus on measuring energy consumption (fuel and electric).
- Perform baseline dynamometer testing of DOE's Advanced Vehicle Testing Activity vehicles before the accelerated fleet testing.
- Test the powertrain systems as well as components of the systems.
- Use a decade of experience in testing vehicles to refine the test procedures and test plans.

Major Accomplishments

- Benchmarked vehicles ranging from idle-stop vehicles to an extended-range plug-in hybrid by comprehensive testing on the chassis dynamometer with complete instrumentation.
- Distributed the test results and analysis through several mechanisms such as reports, presentations, and sharing of raw data.
- The testing activity helped directly in the development of some codes and standards and supported the model development and validation.

Future Activities

- Provide testing and vehicle systems expertise to further contribute to DOE's missions.

III.A.2. Technical Discussion

Introduction

The Advanced Powertrain Research Facility (APRF) at Argonne has been testing advanced-technology vehicles to benchmark the latest automotive technologies and components for the U.S. Department of Energy (DOE). The staff has tested a large number of vehicles of different types such as hybrid electric vehicles (HEVs), plug-in hybrid electric vehicles (PHEVs), battery electric vehicles, and conventional vehicles, including alternative-fuel vehicles.

Over the last decade, the staff has developed a fundamental expertise in the testing of the next wave of energy-efficient vehicles. During this time, the instrumentation of the powertrains has evolved and the test procedures have been refined. Two main levels of testing exist today. The first level involves a basic but complete non-invasive instrumentation of a vehicle, which leaves the vehicle unmarked after the testing. The second level involves an in-depth and comprehensive invasive instrumentation of a vehicle and powertrain components, which leaves the vehicles with irreversible alterations.

This report summarizes the level-1 benchmark activities of FY2011. In the first section the test approach is described, and then the DOE's Advanced Vehicle Testing Activity (AVTA) vehicle tests are presented.

Approach

General Test Instrumentation and Approach

The testing presented in this report is focused on the basic and complete non-invasive level-1 type. Typically, Argonne receives these vehicles on loan from partners; therefore, the vehicles need to leave the test facility in the "as-received" condition. This limits the instrumentation to sensors that can be easily removed without leaving any damage.

Despite this need, Argonne strives to achieve a minimum instrumentation level. If the vehicle has an internal combustion engine, instrumentation is applied to monitor the speed, fuel flow (at least from modal emissions or a fuel flow meter if possible) and engine oil temperature (achieved through dipstick instrumentation). For electrified vehicles, a power analyzer is used to record, at a minimum, the voltage and main current of the stored energy. If the vehicle requires charging, the electric power from the source is recorded. Furthermore, any sensors that can be implemented without permanent damage, such as temperature sensors, are typically included in locations of interest (a battery pack vent, for example). These additional sensors vary from vehicle to vehicle. A final part of the level-1 benchmark is the recording of messages from the vehicle's information buses, and this information will also vary widely from vehicle to vehicle.

In addition to the minimum instrumentation described above, further sensors may be added, depending on the vehicle powertrain and special interests, as long as they are non-invasive.

Purpose of Benchmarking

A major goal of the benchmarking is to enable petroleum displacement through data dissemination and technology assessment. The data generated from the vehicle testing and analyses are shared through several mechanisms, such as raw data, processed data, presentations and reports.

A fundamental gateway to the data is Argonne's Downloadable Dynamometer Database (D^3), which is a public website (http://www.transportation.anl.gov/D3/index.html). The D^3 website provides access to data and reports from vehicles tested on the standard test cycles. The data directly serve the development of codes and standards as well as the development and validation of simulation models. These activities impact the modification of test plans and instrumentation. Further partners in the testing are U.S. manufacturers and suppliers, through the U.S. Council for Automotive Research (USCAR).

Many of the research activities of the DOE rely on the benchmark laboratory and fleet testing results to make progress towards their own

goals. Figure 1 details some of these DOE research activities and partners.

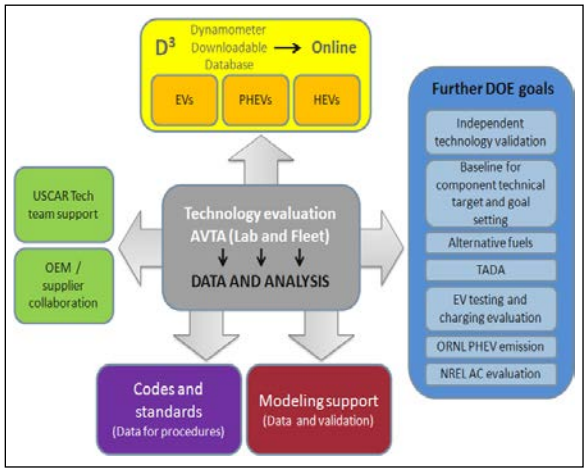

Figure 1. Data dissemination and partners.

The benchmark program leverages DOE's AVTA activities. INL procures new advanced-technology vehicles to test them in accelerated fleet testing. As part of the evaluation, these vehicles are benchmarked in the APRF. Figure 2 illustrates the process.

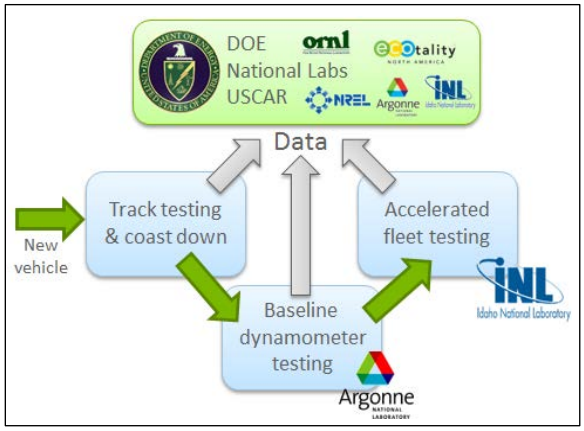

Figure 2. Advanced Vehicle Testing Activity process.

Further information on the AVTA is available at http://avt.inel.gov/.

Background

Overview of ATVA Vehicles Tested

Each year the AVTA partners select a set of vehicles which best represent the new technologies available on the market. For FY2011, the selected vehicles were the 2010 Honda CRZ, a selection of three imported idle-stop vehicles, the 2011 Hyundai Sonata Hybrid, and the Chevrolet Volt. Figure 3 shows pictures of all the AVTA test vehicles on the dynamometer along with the reason for the testing and some further points of interest.

Also included in Figure 3 are comparisons of labeled fuel economy between the tested vehicles and their closest conventional counterparts in the manufacturers' lineups. It appears that the hybrid systems of these vehicles provide a significant efficiency improvement, whereas the fuel-economy improvements of the idle-stop vehicles are modest on the UDDS cycle.

Results

For each vehicle in this report, this section provides a vehicle description, a graph illustrating the powertrain operation, and discussion of some interesting aspects of the results.

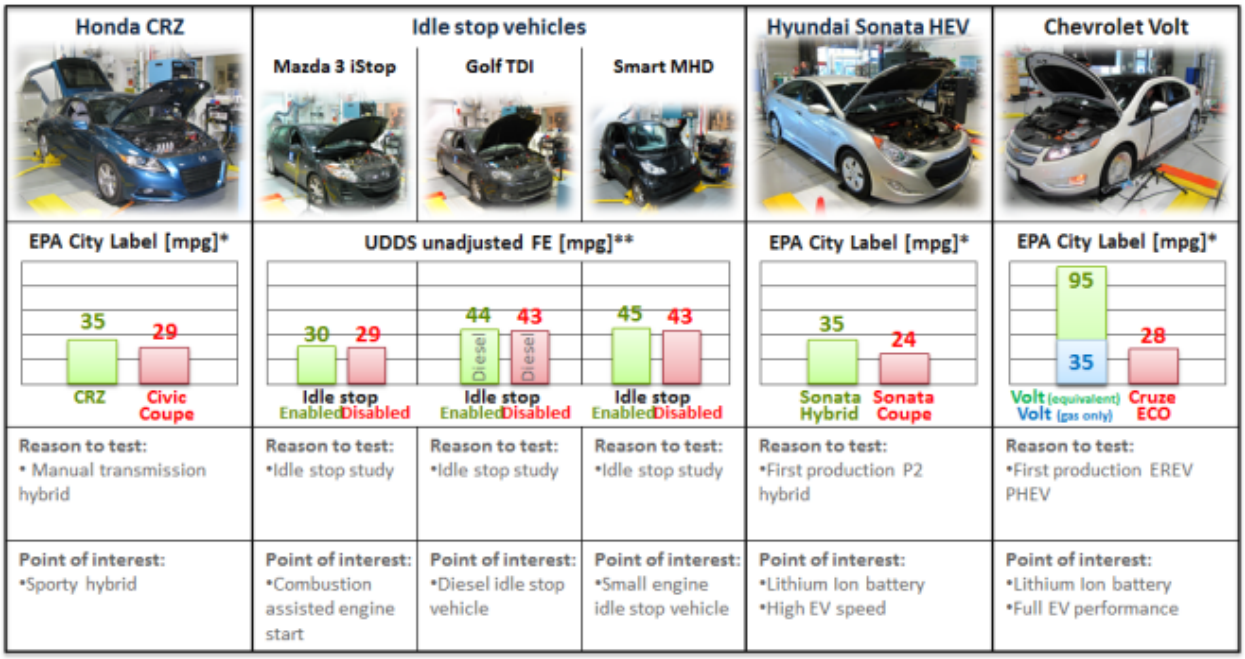

*Source Manufacturer websites to enable comparison
** APRF Test results

Figure 3. Summary of APRF test results and overview of vehicles for level-1 benchmarking in FY2011.

2010 Honda CRZ (Manual Transmission)

Vehicle Description

The CRZ powertrain is based on the second-generation Honda Insight powertrain. The engine is directly coupled to an electric motor and a six-speed manual transmission. Table 1 presents the technical specifications.

Table 1. Honda CRZ powertrain specifications

Architecture	Power Split Hybrid
Engine	1.5-liter I6 (10.4:1) • 91 kW @ 6000 rpm • 174 N•m @ 1000-1750 rpm
Hybrid	Micro hybrid with manual six-speed transmission
Motor	PM motor • 10 kW • 79 N•m
Battery	Nickel metal hydride (NiMH) • 10 kW • 0.58-kWhr capacity • 100.8 V nominal

Vehicle Operation

Figure 4 illustrates the powertrain operation of the CRZ. Honda's Integrated Motor Assist system uses a single small electric machine directly coupled to the engine, which enables engine idle stop, electric assist, regenerative braking and engine fuel cut-off operation. This configuration does not enable electric-only operation.

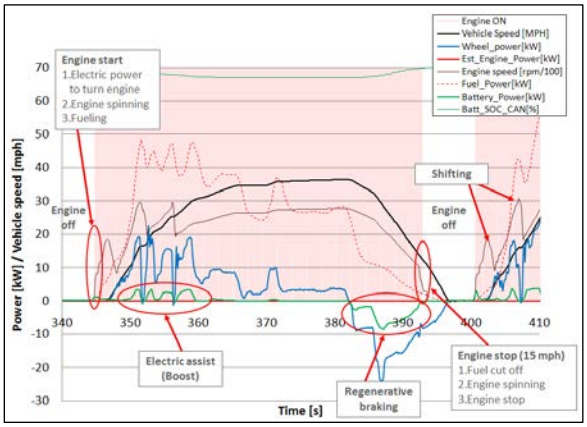

Figure 4. CRZ operation on a section of the UDDS cycle.

With a manual transmission, the engine will turn off when the vehicle is stopped if the

transmission is in neutral, the driver's foot is off the clutch pedal, the driver's foot is on the brake pedal, and the engine is warm (engine oil temperature is above 60°C). The engine is shut off during a deceleration below 15 mph if the above conditions are met. The motor-crank torque to start the engine is 60-65 N•m.

The driver has to shift manually, but a dashboard shift indicator helps the driver to select a gear. Argonne used the shift schedule used for the CRZ's certification. Using the Honda shift schedule, the CRZ achieves a fuel economy of 38 mpg unadjusted. If the dynamometer driver follows the shift light on the dash to shift, the CRZ achieves a fuel economy of 44 mpg. So the shift pattern has a great impact on the fuel economy.

Point of Interest

The CRZ relies on the hybrid system to obtain a performance boost, as shown in Figure 5. When the battery is in a normal or greater state of charge, the motor provides an extra 10 kW of power. If the battery is depleted and the motor cannot provide assistance, an extra 1.3 sec is needed to accelerate to 60 mph.

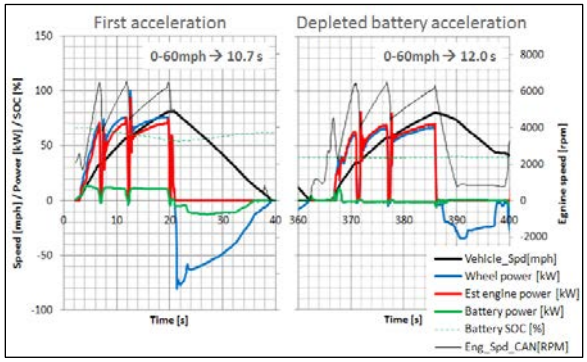

Figure 5. CRZ acceleration performance at different battery states.

Idle-Stop Vehicles

The next three vehicles tested are part of a study to determine the fuel-economy benefits of idle-stop technology. Idle-stop vehicles shut off the engine when the vehicle is at a stop, but all the power to move the vehicle forward comes from the engine. Therefore, idle-stop vehicles are not considered hybrid vehicles.

Each vehicle was tested with the idle-stop feature enabled and disabled to measure the fuel-economy benefit for each of the test cycles. The conclusions on fuel economy will be summarized after all three vehicles and their operations are discussed.

Shift schedule note: All three vehicles required the driver to shift. Argonne developed a shift schedule for each vehicle and each drive cycle. The shift-schedule development is an iterative process. At first, the driver drives the test cycle and shifts gears in accordance with a shift indicator prompt (if available). The shift pattern is then processed from the recorded data into a shift schedule displayed on the driver aid. Finally, the driver repeats the test cycle with this shift schedule and adjusts the schedule several times if needed.

2010 Mazda 3 iStop

Vehicle Description

The Mazda 3 iStop is based on the Mazda 3 hatchback with a 2-liter direct-injection gasoline engine and a six-speed manual transmission. Table 2 presents the technical specifications. It is interesting to note that Mazda opted to use a second 12-V battery dedicated to the 12-V starter system.

Table 2. Mazda 3 iStop powertrain specifications

Architecture	Power Split Hybrid
Engine	2.0-liter 4-cyl DI (11.2:1) • 111 kW @ 6200 rpm • 191 N•m @ 4500 rpm
Transmission	Manual six-speed
Start System	12-V starter Combustion-assisted engine start (0.35 seconds)
Battery	Secondary power battery for engine starting

Vehicle Operation

With a manual transmission, the engine will turn off when the vehicle is stopped if the transmission is in neutral, the driver's foot is off the clutch pedal, the driver's foot is on the brake pedal, and the engine is warm (engine oil

temperature is above 60°C). The engine is shut off during a deceleration below 3 mph if the above conditions are met.

Mazda developed a "combustion-assisted" engine-start process. When the engine is shut down, the engine is stopped in a particular position with some cylinder just past top dead center on a compression stroke, which is ideal for a restart. Direct injection enables the engine shutoff with no fuel. The start time of the engine is reduced to 0.35 sec from a typical 0.7 sec. Figure 6 illustrates the powertrain operation on a cold-start UDDS cycle.

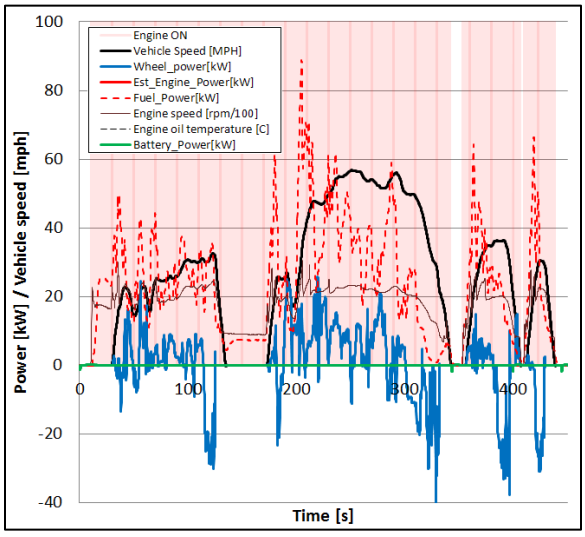

Figure 6. Mazda 3 iStop operation on a cold-start UDDS cycle.

Point of Interest

The frequent starting of the engine could potentially lead to increased emissions spikes. Figure 7 shows the integrated emissions of the Mazda 3 iStop on a cold-start UDDS cycle. The graph compares normal idle-stop operation with disabled idle-stop operation, where the engine never shuts down.

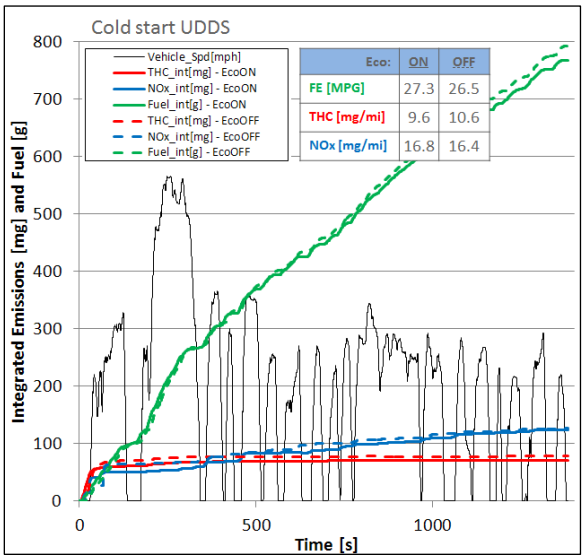

Figure 7. Integrated emissions of the Mazda 3 iStop on a cold-start UDDS cycle.

For the Mazda 3 iStop, the idle-stop behavior does not impact the emissions behavior. The controlled "combustion-assisted" engine start can probably be credited for that achievement.

2010 Volkswagen Golf TDI Bluemotion

Vehicle Description

The Golf uses a 2-liter direct-injected turbo-charged diesel engine. The engine is started with a 12-V starter, which operates on the standard 12-V battery. The engine is coupled to a five-speed manual transmission. Table 3 presents the technical specifications.

Table 3. Golf TDI Bluemotion powertrain specifications

Architecture	Power Split Hybrid
Engine	Diesel 2.0-liter 4-cyl TDI (11.2:1) • 103 kW @ 4200 rpm • 236 N•m @ 1750 rpm
Transmission	Manual five-speed
Start System	12-V starter
Battery	Standard 12-V battery

Compared to a standard Golf TDI, the Bluemotion has a tall final drive and some aero-dynamic changes to improve the fuel economy.

Vehicle Operation

With the manual transmission, the engine will turn off at a vehicle stop if the transmission is in neutral, the driver's foot is off the clutch pedal, and the driver's foot is on the brake pedal. The engine does not have to be warm for the idle stop to work, as illustrated in Figure 8. The engine is shut off at the first vehicle stop (~120 sec) despite an engine oil temperature of only 40°C. The vehicle has to be at a complete stop for the engine to shut off.

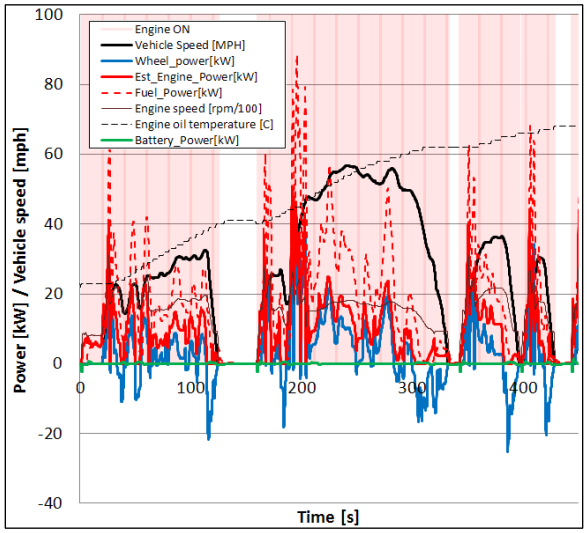

Figure 8. Golf operation on a cold-start UDDS cycle.

Point of Interest

Figure 9 shows the integrated emissions of the Golf on a cold-start UDDS cycle. The graph compares the normal idle-stop operation to the disabled idle-stop operation, where the engine never shuts off. The Golf obtains better fuel economy and lower emissions with the idle-stop feature enabled. The Golf's emissions levels are higher than those of the Mazda 3, especially for NOx.

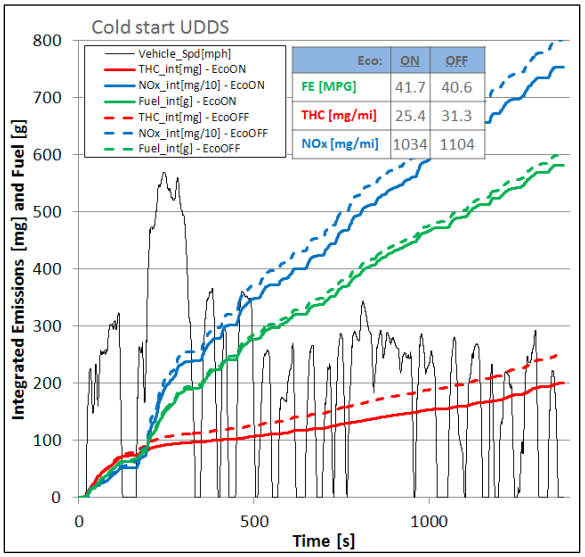

Figure 9. Integrated emissions of the Golf on a cold-start UDDS.

2010 MCC Smart MHD

Vehicle Description

The Smart is a small two-seat vehicle designed for city driving. The 1-liter engine is located under the trunk floor and is coupled to a five-speed automated sequential gearbox which drives the rear wheels. The driver has to pull or push the shift lever in the vehicle to change gears. The engine is started through a belted starter generator system which operates on 12 V from the standard 12-V battery. Table 4 presents the technical specifications.

Table 4. Smart MHD powertrain specifications

Architecture	Power Split Hybrid
Engine	1.0-liter 3-cyl • 52 kW @ 5800 rpm • 92 N•m @ 4500 rpm
Transmission	Five-speed manual sequential
Start System	Belt-start alternator system
Battery	Standard 12-V battery

Vehicle Operation

The engine will turn off at a vehicle stop if the driver's foot is on the brake pedal and the engine is warm (engine oil temperature is above 60°C). The engine is shut off below 5 mph during a deceleration if the above conditions are met.

This is the highest shut-off speed of all three cars. Figure 10 shows the vehicle operation on a cold-start UDDS cycle.

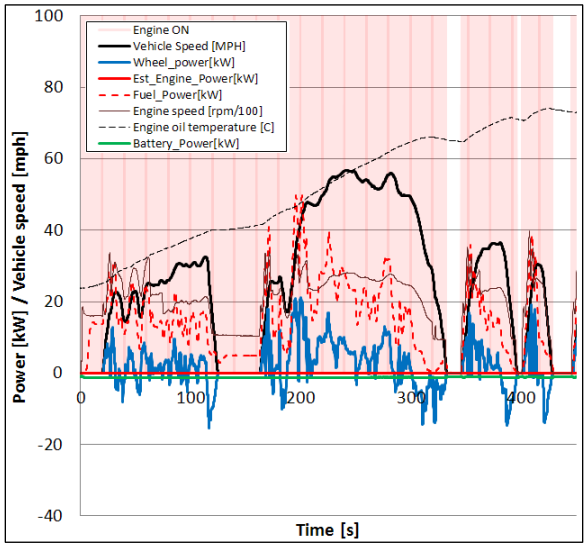

Figure 10. Smart operation on a cold-start UDDS cycle.

Point of Interest

Figure 11 shows the integrated emissions of the Smart on a cold-start UDDS cycle. The graph compares the normal idle-stop operation to the disabled idle-stop operation, where the engine never shuts down. Both the total hydrocarbon (THC) and the NOx levels are higher when the idle stop is operational. The initial engine start causes the biggest difference in the THC measurement between the two operating modes. But in both cases, the engine is cranked after a 12 hour soak period, so the initial THC spike is not caused by the idle-stop feature. Once the test is started, the THC levels stay relatively low and parallel; therefore it seems that the idle-stop operation does not have a large impact on THC production. On the other hand, the frequent engine starts do cause high NOx levels.

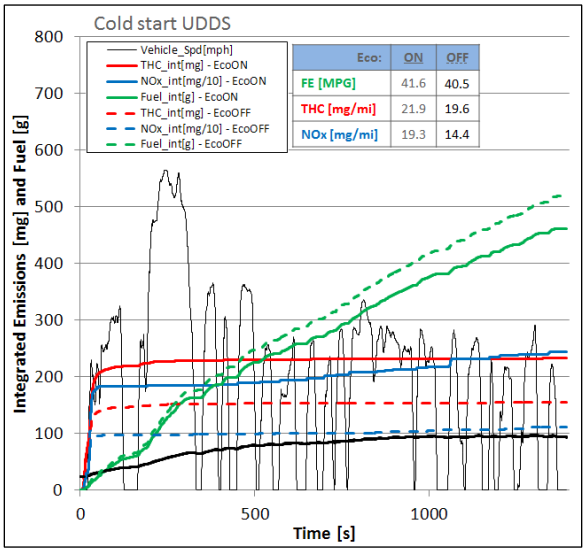

Figure 11. Integrated emissions of the smart on a cold-start UDDS cycle.

Idle-stop Vehicle Conclusions

The benefit of the idle-stop technology will depend on the type of drive cycle it is tested on. Figure 12 and Figure 13 show the fuel consumption with and without the idle-stop feature enabled for the U.S. and European certification cycle, respectively. The average fuel-consumption benefit of the idle-stop technology for the UDDS (U.S. city) cycle, in which a vehicle is stopped for less than 18% of the time, is 4%. The average fuel-consumption benefit of the idle-stop technology for the European city cycle, in which a vehicle is stopped for more than 30% of the time, is 10%. Idle-stop technology has a much larger benefit for the European certification cycle, owing to that test cycle's longer total vehicle stop time.

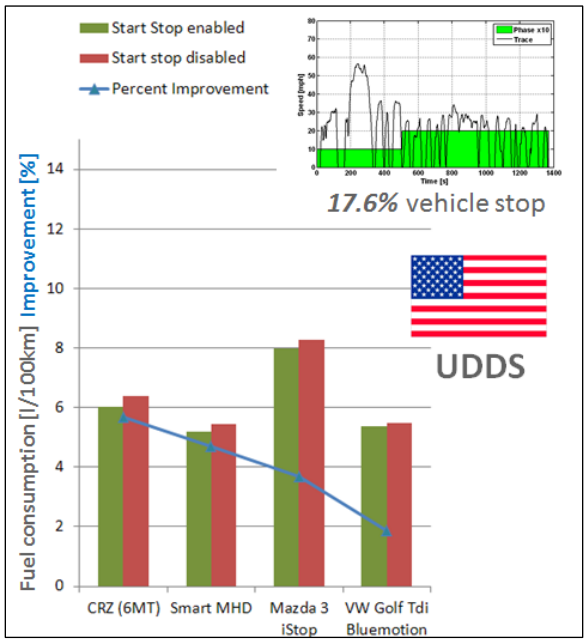

Figure 12. Idle-stop fuel-consumption benefits on the UDDS cycle.

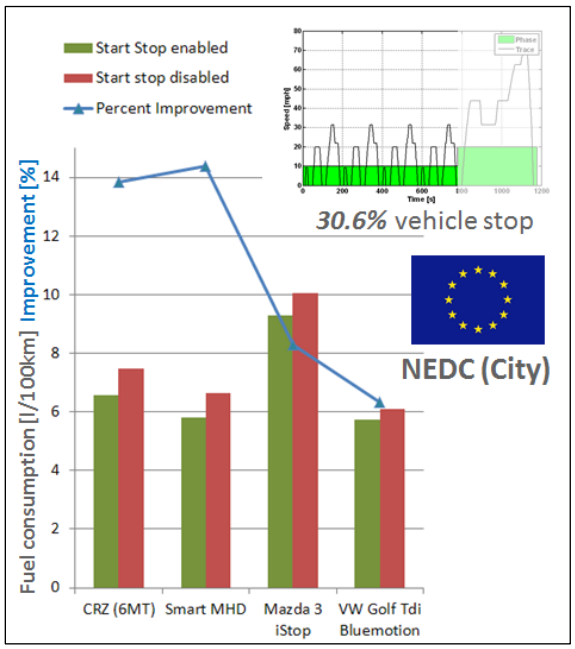

Figure 13. Idle-stop fuel-consumption benefits on the city portion of the NEDC cycle.

Figure 14 illustrates the fuel-consumption benefits of the idle-stop technology for many different cycles as a function of the drive cycles' idle-time proportion. The graph shows a logical correlation between fuel-consumption benefit and vehicle stop time.

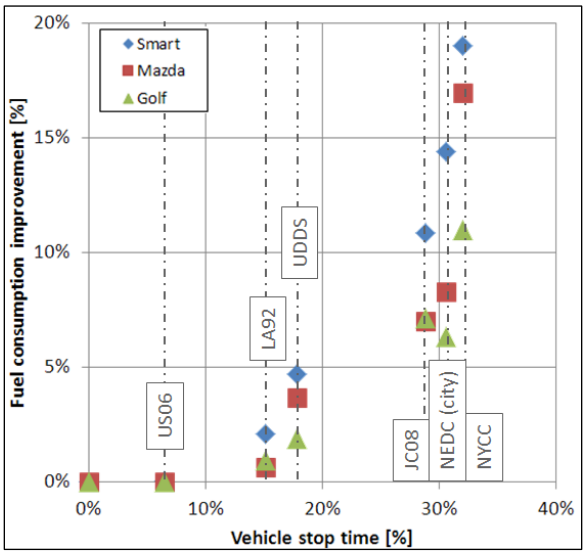

Figure 14. Fuel-consumption benefit of idle-stop technology for different drive cycles.

The smaller the vehicle, the larger the benefit, since the average fuel power required to move the vehicle is lower than the average fuel power required to idle the engine. The Smart is also helped by a high speed threshold under which the engine will turn off.

The 2-liter diesel engine idle fuel flow rate is 1.2 g/s once the engine is at operating conditions. In comparison, the 2-liter gasoline engine requires almost 0.2 g/s of fuel to idle. So the reason for a lower fuel-consumption benefit for the Golf diesel compared to the gasoline Mazda 3 is the already fuel-efficient idle of the diesel engine.

2011 Hyundai Sonata Hybrid

Vehicle Description

The Sonata hybrid is the first production hybrid to use a single-traction motor with a clutch between the motor and the engine. This approach has a cost advantage, with lower hardware complexity compared to a power split hybrid, while maintaining significant EV operation. The engine is belted to a starter alternator motor which enables the engine idle stop. A six-speed automatic transmission delivers the power to the front wheels. Table 5 presents the technical specifications.

The lithium polymer battery is a new technology for a charge-sustaining full hybrid vehicle.

Table 5. Hyundai Sonata Hybrid powertrain specifications

Architecture	P2 hybrid. Single-traction motor directly coupled to the trans-mission with a clutch to the engine to enable EV operation. Belted alternator start motor
Engine	2.4-L in-line 4-cylinder DI CVVT Atkinson-cycle • 166 bhp @ 6000 rpm • 154 ft•lb @ 4500 rpm
Transmission	Six-speed automatic
Motor	PM AC synchronous motor • 40 hp (30kW) • 153 ft.lb (142 N•m)
Battery	Lithium polymer battery • 35 kW • 5.3 A-hr rated capacity • 270 V nominal

Vehicle Operation

The Sonata uses its 30-kW electric motor to launch in electric mode while the clutch between the engine and the motor is open. If the engine is needed, the belted starter starts the engine and the clutch between the engine and motor is closed. When the engine is engaged, the motor can be used to assist in the propulsion or adjust the engine load. Figure 15 shows the Sonata's operation on a cold-start UDDS cycle.

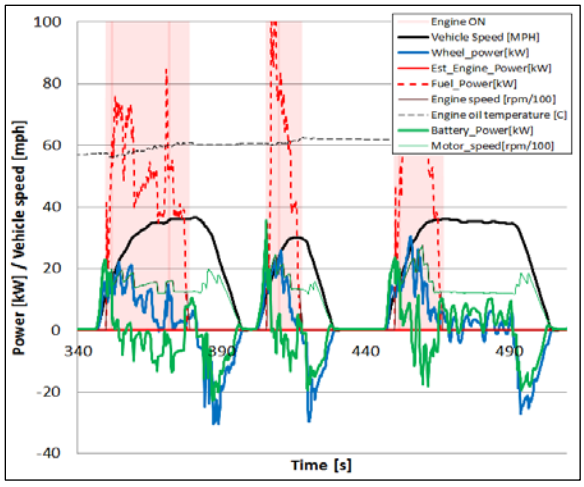

Figure 15. Sonata Hybrid operation on a section of a cold-start UDDS cycle.

The regenerative breaking is performed by the main motor. Note that the transmission is downshifting while the motor applies negative torque during a deceleration, as shown in Figure 15.

Point of Interest

Once the engine is declutched from the powertrain, the 30-kW motor with the six-speed transmission can move the vehicle using only battery power. This combination enables the Sonata to reach very high EV speeds as compared to power split hybrids, which have lower EV speeds because of mechanical limitations. Figure 16 shows the electric-mode envelope as a function of vehicle speed. Each point on the graph is a wheel tractive effort and vehicle speed point from a UDDS, HWY or US06 cycle. The color-coded points represent the electric mode operation in the different gears.

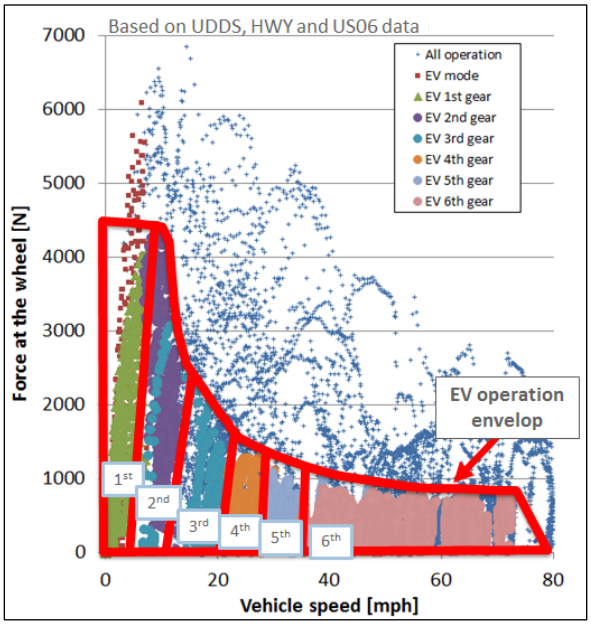

Figure 16. Sonata electric-mode operation envelope.

The highest EV speed was achieved by testing steady-state speeds. The Sonata demonstrated electric operation at 81 mph steady state speed for 40 seconds. The battery pack provided a continuous 25 kW during that speed.

Hybrid Architecture Comparison: Power split compared to single motor with clutch

Within this vehicle evaluation activity an additional subtask was to perform analysis comparing the Sonata's unique P2 type hybrid architecture to the more prevalent power-split type architecture. While it is difficult to compare vehicle architectures based solely on vehicle testing due to the compounding of design choices and true architectural differences, some clear differences do exist. Moreover, the ability to observe the different powertrain architectures implemented in real vehicles helps ground future analysis and provides a good starting point for evaluating future vehicle technologies and powertrain architectures. While the architecture comparison and related analysis is outside the scope of this brief summary section, the following paragraphs seek to highlight some observations from the research.

One of the more noteworthy differences between the architecture of the Sonata and the power-split architecture of a vehicle such as the Toyota Prius is the Sonata's use of a discrete ratio transmission as opposed to the Prius' e-CVT type transmission. An e-CVT transmission similar to the Prius' provides increased flexibility in terms of possible component speeds as well as some additional benefits. In contrast to the Prius, the Hyundai Sonata Hybrid uses a 6-speed transmission mated to the main traction motor for the Sonata's hybrid architecture. While it should be noted that it is possible to operate a P2 type system mated to a CVT, the analysis examples provided in this report focus on a conventional automatic transmission that has fixed ratios.

One of the largest consequences of having a fixed ratio transmission is the need to shift during vehicle operation. This issue leads to several challenging vehicle dynamics issues relative to operating the vehicle while simultaneously managing shifting and hybrid functionality. Figure 17 shows the tractive effort for the Sonata and Prius during an aggressive acceleration and exemplifies one of these driving dynamics related issues. The Prius shows a fairly smooth tractive effort envelope, whereas the Sonata's tractive envelope has a fair amount of variability due primarily to transmission shifting. Other changes in tractive effort appear to be related to engine operation, most likely enrichment. Engine speed is also plotted for the Sonata and can be used to identify transmission shift points which correspond to most of the decreases in tractive effort. There are numerous additional situations where the shifting of the transmission must be coordinated with the hybrid system. For example, during aggressive regenerative braking, the transmission may also need to shift which will likely temporarily reduce the amount of regeneration capability and/or produce battery current spikes.

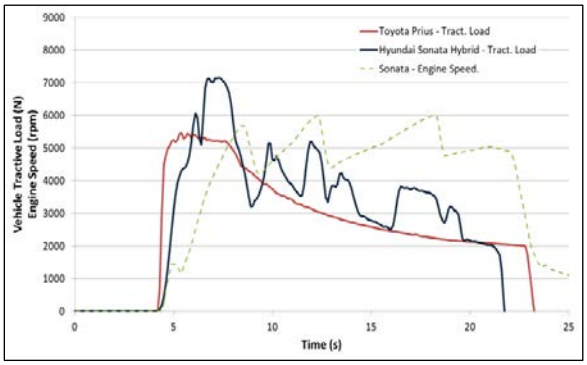

Figure 17. Tractive load comparison during aggressive acceleration.

Another obvious but equally important consequence of fixed transmission ratios is the inability to have full speed control over engine operation. In a power-split type system there is no required relationship between vehicle speed and engine speed, whereas the Sonata must adhere to its six ratios during normal operation. As more transmission speeds are added, the discrete ratios become a closer approximation to the continuous capability of an e-CVT (or CVT), but this is typically at the expense of increased transmission losses. Figure 18 contrasts the observed engine versus vehicle speeds for the Prius and Sonata while operating on the US06 cycle. The difference in engine speed flexibility is clearly illustrated by the different scatter plot results. The dashed lines provided for the Sonata engine operation roughly highlight the fixed ratios for the transmission, but are intended for illustration purposes and do not show all the possible ratios. In contrast to the Sonata, the Prius shows a wide range of engine speed

variability at the same vehicle speed. The Sonata does show some operation outside of the fixed ratios, but this is typically during engine restarting (and clutch slipping) or during shift events.

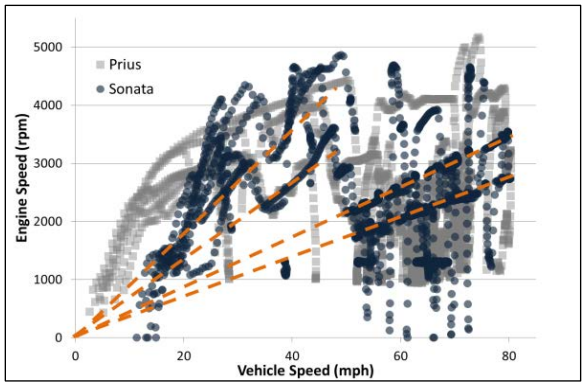

Figure 18. US06 engine speed versus vehicle speed for the Sonata and Prius.

The previous analysis represents a small fraction of the comparisons between these two types of hybrid architectures. Issues such as "series" operating capability, engine restarting, component sizing, required components, and vehicle driving dynamics also are critical in differentiating between these hybrid architectures.

2011 Chevrolet Volt

Vehicle Description

The Volt is the first dedicated mass-produced plug-in hybrid available from a major OEM. The Volt is considered to be an extended-range plug-in hybrid because it achieves full performance in the charge-depleting mode, i.e., it achieves full performance without needing to use its engine. Table 6presents the technical specifications.

Table 6. Volt powertrain specifications

Architecture	Extended-range Plug-in Hybrid
Engine	1.4-L in-line 4-cylinder DI VVT-i Atkinson-cycle • 83 bhp
Motor	Traction PM motor • 149 hp • 273 ft•lb Generator • 80 hp
Battery	Lithium ion battery • 16 kWh capacity (10.4 kWh usable)

Vehicle Operation

The Volt has two distinct operating modes. The first mode is the charge-depleting mode, where the vehicle operates in electric-only mode using only electric power and therefore depleting the battery. The second mode is the charge-sustaining mode, which occurs only after the battery is depleted. In the charge-sustaining mode, the Volt operates similarly to a charge-sustaining hybrid, relying on the burning of fuel for energy.

Figure 19 shows the charge-depleting operation: the Volt operates in electric mode while depleting the battery.

Figure 20 shows a cold-start UDDS cycle in charge-sustaining mode. The Volt starts the cycle in electric mode. Since the powertrain can provide all the tractive effort from the electric motor, the engine is completely isolated from the power needed at the wheels. In fact, the engine is maintained at 1400 rpm for the first 60 seconds with a 6-kW load. This allows a very clean and controlled warm-up of the exhaust after-treatment system. Even in charge-sustaining mode, the Volt appears to operate in EV mode frequently, using the engine to regulate the battery state of charge.

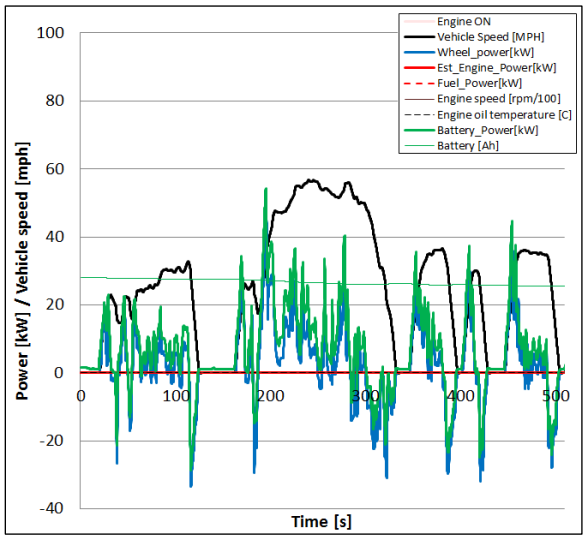

Figure 19. Volt operation on a cold-start UDDS cycle in electric mode with a fully charged battery

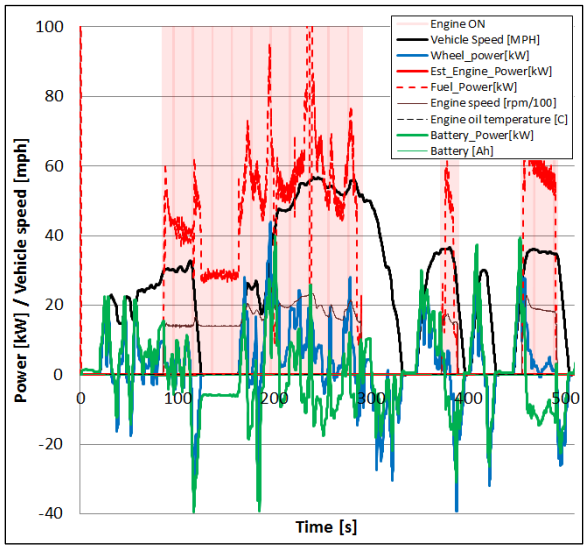

Figure 20. Volt operation on a cold-start UDDS cycle in charge-sustaining mode with a depleted battery.

Point of Interest

The Volt is the first production extended-range plug-in hybrid tested at Argonne. Argonne used the full-charge test approach recommended in SAE J1711 for the testing of the Volt. The fuel and energy consumption results for the different drive cycles are shown in Figure 21.

The Volt displaces 100% of the fuel during the charge-depleting phase. The Voltage uses 225 DC Wh/mi for the UDDS cycle and 320 DC Wh/mi for the aggressive US06 cycle. During a cold start with a fully charged battery, the Volt uses 250 DC Wh/mi, which is an increase in energy consumption of 10%. The start test penalty is only 4%.

The electric ranges for the Volt are 44.5 miles, 41.9 miles and 30.1 miles for the UDDS, highway, and US06 cycles, respectively. The electric range is significantly reduced under aggressive driving conditions.

Obtaining a charge-sustaining fuel-consumption result requires a repetition of several cycles to ensure that the net energy change of the battery over the cycle is less than 1% of the fuel energy used. The large battery and prominent EV operation may contribute to that behavior.

The Volt has full electric performance in the charge-depleting mode. Figure 22 shows the acceleration of the Volt at different battery states of charge. The electric propulsion power is 73 kW with a full battery pack, and it drops to 69 kW with a close-to-depleted battery pack. The drop in power is caused by the lower battery-pack voltage of the depleted battery. Figure 23 shows the performance envelope of the electric propulsion system. The Volt has slightly better performance in the charge-depleting electric mode compared to the charge-sustaining mode.

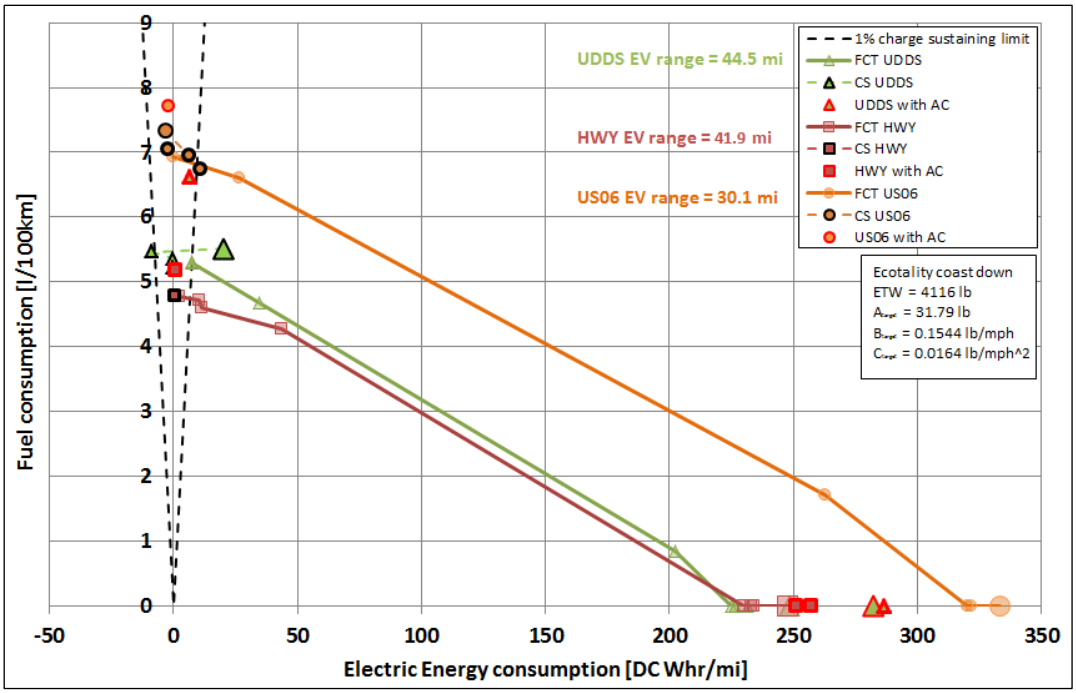

Figure 21. Fuel and energy consumption of the Volt in full-charge tests on the UDDS, highway and US06 cycles.

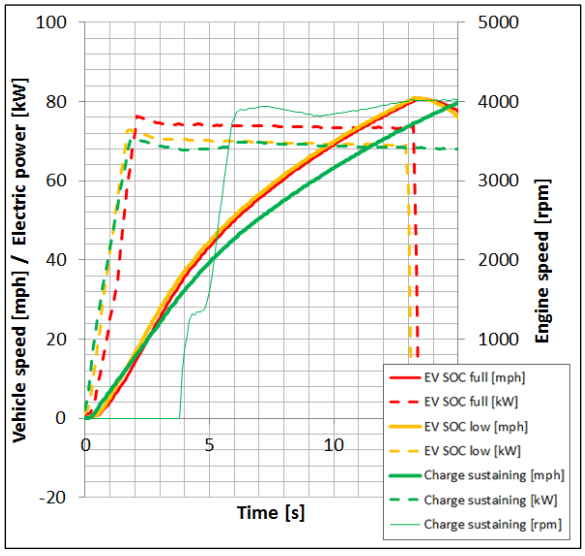

Figure 22. Maximum acceleration of the Volt at different battery states.

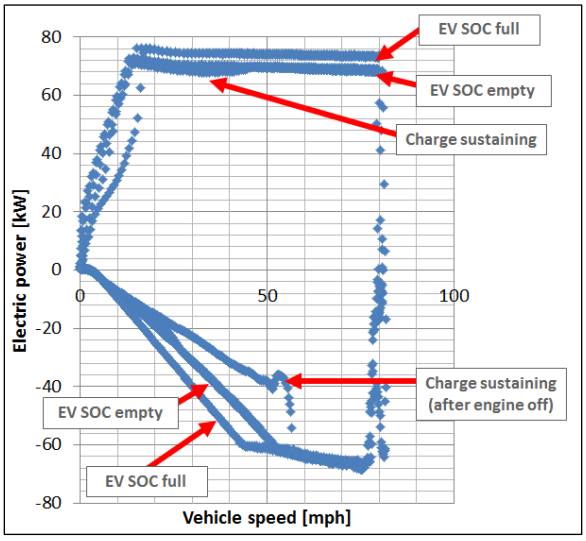

Figure 23. Electric propulsion envelope for the Volt.

Comparison of In-situ Battery Data Across Vehicles

The polarization curves of the batteries of the different test vehicles are shown in Figure 24. The Volt battery, the Sonata battery and the S400h battery are lithium-based battery packs, which have the lowest system resistance.

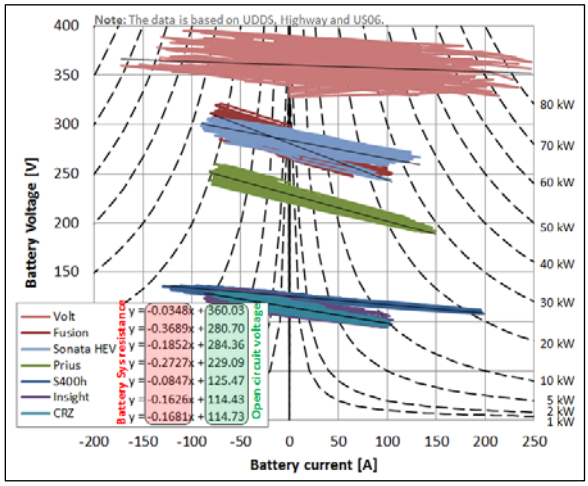

Figure 24. Battery polarization curves from the different vehicles tested.

The Volt has the highest battery system voltage, which enables the high discharge and charge power needed for the Volt's electric operation. The wide spread of the voltage on the Volt is cause by the large capacity of the pack that is used in the charge-depleting mode.

An interesting comparison is between the Fusion HEV and the Sonata hybrid. Both battery systems have similar system voltages. The Fusion has a nickel metal hydride battery and the Sonata uses a lithium polymer pack. The lithium pack has a lower system resistance, which lowers the losses. The lithium pack also has a voltage that stays steadier as the current changes, which has a positive impact on the system hardware and control.

Conclusions

Argonne benchmarked vehicles ranging from idle-stop vehicles to an extended-range plug-in hybrid through comprehensive testing on the chassis dynamometer and with complete vehicle instrumentation. The test results and analyses were distributed through several mechanisms such as reports, presentations, and sharing of raw data. The testing activity helped directly in the development of some codes and standards and supported the model development and validation.

This report summarizes Argonne's basic vehicle benchmark activity for FY2011. For more detailed information on each vehicle and further analysis, the reader is encouraged to read the vehicle reports.

III.B. Extended Level 2 Benchmarking of Advanced Technology LD Vehicles – Hyundai Sonata Hybrid, VW Jetta TSI, and Chevrolet Volt

Principal Investigator: Eric Rask
Argonne National Laboratory
9700 South Cass Avenue
Argonne, IL 60439
(630) 252-3110; erask@anl.gov

DOE Program Manager: Lee Slezak
(202) 586-2335; Lee.Slezak@ee.doe.gov

III.B.1. Abstract

Objective

- Establish work plans that involve thorough vehicle instrumentation, testing, and analysis for the selected vehicles (Hyundai Sonata Hybrid, VW Jetta TSI, and Chevrolet Volt PHEV). Data collected will be used for a wide range of tasks, including technology benchmarking and evaluation, simulation validation, advanced vehicle component evaluation, and vehicle testing procedure/methodology development.

Approach

- Purchase vehicle, service manuals, and diagnostic tools for the vehicle tested
- Leverage previous high-level data collection and insight
- Install engine and drive shaft torque sensors
- Perform significant instrumentation development, creation, and installation
- Record Controller Area Network (CAN) signals through testing as a means of measuring parameters that would otherwise be too difficult, too expensive, or impossible to obtain
- Run a broad range of tests for cycle fuel economy, energy consumption, performance, and steady-state operation for vehicle assessment, component evaluation, and technology benchmarking

Major Accomplishments

- Successfully conducted significant vehicle/component testing and analysis for selected vehicles
- Evaluated a wide range of advanced vehicle technologies
- Significantly improved CAN bus data collection through new tool development
- Continued node-based thermal instrumentation for improved data dissemination and real-world fuel economy research

Future Activities

- Continued data collection, leveraging installed vehicle instrumentation. Areas of particular interest include improved component efficiency testing/mapping and vehicle temperature sensitivity testing when exposed to more extreme ambient conditions.

III.B.2. Technical Discussion

Background

This work revolves around in-depth instrumentation, testing, and analysis of new and emerging vehicle technologies. Vehicles are selected for evaluation on the basis of technical merit for technology assessment and data collection. Vehicles are tested primarily on a chassis dynamometer using state-of-the-art instrumentation and data analysis equipment. Testing and instrumentation plans are specifically developed for each vehicle and reflect its particular technical merits and unique features.

Introduction

The first of three vehicles to be discussed in this report is the Hyundai Sonata Hybrid. Unlike the majority of two-motor, power-split-based hybrid vehicles currently on the market, the Hyundai Sonata Hybrid utilizes a conventional six-speed automatic transmission mated to a single 30-kW motor. This transmission/motor assembly is then mated to a clutch which is then connected to the engine. This configuration allows for a significant amount of electric operation by decoupling the vehicle's engine when operating in electric mode, but also allows the electric machine to supplement engine torque when the clutch is closed. Regenerative braking is also accomplished using the main traction motor and six-speed transmission. In addition to the main motor, the Sonata also utilizes a Hybrid Starter Generator (HSG) connected to the engine though a belt for engine restarting, allowing for electric-only operation and idle engine stop. Given this alternative transmission architecture for a full hybrid, the Sonata provides an opportunity to collect and analyze recent hybrid-vehicle data for technology assessment and benchmarking. Also, it provides a unique opportunity to evaluate some of the trade-offs between two types of hybrid architectures. Figure 1 shows the Hyundai Sonata Hybrid at Argonne's facility.

Figure 1. Hyundai Sonata Hybrid

The second vehicle selected for this in-depth testing activity is the VW Jetta TSI. This vehicle uses a significantly downsized 1.4-L SI engine, which is boosted to provide roughly 90 kW of engine power. This advanced engine is mated to a seven-speed dual clutch transmission (DCT), which offers a wide range of operating ratios while reducing losses, owing to the DCT's lower losses as compared to a conventional automatic transmission. Unlike the Sonata, this vehicle is not a hybrid, but does feature a very advanced engine and transmission, which is important for performing technology assessments and understanding advances in all vehicle technologies as opposed to only hybrid technologies. Moreover, several manufacturers have recently begun to offer downsized/boosted engines and DCTs in order to improve fuel economy; thus, the information gained from this testing is particularly relevant. Figure 2shows the Jetta vehicle in the Argonne test facility prior to being removed from the chassis dynamometer.

Figure 2. VW Jetta TSI Test Vehicle

The final vehicle discussed in this report is the Chevrolet Volt. As one of the first available OEM-developed plug-in hybrid electric vehicles (PHEVs), this vehicle represents a major testing milestone. The Volt provides full electric propulsion during charge-depleting (CD) operation and switches over to a more traditional charge-sustaining-type operating strategy when operating in charge-sustaining (CS) mode. Given this full EV traction capability, the Volt is commonly referred to as an Extended Range Electric Vehicle (EREV), but this term simply means the vehicle has full electric traction capability, which is not necessarily exclusive to the Volt's architecture. While much has been written regarding the Volt, testing the vehicle in depth on a dynamometer provides significant insight for vehicle technology benchmarking, standards development, and component evaluation. Figure 3 shows the Volt on ANL's chassis dynamometer.

Figure 3. Chevrolet Volt Test Vehicle

Approach

As discussed in the Background section, vehicles were outfitted with a significant number of sensors to provide a range of information from temperatures to mechanical and electrical power flows. Specific test plans were developed to evaluate the particularly interesting facets of each vehicle technology. Testing was done using a chassis dynamometer and sophisticated instrumentation under laboratory conditions to aid in repeatability, accuracy, and sensitivity.

Results

The following sub-sections discuss some of the noteworthy findings related to the testing of these vehicles. These discussion items represent a small fraction of the information and insight gained during the testing of these advanced vehicles.

Hyundai Sonata Hybrid: Selected Results

Electric Machine Usage Envelope: Unlike the power-split-based hybrids currently on the market (Toyota Prius, Ford Fusion, GMC Tahoe, etc.), the Hyundai Sonata Hybrid uses a single electric machine mated to an automatic transmission for the majority of hybrid functionality. In addition to this fairly large machine, the Sonata also uses an Hybrid Starter Generator (HSG) for engine restarting, torque smoothing, and minimal hybrid functionality. Both electric machines are permanent-magnet-type motors despite their significantly different usage profiles and capabilities. The main motor covers a wide range of hybrid capabilities such as vehicle assist, engine-off operation, and regenerative braking. With these capabilities in mind, this motor features a fairly large bandwidth of available power and torque. Figure 4 shows the traction motor usage for the Urban (UDDS), Highway, and US06 cycles as well as over aggressive accelerations. This usage is also a reasonable estimate for peak capability during nominal operation, which results in a peak observed torque of 200 Nm and peak power of roughly 40 kW. The limited usage of near-peak torque below 1,000 rpm operating speed is most likely due to vehicle/transmission operating constraints, as opposed to any capability issue.

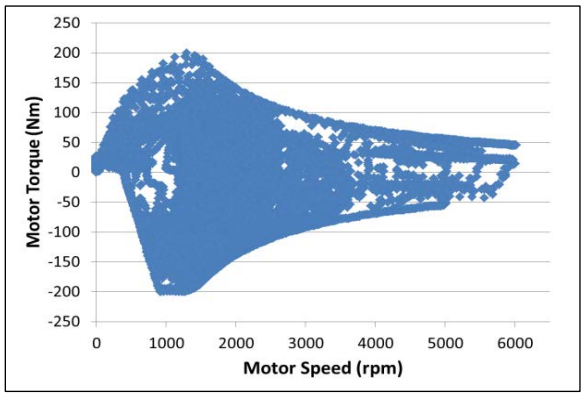

Figure 4. Main Traction Motor Usage during UDDS Cycle

Similarly, Figure 5 shows the usage of the HSG over the same cycles and repeated accelerations. The HSG's primary function of engine restarting can be observed in the fairly low levels of torque at low speeds. Since the HSG is connected to the engine through a belt, the HSG can also be seen operating at very high speeds but low torque levels. Minimal levels of negative torque, which likely represent torque smoothing, can also be seen in the figure. Peak observed torque for the HSG is 40 Nm and peak observed power is roughly 8.5 kW

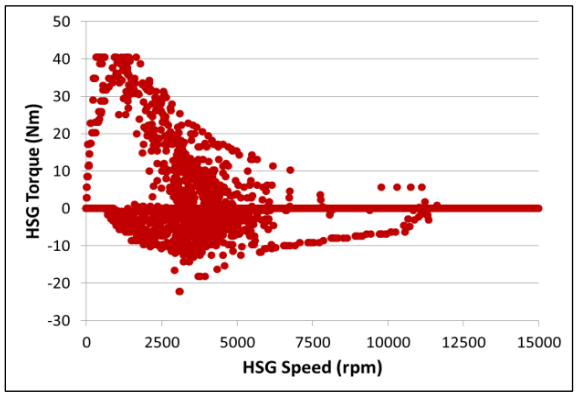

Figure 5. HSG Motor Usage

Basic Battery Characterization and De-rating: In addition to its single-motor hybrid system, one of the most noteworthy features of the Sonata Hybrid is its lithium polymer battery pack. This pack is one of the first lithium polymer packs available in a full hybrid vehicle and represents a significant reduction in weight, size, and resistance as compared to the nickel metal hydride (NiMH) packs currently used in most hybrid vehicles.

One of the most basic yet useful ways to characterize a battery under nominal operating conditions is to create a simple scatter plot of terminal voltage versus current while the battery is being used. This basic plot can be used to glean several important pieces of information related to a battery's basic characteristics. By creating a best-fit regression line of voltage versus current and observing the zero-crossing, a rough approximation for nominal voltage at nominal state of charge can be made. Additionally, the slope of this line can be used as an estimate of pack resistance at nominal operating conditions. Figure 6 shows this scatter plot and analysis for both the Hyundai Sonata and the Ford Fusion Hybrid. Although both packs have a similar zero-crossing nominal voltage estimate, the Fusion pack shows a much larger pack resistance, as evidenced by the steeper slope. This result is expected, given the Fusion's NiMH pack in contrast to the Sonata's lithium polymer pack.

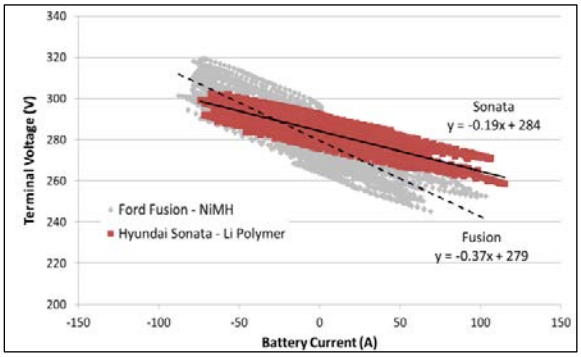

Figure 6. Terminal Voltage vs. Current for the Hyundai Sonata and Ford Fusion

Another interesting research finding relates to the Sonata's battery de-rating strategy. By leveraging information on the vehicle's communications bus, one can observe the battery temperature as well as available charge and discharge power during testing. This technique helps in understanding the Sonata's de-rating strategy to protect the battery pack from operating at too high a temperature. Typically, a vehicle's pack will operate at full or nearly full capacity until the pack reaches a

particular temperature. Once this temperature has been reached, the pack begins to scale back the charge and/or discharge power to reduce the demands on the battery and allow it to cool. By running aggressive US06 cycles followed by back-to-back aggressive accelerations, the pack de-rating strategy can be observed. During initial operation, the Sonata has very consistent available discharge power and fairly consistent charge power. As the battery warms during the accelerations, both available charge and discharge power begin to de-rate at around 45°C. Following this initial de-rating, the battery continues to increase in temperature and the available discharge power is scaled back considerably. Moreover, the discharge power appear to be adjusted dynamically in this temperature range (48°C+). This adjustment appears to provide additional power at low vehicle speeds and then reduces power at elevated speeds. Figure 7 shows the available power for the duration of the cycles and accelerations. Figure 8 highlights the discharge power adjustment during a period of fairly aggressive de-rating and shows the variability of available discharge power relative to vehicle speed.

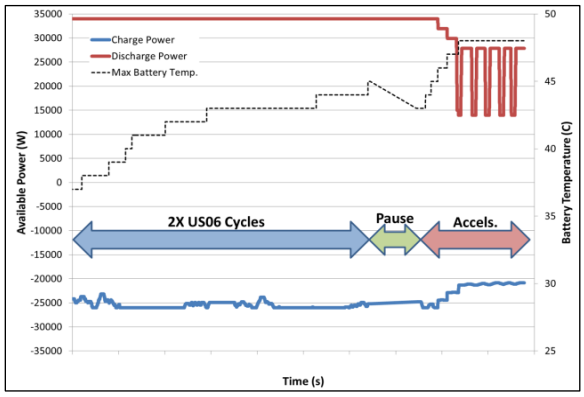

Figure 7. Battery De-rating with Temperature

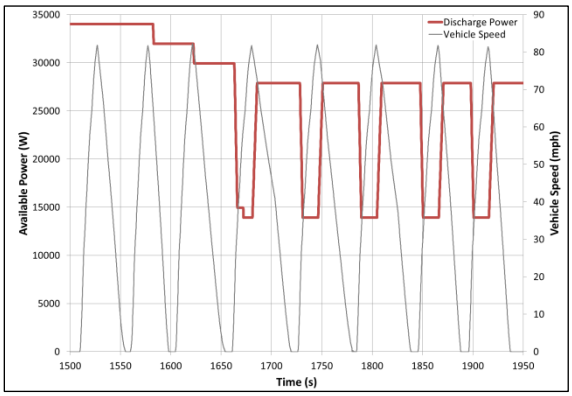

Figure 8. Battery Discharge Power During Aggressive De-rating

Electric-only Operating Capability Envelope: One of the Sonata's unique operating characteristics is its large envelope of electric-only, engine-off capability. Through the mating of a moderately sized electric machine with a six-speed transmission, the Sonata can operate over a wide range of fairly high torques and speeds. In fact, EV operating speeds of roughly 75 mph were observed during testing over standard drive cycles. The shape of the Sonata's EV operating envelope is also unique because of its six-speed transmission, which facilitates a wide range of engine-off operation ranging from high launch torque to high-speed assist. To better illustrate these points, Figure 9 shows a scatter plot of the Sonata's engine-off operating points over the UDDS, Highway, and US06 cycles.

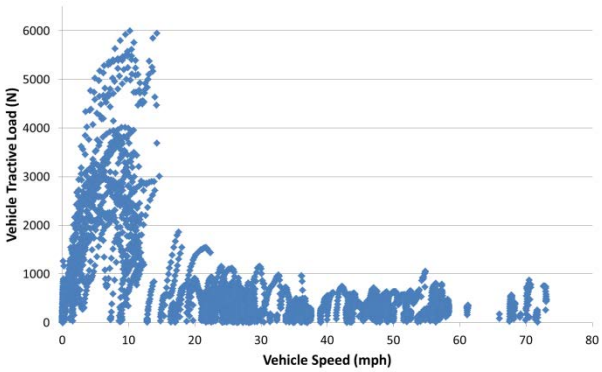

Figure 9. Sonata Hybrid EV Operation Points over UDDS, Hwy and US06 Cycles

VW Jetta TSI: Selected Results

Aggressive Deceleration Fuel Cut-off: Although the Jetta is a conventional fuel-only vehicle, it does have the ability to operate unfueled under certain operation scenarios. During vehicle decelerations, the vehicle can cut fuel to the engine while keeping the engine spinning through the force of the road. Once the vehicle reaches zero speed, the engine must again begin operating with fuel in order to stay active. The deceleration fuel cut-off (DFCO) behavior is an enabler for improved conventional-vehicle fuel economy, since it shuts off fuel normally used during vehicle decelerations. In the case of the Jetta, the vehicle uses DFCO very aggressively and cuts fuel for the majority of vehicle decelerations. This type of behavior is an important technical trend since it not only directly improves conventional-vehicle fuel economy, but also decreases the real-world benefit of hybrids over conventional vehicles. Figure 10 shows the Jetta's fuel usage for a segment of the UDDS drive schedule. As can be clearly seen in the figure, the fuel usage rate is zero during the majority of the decelerations shown. In fact, the vehicle operates without fuel for nearly a minute near the 300-second mark during the long deceleration back to zero speed.

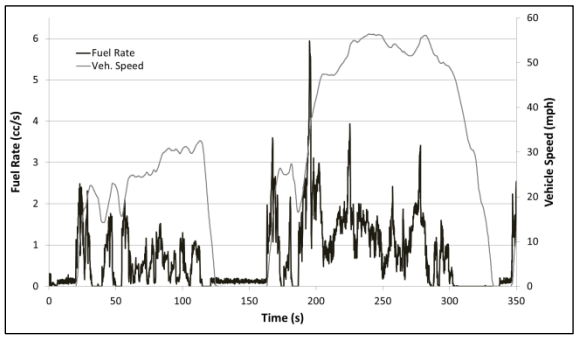

Figure 10. VW Jetta TSI DFCO on the UDDS Cycle

Seven-Speed Dual Clutch Transmission Operation: Another interesting facet of the Jetta is the gear usage related to its advanced seven-speed DCT. To illustrate the general usage and shift patterns of the vehicle, Figure 11 shows the engine speed relative to vehicle speed, which can then be used to better understand the transmission operation. In this figure, the ratios for each gear can be estimated relative to engine/vehicle speed. In addition, it can be seen that the vehicle very frequently operates in the highest (7^{th}) gear, which reduces engine speed and allows for improved fuel economy.

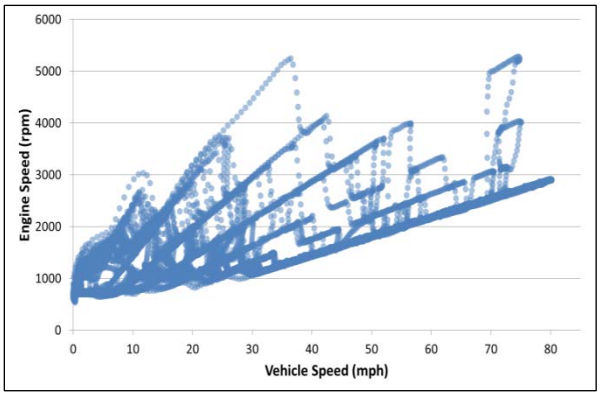

Figure 11. VW Jetta TSI Engine Speed vs. Vehicle Speed

Engine Oil Warm-up Comparison: Another interesting observation from the Jetta is the rapid rise in engine temperature as compared to a hybrid vehicle. As would be expected, given the increased amount of engine operation relative to a hybrid vehicle, the Jetta's engine oil warms much more quickly as compared to that of a hybrid such as the Toyota Prius. Furthermore, once the engine oil is warm, it remains warm; whereas a hybrid may run with the engine off long enough that the oil begins to cool. Figure 12 contrasts the engine dipstick oil temperature for the Jetta and the Toyota Prius during UDDS cycle operation. Both vehicles begin at "cold-soak" conditions and quickly begin to warm, but following this initial warm-up, the Jetta oil temperature continues to increase and stabilizes at a much higher temperature.

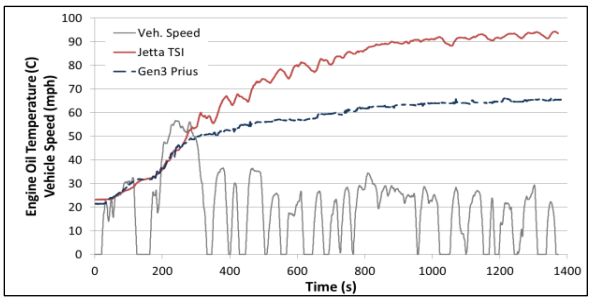

Figure 12. Engine Oil Warm-up Comparison

Chevrolet Volt: Selected Results

As discussed in the introduction, the Chevrolet Volt is a unique vehicle that offers the ability to run in all-electric mode during CD operation and to operate more traditionally in CS mode. Along with fully electric vehicles, the Volt represents emerging technology that can be used to significantly impact fuel usage though greater vehicle electrification. Figure 13 shows battery power over the aggressive US06 cycle during EV operation. As can be seen in the figure, peak positive battery power during this cycle is roughly 75 kW and peak regenerative (negative) battery power is on the order of 55 kW.

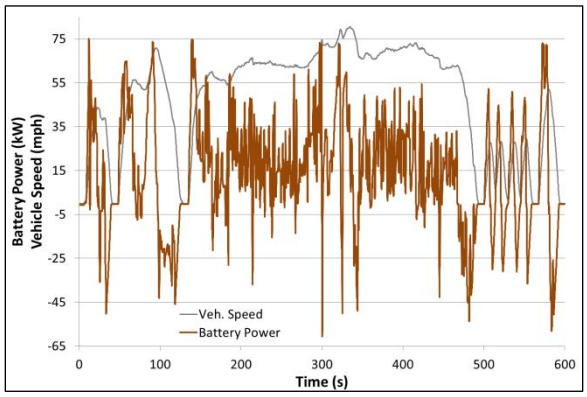

Figure 13. Chevrolet Volt US06 Battery Power During EV Operation

Figure 14shows the accumulated battery current for the Volt operating over repeated Highway cycles. Following roughly four Highway cycles, the vehicle begins to transition to CS operation. An important finding related to estimating battery-current trends is also shown in the figure. Several Argonne-developed PHEV evaluation methodologies rely on estimating accumulated current trends using only the starting and ending values of each cycle. This estimate has been overlaid on the actual accumulated current trace in the figure. Fortunately, the actual accumulated current does not stray too far from the estimate, thus helping to validate the procedural estimate for this type of operating scenario.

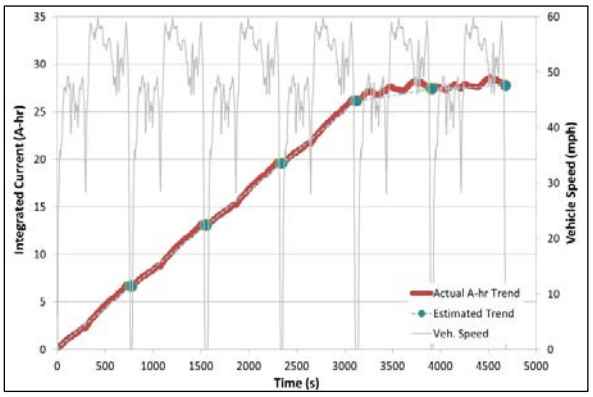

Figure 14. Chevrolet Volt Accumulated Current During CD Operation

Another important dataset for this type of vehicle is the actual load on the power grid when the vehicle is recharging. This information can help inform decision-makers on a range of topics related to power-grid noise, stability, and additional demand. Figure 15 shows the actual AC power taken from the "wall" while the Volt is recharging following CD operation.

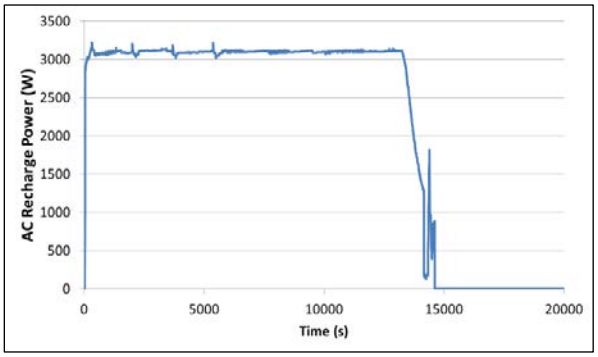

Figure 15. Chevrolet Volt Recharge Power

While the CD operation of the Volt is the major research interest, this vehicle's behavior during CS operation is of interest as well. Research was done to understand how the Volt's highly capable electrical propulsion system is leveraged during CS operation. While fully explaining the operation of the Volt is outside of the scope of this brief summary report, Figure 16 shows a basic scatter plot of the vehicle's engine operation versus vehicle speed. The figure shows a wide range of vehicle speeds run with a fairly similar band of engine operation. This highlights the Volt powertrain's ability to adjust engine loading when operating in CD mode.

Furthermore, the spread of engine speed and the maximum engine speed appear to increase with vehicle speed. This suggests that noise or dynamics may also be a consideration to the engine operating strategy in addition to the need for additional engine power.

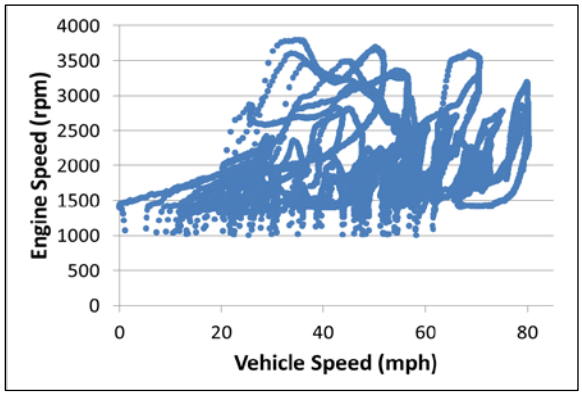

Figure 16. Chevrolet Volt Engine Operation vs. Vehicle Speed

Conclusions

A significant amount of time and effort was spent on the instrumentation, testing, and analysis of three selected model-year 2011 vehicles: the Chevrolet Volt, the Hyundai Sonata Hybrid, and the VW Jetta TSI. Specific instrumentation was developed to evaluate the most noteworthy aspects of these vehicles. Additionally, testing was tailored to the vehicles in order to efficiently and effectively benchmark and evaluate these advanced-technology vehicles. The results and analysis contained in this report represent a small but important subset of the entire project. Research regarding these as well as additional hybrid vehicles should continue, given the ever-charging dynamics of the advanced vehicle marketplace.

III.B.3. Products

Publications

Rask E., Duoba M., Lohse-Busch H., Recent hybrid electric vehicle trends and technologies, Vehicle Power and Propulsion Conference (VPPC), 2011 IEEE, Chicago, IL, Sept. 6–9, 2011.

Several presentations to Vehicle Systems Analysis Technical Team

III.C. Extensive Study of Prius under Temperature Extremes

Principal Investigator: Eric Rask
Argonne National Laboratory
9700 South Cass Avenue
Argonne, IL 60439
(630) 252-3110; erask@anl.gov

DOE Program Manager: Lee Slezak
(202) 586-2335; lee.slezak@ee.doe.gov

III.C.1. Abstract

Objective

- Perform vehicle testing and evaluation of the Model Year (MY) 2010 Toyota Prius over a range of more extreme ambient temperatures. This testing is performed under both cold and hot ambient conditions, with and without the HVAC system active. Given some of the Prius's unique components geared toward hot and cold ambient operation, data collected will be used for a wide range of tasks, including technology benchmarking and evaluation, simulation validation, advanced vehicle component evaluation, and vehicle testing procedure development.

Approach

- Leverage highly instrumented MY 2010 Toyota Prius vehicle from previous year's in-depth testing
- Evaluate vehicle over a wide range of ambient temperatures and test cycles
- Record Controller Area Network (CAN) signals through testing as a means of measuring parameters that would otherwise be too difficult, too expensive, or impossible to obtain
- Analyze impact of ambient temperature not only on fuel economy, but also on component efficiency and overall vehicle operation

Major Accomplishments

- Testing done at a range of hot ambient conditions and drive cycles for evaluation of air-conditioner load and fuel-economy impact
- Vehicle evaluated at cold temperatures with and without heater for a range of possible operational strategies and impacts related to cold operation
- Significantly improved understanding of the impacts of extreme-ambient-temperature operation as well as improved understanding of the direction of heat flow for these various conditions

Future Activities

- Continued data collection, leveraging installed vehicle instrumentation and upgraded ANL laboratory facilities. Areas of particular interest include improved component efficiency testing/mapping and vehicle temperature sensitivity to more extreme ambient conditions.

III.C.2. Technical Discussion

Background

The Model Year (MY) 2010 Toyota Prius represents the most recent iteration of Toyota's hybrid system, which began wide-scale production in 1997. As with most hybrid systems, fuel economy and emission gains are enabled through regenerative braking, engine-off at idle, electric operation at low road loads,

electric assist, and the ability to achieve closer to optimal engine operation. In addition to the broad goal of generally achieving improved fuel economy, the technology of the MY2010 Prius also specifically seeks to improve the vehicle's real-world fuel economy, namely, in both hot and cold weather. In addition to this overall vehicle goal, features such as an exhaust-heat-to-engine-coolant exchanger, electric water pump, and ejector-cycle air-conditioning make evaluating the MY2010 particularly interesting over a range of more extreme ambient temperatures.

Introduction

This work leverages the highly instrumented Toyota Prius used in the FY2010 benchmarking task. Given the wide array of instrumentation, (especially temperature sensors) available on the vehicle, the main tasks associated with this project involved developing test plans at alternative testing temperatures that included testing the vehicle over a wide range of both hot and cold conditions, and analyzing and synthesizing the data into conclusions related to technical benchmarking providing an improved understanding of vehicle operation under real-world ambient conditions. To date, the cold-temperature portion of this work has been done in collaboration with Environment Canada at its cold test cell facility in Ottawa. Since the Argonne test cell was being upgraded during a portion of this work, this collaboration with Environment Canada allowed cold ambient testing as well as an exchange of data and best practices. The majority of hot ambient testing was done at Argonne's Advanced Powertrain Research Facility. Figure 1shows Argonne's highly instrumented Prius on the dynamometer at Environment Canada's test facility.

Figure 1. ANL-instrumented Prius in Environment Canada's thermal test cell

Approach

As discussed in the Introduction, this work leverages previously installed instrumentation on Argonne's Level-2 Prius research vehicle. This section provides a brief overview of the thermal instrumentation used for this testing. While not discussing all of the thermal instrumentation included in this vehicle, this section also describes some of the important temperature-sensor locations developed for analyzing the MY2010 Toyota Prius over a wide range of ambient temperatures.

Figure 2 shows an overview of the main cooling system for the MY2010 Prius as well as the sensor placement within the cooling system. The significant amount of temperature information available from this instrumentation allows for a thorough analysis of energy flow within the cooling system from the various components, which is important for understanding the impact of operating temperature on vehicle efficiency. In addition to thermocouples, a flow sensor is also included in the exhaust-heat-recovery system to better understand its operation and efficiency.

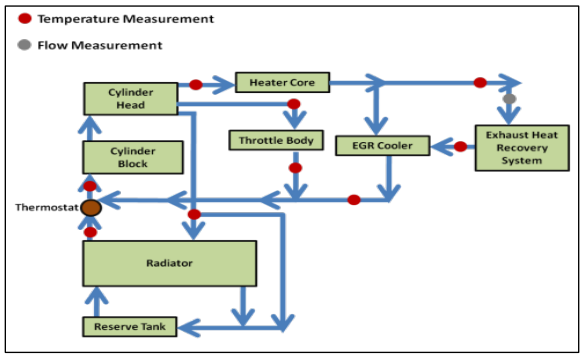

Figure 2. Main cooling system overview and thermocouple placement

In addition to the main cooling system, significant temperature instrumentation has been included in the separate power-electronics cooling loop for the Prius. The Prius uses a separate, stand-alone loop for cooling the vehicle power electronics and one of the electric machines. Given the significant ongoing component coolant research throughout many DOE laboratories and in industry, this information is particularly valuable. Figure 3 shows the power-electronics cooling loop as well as the location of the temperature sensors.

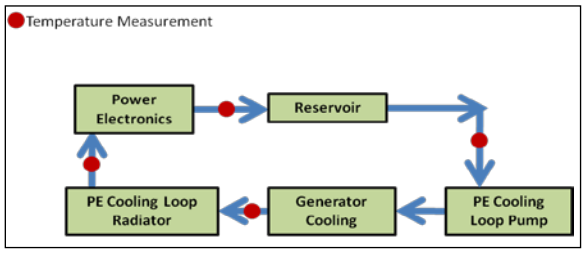

Figure 3. Power-electronics cooling system and thermocouple placement.

In addition to the coolant-temperature sensors shown in Figure 2 and Figure 3, instrumentation was also included to determine exhaust and catalyst temperature for the emissions/exhaust system. Given the importance of understanding emissions for advanced vehicles, these temperature sensors will assist in evaluating emissions strategies in a vehicle with frequent engine stops and starts. Additionally, exhaust pressure sensors were included before and after the exhaust-heat-recovery system to assess the restriction in exhaust flow and thus reduction in power related to the exchanger system. Figure 4 shows the exhaust-system instrumentation.

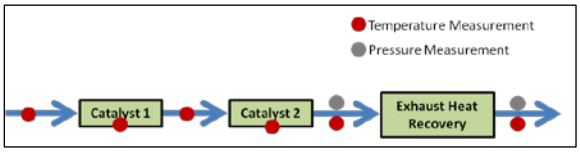

Figure 4. Exhaust-system instrumentation

Engine and transmission oil temperatures are also signals of significant interest. Both engine and transmission temperatures have a significant impact on vehicle fuel economy. Moreover, these working fluids are often particularly sensitive to temperature, i.e. viscosity changes, and thus very relevant to the real-world fuel economy of the 2010 Prius. Figure 5 and Figure 6 show the thermocouple placement for the engine oil and transmission oil, respectively.

Figure 5. Engine-oil temperature sensor

Figure 6. Transmission-oil temperature sensor

Results

The following discussion addresses selected observations related to the Prius during operation under hot or cold ambient conditions.

A wide range of testing was done to analyze the impacts of HVAC system loads as well as general operating temperature on vehicle duty cycle and fuel economy. The discussion items presented in this document represent a small fraction of the information and insight gained during this testing.

Figure 7 shows the normalized fuel-economy results of several back-to-back 50-mph, steady-state runs done at a roughly -10ºC ambient temperature. For this testing, the vehicle initially started in an "unsoaked" state, which means that it had not been started prior to the first test. As would be expected, the vehicle's engine and working fluids warm up during these consecutive runs and fuel economy begins to improve. The runs shown were done using the cabin heater, but runs without the heater were also done. Even for a simplified steady-state drive cycle, the dramatic impact of vehicle warm-up can be observed.

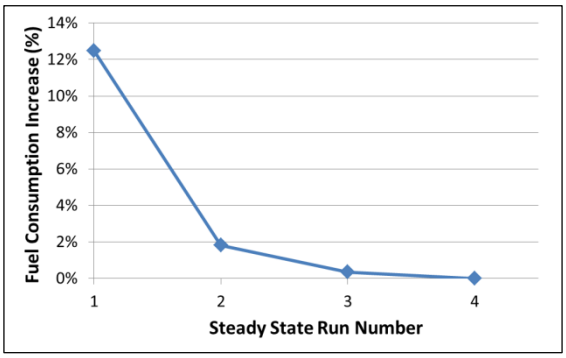

Figure 7. Back-to-back 50-mph, steady-state increased fuel consumption during initial vehicle warm-up at -10C

Figure 8 shows the average engine-oil and transmission-oil temperatures for each of the four steady-state runs. Both averages can be seen to increase with vehicle operation, but the engine oil heats much more quickly compared to the transmission oil. This is as expected because the engine produces much more heat compared to the Prius's transmission, but it is important to consider that certain vehicle components are likely still warming during the second and perhaps third steady-state run.

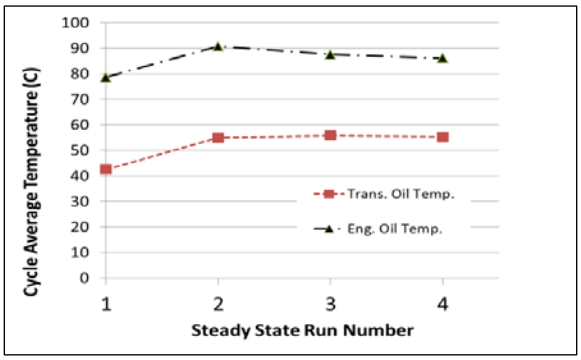

Figure 8. Back-to-back 50-mph, steady-state average engine and transmission oil temperatures at -10C

Steady-state vehicle operation is particularly helpful in evaluating vehicle warming trends, since the additional complexities of transient vehicle operation are removed from the testing. The removal of these additional complexities allows one to focus on the high-level trends and flows of thermal energy as the vehicle warms. This information and insight can then be applied to more complicated transient vehicle operation on a drive cycle or during real-world driving. For example, Figure 9 shows the gradient of coolant into and out of the Prius's exhaust-heat-recovery system for both a cold start and a preconditioned cycle. During initial cold operation, a significant temperature gradient can be observed across the heat-recovery system. Once the vehicle begins to warm (~800 s of cold running), the system begins to pull less heat off the exhaust and thus a smaller temperature difference is seen across the system. Moreover, the warm run shows a diminished amount of heat recovery.

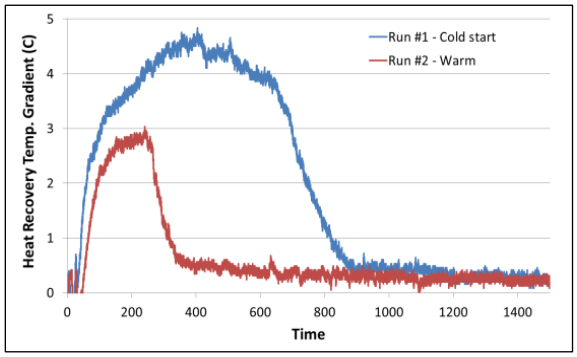

Figure 9. Exhaust-heat-recovery temperature gradient

Figure 10 shows the current for the electric-engine coolant pump over the previously discussed back-to-back steady-state runs. This figure demonstrates one of the major advantages of an electric water pump. During initial vehicle operation and warm-up (refer to the blue series), the pump current remains low for the entire cycle. Later runs, which begin much warmer and continue to increase in temperature, show a run-up in pump current. This observation is likely due to the need for increased circulation and cooling due to continued engine operation.

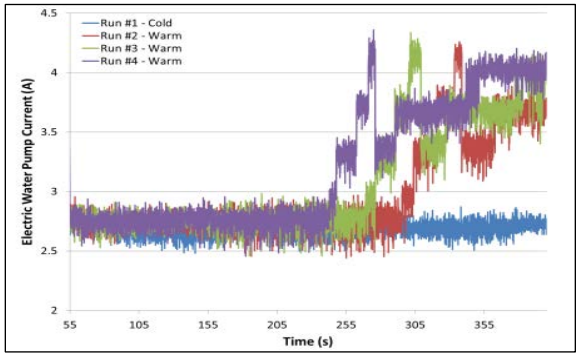

Figure 10. Electric-water-pump current for consecutive runs

Although the previous discussion focused on easy-to-understand, steady-state operation, numerous runs were also done using a mix of regulatory drive cycles. One of the most interesting observations from testing the Prius at cold ambient conditions is the dramatic observed difference in vehicle operation depending on the heater selection. Figure 11 shows the engine-outlet coolant temperature for two cold-start UDDS runs, one with the heater in use and one without. The blue line shows the coolant temperature for a run without the heater and the red line shows coolant temperature with the heater active. While the temperatures are fairly similar for the initial ~400 sec of operation, the coolant trends begin to diverge thereafter, suggesting differences in vehicle operation. Vehicle operation without the heater appears to have a much more jagged coolant trace, which indicates the vehicle is operating with the engine off and thus cooling down in the cold ambient temperature. In contrast, the heater-on trace shows some cooling during long engine-off periods, but is much less jagged, suggesting less engine-off operation.

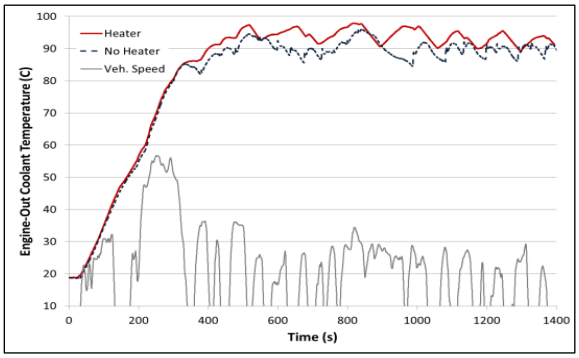

Figure 11. Cold-ambient, "cold"-start coolant temperature with and without heater during UDDS cycle

Figure 12 shows the temperature difference across the vehicle's heater core. As expected, the temperature gradient is much larger for heater-on operation, but quite a bit of temperature is still lost across the heater core when operating with the heat off. As vehicle thermal analysis begins to consider loads other than simple engine-heat loss and ambient temperature, insights like the amount of heat loss in a vehicle's heater core will assist in creating an improved estimate of overall heat transfer within a vehicle.

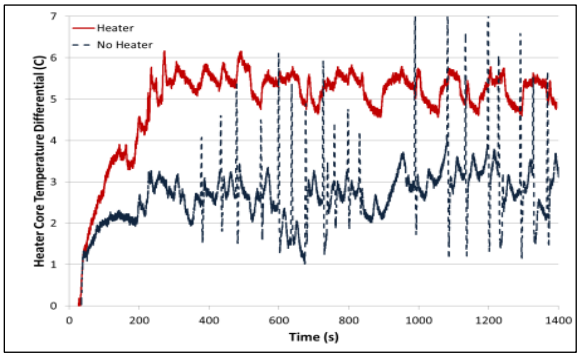

Figure 12. Heater-core temperature gradient with and without heater during UDDS cycle

In addition to the previous discussion related to cold ambient operation, the Prius was also tested at elevated ambient temperatures. The Prius utilizes an electric air conditioning (AC) compressor to increase efficiency when operating with the AC system; thus it is interesting to observe both the AC system power

utilization and the overall response to the additional demands of HVAC loads. Table 1. provides an overview of some preliminary hot ambient tests performed on the Prius. These tests are comprised of standard regulatory cycles at a range of ambient temperatures. Because of test cell limitations, these preliminary runs were done without solar load, but will be repeated with a solar load to examine the differences between the two scenarios. The following discussion briefly addresses some selected findings, which only represent a portion of the analysis and testing performed.

Table 1. Preliminary AC evaluation runs

Drive Cycle	Ambient Temperature (C)
UDDS	22
UDDS	22
Hwyx2	22
SC03	22
UDDS	28
UDDS	28
Hwyx2	28
SC03x2	28
UDDS	33
UDDS	33
UDDS	33
Hwyx2	33
SC03	33
SC03	33
UDDS (AC OFF)	33
UDDS	33
UDDS	33
UDDS	33
A/C Pulldown	33

Figure 13 shows the estimated AC load due to AC operation at three different ambient temperatures. As expected, the warmer temperatures show increased load throughout the drive cycle, as well as a larger and longer initial temperature pull-down period. One particularly interesting result is the load for operation during a 22ºC ambient-temperature run. The AC load appears to be modulated between 0 and roughly 300 W, giving it a fairly low overall power level. This behavior is likely due to the extremely low AC requirements during 22ºC ambient operation.

To confirm the behavior shown in Figure 13, Figure 14 shows the directly measured high-voltage battery power during the 22ºC run. As with the AC power load, the battery power can also be seen to modulate, thus confirming the behavior shown in the earlier figure.

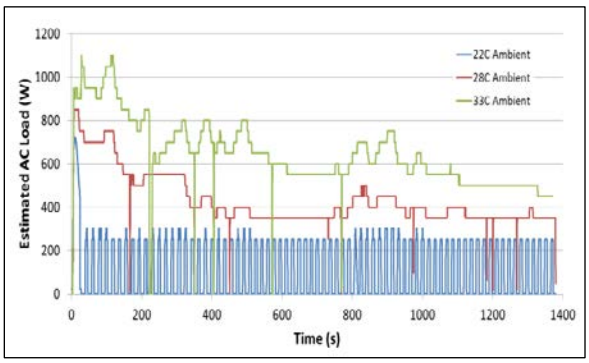

Figure 13. Estimated AC power consumption at various ambient temperatures (72ºC cabin thermostat temperature).

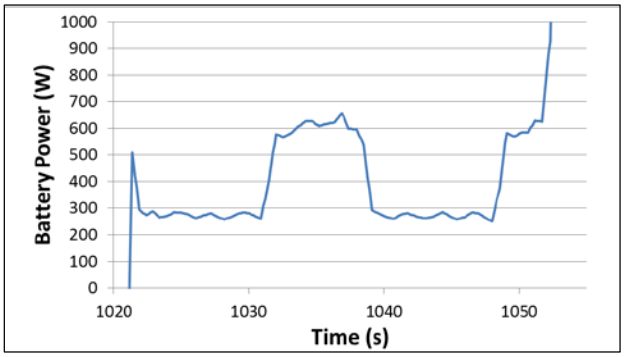

Figure 14. Battery power during AC cycling

Conclusions

Through leveraging the previously instrumented MY2010 Toyota Prius and developing a detailed set of tests at a range of both hot and cold ambient conditions, a significant amount of data and insight has been generated regarding the Prius's operation outside of the traditional testing/evaluation temperature range. Given the automaker's attention to non-standard temperature operation through the use of advanced components such as an exhaust-heat-recovery system, an electric water pump, and an advanced AC system, these trends are likely to spread to more vehicles as real-world fuel consumption reduction becomes an important metric. Furthermore, resource sharing through preliminary collaboration with Environment Canada for cold testing provided an additional means for improving testing capability and insight gained.

III.D. Automated Vehicle Data Bus Decoding for AVTA Vehicle Data Collection

Dan Bocci
Argonne National Laboratory
9700 S. Cass Avenue
Argonne, IL 60439
(630) 252-6788; dbocci@anl.gov

DOE Program Manager: Lee Slezak
(202) 586-2335; Lee.Slezak@ee.doe.gov

III.D.1. Abstract

Objectives

- Develop a toolset to help automate the process of decoding the signals on the vehicle data bus
- Decrease the time and skill level required to decode the signals on the vehicle data bus
- Increase the number signals on the vehicle data bus that can be decoded

Approach

- Use the original equipment manufacturer's (OEM's) scan tool for the vehicle to collect a set of correct data along with raw bus traffic data signals
- Apply some knowledge of digital communications to decode the raw bus traffic data into possible signals that could be useful information
- Use correlation techniques to present the user with the best matching signals for the data from the scan tool
- Let the user then build a database of the signals on the vehicle data bus

Major Accomplishments

- The data bus decoding time was reduced from approximately 5 days to 2 days.
- New data acquisition techniques for the decoding tool allowed additional data collection methods to be used in the Advanced Powertrain Research Facility (APRF).

Future Activities

- Utilize the tool suite for future DOE Advanced Vehicle Testing Activity (AVTA) project vehicles and on the Argonne National Laboratory (Argonne) test vehicles to enable the collection of more data with a minimal investment of time and effort

III.D.2. Technical Discussion

Background

As vehicles have continued to include more computers and controllers, the communications between the controllers have become increasingly critical to vehicle operation. To reduce the number of sensors and amount of wiring, all of the controllers communicate signals between each other by using a common data bus. Modern vehicles typically have multiple communication buses in order to ensure the safe delivery of parameters critical to vehicle operation. Argonne has developed techniques to

decode these communications, thereby facilitating data collection and enhancing the understanding of vehicle operation.

Introduction

The increased complexity of vehicle powertrains and control architectures has led to an ever-increasing level of communications between modules. This communication is typically done over a predefined protocol that specifies physical and data link layers. The most commonly used protocols include Controller Area Network (CAN), Local Interconnect Network (LIN), and Single Wire Controller Area Network (SW-CAN). In most cases, the application layer is defined by the OEM and is not publicly available. One notable exception to this is the On Board Diagnostic II (OBD-II) protocol, which is required by the U.S. Environmental Protection Agency (EPA).

Of the three data protocols commonly used on vehicles, LIN and SW-CAN are relatively low-speed protocols typically used for interior functions, such as the operation of signal lights, door locks, or windows. The CAN protocol provides a significantly higher throughput and is the standard communication protocol for critical powertrain communications. In addition, the EPA has required that all vehicles produced after 2006 use the CAN protocol to implement OBD-II. Modern vehicles may use two or more CAN buses to securely transfer all the required information for powertrain operation among the vehicle's controllers.

Three types of communication are typically seen on a vehicle's CAN bus. The first is the OBD-II protocol. This protocol is published and allows a diagnostic (scan) tool to query the status of various systems in the vehicle and to monitor the vehicle's operation for emissions compliance. The OBD-II protocol centers on emissions compliance and has a limited number of parameters defined. Because of the request/response nature of the OBD-II protocol, the data rates achievable are relatively low, and the update rate of signals decreases as additional signals are monitored. When signals are monitored via OBD-II, typical data rates range from 0.1 to 2 Hz.

The second type of communication typical of a vehicle CAN bus is OEM scan tool communication protocol. The OEM scan tool communicates with the various modules and queries faults and signal values. The major differences between this type of communication and OBD-II communication is that for this one, the protocol is controlled by each OEM and is not typically published in the public domain. The OEM scan tool protocol typically supports significantly more signals that are specific to the operation of the vehicle than does the OBD-II protocol. The OEM scan tool communication protocol centers on the ability of technicians to diagnose and repair the vehicle, and it allows both fault information as well as current signal information from the controllers to be communicated. This information stream is typically limited to speeds of ~0.1 to 10 Hz.

The third type of communication on the CAN bus involves the data that are exchanged between all the controllers within the vehicle during normal operation. Because of the nature of CAN networks, these messages are broadcast and available to all controllers connected to the CAN bus. Data rates for some signals that are critical to powertrain operation can be >100 Hz. The information communicated includes all the signals necessary to coordinate the operation of all the powertrain controllers during vehicle operation. This protocol is defined by the OEM, typically on a per vehicle basis, and is rarely available outside the OEM.

Over the past four years, Argonne has developed techniques to reverse engineer the protocol for communication between modules on the CAN bus. These techniques have been shown to implement effective methods and procedures for reverse engineering vehicle data bus communications; however, they require a significant amount of time and effort. The techniques also require a significant knowledge of vehicle operation and of digital communications.

The data that can be collected from the vehicle data bus are very useful for testing and benchmarking vehicles. Because the vehicle's CAN data bus collects this needed information, it allows many sensors (that otherwise would have been installed in the vehicle or calibrated) to be removed. It also enables the measurement of many powertrain parameters such as torque (whose measurement would otherwise have required invasive instrumentation). An interesting and sometimes useful caveat to this discussion is that the data are a true representation of what the vehicle *thinks is happening* and not necessarily what *actually is happening*. This can be very useful when studying the control techniques a vehicle uses.

Approach

Determine Message Source

The first step in the process of decoding a vehicle data bus is to determine the sources of all the messages on it. Knowing the sources makes it much easier to determine if the results are valid and if the message is a command or measured result and can be mapped like shown in Figure 1. For example, it is unlikely that the antilock braking system (ABS) module would measure engine speed and send this information out on the data bus. This information is typically and most logically handled by the engine control module. A tool has been developed to aid in this step; it monitors the data bus for missing messages by comparing them to a reference message set. Typically the reference messages are set on the basis of the messages that exist during normal operation. The operator can then disable each control module individually and monitor for missing messages, saving the results after each step.

Msg ID	PCM	HCM	MCU	BCM
293			X	
170		X		
203		X		
261	X			
110	X			
260	X			
292	X			
2A0	X			
2A1			X	
2B5	X			
2F0		X		
2F1		X		
440	X			
620				X
671				X

Figure 1. Message source mapping results

Capture Data

The next step is to collect the raw data from the vehicle and the actual data from the vehicle scan tool or another trusted data source. This step creates the source data for the next two steps. This procedure may need to be repeated multiple times depending on the number of data buses in the vehicle and any limitations on recording scan tool data.

The manual data bus decoding methods require the researcher to drive the vehicle on a dynamometer or in a large empty area while watching multiple computers to find correlations between the raw data bus signals and actual values. They often also include driving the vehicle in a nonstandard way to isolate a particular variable. With the new automated method, however, no special drive schedule is needed. The driving and data collection can easily be done on the road. The standard operating procedure is to set up the acquisition computers, start acquisition, and then take a short drive to collect data. During driving, it is not necessary to monitor any of the computers.

Use OCR DAQ Module

A critical component of the data collection effort is the ability to collect the "correct answer" from a trusted data source. It could come from an external sensor or the vehicle's scan tool. Since one objective is to reduce the amount of required instrumentation, it is preferable to use the vehicle's scan tool to collect these data. A survey of many of the OEM scan tools available

clearly revealed that additional tools would be needed to collect data from the scan tool that would be appropriate for use in data bus decoding.

Almost all of the scan tools are designed to work on a personal computer (PC). An optical character recognition (OCR)-based data acquisition (DAQ) software module was developed to collect these data. The OCR DAQ module captures a continuous stream of screen images from the scan tool computer, such as the example in Figure 2. These are then converted to data by using OCR techniques and a configuration file that defines the location of various pieces of information on the screen as shown in Figure 3. This technique has proven to be robust and compatible with most scan tools currently available.

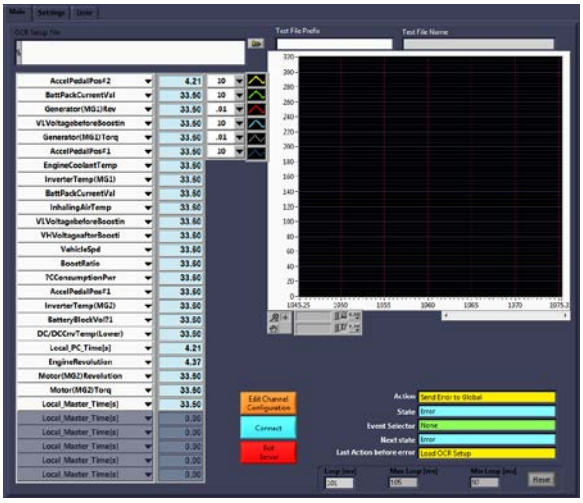

Figure 2. Screen shot of OCR DAQ module in operation

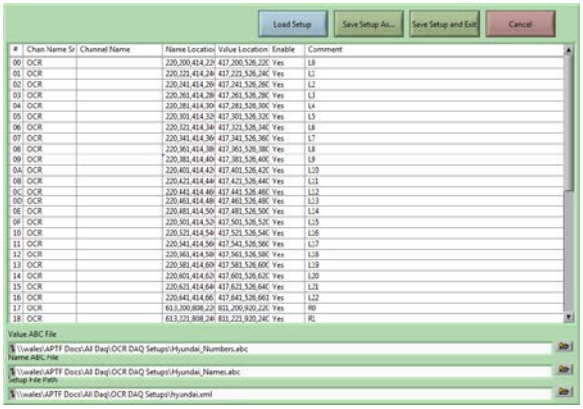

Figure 3. Configuration of the OCR DAQ module, which includes defining the location of the signal name and value on the screen

Merge Data

Once all the raw and trusted data have been collected, they must be merged into a common file and time aligned. When data are collected by using the OCR DAQ module, the time alignment is handled by a common time channel broadcast that is recorded by both data sources. This makes time alignment easy and accurate.

Generate Channels

Next the possible data channels must be constructed from the raw data bus traffic for comparison to the trusted channels. This is done by splitting all the messages on the data bus into many different possible signals. Many of these constructed signals represent a smaller portion of the bits in an actual signal or the concatenation of multiple signals. If the constructed signal is not a true signal, it should not correlate properly with the trusted signals.

The user has a number of options that can be manipulated to control the generation of the possible signals. These parameters are summarized in Table 1. A general knowledge of binary numbers and digital communications is helpful to optimize these parameters; however, the main reason to optimize these parameters is to speed up this step and future steps and thus reduce the number of possible signals. This step generally results in 1,000 to 20,000 possible signals being identified and generated.

Table 1. Tuning parameters used to control possible signal generation

Min Length	Sets the minimum number of bits in a possible signal
Max Length	Sets the maximum number of bits in a possible signal
Min Byte Align	Sets the length at which a signal is required to be byte aligned
Endian	Sets the endian to big, little, or both
Datatype	Sets the data type to unsigned, signed, or both

Perform Correlations

The heart of the automated data bus decoding is performing all the correlations. During this process (Figure 4), the program will perform a linear regression fit of every possible signal to every trusted signal and store the curve fit parameters as well as the quality of the fit. If the correct pairing of the trusted channel to the possible channel is found, the degree of linear relation between the signals will be very high. If the signals being compared are not a match, the value of the fit will be significantly lower. During this step, 30,000 to 250,000 correlations will be performed on a normal data set.

Create Database

The final step is to present the results to the user and allow the user to finish identifying the signals on the CAN bus. The user starts by selecting one of the trusted signals collected during the data collection phase and is then presented with a rank-ordered list of possible signals that is based on the quality of fit. At this point, it is again useful for the user to have some knowledge of or familiarity with digital communications. In some cases, there may be multiple similar versions of possible signals that equally match the trusted signal. For example, if the signal was not exercised to its extremes during the data collection, the 7-bit and 8-bit versions of the signal may be exactly the same. In such a case, the user would have to use his or her knowledge of digital communications to determine the proper alignment and length of the signal. Once the correct possible signal is selected and the correct gain and offset have been confirmed, the signal can be added to the vehicle message database.

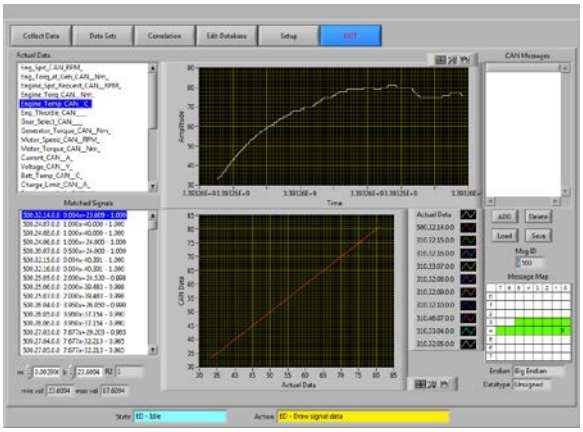

Figure 4. Screen shot of the automated data bus decoder program in the process of performing signal correlation and linear regression fit operations

Results

The tools developed for data bus decoding were used to reverse-engineer the data bus of a 2011 Hyundai Sonata hybrid. All the major powertrain effort and flow signals were identified in 2 to 3 days. Figures 5 and 6 show the result of the engine speed signal determined by the automated tool. The data are plotted versus time and in an XY form.

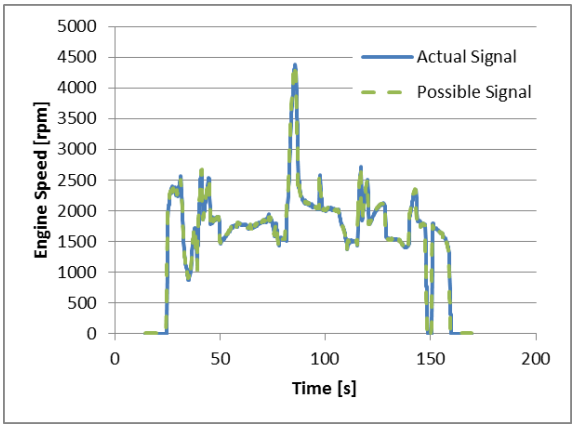

Figure 5. Engine speed signal identified by automated tool plotted versus time

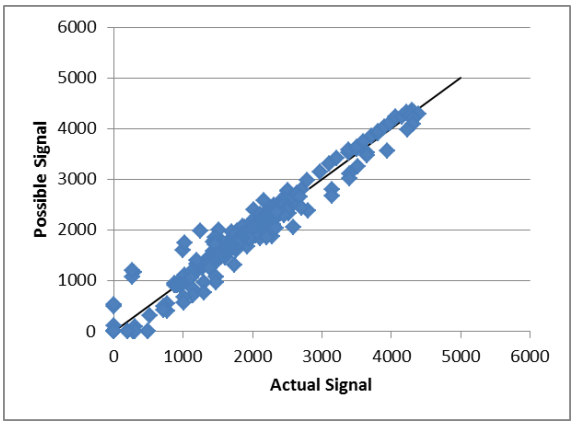

Figure 6. Engine speed signal identified by automated tool plotted versus actual signal

In addition, the automated tool allowed the determination of some signals that would have been exceedingly difficult to find manually. Examples of such signals are the minimum and maximum cell voltages of the battery. During normal operation, these signals are nearly identical, which makes them very difficult to distinguish manually. Another signal that was determined was battery temperature. This signal is an example of one that does not significantly vary and one in which it is difficult to cause rapid variations without disassembling the vehicle. Figure 7 shows that even when there are four changes in the signal, the data bus decoding tool can easily identify the correct signal.

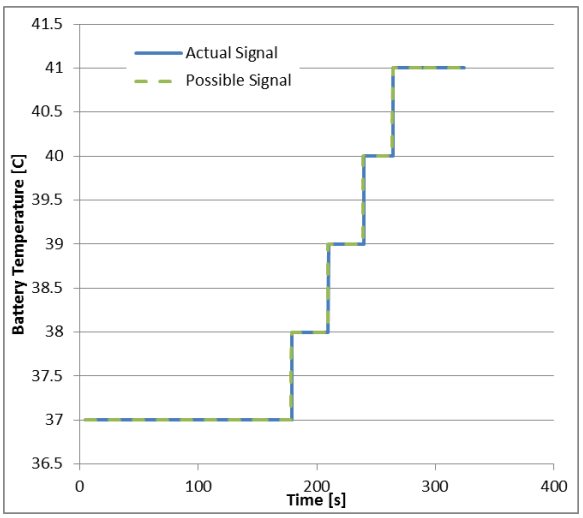

Figure 7. Battery temperature signal identified by automated tool plotted versus time

Conclusions

A toolset that aids in identifying signals on a vehicle's data bus has been developed. This new software application can assist researchers in the identification of signals that otherwise would be very difficult to determine by using manual techniques. The tools also reduce the amount of time needed to decode the signals on the data bus by allowing the operator to drive the vehicle and collect data once with the ability to then process that data for all available signals.

III.D.3. Products

Tools & Data

Software toolset developed to assist and automate the decoding of signals on a vehicle data bus.

III.E. Plug-in Electric Vehicle (PEV) Testing by DOE's Advanced Vehicle Testing Activity (AVTA)

James Francfort (Principal Investigator)
Idaho National Laboratory
P.O. Box 1625
Idaho Falls, ID 83415-2209
(208) 526-6787; james.francfort@inl.gov

DOE Program Manager: Lee Slezak
(202) 586-2335; Lee.Slezak@ee.doe.gov

III.E.1. Abstract

Objective

- Benchmark grid-connected plug-in electric vehicles (PEV) to determine the contribution PEV technologies can make to reduce petroleum consumption in the United States.
- Benchmark individual PEV models from original equipment manufacturers (OEMs).
- Benchmark PEV charging infrastructure, including charging equipment performance and driver recharging patterns.
- Reduce the uncertainties about PEV performance, and battery performance and life.
- Reduce the uncertainties about drivers' recharging practices and PEV acceptance.
- Provide PEV testing results to the U.S. Department of Energy (DOE), vehicle modelers and designers, technology target setters, and industry stakeholders.
- Provide PEV testing results to fleet managers and the general public to support their acquisition and deployment decisions.

Approach

- Document via various testing methods the fuel (petroleum and electricity) use over various trip types and distances.
- Report petroleum and electricity use separately.
- Document PEV electric vehicle supply equipment (EVSE) and fast charger performance (profile and demand), charging times, and infrastructure needs, as well as operator behavior impact on charging times and frequencies.
- Document any environmental factors, such as temperature and terrain that impact PEV fuel consumption.
- Use published testing specifications and procedures developed by the AVTA that are reviewed by industry, national laboratories, and other interested stakeholders.
- Obtain access to Plug-in Hybrid Electric Vehicles (PHEVs), Battery Electric Vehicles (BEVs), Extended Range Electric Vehicles (EREVs), EVSE and fast chargers for testing to the reviewed testing specifications and procedures.
- Perform baseline performance track and laboratory tests, accelerated on-road tests, and fleet demonstrations on vehicles, components and charging infrastructure as appropriate.
- Place vehicles in environmentally and geographically diverse test fleets.
- Continue to use and develop cost-shared partnerships with public, private, and regional groups to test, deploy, and demonstrate vehicles and infrastructure technologies in order to leverage DOE funding resources.
- Expand the use of automated data collection, transmission, analysis, and reporting processes.

- As needed, reach additional cooperative research and development agreements (CRADAs) and non-disclosure agreements (NDAs) in preparation for the testing of vehicles and components from OEMs.

Major Accomplishments

- Collecting and publishing onboard data from a fleet demonstration of 21 Ford Motor Company Advanced Research Escape PHEVs. As FY2011 ended, 377,000 miles of vehicle use and charging profiles, and up to 66% petroleum use reductions were documented.
- Performed baseline performance testing on one Ford Advanced Research Escape PHEV.
- Initiated data collection for more than 100 General Motors Volts EREVs. As FY2011 ended, 247,000 miles of all-electric vehicle operations, charging profiles, and mpg increases of up to 101% were documented were documented by data from 110 Volts.
- Initiated the data collection from a fleet demonstration of 145 Chrysler Ram PHEV Pickups. As FY2011 ended, 70,000 miles of vehicle and charging profiles, as well as mpg increases of up to 33% were documented by data from 70 Chrysler Ram PHEV pickups.
- Completed data collection for fleet demonstrations of 228 Hymotion Prius PHEV conversions. As FY2011 ended 3.3 million miles of vehicle and charging profiles, as well as average mpg increases of 43% were documented.
- Initiated the data collection from approximately 14,000 Level 2 EVSEs and fast chargers from ECOtality North America as part of the EV Project. As FY2011 ended, data had been collected from 2,801 Nissan Leaf BEVs, 21 Chevrolet Volt EREVs, and 2,990 ECOtality EVSE being operated in six states and the District of Columbia. A total of 6.2 million test miles and 178,000 charging events have been documented, and for the Nissan Leafs, there is a complete elimination of in-vehicle use of petroleum for transportation.
- Initiated data collection from approximately 4,500 Coulomb ChargePoint America EVSE. At the end of August 2011, data had been collected from 893 EVSE and 39,000 charge events in twelve states.
- Supported the USPS deployment of electric long-life vehicles (eLLVs) by conducting baseline performance testing on five eLLVs from five different conversion companies. Also initiated the data collection from the same vehicles in USPS mail delivery fleet demonstrations.
- Supported the memorandum of understanding (MOU) between the Departments of Energy (DOE) and Defense (DOD) that specifies DOE technical support to DOD to help DOD reduce petroleum use for non-strategic transportation, by initiating the Micro Climate study of Joint Base Lewis McCord's ability to install EVSE and electric drive vehicles.
- Conducted a workshop and other planning activities to access the needs for codes and standards to support grid-connected vehicle charging. This is being conducted in partnership with the American National Standards Institute (ANSI).

Future Activities

- Continue to report on the performance of 22 Ford Escape Advanced Research PEHVs and report the petroleum reduction capabilities and operations of the same vehicles.
- Continue to report on the performance of up to 145 Chrysler Ram PHEV Pickups and report the petroleum reduction capabilities and operations of the same vehicles.
- Initiate the data collection in partnership with Chrysler from 25 minivan PHEVs and report the petroleum reduction capabilities and operations of the same vehicles.
- Continue to report on the performance of up to 150 General Motors Volts EREVs and report the petroleum reduction capabilities and operations of the same vehicles.
- Continue to report on the performance of up to 8,300 Nissan Leaf EVs and General Motors Volt EREVs being deployed as part of the EV Project as well as approximately 14,000 ECOtality Blink EVSE and fast chargers. Reporting will include recharging and vehicle use patterns, as well as the petroleum reduction capabilities of the charging infrastructure and vehicles.
- Continue to report on the operations of up to 4,500 Coulomb ChargePoint America EVSE.

- Conduct Quantum PHEV Explorer conversion testing in partnership with the South Coast Air Quality Management District in California.
- Complete the initialization of the EDAB test-bed vehicle and obtain electric traction batteries sufficiently developed for onroad and dynamometer testing.
- Continue performing due diligence on potential vehicle, component, and charging infrastructure suppliers and obtain such for testing as appropriate.
- Conduct baseline performance testing on Nissan Leafs, General Motors Leafs and other new PEV testing candidates such as vehicles from Fisker, Tesla, Ford and other manufacturers. Identify additional vehicle models that will be added to the fleet demonstrations in FY 2012.
- Develop additional low-cost vehicle and charging infrastructure demonstration relationships and support the deployment of PEVs and EDVs in these testing fleets.
- Continue to coordinate PEV, EDV, and charging infrastructure testing with industry and other DOE directed entities. This includes supporting the data collection from EVSE deployed via the DOE Clean Cities activities and the development of a NDA with Project Better Place.

III.E.2. Technical Discussion

Background

The U.S. Department of Energy's (DOE's) Advanced Vehicle Testing (AVTA) is part of DOE's Vehicle Technologies Program (VTP), which is within DOE's Office of Energy Efficiency and Renewable Energy (EERE). The AVTA is the only DOE activity tasked to conduct field evaluations of vehicle technologies that use advanced technology systems and subsystems in light-duty vehicles to reduce petroleum consumption. Most of these advanced technologies include the use of electric drive propulsion systems and advanced energy storage systems. However, other vehicle technologies that employ advanced designs, control systems, or other technologies with production potential and significant petroleum reduction potential, are also considered viable candidates for testing by the ATVA.

The AVTA light-duty activities are conducted by the Idaho National Laboratory (INL) for DOE. INL has responsibility for the AVTA's execution, direction, management, and reporting; as well as data collection, analysis and test reporting. The INL is supported in this role by the private sector company ECOtality North America (ECOtality). ECOtality has a competitively awarded contract that is managed by DOE's National Energy Technology Laboratory (NETL). The AVTA sections of the FY 2011 Annual Program Report jointly cover the testing work performed by INL and ECOtality. When appropriate, the AVTA partners with other governmental, public, and private sector organizations to provide maximum testing and economic value to DOE and the United States taxpayers, via various cost sharing agreements.

Introduction

DOE's AVTA is evaluating PEV technology in order to understand the capability of electric propulsion technology to significantly reduce petroleum consumption when vehicles are used for transportation. In addition, many companies and groups are proposing, planning, and have started to introduce PEVs into their fleets.

It should be noted that grid-connected PEVs include several vehicle / energy storage schemes that include: battery electric vehicles (BEVs or simply EVs) such as the Nissan Leaf, plug-in hybrid electric vehicles (PHEVs) such as the Ford Escape and Chrysler Ram PHEVs, and extended range electric vehicles (EREVs) such as the General Motors Volt.

During FY11, a transition occurred from testing mostly PEV conversions to testing PEVs from OEMs. When testing conversion vehicles, the primary focus during FY11 was to study the PEV technology's potential contribution to petroleum reduction and to understand and document charging patterns. The drive to focus on the overall petroleum reduction potential of PEV technology versus testing individual PHEV conversion models was driven by the mostly

conversion nature of the available PEVs during pre-FY 2011 years, and the non-likelihood the conversion vehicles would be the majority of PEV deployments in future years.

This transition in focusing on PEV conversions to focusing on PEVs from OEMs was made possible as several OEMs made available during FY11 PEVs for the first time in about a decade.

The PHEVs available for public purchase in the few years prior to FY 2011 used an HEV as the base vehicle, and either added a second PHEV battery or replaced the base HEV battery with a larger PHEV battery pack, with a 5-kWh PHEV battery size the most typical size to date. However, some PHEVs used a single PHEV battery pack that ranged from 10 to 15 kWh. PHEV control systems and power electronics are also added to the base vehicle to complete the upgrade. These larger additional or replacement battery packs are sometimes recharged by the onboard regenerative braking and generator subsystems, but all of them must also use onboard chargers connected to the off-board electric grid to fully recharge the PHEV battery packs.

Today's OEM PEVs all have 10 to 15 kWh of onboard battery storage in PHEVs and EREVs, and more than 20 kWh of onboard storage for BEVs. However, some other OEMs will introduce PHEVs with smaller battery packs in future years.

Within the AVTA, INL and ECOtality make extensive use of in-vehicle and in-charging infrastructure data loggers to collect a variety of vehicle and infrastructure generated performance parameters. Experience has shown that automated data collection in fleet environments is the only way to ensure accurate data is collected.

The concept of advanced onboard energy storage and grid-connected charging raises questions that include the life and performance of these larger batteries; the charging infrastructure required; how often the vehicles will actually be charged – driver and "smart grid" behavior and controls; and the actual amount of petroleum displaced over various missions, drive cycles, and drive distances.

General Testing Approach

Three basic types of testing methods are used to test vehicles and they discussed below.

- ***Baseline performance testing*** during which a vehicle is track and dynamometer tested. The track testing includes acceleration, range, braking, and fuel use (both electricity and gasoline) at different battery states-of-charge. The vehicles are also coast-down tested to determine dynamometer coefficients, which are used during the urban and highway dynamometer test cycles. Note that the AVTA dynamometer testing is conducted by Argonne or Oak Ridge National Laboratories for the AVTA. This sharing of vehicles also reduces costs to DOE.
- ***Accelerated Testing*** uses dedicated drivers to complete a series of drives and charges (for PEVs) on city and highway streets. This testing is often used to ensure PEVs can accomplish several charge and drive cycles in one day. For some vehicles, this can include more than 5,000 miles of operation per month.
- ***Fleet Testing***. Fleet testing is normally conducted by placing vehicles into fleets with no highly controlled structure to repeatable drive missions. The AVTA partners with government, private, and public fleets for fleet testing as these fleets are often overwhelmingly the earliest adaptors of advanced technology vehicles. Note that the AVTA fleet testing does include some operations by the general public.

For PHEVs and EREVs, these vehicles can operate on gasoline even when the vehicles' battery packs are not charged. Therefore, with some exceptions, the fuel-use result reporting is normally broken down into three operating modes for these vehicle technologies:

- ***Charge Depleting (CD) Mode***: During each entire trip, there is electric energy in the

battery pack to provide either all-electric propulsion or electric assist propulsion.

- ***Charge Sustaining (CS) Mode***: During a trip, there is no electrical energy available in the PHEV battery pack to provide any electric propulsion support.
- ***Combined (or Mixed) Charge Depleting and Charge Sustaining (CD/CS) Mode***: There is electric energy in the battery pack available at the beginning of a trip. However, during the trip, the battery is fully depleted.

Results and Conclusions by Vehicle Model or Technology

Ford Escape Advanced Research PHEV

During FY 2010, the AVTA signed a CRADA with Ford Motor Company that detailed data collection, analysis and reporting by the AVTA for the vehicle performance, fuel use, and charging patterns for 22 Ford Escape Advanced Research PHEVs. This work is being performed to support a grant Ford received from DOE.

Using server-to-server data transmission, the INL receives raw data generated by data loggers installed onboard the 21 Escape PHEVs. With this data, INL generates a series of periodic reports and year to date summary fact sheets which can be accessed at: http://avt.inel.gov/phev.shtml.

The November 2009 to September 2011 report documents 377,000 miles of operation during which the vehicles had an overall fuel economy of 38 mpg. However, when operating in CD mode, the vehicles averaged 53 mpg, which is 66% higher than the 32 mpg result in CS mode operations.

It is evident that ambient temperatures have impacts on mpg results in all operating modes. However, as seen in Figure 1 below, the biggest impact is on CD mode operations where mpg results double during temperatures in the 60 to 75 degrees F operations compared to very hot and cold operations.

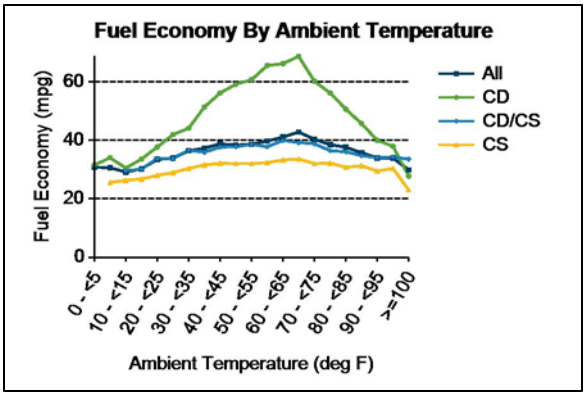

Figure 1. Ford Advanced Research PHEV Explorer mpg impacts at a range of ambient temperatures.

The monthly reports also document seasonal impacts on mpg results with May 2011 reporting 64 mpg in Charge Depleting mode and December 2010 reporting 44 mpg in the same operating mode. See http://avt.inel.gov/library.shtml#F for the monthly results.

Using the May 2011 results, when operating in CD mode during city driving events the mpg is 94% higher (66 mpg) than city driving CS mode (34 mpg). During highway driving in CD mode, the mpg is 116% higher (69 mpg) than highway driving in CS mode (32 mpg).

Ambient temperature impacts are likely the result of auxiliary power settings as well catalyst warming requirements impacts on vehicle control decisions. The auxiliary power impacts where well documented during the baseline performance testing (http://avt.inel.gov/pdf/phev/FordEscapePHEVfact.pdf) when the testing is conducted both with and without the air conditioner (A/C) operating, and with both with cold and non-cold starts. With the A/C off, the vehicle averaged 119 mpg during both CD hot and cold starts. With the A/C on, the hot and cold starts averaged 21 mpg in CD mode. The same testing also reports results in 10 mile increments and during UDDS dynamometer testing the vehicle averaged 118.5 mpg for the first ten miles of operation when the vehicle was in CD mode but only 50.9 mpg for all 200 miles of such operations. This suggests the PHEV technologies best maximizes mpg during shorter trips when operating in CD

modes. In fact, the results were above 115 mpg for the first 40 miles of CD operation with the A/C off.

General Motors Chevrolet Volt EREV

During FY 2011, a NDA was signed with OnStar that detailed data collection, analysis and reporting by the AVTA for the vehicle performance, fuel use, and charging patterns for approximately 150 General Motors Chevrolet Volt EREVs. This work is being performed to support an ARRA grant General Motors received from DOE.

Using server-to-server data transmission, the INL receives raw data generated by OnStar from onboard data loggers installed on the Volts. With this data, which is generated for every key on and off event, INL generates a series of periodic reports which can be accessed at: http://avt.inel.gov/evproject.shtml.

The two reports generated during FY 2011 covered the period May through September 2011, and 247,000 operating miles. Because the Volt is an EREV, the fuel use is reported in different modes than PHEVs. These three reporting modes are overall operations, EV mode operations, and extended range mode operations (ERM) when the gasoline engine is running.

Using the July through September 2011 report for 110 Volts and 208,000 miles, the vehicle averaged 369 AC watt-hours (Wh) per mile with no gasoline used. This operation totaled 50.3% of all 208,000 miles. In ERM operations, the vehicle averaged 37.2 mpg with no electricity used. Overall, the Volts averaged 74.8 mpg and 185 AC Wh per mile.

As Figure 2 shows below, more EV mode trips occurred during shorter distance trips as would be expected. Figures 3 and 4 document the near full battery state of charge (SOC) at the end of each charge event prior to driving events and the SOC at the end of drives prior to charging.

Table 1 below documents the Volt recharging information. It should be noted that the vehicle is being charged 1.3 times per day for those days the vehicle is operated and that a significant amount of recharging must be occurring at Level 1 (110 V) given the 3.4 hours of charging per charging event and the 7.1 AC kWh energy transfer per charging event.

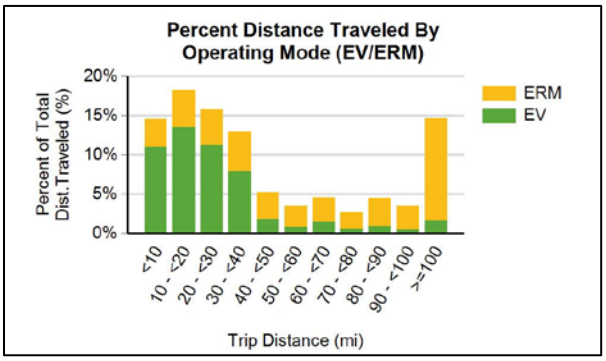

Figure 2. ERM and EV operations for the Volt as measured by the percent of total distance traveled.

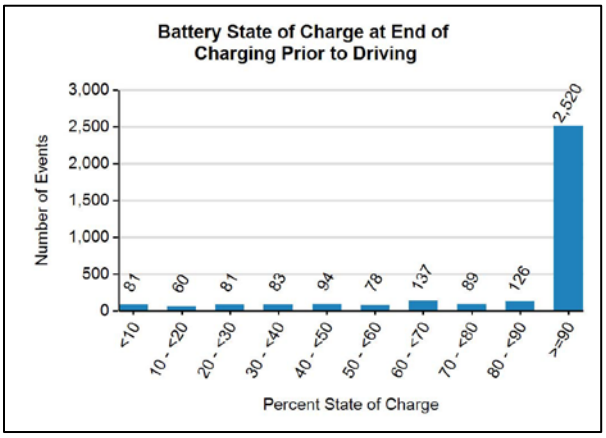

Figure 3. Volt SOC at end of charging events prior to driving events.

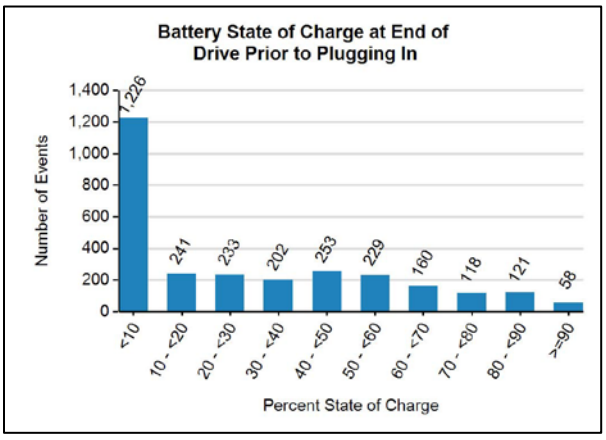

Figure 4. Volt SOC at the end of drives that occur prior to start of charging events.

Table 1. Volt summary charging information for the July through September 2011 reporting period.

Average # charging events per vehicle month	17
Average # of charging event per vehicle day	1.3
Average miles between charging events	44
Average # trips between charging events	3.3
Average hours charging per charging event	3.4
Average energy (AC kWh) per charging event	7.1
Average energy (AC kWh) per vehicle month	119
Total charging energy (AC kWh)	38,593

Chrysler Ram Pickup PHEV

During FY 2011, the AVTA signed an NDA with Chrysler that detailed data collection, analysis and reporting by the AVTA for the vehicle performance, fuel use, and charging patterns for approximately 140 Chrysler Ram PHEV Pickups. This work is being performed to support an ARRA grant Chrysler received from DOE.

Using server-to-server data transmission, the INL receives raw data generated by Chrysler from onboard data loggers installed on the Ram PHEVs. With this data INL generates a series of periodic reports which can be accessed at: http://avt.inel.gov/evproject.shtml.

The reports generated during FY 2011 covered the period July through September 2011, and 32,000 operating miles. The 66 Ram PHEVs providing data at the end of FY 2011 exhibited a 47% increase in mpg when comparing CD trips (22 mpg) to CS trips (15 mpg). As shown in Figure 4, the Ram operating scheme allows the internal combustion engine (ICE) to be off 45% of the time, including 20% engine off while the vehicle was being driven.

The Ram PHEV also exhibits a near linear mpg and aggressiveness driving profile. Figure 5 documents the driving aggressiveness impact on mpg, with less aggressive driving results in an average of approximately 23 mpg while the most aggressive driving results in an average of approximately 11 or 12 mpg.

Table 2 below documents the Ram recharging information. It should be noted that the vehicle is being charged only 0.68 times per day for those days the vehicle is operated.

As FY 2011 ended, the AVTA was starting to receive data from the first of what will be 25 Chrysler Minivan PHEVs.

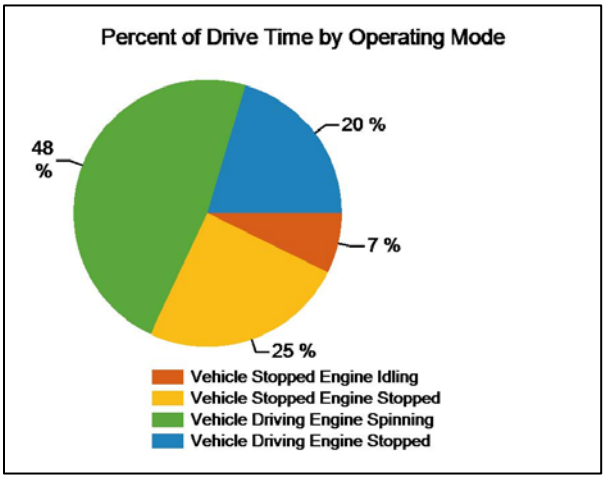

Figure 5. Chrysler Ram PHEV percent of drive time the engine is spinning or stopped by whether or not the vehicle is moving.

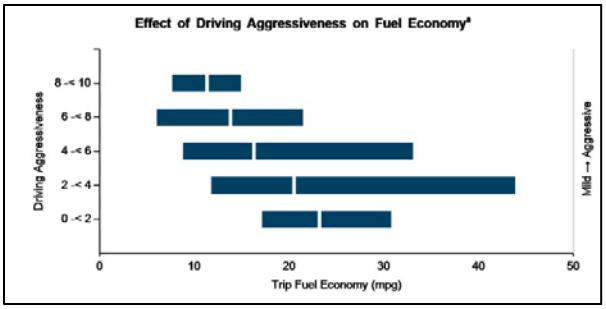

Figure 6. Chrysler Ram Pickup PHEV fuel efficiency impacts from aggressiveness driving.

Table 2. Chrysler Ram PHEV charging information for the July through September 2011 reporting period.

Average # charging events per vehicle month	5.9
Average # of charging event per vehicle day	0.68
Average miles between charging events	40
Average # trips between charging events	7.98
Average hours charging per charging event	1.7
Average energy (AC kWh) per charging event	6.0
Average energy (AC kWh) per vehicle month	35.3
Total charging energy (AC kWh)	4,768

Hymotion Prius PHEV Conversion

Prior to the introduction of PHEVs from OEMs, only relatively small conversion companies were providing PHEVs for sale that used Toyota Prius and Ford Escapes HEVs as the base vehicles, with most conversions based on the Prius. In terms of number of vehicles converted and deployed, the majority were Hymotion Prius PHEVs.

The AVTA partnered originally with Hymotion to collect data via onboard data loggers and the vehicle CAN to collect more than 25 operating vehicle and battery parameters. This joint data collection activity grew to eventually include more than 100 testing partners, operating 228 Hymotion Prius PHEVs in more than 25 states and Canada. The AVTA did collect data on more than 260 PHEVs from twelve different PHEV conversion models (based on battery type) and one OEM. However, these other activities are discussed in previous reports.

The 228 Hymotion Prius data collection activity was completed during FY 2011 and it provided a rich data set that documented operator behaviors, charging profiles, and impacts to mpg; including ambient temperatures, terrain, and driver power demands. The 228 vehicles were broken into two data collection sets, those equipped with data loggers from Kvaser that did not have cellular capabilities for transmitting data and those equipped with data loggers from GridPoint. The Kvaser data loggers required physical removal of storage cards and either data uplifting by internet or the physical mailing to INL of the data cards. This data collection method introduced data collection delays and opportunities to mishandle data. However, this activity started, this was the economical state of the art for collecting data from a smaller set of vehicles. The GridPoint data loggers, which were introduced to the market later than the Kvaser loggers, included cellular communications and GPS tracking in real time. Both data quality and timeliness increased significantly as reliance on humans to collect the storage cards was eliminated.

A complete set of PHEV fact sheets can be found at: http://avt.inel.gov/phev.shtml. A summary fact sheet for the 44 Hymotion Prius without cellular data collection can be found at http://avt.inel.gov/pdf/phev/HymotionPriusKvaserJan08-Dec10Rpt.pdf. These vehicles included a high percentage based in Canada and they exhibited similar results to the GridPoint data logger vehicles with the exception that mpg for all operating modes was lower due to the colder operating climate of Canada.

Table 3 below provides energy use data for the 184 GridPoint equipped Hymotion Prius and this data represents 87% of the 3.3 million miles of documented Hymotion Prius PHEV operations.

Table 3. Hymotion Prius PHEV conversions operations data for vehicles equipped with GridPoint data loggers.

Total vehicles	184
Total miles	2,899,288
Total trips	310,808
All trips mpg	48
Overall AC Wh per mile	52
Overall DC Wh per mile	38
CD mode mpg	62
CD mode DC Wh per mile	142
CD/CS mode mpg	53
CD/CS mode DC Wh per mile	49
CS mode mpg	43

Table 3 documents 45% higher mpg for the CD operations when the vehicles averaged 62 mpg compared to 43 mpg for the CS operations. The delta for city only driving was even higher with the CD operations having 67% higher mpg at 60

mpg than the CS of 36 mpg in city driving. See http://avt.inel.gov/pdf/phev/HymotionPriusV2GreenApr08-Sept11.pdf.

Most of these vehicles were operated by fleets and this impacted their driving and charging profiles. Figure 7 documents the mostly daytime work use of the vehicles. Figure 8 documents the highest time for plugging these vehicles into the grid via a 110 V connection occurred during the early afternoon hours, and this connection time influenced the time of day charging as seen in Figure 9.

These vehicles only received an average of 2.7 AC kWh of energy during their average charge time of 2.7 hours. These are both a reflection of the small battery packs used and the use of 110 V for charging.

The data collection and reporting for these vehicles officially ended at the conclusion of FY 2011. However, a couple of fleets did request a few more months of data collection and reporting for their respective vehicles in order to get a final whole year of data or a final season of data. This was a very highly leveraged data collection activity in that DOE only purchased one of the 228 vehicles and paid for less than 10% of the conversion costs.

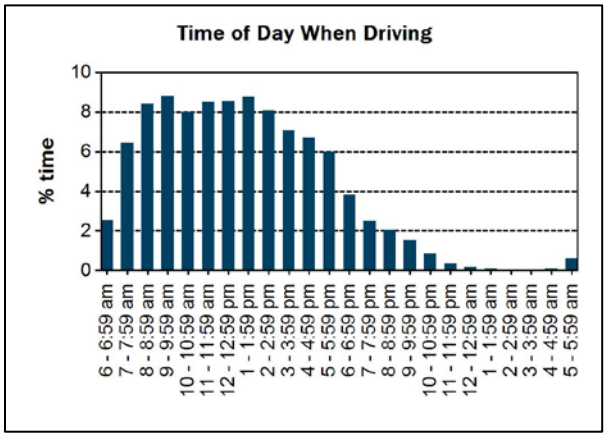

Figure 7. Time of day Hymotion Prius PHEV conversion vehicle operations.

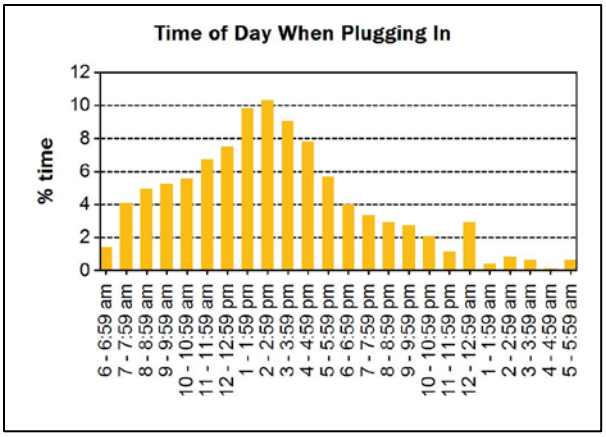

Figure 7. Time of day for plugging in Hymotion Prius PHEV conversion vehicles for charging.

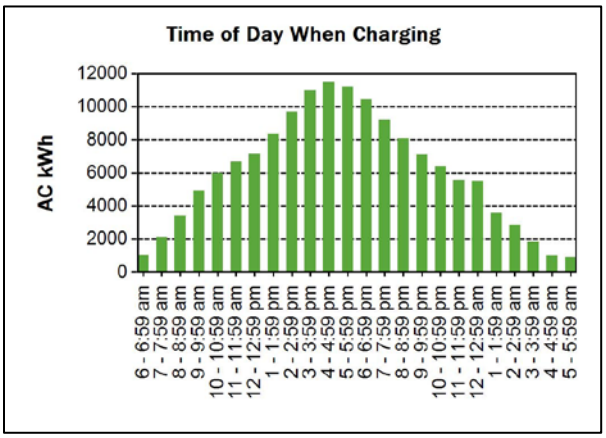

Figure 7. Time of day the Hymotion Prius PHEV conversion vehicles where receiving energy from the grid as measured by AC kWh.

EV Project Charging Infrastructure Demonstration

The EV Project is a DOE funded ARRA project for deploying and testing PEV recharging infrastructure. Lead by ECOtality North America, it is the largest deployment and testing of EVSE and fast chargers ever attempted. Approximately 14,000 Level 2 EVSE and fast chargers, along with approximately 8,000 Nissan Leafs and Chevrolet Volts are being deployed in the major population areas of:

- Phoenix and Tucson, Arizona
- San Diego, San Francisco and Los Angeles, California
- Portland, Eugene, Salem and Corvallis, Oregon

- Nashville, Knoxville and Memphis, Tennessee
- Dallas, Fort Worth and Houston, Texas
- Washington, D.C.

The project intent is to deploy Level 2 EVSE in the residents of each Leaf or Volt purchaser, and Level 2 EVSE and fast chargers in public locations in order to characterize charging infrastructure and vehicle use in diverse topographic and climatic conditions, evaluate the effectiveness of public versus private charge infrastructure, and conduct trials of various revenue systems for public charge infrastructures.

As FY2011 ended, data had been collected from 2,801 Nissan Leaf battery electric vehicles (Figure 8), 21 Chevrolet Volt extended range electric vehicles, and 2,990 ECOtality EVSE were being operated (Figure 9) in six states and the District of Columbia. A total of 6.2 million test miles and 178,000 charging events have been documented on the Project Overview Report for the EV Project to date (http://avt.inel.gov/pdf/EVProj/EVProjOverviewQ32011.pdf).

For the Nissan Leafs, there is a complete elimination of in-vehicle use of petroleum for transportation. For the Volts, see the earlier section in this report on Volt testing which has a larger data set from which to discuss Volt fuel-use results. It should be noted that the reports only contain numbers of EV Project vehicles and charging infrastructure that have provided data to the INL at the end of FY 2011. Actually deployment numbers are actually higher.

The EV Project's Nissan Leaf summary report (http://avt.inel.gov/pdf/EVProj/EVProjNissanLeafQ32011.pdf) provides national and regional Leaf usage statistics for each reporting quarter and this data includes the national vehicle usage data seen in Table 4. Additional data for each region can be found in the same above PDF.

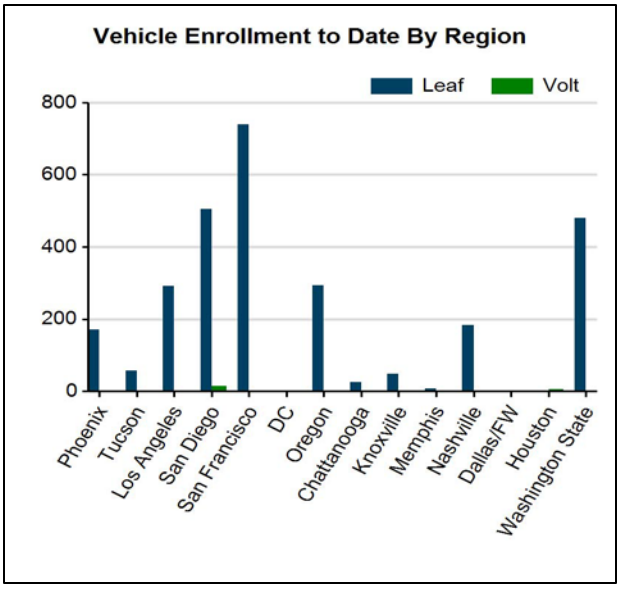

Figure 8. Number of EV Project vehicles providing data and deployment by major cities as of the end of FY 2011.

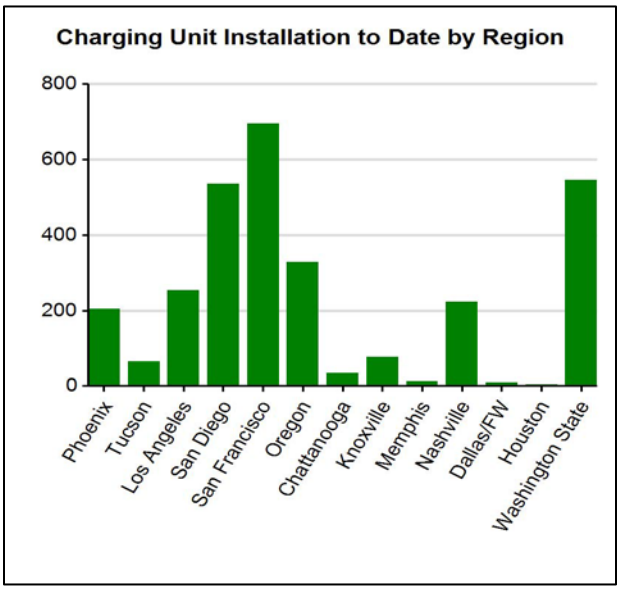

Figure 9. Number of EV Project EVSE deployed and providing data by major cities as of the end of FY 2011.

Figures 10 and 11 document the Nissan Leaf battery SOC before and after charging events. It will be interesting to see if SOC before-charging changes as operators become more familiar with the vehicles and if SOC at end-of-charging changes as drivers use public charging, including fast chargers for shorter periods of time.

Table 4. EV Project Nissan Leaf BEV usage data for the July 2011 to September 2011 quarter.

Number vehicles	2,394
Total miles	3,718,272
Average miles per trip	6.9
Average miles driven per day when driven	30.8
Average number trips between charge events	4.3
Ave miles driven between charge events	30.1
Ave number of charges per day when driven	1.0
Number of at home charging events	98,891
Number away from home charging events	19,219
Unknown charging event locations	5,485

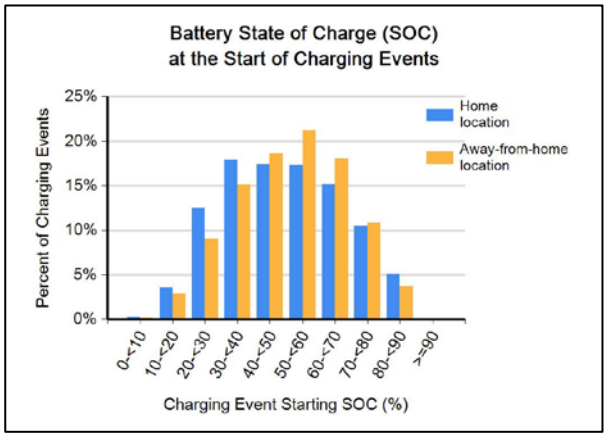

Figure 10. EV Project Nissan Leaf battery SOC at start of charging events.

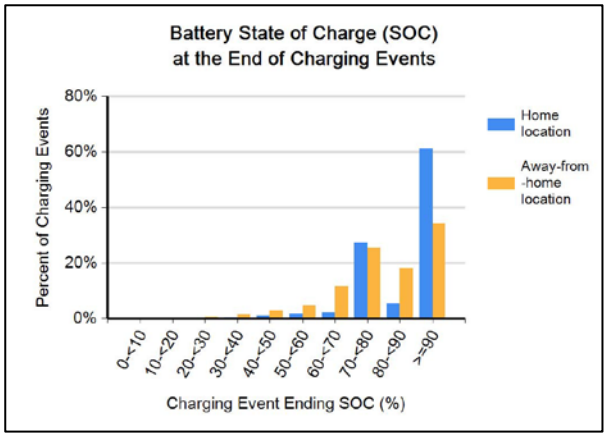

Figure 11. EV Project Nissan Leaf battery SOC at end of charging events.

The July – September 2011 quarterly Infrastructure Summary report documents infrastructure utilization nationally and regionally for residential Level 2 EVSE and publicly available Level 2 EVSE. As additional units are installed, this report will also include Fact Charge data as well as private access, nonresidential Level 2 EVSE. See: http://avt.inel.gov/pdf/EVProj/EVProjInfrastructureQ32011.pdf for the July - September 2011 report.

Figure 12 highlights the percent of all national Level 2 EVSE charging units in 15-minute increments with an EV Project vehicle connected during week days. Figure 13 is the charging profile in AC MWh for all Level 2 EVSE in the EV Project. Note the heavy use of post midnight charging.

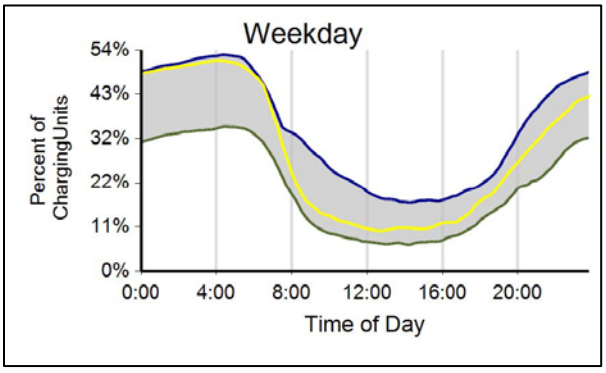

Figure 12. EV Project percent of all national Level 2 EVSE with a vehicle connected during weekdays. Data is in 15-minute increments for any time in the reporting quarter.

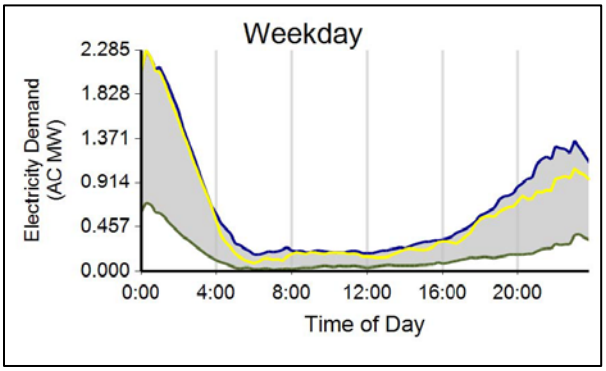

Figure 13. EV Project charging profile based on national energy demand for weekdays. Data is in 15-minute increments for any time in the reporting quarter.

Figure 14 documents the length of time vehicles are connected to residential EVSE. The two sets of peaks suggest short opportunity charging for less than one or two hours, and overnight charging for 10 to 14 hours. Figure 15 shows the same set of vehicles drawing power for much shorter periods of time than when they were connected as shown in Figure 14. Figure 16 matches Figure 15 as would be expected as the distribution of energy consumed would have a similar profile to the length of time the vehicles draw power.

Figure 17 is the charging profile for public access Level 2 EVSE as measured by the number of vehicles connected as a percent. Figure 18 documents a similar work day peak profile when vehicles are connected and start drawing power about 8 a.m. Note that the EVSE at ORNL heavily influences these profiles.

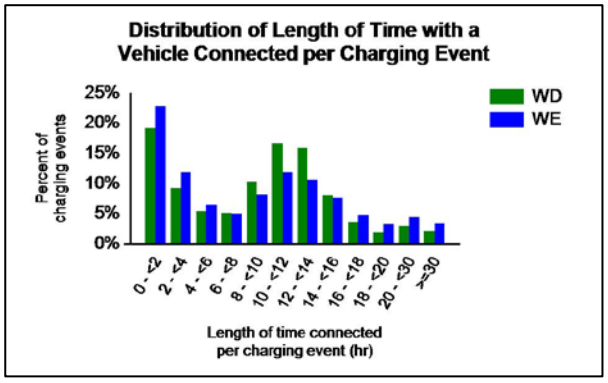

Figure 14. EV Project distribution of length of time with a vehicle connected per charging unit for residential Level 2 EVSE.

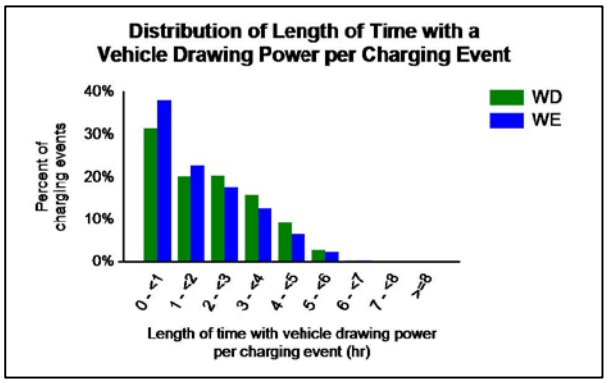

Figure 15. EV Project distribution of length with a vehicle drawing power per charging event for residential Level 2 EVSE.

The EV Project will continue accumulating both vehicle and EVSE data, with the first fast chargers coming on line as FY 2011 ended. As FY 2011 ended, more than one-half a million miles of data was being collected weekly.

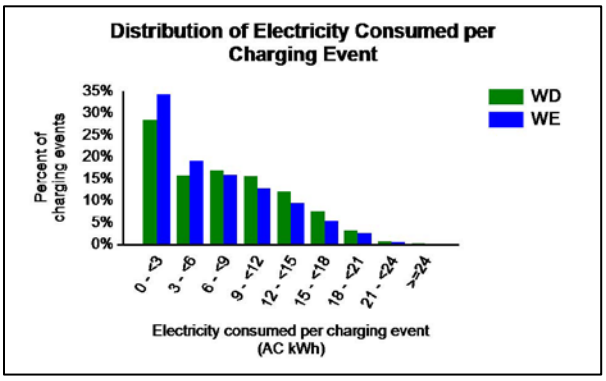

Figure 16. EV Project distribution of electricity consumed per charging event for residential Level 2 EVSE.

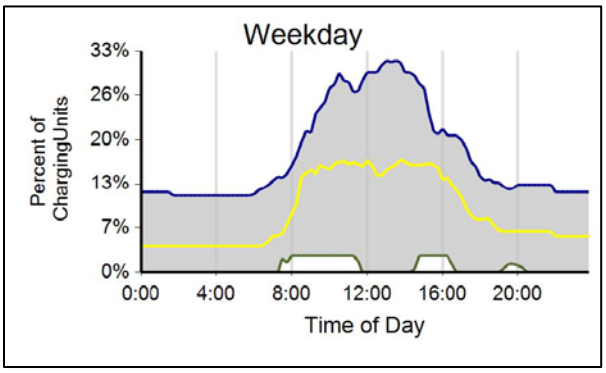

Figure 17. EV Project percent of all publicly available Level 2 EVSE with a vehicle connected during weekdays. Data is in 15-minute increments for any time in the reporting quarter.

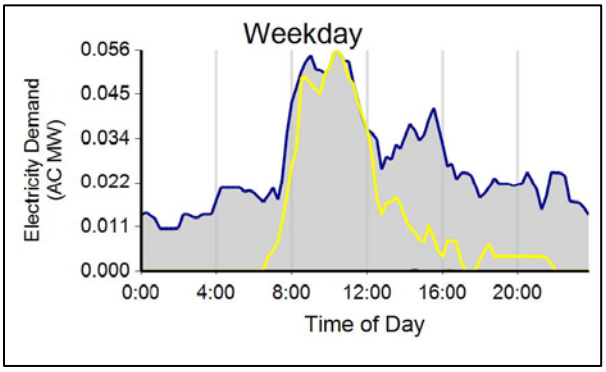

Figure 18. EV Project publicly available Level 2 EVSE charging profile based on energy demand for weekdays. Data is in 15-minute increments for any time in the reporting quarter.

ChargePoint America (Coulomb) EVSE Project

The ChargePoint America project is a DOE funded ARRA project for deploying and testing PEV recharging infrastructure. Lead by Coulomb, it will deploy approximately 4,500 Coulomb EVSE. At the end of August 2011, data had been collected from 893 EVSE, with most deployed in California (Figure 19). The May to August 2011 report documents 36,211 charging events and the use of 237 AC MWh and 39,000 charge events in twelve states. (http://avt.inel.gov/pdf/evse/CoulombMay11-Aug11.pdf) Note that there is no vehicle data as part of this project.

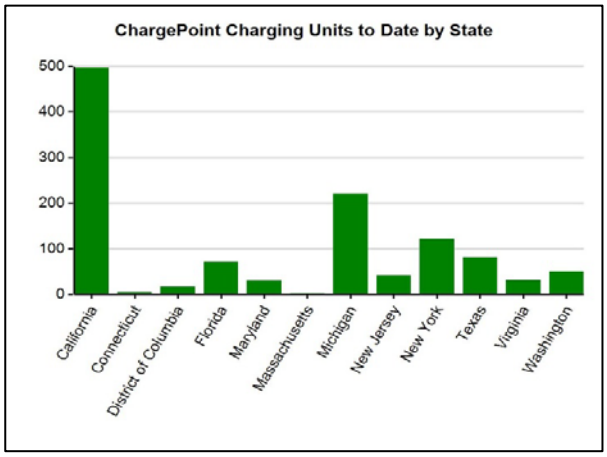

Figure 19. ChargePoint America EVSE deployments as of August 2011.

USPS eLLV Testing Support

DOE, through the AVTA, has been supporting the U.S. Postal Services (USPS) electric long-life vehicle (eLLV) procurement and testing regime by performing baseline performance testing on five conversions of LLVs into eLLVs. The support also includes onboard data collection instrumentation and the documentation of vehicle use in a mail delivery fleet demonstration.

Fact sheets that document baseline performance testing and monthly fleet demonstration results can be found at: http://avt.inel.gov/fsev.shtml.

All five conversion eLLVs met the minimum requirements of the baseline performance testing. However, the fleet demonstration has resulted in less than stellar delivery fleet mileage accumulations as various problems have been encountered with the vehicles.

DOD / DOE MOU Support

During July 2010, DOE and the U.S. Department of Energy signed the Memorandum of Understanding (MOU) "Concerning Cooperation in a Strategic Partnership to Enhance Energy Security", which covers several energy efficiency areas, including transportation, fueling and grid issues. In support of the MOU, the AVTA has initiated a Micro Climate study at Joint Base Lewis McCord in Tacoma Washington. This study takes into account traffic patterns, attractions, transportation hubs, and existing and potential electric infrastructure and charging locations. A subset of the Base's vehicle fleet will also be instrumented to document mission profiles. This work will support the future deployment of charging infrastructure and EDVs on the DOD base. Other bases were under consideration for study as FY 2011 ended.

In addition, the AVTA has initiated support to Andrews Air Force Base for the deployment of PEVs by designing EVSE deployment options.

Codes and Standards for Electric Drive Vehicles

In cooperation with DOE's AVTA, the American National Standards Institute (ANSI) conducted a workshop to examine the standards, codes, conformance programs and education initiatives needed to drive the widespread deployment of EDVs. The overall conclusion was a call for better coordination and harmonization of standardization efforts and the need for a private-public partnership to more this work quickly forward. The workshop report can be found on the workshop webpage: http://www.ansi.org/meetings_events/events/2011/electric_drive_vehicles_workshop.aspx?menuid=8.

As a result, ANSI, supported by the AVTA, formed the Electric Vehicles Standards Panel (EVSP). As FY 2011 ended, the EVSP was working with the many organizations under its codes and standards umbrella, as well as

government groups, to produce a strategic roadmap to define the standards and conformity assessment programs that are needed to accelerate the deployment of PEVs.

III.E.3. Products

Publications

Previous annual reports have identified AVTA's baseline performance testing procedures, vehicle specifications, and testing and demonstration results reports and fact sheets. All of these documents can be found at: http://avt.inl.gov/ and http://www.eere.energy.gov/vehiclesandfuels/avta/light_duty/hev/hev_reports.shtml. The PEV reports published and formal presentations that occurred during FY 2011 are listed below.

1. T. Murphy. July 2011. *Plug-In Electric Vehicle Demonstration Project Status*. Portland, OR. INL/CON-11-22666
2. K. Morrow. September 2011. *Vehicle to Electric Vehicle Supply Equipment Smart Grid Communications Interface Research and Testing Report*. Idaho Falls, ID. INL/EXT-22-23221.
3. J.E. Francfort. November 2010. *INL Electric Drive Vehicle Testing Activities for the ASME – Boise, Idaho*. Boise, ID. INL/MIS-10-19891.
4. J.E. Francfort. October 2010. *DOE / FreedomCAR Directors INL Visit. Advanced Vehicle Testing Activity - Vehicle and Infrastructure Testing and Data Collection*. Idaho Falls, ID. INL/MIS-10-20053.
5. J.E. Francfort. February 2011. *ASME Treasure Valley Section – Electric Drive Vehicles and Infrastructure Overview.* Boise, ID. INL/MIS-10-20383.
6. J.E. Francfort. November 2011. *AVTA FY 2010 Annual Program Report.* Idaho Falls, ID. INL/MIS-10-20477.
7. J.E. Francfort. November 2011. *Alabama Clean Cities Coalition – Electric Drive Vehicles, Charging Infrastructure and ARRA Projects Overview.* Idaho Falls, ID. INL/MIS-10-20557.
8. J.E. Francfort. February 2011. *Electric Vehicle Charging Levels and Requirements Overview.* Idaho Falls, ID. INL/MIS-10-20653.
9. R.B. Carlson. March 2011. *EDAB Project and USPS eLLV Testing- Merit Review 2011.* Washington, D.C. INL/MIS-11-21291.
10. M.G. Shirk. March 2011. *Plug-In Electric Vehicles: Motivation and Progress*. Idaho Falls, ID. INL/MIS-11-21325.
11. J.E. Francfort. May 2011. *Advanced Vehicle Testing Activity – Testing Background and EERE / FEMP Sponsored Federal Fleet characterization Activities*. Washington, D.C. INL/MIS-11-22058.
12. J.E. Francfort. May. *DOE's Advanced Vehicle Testing Activity – ECOtality's EV Project and other Electric Drive Data Collection and Testing Activities*. Idaho Falls, ID. INL/MIS-11-22085.
13. J.E. Francfort. May 2011. *Electric Drive Vehicles – INL Retired Employees' Association*. Idaho Falls, ID. INL/MIS-11-22115.
14. J.E. Francfort. June 2011. *ARRA / TADA Light-Duty Electric Drive Vehicle and Charging Infrastructure Deployment Activities, Data Collection and Reporting*. Golden, CO. INL/MIS-11-22237.
15. J.E. Francfort. July 2011. *Clean Cities 2011 Stakeholders Summit – Electric Drive Vehicles and Charging Infrastructure Demonstrations, Analysis and Lessons Learned*. Detroit, MI. INL/MIL-11-22496.
16. J.E. Francfort. August 2011. *U.S. / China 2011 Workshop – INL / DOE Plug-in Electric Vehicle and Charging Infrastructure Demonstrations and Reporting*. Chicago, IL. INL/MIS-1-22836.
17. J.G. Smart. August 2011. *A First Look at Electric Vehicle Charging Behavior and Impacts on the Electric Grid in the EV Project. Detroit*, MI. INL/CON-11-22696.
18. J.G. Smart. January 2011. *Annual AVTA / EV Project Review (Jan 2011 Phoenix).* Phoenix, AZ. INL/MIS-11-20831.

19. J.G. Smart. April 2011. *EV Project Overview Report.* Idaho Falls, ID. INL/MIS—11-21898.
20. J.G. Smart. April 2011. *Nissan Leaf EV Project*. Idaho Falls, ID. INL/MIS-11-21904.
21. R.B. Carlson. July 2011. *Plug-In Hybrid Electric Vehicle On-road Results from DOE's Technology Acceleration and Deployment Activity*. Idaho Falls, ID. INL/CON-11-22722.
22. M.G. Shirk. August 2011. *Chrysler RAM PHEV Fleet*. Idaho Falls, ID. INL/MIS-11-22875.
23. M.G. Shirk. March 2011. *Plug—IN Electric Vehicles: Motivation and Progress*. Seattle, WA. INL/MIS-11-21325.
24. M.G. Shirk. January 2011. *2010 Analysis for Seattle PHEV Committee*. Seattle, WA. INL/MIS-11-20852.
25. B.R. Stone. September 2011. *Route Type Determination Analysis.* Idaho Falls, ID. INL/EXT-11-23204.
26. R.B. Carlson. March 2011. *2010 Ford Escape PHEV_PHEV America Datasheet.* Idaho Falls, ID. INL/MIS-11-21383.
27. R.B. Carlson. March 2011. *USPS eLLV Fleet Monthly Summary Report.* Idaho Falls, ID. INL/MIS-11-21835.
28. M.L. Kirkpatrick. April 2011. *Creating Plug-in Hybrid Electric Vehicle (PHEV) Locations using ArcMap*. Idaho Falls, ID. INL/MIS-11-21900.
29. R.B. Carlson. September 2011. *EV Charging Systems Testing Overview.* Idaho Falls, ID. INL/MIS-11-23470.
30. B.R. Stone. July 2011. *City or Highway – Vehicle Route Type Determination.* Idaho Falls, ID. INL/MIS-11-22691.

III.F. Hybrid Electric Vehicle (HEV) Testing by DOE's Advanced Vehicle Testing Activity (AVTA)

James Francfort (Principal Investigator), Timothy Murphy (Project Leader)
Idaho National Laboratory
P.O. Box 1625
Idaho Falls, ID 83415-2209
(208) 526-6787; james.francfort@inl.gov

DOE Program Manager: Lee Slezak
(202) 586-2335; Lee.Slezak@ee.doe.gov

III.F.1. Abstract

Objective

- Benchmark hybrid electric vehicle (HEV) petroleum reductions, component performance, maintenance requirements, battery performance, and life-cycle costs.
- Provide HEV testing results to vehicle modelers, DOE, the general public, and technology target setters.
- Eliminate any uncertainties about HEV battery life.

Approach

- Perform baseline performance testing on 22 HEV models and 56 HEVs to date.
- Operate at least two of each HEV model over 36 months to accumulate 160,000 miles per vehicle in fleets to obtain fuel economy, maintenance, operations, battery life and performance, and other life cycle related vehicle data under actual road conditions.
- Test HEV batteries when new and at 160,000 miles.

Accomplishments

- Accelerated testing for the HEV fleet, consisting of 56 individual HEVs and 22 HEV models, exhibited varying fuel economies that ranged from 17.9 mpg for the Chevrolet Silverado to 44.2 for the second and third generation Toyota Prius. The second generation Honda Insight was averaging 40.1 mpg.
- As of the end of FY 2011, 6.1 million HEV test miles have been accumulated.
- Provided HEV testing results to the automotive industry, DOE, and other national laboratories via the DOE Vehicle Technologies Program's Vehicle Simulation and Analysis Technical Team.
- Future Activities
- Benchmark new HEVs available during FY 2011, including new HEVs with advanced batteries and start-stop control technologies.
- Ascertain HEV battery life by accelerated testing at the end of 160,000 miles.
- Continue testing coordination with industry and other DOE entities.

III.F.2. Technical Discussion

Introduction

Today's light-duty HEVs use a gasoline internal combustion engine (ICE), electric traction motors or electric stop-start technology, along with less than 2000 watt-hour (Wh) of onboard energy storage to increase petroleum efficiency as measured by higher mpg results compared to non-HEV models. HEVs are never connected to the grid for charging the battery. The HEV batteries are charged by an onboard ICE-powered generator, as well as by regenerative braking systems.

In addition to providing benchmark data to modelers and technology target setters, the AVTA benchmarks and tests HEVs to document petroleum reduction, maintenance requirements, and life-cycle costs. The AVAT also provides testing results to the public and fleet managers. In addition to the 19 traditional HEVs that have been tested, the AVTA is also testing three micro-hybrid vehicle models (MHV) and these are discussed as part of the HEVs.

Approach

As of the end of FY 2011, AVTA has performed, or is performing testing on 56 HEVs, comprised of 22 HEV models. The HEV models and number of each model tested are listed below:

Generation (Gen) I Toyota Prius - 6
Gen II Toyota Prius - 2
Gen I Honda Insight - 6
Honda Accord - 2
Chevrolet Silverado - 2
Gen I Honda Civic - 4
Gen II Honda Civic - 2
Ford Escape - 2
Lexus RX400h - 3
Toyota Highlander - 2
Toyota Camry - 2
Saturn Vue - 2
Nissan Altima - 2
Chevrolet Tahoe - 2
Gen II Honda Insight - 2
Gen III Toyota Prius - 2
Ford Fusion - 2
Mercedes S400 – 2
Honda CRZ – 2
Smart Fortwo Pure Coupe (MHV) – 3
MAZDA 3 Hatchback (MHV) - 2
Volkswagen Golf TDI (MHV) - 2.

As of the end of FY 2011, the 56 HEVs had accumulated 6.1 million total accelerated and fleet test miles (Figure 1). During FY 2011, the HEVs accumulated a total of 862,000 test miles, averaging 72,000 test miles per month (Figure 2).

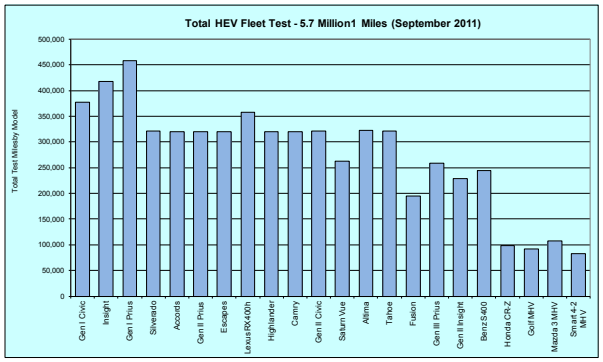

Figure 1. Total HEV test miles by vehicle model..

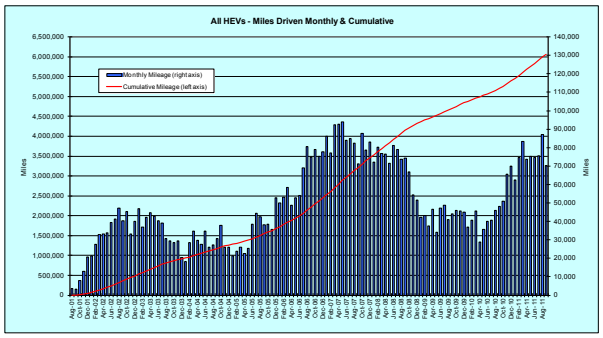

Figure 2. Total and monthly HEV test miles by all models.

The average fuel use per HEV model since testing started ranges from 17.9 mpg for the Silverado to 45.2 mpg for the Gen I Honda Insight (Figure 3). However, among the more recent HEV models the mpg has ranged from 25.8 mpg for the Mercedes S400 to 44.2 mpg for the Generation III Prius (Table 1).

The AVTA continues to collect data that allows it to publish several fact sheets for each HEV (see: http://avt.inel.gov/hev.shtml), including:

- Maintenance Fact Sheet - mileage, date, maintenance event, cost for repair, or if under warranty
- Fleet Testing Summary Fact Sheet – includes operating costs based on purchase, residual, maintenance and operating costs (insurance, fuel and registration), monthly and cumulative mpg, and monthly mileage accumulation.

- Battery Fact Sheets and Testing Reports for when the vehicles are new and at 160,000 miles.
- Fleet Testing Results to date Fact Sheet which is discussed in greater detail below.

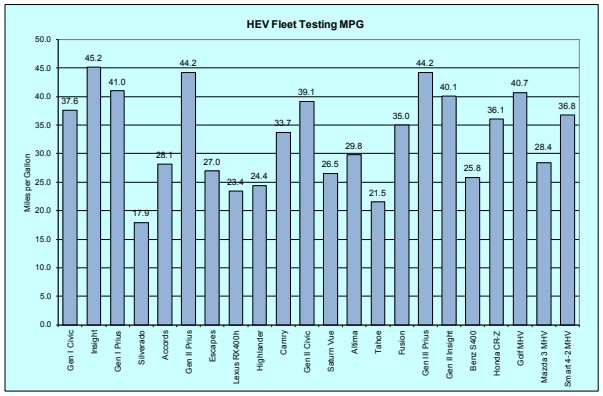

Figure 3. HEV mpg by model.

Table 1. Onroad accelerated testing mpg for the most recent HEV test models, including the micro hybrid vehicles (MHVs) from Europe.

HEV Model	Onroad MPG
Fusion	35.0
Gen III Prius	44.2
Gen II Insight	40.1
Benz S400	25.8
Honda CR-Z	36.1
Golf MHV	40.7
Mazda 3 MHV	28.4
Smart 4-2 MHV	36.8

More recent advances in data collection techniques and costs have allowed the AVTA to provide the more complete analysis of HEV operations as can be found on the Fleet Testing Results to Date Fact Sheet and examples are provided in the next paragraphs for the Generation III Prius.

Figure 4 shows that the Prius gasoline engine is stopped 34% of the time when the vehicle is either moving or stopped. Minimizing ICE operations at least partially contributes to the Prius achieving between 45 and 55 mpg at least half of the time as measured by the percentage of the miles driven (Figure 5).

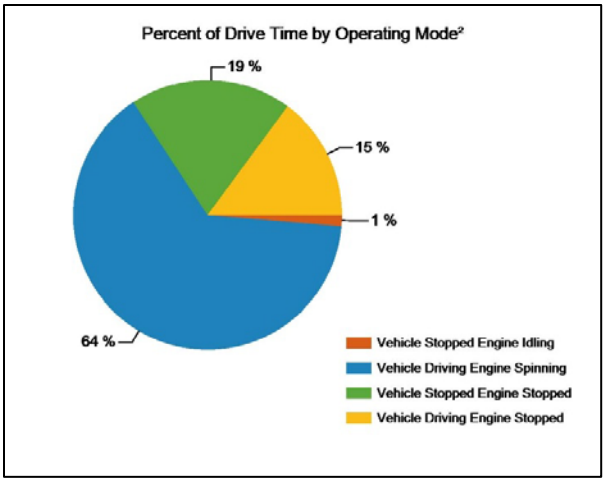

Figure 4. Generation III Prius HEV engine operating mode.

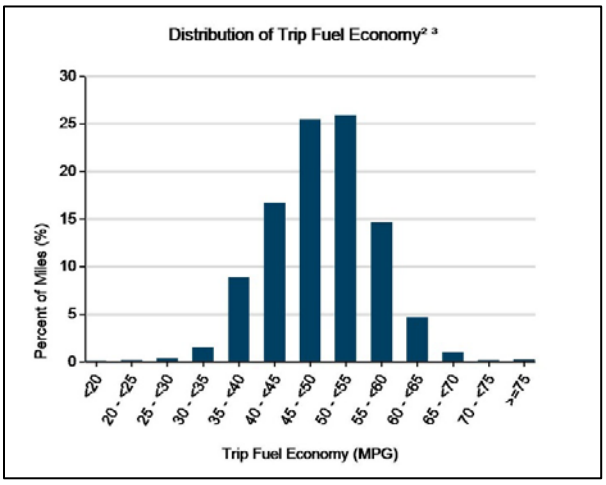

Figure 5. Generation III Prius HEV mpg by percent of miles driven.

Figure 6 clearly documents the vehicle speeds the Prius should be operated at by fleets and private operators seeking to maximize petroleum reduction. However, safe operations should be the primary consideration over operating speed. As seen, the Prius has been averaging nearly 60 mpg when driven at vehicle speeds of 40 to 50 mph.

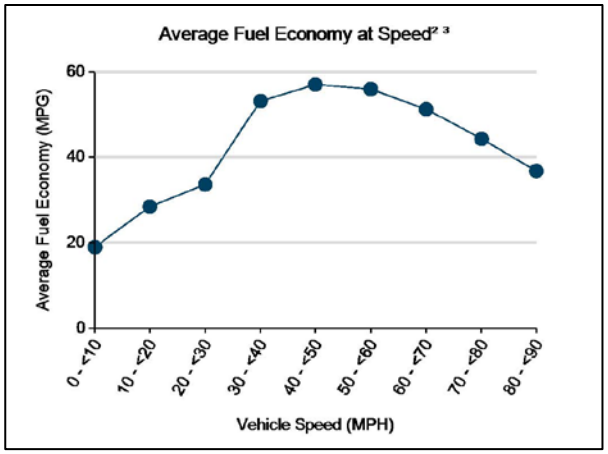

Figure 6. Generation III Prius HEV average mpg at various vehicle speeds.

Ambient temperature also has an impact on mpg. As seen in Figure 7, there is significant decrease in mpg at colder temperatures, especially below refreezing.

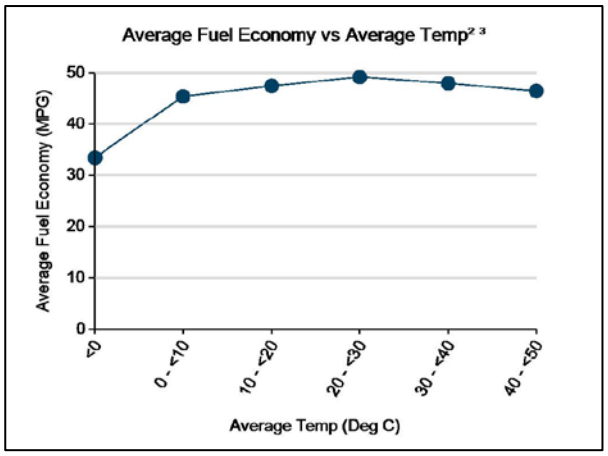

Figure 7. Generation III Prius HEV

Figures 8 and 9 document vehicle operations by both the percent of miles driven are various vehicle speeds (Figure 8) and the percent of trip distances by trip miles (Figure 9).

In addition to the above mpg and vehicle operations profiles, data is also collected on battery use. Figure 10 shows the battery current in amp-hours during battery assistance and regenerative breaking.

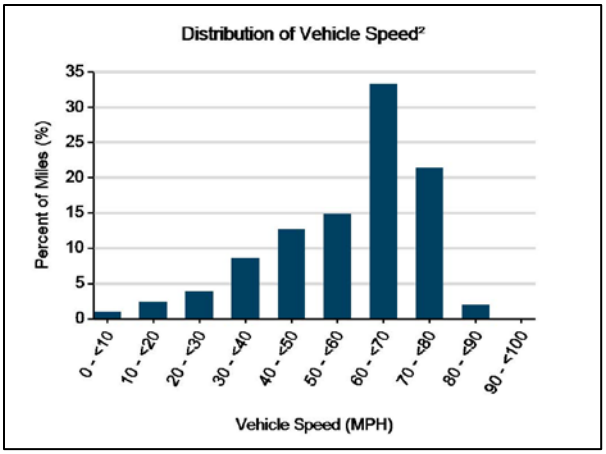

Figure 8. Generation III Prius HEV distribution of vehicle operating speed in fleet testing.

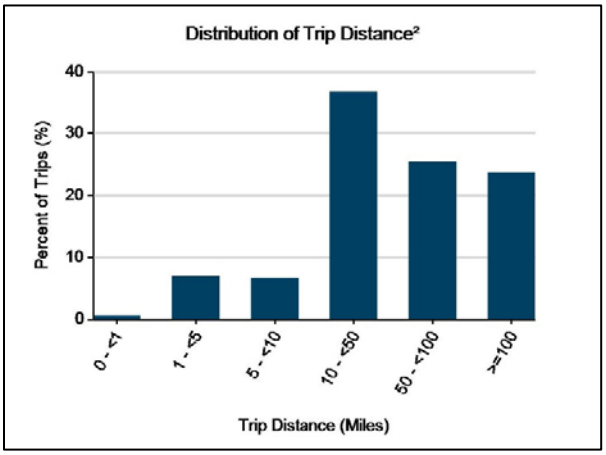

Figure 9. Generation III Prius HEV distribution of vehicle trip distances in fleet testing.

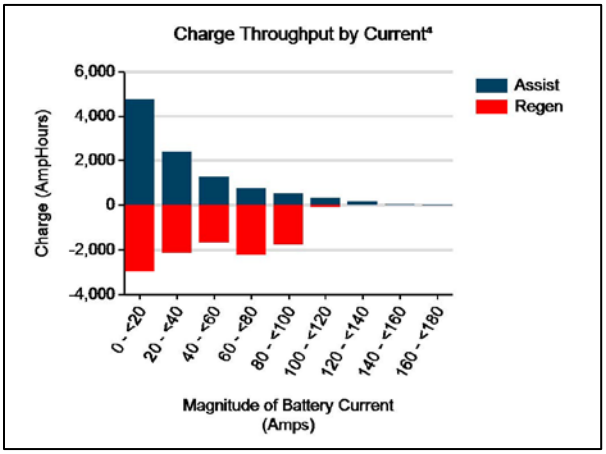

Figure 10. Generation III Prius HEV traction battery throughput by current.

Battery pack charge throughput by battery temperature is documented in Figure 11. Figure 12 shows the significantly higher amount of assistance in amp-hours per mile at various speeds, with the lowest speeds having the largest difference as the vehicle accelerates from zero or very low mph.

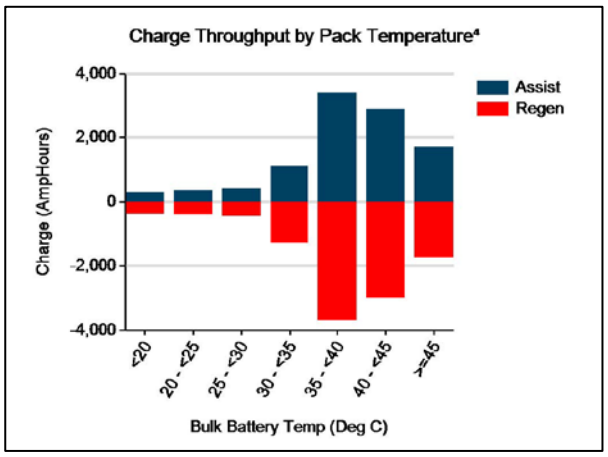

Figure 11. Generation III Prius HEV battery charge throughput by pack temperature.

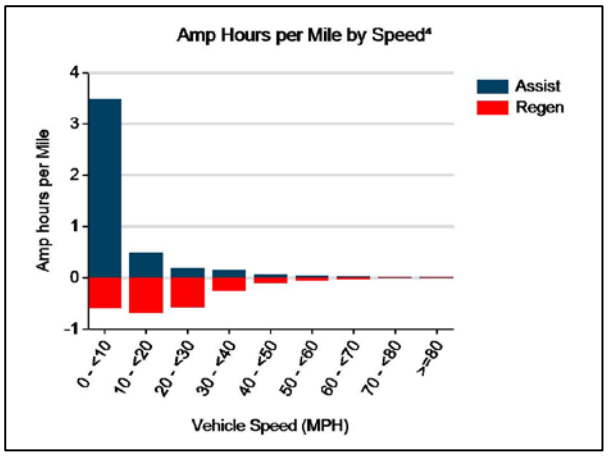

Figure 12. Generation III Prius HEV amp hours per mile by speed.

At the end of FY 2011, the AVTA had published 24 HEV battery tests for when vehicles were new or at 160,000 miles and these can be found at http://avt.inl.gov/hev.shtml

AVTA has partnered with private fleets to conduct the high mileage HEV testing. All 6.1 million HEV test miles have been accumulated with no driver costs to DOE. In addition, several of the HEV models get secondary test value after completing the 160,000 miles of HEV testing. Oak Ridge and Argonne National Laboratories have purchased several used HEVs and they use the HEV power electronics subsystems and other subsystems for end-of-life testing. The EPA has also purchased several HEVs at vehicle testing completion so they can conduct their own end-of-life testing to support their HEV life-cycle models.

New HEVs available from U.S., Japanese, and European manufacturers will be benchmarked during FY 2012. These will introduce advanced technologies such as lithium or advanced lead acid designs. Most new HEVs will be tested to reduce uncertainties about HEV technologies, especially the life and performance of their batteries, and any other onboard energy storage systems, and unique start/stop strategies. Just one example of this is Mazda 3's unique top-of-piston-cylinder-compression restart scheme. While the Mercedes S400 is the first HEV in the United States with a lithium battery, it is anticipated battery chemistries other than NiMH will arrive with new HEV models.

III.F.3. Products

Publications

More than 200 HEV baseline performance, fleet, and accelerated testing fact and maintenance sheets, reports, and presentations have been generated by AVTA and all are available on the AVTA's Web pages. The HEV baseline performance testing procedures and vehicle specifications were also updated and republished on the AVTA's Web pages. The 31 new or updated with additional data reports, papers, fact sheets and presentations published during FY 2011 are listed below.

In addition to the below testing fact sheets, reports, and papers, the maintenance requirements and fuel use fact sheets are generated every three months for all of the HEVs. All of these documents can be found at: http://avt.inl.gov/hev.shtml and http://www.eere.energy.gov/vehiclesandfuels/avta/light_duty/hev/hev_reports.shtml.

1. J.E. Francfort. March 2010. AVTA HEV, NEV, and BEV Demonstrations and Testing (DOE FY10 Merit Review). INL/CON-11-21375. Washington, DC.
2. J.E. Francfort. June 2011. Comparing Energy Costs per Mile for Electric and Gasoline-Fueled Vehicles. Idaho Falls, ID. INL/MIS-11-22482.
3. M.G. Shirk. June 2011. HEV Fleet Testing Results to Date. Idaho Falls, ID. INL/MIS-11-22189.
4. 2011 Honda CRZ VIN 2982 Baseline Performance Testing Fact Sheet. http://avt.inel.gov/pdf/hev/fact2011hondacrz.pdf
5. 2011 Honda CRZ HEV Accelerated Testing Fuel Use. http://avt.inel.gov/pdf/hev/hondacrz_ar.pdf
6. 2011 Honda CRZ VIN 2982 Fleet Testing Fact Sheet. http://avt.inel.gov/pdf/hev/2011crz_2982_Oct2011.pdf
7. 2011 Honda CRZ Vin 2982 Fact Sheet. http://avt.inel.gov/pdf/hev/2982HondaCRZ11factsheet.pdf
8. 2011 Honda CRZ VIN 2982 Maintenance History http://avt.inel.gov/pdf/hev/ms_2982_2011_honda_crz.pdf
9. 2011 Honda CRZ VIN 4466 Fleet Testing Fact Sheet. http://avt.inel.gov/pdf/hev/2011crz_4466_Oct2011.pdf
10. 2011 Honda CRZ Vin 4466 Fact Sheet. http://avt.inel.gov/pdf/hev/4466HondaCRZ11factsheet.pdf
11. 2011 Honda CRZ VIN 4466 Maintenance History http://avt.inel.gov/pdf/hev/ms_4466_2011_honda_crz.pdf

In addition to the above new fact sheets, the below fact sheets were updated during FY 2011.

12. 2010 Mercedes Benz S400 VIN 5883 Fleet Testing Fact Sheet http://avt.inel.gov/pdf/hev/5883MercedesBenz10factsheet.pdf
13. 2010 Mercedes Benz S400 VIN 5883 Maintenance History http://avt.inel.gov/pdf/hev/ms_5883_2010_mercedes_benz.pdf
14. 2010 Toyota Prius VIN 0462 Baseline Performance Testing Fact Sheet. http://avt.inel.gov/pdf/hev/fact2010toyotaprius.pdf
15. 2010 Toyota Prius HEV Accelerated Testing Fuel Use. 1. http://avt.inel.gov/pdf/hev/toyotapriusIII_ar.pdf
16. 2010 Toyota Prius VIN 0462 Fleet Testing Fact Sheet http://avt.inel.gov/pdf/hev/0462ToyotaPrius10factsheet.pdf
17. 2010 Toyota Prius VIN 0462 Maintenance History http://avt.inel.gov/pdf/hev/ms_0462_2010_toyota_prius.pdf
18. 2010 Toyota Prius VIN 6063 Fleet Testing Fact Sheet http://avt.inel.gov/pdf/hev/6063ToyotaPrius10factsheet.pdf
19. 2010 Toyota Prius VIN 6063 Maintenance History http://avt.inel.gov/pdf/hev/ms_6063_2010_toyota_prius.pdf
20. 2010 Ford Fusion VIN 4757 Baseline Performance Testing Fact Sheet. http://avt.inel.gov/pdf/hev/fact2010fordfusion.pdf
21. 2010 Ford Fusion HEV Accelerated Testing Fuel Use. http://avt.inel.gov/pdf/hev/fordfusion_ar.pdf
22. 2010 Ford Fusion VIN 4699 Fleet Testing Fact Sheet http://avt.inel.gov/pdf/hev/4699FordFusion10factsheet.pdf
23. 2010 Ford Fusion VIN 0462 Maintenance History http://avt.inel.gov/pdf/hev/ms_4699_2010_ford_fusion.pdf
24. 2010 Ford Fusion VIN 4757 Fleet Testing Fact Sheet http://avt.inel.gov/pdf/hev/4757FordFusion10factsheet.pdf

25. 2010 Ford Fusion VIN 6063 Maintenance History http://avt.inel.gov/pdf/hev/ms_4757_2010_ford_fusion.pdf
26. 2010 Honda Insight VIN 0141 Baseline Performance Testing Fact Sheet. http://avt.inel.gov/pdf/hev/fact2010hondainsight.pdf
27. 2010 Honda Insight HEV Accelerated Testing Fuel Use. http://avt.inel.gov/pdf/hev/hondainsightII_ar.pdf
28. 2010 Honda Insight VIN 0141 Fleet Testing Fact Sheet http://avt.inel.gov/pdf/hev/0141HondaInsight10factsheet.pdf
29. 2010 Honda Insight VIN 0141 Maintenance History http://avt.inel.gov/pdf/hev/ms_0141_2010_honda_insight.pdf
30. 2010 Honda Insight VIN 1748 Fleet Testing Fact Sheet http://avt.inel.gov/pdf/hev/1748HondaInsight10factsheet.pdf
31. 2010 Honda Insight VIN 1748 Maintenance History http://avt.inel.gov/pdf/hev/ms_1748_2010_honda_insight.pdf

III.G. PHEV and Renewable Integration

Principal Investigator: Michael Kintner-Meyer
Pacific Northwest National Laboratory
P O Box 999, K1-85
Richland, WA 99352
509-375-4306, michael.kintner-meyer@pnnl.gov

DOE Program Manager: Lee Slezak

III.G.1. Abstract

Objective

- Investigate the capabilities of light duty electric vehicles to mitigate the additional balancing requirements associated with the addition of 10 GW of wind generation in the Northwest Power Pool

Approach

- Utilize additional balancing requirements for 2019 wind scenario from another DOE project
- Simulate vehicle population behavior using 2001 National Household Travel Survey (NHTS) driving patterns to determine the number of vehicles required to meet all of the new balancing requirements
- Examine impacts on results for various parameters such as public charging availability, V2GFull, charging levels, and battery size

Major Accomplishments

- Key results indicate the significant resource potential of the emerging electric vehicle fleet in providing balancing services to integrate the growing wind energy capacity.
- Study provided significant insights into the value of smart charging versus vehicle to grid application, the influence of charging levels, battery size and availability of public charging infrastructure.
- Study showed that a relatively small percentage of public charging available (10%) could provide 80% of the benefits of electric vehicle providing grid support. This is an important finding as the question of the size of the public charging infrastructure is being discussed.
- Key findings of this study were presented by DOE/Office of Electricity's Office Director

Future Activities

- Expand study to
  - Rooftop solar technology integration and the role of PHEVs
  - Compare the resource potential of PHEVs to that of stationary energy storage system

III.G.2. Technical Discussion

Background

Many states are deploying renewable generation sources at a significant rate to meet renewable portfolio standards. As part of this drive to meet renewable generation levels, significant additions of wind generation are planned. Due to the highly variable nature of wind generation, significant energy imbalances on the power system can be created and need to be handled. This project examined the impact on the Northwest Power Pool (NWPP) region for a 2019 expected wind scenario. One method for mitigating these imbalances is to utilize plug-in hybrid electric vehicles (PHEVs) or battery electric vehicles (BEVs) as assets to the grid.

PHEVs and BEVs have the potential to meet this demand through both charging and discharging strategies. This report explores the usage of two different charging schemes: V2GHalf (sometimes called G2V) and V2GFull. In V2GHalf, PHEV/BEV charging is varied to absorb the additional imbalance from the wind generation, but never feeds power back into the grid. This scenario is highly desirable to automotive manufacturers, who harbor great concerns about battery warranty if vehicle-to-grid discharging is allowed. The second strategy, V2GFull, varies not only the charging of the vehicle battery, but also can vary the discharging of the battery back into the power grid. This scenario is currently less desirable to automotive manufacturers, but provides an additional resource benefit to PHEV/BEVs by theoretically doubling their capacity value to the grid.

Under these two different charging strategies, electric vehicles have great potential to help integrate renewable generation technologies. Through grid friendly charging, the strategies can meet the additional balancing energy requirements required by the introduction of a significant amount of wind generation.

Introduction

Renewable generation sources are being deployed at a significant rate. The primary driver of the deployment comes from mandated renewable or alternative energy portfolio standards law in 36 states and the District of Columbia [1]. Of all of the renewable generation sources, wind is expected to be most significant component of the new capacity.

One challenge of wind and solar generation sources is the variability in the output [2]. Lulls in the wind and clouds across the photovoltaic panel can significantly reduce the output of such generation sources. Conversely, a sudden gust of wind can create an excess energy output from the resource. These fluctuations can have significant impacts on the power system [3-5]. To stabilize and mitigate these fluctuations, flexible hydro units and combustion turbines are customarily utilized. Energy storage and demand response resources have been more recently discussed as a viable technology solution [6,7].

One method for mitigating the additional variability associated with renewable generation sources is through electric vehicle charging that utilizes varying control of the charge rate in response to grid needs. Many approaches to this problem exist, including centralized and decentralized control schemes [8-10]. Utilizing an autonomous, decentralized control scheme developed at the Pacific Northwest National Laboratory in 2009, various parameters of an electric vehicle population's charging were adjusted to examine their impact on aiding in integrating renewable generation sources.

Approach

The simulation results for this study were centered around the behavior of a 1000-vehicle population randomly selected from a larger population provided by the 2001 National Household Travel Survey. The vehicle population responded to the same grid imbalance data for all different charging scenarios examined.

The additional energy requirements associated with the 2019 wind scenario were obtained from [11]. This signal underwent a simple transformation to change the varying power levels into a grid frequency term. A subset of this new frequency signal is shown in Figure 1. The values obtained represent only the additional balancing energy requirements for the wind generation, and neglect other influences on this portion of the power grid.

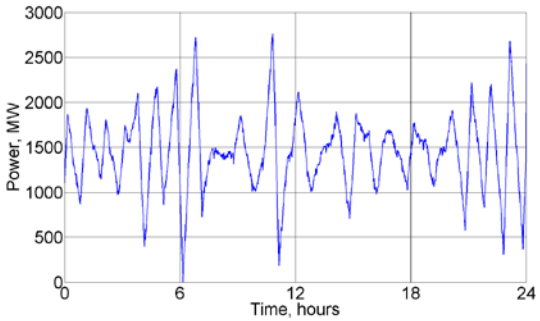

Figure 1. Additional Balancing Energy Requirements for 2019 Wind Scenario

The vehicles of the population utilized drive cycles and energy requirements (in terms of distance) obtained from the 2001 National Household Travel Survey data [12]. Sizing characteristics, such as battery size and drivetrain efficiency, were obtained from [13,14]. Each vehicle was simulated individually and responded independently of all other vehicles. Each vehicle also managed its own individual battery energy levels (state-of-charge) to ensure the behavior was as representative of a true vehicle as possible.

Results

The results of the study can be summarized as follows:

1. The study revealed a significant potential of the emerging electric vehicle fleet toward meeting some of the growing balancing services that grid operators will need to harness the fluctuations in the production of wind energy technologies. While a V2GFull operating mode may have some market acceptance barriers to overcome, V2GHalf would not be encumbered with these issues. V2GHalf strategies only require a modulation of the charging current without violating the users' desire to have the battery fully charged at a certain time.

If about 13% of the existing light-duty vehicle stock (about 2.1 million vehicles) were PHEVs with a 33-mile electric range and applied V2GHalf charging strategies at home and at work, all of the additional balancing requirements of to integrate 10 GW of additional wind power (from 3.4 GW in 2008). (See Table 1).

2. A comparison between V2GFull and V2GHalf confirmed that the individual larger capacity that V2Gfull service offers to the grid, which is theoretically double the capacity of V2GHalf, requires a smaller number of vehicles to meet the additional balancing constraints. The V2GFull service requires, on average, about 30 to 35% fewer vehicles than the V2GHalf approach, across all scenarios.

3. The results are relatively insensitive to the charging level. A comparison between Level 1 and Level 2 charging revealed very little differences. This suggests that the apparent advantage of higher electricity demand of Level 2 charging (3.3 kW) compared to Level 1 charging (1.7 kW), does not reduce the number of vehicles to meet the balancing requirements in the proportion of the charging limits.

4. The results indicate a strong relationship of the charging station availability throughout the day (referred to as "charging at work") on the total number of vehicles required to meet the balancing requirements. The results reveal a behavior of diminishing returns after the vehicle stock is offered a certain amount of charging stations at work. Almost 80% of the improvements by offering public charging stations at work can be achieved with about 10% of public stations (i.e., a public to residential charging station ratio of 1:10). Results of number of vehicles required to meet the balancing requirements is shown as a function of availability of public charging stations (Figure 2).

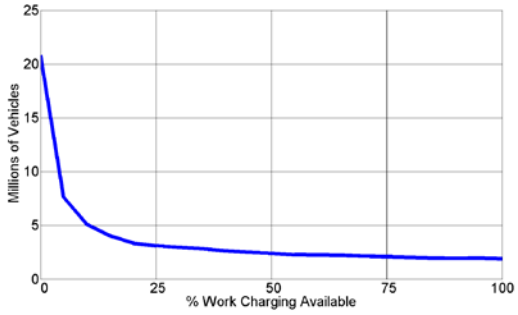

Figure 2. Population required to meet additional energy requirements as work charging availability varied

Table 1. Population of Vehicles Required to Meet Additional Balancing Requirements
(percentages are based on 16.5 million light-duty vehicles in NWPP)

Charging type	Battery Size Scenario				
	Stationary Storage	PHEV 33		PHEV 110	
		Home only	Home and Work	Home only	Home and Work
V2GHalf	-	29.7 mill (180%)	2.1 mill (13%)	20.8 mill (126%)	1.9 mill (12%)
V2GHalf and V2GFull	-	21.8 mill (132%)	1.6 mill (10%)	17 mill (103%)	1.4 mill (8%)
V2GFull	0.6 mill. (4%)	18.6 mill (113%)	1.4 mill (8%)	15.5 mill (94%)	1.3 mill (8%)

5. The size of the vehicle battery matters for supplying balancing services. For the home-only charging option, the larger battery (BEV) reduces the number of required vehicles in the range of 17% to 30% over that for a PHEV33, while for home and work charging options, the improvement potential is only between 7% and 10%.

6. A limiting case was defined that postulated that all electric vehicles be available 24 hours per day – 7 days a week performing V2GFull services. This limiting case is identical to a distributed stationary energy storage system dedicated to perform balancing services. For this limiting case, a total number of about 560,000 vehicles (4% of light-duty vehicle stock) would be necessary with a Level 2 (3.3 kW) charging/discharging technology to provide all of the additional balancing services.

Conclusions

The results indicate that the emerging electric vehicle fleet could make a substantial contribution toward meeting the new balancing requirements associated with the grid integration of growing wind technology deployment. To what degree this potential can be realized in the future will depend on the economics of the implementation and a viable and compelling business model either for the individual electric vehicle owner, or a third-party service provider. Other demand response technologies, particularly residential electric hot water heaters and large industrial customers, are likely to compete for the same market share. While several million hot water heaters are already installed in residential and commercial buildings, electric vehicles still have to prove their market acceptance. However, the international automotive industry has made significant investments in battery and electric vehicle technology, giving rise to the anticipation that electric vehicles will play a role as transportation means. With an optimistic outlook of future market adoption of PHEVs and EVs in the U.S., 10% of the light-duty vehicle stock could be achieved by about 2030 [15].

The analysis explored the incremental improvement of V2GFull over that of V2GHalf and found that improvement potential, in terms of less vehicles necessary for meeting the balancing requirements, are in the range of 30% to 35%. While this range is a significant improvement, the fact that currently all EV and PHEV manufacturers do not allow discharging the transportation battery into the grid without voiding the battery warranty may pose a significant barrier to this strategy, at least for the near-term. V2GHalf, which will never discharge the transportation battery for grid services, will circumvent the warranty issue. In fact, the current SAE standard J1772, which specifies the electric coupler for electric vehicle charging, provides the communication via the Control Pilot to change the rate at which the battery are

charged. Thus, this technology could be implemented in the near-term.

Furthermore, the results of this analysis provide a different perspective to the current discussion about the need and size of a public charging infrastructure. As discussed above, there is a strong diminishing-return relationship with an increase of non-residential charging stations. The study showed that with the first 10% of non-residential charging stations, 80% of the grid balancing value can be provided. These results are strongly dependent on the driving behavior and where and how often the vehicle is used. Unless the driving behavior will change significantly over the next decades, or a larger population will work at home or assume part-time employments, which in turn influences the driving behavior, the 2001 Department of Transportation Household Travel Survey used in this analysis may still provide a reasonable first starting point for this discussion. This result suggests that as long as the need for addressing the range anxiety and the need for charging access is not substantiated, the argument for a large size of non-residential charging infrastructure from a grid service perspective does not hold. A ratio of 1:10 (public to residential charging stations) would enable electric vehicles to provide grid services over a 24-hour period and substantially enhance their value to the grid, compared to charging vehicles only at home.

With ongoing DOE electric vehicle monitoring efforts, more insights into the driving and charging behaviors are expected to be forthcoming. With new data, the needs and value of public charging stations can be further analyzed and investigated.

References

1. Pew Center on Global Climate Change, "Renewable and Alternative Energy Portfolio Standards," February 11, 2011, Accessed March 9, 2011. [Online]. Available: http://www.pewclimate.org/what_s_being_done/in_the_states/rps.cfm.
2. Lauby, M.G., and J. J. Bian, "Accommodating Large Amounts of Variable Generation in North America," in *Proceedings of the 8th International Conference on Advances in Power System Control, Operation, and Management*, pp. 1-5, Hong Kong, CN, November 8-11, 2009.
3. Simburger, E.J. and C.K. Cretcher, "Load Following Impacts of a Large Wind Farm on an Interconnected Electric Utility System," *IEEE Transactions on Power Apparatus and Systems*, vol. PAS-102, no. 3, pp. 687-692, May 1983.
4. Loutan, C., T. Yong, S. Chowdhury, A.A. Chowdhury, and G. Rosenblum, "Impacts of Integrating Wind Resources into the California ISO Market Construct," in *Proceedings of the 2009 PES General Meeting*, pp. 1- 7. Calgary, AB, Jul 26-30, 2009.
5. Makarov, Y. V., C. Loutan, J. Ma, and P. de Mello, "Operational Impacts of Wind Generation on California Power Systems," *IEEE Transactions on Power Systems*, vol. 24, no. 2, pp. 1039-1050, May 2009.
6. Halamay, D.A., T.K.A. Brekken, A. Simmons, and S. McArthur, "Reserve requirement impacts of large-scale integration of wind, solar, and ocean wave power generation," in *Proceedings of the 2010 PES General Meeting*, pp. 1-7, Minneapolis, MN, Jul 25-29, 2010.
7. Ortega-Vazquez, M.A. and D.S. Kirschen, "Estimating the Spinning Reserve Requirements in Systems With Significant Wind Power Generation Penetration," *IEEE Transactions on Power Systems*, vol. 24, no. 1, pp. 114-124, Feb 2009.
8. Saber, A.Y. and G.K. Venayagamoorthy, "Efficient Utilization of Renewable Energy Sources by Gridable Vehicles in Cyber-Physical Energy Systems," *IEEE Systems Journal*, vol. 4, no. 3, pp. 285 - 294, Sep 2010.

9. Han, S., S. H. Han, and K. Sezaki, “Design of an Optimal Aggregator for Vehicle-to-Grid Regulation Service,” in *Proceedings of the Innovative Smart Grid Technologies 2010*, pp. 1 - 8, Gaithersburg, MD, USA, , Jan 19-21, 2010.
10. Kintner-Meyer, M. C.W., “Smart Charger Technology for Customer Convenience and Grid Reliability,” in *Proceedings of the 24th Electric Vehicle Symposium*, Stavanger, NO, May 13-16, 2009.
11. Kintner-Meyer, M. C.W., P. Balducci, C. Jin, T. Nguyen, M. Elizondo, V. Viswanathan, X. Guo, and F. Tuffner, “Energy Storage for Power Systems Applications: A Regional Assessment for the Northwest Power Pool (NWPP),” PNNL-19300, Pacific Northwest National Laboratory, Richland, WA, April 2010.
12. U. S. Department of Transportation, Bureau of Transportation Statistics, *NHTS 2001 Highlights Report*, BTS03-05, Washington, D.C., 2003.
13. Duvall, M., “Comparing the Benefits and Impacts of *Hybrid* Electric Vehicle Options for Compact Sedan and Sport Utility Vehicles,” Final Report 1006892, Electric Power Research Institute, Palo Alto, CA, July 2002.
14. Duvall, M., “Advanced Batteries for Electric-Drive Vehicles,” Final Report 1009299, Electric Power Research Institute, Palo Alto, CA, May 2004.
15. Balducci, P. “Plug-in Hybrid Electric Vehicles *Market* Penetration Scenarios”. PNNL-17441 Report. Pacific Northwest National Laboratory. Richland, WA 2008.

III.G.3. Products

Publications

This work resulted in two different publications.

1. F. Tuffner and M. C.W. Kintner-Meyer, "Using Electric Vehicles to Mitigate Imbalance Requirements Associated with an Increased Penetration of Wind Generation" in *Proceedings of the 2011 IEEE PES General Meeting*, July 24-29, 2011, Detroit, MI.
2. F. Tuffner and M. C.W. Kintner-Meyer, *Using Electric Vehicles to Meet Balancing Requirements Associated with Wind Power*, Pacific Northwest National Laboratory, Technical Report, PNNL-20501, July 2011.

IV. LABORATORY AND FIELD TESTING (MEDIUM & HEAVY DUTY)

IV.A. Grade and Elevation Data Acquisition Accuracy Study

Kevin Walkowicz (Principal Investigator)
National Renewable Energy Laboratory
1617 Cole Boulevard
Golden, CO 80401
(303) 275-4492; kevin_walkowicz@nrel.gov

DOE Technology Manager: Lee Slezak
lee.slezak@ee.doe.gov

IV.A.1. Abstract

Objective

- Determine Requisite Road Grade Accuracy for future fleet analysis applications.
- Evaluate quality of existing road grade data acquisition methods.
- Investigate potential hardware/software solutions.
- Explore potential approaches for reconstruction/repair of previously collected road grade and elevation data.

Approach

- Perform initial literature review to explore any existing and previous research performed in the area.
- Isolate grade dependent components of the road load equation and perform differential analysis to quantitatively report minimum road grade accuracy requirements.
- Collect experimental data to evaluate the quality of existing hardware and approaches

Major Accomplishments

- Determined minimum required road grade accuracy requirements through the differential analysis of road grade influenced uncertainty components found in the vehicle road load equation.
- Confirmed minimum road grade accuracy requirements through vehicle simulation.
- Developed algorithms to reconstruct/repair road grade and elevation information using captured Global Positioning Satellite (GPS) latitude and longitude information.
- Performed local small scale experimentation to evaluate the accuracy of both existing road grade collection methods and Digital Elevation Model (DEM) based reconstruction/repair techniques.
- Expanding on local small scale experimentation results, performed additional analysis on existing GPS data sets gathered as part of previous efforts to further investigate the influence of geography on road grade data acquisition.

Future Activities

- Expand analysis of road load equation and perform vector analysis using required road grade accuracy to determine minimum slope distance (i.e. DEM grid resolution) necessary for accurate DEM based reconstruction.
- Develop an in-house DEM database for enhanced elevation/road grade reconstruction capabilities.

IV.A.2. Technical Discussion

Background

Accurate road grade linked with speed-time duty cycle information is of paramount importance when characterizing real world vehicle operation. As a key component in the traditional road load equation, road grade information coupled with speed-time duty cycle directly influences vehicle tractive power and motive force requirements, both of which affect the development and evaluation of advanced vehicle technologies.

Introduction

Possessing accurate road grade information in addition to speed-time duty cycle is requisite to forming a better understanding of real world vehicle operating behavior, and consequently plays a fundamental role in the development of better computational models, evaluation techniques, regulations, and component designs. However, due to past limitations involving both hardware and software available for the collection of accurate road grade information, this dimension of vehicle operation has often been ignored when determining true in-use vehicle behavior. As current research continues to demonstrate the need for accurate road grade data due to direct correlation of road grade to both vehicle fuel consumption and emissions across operational duty cycles, it is necessary to develop methodologies capable of capturing this fundamental information.

This study was proposed in an attempt to address the problems currently faced when attempting the collection of accurate road grade information in conjunction with vehicle operational speed-time duty cycle. As part of this study, the goal was to determine minimum road grade accuracy requirements for vehicle evaluation and modeling. In addition, an effort was made to analyze existing approaches currently employed for the collection of road grade information using vehicle mounted GPS receivers. Finally, the development of novel methods for producing accurate road grade information was explored based on the results of both the minimum accuracy analysis and current technology evaluation.

Approach

Determining Minimum Accuracy Requirements

Starting with the traditional vehicle road load equation, statistical sensitivity tests were performed to isolate the influence of road grade on vehicle tractive power requirements. Once road grade contributions to vehicle road load had been isolated, the effect of road grade on vehicle performance was evaluated over a range of expected observable road grades. With these values in hand, the minimum required accuracy for road grade measurements was determined

Hardware/Software Solutions Examined

Upon determining the minimum accuracy required for valid road grade measurements, investigators explored currently available hardware and software options to evaluate the viability of present technology to meet the minimum accuracy needs. A number of technologies were explored, such as barometric elevation sensors, inertial measurement systems, multi-antenna GPS receivers, and Geographic Information System (GIS) based software routines. These solutions were judged based on capital cost, ease of installation/integration into existing data acquisition platforms, and available road grade accuracy.

Development of DEM based road grade reconstruction/determination technique

Based on the results of analyzing the existing technologies available for capturing accurate road grade information, a set of novel DEM derived road grade/elevation extrapolation computational algorithms were developed.

Performing Field Test to Evaluate Existing Data Acquisition Approach and DEM Reconstruction

A local field test was performed to evaluate the accuracy of currently employed GPS data acquisition devices used to capture road

grade/elevation data vs. the DEM based algorithms developed as part of this study. As shown in Figure 1, the Golden Field test route consisting of a combination of highway, city, and transitional highway/city driving was developed and testing performed as part of a three lap circuit in an attempt to evaluate the accuracy of both methods across range of common driving conditions. Road grade/elevation information was collected in addition to duty cycle data over the course of the three lap circuit, and the results compared. Comparisons of both raw elevation data and simulated vehicle fuel economy based on collected duty cycle and road grade were performed.

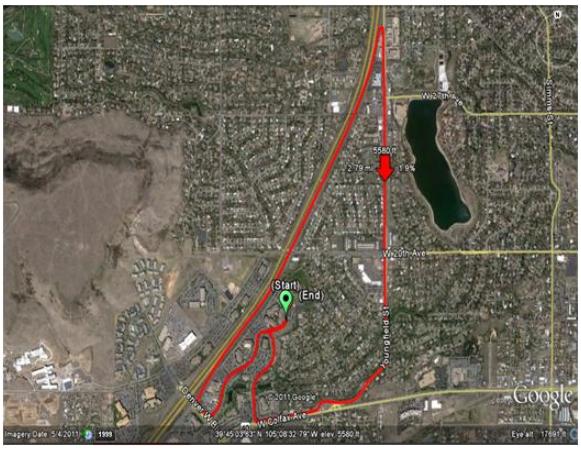

Figure 13. Golden Field Test Route

Results

Determining Minimum Accuracy Requirements

Based on the results of the statistical sensitivity tests performed on the road load equation shown in Figure 2 to isolate the effects of vehicle road grade on tractive power requirements, the minimum accuracy required for less than 5% error in simulated vehicle fuel economy for a given combination of duty cycle and elevation profile was found to be 0.25% road grade or less. In order to achieve an error of less than 1% in simulated fuel economy, 0.05% or less error in road grade measurement is required.

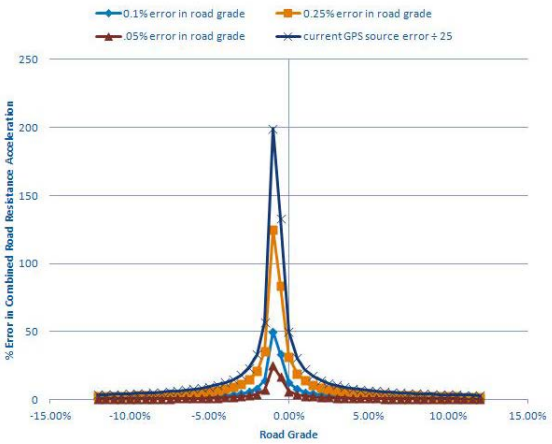

Figure 14. Effects of Error in Road Grade on Combined Road Resistance Acceleration Calculations Assuming a Standard RRC of 0.008

Hardware/Software Solutions Examined

Analysis of available alternative technologies for capturing accurate road grade revealed prohibitive cost, installation, and lack of repeatable measurements for the hardware solutions examined. However, it was found that employing computation algorithms to restore road grade/elevation information from captured latitude and longitude data using publicly available DEM databases such as the United States Geological Survey's (USGS) National Elevation Database (NED) could serve as a viable low cost alternative to upgrading data acquisition hardware. DEM based computational algorithms provide a low cost repeatable solution for meeting the minimum accuracy requirements for road grade/elevation determined as part of this study.

Field Test Results

Results of the Golden Field test reveal significant issues associated with the repeatability of currently employed GPS based road grade/elevation measurements. As shown in Figure 3, it can be seen that when compared to the consistent road grade measurements provided through DEM based extrapolation, existing GPS based road grade measurements fail to produce repeatable results. This is expected given the nature of GPS as a measurement device; however a lack of repeatable measurements becomes a particular issue of interest when examining vehicles

operating on consistent repeated routes. In order to determine true vehicle operation we desire as uniform road grade readings over multiple observations as possible.

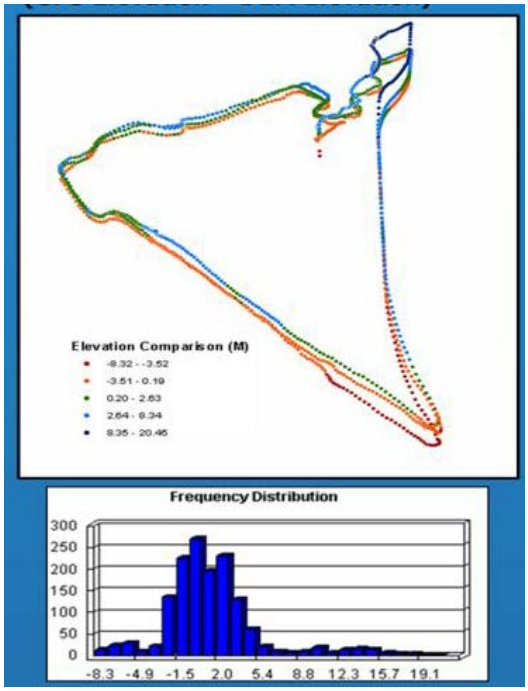

Figure 15. Comparison of GPS and DEM based Elevation Records

Building upon the analysis of the base road grade data collected as part of the field test, vehicle simulations were performed using a variety of generic vehicle models operating on the captured duty cycle and associated road grade profile. Examining the results of the captured duty cycle coupled with DEM based road grade vs. that of the GPS derived road grade and no grade conditions reveals a significant difference in simulated fuel economy between GPS and DEM based approaches. As show in Figure 4, in some cases as much as a 5% simulated fuel economy difference was observed between the GPS and DEM based driving profiles.

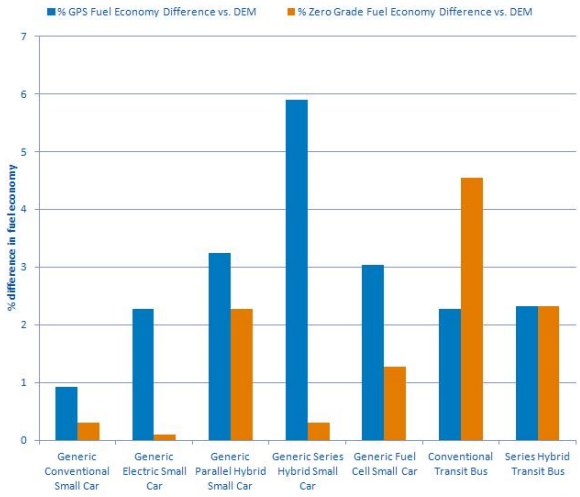

Figure 16. Comparison of simulated fuel economy differences for DEM, GPS, and level road grade cases for Golden field test drive cycle.

Conclusions

Given the costs associated with the integration of additional sensors and new technology into existing data acquisition systems, it is recommended that a software based road grade construction/reconstruction approach using DEM models be further explored for use in future studies. In the experiments performed as part of this study, DEM based road grade data construction/reconstruction has shown to be a reliable, low cost method for gathering road grade information in addition to functioning as a robust method for the repair of existing low quality road grade/elevation data. Additionally, working with DEM information as a source for road grade information provides for consistent, repeatable results which can be employed regardless of data acquisition equipment or approach.

IV.B. MD & HD In-Use performance Evaluations & Near-Term Technology Validation

Principal Investigator: Kevin Walkowicz
National Renewable Energy Laboratory
Center for Transportation Technology and Systems
1617 Cole Boulevard
Golden, CO 80401
(303) 275-4492; Kevin.Walkowicz@nrel.gov

DOE Program Manager: Lee Slezak
(202) 586-2335; Lee.Slezak@ee.doe.gov

IV.B.1. Abstract

Objective

- Validate & document the performance and costs of advanced technologies in medium- and heavy-duty applications;
- Provide 3rd party, unbiased report results for interested parties to further optimize and improve the systems; and
- Facilitate purchase decisions of fleet managers by providing needed information.

Approach

- Work cooperatively with fleets to collect operational, performance, and cost data for advanced technologies;
- Analyze performance and cost data over a period of one year or more;
- Test and analyze in-use performance of advanced technologies in a laboratory setting;
- Produce fact sheets & reports on advanced heavy-duty vehicles in service; and
- Provide updates on new, advanced technology to DOE and other interested organizations, as needed.

Major Accomplishments

- Completed data collection on 36 months of operation for 10 UPS HEV delivery vans in Phoenix, AZ versus 10 conventional vans in the same location. Analyzed drive cycles, fuel consumption, reliability, emissions, and operating cost differences.
- Completed data collection on 12 months of operation for 10 UPS HEV delivery vans in Minneapolis, MN versus 10 conventional vans in the same location. Analyzed drive cycles, fuel consumption, reliability, emissions, and operating cost differences.
- Completed data collection on 12 months of operation for 5 Coca Cola Class 8 HEV tractors versus 5 conventional vans in the same location. Analyzed drive cycles, fuel consumption, reliability, emissions, and operating cost differences.
- Tested and analyzed results from a 40’ transit bus equipped with an advanced electric fan system versus the same bus equipped with a conventional hydraulic fan system.

Future Activities

- Complete evaluations on current fleet vehicles, initiate new evaluations;
- Coordinate modeling and testing activities with other DOE projects such as 21CT as well as other DOE laboratories; and
- Monitor and evaluate promising new technologies and work with additional fleets to test the next-generation of advanced vehicles.

IV.B.2. Technical Discussion

Introduction

Understanding how advanced technology vehicles perform in real-world service, and the associated costs, is important to enable full commercialization and acceptance in the market. The Advanced Vehicle Testing Activity (AVTA) works with fleets that operate these vehicles in medium- and heavy-duty applications. AVTA collects operational, performance, and cost data for analysis. The data analyzed typically covers one year of service on the vehicles to capture any seasonal variations. Because of this, evaluation projects usually span more than one fiscal year. The AVTA team also works on shorter term projects designed to provide updates on current applications to DOE and other interested organizations.

Approach

The AVTA activities for 2011 included:

- ***Fleet evaluations***: 3 locations including HEV's operating in Coca Cola fleet & HEV's operating in 2 UPS fleets. 2 other locations were in started in FY11, but have not yet begun data collection so they are not reported here (BAE lithium equipped buses and FedEx Class 6 HEV box trucks).
- ***Near Term Technology Validation***: Laboratory testing of transit buses equipped with electric cooling fan packages was completed.

FLEET EVALUATIONS:

1) Class 8 HEV Beverage Delivery Truck Evaluation – Coca Cola / Eaton Gen II

In FY10, AVTA began to work with Coca Cola Enterprises (CCE) to evaluate the Eaton Gen II HEV tractors operating in their fleet in Miami, FL to evaluate HEV vs. diesel operation. This work was finished in FY11. CCE currently operates the largest heavy-duty HEV fleet in North America and many of these hybrids are equipped with the Eaton hybrid system. NREL initiated a project with CCE and Eaton to evaluate 5 HEV tractors and compare their performance to 5 diesel counter parts operating in similar service. This work began with a May 2010 kickoff meeting in Miami along with a drive cycle data logging activity. Once the drive cycle data was analyzed, 2 CCE vehicles were shipped to NREL to be tested on drive cycles selected using this on-road data at NREL's ReFUEL laboratory. The 12 month study period was identified to be May 2010- April 2011.

Results

CCE Drive Cycle Collection and Analysis: For a two week period beginning on May 13th, 2010, and then repeated again in Jan 2011 to capture additional information, GPS and CAN data was collected on ten study tractors in the Miami/South Dade Coca-Cola Enterprises fleet. The study vehicles consisted of five Kenworth T370 single axle tractors equipped with a PACCAR PX-6 diesel engine, and Eaton Fuller UltraShift transmission and the Eaton Hybrid System, as well as five Freightliner M2 106 single axle tractors equipped with a Cummins ISC engine and an Eaton Fuller 7-speed manual transmission. Both the Kenworths and the Freightliners were 2007 EPA emissions certified. Additional vehicle details can be found in Table 1.

Table 1. Description of vehicles in CCE Miami Study

Vehicle Information	HEV Tractor	Diesel Tractor
Asset Numbers	643879 643880 643881 643882 643883	644024 644025 644079 644081 644082
Chassis Manufacturer/Model	Kenworth T370	Freightliner M2106
Chassis Model Year	2010	2009
Engine Manufacturer/Model	PACCAR PX-6 260	Cummins ISC-285
EPA Emissions Certification	2007	2007
CARB Emissions Certification	2008 (Clean Idle)	2008 (Clean Idle)
Engine Ratings Max. Horsepower Max. Torque	 280 HP @ 2300 RPM 660 lb-ft @ 1600 RPM	 285 HP @ 2000 RPM 800 lb-ft @ 1300 RPM
Fuel Capacity	56 gallons	80 gallons
Transmission Manufacturer/Model	Eaton Fuller UltraShift Automatic	Eaton Fuller T-14607 Manual 7 speed

Processing the data collected in Miami with a MATLAB based drive cycle tool provided several key drive characteristics of the Miami routes. Using this data and initially considering three duty-cycle characteristics (average speed while driving, percent idle time, and kinetic intensity), the library of heavy-duty standard duty cycles was reviewed to find cycles that most closely represent the CCE fleet data. Data were compared to existing cycles and all data were added to the drive-cycle library. Using these three parameters, the Heavy Heavy-Duty

Diesel Truck (HHDDT), Composite International Truck Local Cycle Commuter (CILCC), and the West Virginia University City (WVU City) cycles were chosen for testing on the chassis dynamometer. Figure 1 illustrates how these three cycles appear to be bracket the field data and can be used to characterize the variation observed in the field.

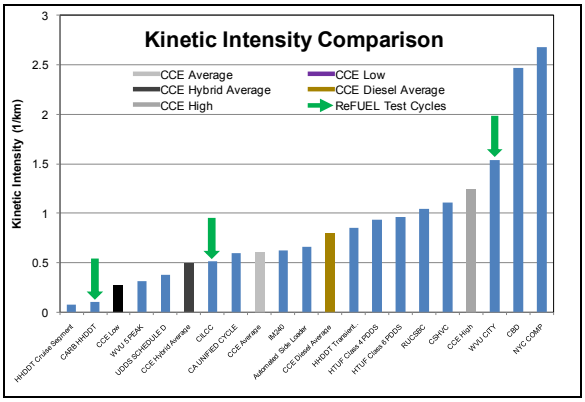

Figure 1. Comparison of CCE field data

To verify that these chose cycles were the correct selection, a HD Truck model was used to run these three standard cycles and the 27 delivery days of CCE data to compare fuel economy. Figure 2 further illustrates how the prediction from these three chosen cycles bracket the CCE data.

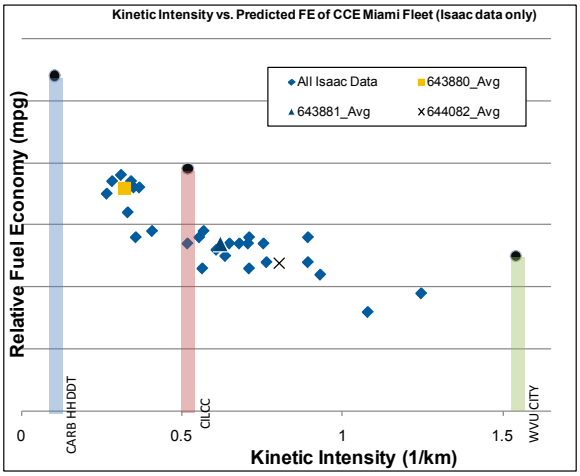

Figure 2. Simulated fuel economy of in-use and standard cycles for CCE vehicles

Laboratory Testing of CCE Tractors: To test these duty cycles at NREL's heavy duty chassis dynamometer facility in Denver, CO, one vehicle from each of the study groups would be needed. Rather than transport both vehicles from Miami, CCE searched their fleet inventory for similar configuration vehicles closer to Denver. A Kenworth hybrid tractor was located in the Denver CCE fleet and the conventional diesel was located in Omaha, NE. These vehicles were exact matches to the tractors in the study fleet. The testing began in August 2010 with the Kenworth hybrid first up on the dynamometer. The first cycle to be tested was the WVU City cycle followed by the CILCC and then the CARB HHDDT cycles. This pattern was followed again for the conventional diesel tractor until testing was completed in FY11.

The emissions results were as expected for Carbon Monoxide (CO), Total Hydrocarbons (THC) and Carbon Dioxide (CO2). The HEV produced fewer of these emissions on each of the three selected duty cycles as detail in Table 2. However, Nitrogen Oxides (NOx) increased for the HEV over the conventional vehicle for each of the tested duty cycles. In fact for the HHDDT cycle, the HEV produced more than double the NOx emissions when compared to the conventional vehicle. This is presented in Table 3 as a percent reduction in emissions for the hybrid over the conventional vehicle. That said, while both engines were 2007 EPA emissions certified they were certified under different NOx emissions limits. The conventional vehicle with the 8.3 L Cummins ISC engine was certified at 1.25 g/bhp-hr and the HEV equipped with the 6.7 L PACCAR PX-6 engine was certified at 1.95 g/bhp-hr. The higher NOx emissions certification is thought to be a major contributor to the increase NOx observed on all three duty cycles tested.

Table 2. CCE Emissions

Drive Cycle	Vehicle	NOx (g/mile)	CO (g/mile)	THC (g/mile)	CO2 (kg/mile)
WVU City	HEV	9.94	1.64	-0.09	1.77
	Conventional	7.70	1.70	0.07	2.31
CILCC	HEV	7.53	0.35	-0.03	1.36
	Conventional	7.16	0.93	0.06	1.66
CARB HHDDT	HEV	5.75	0.49	-0.01	1.66
	Conventional	2.86	0.71	0.03	1.66

Table 3. CCE Hybrid Emissions Reductions

Drive Cycle		NOx	CO	THC	CO2
WVU City	HEV % reduction	-29.1	3.6*	222.7*	23.3
CILCC	HEV % reduction	-5.1	62.3	147.5	18.1
CARB HHDDT	HEV % reduction	-101.3	31.3*	141.9	-0.2*

The fuel economy results were as expected. The HEV demonstrated improved fuel economy on all three tested duty cycles with the lower average driven speed and higher kinetic intensity WVU City cycle producing the most significant difference between the two vehicles with a 30% increase in fuel economy, as seen in Table 4. Table 4 further confirms the relationship between kinetic intensity and hybrid advantage. As such the hybrid advantage, indicated here as percent increase in fuel economy, increased with an increase in the kinetic intensity of the duty cycle. This is illustrated in Figure 3.

Table 4. CCE Laboratory Fuel Economy

Drive Cycle	HEV Fuel Economy (mpg)	Conventional Diesel Fuel Economy (mpg)	HEV Percent Increase (%)	P Value
WVU City	5.79	4.44	30.3%	8.8E-6
CILCC	7.55	6.18	22.2%	1.8E-9
CARB HHDDT	6.17	6.18	-0.14%*	0.88

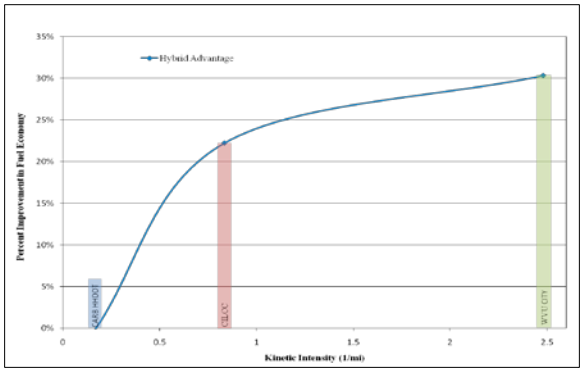

Figure 3. CCE Hybrid Advantage vs. KI

CCE In-Use Data Collection: The in-use study of the CCE South Dade fleet started in May 2010 and continued into June 2011 for a total of 13 months of operation. Fuel consumption data was collected and correlated from two sources:

1) Controller Area Network (CAN) data recorded with data loggers during the two-week study (an integration of the CAN message "EngFuelRat," which will provide cumulative fuel used for each day of the two-week study period). This data was acquired to confirm the longer term Engine Control Module (ECM) data.
2) ECM image downloads provided monthly to NREL by the local CCE ECM service contractor. These images contained a total cumulative fuel used value and will be compared month to month to determine monthly fuel usage.

Data from the ECM image downloads over 13 months was analyzed to report in use fuel economy of the study groups. The hybrid group fuel economy average was 5.63 mpg; 13.7% better than the diesel group's 4.95 mpg. Individual vehicle results are seen in Table 5.

Table 5. CCE In-use Fuel Economy

Fuel Economy Comparison (May 2010 - June 2011)				
Tractor	Powertrain	Mileage Total	Fuel Used	MPG
644024	Diesel	14496.3	2604.1	5.57
644025	Diesel	15842.9	3165.1	5.01
644079	Diesel	12551.1	2373.8	5.29
644081	Diesel	13101.9	2682.5	4.88
644082	Diesel	8965.9	2297.6	3.90
Conventional	**Total**	**64,958**	**13,123**	**4.95**
Conventional	**Average**	**12,992**	**2,625**	**4.93**
643879	Hybrid Diesel	4339.6	698.8	6.21
*643880**	Hybrid Diesel	*3315.4*	*552.9*	*6.00*
643881	Hybrid Diesel	10889.6	1822.2	5.98
643882	Hybrid Diesel	10685.6	2012.8	5.31
643883	Hybrid Diesel	18214.1	3343.7	5.45
Hybrid	**Total**	**47,444**	**8,430**	**5.63**
Hybrid	**Average**	**9,489**	**1,686**	**5.79**

*643880 ECM records from May 2010 to January 2011 only

The ECM images also provided useful insights into vehicle idle time and hybrid effect on DPF regenerations. Hybrids had nearly half as much idle time % as the conventional group, but still used 9% of their fuel at idle. The conventional vehicles used 16% of their fuel while at idle (zero speed, engine on). The hybrids averaged only 11.5 DPF regenerations over the 13 months while the conventional vehicles averaged 42.2 regenerations over the same period. See Table 6 for details.

Table 6. CCE DPF regenerations and idle time

	DPF Regens	Regen Fuel	Idle Time %	Idle % Fuel
Conv Avg	42.2	12.2	61%	16%
Hybrid Avg	11.5	1.8	35%	9%
Hybrid Advantage	-72.7%	-85.5%	-41.9%	-46.8%

In addition to CAN data, maintenance costs were also tracked via fleet records to examine operational costs & reliability of new hybrid components. The hybrid group cumulative maintenance costs per mile were 51% less than the conventional group and can be seen in Figure 4. Overall operation costs (fuel and maintenance) were 21% less for the hybrids over the 13 month period ($1.07/mile for the conventional versus $0.85 for the hybrids).

Conclusions:

A final technical report detailing these results is due out in early 2012.

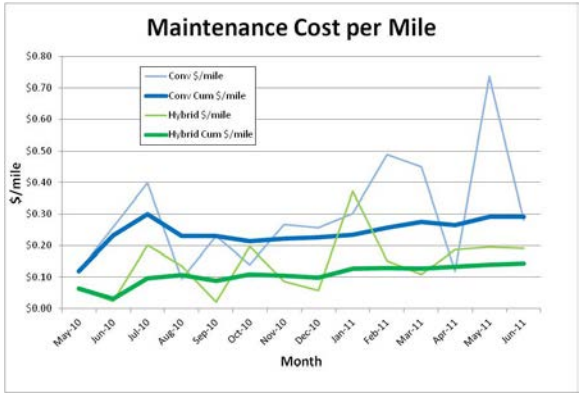

Figure 4. CCE Maintenance Cost

2) Gen II HEV Package Delivery Truck Evaluation - Eaton/UPS - Minneapolis, MN

In June 2010, NREL and UPS kicked off a new 'Gen II study' aimed at evaluating 10 'next generation' Eaton hybrids and 10 conventional technology vehicles in a UPS fleet located in Minneapolis, MN. AVTA initiated this evaluation with a data logging effort from both these study groups, followed by chassis dyno testing on representative cycles and complimented with a planned 12 months of in-use data collection. The overall intent of this new evaluation in Minneapolis was to compare these 'next generation' lithium battery parallel hybrid trucks with conventional diesel powered trucks.

Approach:

A detailed route/duty cycle analysis involving 14 vans instrumented for 3 weeks with GPS and J1939 logging at 5hz was completed in July 2010 followed by a multidimensional statistical analysis. This effort was followed by collecting in-use performance and cost data on each set of vehicles and will be analyzed over a period of 12 months. Daily miles, fueling events, parts cost, maintenance hours will be recorded as part of this effort. ECM image downloads were also obtained at monthly intervals providing fuel consumption, idle time, DPF regenerations and other data. Representative vehicles were tested at the NREL's chassis laboratory (ReFUEL) with 3 duty cycles tested for 4 repetitions of each cycle to ensure some degree of statistical confidence.

Results

Analysis of the assigned routes of the two study groups indicated a large difference in duty cycle, specifically a mismatch of the "stem" portion of the delivery routes as seen in Figure 5. As a result the study was extended to 18 months to enable UPS to switch the routes of the two groups for a more comprehensive analysis. Data from the first 12 months has been analyzed, but post route switch data collection is still underway.

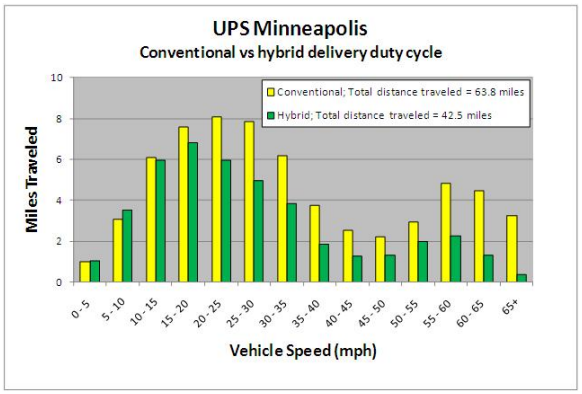

Figure 5. GPS route analysis showing bimodal operation and greater miles traveled by conventional study group.

The detailed drive cycle analysis led to choosing the NYC Comp, HTUF4 and HHDDT standard laboratory duty cycles as representative of and bracketing the measured study group routes. ReFUEL laboratory testing was completed in June 2011 and indicated 21% to 45% improvement in ton-mi./gal fuel economy (13% to 36% mpg improvement) as seen in Table 7.

In-Use fuel economy indicates only a 5% hybrid advantage to date, but this is on very different mileage/drivign routes. The route switch UPS implemented will provide an opportunity to compare fuel economy on similar route hybrids to conventional vehicles and will be included in the final report due out in mid 2012.

Table 7. ReFUEL Laboratory Ton Fuel Economy results

Ton Fuel Economy	NYC Comp	HTUF4	HHDDT
Conventional P100D (ton-mi./gal)	51.1	56.2	72.0
Hybrid P100H (ton-mi./gal)	70.9	81.6	87.2
Hybrid Advantage (%)	39%	45%	21%
Ttest P Value	0.0000	0.0000	0.0001

Conclusions

Although the study is continuing into Dec 2011 to capture the route switch of the two groups, the following are conclusions to date:

- Cumulative miles per van for the hybrids were roughly half as many as for the diesels
- The study groups were on significantly different duty cycles necessitating a route switch between the groups to more accurately compare fuel economy and maintenance costs
- Fuel economy of the hybrid group over these 6 months was 5.3% greater than that of the diesel group, (P value = 0.0428). However, the test groups were on very different routes and a fuel economy comparison after route switches will be more telling
- Total maintenance cost per mile was 89% higher for the hybrids (P value = 0.0063). However, this was only 18% more when considered on a cost per delivery day basis
- Propulsion related maintenance cost per mile was 168% higher for the hybrids (P value = 0.0028). However, this was only 68% more when considered on a cost per delivery day basis
- Total operating costs per mile (assuming $3.43/gal) for the hybrids were 19% more than those for the diesels (P value = 0.0258)
- ReFUEL laboratory testing demonstrated a statistically significant 21% to 45% improvement in ton-mi./gal fuel economy for the hybrids, 13% to 36% on an mpg basis

Final Conclusions are awaiting final post route switch data. Data collection should be complete at the end of December 2011. A final technical report detailing all the findings is due out mid 2012.

3) 36 Month Gen I Package Delivery Truck Evaluation - Eaton/UPS – Phoenix, AZ

In FY10 (December 2009) NREL completed and published an evaluation of the first generation of Eaton's hybrid electric delivery vehicles operating at a UPS facility in Phoenix, AZ. UPS obtained new Eaton 'Gen 1' equipped HEV delivery trucks in their fleet in 2007. AVTA initiated an evaluation for these MD package delivery vehicles equipped with an Eaton's parallel hybrid systems (with lithium battery) to assess the performance and feasibility of this technology in Phoenix, AZ A group of 10 vehicles from both the new and conventional technology was selected for the study. The intent of the project was to compare the lithium battery parallel hybrid trucks with conventional diesel powered trucks. This project is to collect and analyze performance and cost data from years 2 and 3 from the hybrids operating in Phoenix, AZ.

Results

It appears that the conclusions in December 2009 report will remain the same after following up with the study group in years 2 and 3. The hybrids continue to be driven fewer daily miles than the diesels (as shown in Figure 6), but demonstrate a 23.1% fuel economy advantage (as shown in Figure 7). The mileage difference between the two groups show a slight bias toward shorter more urban routes. It would be expected that if the conventional vehicles were

also driven on more urban routes, the fuel economy would decline and a higher fuel economy advantage would be observed. There is still no statistically significant difference between the diesel and hybrid groups for total maintenance cost per mile or propulsion cost per mile (see Table 8)

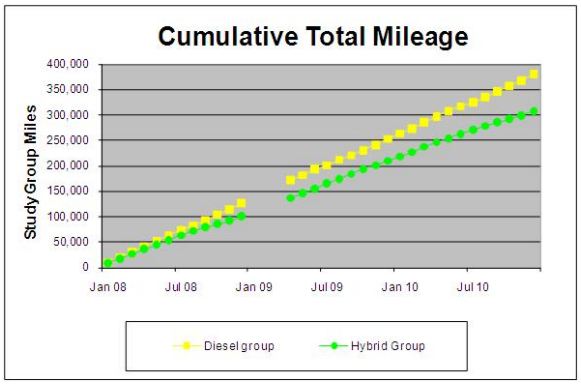

Figure 6. UPS Phoenix hybrid and conventional cumulative miles driven

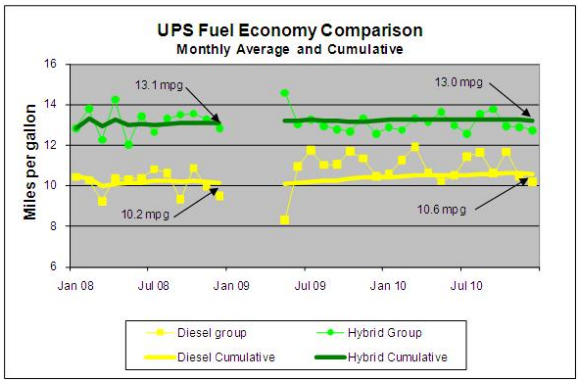

Figure 7. UPS Phoenix hybrid and conventional monthly average and cumulative fuel economy

Table 8. UPS Phoenix hybrid and conventional Propulsion Maintenance Cost Comparison

Propulsion Maintenance Cost Comparison					
Car	PWRTRN	Mileage Total	Labor Hours	Parts Cost	Cost ($/mile)
663982	Diesel	58,475	23	$ 883	$ 0.035
665020	Diesel	66,000	28	$ 526	$ 0.029
665044	Diesel	59,118	23	$ 331	$ 0.025
665086	Diesel	70,613	60	$ 199	$ 0.045
665087	Diesel	68,659	13	$ 474	$ 0.016
665150	Diesel	57,415	20	$ 422	$ 0.025
Total	**Diesel**	**380,280**	**167**	**$ 2,835**	**$ 0.029**
666131	Hybrid Diesel	41,004	28	$ 69	$ 0.035
666132	Hybrid Diesel	59,646	24	$ 103	$ 0.022
666133	Hybrid Diesel	59,323	15	$ 25	$ 0.013
666139	Hybrid Diesel	53,793	53	$ 103	$ 0.051
666142	Hybrid Diesel	46,772	36	$ 407	$ 0.047
666145	Hybrid Diesel	47,193	52	$ 173	$ 0.059
Total	**Hybrid Diesel**	**307,731**	**208**	**$ 878**	**$ 0.037**

Conclusions

- Monthly (and cumulative) miles per van for the hybrids were 18% lower than they were for the diesels. (P value = 0.0191)
- Miles per operational day were 11% lower for the hybrids than they were for the diesels, but this difference was not statistically significant. (P value = 0.27)
- Fuel economy of the hybrid group over these 3 years was 23.1% greater than that of the diesel group. (P value = 0.0009) This is less than the nearly 29% reported after the first year and 31% to 37% shown during laboratory fuel economy testing. The diesels seemed to slightly improve their fuel economy over time while the hybrids did not.
- There still was no statistically significant difference between the diesel and hybrid groups for total maintenance cost per mile (P value = 0.46).
- Total operating costs per mile for the hybrids were 10% less than those for the diesels but were not found to be statistically significant (assuming $3.09/gal).
- The hybrid vehicles continue to perform in years 2 & 3 much the same as they did during the 1st year study. UPS continues to be satisfied with their performance and acquire more Eaton hybrid vehicles. A final technical report is due out in early 2012.

NEAR TERM TECHNOLOGY VALIDATION:

1) *Transit Bus Electric Cooling Fan Performance Evaluation:*

The objective of this project was to evaluate the fuel economy and emissions impacts of using the EMP "Mini-Hybrid" cooling system in place of conventional hydraulic cooling systems commonly found in transit buses.

The approach used for this project included:

- Laboratory chassis dynamometer loading over repeats of standard transit bus duty cycles while concurrently measuring exhaust emissions and fuel consumption for a single

transit bus with a conventional hydraulic fan cooling system and for the same bus following a retrofit with the EMP cooling system.

- Subsequent analysis of test results to determining statistically significant differences from cooling system retrofit.

Cooling systems for diesel engines on transit buses require power from the engine to operate. Most transit buses employ hydraulically powered cooling fans (Figure 8) which place an auxiliary load on the engine in the form of a hydraulic pump. The pump supplies hydraulic fluid under pressure to a hydraulic motor which turns the fan at either the controlled speed or simply "on" at the full speed attainable for the developed hydraulic pressure (engine-speed dependent). Because of the energy losses associated with hydraulic pumps, motors, plumbing, and fan designs, there is potential for reducing the energy expended in meeting engine cooling demands.

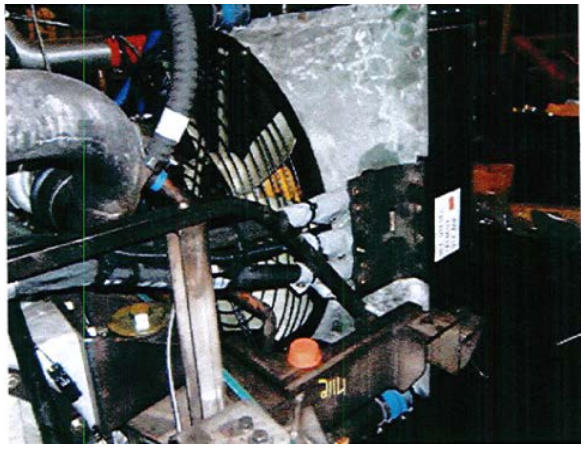

Figure 8. Conventional Hydraulic Cooling Fan.

The EMP Corporation manufactures the electrically-powered "Mini-Hybrid" cooling system (Figure 9) which seeks to improve upon the energy efficiency of conventional cooling systems. In place of a hydraulic pump and motor, a higher capacity alternator is used to provide power for the electric motor driven cooling fans, as well as other vehicle electrical loads. A different radiator and charge air cooler assembly is also used.

Figure 9. EMP "Mini-Hybrid" Cooling Fan.

NREL completed a testing program to evaluate the potential of the EMP "Mini-Hybrid" cooling system as a "near-term" retrofit technology solution for improving the overall fuel economy of transit buses. The testing program was designed to provide results applicable to transit bus operation for various urban areas with different characteristic drive cycles.

To minimize the number of replicate tests needed for a valid comparison, a chassis dynamometer-based laboratory testing program was conducted at NREL's ReFUEL laboratory in Denver, CO. Furthermore, the same bus before and after cooling system retrofit (see Figure 10), the same driver, and same fuel batch were used for all tests. The baseline cooling system of the test bus prior to the retrofit employed a variable speed hydraulic fan. Testing was conducted over the Manhattan, Orange County Transit Authority (OCTA), and heavy-duty UDDS standard drive cycles in case performance differences were dependent on drive cycle.

Figure 10. 2008 40-Foot Gillig Test Bus.

Results

The average measured fuel economies in miles per gallon (MPG) demonstrate a statistically significant difference only in the case of the OCTA cycle (Table 9). The difference is an improvement on that cycle of 1.8% in retrofitting a conventional cooling system with the EMP cooling system. NOx emissions in grams per mile (g/mi) show no statistically significant difference related to cooling system differences.

Table 9. Fuel Economy and NOx Test Results.[1]

Test Cycle	Runs Hyd/EMP	Hyd. MPG	EMP MPG	Diff. (%)	Hyd. NOx (g/mi)	EMP NOx (g/mi)	Diff. (%)
Manhattan	6/3	3.20	3.22	0.0	12.32	12.40	0.7
OCTA	6/5	4.33	4.41	1.8	9.40	9.24	-1.7
HD UDDS	6/4	5.96	5.96	0.0	6.46	6.86	6.3

- A statistically significant improvement of fuel economy of approximately 1.8% on the OCTA cycle was observed following the retrofit of the hydraulic fan cooling system with the EMP cooling system
- A Statistically significant improvement of fuel economy was not observed on either the Manhattan cycle or the heavy-duty UDDS cycle
- A statistically significant difference in NOx emissions attributable to the change in cooling systems was not observed on any of the three cycles

[1] Red background indicates the numerical value is not statistically significant at the 95% confidence level.

Conclusions

Chassis dynamometer testing at the ReFUEL laboratory showed that an improvement in fuel economy of approximately 1.8% could be expected by retrofitting conventional variable speed, hydraulic cooling fan systems to the EMP "Mini-Hybrid" cooling system in the case of transit buses operating over duty cycles similar to the standard OCTA cycle. Fuel economy improvements for buses operating on cycles similar to the Manhattan or heavy-duty UDDS cycles are not expected. Retrofitting variable speed hydraulic systems with the EMP system has no significant impact on NOx emissions. Additional fuel economy improvements could be gained by retrofitting buses without the more advanced 'variable speed' hydraulic fans.

Testing at cold or hot ambient temperatures may also result in significantly different fuel economy improvements. Additional testing is required to demonstrate this.

IV.B.3. Products

Publications

1. Lammert, Mike (March 2011). *"Project Startup: Evaluating Coca-Cola's Class 8 Hybrid Electric Delivery Trucks";* DOE/GO-102011-3172.
2. Lammert, Mike (September 2011). "Project Overview: United Parcel Service's Second-Generation Hybrid-Electric Delivery Vans"; DOE/GO-10-2011-3284.
3. Barnitt, Robb (January 2011). *"FedEx Express Gasoline Hybrid Electric Delivery Truck Evaluation: 12-Month Report";* NREL/TP-5400-48896.
4. Walkowicz, Kevin (May 2011). *"Medium and Heavy Duty Field Evaluations";* Presented at 2011 DOE Annual Merit Review, Washington, DC.

IV.C. MD PHEV/EV Data Collection and Reporting

Kevin Walkowicz (Principal Investigator)
National Renewable Energy Laboratory
1617 Cole Boulevard
Golden, CO 80401
(303) 275-4492; kevin_walkowicz@nrel.gov

DOE Technology Manager: Lee Slezak

IV.C.1. Abstract

Objective

- Securely collect, store, and analyze vehicle data transmitted from medium- and heavy-duty plug-in electric vehicles and equipment being deployed/developed as a part of DOE funded activities (under the ARRA Transportation Electrification Awards and MD PHEV school bus TADA Award).
- Report data and progress of the data collection effort as well as analyzed vehicle/equipment performance data to the DOE and the general public.

Approach

- Provide for secure storage of data on 30 TB capacity storage arrays.
- Create initial data processing routines to easily analyze data sets as they become available as well as provide quality checking and filtering
- Provide data analysis and reporting of initial ARRA vehicles expected to deploy in FY11 (expected to be at the 10-20% levels of total)
- Create data sheets & on-line access for DOE managers and full monitoring of vehicles (4 specific vehicle types)
- More than 25 parameters, recorded each second from each vehicle, will be logged and stored at NREL.
- Drive cycle information will be used in coordination with other DOE laboratories to further refine medium-duty vehicle R&D activities. Motor, power electronics, and battery performance will also be monitored and recorded.
- Additional results, processed to obscure proprietary/private information, will be posted on the NREL website quarterly for public review.

Major Accomplishments

- In FY11, NDAs were signed with two OEM's to exchange vehicle data with NREL. Others are in process in order to collect and analyze data being generated as part of the DOE funded ARRA Transportation Electrification Awards .
- In FY11, NREL received additional data from Zonar (data collection partner) and brought the total number of shifts/days analyzed to 1437.
- Secure data receipt, storage, and backup has been automated and currently serves two fleets (Smith & Navistar)
- Automated analysis and reporting routines are well under way and ready for validation with additional OEM discussions.

Future Activities

- Agreements and plans for remaining ARRA fleets will be finalized.
- Additional raw data processing routines will be created for these upcoming unique platforms.

- Additional analyses dedicated to vehicle batteries and powertrains will be further developed and refined.
- Coordination with other DOE VTP tasks will be established to leverage the processed/desensitized data set in related activities.

IV.C.2. Technical Discussion

Introduction

Understanding how advanced plug-in electric vehicles operate under real-world conditions will enable future refinements and improvements in the industry. Large amounts of data will be made available to NREL to capture and analyze as part of the medium duty projects funded under the American Recovery and Re-Investment Act (ARRA) and funded under the Technology Assessment and Demonstration Activity (TADA) PHEV school bus project. Vehicle data will be collected, analyzed and reported to show the results and general trends observed.

Approach

The MD Data Collection and Reporting activities for 2011 included:

- ***ARRA MD PHEV and EV Vehicles***: FY11 included efforts to begin data collection from 2 deployments of MD EV's: Smith's 'Newton' and Navistar's 'e-Star'.
- T***ADA MD PHEV School Bus analysis***: Data collection on school buses to characterize operational metrics to support development of Navistar's PHEV school bus

1. ARRA MD PHEV & EV DATA COLLECTION:

Background

American Recovery and Reinvestment Act (ARRA) deployment and demonstration projects are helping to commercialize technologies for hybrid electric vehicles (HEVs), plug-in hybrid electric vehicles (PHEVs), all-electric vehicles (EVs), and electric charging infrastructure.

This effort, funded by the DOE Vehicle Technologies Program (VTP) within the Vehicle & Systems Simulation and Testing Activities (VSST), will utilize data collected from some of these ARRA demonstration projects. Data from approximately 1,700 electric vehicles (EVs) and plug-in hybrid electric vehicles (PHEVs) entering fleets in FY11 and FY12 from Smith Electric Vehicles, Navistar, and a collaboration between the Electric Power Research Institute (EPRI) and South Coast Air Quality Management District (SCAQMD) will be collected, compiled, and analyzed. Additionally, data from the Cascade Sierra Solutions anti-idle station installation program will be added to this project when available.

NREL will compile all data from these MD electric drive vehicles in order to directly support DOE Vehicle Technology Program (VTP) goals of developing and deploying plug-in electric vehicles. Collection, storage, and analysis of vehicle data transmitted from each OEM will occur via the NREL Commercial Fleet Data Center (CFDC).

More than 25 parameters, recorded each second from each vehicle, will be telemetered and stored at NREL. Drive cycle information will be used in coordination with other DOE laboratories to further refine medium-duty vehicle R&D activities. Motor, power electronics, and battery performance will also be monitored and recorded.

NREL will securely deliver detailed reports of vehicle performance during an 18-month period of performance to the U.S. DOE. Additional results, processed to obscure proprietary/private information, will be posted on the NREL website quarterly for public review.

This report summarizes the data collected and processed with NREL's Fleet Analysis Toolkit (FAT) thus far and describes the other data products being produced from this project.

Approach

Data recorded (typically via CAN bus on-board the vehicle) is collected by the on-board data

acquisition systems and transmitted wirelessly to the OEM or 3rd-party telemetry provider data warehouse. From there, raw data files are uploaded to NREL secure FTP sites as shown in Figure 1.

Automated software checks the FTP sites every morning for new files and stores them locally (with nearly 30 TeraBytes of capacity) in the NREL Commercial Fleet Data Center (CFDC).

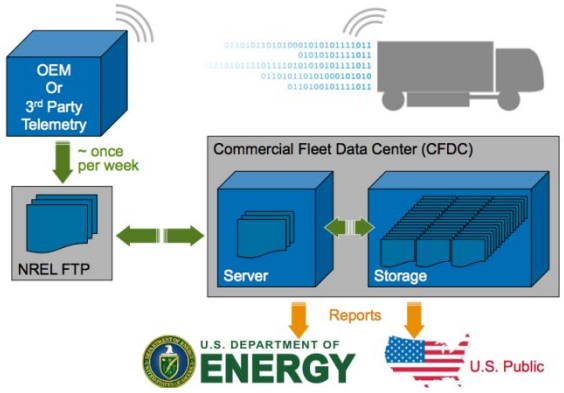

Figure 1. Data Transfer Network Topology

Data is then converted to more useful formats, analyzed, and processed into reports delivered to DOE and the American public.

Within the CFDC, the data is investigated throughout a series of steps. While raw data is never deleted, if some of it is found to be corrupt or unusable, it is quarantined for closer inspection.

The central portion of the analysis takes place after the second-by-second data has been aligned with local time-stamps and separated into driving and charging modes, as shown in Figure 2. The major interest of this program is the effectiveness of these new electrified drive systems in reducing oil consumption and fuel costs for commercial fleets.

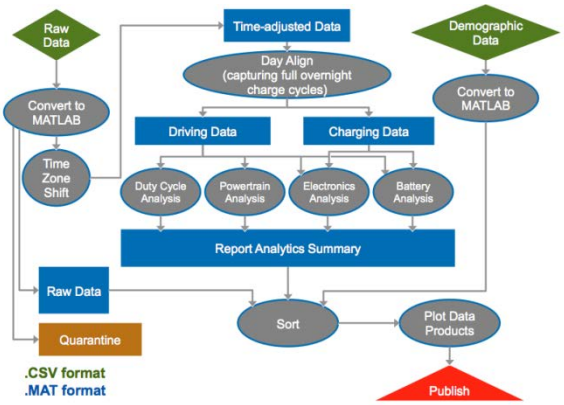

Figure 2. Data Processing Methodology

Throughout the process, routines correlate the data with local demographic data to understand the markets in which these vehicles are used. Additional routines sort the data and produce dozens of individual metrics to produce charts and reports. A list of these metrics is included in Table 1. Some of these metrics may be considered proprietary but some will be published as part of the quarterly updates which will be produced for each project.

Table 1. Reporting Metrics Produced

1	**Time in Service**	Total days of valid data
2	**Vehicle Range**	Miles traveled per trip
3	**Fuel Efficiency**	DC energy out of the battery with respect to total miles traveled (Wh/mi)
4	**Battery Pack & Cell Voltage**	Average voltages at pack and cell levels
5	**Battery Degradation**	Average voltages for fleet each 1000 miles (or 1000 cycles)
6	**Battery Soak Temperatures**	Time spent parked at various temperatures
7	**Time Spent Charging**	Total hours spent charging per vehicle per mile traveled
8	**Arriving/Departing SOC**	Binned SOC % recorded when plugging-in and unplugging
9	**Battery Resting SOC**	Time spent at each range of SOC
10	**Charging Time of Day**	Local time when plugging-in
11	**Powertrain Efficiency**	Compare road-load demand (assuming various GVWs) to DC power out
12	**Charging Efficiency**	Total AC energy in (from the charging cord) vs. total DC energy out (to the motor)
13	**Duty Cycle Impacts to Range**	Variation in energy efficiency (Wh/mi) with respect to Kinetic Intensity
14	**Idling Statistics**	Idle time (key-on zero speed) and power demand during Idle
15	**Drive Temperatures**	Trip duration at various ambient temperatures
16	**Drivetrain Temperatures**	Motor/power electronics temperatures at various DC power levels
17	**Air Conditioner Energy Impacts**	Fuel efficiencies with air conditioner on and off and duration in each mode
18	**Charging Location**	Map of locations where vehicle charge (with bubbles sized proportional to duration)
19	**Effective Vehicle Range**	Estimate total range availability using fuel efficiency and SOC usage windows
20	**Voltage Transients**	Second-by-second deviations in pack voltage
21	**Energy Cost Savings**	Estimate electricity cost by location with respect to diesel equivalent cost
		and more to come…

Results

***Smith**:* Smith EV's began deployment in November 2010, but higher quantity ramp up began in early 2011. Vehicle details include:

Curb Weight	16,535-26,455	pounds
Length	225.6 - 285.6	inches
Width	79.2	inches
Height	78 - 79.2	inches
Peak Motor Power	120	kW
Electric Range	100	miles
Seating	3	
Payload	16,060	pounds
Electric Top Speed	50	mph
Battery Capacity	80 or 120	kWh
Battery Voltage	~350	V nominal
Charging Standards	J1772 or 3-phase	
Transmission	Single Reduction Gear	
Drag Coefficient	~0.5	
Wheel Base	153 - 197	in.
U.S. Debut	2006	

For Smith, which at the time of this publication (Oct. 31, 2011), had enough vehicles producing data on a regular basis and to extract usable information, preliminary data is as follows:

- Number of vehicles reporting: 124
- Number of vehicle days driven: 4135
- Number of operational cities: 62
- Total number of trips recorded: 4051
- Total distance travelled: 174638 miles

The overall gasoline mpg equivalent (based on EPA/NHTSA method) is calculated to be 18.8 mpg for these vehicles. This is shown in Figure 3. Estimates are being made to compare these EV's with their conventional counterparts but this information is not yet available.

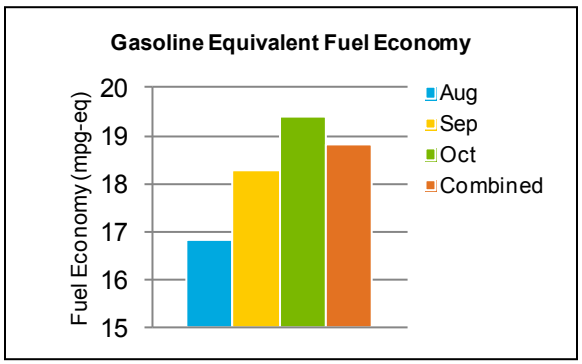

Figure 3. Gasoline Equivalent MPG (Smith)

Smith vehicle driving metrics are also being calculated in order to understand vehicle usage versus vehicle performance. Some basic drive cycle statistics include:

- Average number of stops/trip: 57.1
- Average number of stops/mi: 4.8
- Maximum driving speed: 43.7 mph
- Average driving speed: 11 mph

A chart of vehicle distance travelled at various speeds is shown in Figure 4 and Figure 5 shows time of day when charging for the vehicles.

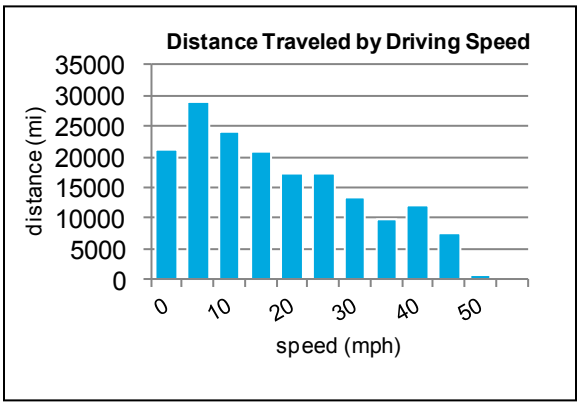

Figure 4. Speeds driven by Smith Vehicles

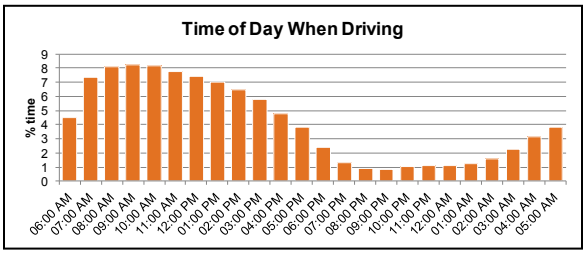

Figure 5. Time of charge for Smith

Additional information will be published on Smith when it becomes available. This information will be available in the quarterly updates (first one planned for December 2011).

Navistar:

Navistar EV's (eStar) began deployment and data transmission in mid 2011. To date, 84 vehicles have been deployed with 42 of those vehicles successfully transmitting data via their on-board loggers. At the time of this publication, the operational use of these vehicles has not yet been verified so limited data analysis has been completed. Additional data will be published in

the quarterly reports planned to start in 2012 for this project.

Navistar vehicle details are as follows:

Curb Weight	12,000	pounds
Length	254	inches
Width	78.75	inches
Height	106	inches
Peak Motor Power	70	kW
Motor Location	Rear	
Electric Range	100	miles
Seating	2	people
Payload	4,000	pounds
Electric Top Speed	50	mph
Battery Capacity	80	kWh
Battery Voltage	~320	V nominal
Charging Standards	J1772	
Wheel Base	141.7	in.
U.S. Debut	2010	

Conclusions / Future Efforts

So far, over 120 Smith Electric Vehicle "Newtons" and over 80 Navistar "eStars" have been deployed and are transmitting data. Though data transfer has recently started to happen consistently, many anomalies in the data are still being investigated and analyzed. It is anticipated that quarterly reports will begin in late 2011 and early 2012 to document Smith and Navistar on a regular basis. Additional sites in FY12 will include the AQMD / EPRI vehicles (bucket trucks and shuttle buses) as well as Class 8 truck stop electrification (from Cascade Sierra).

In FY12, efforts will continue on all 5 vehicle data sets to improve data quality and results fidelity and begin publishing quarterly reports. Additional analyses will be added including:

- power train thermal performance
- battery thermal performance/efficiency
- battery degradation
- fleet charging effects to the grid

Efforts will also include processing drive cycle data for public consumption and incorporating it with Fleet DNA, coordinating with other projects within the VT program, adding PHEV analysis capabilities (Azure + Odyne architectures) to the toolkit and when applicable, sharing publicly available data with Clean Cities to provide guidance to more fleets interested in PEVs.

2. TADA MD PHEV School Bus Analysis:

In order to assist in the development efforts of a MD PHEV school bus, NREL was asked to characterize the true operating behavior of school bus fleets operating across the country. In FY11, NREL researchers finished collecting duty cycle information for 3 unique vehicle fleets using a conjunction of in-vehicle GPS/CAN data acquisition systems, and existing onboard telemetric systems. Performing statistical analysis on the field data, NREL characterized the typical operation of a school bus across the 3 vehicle fleets. In addition, existing chassis dynamometer test cycles were also selected based on the fleet analysis for future vehicle modeling and design applications.

Approach

Employing a combination of Isaac Instruments GPS/CAN data loggers and existing Zonar telemetric systems allowed NREL to capture operating information for 212 unique vehicles operating in 3 fleets spread across the country. This amounted to a total of 1437 individual operational shifts. The fleets examined in this study were located in Lake Washington, Washington, Schenectady, New York, and Adams County, Colorado.

Once the field data had been collected using either NREL installed data acquisition devices, or existing telemetry systems, NREL researchers performed large scale duty cycle statistical analysis to examine underlying trends within the data and to explore both the similarities and differences in vehicle operation between fleets. Based on the results of these analyses, high, low, and average vehicle performance was determined, and standard chassis dynamometer test cycles were chosen to reflect this range.

Results

Performing statistical analysis of the duty cycle information collected as part of this study revealed a number of unique trends among the vehicles examined. Examining the route statistics generated as part of the duty cycle analysis, we can see that there is a strong exponential relationship between the number of stops on a given route and the average driving speed as shown in Figure 6. Additionally, we see that not only is there a strong trend between stops per mile and average driving speed, but when comparing route data across the different fleets, we see typical school bus operation in Schenectady for the vehicles examined displaying significantly higher stops per mile and lower speed than both the Lake Washington and Adams County fleets.

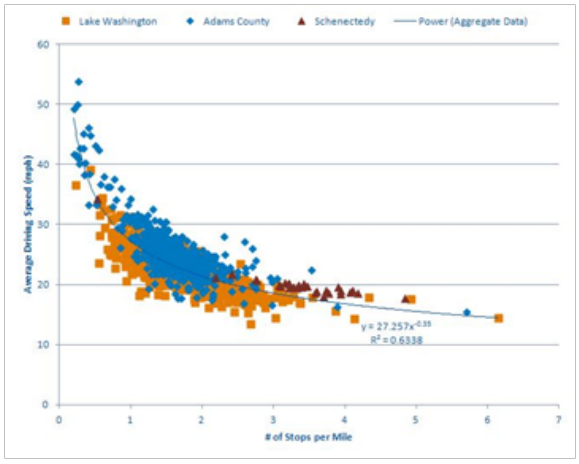

Figure 6. Number of Stops per Mile vs. Average Driving Speed for School Bus Routes

This is of particular interest when we examine the relationship between average driving speed and Kinetic Intensity shown in Figure 7. We can see that due to the high number of stops per mile associated with the buses located in Schenectedy, they tend to display higher kinetic intensity values. Since kinetic intensity is a metric that effectively measures the "stop and go" nature of a duty cycle, we see that the number of stops is the driving force in energy consumption for vehicles located in the area.

In addition to observing the effect of stops per mile on average driving speed and its resulting affect on Kinetic intensity, we can also see that similar to stops per mile vs. average driving speed, average driving speed shows a strong exponential correlation to kinetic intensity as shown in Figure 7. It is interesting to note that compared to Schenecty, Lake Washington's school bus fleet operates at much higher average driving speed with fewer stops per mile, and as a result possesses a much lower kinetic intensity value. In this case, more of the energy consumed by the vehicles in Lake Washington's fleet can be attributed to aerodynamic losses rather than to the losses as a result of stop and go behavior.

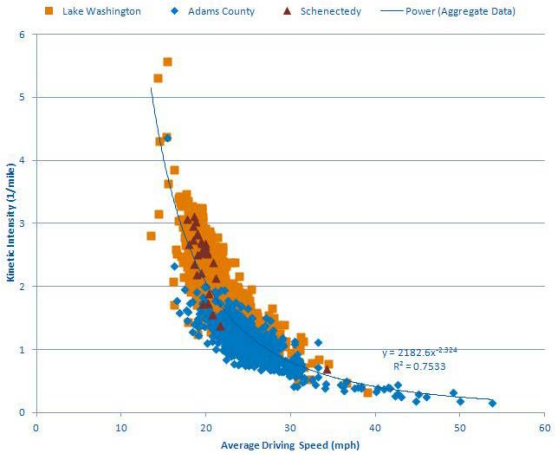

Figure 7. Average Driving Speed vs. Kinetic Intensity for School Bus Routes

If we examine the results of the speed analysis performed on the entire 1437 operational shift set, we can see as shown in Table 2, that as expected, the majority of school bus operation occurs at speed below 40 miles per hour (mph). However, what is of particular note is the significant amount of time spent at zero speed over the course of operation. On average, over 50% of the operating time of the vehicle is spent at zero speed.

Table 2. Operating Shift Speed Distribution

Speed Bin	Data Set Average	Data Set STD	Data Set Max	Data Set Min
zero speed time (%)	53.25	13.38	96.65	5.37
0+ - 5 mph time (%)	3.59	1.32	8.99	0.36
5+ - 10 mph time (%)	5.25	1.90	22.15	0.68
10+ - 15 mph time (%)	5.83	2.07	18.71	0.46
15+ - 20 mph time (%)	5.76	2.37	15.53	0.42
20+ - 25 mph time (%)	6.11	2.66	18.71	0.28
25+ - 30 mph time (%)	5.83	2.82	27.95	0.21
30+ - 35 mph time (%)	5.22	2.45	19.71	0.17
35+ - 40 mph time (%)	3.96	2.24	20.47	0.00
40+ - 45 mph time (%)	2.52	2.10	15.92	0.00
45+ - 50 mph time (%)	1.11	1.40	15.21	0.00
50+ - 55 mph time (%)	0.59	1.27	25.78	0.00
55+ - 60 mph time (%)	0.53	1.29	21.77	0.00
60+ - 65 mph time (%)	0.32	1.01	20.30	0.00
65+ - 70 mph time (%)	0.11	0.74	14.06	0.00
70+ - 75 mph time (%)	0.03	0.47	12.85	0.00
75+ mph time (%)	0.00	0.11	4.32	0.00

This is even more apparent as shown in Figure 8, when a histogram of the speed bins for the average of the 1437 school bus cycles is generated. The majority of operational time is currently spent operating at idle conditions, with the next largest speed bin occurring in the 20-25 mph range and only accounting for approximately 6 percent of total operating time.

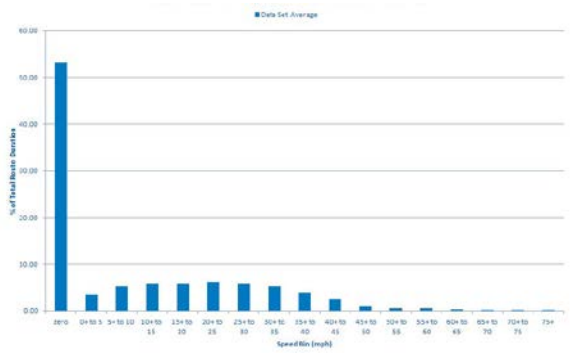

Figure 8. Speed Bin Histogram for Average School Bus Duty Cycle

Looking at a sample duty cycle drawn from the set in Figure 9, it can be seen that these idle times occur as large chunks in between driving events. In the case of PHEV applications, it may be advantageous to perform additional analysis to determine the viability of altering these idle periods for battery charging use.

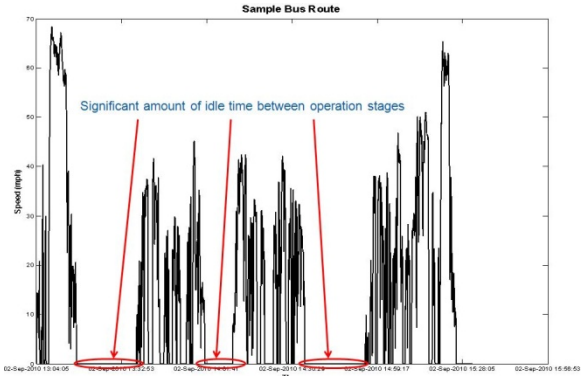

Figure 9. Sample Idle Time Analysis

Conclusions/Future Efforts

Based on the results of the duty cycle analysis performed on the school bus fleet data, is has been shown that a number of interesting relationships appear in the underlying vehicle operation. Strong exponential relationships exist between a number of significant operating metrics, including average driving speed, stops per mile, and kinetic intensity. It addition, basic results correlating the influence of geography on route behavior has been observed. It may be of interest to explore further efforts to greater examine the effect geography plays on vehicle operation, specifically in the area of operational duty cycle.

The data was also analyzed in order to select the 'best fit' drive cycle(s) for the data. Cycle Selection for average cycle based on the average absolute percent difference between standard cycle and aggregate data set average.

High/Low cycle selection focused on absolute percent difference between standard cycle and maximum/minimum driving metrics from data set. (i.e. for high aggressiveness cycle, we would want a cycle with higher stops/mile, higher Characteristic Acceleration, low Aerodynamic Speed, and Low Average Driving Speed, and low Maximum Driving Speed).

Metrics selected based on a minimization of the average of % differences in select operating metrics

List of selection metrics:

- Average Driving Speed (speed >0)
- Maximum Driving Speed
- Standard Deviation of Speed
- Characteristic Acceleration
- Aerodynamic Speed
- # of Stops Per Mile

Recommended test cycles to model average operation are shown below:

- JP-JE 05
- RUSCBC
- CSHVC (CSC)

The data set statistics versus the selected cycles are shown in Table 3 below.

Table 3. Data set statistics versus cycles

Metric	DATA SET AVERAGE	JP - JE05	RUCSBC	CSHVC (CSC)
maximum driving speed (mph)	54.48	54.43	49.70	43.80
average driving speed (speed > 0, mph)	23.32	22.70	26.59	18.44
standard deviation of speed (mph)	14.12	15.94	16.05	13.06
number of stops per mile	1.73	1.62	1.44	1.95
characteristic acceleration (ft/s/s)	0.63	0.40	0.86	0.56
aerodynamic speed (ft/s)	47.63	51.31	51.88	40.66
kinetic intensity (1/mile)	1.63	0.80	1.68	1.79

In addition to observing interesting relationships between duty cycle metrics and geographic influences, it is worthwhile to note the significant idle time occurring as part of typical school bus operation. Due to the large amount of time spent at zero speed as part of daily route operation, it may be of interest to investigate additional idle reduction technologies or charging strategies in the case of PHEV applications.

IV.C.3. Products

Tools & Data

1. Drive-cycle, Rapid Investigation, Visualization and Evaluation Tool (DRIVE), Copyrighted 2011. Tool created to analyze large sets of drive cycle data.
2. Fleet Analysis Toolkit (FAT GUI). Created/modified to input, filter, analyze and visualize large sets of vehicle performance data.

IV.D. CoolCab Test and Evaluation and CoolCalc HVAC Tool

Principal Investigator: Jason A. Lustbader
National Renewable Energy Laboratory
1617 Cole Boulevard
Golden, CO 80401
(303) 275-4443; E-mail: Jason.Lustbader@nrel.gov

DOE Program Managers: Lee Slezak and David Anderson
(202) 586-2335; Lee.Slezak@ee.doe.gov and 202-287-5688; David.Anderson@ee.doe.gov

IV.D.1. Abstract

Objective

- Help industry overcome barriers to the adoption of market-viable and efficient thermal management systems that keep the cab comfortable without the need for engine idling, helping to reduce the 838 million gallons of fuel used for truck overnight idling
- Investigate the potential to reduce truck cab thermal loads through testing and analysis
- Develop tools to help predict heating, ventilation, and air conditioning (HVAC) load reduction in truck cab/sleepers
- Reduce parasitic climate control loads needed for idle rest periods

Approach

- Develop analysis tools and test techniques to assess the impact of technologies that reduce the thermal load, improve climate control efficiency, and reduce vehicle fuel consumption
- Work with industry partners to research, evaluate, and develop commercially viable advanced idle-reduction technologies and systems
- Develop, validate, and apply CoolCalc, a long-haul truck thermal load modeling tool
- Collaborate closely with original equipment manufacturers (OEMs) and their suppliers

Major Accomplishments

- Improved and leveraged CoolCalc to identify opportunities to reduce loads and lead research efforts
- Experimentally characterized a 36% reduction in heavy vehicle heating loads using advanced insulation
- Achieved a 34% reduction in electric air conditioning (A/C) system energy consumption in Colorado test conditions by improving cab thermal performance
- Wrote CoolCalc user's guide

Future Activities

- Collaborate closely with industry partners to develop and evaluate idle and thermal load reduction systems
- Apply CoolCalc to simulate vehicle thermal performance across a broad range of operating conditions
- Develop advanced idling and HVAC testing capabilities to evaluate idle reduction systems
- Research advanced and innovative thermal and idle load reduction technologies

IV.D.2. Technical Discussion

Background

Heating and air conditioning are two of the primary reasons for long-haul truck main engine operation when the vehicle is parked. In the United States, trucks that travel more than 500 miles per day use 838 million gallons of fuel annually for overnight idling [1]. Including workday idling, over 2 billion gallons of fuel are used annually for truck idling [2]. By reducing thermal loads and improving efficiency, there is a great opportunity to reduce the fuel used and emissions created by idling. Enhancing the thermal performance of cab/sleepers will enable cost-effective idle reduction solutions. If the fuel savings from new technologies can provide a 1- to 2-year payback time, fleet owners will be economically motivated to incorporate them. This provides a pathway to rapid adoption of effective thermal and idle load reduction solutions.

Introduction

The U.S. Department of Energy's (DOE's) National Renewable Energy Laboratory (NREL) CoolCab project is researching efficient thermal management systems that keep the cab occupants comfortable without the need for engine idling. The CoolCab research approach is to reduce thermal loads, concentrate on occupant thermal comfort, and maximize equipment efficiency. By working with industry partners to develop and apply commercially viable solutions that reduce idling fuel use, both national energy security and sustainability will be improved.

Approach

NREL is closely collaborating with OEMs and suppliers to develop and implement a strategic approach capable of producing commercially viable results to enable idle reduction systems.

This strategic, three-phased approach was developed to evaluate commercially available and advanced vehicle thermal management and idle reduction technologies. The three phases are baseline characterization and model development, thermal performance enhancement, and idle reduction, each featuring applications of NREL's suite of thermal testing and analysis tools. The test procedures conducted include: thermal soak, overall heat transfer (UA), idle air conditioning (A/C), infiltration rate, and infrared imaging.

Thermal soak tests were conducted to evaluate the impact of technologies in an engine-off solar loading condition. This test procedure is used to characterize technology impacts on modified truck interior air temperatures (compared to baseline truck interior air temperatures . A test parameter (β) was developed to quantify the maximum possible reduction in interior air temperature rise above ambient as described in equation 1.

$$\beta = \frac{\overline{T}_{baseline} - \overline{T}_{modified}}{\overline{T}_{baseline} - \overline{T}_{ambient}} \cdot 100\% \quad (1)$$

Overall heat transfer (UA) tests were conducted to quantify baseline heat loss and the impact of adding commercially available and advanced insulation. The test was conducted at night with a 1-kW heat source in each vehicle. The sleeper curtain was closed, and the average interior air temperature was calculated by averaging eight k-type thermocouples with six located in accordance with the Technology Maintenance Council's recommended practice RP422A [3]. The UA value was calculated by measuring the heater power (Q) and the temperature difference (ΔT) between the interior air and ambient as described in equation 2.

$$UA = \frac{Q}{\overline{T}_{sleeper} - \overline{T}_{ambient}} \quad (2)$$

A new test capability was developed to evaluate a Dometic Environmental Corporation battery powered A/C system. The A/C systems were used to characterize the impact of thermal load reduction technologies on A/C power requirements. Each vehicle was equipped with an A/C unit controlled to a setpoint of 73°F and connected to a data logger that recorded current, voltage, and power.

The test program was conducted at NREL's new Vehicle Testing and Integration Facility (VTIF), shown in Figure 1, during the months of May through September. The facility is located in Golden, Colorado, at an elevation of 5,997 feet at latitude 39.7 N and longitude 105.1 W. The experimental setup included a test vehicle provided by Volvo Trucks North America and an NREL-owned control vehicle. The vehicles were oriented south and separated by a distance of 25 feet to maximize solar loading and minimize shadowing effects. A National Instruments data acquisition system was developed to record instrumentation measurements at a sampling frequency of 1.0 Hz averaged over one-minute intervals. The instrumentation for each vehicle included 52 calibrated k-type thermocouples featuring 30 air and 22 surface locations with a maximum measurement uncertainty, U_{95} of ± 0.18°C.

Figure 1. NREL's Vehicle Testing and Integration Facility, *Photos by Dennis* Schroeder*, NREL*

CoolCalc, a long-haul truck thermal load estimation tool, was improved and leveraged to identify opportunities to reduce thermal loads and to lead research efforts. Enhancements were made to CoolCalc to make it more robust and improve usability. The new version was provided to industry partners. A user's guide was written to help the user through the entire simulation process, from installing the software to processing simulation results. It helps new users learn CoolCalc and serves as a reference for experienced users. The approach for both heating and cooling load estimation was also improved. CoolCalc was used to assist partners on both DOE- and industry-funded projects for Oshkosh Truck, Volvo, Aerospace Corporation, and a Daimler Trucks SuperTruck project.

Technologies researched this year using the three-phase approach include a battery-powered A/C system, a solar reflective film, multiple configurations of insulation, and a truck featuring both film and insulation.

Results

Phase I research, Baseline Characterization, characterized the production performance of OEM vehicles, calibrated the control vehicle to represent a baseline test vehicle, and collected data for the development of a CoolCalc truck model. This calibration was achieved by collecting several days of baseline data with unmodified vehicles. Figure 2 illustrates the accuracy of the calibrated control truck compared to the measured test truck during baseline thermal soak tests.

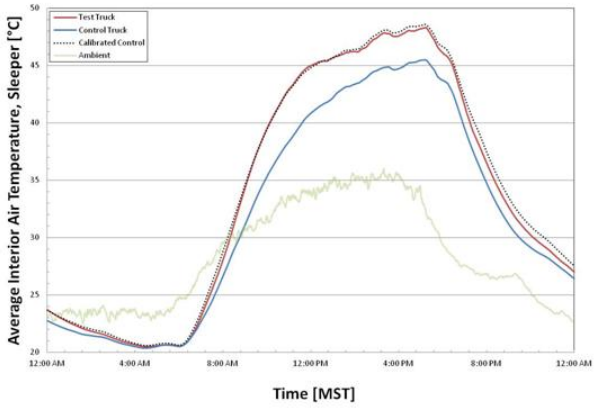

Figure 2. Baseline thermal soak calibration check on verification day

Baseline UA characterization testing was conducted to determine the overall heat transfer differences between test and control vehicles. On average, the control truck tested 20.8 W/K

higher than the test truck. Therefore, on modified test days, the measured control truck UA value was reduced by 20.8 W/K. Two calibration check days were used to verify that the adjusted control truck UA matched the measured test truck data. Table 1 summarizes the results of the verification days.

Table 1. Baseline Characterization of Overall Heat Transfer, UA

Truck	Check 1 UA [W/K]	Check 2 UA [W/K]	Mean UA [W/K]
Measured Control	70.3	70.2	70.3
Calibrated Control	49.5	49.4	49.5
Measured Test	48.9	49.8	49.4

Baseline A/C system test results, Figure 3, showed that the A/C systems did not operate overnight at the set point and weather conditions tested. Therefore, a 10-hour daytime A/C-on test period, from 9 a.m. to 7 p.m., was specified.

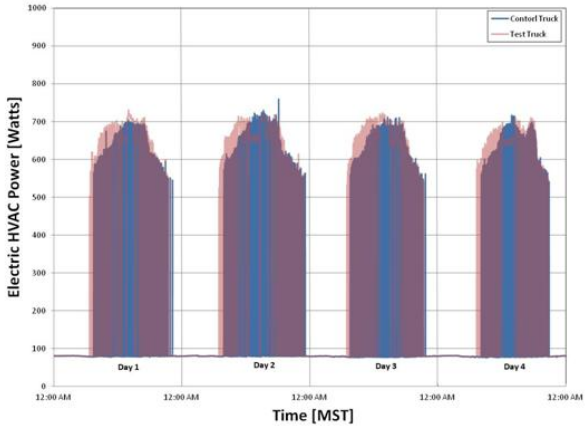

Figure 3. Baseline engine-off A/C test results

Phase II research focused on reduction of vehicle thermal loads. Infrared imaging and CoolCalc analysis were used to identify promising load reduction strategies. The CoolCalc tool characterized an opportunity to reduce thermal loads by as much as 25% with a generic truck model, through application of exterior glazings such as reflective paints, films, or radiant barriers as illustrated in Figure 4.

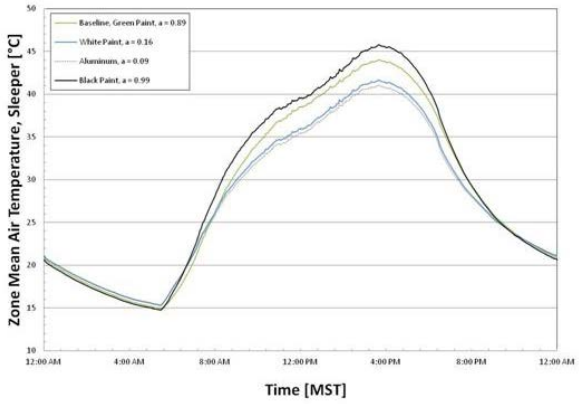

Figure 4. CoolCalc paint and radiant barrier study

Nighttime infrared imaging identified opportunities to enhance heat transfer performance of the vehicle. During infrared imaging, a heater equipped with a fan was placed in each vehicle to supply a uniformly distributed heat source. High temperature exterior surface areas, illustrated in Figure 5, resulted from high heat transfer through the walls. This demonstrated an opportunity to reduce the conduction by applying commercially available and advanced insulation packages.

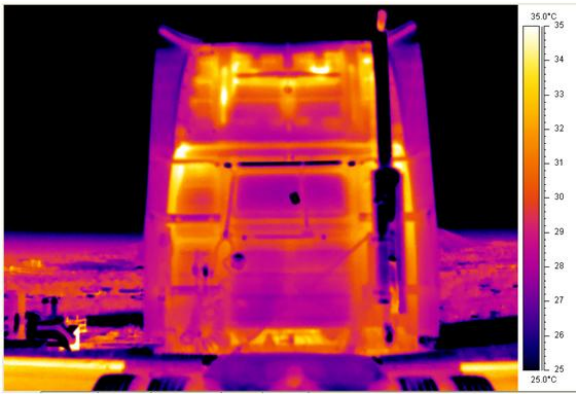

Figure 5. Infrared image of back exterior wall

Field evaluation of R-19 insulation and a highly reflective radiant barrier was conducted to identify idealized thermal load reductions as a benchmark for commercially available and advanced technologies. A 5°C temperature reduction or β value of 32%, equation 1, was achieved with the reflective barrier, while a 20% reduction in the overall heat transfer coefficient, UA, was achieved from insulating the cab and sleeper with the sleeper curtain open.

Experimental results from the radiant barrier shown in Figure 6 were comparable to analytical results from the CoolCalc generic truck model shown in Figure 4.

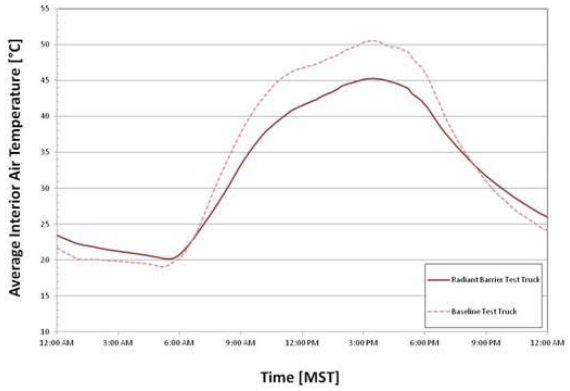

Figure 6. Thermal soak results with radiant barrier

Phase III of research involved close collaboration with OEMs and suppliers to select commercial and advanced technologies for further evaluation with an idle reduction system on-board. NREL collaborated closely with engineers at Volvo Trucks North America, 3M's Renewable Energy Division, EAR Thermal Acoustic Systems, and Dometic Environmental Corporation. Several configurations were selected for evaluation, including commercially available and advanced insulation packages, a solar reflective film, and a truck configuration featuring both commercial insulation and film.

The baseline test data for an unmodified vehicle was compared to the OEM vehicle modified with the different packages. Thermal soak, UA, and idle A/C tests were repeated to determine rest period temperature impacts, heat transfer improvements, and A/C load reductions.

Table 2. Climate Control Reduction Summary

Test Configuration	Heating Reduction [% of UA]	Cooling Reduction [% of A/C]
Curtain Closed	19%	3%
Solar Reflective Film	-	8%
Insulation and Film	-	22%
Commercial Insulation	26%	20%
Advanced Insulation	36%	34%

Table 2 summarizes the impact of the technologies on climate control systems. The truck modified with solar reflective film had an average interior air temperature reduction of 1.5°C from the baseline or β value of 8%. This reduction would have been significantly larger if comparing the technology to a higher absorptivity exterior than the baseline truck's silver color.

Overall heat transfer tests for the advanced Thinsulate™ insulation package demonstrated an increase in interior air temperature of 7°C resulting in an overall heat transfer coefficient reduction of 23 W/K. This equates to a 36% savings on heating loads required to maintain the baseline interior air temperature.

Modified engine-off idle A/C tests characterized the impact of thermal management technologies on an idle reduction system. A/C energy requirements were monitored over a 10-hour daytime test period from 9 a.m. to 7 p.m. A 2-kW battery-powered idle A/C system was used during the evaluation. Energy consumed in watt-hours was determined by integrating the A/C load over the 10-hour test period. Hourly energy consumption for the baseline vehicle compared to the vehicle modified with an advanced insulation package is shown in Figure 7.

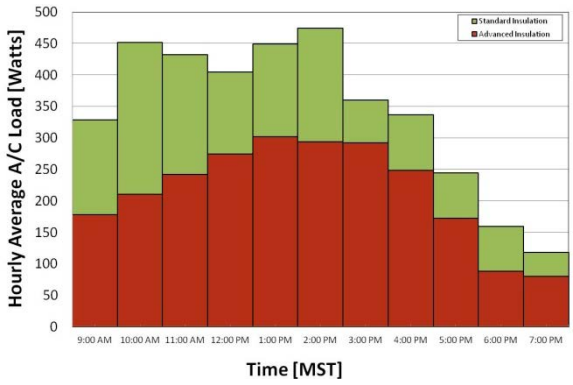

Figure 7. A/C test results for advanced insulation

A 34% reduction in A/C load was achieved with the advanced insulation package applied to the vehicle. This equates to approximately 1,400 W-hr of energy saved over the 10-hour rest period. Savings for other configurations are summarized in Table 3.

Table 3. A/C Electrical Load Reduction Summary

Test Configuration	Battery Energy Saved [W-hr]
Curtain Closed	160
Solar Reflective Film	430
Insulation and Film	1200
Commercial Insulation	900
Advanced Insulation	1400

Conclusions

Heating and cooling loads required for idle reduction systems were reduced by as much as 36% and 34%, respectively, through application of commercially available and advanced vehicle thermal management technologies. An energy savings of 1400 W-hr was achieved during a 10-hour daytime rest period while operating a battery-powered idle A/C system under

Colorado ambient conditions. For this specific auxiliary A/C system this equates to a 23% reduction in battery pack capacity. Reductions in battery pack capacity lead to lower initial costs, operating costs, mass, and volume of idle reduction systems.

Working closely with industry partners and applying both modeling and testing tools, NREL has shown that systematically packaging vehicle thermal management and idle reduction technologies together can reduce climate control loads needed for heavy vehicle hotel load idling. This can reduce cost, weight, and volume of idle reduction systems, improving payback time and increasing economic motivation for fleet owners and operators to consider idle reduction systems.

IV.D.3. Products

Publications

1. Lustbader J., Rugh, J., Rister, B., Venson, T. "CoolCalc: A Long-Haul Tuck Thermal Load Estimation Tool," SAE World Congress, Detroit, Mi, April 12-14, 2011, Paper Number 2011-01-0656

References

1. Stodolsky, F., Gaines, L., Vyas, A. *Analysis of Technology Options to Reduce the Fuel Consumption of Idling Trucks.* Argonne National Laboratory, ANL/ESD-43, June 2000.
2. Gaines, L., Vyas, A., Anderson, J., "Estimation of Fuel Use by Idling Commercial Trucks," 85th Annual Meeting of the Transportation Research Board, Washington, D.C., January 22–26, 2006, Paper No. 06-2567.
3. "Cab Insulation Testing Methodology," RP422A-1-9, in *Technology and Maintenance Council's Recommended Maintenance Practices Manual, 2010-2011 edition,* Arlington, VA: American Truckers Association, p. RP422A-1

Tools & Data

CoolCalc rapid HVAC load estimation tool version 1.0. Only available to industry and laboratory partners at this time.

Acknowledgements

- Co-author: Travis Venson (NREL)
- Additional thanks to: John Rugh and Matt Jeffers (NREL)

Special thanks to: Our industry partners (Volvo, Daimler, PACCAR, Oshkosh, Dometic, 3M, EAR)

\

IV.E. Medium Truck Duty Cycle (MTDC) and Performance Data Base

Principal Investigator: Gary Capps
Oak Ridge National Laboratory (ORNL)
National Transportation Research Center
2360 Cherahala Boulevard
Knoxville, TN 37932
(865) 946-1285; cappsgj@ornl.gov
Fax: (865) 946-1381

Gratis Fleet Partner: Fountain City Wrecker Service
President: Joel Smith
(865) 688-0212; fcwreckerservice@bellsouth.net

Gratis Fleet Partner: Knoxville Utilities Board
Fleet Supervisor: Chris Wilson
(865) 558-2408; Chris.Wilson@kub.org

Federal Agency Partner: Federal Motor Carrier Safety Administration
General Engineer: Chris Flanigan
(865) 558-2408; chris.flanigan@dot.gov

DOE Technology Development Manager: Lee Slezak
(202) 586-2335; lee.slezak@ee.doe.gov

IV.E.1. Abstract

Objective

- To collect and analyze real-world heavy- and medium-truck duty cycle (HTDC, MTDC) and performance data to support: PSAT/Autonomie modeling, DOE technology investment decisions, heavy- and medium-truck fuel efficiency research, and to outreach to other federal and private stakeholders for collaboration and joint project execution.

Approach

- Identify relevant performance measures (e.g., location, speed, fuel consumption, gear, grade, time-of day, congestion, idling, weather, weight, etc.). Note: no emissions data is currently being collected.
- Design/test a data acquisition system to collect identified performance measures (i.e., field hardened and tested, able to interface with the test vehicle's on-board databus and other sensors, communicates data wirelessly/daily/securely).
- Find fleets willing to participate without direct funding (i.e., gratis partnerships). Incentives for partners include: better introspective data to improve fuel efficiencies, public exposure, and public goodwill.
- Instrument and "shake-down" test vehicles; i.e., six test vehicles per year in two vocations per year over two years
- Manage data in a cost effective and secure manner (e.g., automatic quality assurance programs to look for data that is out-of-range, missing data, etc.).
- Develop specialized data manipulation and analysis software; e.g., the prototype real-world-based duty-cycle generation tool – DCGenT will generate duty cycles of user specified duration based on user-selected duty cycle characteristics (e.g., grade, payload, type of roadway, weather, time-of-day, etc.).

- Outreach to other agencies/programs for cost leveraging. A recent major MTDC success involves a DOE/DOT partnership agreement for the collection of brake and tire performance data. DOT provided funding for all sensors and labor associated with their brake and tire interests and by doing this in conjunction with DOE's MTDC efforts reduced the amount of funding required to conduct this research. The benefit to DOE is that the brake and tire performance data adds to the DOE's data store of medium-truck performance data; already the largest known data store of medium-truck performance data from real-world operating environments, in the world.

Major Accomplishments

- Instrumentation of the utility vehicles was completed and FOT data collection started
- Began the MTDC Part-2 data collection effort on towing and recovery vehicles and utility vehicles
- completed the MTDC Part-1 interim report
- Partnered with the Department of Transportation's (DOT's) Federal Highway Administration (FHWA) Office of Freight Management and Operations to study the weight and grade effects on fuel economy based on HTDC data. A final report was submitted to FHWA in July 2011
- At industry's request provided specific information derived from the HTDC and MTDC databases (e.g., histograms of engine torque vs. engine speed for given load levels and different time of the year). Also provided specific information to ANL to support their research and development efforts (e.g., transit vehicle duty cycles)
- A set of software tools were developed and finalized. These tools are used to interrogate potential vehicles, wirelessly transfer data from the vehicles, validate data, selection data segments for analysis and to create synthetic duty cycles from the data

Future Activities

- Complete the MTDC Part-2 data collection and analysis
- Complete the MTDC final report
- Develop a MTDC and HTDC public website for summarized and analyzed data
- Broaden the data collection suite to include aerodynamics, parasitic energy losses, rolling resistance measures, and emissions
- Broaden the data collection efforts to include duty cycle data for heavy- and medium-truck hybrids.
- Complete the Duty Cycle Generation Tool (DCGenT) with the capability of estimating energy demand including truck-based energy demands involving real-world event such as idling, coasting, and congestion

IV.E.2. Technical Discussion

Background

The MTDC project, like the previous Heavy-Truck Duty Cycle (HTDC) project, is an important DOE Vehicle Technologies Program (VTP) effort. It is providing important data and information related to fuel usage, engine parameters, speed, direction of travel, time-of-day, geographic position, grade, and weather and road conditions for Class-6 and 7 vehicles operating in real-world environments. Through the use of the DCGenT users are able to generate, based on user-specified criteria, real-world-based duty cycles for use by vehicle fuel economy modeling development in support of VTP, private industry studies, and studies by the heavy-truck research community. For example, an analyst might be interested in duty cycles for metropolitan areas during peak travel times; or a duty cycle that is characteristic of rural freeways with steep grades. Upon completion of the DCGenT, analysts will be able to specify various performance shaping factors to generate customized duty cycles based on data collected from real-world experience. Lastly, with more than one year's worth of Class-8 data in DOE's Truck Performance Database, and Class-7 data being collected daily, specialized studies of energy efficiency are being conducted, and

support for the development of a standardized heavy truck duty cycle for emissions studies can be provided, including possible collaboration with the Environmental Protection Agency (EPA). The parameters for which data have, and will continue to be collected are based on parameters of importance for vehicle fuel economy modeling development in support of the DOE Vehicle Technologies Program.

The MTDC effort is leveraging the prior HTDC work that has led to the development of a customized data acquisition suite, the collection of a significant database of Class-8 real-world performance data, and the development of DCGenT. MTDC, which involves an emphasis on Class-6 and 7 trucks, was initiated in the latter half of FY 2008. The MTDC effort involves designing and implementing a 36-month data collection, analysis and reporting effort for Class-6 and 7 trucks. The effort is further subdivided into two parts: Part 1 involved the data collection effort for transit buses and combination delivery vehicles which was just completed; and Part 2 will involve similar efforts for utility trucks and towing and recovery trucks. A list of the data channels gathered in the MTDC effort is provided in Table 1.

Table 1. MTDC Data Channels

No.	Description
1	Total Vehicle Distance
2	Road Speed Limit Status (On/Off)
3	Wheel-Based Vehicle Speed/Road Speed
4	Front Axle Speed
5	Engine Speed
6	Current Gear
7	Selected Gear
8	Actual Gear Ratio
9	Output Shaft Speed
10	Transmission Selected Range
11	Transmission Current Range
12	Engine Oil Temperature
13	Intake Manifold Temperature
14	Engine Coolant Temperature
15	Boost Pressure
16	Fuel Rate
17	Instantaneous Fuel Economy
18	Actual Engine - Percent Torque
19	Percent Accelerator Pedal Position
20	Percent Load at Current Speed
21	Driver's Demand Engine - Percent Torque
22	Nominal Friction Percent Torque
23	Brake Switch
24	Clutch Switch
25	Cruise Control Accelerate Switch
26	Cruise Control Active
27	Cruise Control Coast Switch
28	Cruise Control Enable Switch
29	Cruise Control Resume Switch
30	Cruise Control Set Switch
31	Cruise Control Set Speed
32	Power Takeoff Governor/Status Flags
33	Power Takeoff Set Speed
34	Total Power Takeoff Hours
35	Battery Voltage
36	Fan Drive State

No.	Description
37	AC High Pressure Fans Switch
38	Barometric Pressure
39	Latitude
40	Longitude
41	Altitude
42	Vertical Velocity
43	Velocity over Ground
44	Longitudinal Acceleration
45	Lateral Acceleration
46	Heading
47	Satellites
48	Time UTC
49	Distance
50	Steer Axle Weight
51	Drive Axle Weight
52	Wiper Switch Position (On/Off)
53	Brake Actuator Status - Left Front
54	Brake Actuator Status - Right Front
55	Brake Actuator Status - Left Rear
56	Brake Actuator Status - Right Rear
57	Lining Status - Left Front
58	Lining Status - Right Front
59	Lining Status - Left Rear
60	Lining Status - Right Rear
61	Brake Application Pressure
62	Tire Pressure - Left Front
63	Tire Pressure - Right Front
64	Tire Pressure - Left Rear Outside
65	Tire Pressure - Left Rear Inside
66	Tire Pressure - Right Rear Inside
67	Tire Pressure - Right Rear Outside
68	Tire Temperature - Left Front
69	Tire Temperature - Right Front
70	Tire Temperature - Left Rear Outside
71	Tire Temperature - Left Rear Inside
72	Tire Temperature - Right Rear Inside

No.	Description
73	Tire Temperature - Right Rear Outside

Approach

This is an ongoing effort with Part 1 of the data collection complete as well as the Part 1 Interim Report. For Part 2 of the effort, six (6) vehicles were instrumented and data is being collected as called out in the Background section of this report. They are as follows: three (3) Class-6 roll-back vehicle recovery trucks and three (3) Class-8 utility bucket and derrick trucks. Representative images of these vehicles are shown in Figures 1 and 2. Data from these vehicles is being wireless collected from the on-board DAS, validated and cleansed, and stored for analysis.

Figure 1. Class-8 Bucket Truck

Figure 2. Class-6 Flat-Bed Recovery Vehicle

Results

The data collection effort for Part 2 of the MTDC project is currently underway and it is expected to conclude at the end of November 2011, at which point the analysis of the information gathered in the project will start. For MTDC Part 2, data has been collected at a rate of approximately 7.5 GB per month and at the end of this phase of the project it is expected to have over 95 GB of data (approximately 38 GB collected by the utility bucket and derrick trucks, and 57 GB by the recovery trucks). For the overall MTDC project (Parts 1 and 2), the total data collected will be approximately 290 GB, similar to the amount of data collected in the HTDC project. This will result in a 1.2 billon-record database of heavy and medium size vehicle information.

Conclusions

The MTDC (and HTDC) efforts are producing a rich database of duty cycle and vehicle performance data that is available nowhere else in the world. To date, this duty cycle data has been provided to Argonne National Laboratory to support PSAT/Autonomie modeling efforts for class-7 and 8 trucks. The effort has demonstrated the ability and value of cross-agency cooperation and partnerships (DOE/VTP and DOT/FMCSA) which has produced a win-win situation for both agencies. More and greater cooperation with DOT/FHWA in Part-2 of the MTDC effort and future duty cycle efforts is expected. This effort has shown the need for more data based on vocations within a given class in order to characterize the variability inherent within particular vocations. Currently, a feasibility study for a large scale, low-cost duty cycle effort is being conducted to assess within-vocation duty cycle variability. Additionally, methods for synthetically generating emissions data are being discussed and a potential partnership with EPA is being explored.

IV.E.3. Products

Publications

WBIR, a local Knoxville news station, interviewed ORNL and KUB personnel for a segment on the Medium Truck Duty Cycle research. The segment, which aired on the local 11:00pm news on Wednesday, November 17, 2010, can be accessed via the following link:

http://www.wbir.com/news/local/story.aspx?storyid=143220.

Effect of Weight and Roadway Grade on the Fuel Economy of Class-8 Freight Trucks; Franzese, Davidson; August 2011

Patents

None.

Tools & Data

A suite of software tools have been develop or further refined to aid in the collection, analysis, and application of the duty cycle data.

First, the Data Bus Utility (DBAU) is used to access the data available on a candidate vehicle. The BDAT is a Matlab-based tool that provides a graphical representation of the data available, is able to look for specific messages on the data bus, and allows for the modification of parameters used to interpret the data. Typically, a vehicle can be fully assessed in only one interrogation session. A snapshot of the BDAU is shown in Figure 3.

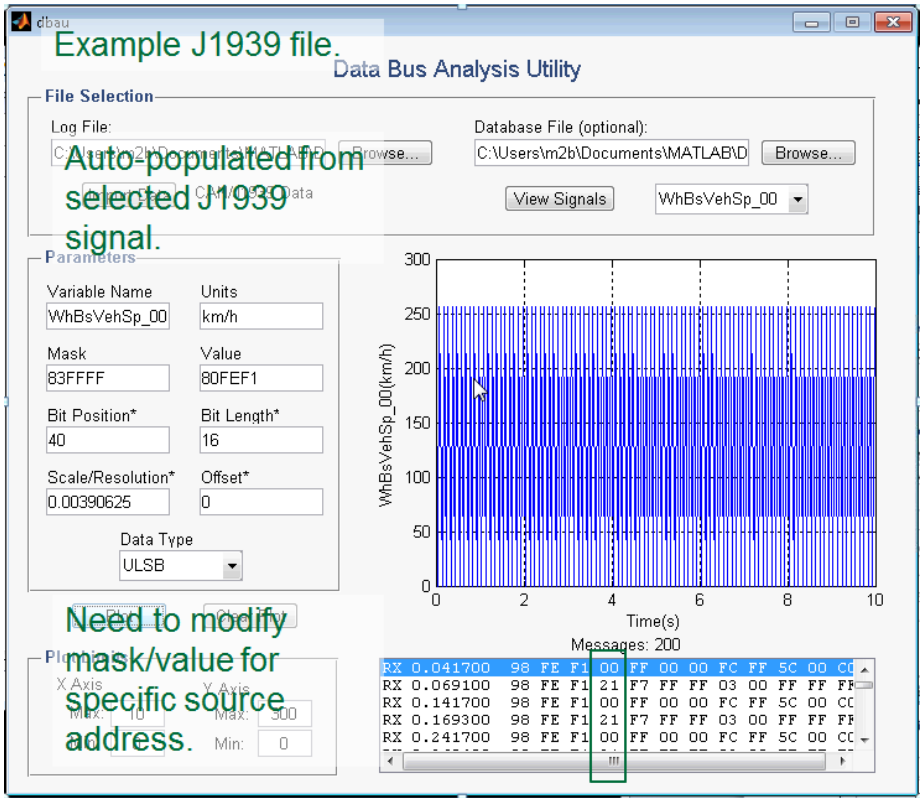

Figure 3. BDAU User Interface with Auto-Populated Data

Once a candidate vehicle is chosen and instrumented, the Wireless Data Download Tool (WDDT) is used to retrieve the data automatically from the data acquisition system (DAS) on-board the vehicle. The WDDT also increases data security and integrity and provides an e-mail summary of the data to ORNL researchers. The WDDT architecture is shown in Figure 4.

Next, the Data Quick Look Tool (DQLT) is used to spot-check the data once is has been retrieved. The DQLT allows the user to choose a file, then the associated file(s), and then plot the data for inspection. The user interface for the DQLT is shown in Figure 5.

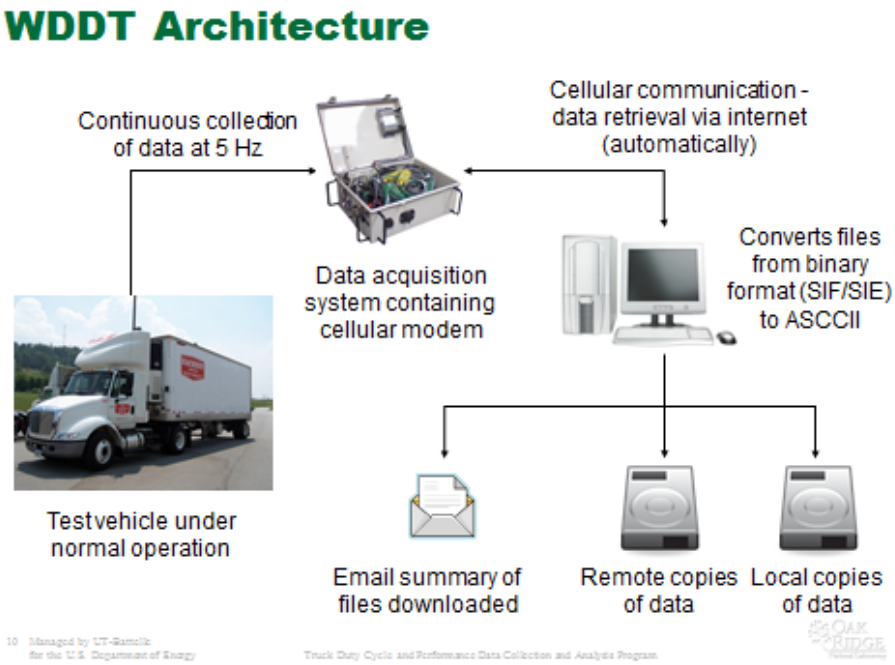

Figure 4. WDDT Architecture

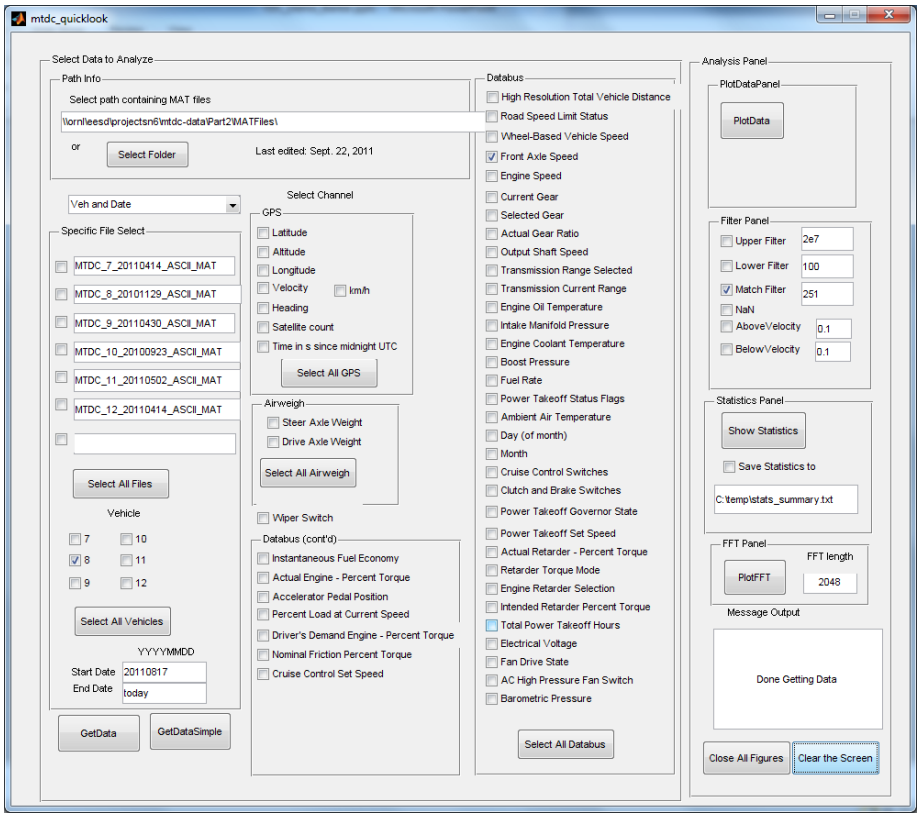

Figure 5. DQLT User Interface

In order to select duty cycle data from the data base to be used for analysis purposes, the data must be extracted based on some initial parameters. These parameter allow the user to reduce the data set down to a manageable set of files and allow for the selection of parameters of interest. This process is managed through the Data Extractor and Analysis Tool (DEAT). The DEAT user interface is shown in Figure 6 for the HTDC database. The available parameters for data selection (in the case shown in the figure) are:

- Time of day
- Speed
- Topography
- Transmission
- Temperature
- Precipitation
- Roadway type
- Location
- Tires
- Wind speed
- Dynamic condition
- Tractor and/or trailer
- Weight

In additional to the DEAT, ORNL has also developed the Spatial Data Extractor and Analysis Tool (SDEAT). The SDEAT allows the use to spatially display, select, and extract collected data. The SDEAT is a web-based analysis application that is able to access both the medium and heavy truck data and provided analysis tables and charts of the selected data. Figure 7 shows the SDEAT with a route selected in Tennessee.

A major component of the medium and heavy truck duty cycle data collection effort is the use of the data for modeling where real-world data input is desired. In support of this modeling need, the Duty Cycle Generation Tool (DCGenT) has been developed to produce a synthetic duty cycle statistically representative of the original duty cycle. These synthetic duty cycles can be much smaller than the original duty cycle making analysis and modeling faster while given the same or similar results. The inputs for the DCGenT at present are:

- Engine torque
- Altitude
- Engine speed
- Fuel rate
- Velocity
- GPS Coordinates

The DCGenT creates the synthetic duty cycle by breaking up the original duty cycle into smaller sections and segments based on stopped, start-stop, acceleration, and deceleration sections. Next, the original duty cycle data is place into bins on a bivariate histogram to create synthetic segments. These segments are stringed together and further refined and then compared with the original. This comparison is shown in Figure 8.

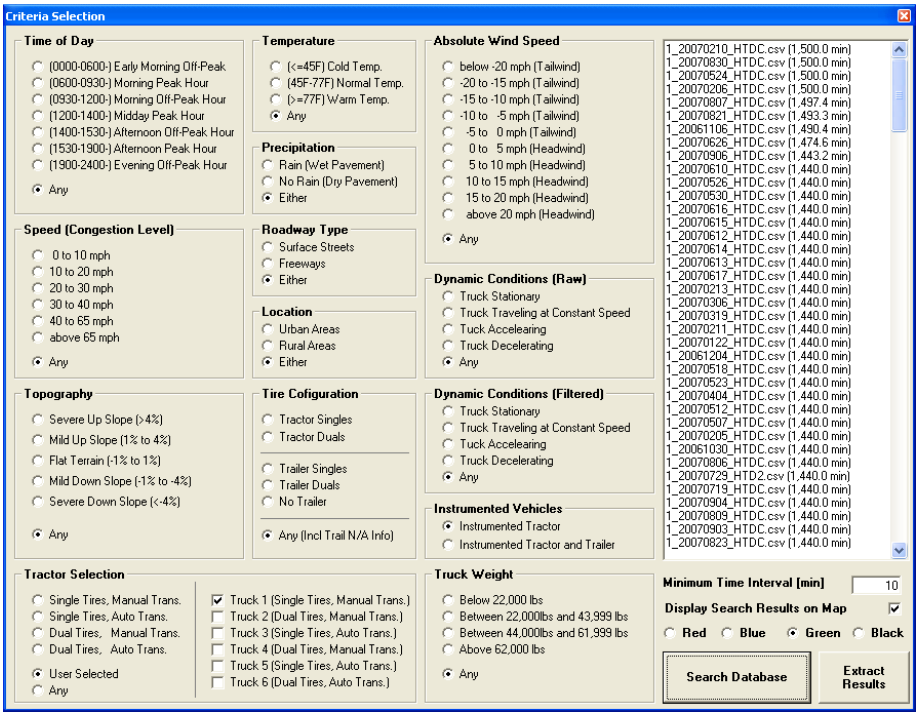

Figure 6. DEAT User Interface

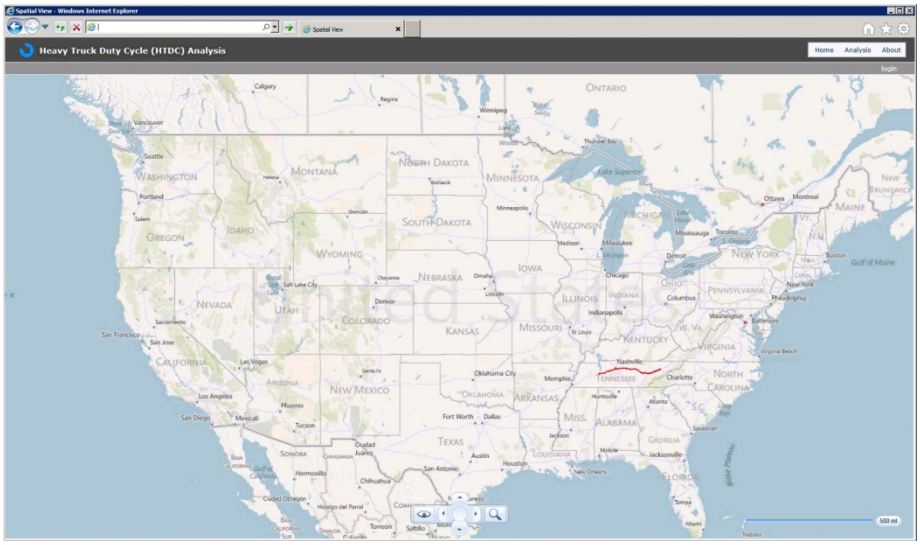

Figure 7. Data Set Selected in Tennessee (I-40) Using the DEAT

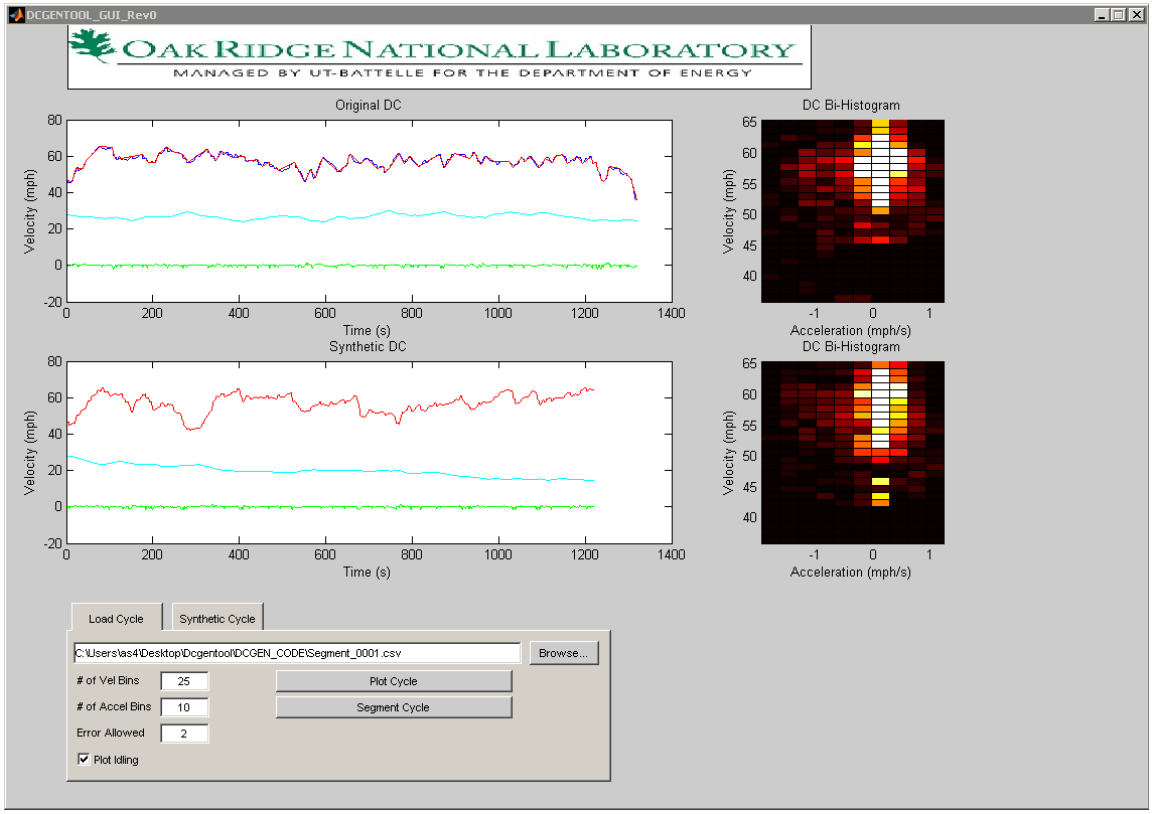

Figure 8. DCGenT Comparison of Original and Synthetic Duty Cycles

IV.F. Large-Scale Duty Cycle (LSDC) and Performance Database

Principal Investigator: Tim LaClair
Oak Ridge National Laboratory (ORNL)
National Transportation Research Center
2360 Cherahala Boulevard
Knoxville, TN 37932
(865) 946-1305; laclairtj@ornl.gov
Fax: (865) 946-1314

IV.F.1. Abstract

Objective

- Characterize the real-world usage of medium- and heavy-trucks in a broad range of trucking applications in the United States and conduct analyses to assess the fuel savings potential of employing advanced energy efficiency technologies. This research will help provide guidance to technology developers, fleets and individual truck owners in creating and employing those technologies that provide the greatest fuel savings for each application in real-world use, and will assist the DOE and other agencies in setting transportation research and policy priorities.

Approach

- Identify a technical approach for the cost-effective measurement of duty cycles from 3000-5000 trucks among 12-15 trucking vocations.
- Obtain vehicles to participate in the study for each vocation from across the U.S., and conduct duty cycle measurements over a 12-month period to comprehensively characterize the vehicles' normal usage.
- Perform statistical analysis of the duty cycle data for each vocation and develop a set of characteristic duty cycles that are highly representative of the use for each trucking vocation/application.
- Conduct analyses using the representative duty cycle data to quantify the fuel savings that can be achieved by implementing advanced energy efficiency technologies, individually or in combinations, on trucks in the U.S. fleet.
- Develop web-based tools that will allow users to estimate the fuel savings that can be realized with any combination of selected technologies for each application, based on analysis results of the characteristic duty cycles from the project or allowing the input of user-specific drive cycle data.

Major Accomplishments

The Feasibility Study for the project was completed in FY11:

- ORNL has gained critical support from the Technology & Maintenance Council (TMC) of the American Trucking Associations (ATA) for identifying and recruiting participants for the LSDC data collection effort.
- A novel approach has been developed for estimating the fuel savings that can be achieved by implementing advanced fuel efficiency technologies, either individually or with combinations of technologies. The approach is based on a tractive energy analysis using only measured duty cycle data along with several fundamental vehicle parameters. This methodology, which was demonstrated by analyzing a variety of previously measured duty cycle data, is the same approach that will be used for performing the fuel savings evaluations when the characteristic duty cycle data is collected from all of the vocations of interest.
- Cost estimates were obtained for the telematics data collection activities by issuing a Request for Proposal (RFP) to data collection service providers. The desired duty cycle measurements for the project can be completed at a cost of approximately $50/month/truck.

Future Activities

- Proof of concept (POC) testing of 10-20 vehicles during a one-month period will be performed to demonstrate that the required measurements can be made on a continual basis at the specified 1 Hz sampling rate.
- ORNL will develop the tools needed to receive measured data in large quantities and automate the data validation, processing and database transfer requirements, in preparation for the Full-System Pilot Test (FSPT).
- The FSPT will be performed with 50-100 vehicles from a selected vocation tested for a duration of six months. This will serve to verify and refine the automated data collection, verification, and processing procedures, in preparation for the Field Operation Test (FOT).
- The FOT will be conducted to measure duty cycles of the remaining vehicles from all vocations selected for the project. This is the primary measurement activity, and will include measurements from thousands of medium- and heavy-duty trucks during a period of a full year.
- Statistical analysis of all of the collected data will be performed to generate characteristic duty cycles representing each of the vocations for which the duty cycle data is collected.
- Web-based Decision Support Tools will be developed to make the analysis results and characteristic duty cycle data available to fleets and other users.

IV.F.2. Technical Discussion

Background

The LSDC project was launched as a research effort aimed at characterizing the usage of medium- and heavy-duty trucks throughout the United States by collecting basic duty cycle data (velocity, acceleration and elevation) over a one-year period during normal operations. The measured data will be analyzed to develop a broad understanding of truck fuel economy and emissions in normal everyday use, to identify advanced efficiency technologies that offer the greatest potential for improving truck efficiencies in each trucking application and to understand the variations in drive cycles that exist among vehicles within the same application. Tools will be developed to allow fleets and owner operators to evaluate the benefits that can be expected with any technology or combination of technologies for their particular application. Key objectives of this research include developing representative duty cycles for each truck vocation and evaluating the fuel savings potential for advanced efficiency technologies for different trucking applications. The term "representative drive cycle" in this case means that the drive cycles that will be developed should represent, in a statistical sense, the average driving characteristics for all trucks within each trucking application/vocation. The representative, or characteristic, drive cycles will therefore be developed by accumulating statistics for accelerations, velocities and loads, among all of the vehicles measured in the project, and developing drive cycles for each vocation that have characteristics as close as possible to those of the complete set of data collected.

For the main testing phase of the project (the FOT), the goal is to measure the duty cycles of 100-500 separate vehicles among each of 12-15 selected truck vocations—for a total of 3000-7500 trucks—during a period of approximately 12 months. The measurements to be made will consist primarily of vehicle speed and route, with readings taken once every second of vehicle operation. The route information, based on real-time GPS coordinates, will allow road elevation data to be determined. Additional information will be collected for engine speed, torque and instantaneous fuel consumption, if possible, but the core drive cycle information is the primary data of interest.

This research will help provide guidance to technology developers, government agencies, and fleets and individual truck owners for

investing in technologies that are best suited to real-world use. The data collected from this study will also benefit many other areas of transportation research since it will provide a detailed view of traffic encountered throughout the U.S. transportation network over an extended time period and it will contain information about driving behavior among a diverse set of trucking applications.

In FY2011, the primary project activities consisted of obtaining detailed cost information for the data collection, and the development and demonstration of an analysis approach for evaluating the fuel savings attainable when advanced vehicle technologies are employed for each trucking application/vocation. The analysis, which uses characteristic duty cycle data as an input, will allow users to quantify the expected fuel efficiency improvements from any technology, or from combinations of technologies, and thus users can identify the technology, or set of technologies, that will provide the greatest benefits and value for the particular vehicle use. The remainder of this report presents a summary of the analysis approach and provides several results from the analyses performed.

Approach

Fuel savings technologies function, in general, by reducing parasitic energy losses that the vehicle must overcome, and each technology has certain energy losses that they reduce or recover (e.g. aerodynamic drag, tire rolling resistance, braking energy losses, drivetrain frictional losses, or accessory power consumption). Analyzing the tractive energy required to overcome the various forces acting on the vehicle and accounting for the contribution of different parasitic losses during different regimes of the drive cycle provides a means to assess the energy savings potential of these technologies. Figure 1 below shows a drive cycle for which the speed (black curve) characteristics vary significantly over the duration of the drive cycle, with nearly constant highway speeds, followed by off-freeway operation that is more characteristic of an urban vehicle usage. In spite of the different operating characteristics over the cycle, the measured cumulative fuel consumption (blue curve) is very nearly proportional to the cumulative tractive energy (green curve) over the drive cycle.

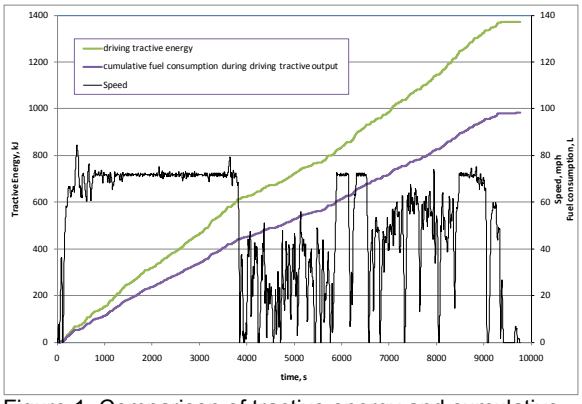

Figure 1. Comparison of tractive energy and cumulative fuel consumption during periods of positive tractive power during a measured drive cycle.

This linearity of the fuel consumption and tractive energy is very evident in Figure 2, in which these two data sets are cross-plotted. The fact that the tractive energy linearly correlates to the vehicle fuel consumption is the basis for this analysis, since this permits fuel savings to be estimated relatively precisely from any changes

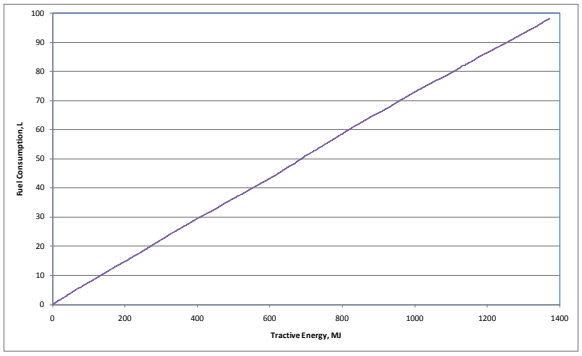

Figure 2. Cumulative fuel consumption vs. tractive energy requirement.

to the overall tractive energy requirements—regardless of the source of the tractive energy variation.

The analysis is completed through a series of calculations, as follows: (1) Both the driving and braking tractive energies are first calculated for the input drive cycle, and the relative contributions to the tractive energy from tire

rolling resistance, aerodynamic drag and braking are determined. (2) Sensitivity values associated with each of the energy loss factors, in addition to that associated with the vehicle mass, are calculated. (3) Once the tractive energy impacts are quantified in this way, variations in the tractive energy can be very easily estimated using the calculated sensitivity parameters. (4) With the total tractive energy, the fuel consumption is calculated for the drive cycle by applying values for the average engine efficiency, transmission efficiency, and average accessory power. (5) Fuel consumption during idling can be quantified in a final step, which allows the benefits of idling reduction technologies to be quantified. With this model, key parameters that characterize rolling resistance, aerodynamic drag, engine efficiency, transmission efficiency, hybrid regenerative braking, accessory power and idling can be modified in a series of basic calculations to determine the effects of any combination of parameter changes on the fuel consumption. This provides a relatively simple but powerful method to estimate the fuel savings that are possible with different technologies without the need to perform very detailed and time-consuming analyses, and it provides a means to identify those technologies with the greatest potential for trucking applications for which the vehicle usage is known, i.e. when representative drive cycles are available for the application or trucking vocation.

Results

Duty cycle data collected as part of an earlier DOE funded effort, the Heavy Truck Duty Cycle (HTDC) project, was evaluated using the tractive energy analysis approach to demonstrate the operation of the tool and to show the fuel efficiency benefits for a variety of duty cycles. For the current discussion, only one case is presented for brevity. Figure 3 shows the drive cycle considered.

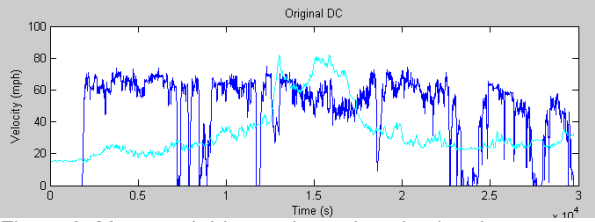

Figure 3. Measured drive cycle analyzed using the tractive energy method. The cyan curve is the elevation in meters (x10), while the dark blue curve is the velocity profile.

Using the tractive energy approach, the sensitivity of the fuel consumption to changes in various physical parameters is calculated as shown in Table 1.

Table 1. Calculated sensitivity of driving and braking tractive energy to rolling resistance, aerodynamic drag, and vehicle mass.

Sensitivity Factors	Value
$S_{RR,drive}$ (% per kg/T reduction in C_{RR})	4.4
$S_{RR,braking}$ (% per kg/T reduction in C_{RR})	1.4
$S_{aero,drive}$ (% per 10% aero drag reduction)	3.0
$S_{aero,brake}$ (% per 10% aero drag reduction)	0.9
$S_{brakes,drive}$ (% of E_{trac})	18.3
$S_{mass,drive}$ (% per 1,000kg)	2.7
$S_{mass,braking}$ (% per 1,000kg)	-1.1

By applying these sensitivity factors to the tractive energy over the drive cycle, the potential savings in tractive energy is determined both with and without regenerative braking for a set of assumed variations in the vehicle mass, aerodynamic drag and rolling resistance, as well as for regenerative braking, as shown in Figure 4 below. The fuel savings due to any combination of the technologies considered is determined using this data but is slightly lower than the tractive energy reductions.

The fuel savings associated with regenerative braking, assuming an 80% efficiency of the system, is about 13.0% for this drive cycle. If we consider the energy savings potential when regenerative braking is used simultaneously with the other technologies impacting the tractive energy, the overall benefits are quite impressive. The total reduction in tractive energy is 28.2%

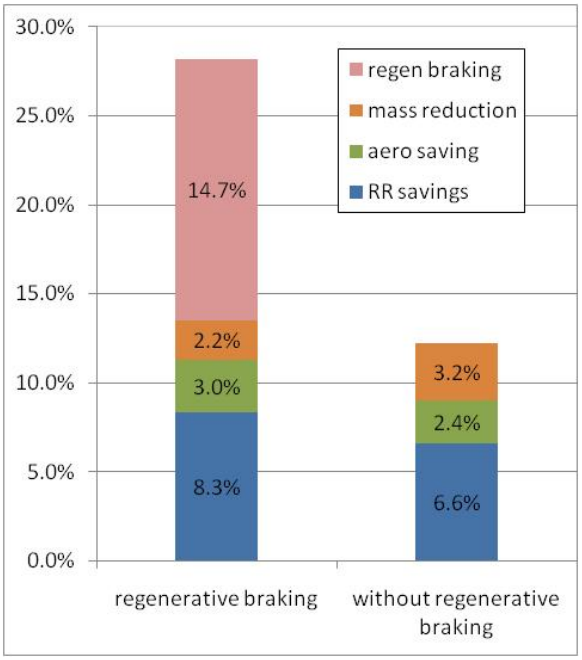

Figure 4. Comparison of the relative reduction in driving tractive energy, with and without regenerative braking, when the rolling resistance coefficient is reduced by 1.5 kg/T, the aerodynamic drag coefficient is reduced by 8% and the mass reduced by 1200 kg for the measured drive cycle.

for the full combination of technologies (8% reduction in aerodynamic drag, improvement in the tire rolling resistance coefficient by 1.5 kg/T and a 1200 kg reduction in mass) and the corresponding fuel savings is 25.0%. For the case where regenerative braking is used simultaneously with the other technologies, the rolling resistance and aerodynamic drag reductions provide an extra 2.3% savings in the tractive energy requirement relative to the non-hybrid case, showing the synergies that can occur when various technologies are combined. This increases the benefits from the low rolling resistance and aerodynamic drag reductions by about 25% relative to the savings they generated without regenerative braking.

The energy savings potential from regenerative braking for this drive cycle, even though it is almost entirely freeway driving, is at a level that employing hybrid technology should receive serious consideration. If this level and frequency of braking is common among long-haul operations, the fuel savings potential of hybridization could be much greater than what is generally believed. Several of the drive cycles evaluated for this study showed braking contributions to the tractive energy of 6% or higher, and it appears that there is at least a modest fuel savings potential for regenerative braking in long-haul trucking. A more complete evaluation of the range of drive cycles that are experienced in each trucking application/ vocation is needed to determine which technologies can provide significant improvements in fuel efficiency for the set of vehicles used in that application. This is the main objective of the LSDC project, and detailed analysis of the tractive energy results, using the approach demonstrated here, will be conducted as part of the project to determine the energy savings potential associated with various advanced technologies for each trucking application.

Conclusions

An analysis of measured drive cycle data from the HTDC project was performed and several results were presented that illustrate how the analyses using the tractive energy approach are carried out. These cases serve as examples of the type of fuel savings estimates that can be performed using the tractive energy analysis of drive cycle data. These results clearly demonstrate how the intended analysis for the LSDC project will be completed using the set of data that the project team intends to have measured during the project. This tractive energy analysis approach provides a relatively simple means to quantify the fuel savings potential of various technologies and combinations of technologies for any given drive cycle. This analysis approach, coupled with detailed drive cycle measurements from a broad set of trucking applications/vocations, will enable better decisions to be made regarding the technologies that can provide the greatest benefits for fuel efficiency in each trucking application (including cost-benefit analyses), and realistic estimates of the fuel savings potential can be made for different technologies and technology combinations for each application/vocation.

IV.F.3. Products

Publications

1. T. LaClair, *Large Scale Duty Cycle (LSDC) Project: Tractive Energy Analysis Methodology and Results from Long-Haul Truck Drive Cycle Evaluations*, Project Report submitted to DOE, June 2011.
2. T. LaClair, "Application of a Tractive Energy Analysis to Quantify the Benefits of Advanced Efficiency Technologies Using Characteristic Drive Cycle Data," Submitted to SAE for presentation and publication at the *2012 SAE World Congress*.

Patents

None.

Tools & Data

The Tractive Energy Efficiency Assessment (TEEA) tool has been implemented as a prototype tool in MS Excel, and relies on macros and functions to perform all of the calculations for the fuel efficiency technology evaluations. The results presented in this report were created using this version of the tool. Many of the functions have been converted to a Matlab-based tool and it is planned to integrate this functionality with the Duty Cycle Generation (DCGen) tool that has been developed as part of the Medium Truck Duty Cycle (MTDC) project.

V. SIMULATION AND MODELING

V.A. Advanced Light Duty HEV Validation

Namdoo Kim (Project Leader), Aymeric Rousseau
Argonne National Laboratory
9700 South Cass Avenue
Argonne, IL 60439-4815
(630) 252-7261; arousseau@anl.gov

DOE Technology Managers: David Anderson, Lee Slezak

V.A.1. Abstract

Objectives

- Validate the latest conventional, hybrid, and plug-in hybrid vehicles in Autonomie.

Approach

- Gather component and vehicle assumptions.
- Develop the vehicle-level control strategy.
- Validate the model by comparing with available test data.

Accomplishments

- Validated heavy-duty conventional vehicles.
- Validated hybrid electric vehicles (HEVs) and plug-in hybrid electric vehicles (PHEVs) using proprietary data.

Future Directions

- Continue to validate models of the latest powertrain technologies.
- Improve models for accessory loads for medium and heavy duty applications

V.A.2. Technical Discussion

Introduction

The Prius, a power-split hybrid electric vehicle from Toyota, has become synonymous with the word, "Hybrid." As of October 2010, two million of these vehicles had been sold worldwide, including one million vehicles purchased in the United States. In 2004, the second generation of the vehicle, Prius MY04, enhanced the performance of the components with advanced technologies, such as a new magnetic array in the rotors. However, the third generation of the vehicle, Prius MY10, features a significant configuration — an additional reduction gear has been added between the motor and the output of the transmission. In addition, a change of the energy management strategy has been found by analyzing a number of testing results performed at the Advanced Powertrain Research Facility (ARRF) at Argonne National Laboratory. Whereas changes of the configuration, it is not easy to determine the effect of the energy management strategy because the supervisory control algorithm is proprietary. Based on extensive experience in designing the controllers of power-split hybrid electric vehicles in Autonomie, the objective is to identify the supervisory control algorithm by analyzing the vehicle test results. A vehicle

model and a control model for Prius MY10 have been developed to reproduce the real-world behaviors, and the simulation results are compared with test data.

Vehicle Description

The system configuration and the differences compared with the previous version will be briefly introduced in this section.

Powertrain Configuration

The transmission of Prius MY10 is composed of two planetary gear sets, whereas the previous version, Prius MY04, only had one. One of the two planetary gear sets splits the power flow from the engine as well as the previous version, and the other one is operated as a reduction gear for the motor, as shown in Figure 1.

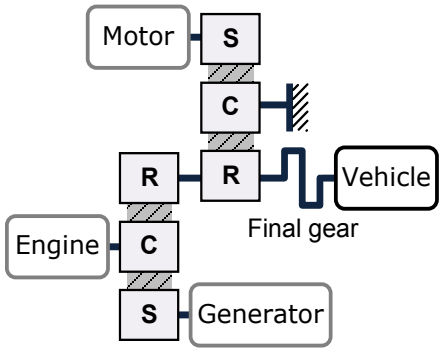

Figure 1. A configuration of Prius MY10

The high-speed permanent magnet synchronous motor is able to produce power up to 60 kW, but the available power for the pure electric driving is less than half of the power because the battery can only provide 28kW of electric power. One of the differences between the MY04 and MY10 models is an increased component power level as shown Table 1. The new components lead to better vehicle performance despite increase weight.

Table 1. Power capacity of the components and vehicle performance of Prius MY10 [5]

	MY04	MY10
Engine power (kW)	57	73
Motor power (kW)	50	60
Net power (kW)	80	100
Fuel economy, sticker (MPG) (City/Highway)	48/45	51/48
Fuel economy, estimated	34/67	35/74

The planetary gear set added between the output of the transmission and the motor allows a smaller final drive compared to the MY04. The influence of the change will be discussed in the following section.

Prius MY10 vs. Prius MY04

The lower final drive ratio allows the transmission output to operate at a relatively lower speed than MY04. A lower output speed means that the generator could also have a different speed. One of the drawbacks of Prius MY04 is that the system efficiency of the vehicle rapidly declines when the vehicle is running on the highway because the generator speed is reversed, and the power conversion loss is rapidly increased in the situation. The generator speed in Prius MY10 is, however, reduced by the changed gear ratio of the final drive, as shown in Figure 2.

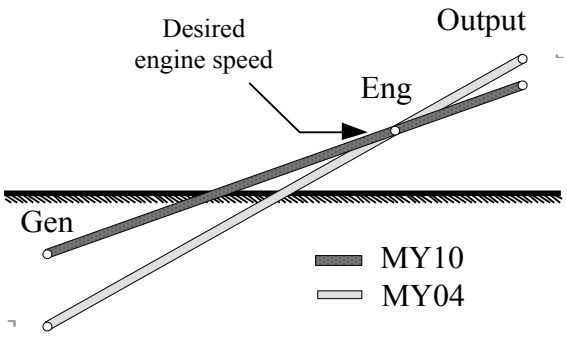

Figure 2. A lever system showing the different operating speed for Prius MY10

Based on the testing results, a recent study showed that the conversion loss for Prius MY10 is reduced by 12% compared with the loss for Prius MY04. On the other hand, the study also shows that the battery in Prius MY10 is less used than the battery in the Prius MY04, as

shown in Figure 3, which is caused by the change of the energy management strategy.

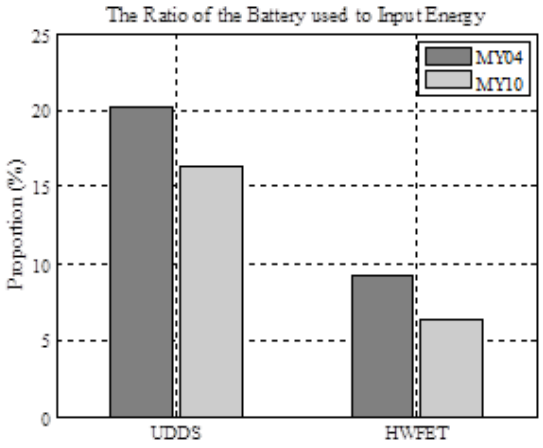

Figure 3. The difference in the use of energy from the battery [9]

The reduced battery usage could be helpful to extend the lifetime of the battery, but a number of tests should be conducted to determine the exact influence of the change of the energy management strategy to the battery life.

Vehicle Control Strategy Analysis

Vehicle Testing

The Toyota Prius MY10 was tested on 25 various driving schedules on the APRF dynamometer. For vehicle control strategy analysis, steady speed testing results were primarily used to understand basic control patterns and establish control rules. The testing results obtained from various driving schedules are used to verify the established rules.

Analysis of Testing Results

Three main strategies were introduced to understand and reproduce the vehicle level control

Engine-on Condition

The operation of the engine determines the mode, such as pure electric vehicle mode (PEV mode) or HEV mode. The engine is turned ON when the driver's power demand exceeds a pre-defined threshold, as shown in Figure 4, where the demand power is determined by the pedal signal and the current vehicle speed.

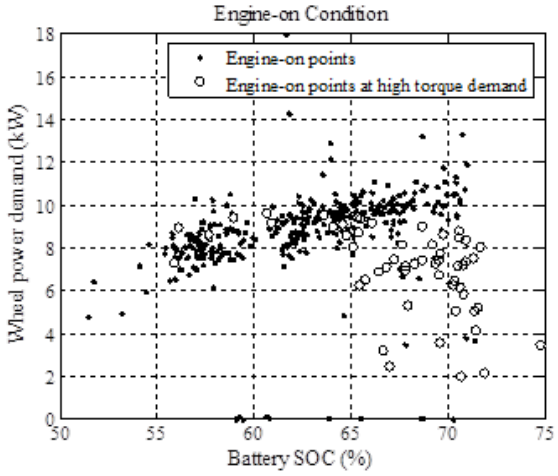

Figure 4. The engine-on condition (The engine is turned on when the driver's demand power is over the threshold line [JPS])

In Figure 4, the engine is turned ON early if the SOC is low, which means that the system is changed from PEV mode to HEV mode to manage the SOC. On the other hand, the engine is turned ON during conditions that are not expected, such as the circles shown in Figure 4. The circles indicate the points when the driver requires a high torque larger than 900 Nm, which means that the engine provides propulsion power if the motor does not cover the desired performance, even though the power demand is lower than the threshold.

SOC Balancing

The desired battery power is strongly related to the energy management strategy. We found that the battery power is mainly determined by the current SOC, as shown in Figure 5, when the vehicle is in HEV mode. The results are obtained by extracting the testing data when the vehicle is in HEV mode and when the effect of target tracking torque is minimized. The motor and generator could consume additional power when they need to trace a target. The testing results are not considered for the control target if a significantly transient dynamic behavior exists in the transmission.

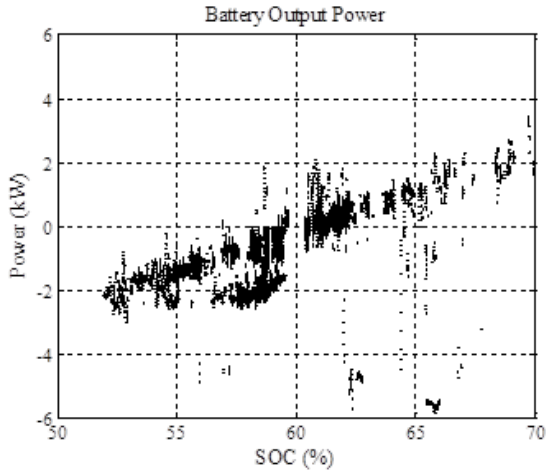

Figure 5. The battery output power (The desired battery power is determined by the current SOC.)

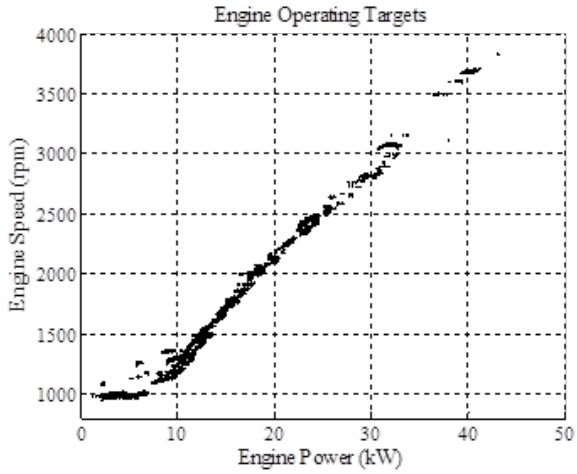

Figure 6. The engine operating targets (The engine speed is determined by the desired engine power.)

The overall trend shows that the energy management strategy tries to bring SOC back to a regular value of 60%. With the engine turn-on condition, the control idea is the main approach of Prius MY10 to manage the SOC. If the SOC is low, the engine is turned on early, and the power-split ratio is determined to restore the SOC to 60%, so that the SOC can be safely managed without depletion.

Engine Operation

The two control concepts previously stated could determine the power-split ratio. It, however, does not generate the target speed or torque of the engine because the power-split system could have infinite control targets that produce the same power. Therefore, an additional control concept to determine the operating target is needed. Figure 6 shows how the engine speed can be determined based on the requested engine power.

To obtain the points, we excluded the engine operating points when the engine temperature is low, and instantaneously steady targets are considered only from the testing results, as we did for analyzing the SOC balancing.

Vehicle Model

Vehicle model

A vehicle model was developed in Autonomie based on collected powertrain configuration and component data information (Figure 7).

Figure 7. The vehicle system loaded on Autonomie

Simulation Results

Simulation was performed on the the Urban Dynamometer Driving Schedule (UDDS) and the Highway Fuel Economy Test (HWFET). The simulation results were compared with the vehicle testing results. First, simulation results of the vehicle speed, the engine speed, and the engine torque on UDDS are compared with the testing results (Figure 8).

Since the engine thermal model is not considered in this version, the first 200 seconds of the simulation do not match as well with the testing results. Even if the test is supposed to start under engine warm conditions, the 10 minutes soak time between tests is sufficient to trigger a different vehicle level control strategy.

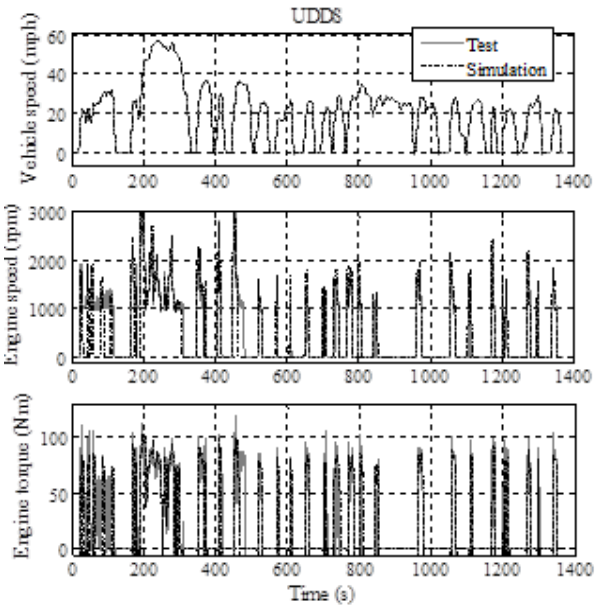

Figure 8. The simulation results and testing results on UDDS

The other simulation results on HWFET are compared with the testing results, as shown in Figure 9. One notices that the engine speed and torque match very well with the vehicle test data.

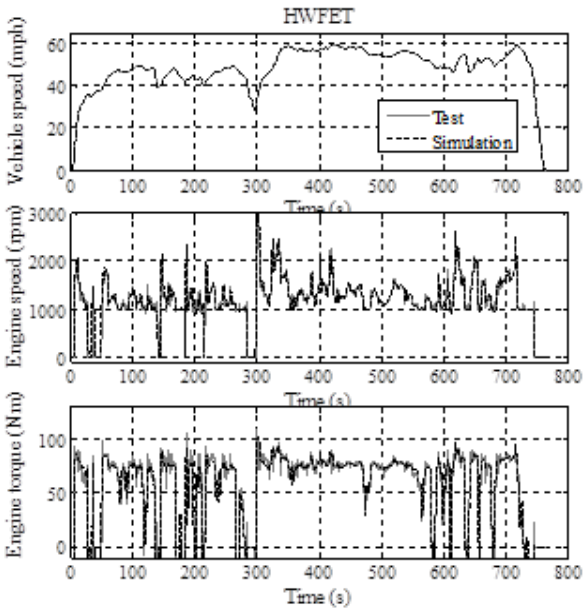

Figure 9. The simulation results and testing results on HWFET

Figure 10 compares the battery SOC from simulation and test both for the UDDS and HWFET drive cycles. As one notices, the signals are very close one to another, with the exception of the first 200 seconds of the UDDS drive cycle. This is due to the fact that the engine is operated differently to be warmed-up.

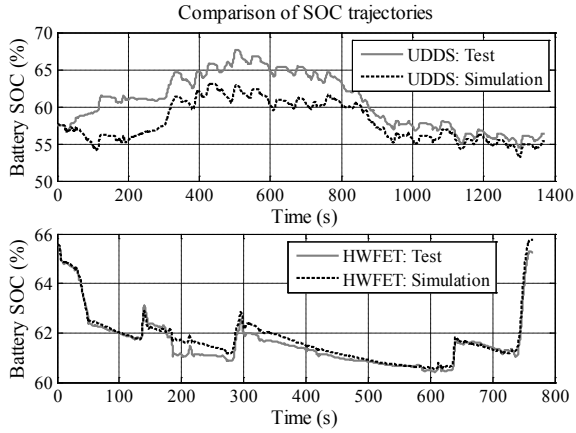

Figure 10. The comparison of SOC trajectories for each driving schedule

By matching the component operating conditions (i.e., engine ON/OFF, torque and speed operation, SOC control…), we were able to achieve a fuel consumption differences of 3.4% for UDDS and 4.1% for HWFET.

Conclusions

One advantage of using simulation instead of real-world testing is that the simulation minimizes the effort and costs of evaluating vehicle performance. To be able to trust simulation results, entire vehicle validation of state-of-the-art powertrain, component and controls is necessary. The results obtained from the MY10 Prius simulation show close performances for fuel economy, within 5%, and the operating patterns for the components are well matched with the real vehicle's patterns. Although the study is focused on the model validation in Autonomie, the validated vehicle model will support numerous studies for the U.S.DOE

V.A.3. Products

Publications/Presentations

1. Kim, N., Rask, E., Rousseau, A., "Vehicle Level Control Strategy Comparison between MY2004 and MY2010 Toyota Prius," Presentation to US DOE, May 2011
2. Kim, N., Rask, E., Rousseau, A., "Toyota Prius MY10 Validation," Presentation to US DOE, September 2011
3. Kim, N., Rask, E., Rousseau, A., "Toyota Prius MY10 Validation," SAE World Congress, April 2012

V.B. Simulation Runs to Support GPRA

Namdoo kim (Project Leader), Ayman Moawad, Aymeric Rousseau
Argonne National Laboratory
9700 South Cass Avenue
Argonne, IL 60439-4815
(630) 252-7261; nkim@anl.gov

DOE Technology Managers: David Anderson, Lee Slezak

V.B.1. Abstract

Objectives

- Simulate multiple vehicle platforms, configurations, and timeframes to provide fuel economy data for analysis in support of the Government Performance and Results Act (GPRA).

Approach

- Validate component and vehicle assumptions with DOE national laboratories and FreedomCAR Tech Teams.
- Use automatic component sizing to run the study.

Accomplishments

- Simulated and sized more than 2,000 vehicles both for light and heavy duty applications
- Simulated new vehicles when assumptions or platforms were revised or when additional configurations or timeframes were requested.

Future Directions

- Continue to provide analytical data to support GPRA in 2011.

V.B.2. Technical Discussion

Introduction

Through the Office of Planning, Budget, and Analysis, DOE's Office of Energy Efficiency and Renewable Energy (EERE) provides estimates of program benefits in its annual Congressional Budget Request. The Government Performance and Results Act (GPRA) of 1993 provided the basis for assessing the performance of federally funded programs. Often referred to as "GPRA Benefits Estimates," these estimates represent one piece of EERE's GPRA implementation efforts — documenting some of the economic, environmental, and security benefits (or outcomes) that result from achieving program goals. The Powertrain System Analysis Toolkit (PSAT) was used to evaluate the fuel economy of numerous vehicle configurations (including conventional, hybrid electric vehicles [HEVs], plug-in HEVs [PHEVs], electric), component technologies (gasoline, diesel, and hydrogen engines, as well as fuel cells), and timeframes (current, 2010, 2015, 2020, 2030, and 2045). The uncertainty of each technology is taken into account by assigning probability values for each assumption.

Methodology

To evaluate the fuel efficiency benefits of advanced vehicles, the vehicles are designed on the basis of component assumptions. The fuel efficiency is then simulated on the Urban Dynamometer Driving Schedule (UDDS) and Highway Fuel Economy Test (HWFET). The vehicle costs are calculated from the component sizing. Both cost and fuel efficiency are then used to define the market penetration of each

technology to finally estimate the amount of fuel saved. The process is highlighted in Figure 1. This report focuses on the first phase of the project: fuel efficiency and cost.

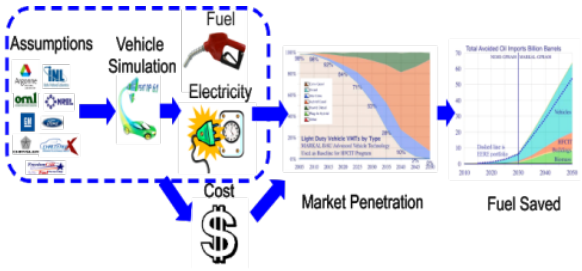

Figure 1. Process to Evaluate Fuel Efficiency of Advanced Technology Vehicles

To properly assess the benefits of future technologies, the following options were considered, as shown in Figure 2:

- Different vehicle classes: compact car, midsize car, small sport utility vehicle (SUV), medium SUV, pickup truck, as well as medium and heavy duty applications
- Four timeframes: 2010, 2015, 2020, 2030, and 2045
- Five powertrain configurations: conventional, HEV, PHEV, fuel cell HEV, and electric vehicle
- Four fuels: gasoline, diesel, hydrogen, and ethanol

Overall, more than 2,000 vehicles were defined and simulated in Autonomie. The current study does not include micro- or mild hybrids and does not focus on emissions.

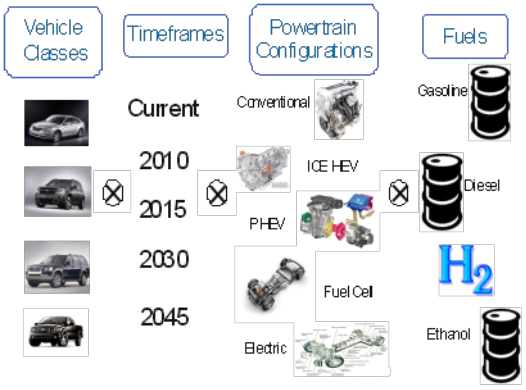

Figure 2. Vehicle Classes, Timeframes, Configurations, and Fuels Considered

To address uncertainties, a triangular distribution approach (low, medium, and high) was employed, as shown in Figure 3. For each component, assumptions (e.g., regarding efficiency, power density) were made, and three separate values were defined to represent the (1) 90th percentile, (2) 50th percentile, and (3) 10th percentile. A 90% probability means that the technology has a 90% chance of being available at the time considered. For each vehicle considered, the cost assumptions also follow the triangular uncertainty. Each set of assumptions is, however, used for each vehicle, and the most efficient components are not automatically the least-expensive ones. As a result, for each vehicle considered, we simulated three options for fuel efficiency. Each of these three options also has three values representing the cost uncertainties.

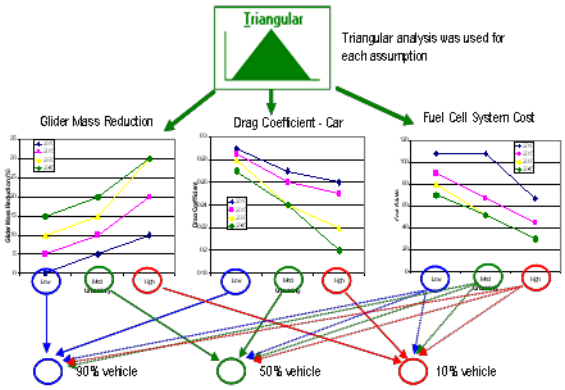

Figure 3. Uncertainty Process

Vehicle Technology Projections

The assumptions described below have been defined on the basis of inputs from experts and the FreedomCAR targets (when available).

Engines

Several state-of-the-art internal combustion engines (ICEs) were selected as the baseline for the fuels considered: gasoline (spark ignition or SI), diesel (compression ignition or CI), ethanol (E85), and hydrogen (H2). The gasoline, diesel, and ethanol engines used for reference conventional vehicles were provided by automotive car manufacturers, while the port-injected hydrogen engine data were generated at Argonne. The engines used for HEVs and PHEVs are based on Atkinson cycles, generated

from test data collected at Argonne's dynamometer testing facility. Table 1 shows the engines selected as a baseline for the study.

Table 2. Engines selected

Fuel	Source	Displacement	Peak
SI	Car	2.4	123
CI	Car	1.9	110
H2	Argonne	2.2	84
E85	Car	2.2	106
SI/E85	Argonne	1.5	57

Fuel Cell Systems

Figure 4 shows the evolution of the fuel-cell system peak efficiencies. The peak fuel-cell efficiency is assumed to be at 55% currently, and it will increase to 60% by 2015. A value of 60% has already been demonstrated in laboratories and therefore is expected to be implemented soon in vehicles. The peak efficiencies will remain constant in the future, as most research is expected to focus on reducing cost and increasing durability.

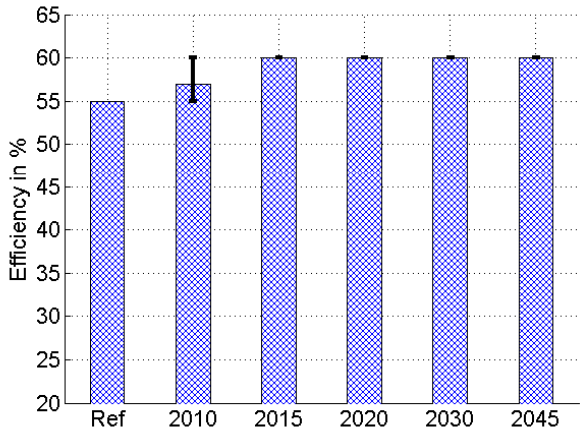

Figure 4. Fuel-cell system efficiency

Hydrogen Storage Systems

The evolution of hydrogen storage systems is vital to the introduction of hydrogen-powered vehicles. As in the case of the fuel-cell systems, all the assumptions used for hydrogen storage were based on values provided by DOE. Overall, the volumetric capacity dramatically increases between the reference case and 2045

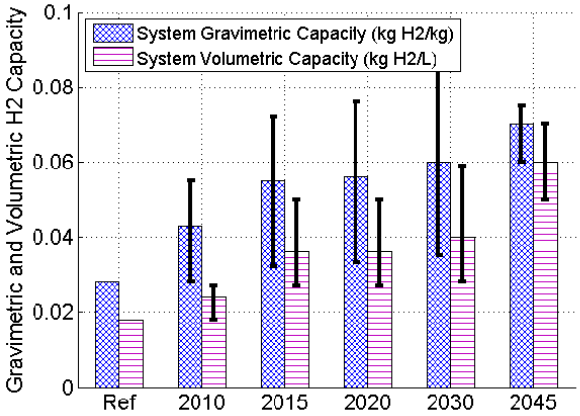

Figure 5. Hydrogen Storage Capacity in Terms of Hydrogen Quantity

Electric Machines

Two different electric machines will be used as references in the study:

- The power-split vehicles run with permanent magnet electric machine (similar to Toyota Camry) which has a peak power of 105 kW and a peak efficiency of 95%.
- The series configuration (fuel cell) and electric vehicles use an induction electric machine with a peak power of 72kW and a peak efficiency of 95%.

Energy Storage System

The battery used for the HEV reference case is a NiMH battery. It is assumed that this technology is the most likely to be used until 2015. The model used is similar to the one found in the Toyota Prius. For PHEV applications, all the vehicles are run with a Li-ion battery from Argonne.

After a long period of time, batteries lose some of their power and energy capacity. To be able to maintain the same performance at the end of life (EOL) compared to the beginning of life (BOL), an oversize factor is applied while sizing the batteries for both power and energy. These factors are supposed to represent the percentage of power and energy that will not be provided by the battery at the EOL compared to the initial power and energy given by the manufacturer. The oversize factor is decreased over time to reflect an improvement in the ability of batteries

to uniformly deliver the same performance throughout their life cycles.

Vehicle

As previously discussed, five vehicles classes were considered, as listed in Table 2.

Table 3. Vehicle Characteristics for Different Light Duty Vehicle Classes

Vehicle Class	Glider Mass (Ref) (kg)	Frontal Area (Ref) in (m^2)	Tire	Wheel Radius (m)
Compact Car	800	2.15	P195/65/R15	0.317
Midsize car	990	2.2	P195/65/R15	0.317
Small SUV	1000	2.52	P225/75/R15	0.35925
Midsize SUV	1260	2.88	P235/70/R16	0.367
Pickup	1500	3.21	P255/65/R17	0.38165

Because of the improvements in material, the glider mass is expected to significantly decrease over time. Although frontal area is expected to differ from one vehicle configuration to another (i.e., the electrical components will require more cooling capabilities), the reduction values were considered constant across the technologies.

Vehicle Powertrain Assumptions

All the vehicles have been sized to meet the same requirements:

- 0–60mph in 9 s +/-0.1
- Maximum grade of 6% at 65 mph at gross vehicle weight
- Maximum vehicle speed of >160 km/h

For all cases, the engine or fuel cell powers are sized to complete the grade without any assistance from the battery. For HEVs, the battery was sized to recuperate the entire braking energy during the UDDS drive cycle. For the PHEV case, the battery power is defined as its ability to follow the UDDS in electric mode for the 10 and 20 miles cases and the US06 for the 30 and 40 miles cases, while its energy is calculated to follow the UDDS for a specific distance regardless of distance.

Input mode power-split configurations, similar to those used in the Toyota Camry, were selected for all HEV applications and PHEVs with low battery energies. Series configurations were used for PHEVs with high battery energies (e.g., 30 miles and up in EVs on the UDDS). The series fuel cell configurations use a two-gear transmission to allow them to achieve the maximum vehicle speed requirement.

Vehicle Simulation Results

The vehicles were simulated on both the UDDS and HWFET drive cycles. The fuel consumption values and ratios presented below are based on unadjusted values.

EVOLUTION OF HEV VS. CONVENTIONAL

The comparisons between power-split HEVs and conventional gasoline vehicles (same year, same case) in Figure 6 show that the ratios increases slightly for diesel, gasoline, and ethanol. However, the hydrogen case shows a decrease over time; the Hydrogen HEV consumes 31% in 2010 and 40% less in 2045 meaning that hydrogen vehicles will benefit more from hybridization in the future than will comparable conventional vehicles.

In summary, the advances in component technology will not significantly benefit conventional and HEVs, except for the hydrogen engine, because of the additional benefits of hydrogen storage.

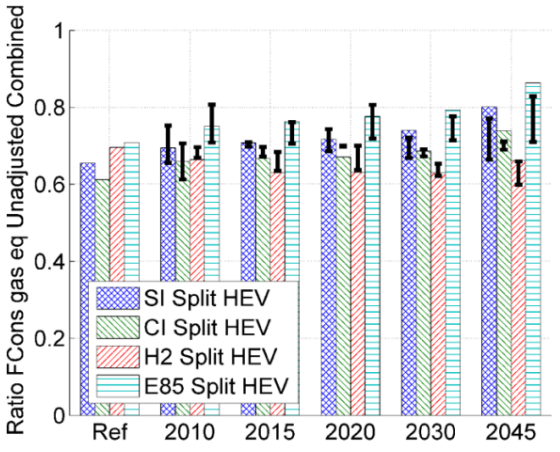

Figure 6. Ratio of Fuel Consumption Gasoline Equivalent Unadjusted Combined in Comparison to the Conventional Gasoline Same Year, Same Case, for Midsize

Figure 7 shows the vehicle cost ratio between HEV and conventional vehicles. As expected, HEVs remain more expensive than conventional vehicles, but the difference significantly decreases because costs associated with the battery and electric machine fall faster than those for conventional engines.

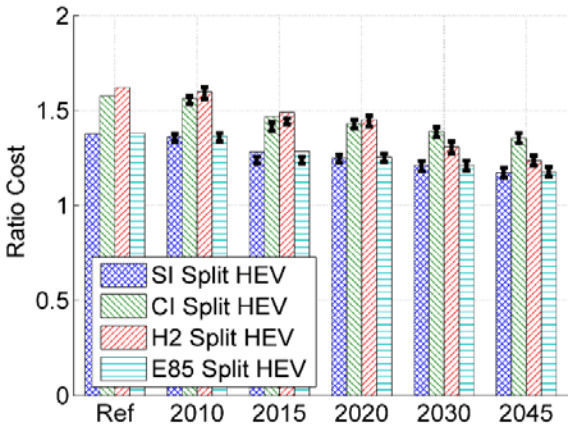

Figure 7. HEV Vehicle Cost Ratio Compared to Gasoline Conventional Vehicle of the Same Year

EVOLUTION OF HEV VS. FUEL CELL

Figure 8 shows the fuel consumption comparison between HEVs and FC HEVs for the midsize-car case. First, note that technology for fuel cell vehicles will continue to provide better fuel efficiency than the technology for the HEVs, with ratios above 1. However, the ratios vary over time, depending upon the fuel considered. The ratio for the gasoline HEV increases over time because most improvements considered for the engine occur at low power and consequently do not significantly impact the fuel efficiency in hybrid operating mode. Both diesel and ethanol HEVs follow the same trend than the gasoline.

Because of the larger improvements considered for the hydrogen engine, the hydrogen power split shows the best improvement in fuel consumption in comparison to the fuel cell technology. Indeed, in 2010, the hydrogen HEV vehicle consumes nearly 18% more fuel than the fuel cell HEV vehicle, but in 2045, this difference is reduced to 9%.

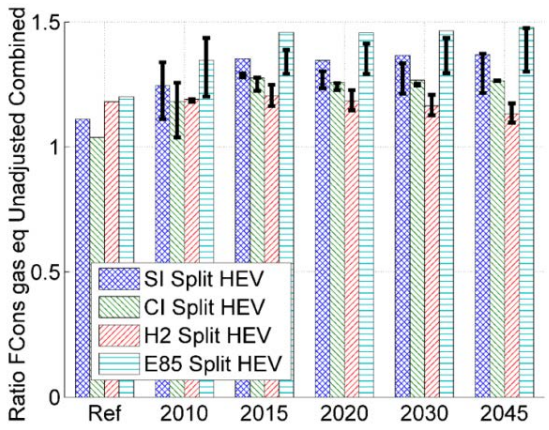

Figure 8. Ratio of Fuel Consumption Gasoline Equivalent Unadjusted Combined in Comparison to the Fuel Cell HEV Same Year, Same Case for Midsize Vehicles

Figure 9 shows the vehicle cost comparison between HEVs and FC HEVs. Note that the cost difference between both technologies is expected to decrease over time. The diesel fuel will become more expensive for all technology uncertainties cases with a ratio ranging from 1.02 to 1.1.

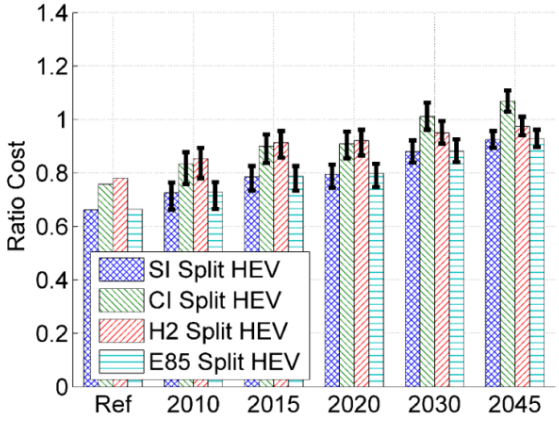

Figure 9. HEV Vehicle Cost Ratio Compared to FC HEV Vehicle of the Same Year

EVOLUTION OF PHEVS

The fuel-consumption evolution for power-split PHEVs is similar to that for power-split HEVs, gasoline engine.

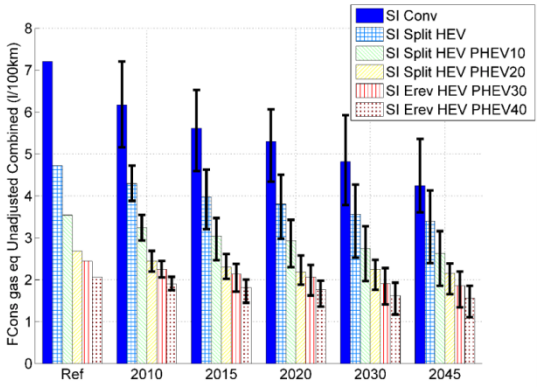

Figure 10. Fuel consumption evolution for PHEVs, gasoline engine, midsize car

Table 3 shows and confirms that PHEVs improvement ranges from 10% to 50% for gasoline engine as for the HEV powertrain.

Table 4. Fuel Consumption of PHEVs for gasoline engine for midsize vehicle

	Ref	Low	High	Percentage	
				Low	High
Conventiona	7.2	3.6	5.35	26	50
HEV	4.7	2.3	4.12	12	49
PHEV10	3.5	1.8	3.15	11	47
PHEV20	2.6	1.6	2.38	11	38
PHEV30	2.4	1.3	2.19	10	45
PHEV40	2.0	1.0	1.84	11	47

Electric consumption trends to decrease overtime for all PHEV ranges; however it can be noticed that EREV electric consumption is almost twice as much as split. This is due to the configuration itself in addition to the fact that they are being sized on US06 drive cycles.

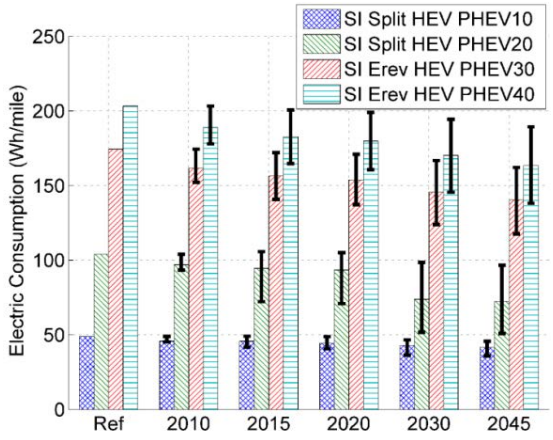

Figure 11. Electric consumption for PHEVs, gasoline engine, midsize car

Figure 12 shows that there is a linear relationship between vehicle mass and electric consumption: the bigger the vehicle, the higher the electrical consumption. It can be said that for every 200 kg decrease in mass, there is a 50Wh/mile decrease in electric consumption.

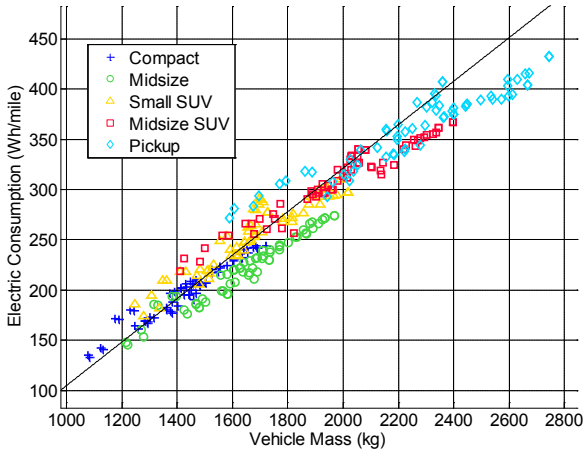

Figure 12. Electric consumption in CD+CS mode for gasoline-powered-split PHEVs.

TRADE-OFF BETWEEN FUEL EFFICIENCY AND COST

Figure 13 shows similar trends for HEVs independently of ICE technology. The overall trend is decreasing, which means lower fuel consumption and lower cost. Gasoline and ethanol HEVs offer the best trade-offs over time, with the hydrogen HEV becoming competitive in the 2045 timeframe.

Figure 14 shows a comparison of all the powertrains, considering gasoline fuel only. The main conclusion is that conventional vehicles are more likely to improve in fuel efficiency than in cost, whereas the higher the electrification level, the more the improvement focuses on cost. For example, the incremental cost for the PHEV40 decreases from $31,950 to $6,236 between 2010 and 2045, whereas the incremental cost for the conventional gasoline vehicle increases from $0 to $845 over the same period.

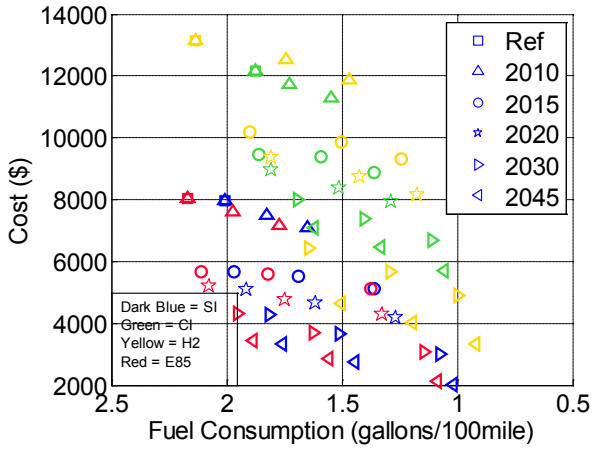

Figure 13. Incremental Cost vs. fuel consumption for Midsize HEV

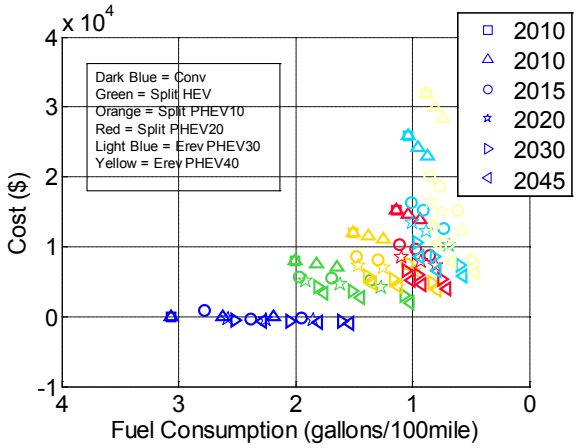

Figure 14. Incremental cost (in comparison to the reference conventional gasoline vehicle manufacturing cost) as a function of fuel consumption for gasoline vehicles

Figure 15 shows the trade-offs between fuel consumption and increased costs for all powertrains and fuels compared to the conventional gasoline reference. Overall, the vehicles on the bottom right would provide the best fuel consumption for the least additional cost. All years, all cases, and all fuels are presented.

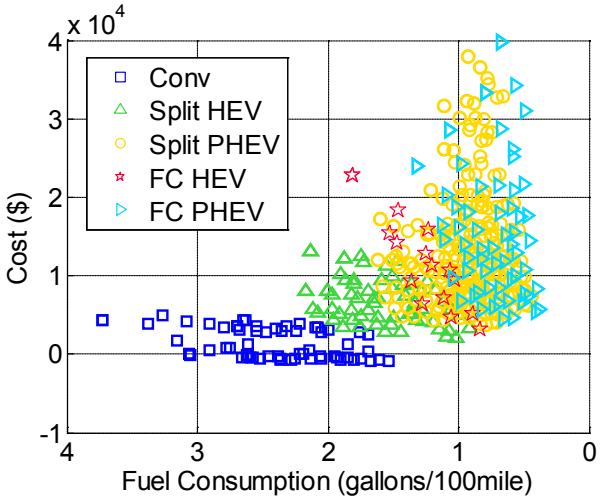

Figure 15. Incremental cost (in comparison to the gasoline conventional reference vehicle) as a function of fuel consumption for all powertrains.

Conclusions

More than 2000 vehicles were simulated for different timeframes (up to 2045), powertrain configurations, and component technologies. Both their fuel economy and cost were assessed to estimate the potential of each technology. Each vehicle was associated with a triangular uncertainty. The simulations highlighted several points:

- From a fuel-efficiency perspective, HEVs maintain a relative constant ratio compared to their conventional vehicle counterparts. However, the cost of electrification is expected to be reduced in the future, favoring the technology's market penetration.
- Ethanol vehicles will offer the best cost - fuel consumption ratio among the conventional powertrains in the near future, which is driving the interest in bio-fuels development.
- Fuel cell HEVs have the greatest potential to reduce fuel consumption.
- Hydrogen engine HEVs, through direct injection, will offer significant fuel improvements and, because they offer lower cost than fuel cell systems, appear to be a bridging technology, which would help the infrastructure

V.C. Autonomie Large Scale Deployment

Shane Halbach (Project Leader), Larry Michaels, Phil Sharer, Ram Vijayagopal, Aymeric Rousseau
Argonne National Laboratory
9700 South Cass Avenue
Argonne, IL 60439-4815
(630) 252-7261; arousseau@anl.gov

DOE Technology Managers: David Anderson, Lee Slezak

V.C.1. Abstract

Objectives

- Develop and implement large scale deployment process for Autonomie

Approach

- Enable efficient, seamless math-based control system design process.
- Enable efficient reuse of models.
- Enable sharing of modeling expertise across the organization.
- Establish industry standard for architecture and model interfaces.

Accomplishments

- Developed user support, issue management system, automated release generation and automated testing
- Developed, implemented and tested generic process (i.e., SIL)

Future Directions

- Complete Autonomie commercialization
- Expand the use of Autonomie within GM and other original equipment manufacturers (OEMs).

V.C.2. Technical Discussion

Introduction

Building hardware is expensive. Traditional design paradigms in the automotive industry often delay control system design until late in the process — in some cases requiring several costly hardware iterations. To reduce costs and improve time to market, it is imperative that greater emphasis be placed on modeling and simulation. This only becomes more true as time goes on because of increasing complexity of vehicles, a greater number of vehicle configurations, and larger numbers of people working on projects, which complicates design choices. To fully realize the benefits of math-based design, the models created must be as flexible and reusable as possible.

Greater reliance on modeling and simulation does come at some cost. New processes must be put in place to facilitate communication among the many model creators and consumers, and to handle the increase in files, which can be quite significant and overwhelming.

Several tools already exist to develop detailed plant models, including GT-Power, AMESim, CarSim, and SimScape. The objective of Autonomie is not to provide a language to develop detailed models; rather, Autonomie supports the assembly and use of models from design to simulation to analysis with complete plug-and-play capabilities. Autonomie provides a plug-and-

play architecture to support this ideal use of modeling and simulation for math-based automotive control system design.

The objective of the project is to develop and implement a process to support large scale deployment ahead of the tool commercialization.

Top Level Process Workflow

Figure 1 shows the top level workflow that was developed and implemented. Several work flow have also been developed for the main tasks, including Work Period, regression testing… The entire process was reviewed by both external and internal CMMI experts.

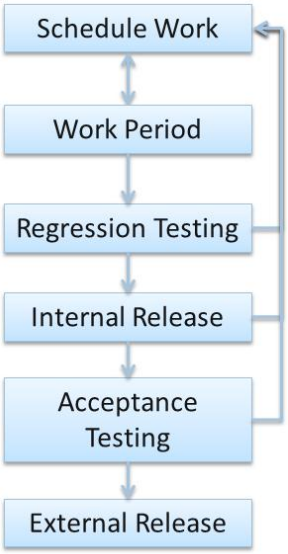

Figure 1. Top Level Workflow

User Support

One of the critical components of large scale deployment is the ability to support users. Figure 2 shows the different support types ranging from Emails, to phone call or webinars… A pre-approved paid contract has also been developed to support specific user applications.

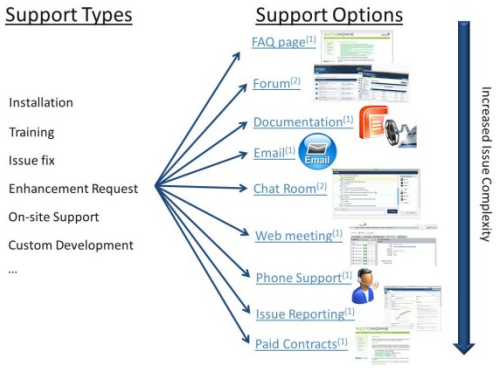

Figure 2. User Support

All the main information is stored into Autonomie website (www.autonomie.net). Figure 3 shows the FAQ page.

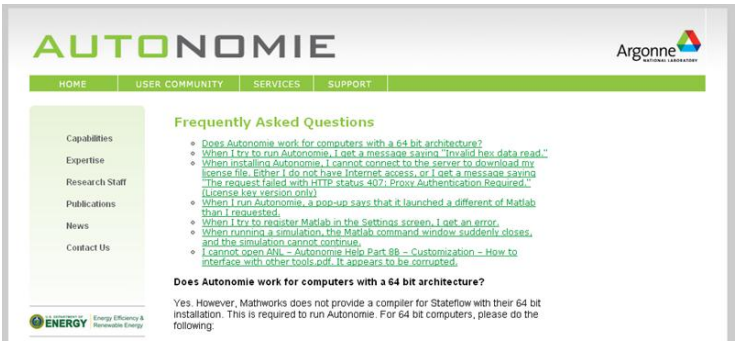

Figure 3. Website FAQ Page

Issue Tracking

The ability to track and schedule issues is at the center of large scale deployment. The tracking system that was adopted allows users to enter and track any of their issues directly. An issue is considered a bug, an enhancement or a new feature. This capability is unique in a sense that most companies do not provide any access.

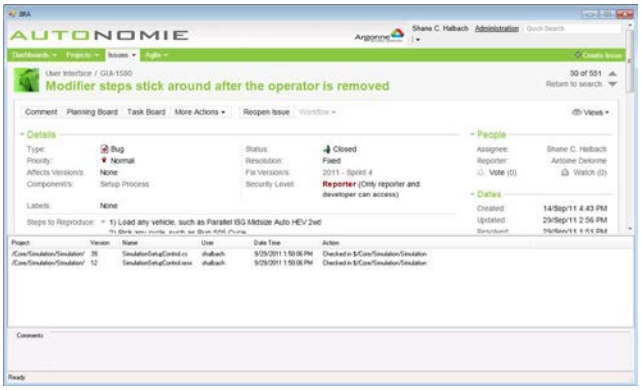

Figure 4. Tracking System

Autonomie Release Generation

Due to the fact that several releases need to be generated (i.e., public, demonstration, Heavy duty regulations…) and users might have specific proprietary data and processes, a process was developed to ensure quick and reliable release generation as shown in Figure 5.

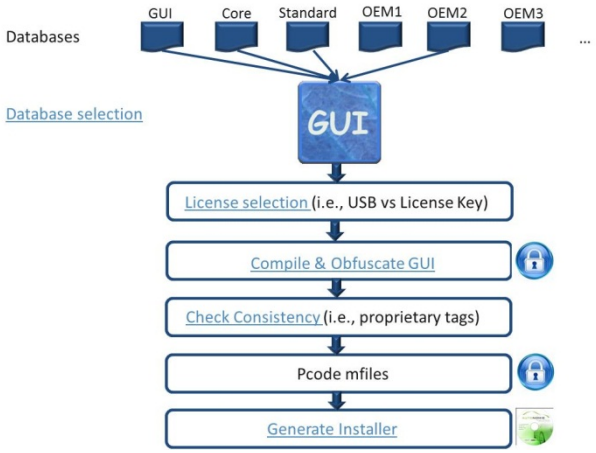

Figure 5. Release Generation Process

To be able to implement the process and considering the specificities of the release generation, a tool was developed in-house as shown in Figure 6. The tool ensures that no proprietary files are sent to other companies or that vehicles are complete.

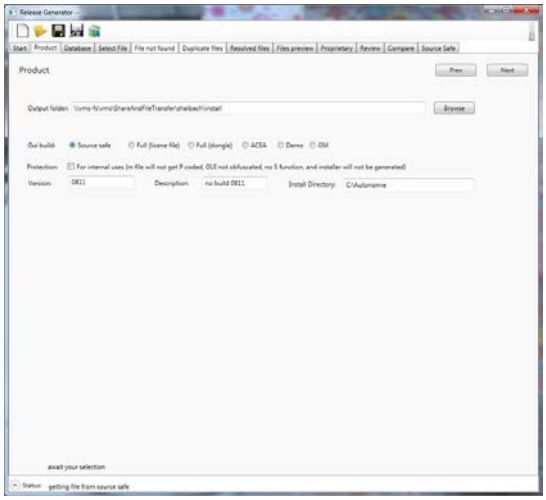

Figure 6. Automated Release Generation

Autonomie Release Testing

One of the main objectives is to provide stable releases over time, especially considering when Autonomie is used to support production development. To do so, a generic process, described in Figure 7, was adopted to handle both GUI and Matlab test cases.

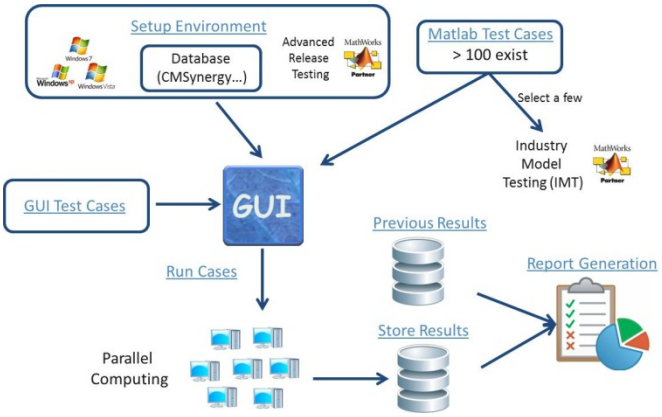

Figure 7. Automated Testing Process

After each test case, reports are generated to provide information (i.e., Pass / Fail). Figure 8 shows how the HP tool automatically provides reports for all GUI test cases. HTML reports have been developed in-house to handle results for the Matlab test cases.

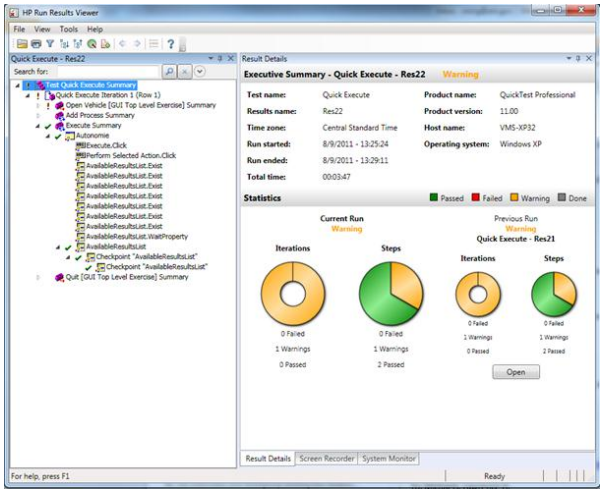

Figure 8. Automated GUI Testing Reports

Conclusions

An overall process for software development has been defined, reviewed by experts and implemented to ensure large scale deployment success. Autonomie is now ready to be provided to a commercial partner for worldwide utilization.

V.D. Autonomie Maintenance and Enhancements

Aymeric Rousseau (Project Leader), Shane Halbach, Phil Sharer
Argonne National Laboratory
9700 South Cass Avenue
Argonne, IL 60439-4815
(630) 252-7261; arousseau@anl.gov

DOE Technology Manager: David Anderson, Lee Slezak

V.D.1. Abstract

Objectives

- Enhance and maintain Autonomie as needed to support DOE, the user community, and hardware-in-loop/rapid control prototyping (HIL/RCP) projects.

Approach

- Use the feedback from Autonomie users to implement new features
- Enhance Autonomie capabilities to support DOE studies

Accomplishments

- Validated the use of Autonomie for new MathWorks releases
- Added state-of-the-art component data from national laboratories and original equipment manufacturers (OEMs)
- Added new powertrain configurations
- Modified the tool to enhance medium- and heavy-duty capabilities
- Included J1711 plug-in hybrid electric vehicle (PHEV) test procedure utility factor

Future Directions

- Continue to enhance Autonomie to support US DOE and technical transfer

V.D.2. Technical Discussion

Introduction

To better support the U.S. Department of Energy (DOE) and its users, several new features have been implemented in Autonomie. Some of the most significant accomplishments are described below.

Operating Systems

A significant amount of work was done to ensure that Autonomie runs on several Operating Systems (OS), including Windows 7 and 64 bits.

Some special attention was paid to solve issues between MathWorks and Windows interactions since Autonomie launches Matlab.

Graphical User Interface

In addition to supporting issues reported by users, one of the main additions to the software is the implementation of the preliminary European PHEV test procedure.

That new feature was implemented to support the work performed under the IEA Annex XV agreement.

The other main new feature developed for the GUI was the ability to visually represent the energy balance after any simulation.

Additional Powertrain Configurations

Several new powertrain configurations were implemented on the basis of specific DOE needs.

In addition, two configurations currently in production were added:

- Voltec System (Figure 1, Figure 2)
- Ability to have multiple energy storage systems (i.e., battery and ultracapacitor) for any of the existing configurations

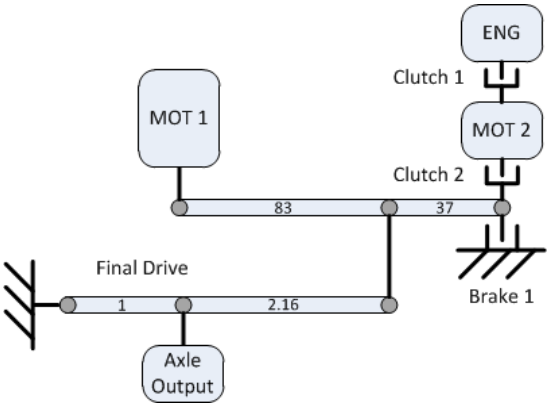

Figure 1. Voltec Configuration

Component Data

State-of-the-art component data were implemented from both universities and companies.

Companies using Autonomie provided proprietary engine (i.e., CNG, gasoline), battery, and electric machine data.

Most of the focus was on gathering state-of-the-art data for medium- and heavy-duty applications. Since few data are publicly available, the data were provided by the OEMs. This effort will continue in the future, focusing especially on missing information, such as accessory loads.

EcoCAR2 Competition

Because of the emphasis on modeling and simulation during the early stages of the competition, GM provided a significant amount of data to the different teams. All of the models were modified to follow Autonomie nomenclature and then implemented into Autonomie.

The reference conventional vehicle model was developed by using component and vehicle data from GM. The vehicle model is used by the teams as reference for any further improvements.

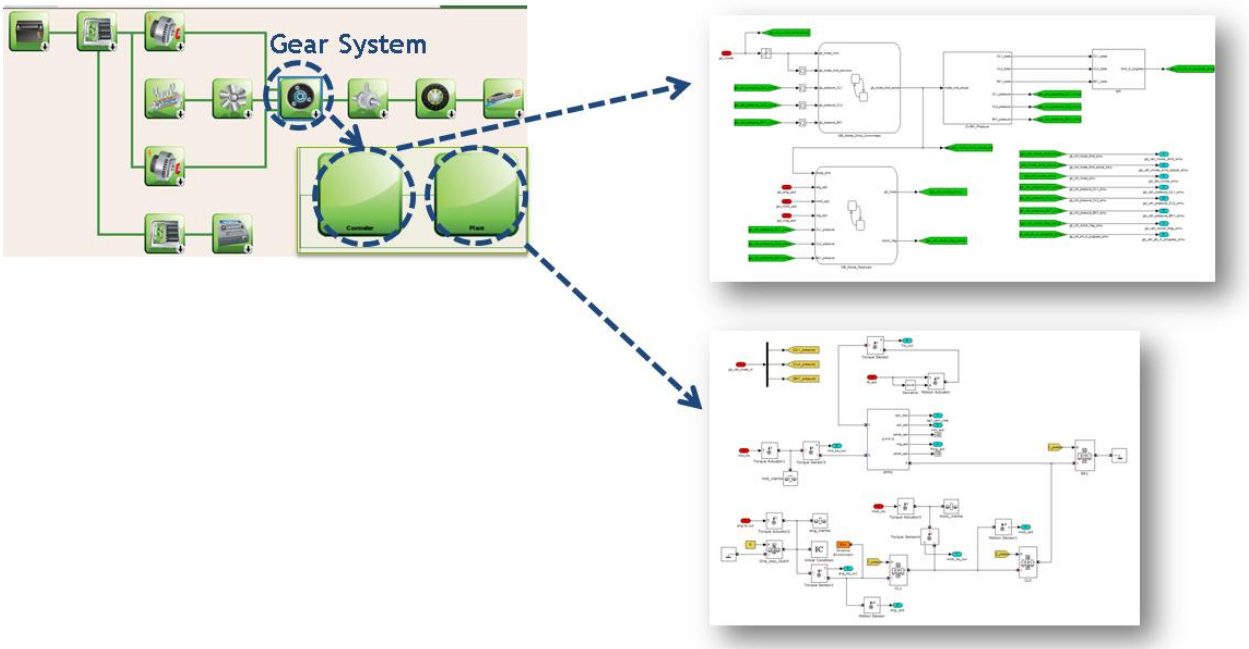

Figure 2. Voltec Transmission Model Development

Control Strategies

A vehicle level control strategy was developed for the Voltec system.

The rule based control strategy was developed by analyzing vehicle test data and follows the logic below:

- In EV operation
  - One-Motor EV (EV1) : The single-speed EV drive power-flow, which provides more tractive effort at lower driving speeds.
  - Two-Motor EV (EV2) : The output power-split EV drive power-flow, which has greater efficiency than one-motor EV at higher speeds and lower loads.
- In extended-range
  - Series One-Motor ER (Series) : The series extended-range power-flow that provides more tractive effort at lower driving speeds.
  - Combined Two-Motor ER (Split) The output power-split extended-range power-flow that has greater efficiency than series at higher speeds and lighter loads.

The rules implemented allowed us to develop a vehicle level control strategy that matched vehicle test data as shown in Figure 3.

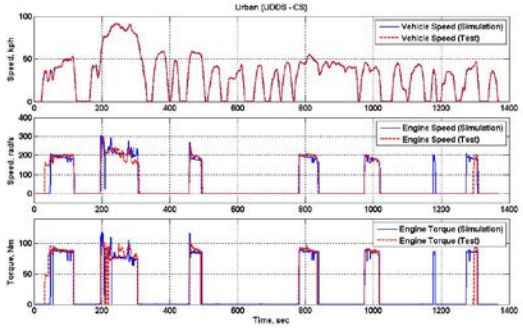

Figure 3. Voltec Vehicle Level Control Strategy

Several changes and new control strategies were implemented for hybrid electric vehicles (HEVs), including an instantaneous optimization algorithm for the single mode power split. The algorithm selects the proper mode and the operating points of the different components within each one to minimize fuel consumption while maintaining acceptable SOC.

Users' Community

The Autonomie users' community has been continuously increasing and currently reaches more than 125 companies worldwide with more than 750 users. More than 80% of the PSAT users have switched to Autonomie one year after its first release.

The Autonomie development effort has focused on understanding the needs of its users and to develop features that would allow researchers to be more efficient and consequently introduce advanced technologies to the market faster.

Conclusions

The latest version of Autonomie includes numerous new features that were developed on the basis of feedback from DOE and the user community.

These enhancements are focused on component models and data, as well as vehicle control strategies.

V.D.3. Products

Tools & Data

DOE Version of the Autonomie Simulation Model

V.E. Heavy Duty Fuel Displacement Potential on Real World Drive Cycles

Aymeric Rousseau (Project Leader), Vikesh Napal
Argonne National Laboratory
9700 South Cass Avenue
Argonne, IL 60439-4815
(630) 252-7416; arousseau@anl.gov

DOE Technology Manager: David Anderson, Lee Slezak

V.E.1. Abstract

Objectives

- Evaluate the fuel consumption benefits of two powertrain configurations (series and power split) for a transit bus on a series of real world drive cycles

Approach

- Develop vehicle level control strategies for each of the powertrain considered
- Size all the vehicles to meet the same vehicle performance
- Run the simulation on the real world drive cycles

Accomplishments

- The fuel consumption of several powertrain configurations was compared for a transit bus application over a series of real world drive cycles provided by NREL and ORNL
- The study demonstrated the advantage of the power split configuration over the series and the conventional vehicles

Future Directions

- Consider new powertrain configurations for transit applications
- Consider other medium and heavy duty applications

V.E.2. Technical Discussion

Introduction

Hybrid electric vehicles have the potential to significantly reduce petroleum consumption for medium and heavy duty vehicles. Several powertrain configurations have been introduced to the market and tested in fleets, but due to the fact that the vehicles do not have the same performances and characteristics, it is very difficult to evaluate the benefits of different options.

The objective of the study is to compare the fuel consumption benefits of two powertrain configurations (series and power split) for a transit bus on a series of real world drive cycles.

Vehicle Descriptions

Conventional Vehicle

The conventional bus chooses for the study, is the default Autonomie's Conventional Class 8 Bus with an automatic gearbox, with a test weight of 19230 Kg. This design is of the Orion V. The manufactures of this bus started in 1989 and was discarded in 2009. It has been used in nearly 90 transit agencies in the United States and over 50 agencies in Canada. The gearbox and the ICE used in the design are the following:

- Engine Diesel Corp. Series 50

- Automatic Gearbox Alisson B500 gearbox

The Table 1 gives some of the specifications of the bus:

Table 1. Conventional Bus Specifications

Components	Value
Final Drive	4.33
Engine Power	243 kW
Test Weight	19230 kg

Series Vehicle

The series transit bus is based on the Orion VII model, which was marketed for the North American continent between 2001 and 2007. The bus was sized accordingly to a target test weight (20230 kg

The powertrain of the series transit bus is composed of the following components:

- Engine: Cummins ISB 260
- Transmission: BAE HybriDrive

The Table 2 gives a quick overview of the different powertrain components key value:

Table 2. Series Bus Specifications

Components		Sized Values
Final Drive		4.1
Engine Power (kW)		184
Motor Power (kW)		203 peak
Generator Power		173.2 peak
Energy Storage	Type	Li-ion
	Power (kW)	200
Test Weight (Kg)		20231

Power Split Vehicle

The Split 2-mode transit bus selected for the study is based on the New Flyer DE60LF. It has been introduced in transit agencies in 2002, and discarded in 2010. It was first launched with the King County Metro.

The King County Metro (KCM) RWDC were acquired via the DE60LF, or the non-hybrid version, the D60LF's journey. Therefore using a DE60LF model is the best way to achieve to a parametrically tuned model that will be the closer to a parametrically tuned vehicle. Using an advanced hybrid powertrain offers the possibility to fine-tune a bigger set of components such as:

- Test Weight
- Engine Power
- Motor and Generator Power
- Battery Capacity
- State of Charge Target

The New Flyer DE60LF is a hybrid vehicle powered by GM Global Hybrid Cooperation. This configuration is defined as a Split 2-mode without fixed gear. The powertrain is composed of the following components:

- Engine Caterpillar C9
- Motor
- Generator
- Energy Storage System
- Dual Power Inverter Module

Table 3. New Flyer DE60LF Specifications

Components		Value
Final Drive		3.42
Engine Power (kW)		246.1
Motor Power (kW)		75 nominal, 150 peak
Generator's Power		75 nominal, 150 peak
Energy Storage	**Type**	Li-ion
	Power (kW)	164
Test Weight (in Kg)		20230

Real World Drive Cycles

NREL Drive Cycles

From April 1, 2005 to March 31, 2006, the National Renewable Energy Laboratory ran an evaluation study on King County Metro Transit buses. The KCM tested fleet contained 30 conventional (D60LF model) buses and 235 hybrid buses (DE60LF model).

The data accessible for the current study is a set of 8 cycles. However the data do not contain any grade information or road type, thus the data are

not as accurate as they could be. Grade information does affect the overall vehicle fuel consumption. Figure 1 shows an example of the real world drive cycles.

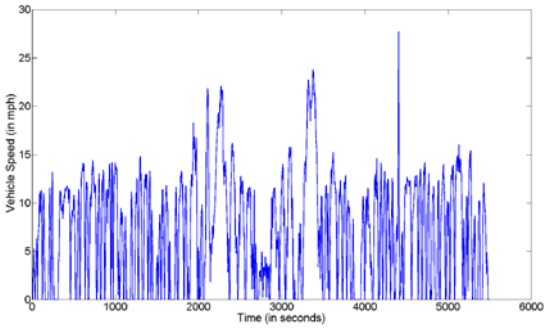

Figure 1. NREL Cycle Example

The table below shows the different values for each cycle and the mean/median for these values.

From the 8-day cycles, 22 actual cycles where extracted, those cycles' varies from 7.41 minutes to over 14 hours. Detailed description of the cycles can be seen in the table below.

Table 4. ORNL RWDC Summary

	Duration	Distance	Average Speed	Stop Duration	Stop Duration	Average V^3	RMS Acceleration	Average Acceleration	Average Deceleration	Braking Time
	min	miles	mph	min	% total	[mph]^3 x0.0	m/s^2	m/s^2	m/s^2	%
①	509.8	65.63	7.7240595	175.0783	34.34098	2.11895	0.38183986	0.4582725	-0.476303016	47.24055
②	247	31.86	7.7399462	71.28667	28.86528	1.4181	0.26D09547	0.405424451	-0.363211778	50.50885
③	46.35	6.71	8.6858252	18.18167	39.2269	3.12291	0.452311A6	0.472487544	-0.581133742	49.06508
④	83.57	17.7	12.774665	38.53167	46.10522	12.3572	0.24867505	0.29322571	-0.385697451	38.68858
⑤	26.78	7.602	17.029432	5.493333	20.51282	13.1269	0.29846709	0.334276623	-0.434369468	41.82226
⑥	86.44	23.15	16.069518	24.46	28.29599	16.1912	0.33241269	0.401352222	-0.467823208	43.83025
⑦	7.41	0.327	2.6466799	4.311667	58.18713	0.24674	0.17426532	0.352470453	-0.339999894	79.73459
⑧	77.15	21.2	16.489329	20.48	26.54569	15.9584	0.3525398	0.443211158	-0.460655345	45.06157
⑨	214.2	34.23	9.5863651	51.80167	24.18115	3.1621	0.40602708	0.502500765	-0.454903468	54.29536
⑩	135.7	22.63	10.007729	32.25667	23.777	3.38087	0.44141169	0.513244388	-0.508790567	53.76668
⑪	318.1	59.53	11.229003	121.2633	38.12154	9.61439	0.2694369	0.378553763	-0.363511684	51.49745
⑫	749.3	176.7	14.14983	291.6983	38.93031	15.5707	0.48967256	0.455071416	-0.549741497	47.1297
⑬	601.5	105.5	10.528317	226.5533	37.66577	11.6148	0.25717629	0.386354054	-0.373643579	49.66472
⑭	161.2	72.32	26.918549	39.60333	24.56986	63.2586	0.22400726	0.350138479	-0.302224917	48.39317
⑮	822.8	225.7	16.458261	201.33	24.46998	14.2466	0.42322618	0.467962024	-0.491337634	50.20014
⑯	877	215.7	14.755755	247.5783	28.23121	11.4694	0.38091306	0.412158888	-0.421624059	53.43932
⑰	652.7	172.2	15.832288	184.1767	28.21838	15.0813	0.48372443	0.496857714	-0.528203946	47.55394
⑱	176	48.06	16.388773	52.32833	29.73933	17.6653	0.41644884	0.438539652	-0.529338355	50.07388
⑲	269.2	38.34	8.5599149	97.42667	36.19746	2.84295	0.41728096	0.486674211	-0.462279536	49.34238
⑳	209.9	28.97	8.2803577	67.805	32.30604	2.77964	0.38355624	0.479719636	-0.425779504	52.42992
㉑	135.4	31.24	13.844088	27.94833	20.64233	8.83615	0.55513517	0.519075859	-0.56080703	47.09242
㉒	418.4	87.94	12.610703	123.2133	29.44729	6.81481	0.4827514	0.508530676	-0.49541074	52.43535
average	310.3	67.88	12.650427	96.49121	31.75353	11.4035	0.36960795	0.434368282	-0.453463201	50.14846
mean	212.1	36.29	12.692684	60.06667	29.15628	10.5419	0.38269805	0.449141287	-0.46146744	49.50355
min	7.41	0.327	2.6466799	4.311667	20.51282	0.24674	0.17426532	0.29322571	-0.581133742	38.68858
max	877	225.7	26.918549	291.6983	58.18713	63.2586	0.55513517	0.519075859	-0.302224917	79.73459

ORNL Drive Cycles

In addition, several "standard" drive cycles were considered, including the UDDS, Manhattan and

Table 5. NREL RWDC Summary

	Duration	Distance	Average S	Stop Dura	Stop Dura	Average V	RMS Acceleration	Average Acceleration	Average Deceleration	Braking Time
	min	miles	mph	min	% total	[mph]^3 x	m/s^2	m/s^2	m/s^2	%
①	91.55	23.46	15.38	20.9	22.83	11.69	0.50762502	0.560833541	-0.637057941	58.29237
②	113.1	22.12	11.74	46.58	41.21	9.254	0.42258552	0.594030086	-0.659586764	68.53899
③	19.35	3.661	11.35	8.3	42.89	8.434	0.62200989	0.752527241	-0.901566727	68.13092
④	90.97	18.38	12.12	37.82	41.57	11.72	0.42114367	0.576669737	-0.690208907	67.57054
⑤	119.5	24.31	12.21	44.55	37.3	10.15	0.57087537	0.659463095	-0.799686444	64.89466
⑥	109.4	20.64	11.33	51.03	46.67	8.947	0.35644292	0.591681906	-0.714994709	70.20271
⑦	158.1	37.64	14.28	59.33	37.52	14.16	0.55454206	0.630787847	-0.877357196	62.97428
⑧	48.47	7.661	9.484	23.2	47.87	6.709	0.41861945	0.655265396	-0.743112193	71.45805
average	93.79	19.74	12.24	36.46	39.73	10.13	0.48423049	0.627657356	-0.75294636	66.50782
median	100.5	21.38	11.93	41.18	41.39	9.703	0.46510527	0.612408967	-0.729053451	67.85073
min	19.35	3.661	9.484	8.3	22.83	6.709	0.35644292	0.560833541	-0.901566727	58.29237
max	158.1	37.64	15.38	59.33	47.87	14.16	0.62200989	0.752527241	-0.637057941	71.45805

Threw the Medium-Truck Duty Cycle Project (MTDC) of Oak Ridge National Laboratory, access was given to daily transit buses' RWDCs. These cycles have been acquired through a partnership with the Knoxville Area Transit, who has a fleet composed of diesel, CNG/LNG and hybrid buses. The data accessible for the current study is a set of 20 daily RWDCs. The data contained the bus vehicle speed, the road's grade (in percent), and the type of road (freeway or a surface street).

OCTA.

Individual Powertrain Fuel Economy Results

Conventional Vehicle

As shown in Figure 2, the fuel economy average of the conventional powertrain ranges from 3 to 4.5 miles per gallon. The maximum occurrences are obtained for a Fuel Economy of 3 mpg and the mean value is .

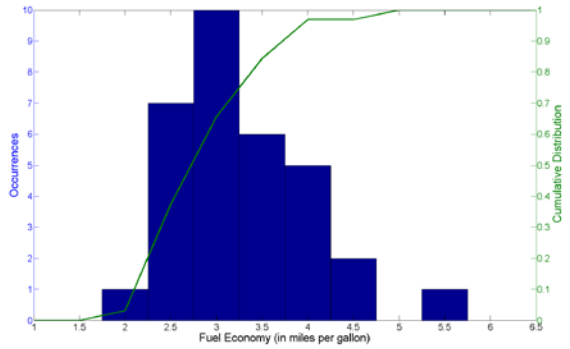

Figure 2. Fuel Economy (Conventional)

Figure 3 shows the average engine power across all cycles. The engine mean power value ranges from 50 kW to 70 kW. Since the vehicle is only propelled by the engine, its output power is closely related to the vehicle speed. A quick conclusion would be to underpower the vehicle to get a lower peak and best-fuel-efficiency point, but this is not the case since bus manufacturing is dictated by:

- Requirements defined by the Federal Transit Agency (http://www.fta.dot.gov/)
- Components made available by OEM

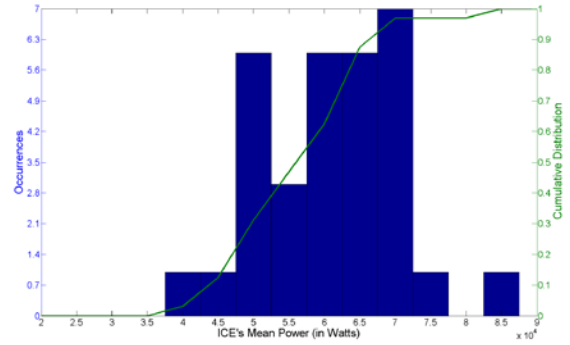

Figure 3. Average Engine Power (Conventional)

The shifting-events-per-minute distribution (Figure 4) can be characterized as bell-shaped, so the mean value can be assumed to be around 225 and 250 events per hour.

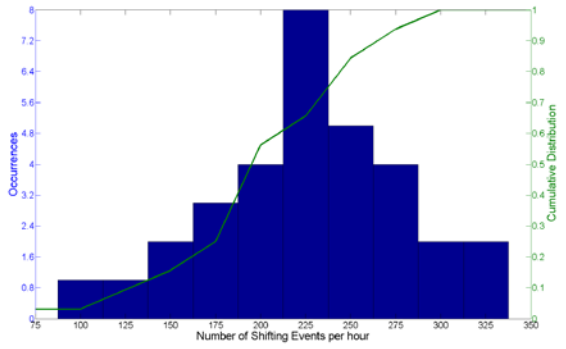

Figure 4. Number of Shifting Events (Conventional)

Series Vehicle

The fuel economy for the series hybrid (Figure 5) is close to 4 miles per gallon. Compared to the Conventional (Figure 2), it is not simply an upward translation of the pattern. Since the engine is not directly connected to the wheels, its output power can be operated more freely (Figure 6), also during stops and decelerating time, the ICE can be switched off (Figure 7). So to summarize, fuel economy comes from a better efficiency of the engine for each step, the possibility to switch off the engine and not to forget the possibility to regenerate from braking.

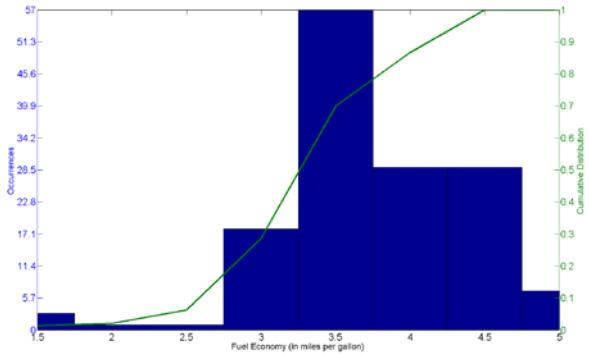

Figure 5. Fuel Economy (Series)

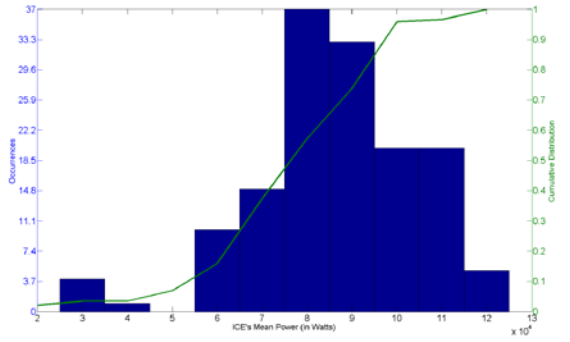

Figure 6. Average Ice Power (Series)

The average percentage of ICE on/off (Figure 7) for the series hybrid is around 77%. The design and vehicle controller regulates the switch of the engine: whenever the battery state of charge is below 50 percent, the engine is turned on. Depending on the battery capacity, the engine could be turned off more often, since the capacity would be higher and/or the switching percentage can be lowered.

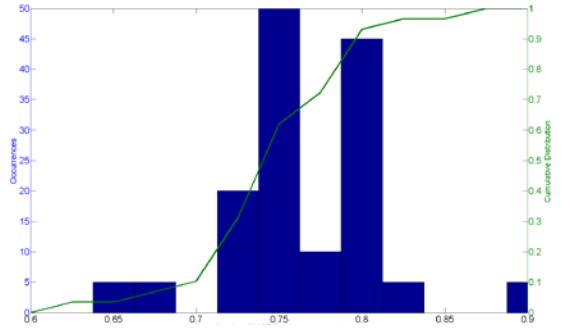

Figure 7. Number of ICE ON (Series)

Power Split Vehicle

For the split 2-mode, the fuel economy (Figure 8) ranges from 4 to 6.5, with an average value of 5.2 miles per gallon. The Fuel economy distribution is bell-shaped, so the fuel economy occurrences are quite normally distributed around the mean value. As a difference with the two previous powertrain technologies studied before, the fuel economy is somewhat independent of the cycle's speed/grade. This is achieved by the powertrain structure and the overall functioning of the vehicle. The strategy of the split 2-modes enables the engine to work, most of the time, in his best efficiency area.

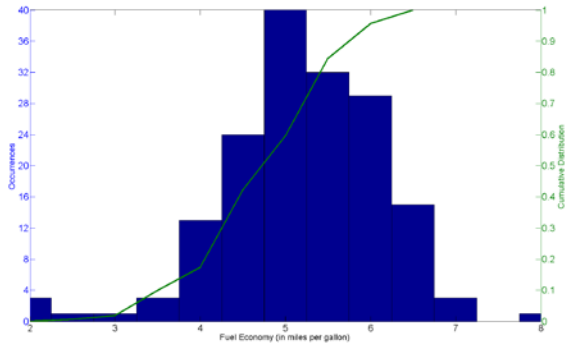

Figure 8. Fuel Economy (Split)

As stated before, the vehicle designed is based on the New Flyer DE60LF, used by the KCM transit agency in Seattle. The table below summarizes the result for fuel economy of the conventional and the split for the simulation and from the KING COUNTY METRO TRANSIT HYBRID ARTICULATED BUSES: FINAL EVALUATION RESULTS by K. Chandler & K. Walkowicz.

Table 6. Comparison with NREL RWDC

	Conv	HEV	Improvement
NREL	2.50	3.46	38.4%
Simu	3.76	5.18	37.5%

As shown in Figure 9, the maximum number of engine ON occurrences is located between 30 and 50 percent.

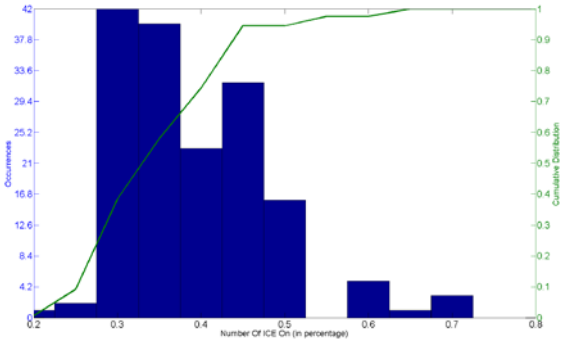

Figure 9. Number of Engine ON (Split)

Figure 10 shows that the average engine power is close to 120 kW for all the cycles. The distribution is bell-shaped, the different values are normally distributed around the mean. The mean engine power is quite high since the split 2-mode design enables the engine to operate

within its best-fuel-efficiency area: the engine feeds the battery close to its best efficiency and propel the vehicle when both speed (engine and vehicle) are close.

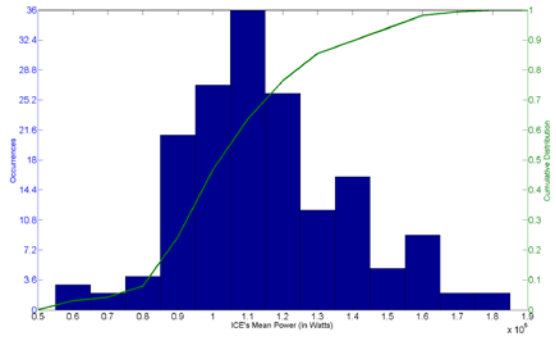

Figure 10. Average Engine Power (Split)

Fuel Economy Results Comparison

Fuel Consumption

The fuel economy for the power split configuration is better than the series, which is better than the conventional. The improvement from the split to the series is 21%, and the improvement from the conventional is 36%. The series improvement from the conventional is 12%. The split fuel economy is significantly higher than the two other vehicles, but the distribution is flatter, which means that there is a fewer probability, that among the 33 cycles, the fuel economy for the split is close to the mean, in comparison with the conventional or the series.

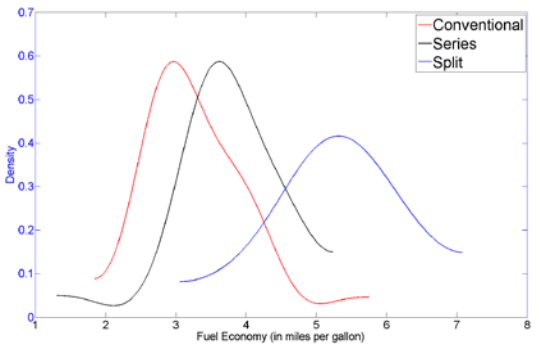

Figure 11. Fuel Consumption (different Powertrain)

Table 7 below shows the mean fuel economy values:

Table 7. Mean Fuel Economies

Technology	Value (in mpg)
Conventional	3.76
Series	4.2
Split	5.1

Number of Engine ON Events

Despite the fact that the standard deviation of the split is higher, it is clear that for the entire set of data, the split engine on/off ratio is lower than for the series (about 80% reduction compared to the Mean).

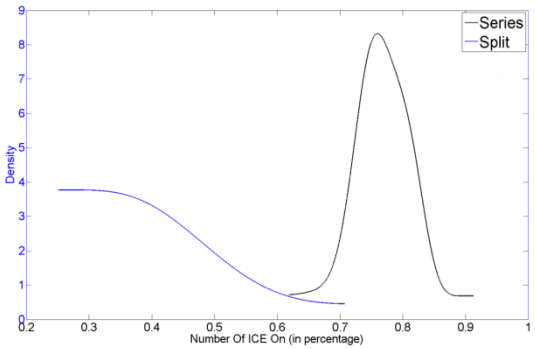

Figure 12. Number Of ICE ON (different Powertrain)

Average Engine Power

The conventional vehicle demonstrates the lowest average engine power. The engine in the power split shows a 70% higher engine average power compared to the conventional vehicle. The Series average engine power is only 85 kW, but the engine peak power is also lower than the two other technologies (around 245 kW). The reduction from peak power to mean power is about 53%, which is close to the reduction for the split (55%), and both are lower than the conventional (73%).

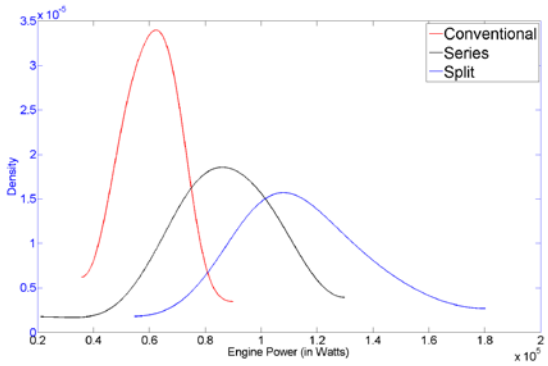

Figure 13. ICE's Power (different Powertrain)

Table 8. Ice Mean power for Each Technology

Technology	ICE Mean Power (kW)	ICE Peak Power
Conventional	65	243
Series	85	184
Split	110	246

Percentage Regenerative Energy at the Battery

The regeneration factor for the split ranges from 40% to 95% and for the series from 40% to 60%.

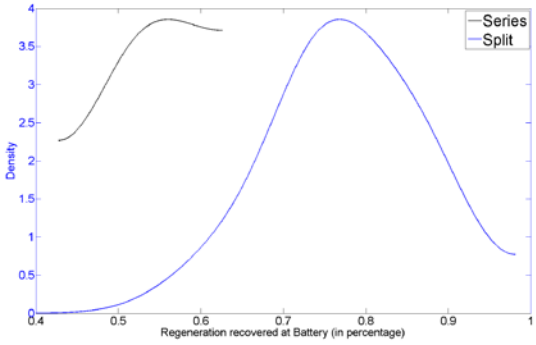

Figure 14. Regeneration at Battery (Series & Split)

Fuel Economy as a Function of Cycle Aggressiveness

For every technology, the fuel economy decreases with a more aggressive cycle. The fact that the conventional decreases quicker than the hybrids shows the benefits of hybridization and regenerative braking. For all data sets, the fuel efficiency of the split 2-mode is better, but it appears that for the most aggressive cycles, the series fuel economy could be better.

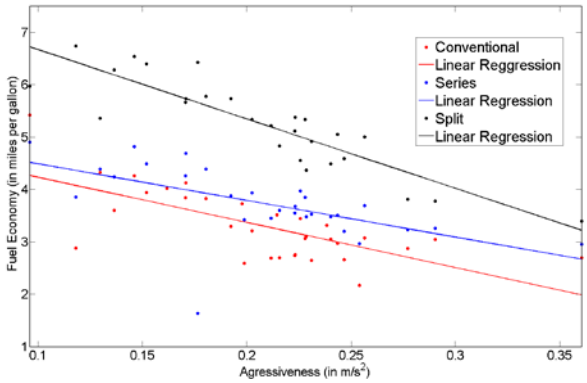

Figure 15. Fuel Economy Against Agressiveness

Fuel Economy as a Function of Vehicle Speed

Figure 15 shows that for both conventional and series technologies, the fuel economy increases with higher vehicle speed, the improvement being more important for the conventional. Similar behaviors have been noticed for light duty vehicles where the least efficient powertrains are more sensitive.

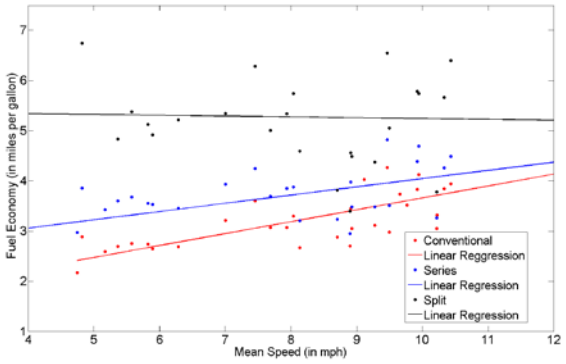

Figure 16. Fuel Economy Against vehicle Mean Speed

Fuel Economy as a Function of Distance

For all technologies, the fuel economy improves with the cycle distance. This improvement is of the same order of magnitude for both the hybrids but is slower (even flat) for the conventional.

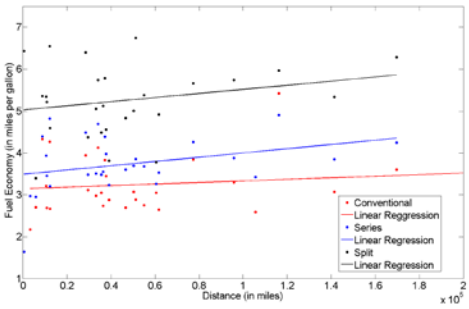

Figure 17. Fuel Economy against Distance

.

Conclusions

Three powertrain technologies (conventional series HEV and power split HEV) have been simulated for transit buses on other 30 real world drive cycles. The behavior is representative to driving one of these cycles and could be generalized to be representative of transit buses real journeys. The split 2-mode revealed to be the more efficient from a fuel-economy point of view.

Both the hybrid proved to have a significant fuel economy over conventional propulsion.

V.F. Class 8 Line-Haul Hybridization

Jason Kwon (Project Leader), Ram Vijayagopal, Aymeric Rousseau
Argonne National Laboratory
9700 South Cass Avenue
Argonne, IL 60439-4815
(630) 252-7261; arousseau@anl.gov

DOE Technology Managers: David Anderson, Lee Slezak

V.F.1. Abstract

Objectives

- Evaluate hybridization potential of class8 line haul applications using real-world driving cycles.

Approach

- Size and design class 8 line-haul applications for conventional, parallel ISG, parallel pre-transmission and series-parallel HEVs using Autonomie
- Understand impact of hybridization of class 8 line-haul on fuel savings over various real-world driving patterns
- Understand impact of different electrical accessory load power during idle and payloads on fuel savings for line-haul hybrid applications.

Accomplishments

- Developed the realistic parallel hybrid applications for class 8 line-haul truck models and controls with the variation of hybridization degree.
- Understand the fuel saving sensitivity to electric accessory load at stops (idle) and payloads on real-world driving cycles

Future Directions

- Understand the impact of different number of gears and limitation of regenerative braking on fuel savings and hybridization on real-world driving cycles.
- Understand the potential fuel saving obtained by use of independent APU (Fuel Cell) on real-world-driving cycles and over-night idling

V.F.2. Technical Discussion

Introduction

Hybridization can lead to significant fuel consumption reduction, which has now demonstrated numerous heavy duty applications. Previously, The fuel savings for heavy-duty vehicle applications from class 2b to class 8 were evaluated with respect to the impact of component efficiencies, new technologies, and their combinations at various steady-state speeds and it concluded aerodynamic improvements and hybridization appeared to be the two technologies resulting in the greatest fuel savings.

This work is the extension of previous hybridization evaluation of class 8 line haul, attempts to understand the impact of hybridization of class 8 line-haul applications on fuel savings over real-world driving cycles and also help to understand the sensitivities of electrical accessory load at idle and payload on various real-world driving patterns. We will finally evaluate the amount of fuel saved by the

hybridization under different state of real-world driving conditions.

Hybrid Configurations

The baseline conventional line-haul truck model used in this study was a Kenworth T660 with a Cummins ISX 425 engine and an 10-speed manual transmission.

In general, A hybrid vehicle can have one or more electric machines that can be positioned at various points of the powertrain, leading to a large number of configurations. The main configuration families used in this study are : Parallel ISG mild hybrid, parallel pre-transmission full hybrid, and series-parallel full hybrid, which represent the spectrum of hybridization of 14% , 39% and 45% respectively.

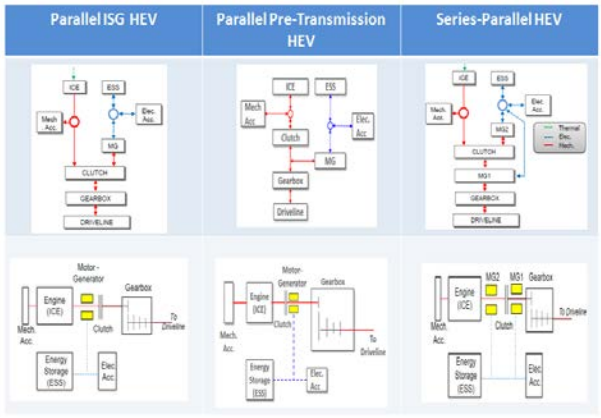

Figure 1. Schematics of parallel hybrids

Hybrids use a variant of the parallel configuration, which was selected over other configuration (s.a. series, power-split) because of the efficiency of its engine-to-wheel path at cruising speeds – were such trucks operate the most. Figure 1 illustrates the schematics of each hybrid used in this study.

Vehicle Specifications

For light-duty applications, typical sizing requirements are made of three criteria: acceleration (e.g. time to reach 60mph), gradability at a given speed (65mph with 6% grade) and top speed. The same type of requirements could be applied to line-hauls. However, there is no industry-wide standard, because trucks are customized to fleet requirements. Another major difference between the two applications is that heavy-duty vehicles often operate at maximum power, especially during grades. Starting from a conventional truck, no engine downsizing can be done because the battery energy is limited to a short duration. In this study the engine size is therefore the same as in the conventional counterpart. The components sizing results are as follows:

Table 1. Vehicle specifications

Configuration		Conventional	Parallel ISG HEV	Parallel Pre-Tx HEV	Series-Parallel HEV
Engine	Cummins ISX	317kW			
Motor 1	UQM PM		50kW	200kW	200kW
Motor 2	UQM PM				50kW
Battery	Shaft LI-Ion		75kW	230kW	230kW
			2.5kWh	25kWh	25kWh
Transmission	AMT 10 Speed	12.69, 9.29, 6.75, 4.90, 3.62, 2.59, 1.90, 1.38, 1.00, 0.74			
Final Drive		Ratio = 3.36			
Wheel	Bridgestone	Radius = 0.3175			
Vehicle		Coeff_Drag = 0.585, Frontal_Area = 10.38m^2			
Accessory	Mech/Elec	5.2kW/0.3kW	3.7kW/1 kW	1kW/3.3kW	1kW/3.3kW
Torque Coupling		Ratio = 2.5 between engine and motor			
Transfer Case		Ratio = 1			
Degree of Hybridization *		0%	14%	39%	45%
Mass		Curb Weight = 15700kg (including empty trailer), GVWR=36280kg , Cargo Mass = 20880kg Simulation Mass = 26140 kg (w/ 50% Payload as a default)			

The mild-hybrid truck is based on a parallel configuration with the electric machine in a starter-alternator position; this allows start/strop engine operations, a mild level of torque assist and a limited of regenerative braking. With only one relatively small, motor (50kW) small battery (5kWh), the mild-hybrid is a less-costly option.

Two full-hybrid trucks are used in this study. The one is based on parallel pre-transmission configuration with one electric machine is mounted between engine and dry-clutch. The other full-hybrid is based on a series-parallel configuration with two electric machines: one in a starter-alternator position and another one between the clutch and the gearbox. These two full-hybrid truck can run in electric propulsion mode at low speed/low power, and the engine is either shut down. The one of the main differences is that series-parallel can run in series mode to charge the battery when the electric motor has more advantage in efficiency during propelling, which provide more degrees of freedom to optimize entire hybrid system. The main traction motor is 200kW and the

additional generator is 50kWfor series-parallel configuration. They are paired to 25kWh battery-enough to provide an average 21.5kW for 10 hours within the 90-30% battery state of charge (SOC) operating window.

In all cases, the gearbox is the same as in the conventional truck, while the accessory load has changed from 5kW mechanical/0.3kw electrical (conventional) to 1kW mechanical/3kW electrical (series-parallel). This is justified by the electrification of accessories, although more investigation would be needed to estimate those values more accurately.

The GVWR is 36280kg including empty trailer and payload is 20880kg. The mass used in the simulation is 26140kg with 50% of payload.

Vehicle-Level Control Algorithms

The vehicle level controller manages the different hybrid powertrain components: engine, electric motors, and transmission (clutch and gearbox) in order to optimize fuel consumption, while maintaining the battery state-of-charge within appropriate levels. Major characteristics of vehicle level controls for hybrids are as follows:

- ON if the power request is above a certain threshold or if motor is saturating. OFF if the power request is below a certain threshold, and below a vehicle speed threshold
- If SOC is below a threshold, engine is ON and charges the battery until the SOC reaches a higher threshold
- Series mode at low speeds, parallel otherwise. Clutch open when engine is off.
- Motor torque is defined by difference between request torque and peak engine torque if the engine is saturating.
- Engine fuel is cut off.

Real-World Driving Cycles (RWDC)

5 real-world driving cycles were provided by Oak Ridge National Laboratory (ORNL) and used in this study. Figure 2 illustrates the RWDC overview.

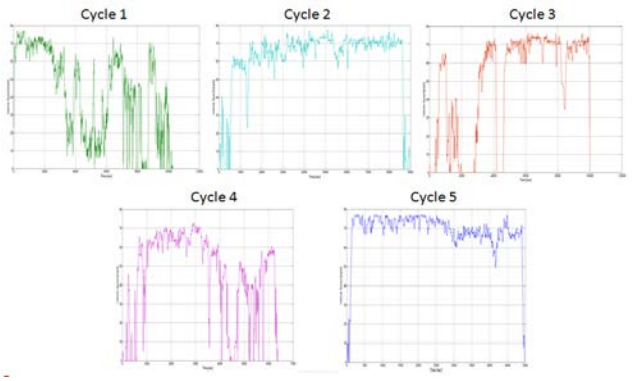

Figure 2. Real-world driving cycle overview

Based on their characteristics, each cycle may roughly be defined as :

Cycle 1 : Urban Driving
Cycle 2 : Highway Accelerating
Cycle 3: Urban to Highway
Cycle 4 : Highway to Urban
Cycle 5 : Highway Cruising

It is important note that the grade information on each cycle were not provided with speed information. The up-and-down behaviors on highway cruising of cycle 5 could be explained by this.

When simulating a hybrid vehicle, it is necessary to ensure that the results are not biased by the battery energy used during the cycle – simulation needs to be "charge balanced". Several iterations of the same cycles were run, so that difference in battery SOC (between the start and the end of the simulation) and therefore the difference in used battery energy become negligible. Thus the total number of simulations would be the scale of hundred iterations. Table 2 shows the main characteristics of 5 real-world driving cycles.

Table 2. Main characteristics of RWDC

	Max Speed	Average Speed	Max Accel	Max Decel	Number of Stop	Duration Of Stop	% of Stop	Total Time	Total Distance
Cycle1	76.9mph	42.3mph	1.68m/s^2	1.86m/s^2	27	667sec	6.48%	10290sec	120mi
Cycle2	72.9mph	45.6mph	1.75m/s^2	1.86m/s^2	15	555sec	8.17%	6370sec	80mi
Cycle3	76.5mph	48.8mph	0.91m/s^2	1.31m/s^2	9	1677sec	3.04%	10017sec	135mi
Cycle4	77.8mph	61.4mph	1.01m/s^2	1.55m/s^2	9	273sec	3.05%	8963sec	152mi
Cycle5	77.1mph	68.6mph	1.03m/s^2	1.54m/s^2	0	0	0	4981sec	94mi

Fuel Consumption Benefits of Hybridization of Class8 Line-Hauls on RWDC

To quantify the impact of hybridization on line-haul tractor-trailers fuel consumption, three types of hybrids were simulated on 5 real-world driving scenario described in previous section and compared against baseline conventional truck.

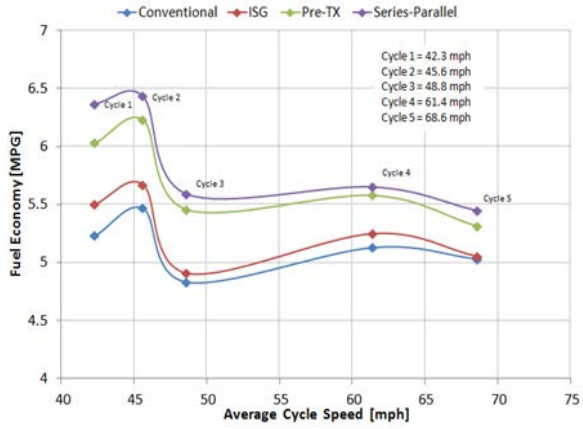

(a) Fuel Economy

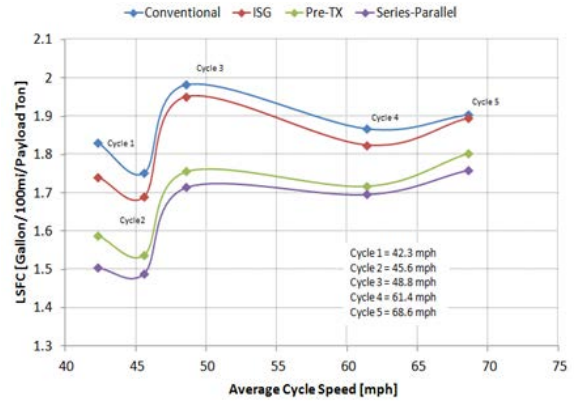

(b) LSFC

Figure 3. Fuel Economy and Load Specific Fuel Consumption on RWDC

At first glance, the fuel economies of conventional line-haul (highlighted in blue) on urban cycles (cycle 1 and cycle 2) are slightly higher than the one on the highway cycle (cycle 4 and cycle 5) even with more efficient operation of engine at cruising speed. It is explained by higher aero-drag loss due to approximately over 70 mph cruising from real-world driving pattern. .

The simulation results are shown in Figure 3 (a)-(b). Hybridization reduces fuel consumption the most in the urban cycle as shown Figure 4(a)-(b). This reduction is explained by the inefficiency of the conventional truck in such a driving scenario: idling, stop-and-go driving, and low-speed/low-load operation as shown in Figure 5 – (a). The hybrid system improves the efficiency of operation significantly from low-torque/low-efficient area to optimum area over the urban driving cycle as shown in Figure 5-(b).

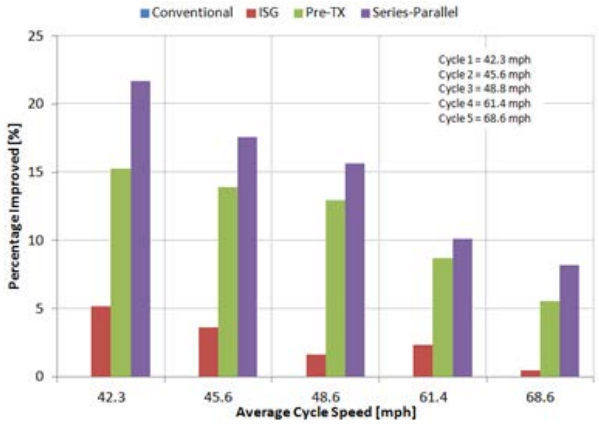

(a) Percentage Fuel Saved Vs. Average Cycle Speed on RWDC

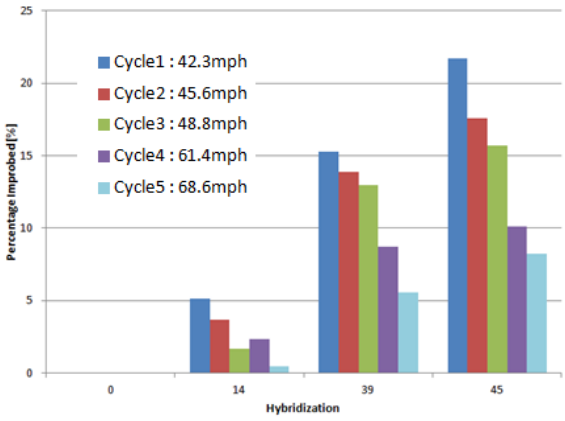

(b) Percentage Fuel Saved Vs. Hybridization on RWDC

Figure 4. Percentage Fuel Saved on RWDC

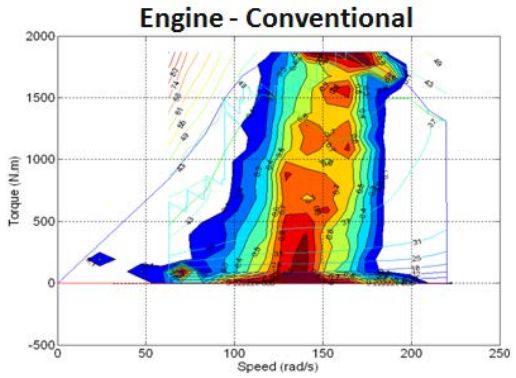

(a) Engine operating points of conventional line-haul

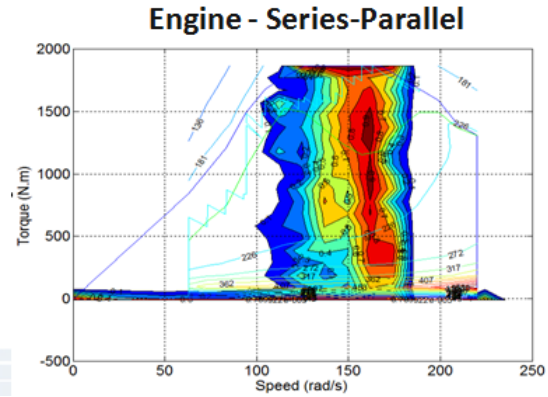

(b) Engine operating points of series-parallel hybrid

Figure 5. Engine operating points over urban driving (cycle 1)

As shown in Figure 4(b), the fuel consumption reduction improves as the degree of hybridization increases regardless of driving patterns. The recovered braking energy can be used for the accessories, which can therefore rely less on the engine. The ISG hybrid (mild, 14% hybridization) shows fewer savings than the series-parallel (full, 45% hybridization), peaking at 5%, while the series-parallel full-hybrid can save up to 22% on urban driving cycle (cycle1). Thanks to its bigger battery, the full hybrid can recover more energy during braking and can also run in electric-only mode when the vehicle starts moving. On the highway, savings are not as large, because conventional vehicle is already efficient at cruising speed, and braking events are rare. The amount of regenerative braking energy recovered by the battery is shown in Figure 6-(a) and average operating efficiencies of components are shown in Table 3.

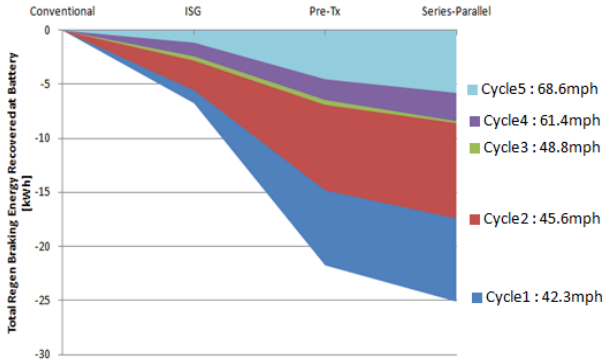

(a) Regenerative braking energy recovered at battery

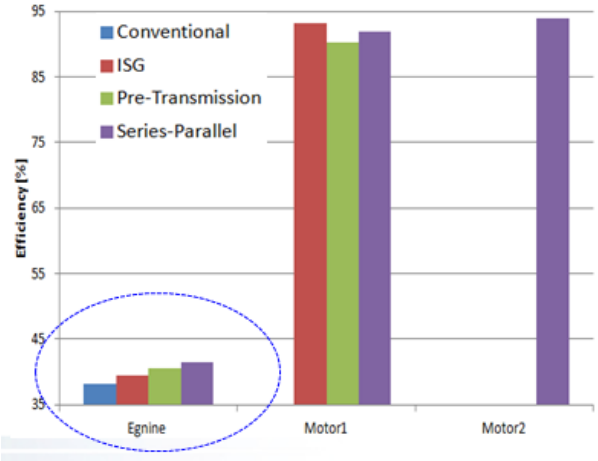

(b) Major component efficiency

Figure 6. Regenerative Braking Energy

Recovered at Battery Vs. Major Component Efficiency on RWDC

Table 3. Component Efficiency over Urban Cycle (cycle1)

	Conventional	ISG	Pre-Transmission	Series-Parallel
Engine	38.18	39.47	40.52	40.54
Motor 1		93.2	89.28	91.86
Motor 2				93.85

Impact of Electrical Accessory Load on Fuel Consumption

Accessories can create a substantial load that requires the engine to idle while the vehicle is at rest. Intuitively, this situation is less than optimal, as a powertrain designed to output 317 kW or more can be running to produce a few

kilowatts for hours at a time. The result is that the engine efficiency ranges between 5and 15% at idle, compared to the 35-40% that can be seen of diesel engines operating at full load for conventional case. Figure 7 shows the energies used over the entire cycle as well as idle for conventional vehicle, which explaining the energy losses due to duration of stops. The average efficiency of engine over the entire driving is sensitive to neither aggressive of cycle or duration of stops. However, pure energy loss generated by engine due to idling is sensitive to the size of electrical accessory load and the duration of stop. Note that the efficiency of engine improves as the size of electrical accessory load increase since the bigger accessory load allows the engine to operate toward its optimum.

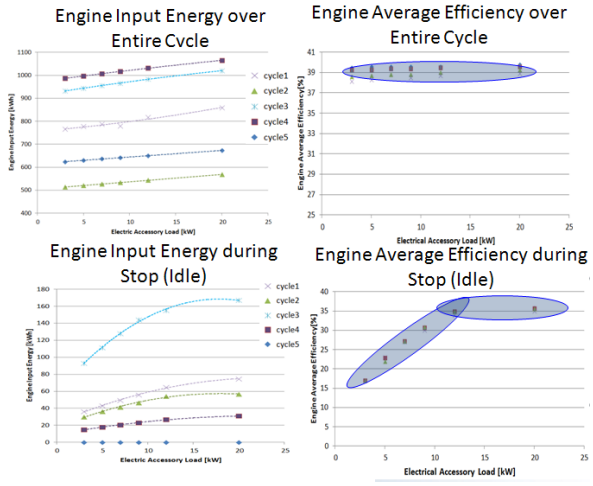

Figure 7. Energy consumption during driving and stopping for conventional Class 8 Line Haul on RWDC

Figure 8-(a)-(e) compare the fuel economy and % improved from conventional counterpart under different electrical accessory load scenario. Each class 8 line-truck was simulated with various electrical accessory loads (3,5, 7,9,12, 20) on 5 real-world driving cycles.

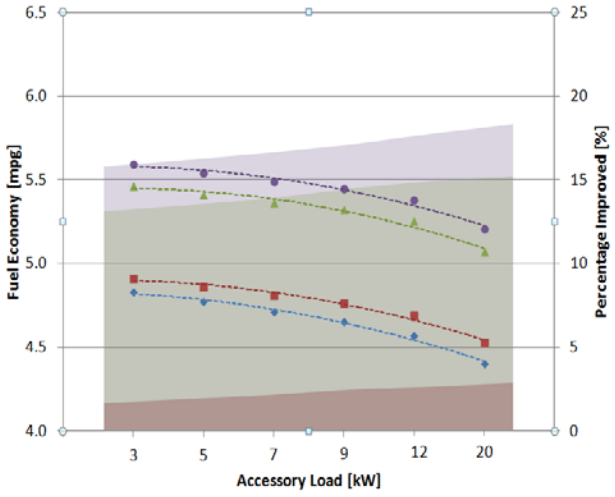

(a) Cycle 3
Stop Time = 1677 sec, Average Speed = 48.4 mph

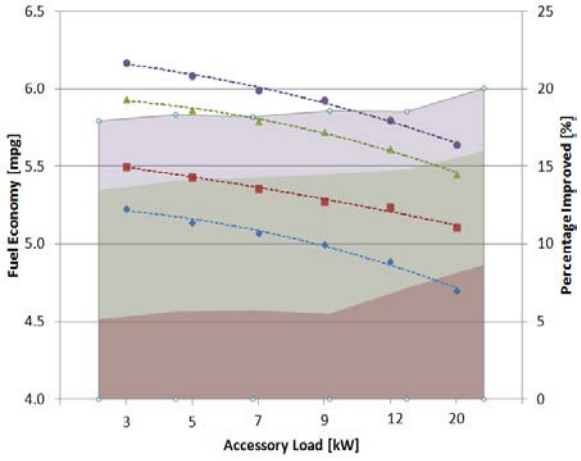

(b) Cycle 2
Stop Time = 667sec, Average Speed = 42.3mph

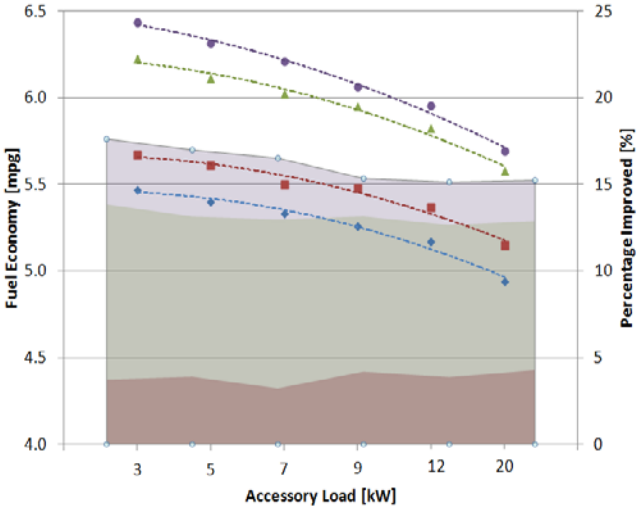

(c) Cycle 5
Stop Time = 555sec, Average Speed = 45.6mph

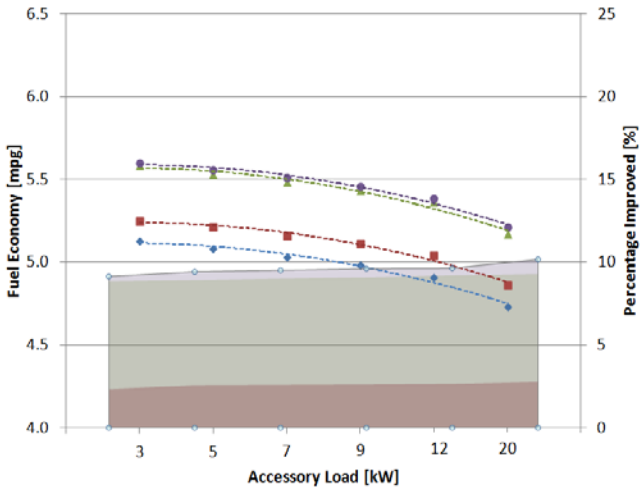

(d) Cycle 4
Stop Time = 667sec, Average Speed = 61.4mph

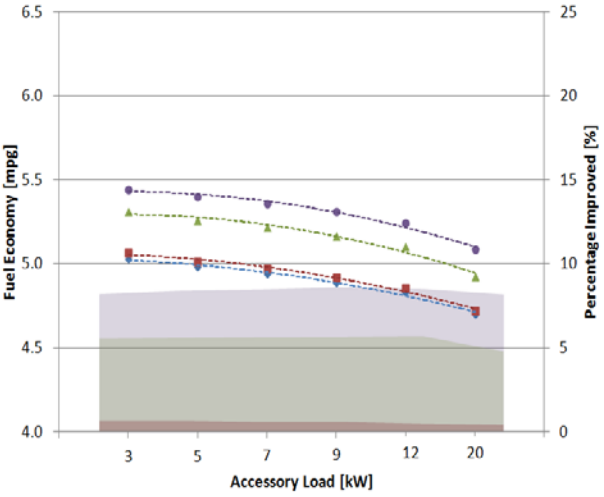

(e) Cycle 1
Stop Time = 0sec, Average Speed = 68.6mph

Figure 8. Impact of electrical accessory load on fuel consumption on various class 8 line-haul hybrid applications over RWDC

Hybridization reduces fuel consumption the most in the urban cycles (cycle3 and cycle2) as shown Figure 8. This reduction is explained by the duration of idling time presented in the cycle. The longer idle time the cycle has, the more fuel consumption reduction the vehicle can be achieved. Also the higher hybridization the vehicle (parallel pre-transmission and series-parallel hybrids) , the more fuel consumption reduction can be achieved. It can be explained by the engine is never turned on during stop (idling) due to the sufficient energy capacity of battery (25kWh) which can even support the power for 20kW electrical accessory load cases over the duration of stops. The engine operation at the low efficiency area (low torque) can be replaced by the large energy capacity battery pack acting as an APU during frequent idling, stop-and-go driving, and low-speed/low-load operation. Higher hybridization implies the battery has more capacity to support the use of electrical accessory loads during idle and this improves the fuel savings significantly for daily driving conditions.

Table 4 shows the number and duration of idle presented in the real-world driving cycles. Cycle 3 has about 30 minutes, cycle 1 has 12 minutes, and cycle 2 has 9 minutes of idling time. In summary, the impact of electrical accessory load is greatest at urban cycle with longer idle time and higher degree of hybridization (i.e. series-parallel hybrid)

Table 4. Idle number and duration

	Cycle1	Cycle2	Cycle3	Cycle4	Cycle5
Number of Stop	27	15	9	9	0
Duration Of Stop	667 sec	555sec	1677sec	273sec	0sec

Impact of Payloads on Fuel Consumption

Another important real-world factor to take into account is the variations in payload. Figure 9 compares the fuel economy and LSFC for different payloads. In this case. A class 8 line haul trucks were simulated at various weights (0, 10%, 20%, 30%, 40%,….100% payload) on 5 real-world driving cycles and their fuel economy as well as LSFC were reported on Figure 9-(a) and -(b). Note that in order to avoid division by zero, the LSFC starts at 10% payload. When solely looking at the fuel economy, Figure 10 would tell us that carrying an empty trailer or the full load would only have change of 25% in the fuel efficiency. However if LSFC is considered, the change in fuel consumption between 10% payload and 100% payload (i.e. GVWR) is nearly 85%. The better depicts the impact of the payload on the consumption of the work done by the truck as shown in Figure 11.

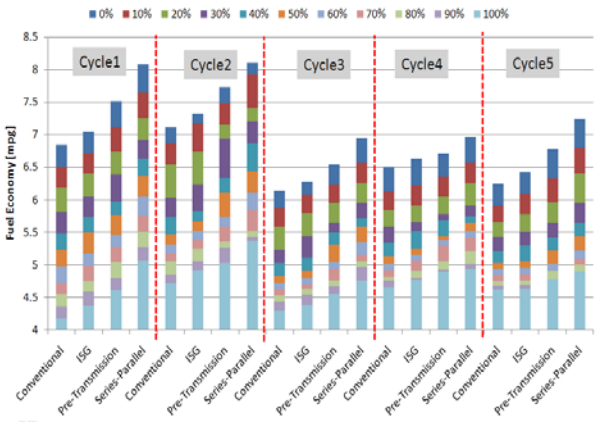

(a) Fuel economy

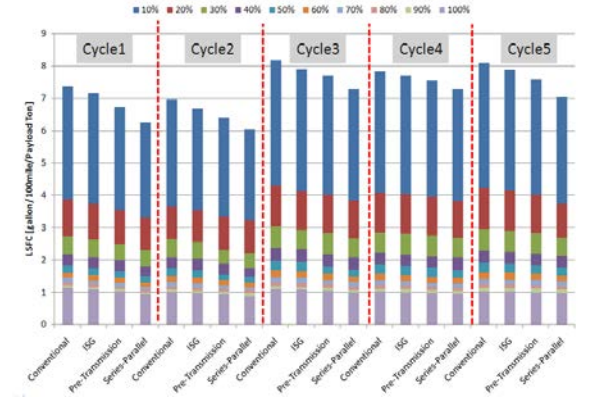

(b) Load specific fuel consumption (LSFC)

Figure 9. Impact of payloads on fuel consumption on various class 8 line-haul hybrid applications over RWDC

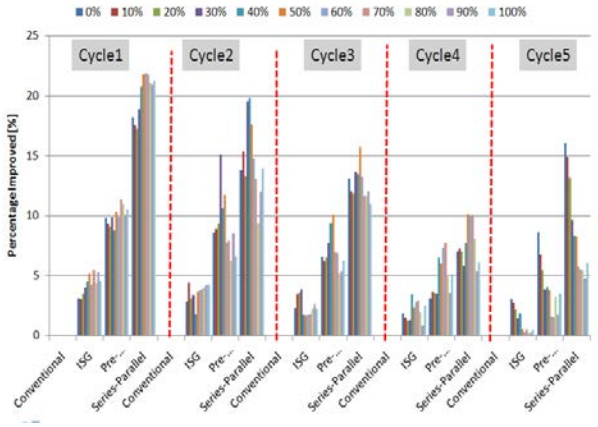

Figure 10. Percentage Fuel Saved on RWDC

At the urban driving(cycle1 & cycle2), the impact of payload is the most significant. 5% to 22% fuel savings were achieved as the degree of hybridization and the percent of payload increase. At the highway cruising (cycle 5), it appeared that the fuel savings due to hybridization are diminished as the payload increases. The impact of hybridization becomes negligible (less than 4%) at GVWR.

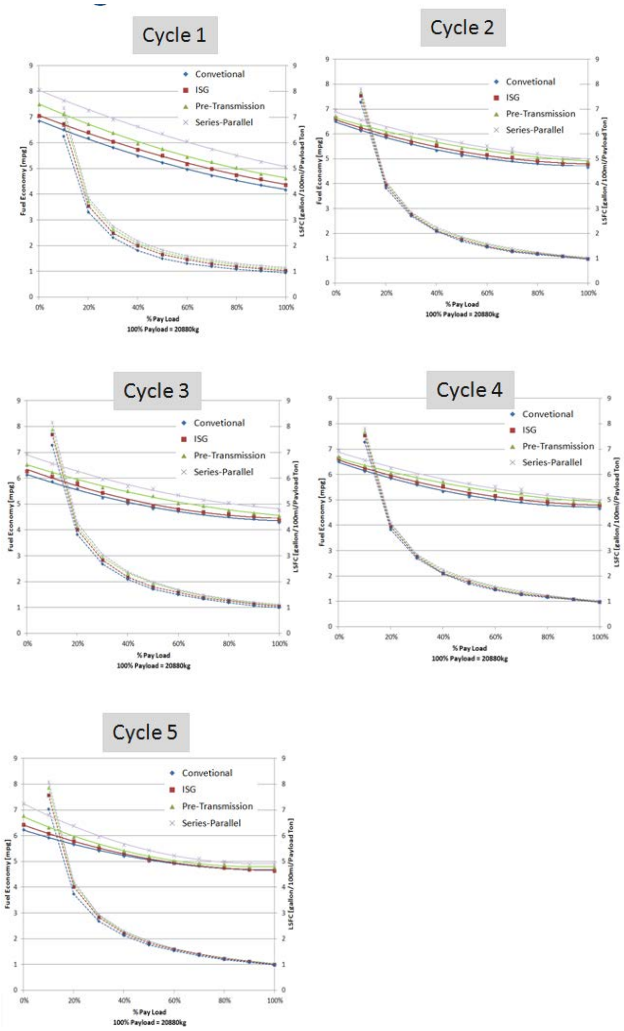

Figure 11. Fuel Economy Vs. LSFC results with various payloads.

Figure 12 shows the impact of payload and hybridization on engine efficiency over urban driving pattern. The motor assists the engine to operate in the efficient area as long as possible by assisting/generating depending on the state of charge of battery during the frequent stop and go driving conditions. At the urban driving, the fuel savings can be achieved as high as 22% with series-parallel hybrid (45% of hybridization), At the highway driving, however, the overall fuel savings becomes negligible less than 4%. It is because the excessive friction losses and grade

force diminish the benefit of engine efficiency improvement achieved by high degree of hybridization (45%).

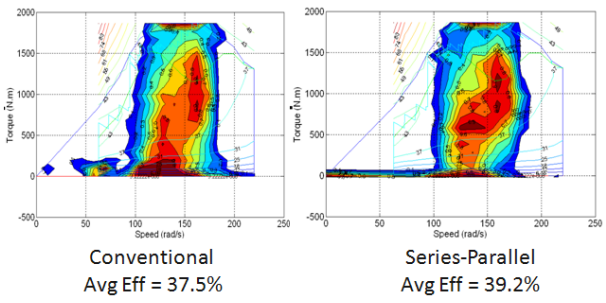

(a) Engine operating points at 0% payload

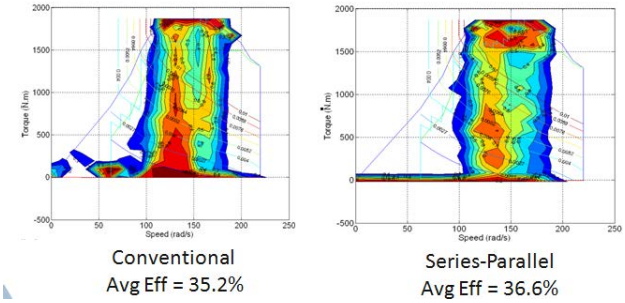

(b) Engine operating points at 100% payload

Figure 12. Engine operating points on Urban driving – cycle 1

Figure 13 clearly shows that the impact of payload on fuel economy over two opposite driving conditions (urban vs. highway) for class 8 line-haul hybrid applications. The slopes of fuel efficiency change due to increase of payload on highway driving is steeper than the urban driving. It is explained by the hybrid system goes beyond its area where the motor is no longer able to control the engine to operate in efficient area. However, on urban driving, the hybridization is still very effective to improve fuel efficiency at GVWR. Especially, the excessive power from two motors of series-parallel hybrid system can provide enough torque at low speed to improve the efficiency of engine operation.

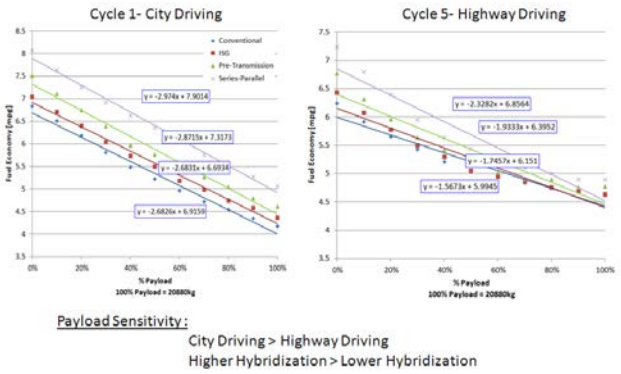

Figure 13. Payloads Sensitivity to hybridization: Urban vs. Highway

Conclusions

In this work, we discussed the implementation of three vehicle models of a class 8 line haul truck in Autonomies . For each of them, we mainly evaluate the fuel consumption reduction potential of hybridization over 5 real-world driving cycles measured and provided by Oak Ridge National Laboratory. Engine efficiency improvements and free regenerative braking energy appeared to be the two major factors to improve the fuel consumption when the vehicle is hybridized, resulting in the greatest fuel savings. Under highway conditions, a 14% degree of hybridization of parallel ISG system could yield fuels savings of up to 3%, but it can improve as much as 6% in fuel savings at urban driving. With higher degree of hybridization leads the more fuel savings due to bigger motor and battery which allows the power train to operate more efficiently. We found that class 8 hybridization benefits were highly dependent on the drive cycle.

The one of the many advantage of hybrid system is to use battery as an APU during idle. It is very effective to improve fuel saving for class 8 line-haul application as the vehicle have frequent idling, stop-and-start, and low-speed/low-low operation, which can be defined as urban driving. The longer idle time the driving cycle has and the higher hybridization the vehicle has, the more fuel consumption reduction can be achieved. Finally the impact of hybridization of class 8 line-haul trucks over real-world driving could be diminished as the payload increases, especially at highway cruising.

Finally, the analysis presented in this paper shows that the potential reduction in fuel consumption by heavy-duty vehicles is significant, and that the use of modeling and simulation tools can allow a better selection of the technologies for implementation in each application.

V.G. Assessment by Simulation of Benefits of New HEV Powertrain Configurations

Namdoo Kim (Project Leader), Aymeric Rousseau
Argonne National Laboratory
9700 South Cass Avenue
Argonne, IL 60439-4815
(630) 252-7261; nkim@anl.gov

DOE Technology Managers: David Anderson, Lee Slezak

V.G.1. Abstract

Objectives

- Understand the advantage and drawbacks of different powertrain configurations for several vehicle applications (i.e., HEVs, PHEVs)

Approach

- Select the main powertrain configurations currently considered for both HEVs and PHEVs
- Define vehicles to meet the same Vehicle Technical Specifications.
- Run the simulations and analyze results on the standard US drive cycles

Accomplishments

- Two powertrain configurations compared for HEVs (single and multi-mode power split) and two other for PHEVs (Voltec and series)

Future Directions

- Evaluate the powertrain configurations considered in this study on additional drive cycles (other standards as well as real world)
- Evaluate additional powertrain configurations

V.G.2. Technical Discussion

Introduction

Various hybrid electric vehicle (HEV) architectures have been proposed, though one of the earliest and most commercially successful systems has been the power split, as used on all three generations of the Toyota Prius, other Toyota/Lexus models, as well as on the Ford Escape. The powertrain configuration of the power-split hybrid system, sometimes referred as the parallel/series hybrid, combines the previous two configurations with a power split device. A major advantage of this configuration stands in the possibility to de-couple the ICE and wheels speed as long as the output power demand is met, which gives much more flexibility to choose the ICE working point in order to optimize fuel consumption.

However, in the power-spilt configuration, the internal power circulation occurs along the closed loop depending on the speed ratio, and sometimes the circulated power increases enormously. This power circulation can lead to high losses and thereby to a low efficiency of the power transmission. Such drawbacks can be addressed by combining several EVT (electro-mechanical infinitely variable transmission) modes in to one multi-mode hybrid system, thereby increasing the number of mechanical points and allowing greater operation flexibility. Various multi-mode EVT design configurations

have been proposed, as indicated by patents and publications.

In HEV, as the battery is charged only by the engine without plugging in, it has a limitation in electric driving due to its relatively small battery capacity. Compare to the common HEV, plug-in hybrid electric vehicle (PHEV) has greater potential for fuel efficiency improvement and emission reduction because it allows full electric driving and can easily obtain electric power from the home electricity grid. PHEV is also capable of long-distances, with its HEV function. PHEV are gaining more attention in the automobile industry due to their advantages, but there have been few comparative studies on their powertrain because a different control algorithm is required depending on the configuration of the PHEV.

When designing a vehicle for a specific application, the goal is to select the powertrain configuration that maximizes the fuel displaced and yet minimizes the sizes of components. In the first part of this study, we evaluate the benefits of several multi-mode powertrain configurations with regard to size and fuel consumption for HEV. Each powertrain is sized to represent a small-size sport utility vehicle (SUV) application, following the same vehicle technical specifications, such as acceleration and gradeability. In the second part, a comparative study was also conducted on GM Volt and series plug-in hybrid for PHEV. Two vehicle powertrain configurations are sized to achieve similar performance for all electric range (AER) approaches based on mid-sized vehicle application. The component sizes and the fuel economy of each option are examined.

Powertrain System Description

HEV Powertrain System

Single-mode EVT

Figure 1 is a schematic diagram of the single-mode power split transmission (TM) with a reduction gear (RG). Since the input power from the ICE is split at the planetary gear which is located at the input side, and the power transmission characteristic is represented by a single relationship for the whole speed range, this power-split configuration is called the "input-split type" or "single- mode EVT." This input-split configuration consists of two planetary gears, and two electric machines (MC1 and MC2). The larger electric machine on the right (MC1) is connected to the output shaft through the second planetary gear and does not affect the speed ratio. Therefore, for this particular EVT arrangement, which maximizes the output torque, the speed of the output is the weighted average of the speed of the input and the speed of MC2. The second planetary gear set multiplies the torque from the input and both of the electric motors during input-split operation. For comparison, the single mode powertrain without RG is also investigated in this study.

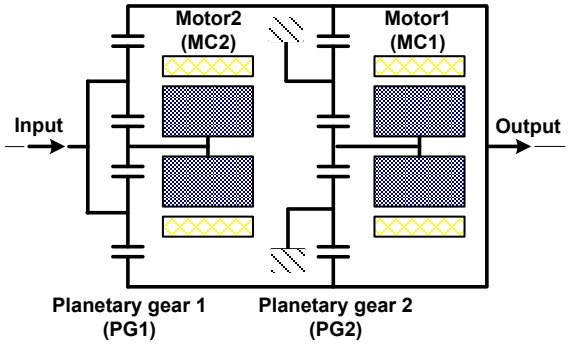

Figure 1. Schematic of the single-mode EVT

In Figure 2, the electro-mechanical power ratio and the EVT system efficiency (η) are plotted with respect to the speed ratio (SR). In this analysis, it is assumed that there is no power loss through the all-mechanical path and only electric machine loss is considered by using the efficiency maps of electric machines. The power ratio is defined as the ratio of the electro-mechanical power to the ICE input power and the SR is defined as the ratio of the ICE input speed to output speed. In high SR range, the system efficiency is low because the electrical machines have relatively low efficiency. This low system efficiency can be avoided by propelling the vehicle by using the electric motor directly instead of using the engine. When SR=0.7, the electro-mechanical power ratio becomes 0, and all the power is transmitted through the mechanical part. This point is called the mechanical point (MP). The system efficiency shows the highest value at the MP. For SR<0.7, the electro-mechanical power ratio has a negative(-) value, which means that the

power is circulating along the closed path. It is apparent that the circulated power increases as the SR decreases. Once the power circulation occurs, the EVT efficiency decreases due to the relatively low efficiency of the electro-mechanical power path. The high circulated power results in the decreased transmission efficiency and requires large electric machines. In addition, this high power requires consideration of the mechanical part design. The analysis results demonstrate why the Toyota hybrid system (THS), a typical example of the input-split HEV, adopts large capacity electric machines.

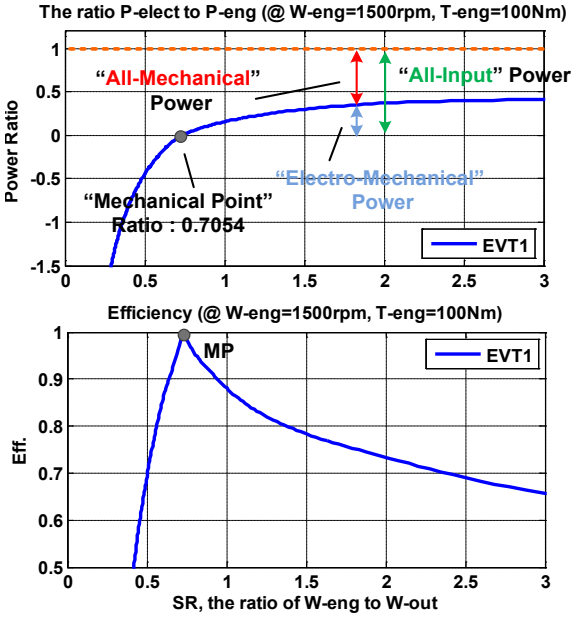

Figure 2. Power characteristics of the single-mode EVT

Two-mode EVT with Fixed Gear Ratios

Figure 3 is a schematic of the two-mode hybrid, which is called the General Motors Advanced Hybrid System2 (AHS2) for front-wheel drive (FWD) [5]. This system has an additional stationary clutch and an additional rotating clutch. Through engaging or disengaging the four clutches, it realizes six different operation modes including two EVT modes and four fixed gear (FG) modes. When operated in any of the four fixed gear modes, the vehicle is comparable to a parallel pre-transmission HEV.

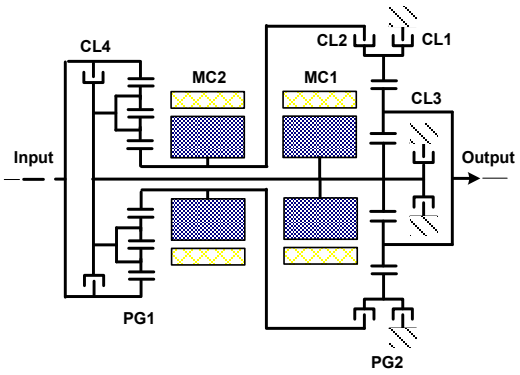

Figure 3. Schematic of the two-mode EVT with FGs

In Figure 4, the two-mode EVT already has a native fixed gear ratio, the synchronous shift ratio, where the action of two clutches at the same time provides a fixed ratio. For the two-mode hybrid, one fixed gear was added within the ratio range of the first EVT mode, and two more fixed gears were added within the ratio range of the second EVT mode. So, for the two-mode hybrid the native fixed gear between the two EVT modes is fixed gear 2 (FG2). The top fixed gear ratio, fixed gear 4 (FG4), was added by putting a stationary clutch on one of the motors that regulates the speed ratio through the transmission, MC1. Fixed gear 1 (FG1), and fixed gear 3 (FG3), were both added with a rotating clutch. The FG1 comes from locking up the input-split mode, so the speed, torque, and power from the engine go through the torque multiplication of the second planetary gear set. The FG3 comes from locking up the compound-split mode, so the speed, torque and power from the engine are coupled directly to the output. This study also investigates the additional two-mode EVT with fixed gears, which is called AHS2 for rear-wheel drive (RWD). A two-mode EVT with both an input-split mode and a compound-split mode fundamentally lowered the requirement for motor power, thus allowing the EVT to be selected as a sound basis for large cars and trucks.

System Operation Schedule			
Mode	BK1	CL1	CL2
EV1	On	Off	Off
EV2	Off	Off	On
Series	On	On	Off
Power split	Off	On	On

By setting the engagement and disengagement of the clutches and brake as shown in Table 1, GM Volt is driven in four modes: the EV1, EV2, series, and power-split modes. The EV1 and EV2 modes are called “charge-depleting (CD) modes” while the series and power-split modes are called “charge-sustaining (CS) modes”. In the CD mode, the battery is the only power source, and the vehicle operation depends on the energy from the battery. In the CS mode, the engine serves as the main power source while sustaining the battery SOC.

In Figure 6, in low SR range, the system efficiency is low because the electrical machines have relatively low efficiency. This low system efficiency can be avoided by propelling the vehicle by using the series mode instead of using the split mode.

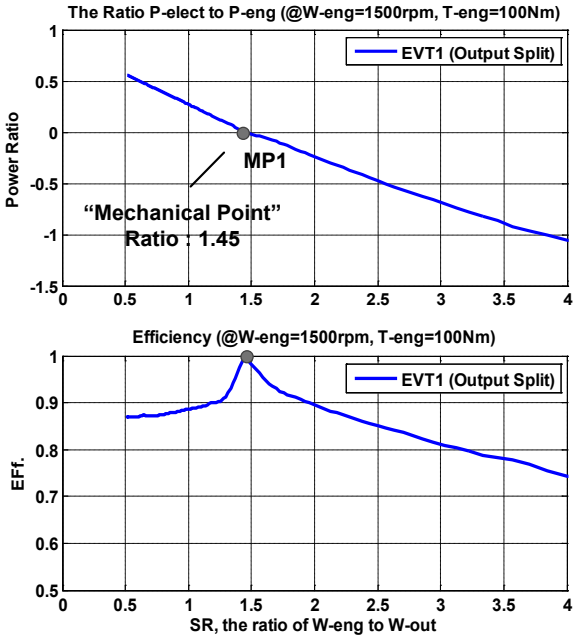

Figure 6. Power characteristics of the GM Voltec

Component Sizing

Modeling the Vehicle in Autonomie

Autonomie is a forward-looking modeling tool that can simulate a broad range of powertrain configurations. The driver model computes the torque demand needed to meet the vehicle speed trace. The torque demand is interpreted by a high-level controller that computes the component's torque demands while ensuring that the system operates within its constraints. Detailed transmission models were developed by using SimDriveline, including specific losses for gear spin and hydraulic oil, as shown in Figure 7. Such a level of detail is necessary to properly assess the trade-off between complexity and efficiency.

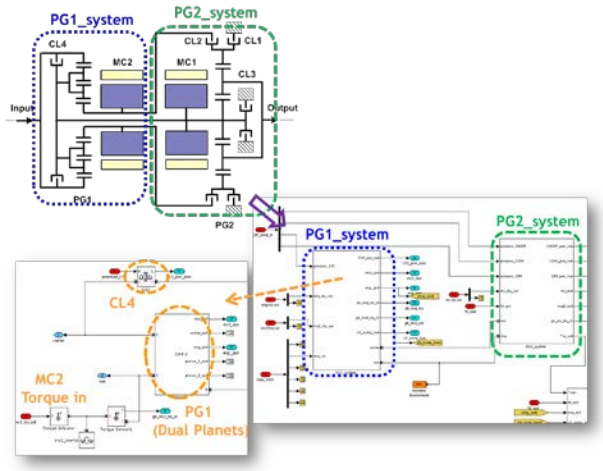

Figure 7. Transmission model for the AHS2 FWD

Mode Selection During Acceleration

The powertrain must be operated in such a way that the output shaft can transmit the maximum torque from the powertrain to the final drive. This can be regarded as an optimization problem, and it is solved for the corresponding vehicle speed. An off-line computation was used to generate the maximum powertrain torque that could be used in Simulink, indexed by gearbox output speed and battery power. To compute that look-up table, a brute-force algorithm is used, possibly several hundreds of times, along an output speed grid ranging from 0 to its maximum.

The maximum powertrain torque curves are obtained along the scheme and displayed in Figure 8. In acceleration simulations, the mode that allows the maximum output torque is selected. Figure 8 shows the tractive capability of the system with fixed gears, based on the optimum selection of engine speed to provide the highest level of tractive output. From this graph, in Figure 8a, it can be seen that FG1 increases the vehicle tractive capability significantly in the range of 10-45 mph. The use of FG1 over a large range of vehicle speeds eliminates the need to use the motors for processing engine power, thereby freeing up capacity to boost acceleration.

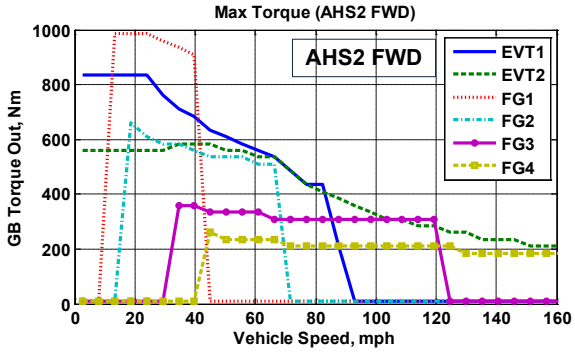

(a) Two-mode EVT with FGs (AHS2 FWD)

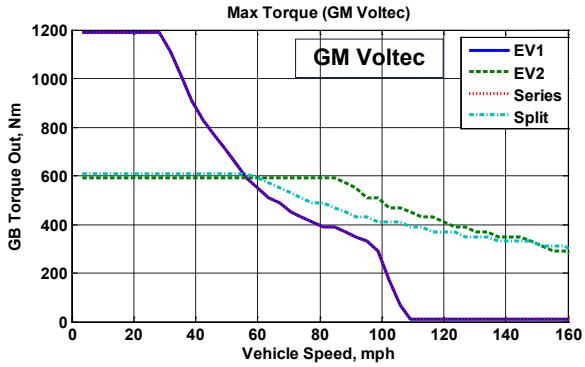

(b) GM Voltec

Figure 8. Max torque during acceleration

Sizing Process

To quickly size the component models of the powertrain, an automated sizing process was used [13]. The sizing process defines the peak mechanical power of the electric machine as being equal to the peak power needed to follow the acceleration constraints. The peak discharge power of the battery is then defined as the electrical power that the electric machine requires to produce its peak mechanical power. The sizing process then calculates the peak power of the engine by using the power of the drivetrain required to achieve the gradeability requirement of the vehicle.

As detailed previously, the component's characteristics determine the constraints. The main vehicle characteristics used in this study are summarized in Table 2. Particularly, the ratios of planetary gear sets are from patents and references. The 0-60 mph performance requirement for the vehicle is satisfied implicitly by the constraints on the peak motor power and the peak engine power. The power required by the motor for the vehicle to follow the UDDS cycle added to the power required by the engine for the vehicle to drive up a 13% grade at 65 mph exceeds the power that the vehicle needs to go from 0 to 60mph in 7.8 sec.

To meet the AER requirements for PHEV, the battery power is sized to follow the Urban Driving Dynamometer Schedule (UDDS) driving cycle while in all-electric mode. We also ensure that the vehicle can capture the entire energy from regenerative braking during decelerations on the UDDS. Finally, battery energy is sized to achieve the required AER of the vehicle. The AER is defined as the distance the vehicle can travel on the UDDS until the first engine start. Note that a specific control algorithm is used to simulate the AER. This algorithm forces the engine to remain off throughout the cycle, regardless of the torque request from the driver.

Table 2. Specifications of the small-size SUV for HEV

Body and chassis mass	1180 kg	**Frontal area**	2.64 m^2
Drag coefficient	0.37	**Wheel radius**	0.3423 m
Final drive ratio	Single mode : 4.11 Multi mode : 3.02		
PGs ratio (Zr/Zs)	Single mode : 2.6 Single mode with RG : 2.4, 2.0 AHS2 FWD : 2.36, 2.24 AHS2 RWD : 1.93, 1.97, 2.6		

The selected vehicle class for PHEV represents a midsize sedan. The main characteristics are defined in Table 3.

Table 3. Specifications of the mid-size sedan for PHEV

Body and chassis mass	950.2 kg	**Frontal area**	2.22 m^2
Drag coefficient	0.275	**Wheel radius**	0.317 m
Final drive ratio	Series PHEV : 4.44 GM Voltec : 3.02		
PGs ratio (Zr/Zs)	Series PHEV (Manual 2spd) : 1.86, 1 GM Voltec : 2.24		

The components of the different vehicles for PHEV were sized to meet the following vehicle performance standards:

- 0–60 mph < 9 s
- Gradeability of 6% at 65 mph
- Maximum speed > 100 mph

Sizing Results

Single-mode EVT vs. Multi-mode EVT

For comparison, two single-mode EVT hybrid systems and two multi-mode EVT hybrid systems are investigated, and the results are presented. As noted in the introduction, the multi-mode system results in significant improvements in dynamic performance at reduced capacities of the electro-mechanical power. As can be seen in Figure 9, the amount of capacities that saved by the multi-mode system ranges from 31.7% to 64.3%, relative to the single-mode. The main contributor is the addition of the EVT mode, which causes the difference between the single-mode and multi-mode systems.

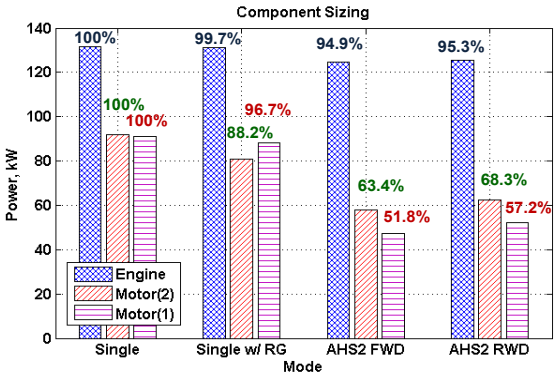

Figure 9. Component sizing results

Series PHEV vs. GM VOLTEC

The main characteristics of the sized vehicles are described in Table 4. Note that engine power is similar for the series and GM Voltec. The sizing result shows that the GM Voltec powertrain requires small component power to meet the VTS than a series system due to the use addition of driving mode. Because the electric machine is the only component used in the series to propel the vehicle, its power is also higher than that in the GM Voltec configuration.

Table 4. Component Size – 40 mi AER case

Parameter	Plug-in Series	GM Voltec
Engine Power (kW)	77.1	69.9
MC1 Power (kW)	129.4	125.8
MC2/Generator (kW)	74.8	69.9
Battery Capacity (kWh)	17.6	16.8
Vehicle Mass (kg)	1900	1865

Vehicle Control Strategy

Mode Shift Strategy

In order to evaluate the benefits of several multi-mode powertrain configurations from the standpoint of fuel consumption, a control strategy is required first. One of the major challenges of the multi-mode control strategy is to properly select the operating mode. In order to develop mode shift strategy, a brute-force algorithm is used. The algorithm generates an optimal input speed and torque for each EVT mode, indexed by gearbox output speed, battery power, and gearbox output torque. The knowledge of these parameters allows us to compute the fuel power and to compare it with that in the other EVT modes. Meanwhile, obtaining a candidate input set for FGs is same as conventional way.

Figure 13a depicts the optimal mode selections for various output load conditions. If we convert these results into new map by using vehicle speed and engine speed indexes, the mode selection rule is defined based on the speed ratio. The reason for this is because the selected optimal mode could be divided according to the speed ratio, which is defined as the ratio of the target engine speed to the output speed. When in propelling mode, the target engine speed previously computed by the simplified system-optimal-operating-line for driver power demand. In Figure 10b, the FG2 mode appears in the transition area between the EVT1 and EVT2 modes. The FG2 mode is inherent modes needed for the synchronous shift between the two EVT modes. The FG4 mode supplements the EVT2 mode. The logic was validated for both single-mode and two-mode hybrid systems by using vehicle test data. Similar algorithms were implemented for the GM Voltec configurations.

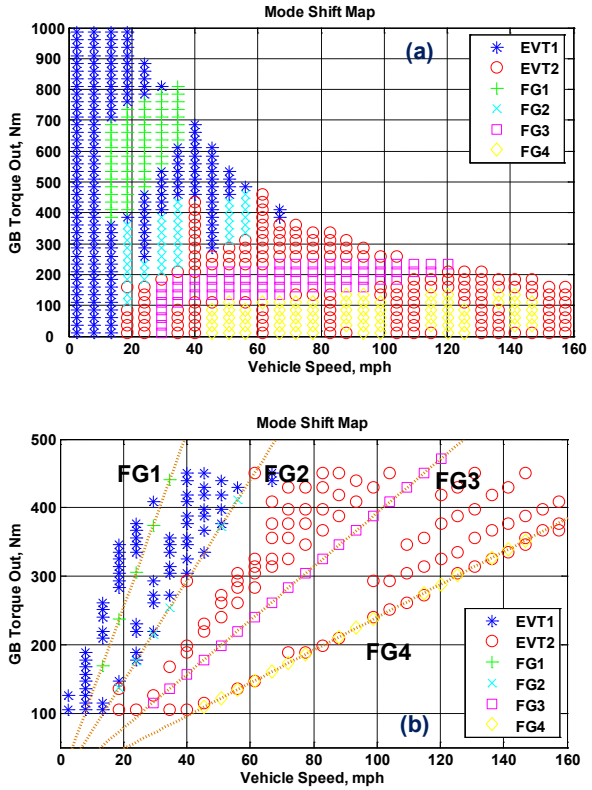

Figure 10. Mode shift Maps for AHS2 FWD

Energy Management Strategy for PHEV

According to sizing results, the average all-electric range of PHEV is almost 40 mi. To achieve this electric driving range, an energy management strategy must be developed.

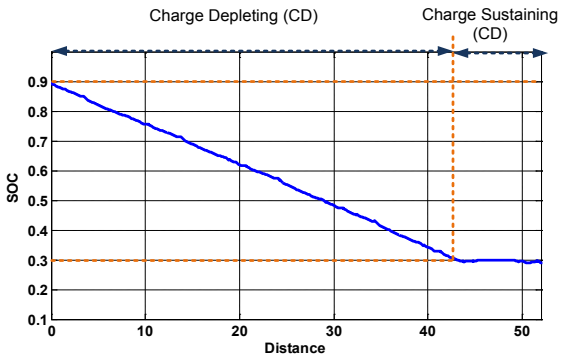

Figure 11. Control Strategy SOC Behavior

The developed energy management strategy is shown in Figure 11. When the battery is being charged, the upper SOC threshold is set at 0.9 due to the efficiency problem. When the initial battery SOC is 0.9, the vehicle is driven in the CD mode at engine start. In the CD mode, the GM Voltec is driven in the EV1 or EV2 mode, depending on the driving condition. The battery is the only power source in the CD mode. When the battery SOC decreases and reaches 0.25, the vehicle operation mode switches to the CS mode. The engine now works as the power source. The engine supplies the demanded vehicle power and maintains the battery SOC at around 0.25. When the battery SOC reaches 0.3, the driving mode of the vehicle is reverted back to the CD mode. Using this algorithm, as much electric energy as can be consumed is consumed to obtain better fuel efficiency.

For GM Voltec configuration, driving mode is an integral part of the energy management strategy. For the CD mode, the transmission efficiency map of EV1 and EV2 mode can be calculated by considering the motor efficiency and transmission loss. Based on the efficiency map, the shift map can be constructed for the CD mode. As a results, the EV1 or EV2 mode can be selected by the battery SOC, vehicle velocity and drive demand torque.

Simulation Results

Comparative Analysis of HEVs

With the transmission models and controller described in the previous section, the vehicle was simulated on standard drive cycles: the urban dynamometer driving schedule (UDDS); the highway fuel economy test (HWFET) cycle; the new European driving cycle (NEDC); a more aggressive urban cycle with some short highway cycles (LA92); and a highly aggressive cycle, predominantly at high speed (US06). The fuel economy results are reported in Figure 12. For urban driving, the single-mode hybrid system has relatively high fuel economy compared with that of the multi-mode hybrid system. On the other hand, the trend shown by the different cycles indicates that the higher the speed of the driving pattern, the greater the advantage of the multi-mode hybrid system. As a consequence, the AHS2 FWD provides a greater fuel consumption advantage for the vehicle application considered on the small-size SUV specification.

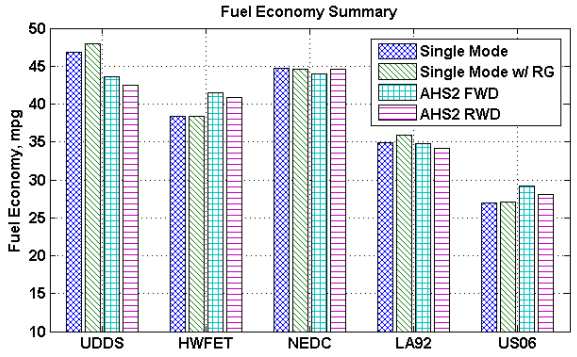

Figure 12. Fuel economy summary

Figure 13 reports the operating points of the powertrain for urban and highway driving. It is remarkable how the vehicles operate in the regions of higher efficiency to reduce fuel consumption. As shown in the figures, the single-mode hybrid system has relatively lower system efficiency in the primary operating region, for highway driving. This occurs because the electro-mechanical power increases sharply as the transmission reaches higher overdrive (Figure 2). The operating points of the multi-mode hybrid system are between the mechanical points to achieve the high EVT efficiency. For the multi-mode hybrid system, highway cycles favor the use of fixed gears.

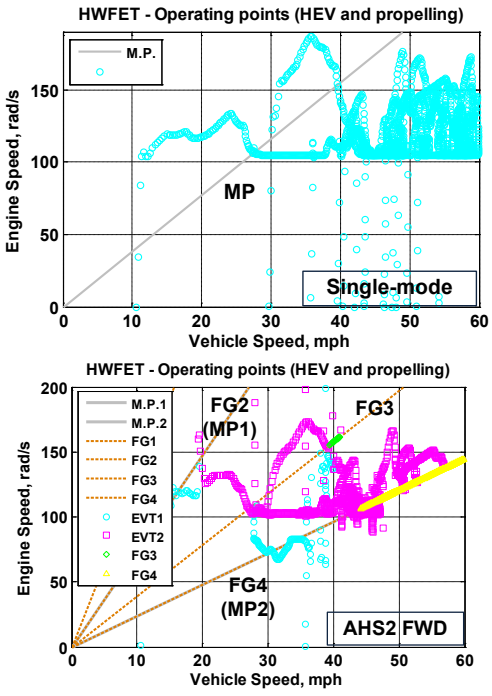

Figure 13. Operating points for HWFET

Table 5 shows the efficiencies of all three power sources and powertrains. The transmission efficiency refers only to the-all-mechanical path. The single-mode hybrid system has the highest transmission efficiency, since there is no need for more planetary gears or clutches. For the multi-mode system with the fixed gear, it is interesting to note that the efficiencies of the ICE are not particularly high. This effect is due to the fixed gear, which improves the highway fuel economy by avoiding the lower system efficiency region to maintain holding torque at the second mechanical point.

Table 5. Component average efficiencies, %

UDDS	S1	S2	M1	M2
Engine	33.3	33.4	30.9	31.1
MC1	87.0	87.5	86.5	86.7
MC2	86.2	86.1	86.0	86.0
TM	96.1	96.4	90.5	89.5
PT	33.5	33.6	31.6	30.9
HWFET	**S1**	**S2**	**M1**	**M2**
Engine	33.8	33.7	31.6	30.6
MC1	91.4	89.9	86.6	87.2
MC2	86.5	86.5	86.6	86.6
TM	94.7	93.4	89.0	88.9
PT	25.9	26.0	26.7	26.2

(S1: single mode; S2: single mode with RG; M1: AHS2 FWD; M2: AHS2 RWD; TM: transmission; PT: powertrain)

Comparative Analysis of PHEVs

The series is mainly driven in the EV and HEV modes, but GM Voltec has four driving modes. In the CD mode, GM Voltec has the EV1 and EV2 modes to drive the vehicle at low and high speed. In GM Voltec, only MC1 is used to propel the vehicle, and MC2 does not work in the EV1 mode. Furthermore, MC2 and MC1 propel the vehicle together in the EV2 mode. In Figure 14a, it can be seen that the MC1 torque shows a similar performance even if the vehicle is driven in a different driving mode. This shows that the MC1 torque of GM Voltec is determined only by the demanded wheel torque and is operated regardless of the driving mode, which implies that MC1 should have a power capacity that is large enough to drive the vehicle while satisfying the demanded power. This explains why the capacity of MC1 in GM Voltec is 125 kW, which is the similar with the capacity of

MC1 in the plug-in series. In the plug-in series, as shown in Figure 14a, in the EV mode, only MC1 is used to propel the vehicle, and MC2 does not work.

In the CS mode, GM Voltec has the series and power-split modes at low and high vehicle speeds. When GM Volt is driven in the series mode, MC2 works as a generator and supplies the electric power required for MC2 to propel the vehicle. In the power-split mode, even if MC2 can be used for optimal engine operation for both PHEV, the role of MC2 in GM Voltec is different from that in the plug-in series. In GM Voltec, MC2 assists the engine to produce the demanded torque at the ring rear, and propels the vehicle together with MC1. In the plug-in series, MC2 works as a generator, to generate electric power, while MC1 is only used to propel the vehicle.

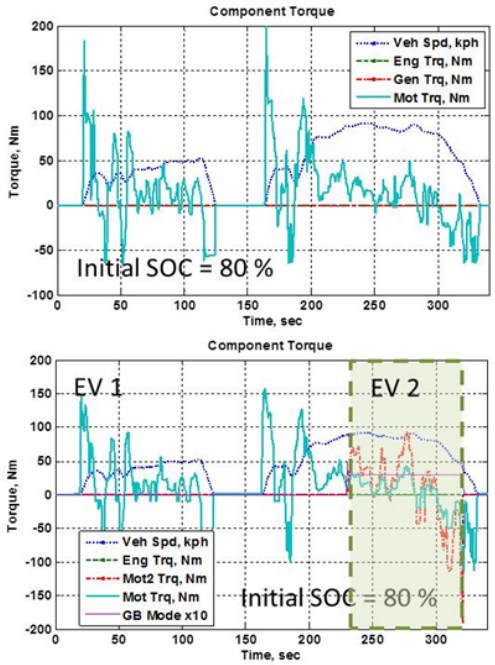

(a) Initial SOC = 80 %, (up = Series, bottom = GM Volt)

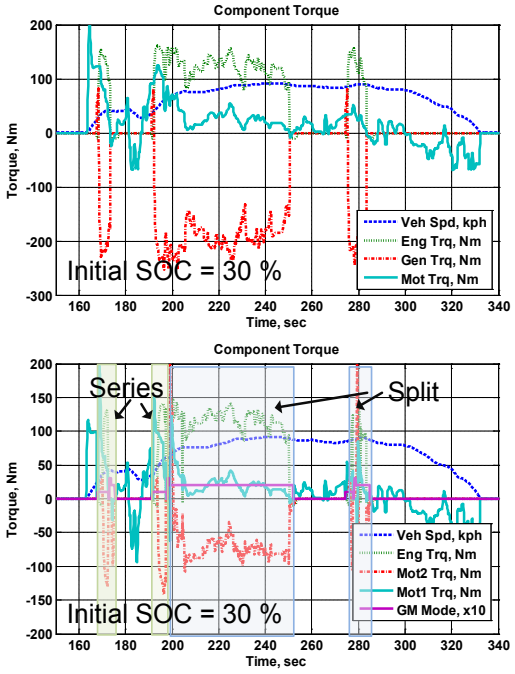

(b) Initial SOC = 30 %, (up = Series, bottom = GM Volt)

Figure 14. Comparison of Components Torque

The J1711 procedure is used in order to calculate the fuel economy of PHEVs. Table 6 shows the electrical consumption and fuel economy results for each powertrain configuration. GM Voltec provides the better

electrical consumption in CD mode. The higher efficiency of the power transfer from engine to wheels benefits the plug-in series due to the use of two electric machines. GM Voltec has also the better fuel economy in CD mode. The series configuration suffers from dual power conversion – from mechanical (engine) to electrical (generator) and back to mechanical (electric machine). The GM Voltec configuration performs better under the conditions of highway driving than under the conditions of urban driving due to the power split operation. The power split allows the engine to be operated close to its most efficient point without the engine sending all of its power through both electric machines, as shown in Figure 6. High engine efficiency and the ability to send mechanical power directly to the wheel allow this configuration to provide the better CS fuel economy.

Table 6. PHEV Fuel Economy Results

Electrical Consumption & Fuel Economy			Plug-in Series	GM Voltec
UDDS	CD	Wh/mile	265.0	251.7
	CS	MPG	44.5	46.8
	CD+CS	Wh/mile	195.0	185.9
		MPG	111.3	117.0
HWFET	CD	Wh/mile	250.7	240.3
	CS	MPG	44.5	49.4
	CD+CS	Wh/mile	197.2	193.1
		MPG	120.1	133.6

Conclusions

This study examined several powertrain configurations, including single-mode EVT, multi-mode EVT, series and GM Voltec, and vehicle-level controls developed in Autonomie. Detailed transmission models were implemented to allow a fair assessment of the benefits these different powertrain architectures by comparing component sizes, system efficiency and fuel consumption over several drive cycles.

First, single-mode EVT and multi-mode EVT were sized to represent a small-size SUV HEV application, following the same vehicle technical specifications, such as acceleration and gradeability. The results predicted that the multi-mode system would have better acceleration performance than a single-mode system, since the additional EVT modes significantly lower the requirement for the electric machine power. In addition, simulations were performed on a small-size SUV to characterize the impact on component operating conditions and fuel consumption for several driving cycles. It was determined that the multi-mode system has more fuel economy advantage during the high-speed cycle due to the relatively higher system efficiency.

A comparative study between the PHEVs powertrains GM Votlec and series was also performed. The sizing results show that the GM Voltec powertrain requires small component power to meet the VTS than a series system as a result of the many component efficiencies between the engine and the wheel. In addition, simulations were performed on a midsize vehicle to characterize the impact on component operating conditions and fuel consumption on urban and highway driving. The series mode in GM Voltec implies that a relatively larger MC2 is required for the vehicle's power requirement. In the power-split mode, MC2 is used to assist the engine in GM Voltec while in the plug-in series, MC2 works as a generator. It was determined that the GM Voltec powertrain achieved lower fuel consumption during all driving condition modes compared to a pure series configuration.

Publications/Presentations

Kim, N., Rousseau, A., "Assessment by Simulation of Benefits of New HEV Powertrain Configurations" , RHEVE Conference, Paris, December 2011

V.H. U.S. DOE Vehicle Technologies Program Support

Aymeric Rousseau (Project Leader), Ayman Moawad
Argonne National Laboratory
9700 South Cass Avenue
Argonne, IL 60439-4815
(630) 252-7261; arousseau@anl.gov

DOE Technology Managers: David Anderson, Lee Slezak

V.H.1. Abstract

Objectives

- Support any specific request from Vehicle Technologies Program occurring throughout the year.

Approach

- Gather component data for technologies to be evaluated
- Run simulations to address specific questions

Accomplishments

- Evaluated the benefit of HCCI engine for several powertrain configurations
- Assessed line haul fuel consumption for several steady-state vehicle speeds for different payloads
- Evaluated impact of displacement on engine idle fuel rate

Future Directions

- Continue to support any unplanned Vehicle Technologies requests.

V.H.2. Technical Discussion

Introduction

The objective of the project is to support any request from the Vehicle Technologies program that may occur throughout the year.

In the past, studies have been performed to assess the fuel consumption impact of component technologies (i.e., SIDI, HCCI), powertrain configurations and vehicle applications (i.e., heavy duty). Requests have also been made to evaluate the technologies required to meet CAFÉ standards.

Though several requests have been made during fiscal year 2011, the main request focused on the impact of vehicle performance on cost effective way to meet CAFE 2017-2025. In September 2010, the U.S. Environmental Protection Agency (EPA) and the National Highway Traffic Safety Authority (NHTSA) released the Interim Joint Technical Assessment Report, *Light-Duty Vehicle Greenhouse Gas Emission Standards and Corporate Average Fuel Economy Standards for Model Years 2017–2025*. The objective of the study is to determine the most cost-effective technology options to meet the 3 and 6% fuel consumption improvements proposed for different acceleration performances. To take into account uncertainties, three cases have been considered: low (90%), medium (50%), and high (10%). The low case represents "business as usual," while the high case is based on targets from the U.S. DOE Vehicle Technologies Program. The study, based on Argonne's Autonomie vehicle simulation tool, demonstrates that improving vehicle performance benefits the introduction of electric drive vehicles.

CAFE 2017–2025 Targets

CO2 Targets

Because CAFE is attribute-based and we cannot simulate all the vehicle footprints at the level of detail considered, we will assume that all vehicles will achieve the same improvements in fuel consumption. As a result, we will only consider a single vehicle class: midsize car.

The average GHG level for midsize cars of the MY 2016 fleet is 230 g/mi (Table 1), which represents the CO_2 value including the projected use of air conditioning (A/C) credits by manufacturers. The power necessary to operate an A/C compressor places a significant additional load on the engine, thus reducing fuel economy and increasing CO_2 tailpipe emissions. Since CAFE does not include such credits (only EPA does), 10 g/mi is added to its analysis, resulting in a 240-g/mi GHG level projected for the MY 2016 fleet (midsize car). The fuel economies shown in Table 1 are referred as "EPA MPG," while the fuel economy without credits can be called "CAFE MPG." In the remainder of the report, all the numbers are "CAFE MPG."

Table 1. MY 2016 CO_2 and Fuel Economy Targets for Various Vehicle Types, including credits

Vehicle Type	Example Models	Example model footprint (ft^2)	CO_2 emissions target (g/mi)	Fuel Economy target (mpg)
Example Passenger Cars				
Compact Car	Honda Fit	40	206	41.1
Midsize Car	Ford Fusion	46	230	37.1
Fullsize Car	Chrysler 300	53	263	32.6

Table 2 shows the possible CO_2 values for a midsize car for the four scenarios selected to reach the CAFE goal. Only two cases were analyzed in this study: the worst-case estimation (Scenario A: 3%/yr CO_2 decrease) and the best-case estimation (Scenario B: 6%/yr CO_2 decrease).

Table 2. 2017–2025 CO_2 Scenarios

Year	CO_2 (g/mi)			
2016	240			
	3%	4%	5%	6%
2017	232.8	230.4	228.0	225.6
2025	182.4	166.2	151.3	137.5

2017/2025 Fuel Economy/Fuel Consumption Equivalent Target

Table 3. 2017 CAFE MPG for Two scenarios A and B

2017/2025	Scenario A: 3%	Scenario B: 6%
CO_2 (g/mi)	232.8/182.5	225.6/137.5
Fuel Economy (mpg)	38.3/48.9	39.5/64.9
Fuel Consumption (L/100 km)	6.13/4.8	5.94/3.62

The attribute-based target was introduced for CAFE beginning with MY 2011 fleet vehicles, so there is no footprint-based regulation before that year. Therefore, it would be difficult to simulate the current (2010) CAFE standard on the basis of a midsize car only. The 2010 unadjusted fuel economy value of a typical midsize car (Ford Fusion) has been used as our reference (see Table 4). According to Table 4, we can assume the current 2010 CAFE standard associated with a midsize car (footprint 46 ft^2) would be set to 27.5 mpg.

Table 4. 2010 CAFE Reference for a midsize car

Ford Fusion 2010 (MPG)	EPA (UDDS)	EPA (HWFET)
Adjusted	18	27
Unadjusted	22.5	37.7
Combined Unadjusted	27.5	

As shown in Table 5, improvements in fuel consumption of 28.1% and 30.3% are needed for Scenarios A and B, respectively, by 2017, and fuel consumption improvements of 43.5% and

57.6% are needed for Scenarios A and B, respectively, by 2025

Table 5. Fuel Consumption and Fuel Economy improvements from 2010 to 2017–2025

	Scenario A	Scenario B
2010 CAFE (mpg)	27.5	
2017/2025 CAFE (mpg)	38.3/48.9	39.5/64.9
Improvement (%)	39.1/77.5	43.6/135.5
2010 CAFE (L/100 km)	8.5	
2017/2025 CAFE (L/100 km)	6.1/4.8	5.9/3.6
Improvement (%)	-28.1/-43.5	-30.3/-57.6

Study Methodology

This section assesses the fuel economy potential and cost of several component and powertrain technologies that would support both Scenarios A and B — 28.1% and 30.3% fuel consumption improvement — compared with current technologies (MY 2010). The simulations were performed with Autonomie by using drive cycles and calculations similar to NHTSA's:

- • Two drive cycles (UDDS and HWFET)
- • Cycle weighting of 55/45
- • Unadjusted fuel consumption

The plug-in hybrid electric vehicle (PHEV) fuel economies were defined on the basis of the SAE J1711 standard testing procedure by using the NHTSA utility factors.

The following powertrain configurations were considered, on the basis of existing and planned vehicles:

- • Conventional
- • Full hybrid electric vehicles (HEVs)
- • PHEVs — Power-split technology was considered for 10- and 20-mi all-electric range (AER) applications, whereas series technology was used for 30- and 40-mile AER.

Fuel Economy/Fuel Consumption and Manufacturing Cost Results

Figure 1, Figure 2, Figure 3 and Figure 4 show the impact of the different vehicle powertrain performance on the fuel consumption evolution.

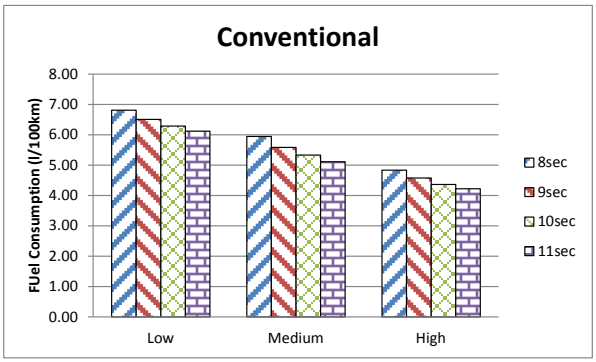

Figure 1. Impact of conventional vehicle performance on fuel consumption

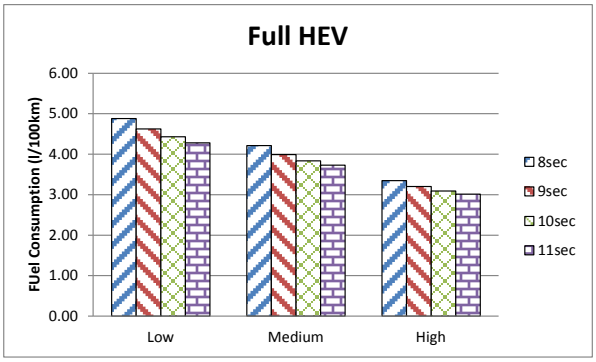

Figure 2. Impact of HEV vehicle performance on fuel consumption

Vehicle performance has a greater impact on fuel saved for conventional and hybrid vehicles than for PHEVs. More fuel is saved for conventional vehicles and HEVs with lower vehicle performance.

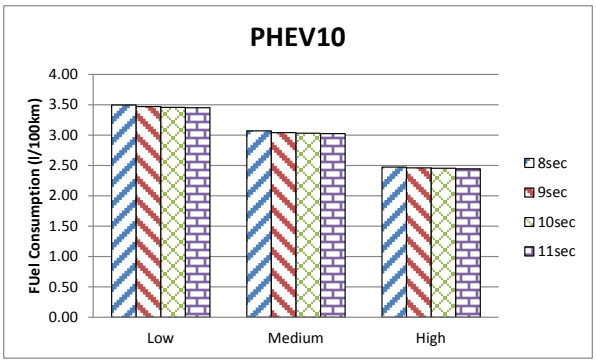

Figure 3. Impact of PHEV10 vehicle performance on fuel consumption

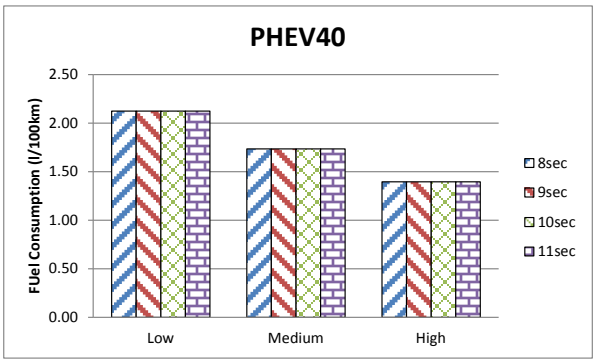

Figure 4. Impact of PHEV40 vehicle performance on fuel consumption

The impact of vehicle performance decreases with higher hybridization degree. The requirements to follow the UDDS in electric-only mode combined with the requirement that the engine meet gradeability leads to a high-performance vehicle. As a result, modifying the performance requirement for PHEVs from 11 to 8 s does not modify the fuel consumption.

8-seconds acceleration sizing

The following tables summarize manufacturing costs ($) for 4 different vehicle acceleration performances: 8 s, 9 s, 10 s, and 11 s. Reference conventional 2010 combined unadjusted FE: 31.2 mpg — 7.55 L/100 km

Table 6. Manufacturing Cost for 8-s Acceleration Performance

Drivetrain Configuration	Low	Medium	High
GASOLINE			
Conventional	14961	13967	14030
Full HEV	18259	18193	17824
PHEV 10	19930	19632	19202
PHEV 20	21102	20699	20007
PHEV 30	24509	23768	22103
PHEV40	26906	25899	23664

9-seconds acceleration sizing

Reference 2010 combined unadjusted FE: 32.9 mpg — 7.1 L/100 km

Table 7. Manufacturing Cost for 9-s acceleration performance

Drivetrain Configuration	Low	Medium	High
GASOLINE			
Conventional	13813	13744	13790
Full HEV	17531	17225	16915
PHEV 10	18882	18626	18315
PHEV 20	19668	19276	18823
PHEV 30	22523	21813	20526
PHEV40	24423	23504	21687

10-seconds acceleration sizing

Reference 2010 combined unadjusted FE: 34 mpg — 6.92 L/100 km

Table 8. Manufacturing Cost for 10-s acceleration performance

Drivetrain Configuration	Low	Medium	High
GASOLINE			
Conventional	13730	13668	13715
Full HEV	17234	16952	16688
PHEV 10	18753	18502	18208
PHEV 20	19553	19174	18734
PHEV 30	22523	21813	20526
PHEV40	24423	23504	21687

11-seconds acceleration sizing

Reference 2010 combined unadjusted FE: 34.98 mpg — 6.72 L/100 km

Table 9. Manufacturing Cost for 8-s acceleration performance

Drivetrain Configuration	Low	Medium	High
GASOLINE			
Conventional	13656	13600	13660
Full HEV	17001	16753	16485
PHEV 10	18660	18425	18135
PHEV 20	19449	19098	18660
PHEV 30	22523	21813	20526
PHEV40	24423	23504	21687

Recalculation of CAFE Targets based on Autonomie results

Since the results from Autonomie are not based on the 2010 Ford Fusion reference values, the first step in answering this question is to calculate updated goals on the basis of the assumptions used in Autonomie. It is important to focus on the percentage increases to obtain useful comparisons between real-world and simulation results. Autonomie simulation results have different fuel economy values. We need to achieve improvements of 39.1% and 43.6% in 2017 and 77.5% and 135.5% in 2025, respectively, for scenario A and scenario B on the basis of these simulation results, regardless of the initial fuel economy. Table 10 shows the new CAFE-targets equivalent on the basis of Autonomie simulation results.

Table 10. Autonomie-equivalent CAFE targets

Initial Autonomie FE result	32.9 mgp
2017 Scenario A (39.1%)	45.8 mpg
2017 Scenario B (43.6%)	47.2 mpg
2025 Scenario A (77.54%)	58.4 mpg
2025 Scenario A (135.56%)	77.5 mpg

Optimal Combination Method

To define the most cost-effective way to meet CAFE, we need to find the best combination of technologies with the lowest manufacturing cost to reach fuel economy of 44.5 mpg and 45.9 mpg. The problem is equivalent to maximizing fuel economy over minimizing cost.

Our analysis assumes that in 2017, fleet vehicles on the market will consist of six powertrain technologies: conventional, HEV, PHEV 10, PHEV 20, PHEV 30, and PHEV 40. Each technology is translated to an X variable in the following equations.

Constraint number 1:

$$(1) \qquad \sum_{i=1}^{n} X_i = 1$$

The mean Fuel Economy of these cars is the objective of CAFE2017 and CAFE2025:

Scenario **A**: $FE_{CAFE\_simu\,2017} = 45.75\ MPG$

Scenario **A**: $FE_{CAFE\_simu\,2025} = 58.38\ MPG$

Scenario **B**: $FE_{CAFE\_simu\,2017} = 47.22\ MPG$

Scenario **B**: $FE_{CAFE\_simu\,2025} = 77.45\ MPG$

Constraint number 2:

$$\frac{1}{\sum_{i=1}^{n} \frac{X_i}{FE_i}} = FE_{CAFE2017}$$

$$(2) \qquad \sum_{i=1}^{n} \frac{X_i}{FE_i} = \frac{1}{FE_{CAFE2017}}$$

Constraint number 3:

$$(3) \qquad \forall i \in \mathbb{N}^*, 0 \leq X_i \leq 1$$

The Cost function that need to be minimized, where $\forall i \in \mathbb{N}^*, C_i \geq 0$ represents the cost of each vehicle technology:

$$(4) \qquad J_\alpha = \sum_{i=1}^{n} C_i X_i$$

Several methods could be used to solve that minimization problem since it is a linear problem: using the Simplex method or Lagrange multipliers or applying the Karush-Kuhn-Tucker conditions. The last method seems to be the most appropriate choice since one of the constraints is an inequality constraint. Solutions might only be local solutions. However, using an adapted numerical optimum algorithm based on these theories to achieve results is discussed in the next section.

Results

2017 CAFE TARGET

Scenario A (3%)

Figure 5 shows the vehicle breakdown for the low-technology case. Overall, the percentage of conventional drivetrains increases with vehicle performance time sizing. The introduction of PHEVs for the 8-s and 9-s cases creates a discontinuity. This is due to the low FE/cost ratio. The slower the car, the more efficient it is, and so the proportion of electric vehicles in the optimal breakdown is lower. For the 8-s and 9-s cases, HEVs are completely absent, giving priority to more than 35% to 40% of PHEV 20.

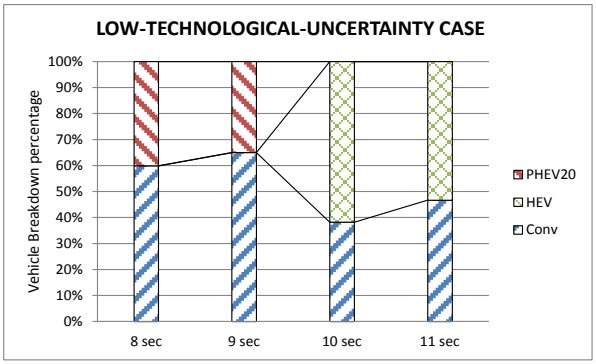

Figure 5. Vehicle breakdown for low-technology case: 2017 Scenario A

The medium-technology case (Figure 6) shows that the percentage of conventional drivetrains increases when vehicle performance decreases. The 8-s case has less than 25% of PHEV 20, whereas all of the vehicles are conventional cars for the 11-s case.

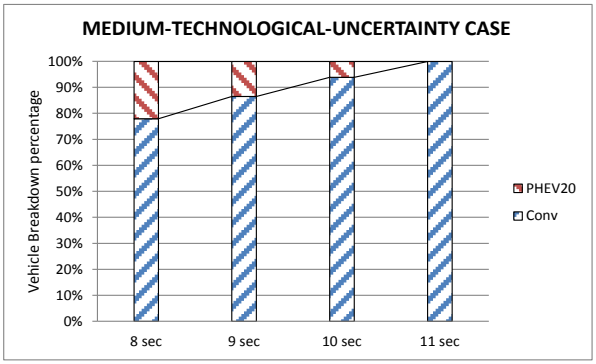

Figure 6. Vehicle breakdown for medium-technology case: 2017 Scenario A

The high-technological-uncertainty case illustrated in Figure 7 demonstrates that if one achieves significant advances in technology, conventional cars alone can meet the CAFE target.

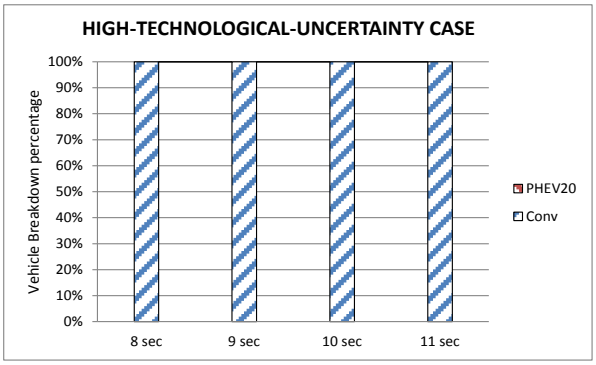

Figure 7. Vehicle breakdown for medium-technological case: 2017 Scenario A

Figure 8 shows that optimal cost decreases with performance. In fact, the slower the vehicle, the less powerful it is, and so its components cost less.

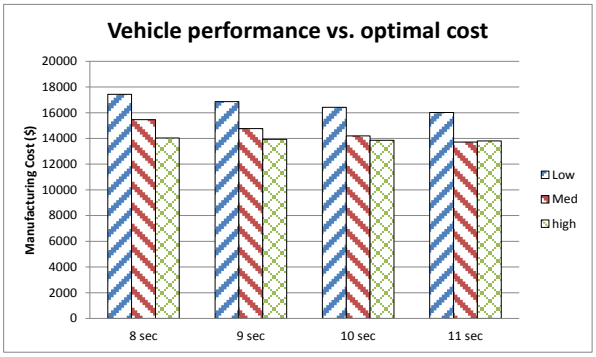

Figure 8. Impact of vehicle performance on optimal cost: 2017 Scenario A

Scenario B (6%)

The scenario B confirms the trend. In that case, the higher fuel-consumption target changes the distribution of the technologies, but the trend remains the same. Figure 9 shows that the share of electric drive vehicles required to meet the target increases. For the 8-s case, the share of PHEV 20 increases from 40 to 45%.

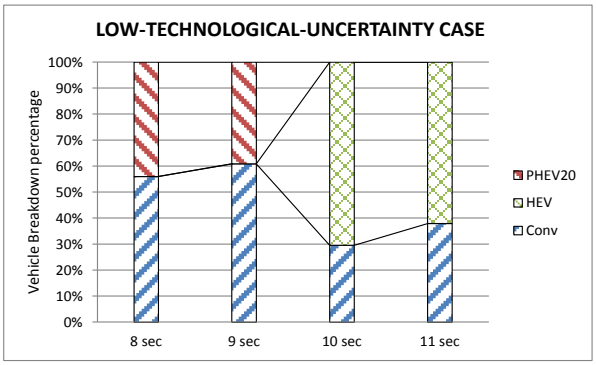

Figure 9. Vehicle breakdown for low-technological case: 2017 Scenario B

Figure 10 shows that by comparing the last scenario, an exception can be noted for the medium-technological-uncertainty case, in which the 11-s vehicle has a small percentage of PHEV 20 introduced (4.5%).

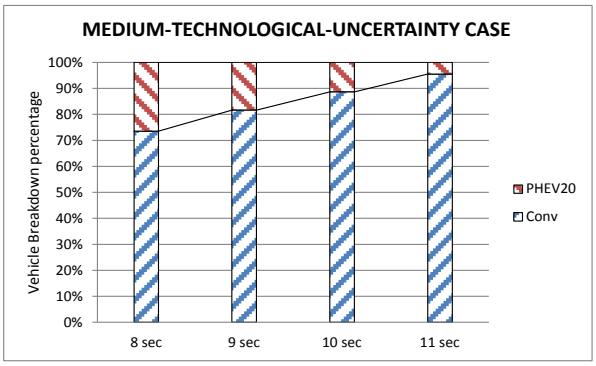

Figure 10. Vehicle breakdown for medium-technological case: 2017 Scenario B

The high-technological case remains the same because only conventional vehicles are shown in Figure 11.

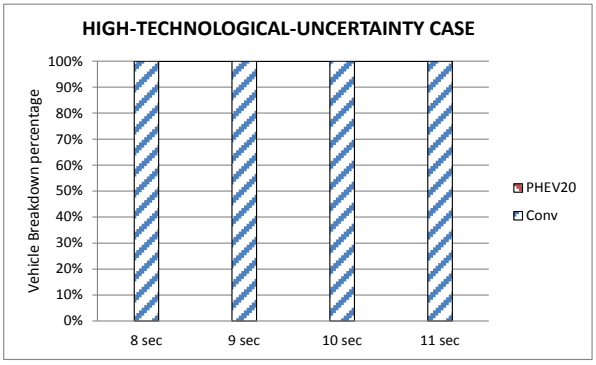

Figure 11. Vehicle breakdown for high-technological case: 2017 Scenario B

Figure 12 shows that optimal cost decreases with performance, as in the previous scenario. The main difference would be in cost values as optimal cost has slightly increased as a result of the higher amount of PHEVs needed on the market.

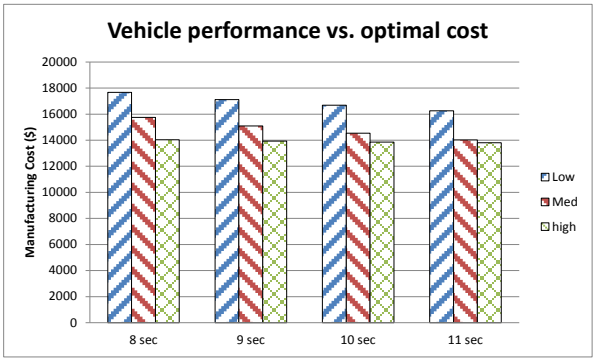

Figure 12. Impact of vehicle performance on optimal cost: 2017 Scenario B

2025 Cafe Target

Scenario A (3%)

As we discuss in this section, the target in this case is more aggressive, which means help from alternative hybrid configurations is needed to reach the goal. For this reason, PHEVS 20 (and especially PHEVs) proportions are higher than in 2017. Note that although HEVs were present in previous results for the low case, the case for 2025 centers the breakdown between conventional cars and PHEVs (PHEV20 in that case), except for the high case. Thus, in 2025, when the CAFE MPG target would be very high, PHEVs would be more likely to be in the market, with PHEV 20 being the best candidate.

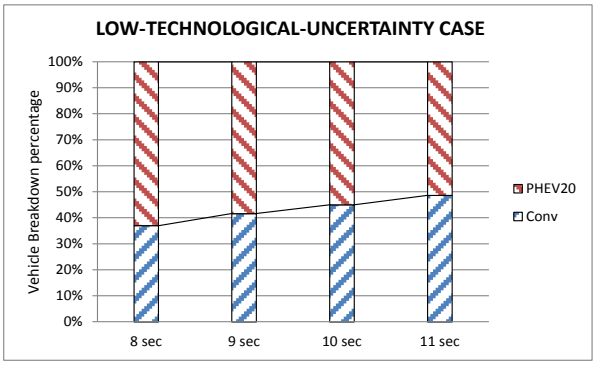

Figure 13. Vehicle breakdown for low-technological case: 2025 Scenario A

In general, comparing 2025 with 2017, shows that the amount of PHEV20 almost doubled for low and medium cases.

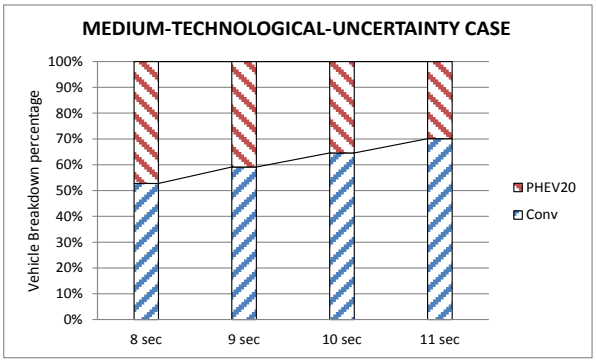

Figure 14. Vehicle breakdown for med-technological case: 2025 Scenario A

Figure 15, which shows the high-technological uncertainty case, first note the introduction of PHEVs in the breakdown. Also note that in the 11-s case, about 6% of the breakdown is HEV cars. Overall, electric vehicles are needed for the high-technological case, in contrast to 2017.

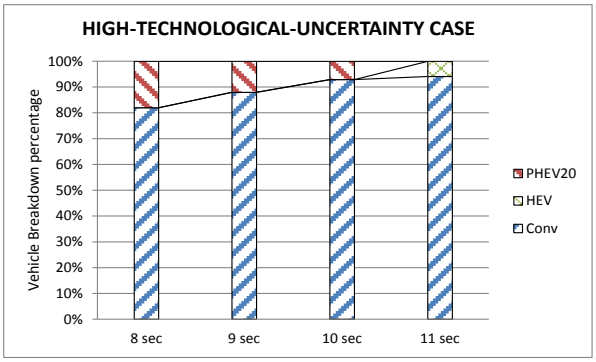

Figure 15. Vehicle breakdown for high-technological case: 2025 Scenario A

Figure 16 shows that optimal cost decreases with performance as in the previous scenarios and year. The trend is the same, but as the PHEV20 percentage is increased, optimal cost increases, as well with higher targets.

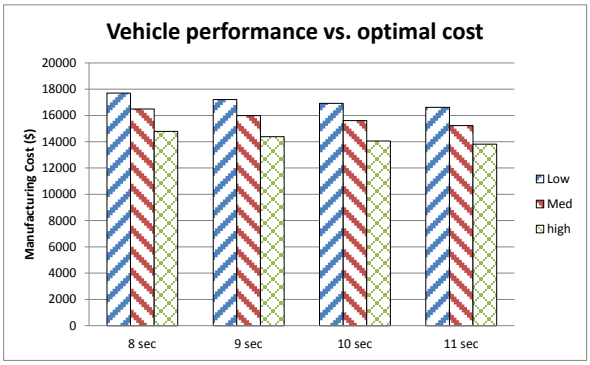

Figure 16. Impact of performance on optimal cost

Scenario B (6%)

Figure 17 shows that more than 85% of the breakdown is composed of PHEV20.

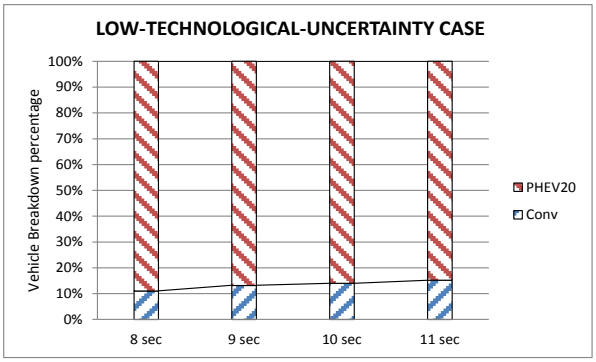

Figure 17. Vehicle breakdown for low-technological case: 2025 Scenario B

Figure 18 shows that around 70–75% of the breakdowns are PHEV20.

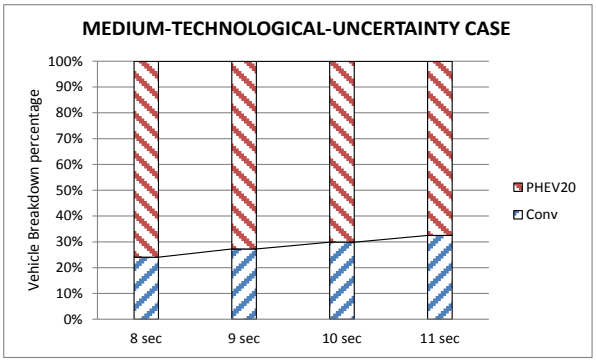

Figure 18. Vehicle breakdown for medium-technological case: 2025 Scenario B

Figure 19 shows that compared to the scenario A, the proportion of PHEV 20 more than doubles. In addition, the percentage of HEVs increases from 5% to 82% of the breakdown for the 11-s case.

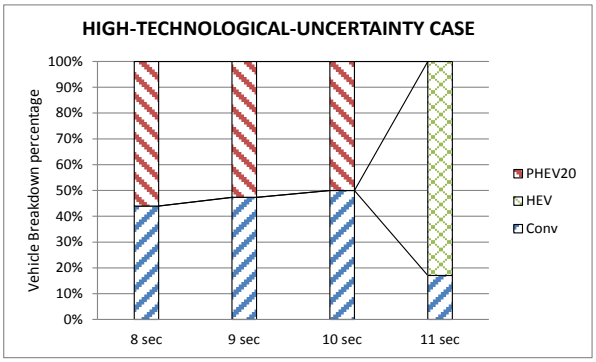

Figure 19. Vehicle breakdown for high-technological case: 2025 Scenario B

Figure 20 shows that optimal cost decreases with performance. However, in 2025, the introduction of a higher percentage of alternative vehicle technologies will lead to higher costs, regardless of the technological uncertainty case forecasted.

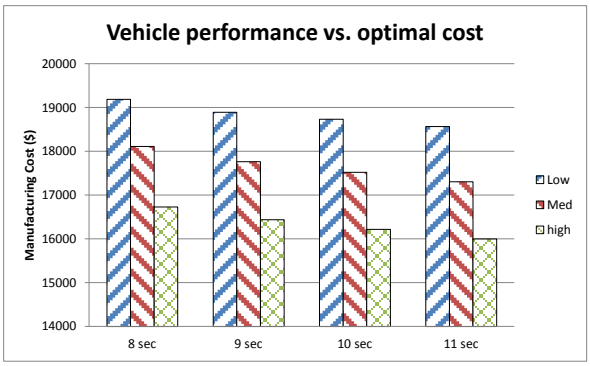

Figure 20. Impact of vehicle performance on optimal cost: 2025 Scenario B

Conclusion

A process has been developed to evaluate the most cost-effective technologies to meet CAFE requirements under different timeframe and vehicle performance scenarios. The study demonstrated that:

- Electric drive penetration could be increased by increasing vehicle performance (i.e., 0–60 mph).
- Increased vehicle performance leads to additional manufacturing cost and impacts the overall choices in powertrain.
- Significant advances related to conventional vehicle technologies (i.e., engine, transmission, lightweighting) would delay the need for electric drive, as demonstrated by the high-uncertainty scenario.
- In 2017, conventional vehicles can meet the requirements for the high-technology case for both 3% or 6% scenarios, while the low-technology case requires hybrid electric vehicles (HEVs) and also plug-in HEVs (PHEV20). The medium-technology case requires from 0% to 26% of PHEV20, depending on vehicle performance and scenario.
- By 2025, a significant number of electric drive vehicles could be necessary (up to 85%) to meet the most aggressive CAFE target.

The results from this paper depend on the assumptions selected (i.e., requirements, efficiencies, cost) and should not be generalized. In addition, this study was based on a single

vehicle class (midsize car), whereas CAFE values are based on entire fleets. Because each vehicle class is impacted differently by technologies, additional vehicle classes should be considered to refine the results.

The combination of the technology improvements leads to significant fuel consumption and cost reduction across light-duty vehicle applications. Because of the uncertainty associated with the evolution of the technologies considered, research should continue to be conducted in areas showing high-fuel-displacement potential.

V.H.3. Products

Publications/Presentations

1. Moawad, A., Rousseau, A., "Cost-Effective Way to Meet 2017–2025 CAFÉ - Update", Report to DOE, September 2011
2. Moawad, A., Rousseau, A., "Impact of Vehicle Performance on Cost Effective Way to Meet CAFE 2017–2025", VPPC Conference, September 2011
3. Moawad, A., Rousseau, A., "Cost-Effective Way to Meet 2017–2025 CAFE", Report to DOE, February 2011
4. Moawad, A., Rousseau, A., "Cost-Effective Way to Meet 2017–2025 CAFE", Presentation to DOE, February 2011

V.I. Medium Duty HEV Validation

Ram Vijayagopal (Project Leader), Aymeric Rousseau
Argonne National Laboratory
9700 South Cass Avenue
Argonne, IL 60439-4815
(630) 252-7261; ram@anl.gov

DOE Technology Managers: David Anderson, Lee Slezak

V.I.1. Abstract

Objectives

- Understand and simulate a heavy-duty vehicle prototype developed by Navistar.

Approach

- Utilize the basic vehicle information, as well as the data logged from test drives, provided by Navistar.
- Analyze the test data to obtain information about:
  - Component sizes,
  - Outline of control logic, and
  - Test drive cycles.

Accomplishments

- Developed the HEV model based on published information and the test data provided by Navistar.
- Modified the default Autonomie HEV control logic based on the test data analysis.
- Validated the model against the available test data.

Future Directions

- Work with original equipment manufacturers and other national laboratories to define the road tests and data to be measured to determine the vehicle component characteristics and control logic.
- Develop more automated processes to identify control parameters from the test data.

V.I.2. Technical Approach

Introduction

This study is an effort to understand and simulate a heavy-duty vehicle prototype developed by Navistar. Navistar has provided the basic information about the truck, but the nature of the project prevents the sharing of all the information required to accurately simulate the vehicle. Therefore, in this study, the team has made reasonable assumptions whenever it was considered necessary.

Based on the test data provided by Navistar, an effort is made to size the components as closely as possible to the prototype vehicle. Since this plant model may not be accurate, the focus of this study centers on the supervisory control logic used by Navistar, rather than on the numerical accuracy of the model.

Navistar HEV

From the vehicle data shared by Navistar, it is inferred that a pre-transmission architecture is adopted for the Class 6 pickup and delivery truck. It is also known that the architecture is the same, or close to, the system put forward by Eaton, shown in Figure 1.

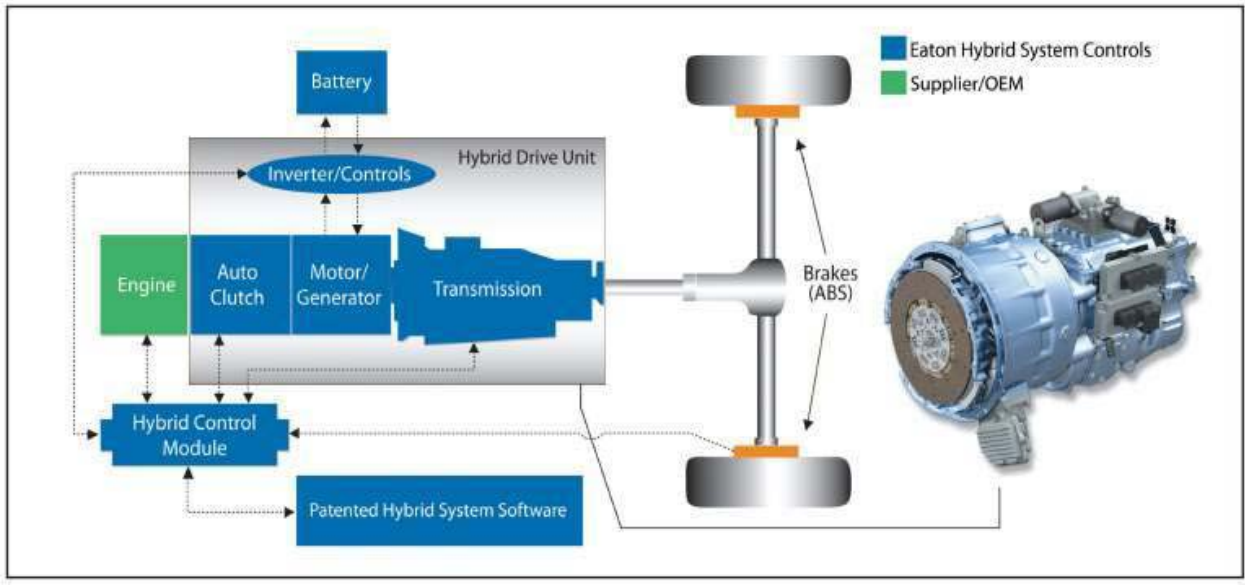

Figure 1. Eaton hybrid system

Vehicle Test Data Analysis

The signals that are logged from the test vehicle are presented in Table 1. For our initial analysis, we used the highlighted signals. Those signals provide the approximate sizes of the components or an overview of the control logic.

Vehicle speed data were logged in either kmph or mph in each test. The speed data logged by GPS closely followed the wheel-based vehicle speed estimation. These data were converted to m/s and used to form the drive cycles.

Engine torque was measured either as Nm or as a percentage of the maximum possible torque, but both the signals never were measured simultaneously. This prevents the direct back calculation of the maximum engine torques at each speed. However, since a few test cases give us the actual torque values, we sized the engine to be capable of providing those torque peak values.

Engine speed was recorded, but the motor speed was not available. In a pre-transmission hybrid, motor speed is either the same as the engine speed or is always directly proportional. Figure 1 shows the Eaton hybrid system, which Navistar is said to be using. Based on that information, we assumed that the motor speed is same as the engine speed when the clutch is engaged.

The selected **gear** shows the gear number. We assumed the vehicle to have an automated manual transmission or an automatic transmission, as the test data showed whether the vehicle was in neutral or gear.

Table 1. List of available signals

vehicle data	driver data
vehicle_speed (kph)	accelerator_position (%)
engine_torque (%)	brake_switch (bit)
engine_coolant_temp. (C)	cruise_control_active (bit)
engine_oil_temp (C)	selected_gear (gear value)
engine_speed (rpm)	shift_in_process (bit)
total_idle_hours (hr)	
hybrid data	**environment data**
motor_torque (N*m)	time_stamp
motor_torque_sign	time_vector (ms)
state_of_charge (%)	ambient_air_temp. (C)
battery_potential (Volts)	pressure (kPa)
	gps locations data

Motor torque was measured in Nm and was used as it is. The lack of motor speed data was acutely apparent in analyzing the control logic — especially as to how and when the clutch is used.

State of charge (SOC) of the battery was recorded in two signals. One of the measured signals had a least count of 10%, and another signal had a least count of 5%. The factor that led to the measurement of these two separate signals is unclear, but if used together appropriately, they can give an SOC estimate within a +/-2.5% error.

Autonomie Model

The Autonomie representation of a pre-transmission vehicle similar to the Navistar prototype is shown in Figure 2. The individual components are separated into different systems. The sizing and initialization information required for each system is calculated from the test data, and in cases where the available data are insufficient, reasonable assumptions are made.

Component Sizing

Battery: Some of the tests conducted by Navistar showed instances where the vehicle was stationary for long periods. The battery becomes discharged within about 15 minutes under those circumstances, since there are electrical loads present in the vehicle that are met from the battery. The nature of this load and the reason for depleting the battery to very low levels in a relatively short time are not known.

When the battery SOC reaches very low levels, the engine is turned on to charge the battery. The SOC variation observed during this test, combined with the engine speed and motor torque, provide enough information to approximate the battery size and the auxiliary electric loads.

Figure 3 shows that the engine runs at a steady 1100 during this charging process, and the motor torque is at -120 Nm. If the motor is spinning at the same speed as the engine, then we have about 12 kW of charging power (assuming about 85% overall charging efficiency).

With about 270 seconds of charging, the SOC goes up to 70%. This indicates that the energy put into the battery during this time accounts for 70% of the battery capacity. Similarly, the battery becomes depleted by auxiliary electric loads in about 17 minutes, as shown in Figure 3. This would suggest an approximate 3.3 kW of average electric load. The motor is used to drive some devices during this period. Intermittent torque bursts from the motor show that the auxiliary loads are not all electric.

This information is used to size the battery. However, more detailed test data are needed to understand the variations in this auxiliary load.

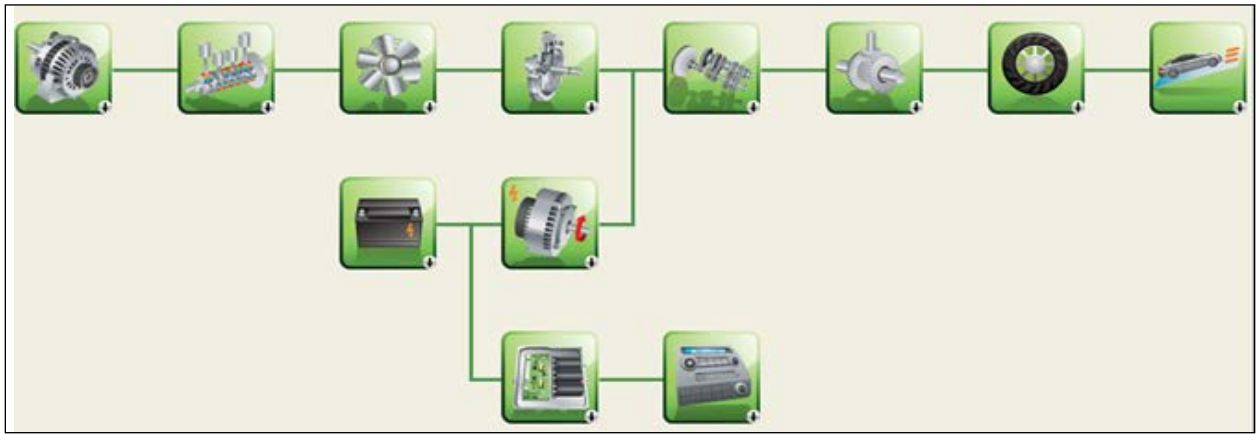

Figure 2. Autonomie powertrain architecture

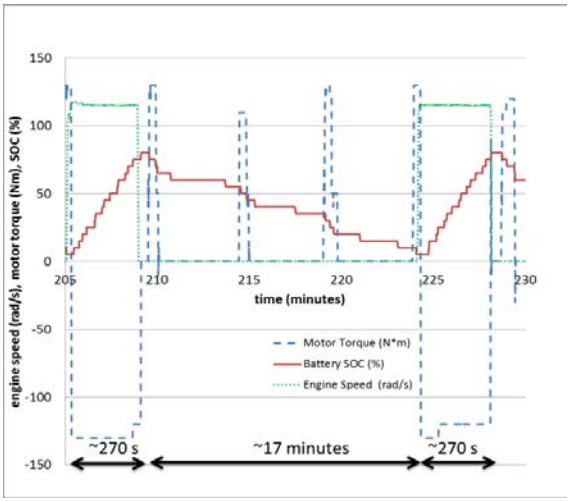

Figure 3. Engine-assisted charging of battery

Engine and Motor

It is known that the engine in this truck belongs to the "Maxxforce-7" series, but the power rating, torque calibration, and fuel consumption data of the engine are considered as proprietary information and thus was not shared by Navistar. The motor size, torque, and efficiency characteristics also were not available.

The test data were analyzed to determine the maximum power output from the motor and the engine. This would ensure that the components chosen for the simulation model are capable of driving the vehicle over the speed trace obtained in the tests. The motor is sized to ensure that it is capable of producing the torque and speeds observed during the test. Simulation data can be used to confirm the power output obtained from the selected components.

Wheel Size

The wheel size was assumed on the basis of previous studies conducted on Class 6 vehicles.

Gear Ratios

The ratio between engine speed and wheel speed provides a fair indication of the gear ratios. The presence of a clutch/torque converter can corrupt this calculation, but we can estimate the most common, steady ratios from this test data. Based on the calculations, the six gear ratios and a final drive ratio were chosen. The error brought into this estimate by the lack of actual speed input to the gears is significant, but this would suffice for analyzing the steady-state performance of the truck.

Deducing Control Logic from Test Results

It is a challenging task to deduce the exact control logic from tests, even when they are conducted under a controlled environment on a dynamometer. The use of tests that are designed to exercise the different aspects of controls is preferable. However, in this case, the Navistar test data seem to be taken from random driving tests of the vehicle. Data for 47 different driving segments were provided, out of which 39 had non-zero vehicle speeds.

The tests had a fair representation of highway driving and urban driving scenarios. The distribution of the duration of the tests is presented in Figure 4.

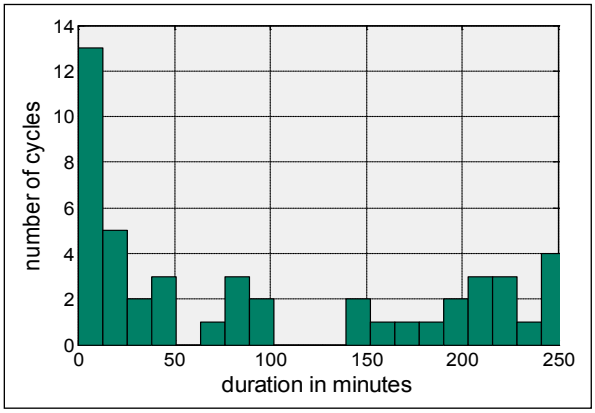

Figure 4. Distribution of test cycles based on duration

The speed trace and the initial SOC values were noted for each test cycle. The shorter duration tests typically involve low-speed, short-distance runs. The longer duration tests generally give the highway cycles. There are a few cycles where the vehicle was stationary or idling. As mentioned previously, one such cycle was used for sizing the battery.

In the case of this HEV, the major part of the control is to identify the speed and torque outputs from the engine and motor. Charging and discharging of the battery will determine the torque provided by the motor. This will, in turn, determine the torque demanded from the engine. The operating speed of the engine and the motor

is determined by the vehicle speed, the wheel size, the final drive ratio, and the gear ratio. Therefore, we can safely establish that the energy management logic and the gear shifting logic constitute the major part of this study.

Energy Management

The decision to turn off the engine seems to be determined by the driver. In most tests, the engine is on all the time during normal running. The engine is turned off only when the vehicle is stationary for a long period of time.

The test data include a few very long drive cycles, which test the vehicle when it is stopped for many hours. The engine also is turned off, and in those cases, some electrical loads are met by the battery. When the battery becomes depleted to very low levels (about 5% to 10% SOC), the engine is used intermittently (once in 15 minutes or so) for about 5 minutes to charge the battery to its upper limit of 80% SOC. This electrical load is not recorded separately in any of these tests.

The plot shown in Figure 5 indicates the variation of vehicle speed, motor torque, and SOC for a test cycle. Interestingly, the control logic chooses not to charge by using engine power, even when the SOC is low (around

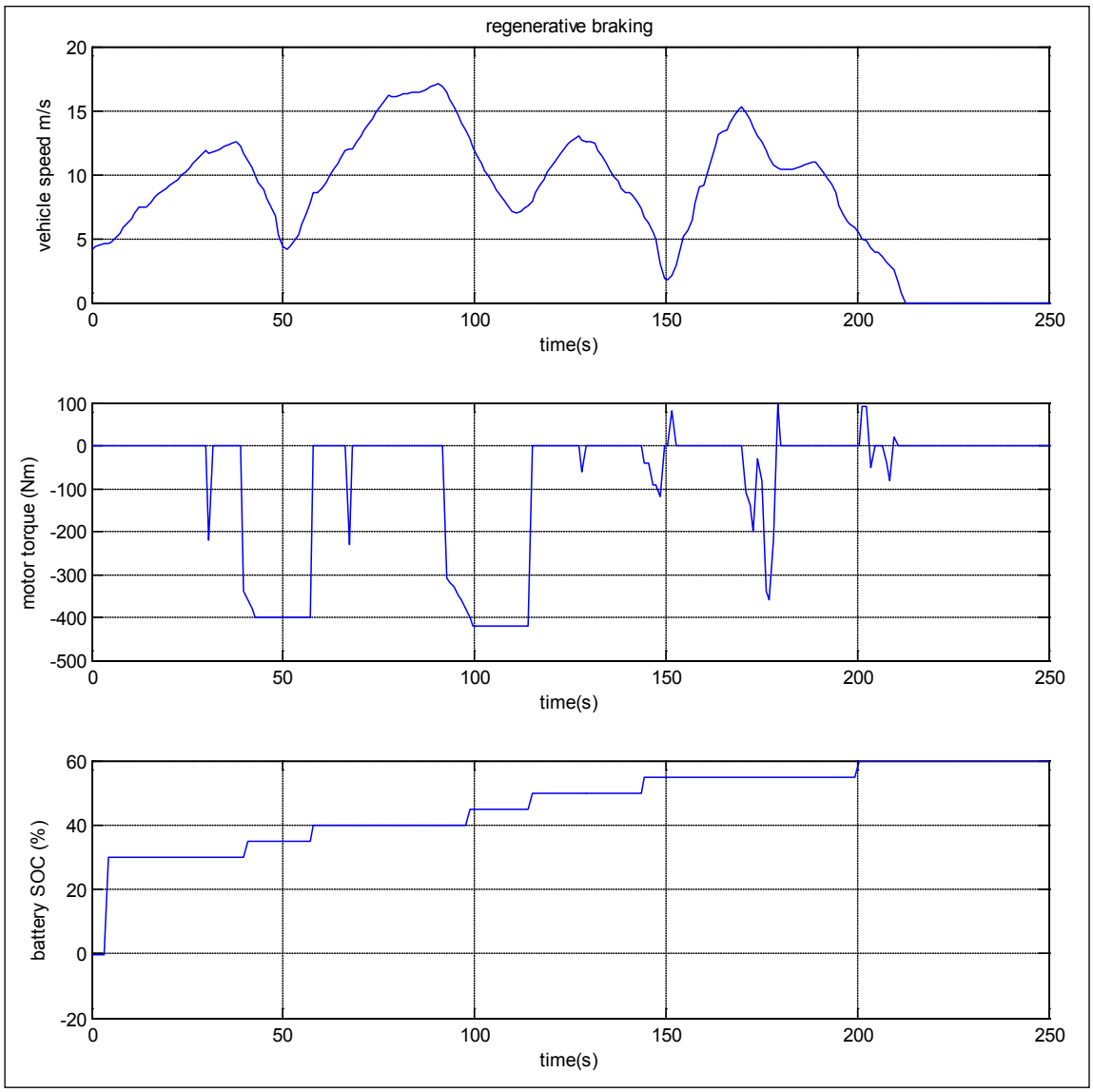

Figure 5. Analysis of when the battery is charged and discharged

30%). Regenerative braking seems to be the only way of charging the battery while the vehicle is running.

Discharging of the battery to assist the engine or to drive the vehicle is observed only after the battery reaches 55% to 60% SOC, after the 150th second in this plot. The battery charge-discharge patterns were checked for many such test cycles.

Gear Shifting Logic

In an automatic transmission, the shifting of gears follows a very specific logic. It is difficult to determine which parameters affect this shifting. However, once that is determined, the shifting can be exactly replicated over every drive cycle. In a manual transmission or an automated manual transmission, the driver can initiate a shift, and that may not be exactly reproducible.

In the case of this test data analysis, the shift map generation is particularly challenging, since we do not factor in the road conditions, the grade, and the information available to the driver or the vehicle controller when the shift was initiated. Based on the test data, MATLAB scripts are written to automatically generate up-shift and down-shift maps.

All the gear shifting points were noted from the test data, and a lookup table was automatically written for the up-shift and down-shift maps. The script looks at all available test cycles and notes down the accelerator position, speed, and gear number for every gear shift event. This information is later converted to a lookup table that can be used in Autonomie. Detailed information about the test data and the logging delays is necessary to ensure complete automation of this map generation. In this case, since such information was not available, the shift maps were inspected for inconsistencies and modified wherever it was deemed necessary. The shift map thus derived is shown in Figure 6.

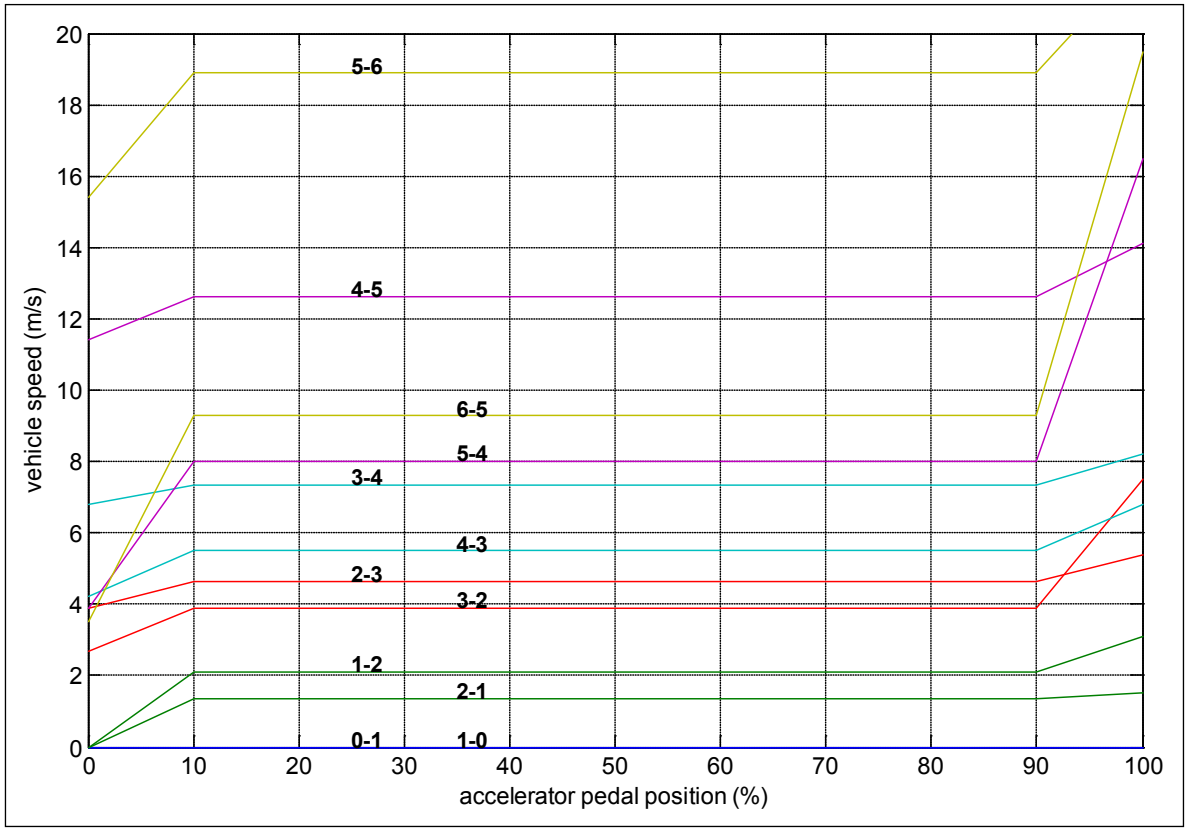

Figure 6. Shift map produced automatically by test data analysis

Engine Operation

The engine is allowed to idle when it is not used for propulsion. The emission implications of frequent stops and starts may have led to this control logic. The default Autonomie HEV control logic does not follow this procedure, so it was modified to ensure that the engine remained idling when it was not being used for propulsion.

Testing with Drive Cycles

The shifting logic and the regenerative braking logic are verifiable in cycles that represent urban driving. One such test cycle is shown in Figure 7. This cycle provides considerable opportunity for charging the battery. The role of the driver in such a test data comparison is significant.

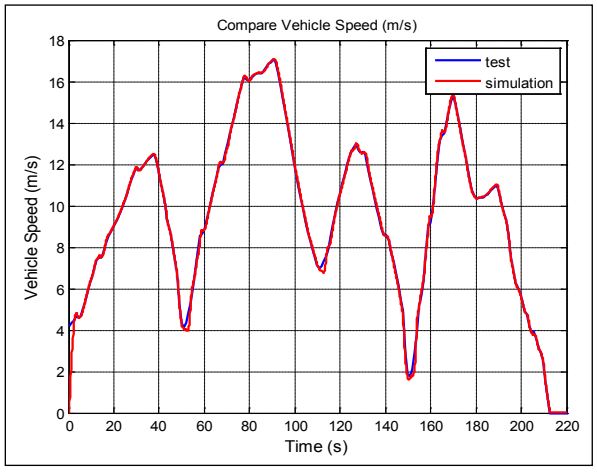

Figure 7. Vehicle speed trace matched during simulation

The proof for the energy management strategy verification would come from the comparison of the SOC profile, as depicted in Figure 8. This comparison would provide information about the use of the engine and motor and the different stages of the cycle. It also would give a reasonable indication of the magnitude of energy that is charged or discharged from the battery.

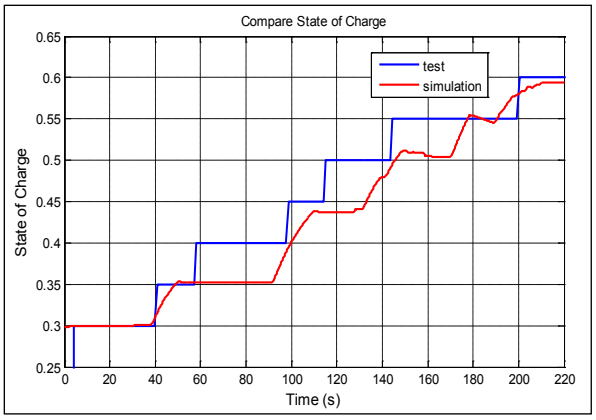

Figure 8. SOC comparison to verify energy management

The SOC measurement has a least count of 5%, since the value of the initial SOC can vary by +/- 0.025, and at least that much error should be expected from the simulation data as well. Here we find that the SOC estimation from the simulation is within the margin of error.

In addition, the torque output of the motor was studied, and that also showed reasonably good matching between the test and the simulation (Figure 9). The presence of electrical and mechanical loads was not accounted for in this simulation because of the lack of measured test data. When we add the auxiliary loads, these characteristics could change, and the vehicle controller must be updated to ensure that those loads are also met by either the engine or motor.

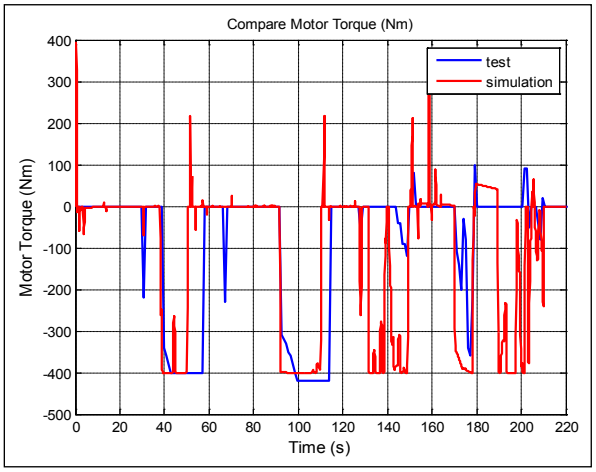

Figure 9. Torque comparison

This simulation result indicates that the vehicle controller chooses to do maximum regenerative

braking at low SOCs. Further, there are not many cases of the motor assisting the engine when the battery SOC is below 50%.

The default Autonomie controller parameters were tuned so they would imitate the test vehicle. A closer matching would require specific testing data meant for understanding the detailed control logic.

The next major feature that was generated automatically from the test data was the shift map for the vehicle. An automatic transmission was adopted for the vehicle, since the test data include notations such as "Drive" and "Neutral" for the gear mode. The shifting pattern did not indicate the presence of a neutral gear between the gear shifts, thereby suggesting an automatic transmission or at least an automated manual transmission. The test data show that the vehicle spends a considerable amount of time in neutral when it is idling. This suggests a possible automated manual transmission. Hence, both cases were modeled. The automatic transmission gear shifting is detailed in Figure 10. The pattern in a manual or automated manual transmission is shown in Figure 11.

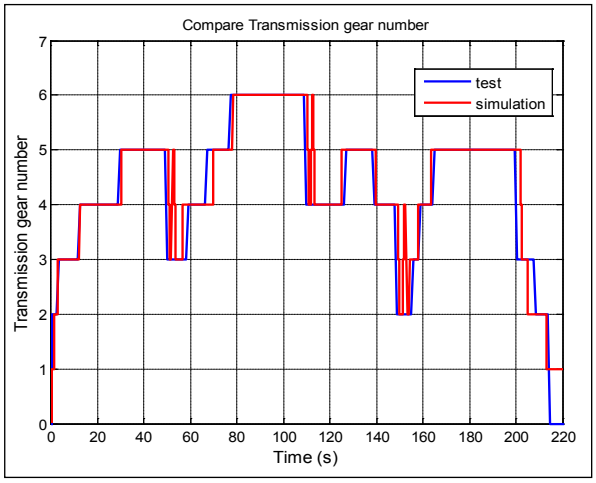

Figure 10. Shift pattern for an automatic transmission

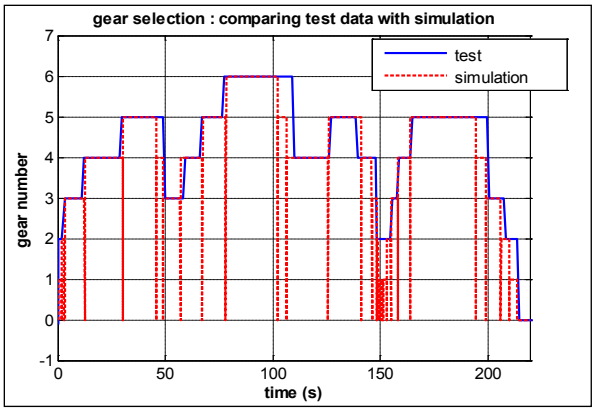

Figure 11. Shift pattern for a manual or automated manual transmission

A similar analysis was conducted with test cycles that presented a highway driving scenario. That comparison is illustrated in Figure 12.

Conclusion

A pre-transmission hybrid model has been built, based on the information that could be gained from road test data generated in a Navistar prototype vehicle. The components are sized on the basis of the operation region attained in these tests. Some of the major control logic features also are incorporated into the model. This is different from the default control logic in Autonomie. However, we expect that the differences are due to drivability issues and other considerations in the use of the vehicle.

A procedure has been developed to extract a shifting map from such test data. The accuracy of such a map also has been verified in this study.

Situations where the vehicle is parked for a long time are not simulated, and the management of hotel loads has been observed in some of the cycles. However, to model this we need more specific test data that measure the different electric and mechanical loads. This could be attempted as a future study, if such data are available

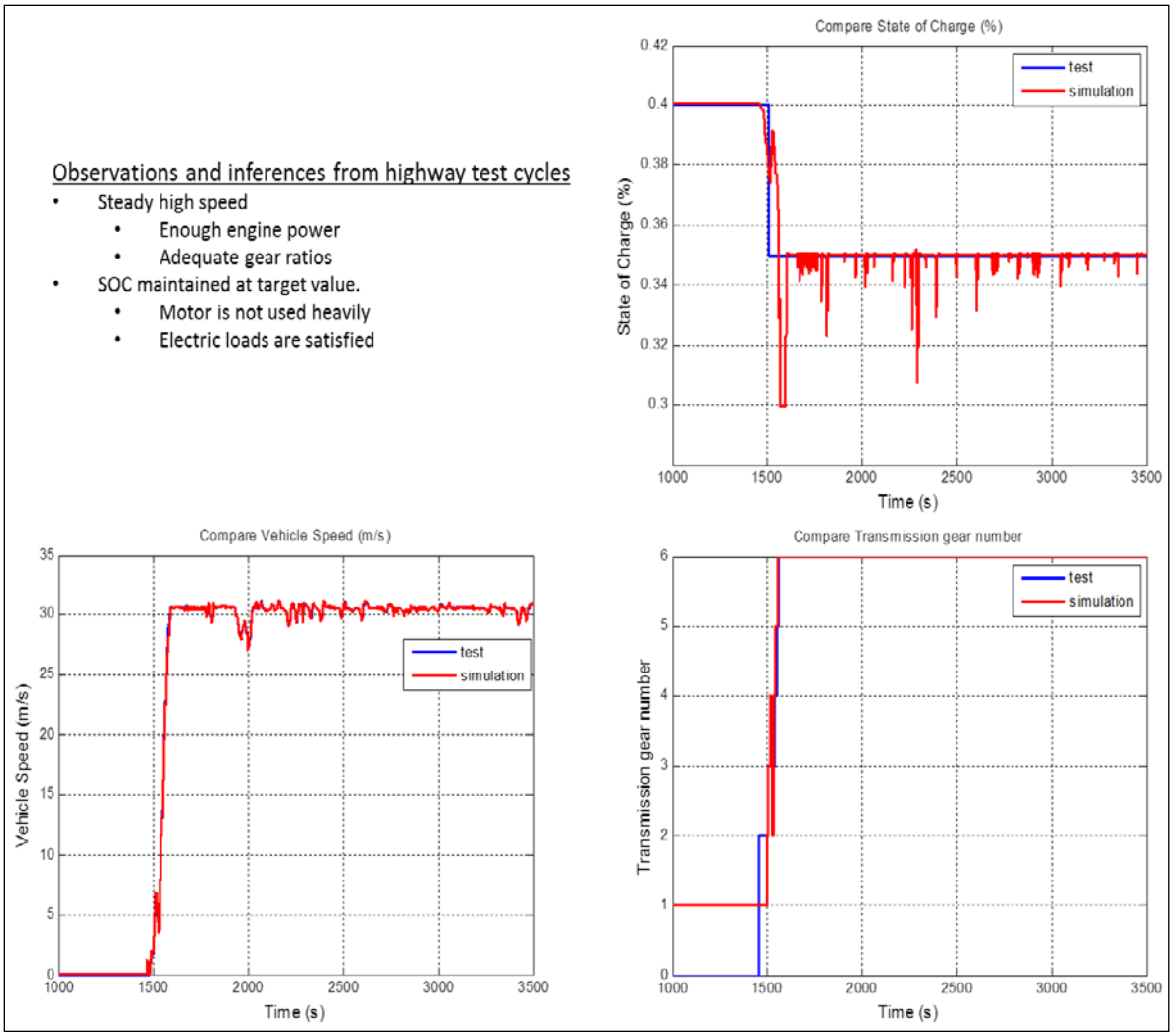

Figure 12. Comparison of vehicle speed, SOC, and gears for a highway cycle

V.J. Heavy Duty Vehicle Sizing Algorithm

Aymeric Rousseau (Project Leader), Clement Fauvel
Argonne National Laboratory
9700 South Cass Avenue
Argonne, IL 60439-4815
(630) 252-7261; arousseau@anl.gov

DOE Technology Managers: David Anderson, Lee Slezak

V.J.1. Abstract

Objectives

- Develop generic algorithms allowing to quickly size medium and heavy duty vehicles for specific applications and requirements

Approach

- Evaluate specific requirements of Medium and Heavy duty vehicles
- Adapt algorithms initially developed for light duty vehicle applications

Accomplishments

- Generic sizing algorithms have been developed for several powertrain configurations
- Each algorithm has been tested and validated

Future Directions

- Validate current algorithms for additional applications
- Adapt other powertrain configuration algorithms for medium and heavy duty

V.J.2. Technical Discussion

Introduction

Numerous hybrid electric powertrain configurations have been introduced in the market for medium and heavy duty vehicles. However, it remains unclear how each component should be sized to maximize fuel displacement while minimizing cost. The objective of the study is to develop algorithms that could be used to size different powertrain configurations for medium and heavy duty vehicles to assess their fuel consumption displacement.

The transit bus application will be used as the main example to develop and test the algorithms.

Transit Bus Requirements

The American Public Transportation Association (APTA) aims to organize and activate communication around all public transportation (bus, light rail, transit bus) in America. Regularly, they publish a Standard Bus Procurement Guideline suggesting multiple requirements for Transit Bus vehicles as components mileage life or performance limit. In the October, 2010 release, APTA recommends two performances test at Gross Vehicle Weight Rating (GVWR), acceleration and gradeability with few different levels.

The Texas Department of Public Safety publishes also each year a Specification Paper for School Bus. Comparing to APTA performance tests, only their gradeability requirements are changing by the speed test. Beside these modifications, both entities suggest a very similar guideline.

As APTA is a federal association, their results were taken as reference values to test and sized our vehicles. We would see later that these requirements are largely overpass by the majority of School and Urban Bus.

Table 1. Performance Requirements: (left) APTA, (right) Texas

Acceleration (s)	
0-10 mph	5
0-20 mph	10
0-30 mph	18
0-40 mph	30
0-50 mph	60
Max Speed	>65mph
Gradeability	
15 mph	10%
40 mph	2.50%

Acceleration (s)	
0-10 mph	5
0-20 mph	10
0-30 mph	18
0-40 mph	30
0-50 mph	60
Max Speed	>65mph
Gradeability	
>0 mph	20%
25 mph	5%
50 mph	1.50%

In order to make a relevant sizing, algorithms need representative cycles. Three chassis dynamometers from United States have been selected for this study: UDDS, Manhattan, and Orange County Transit Authority (OCTA)

Vehicle Sizing

As the light-duty sizing algorithms were not adapted to design medium and heavy duty applications, several new codes have been developed. As the main philosophy is similar, new features have been added to allow the user a greater flexibility. Several powertrains were considered as described below.

Conventional Powertrain

Since the conventional vehicle is mainly defined by is engine, the sizing rule will be focused on calculating the mechanical power to match the requirements. The algorithm has been defined to meet the different performance targets provided by APTA.

First, the grade power on each level is computed. Contrary to light duty code, this sizing allows the user to define several grade levels. Then, the sizing enters an acceleration loop. At the end, the time to reach the target (i.e. 50 mph in 60 second) is compared with the simulated data. At that time, the engine power might be updated. Because any component variation influences the overall weight, the same step has to be run again to check if the requirements are valid. The tests and component tuning will be done on each level and the engine will be sized with the maximum value. Finally, the grade requirements are verified with the updated mass. This is the main condition to exit the routine.

Table 2 shows the validation of the conventional vehicle sizing algorithm compared to the Blue Bird Vision.

Table 2. Blue Bird Vision Specifications

Blue Bird Vision			
	Reference	Sized	error (%)
General information			
GVWR (lbs)	29000	class 6	
SLW (lbs)	23250	23296	0.20
Seat	27		
Engine			
Model	Cummins ISB		
Fuel Type	Diesel		
Displacement	6.7 l		
Power (W)	178968	179355	0.22

Series Powertrain

Since the series powertrain is more complicated, so is its sizing rule. Figure 1 shows the entire routine which can be separated in four parts.

The first one, called here "*UDDS Constraint*", is the motor power computing part. The engine power is defined to match grade requirement while the motor and the battery powers are oversized to allow the vehicle to run the cycle without issues. The objective is then to calculate the minimum motor power value to let the vehicle run the referent cycle without missing the trace. At the end of the simulation, power motor's signal is saved. Once the first step is completed, the vehicle viability is checked by an *Acceleration Test*. If acceleration test fails, second test is performed. Following the results, the code enters an *Acceleration Loop* and updates the component power and weight. The global philosophy of this loop is close to the one used for a conventional vehicle.

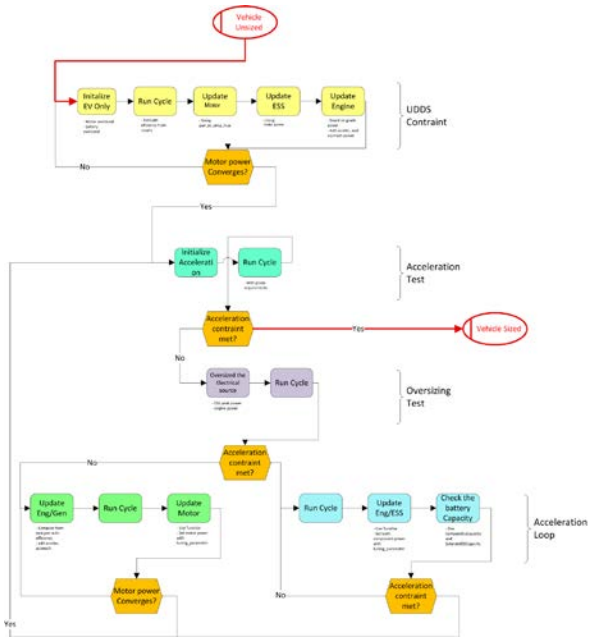

Figure 1. Series Algorithm

Since it is not possible to capture all the regenerative braking during a cycle, a regenerative power rate is available to set the percentage of the power catch by the motor during the cycle. The sizing rule ends when the vehicle meets both acceleration and cycle requirements.

Two Mode Powertrain (No Fixed Gear)

Several modifications were performed compared to the light duty vehicle sizing algorithm. While the light duty algorithm was developed for PHEV vehicles, heavy duty transit buses do not need to be able to accelerate in Electric Mode Only.

The algorithm was also modified to tolerate the cycle as an input. In this way, the motor power computed is the one needed to do the reference cycle. Because same issues as for series routine were encountered, a *motor power rate* was added as well. This parameter's aim is to filter peak power during the cycle and avoid an oversizing of the motor.

Also, in prevision of a future study, an *engine power rate* was added in the script. So far, the motor 1 power was computed to do the cycle with the engine at its maximal peak power. Here the rate is defined as a percentage of the maximal peak power used to follow the cycle. The closer the value is from 1, the more engine power is consumed during the cycle.

Motor Power Rate Impact on Series Sizing

Based on the *series sizing rule* and the OrionVII baseline, different buses have been sized with multiple rate of motor power. Since buses are designated to specific towns, it is necessary to adopt sizing rules which are able to compute motor, engine and battery power for dedicated cycles.

Figure 2 displays OrionVII's motor power on a Manhattan cycle.

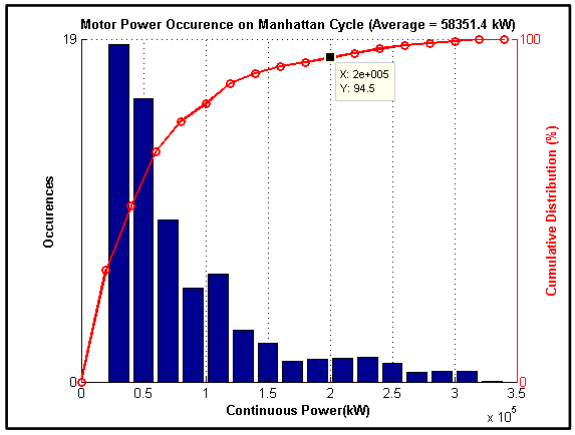

Figure 2. Motor Power

We notice that the maximum value (i.e. 340kW) occurred only a few times. In addition, only 5% of the simulation points need more than 200kW of motor power. The percentage of occurrence displaying on the vertical axes would be defined as the motor power rate and could be set by the users.

In this study, this rate has been decrease from 100% by step of 5%. Sizing has been done considering that the vehicle has to regenerate 100% braking power available and has to be able to run *"UDDS_truck"*, *"Manhattan'* and *"OCTA"* cycles with less than 1% trace missed. Based on this condition, the rate cannot be lower than 70% without impacting the regenerative rate. The six sized vehicles have been simulated on the 33 Real World Drive Cycles available for Transit Bus.

Figure 3 shows the impact on performance of decreasing the electric machine power (performance increases from 28 second to 37 second). We observe that the curb slope is higher with small rate than high rate which means accelerations test would be quickly failed if the rate still drops.

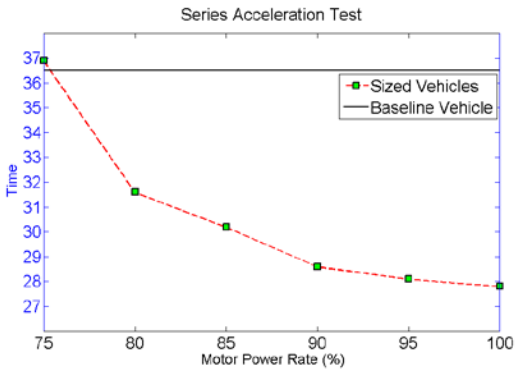

Figure 3. Acceleration Results

Comparing each vehicle in Figure 4, one observes that there is not a significant difference in the fuel consumption for each vehicle.

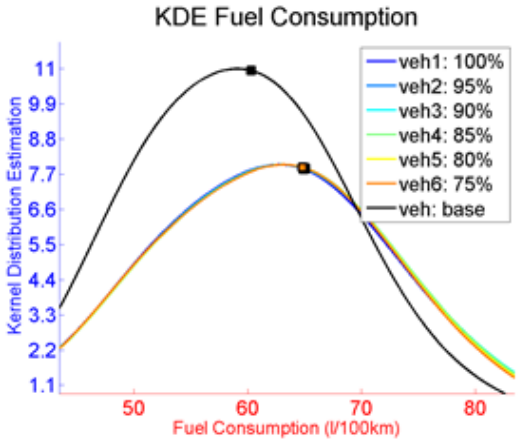

Figure 4. Fuel Consumption Results

Figure 5 shows the impact of electric machine sizing on the percentage of time the trace is missed by 2%. As one notices, the electric machine size can be significantly decreased without incurring a large increase in percentage of time the trace is missed. As a consequence, the algorithm may not need to use the maximum value of the drive cycle to calculate the electric machine peak power.

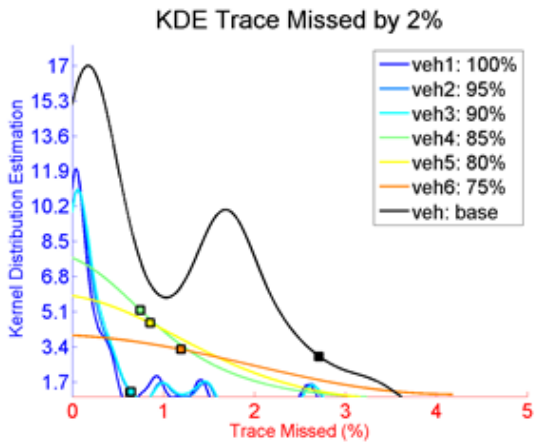

Figure 5. Time Trace Missed

Conclusion

Several vehicle sizing algorithms were developed to automatically size different powertrain configurations for medium and heavy duty applications. While the philosophies remain similar as the light duty algorithms, specific implementation have been performed, including:

- Ability to select any drive cycle
- Ability to size the electric machine and the energy storage system to capture only a percentage of the regenerative braking or to perform a portion of the cycle in EV mode
- Ability to consider multiple performance and grade requirements

V.K. Evaluation of Ethanol Blends for PHEVs Using Simulation and Engine in the Loop

Neeraj Shidore (Project Leader), Ram Vijayagopal, Aymeric Rousseau
Argonne National Laboratory
9700 South Cass Avenue
Argonne, IL 60439-4815
(630) 252-7416; nshidore@anl.gov

DOE Technology Manager: David Anderson, Lee Slezak

V.K.1. Abstract

Objectives

- Investigate the impacts of using different levels of ethanol-gasoline blends on the fuel consumption of a conventional vehicle versus a series plug-in hybrid electric vehicle (PHEV) and a power-split PHEV.

Approach

- Leverage existing engine in the loop (EIL) set-up, AUTONOMIE power-split and series PHEV models, and expertise in bio-fuel combustion at Argonne.
- Maintain stoichiometric engine operation across all ethanol fuel blends
- Use the same vehicle energy management for the different fuel types, to ensure that engine utilization remains the same for a particular vehicle configuration running on all the different fuel blends

Accomplishments

- Quantified the energy density impact of E50 and E85 on the fuel economy of a conventional vehicle
- Demonstrated that the operation of a series PHEV has a lower energy density impact than does the operation of a conventional vehicle, suggesting improved engine efficiency due to high-load operation
- Demonstrated that the operation of a default power-split PHEV does not have a lower energy density impact than does the operation of a conventional vehicle, since the engine operation is not in the efficiency gain regions when ethanol blends are used
- Demonstrated that the energy density impact of the ethanol blends used in the power-split PHEV could be reduced by optimizing the vehicle system, which would result in engine operation in the efficiency gain regions when E50 and E85 are used

Future Directions

- In simulations, use system-level optimization, accompanied by EIL validation for emissions constraints, to identify a suitable vehicle control strategy for PHEVs running on ethanol blends.

V.K.2. Technical Discussion

Introduction

Because of the lower energy density of ethanol and ethanol–gasoline blends, vehicles consume more fuel when they use them than when they use gasoline. Moreover, when higher-level ethanol blends are used, their higher latent heat of vaporization can result in cold-start issues. On the other hand, a higher octane number, which indicates resistance to knock and potentially enables more optimal combustion phasing, results in better engine efficiency, especially at higher loads. Table 1 shows relevant properties of ethanol-gasoline blends and their engine- and vehicle-level impacts.

Table 1. Ethanol and gasoline blend properties and their engine and vehicle impacts

Fuel properties of ethanol-gasoline blends (compared with gasoline)	Engine-level impact	Vehicle-level impact
Lower energy density	Higher volumetric fuel flow for the same shaft power	Higher fuel consumption
Higher latent heat of vaporization	Unreliable cold start for higher blend ratios	Higher emissions on account of failed combustion; issue might be aggravated for blended mode PHEV operation
Better knock properties	More efficient operation at high loads	Lower fuel consumption at high loads can be advantageous for hybrid operation

Figure 1 shows the "efficiency gain" map (i.e., efficiency difference map) for E85 compared with gasoline (E0). This map was generated from steady-state tests of a 2.2-L spark-ignition direct-injection (SIDI) engine, which is used for the EIL tests. The map clearly shows the islands of improved efficiency, at high loads, for E85. The map also shows the peak and minimum torque curves for the engine being studied.

This study compares the fuel consumption and emissions that result from using two ethanol blends (E50 and E85) and gasoline in conventional (nonhybrid) vehicles and series and power-split type PHEVs. Stoichiometric operation for E50 and E85 is ensured by increasing the fuel injection time for the ethanol blends. The emissions control unit (ECU) of the 2.2-L engine is fully accessible for calibration. Knock sensors on the engine also enable the ECU to retard spark timing when knock is detected. For a given configuration, vehicle operation is exactly the same for the different fuel blends, thus making this study a fuel comparison exercise. Fuel consumption for the series and the power-split PHEV is calculated over consecutive urban dynamometer driving schedule (UDDS) cycles. The vehicle models are developed in AUTONOMIE to represent conventional vehicles and PHEVs in the small sport utility vehicle (SUV) class, with an approximate equivalent electric range of 20 mi.

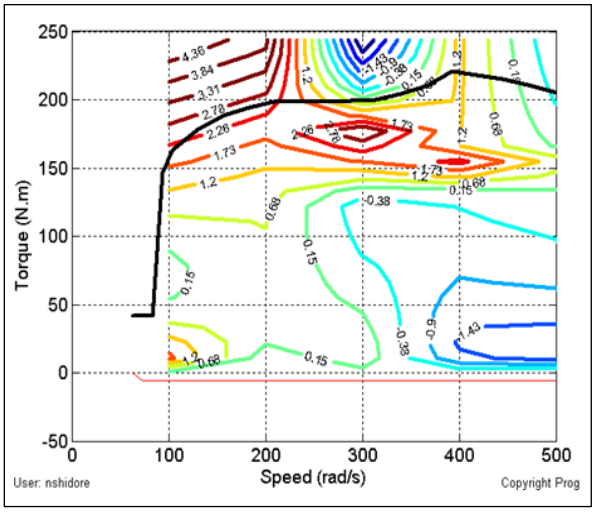

Figure 1. Efficiency gain map of E85 with respect to gasoline

Impact of Ethanol Gasoline Blends on the Fuel Consumption of a Conventional Vehicle

Table 2 shows the percentage increase in fuel consumption that results from using E50 and E85, with respect to gasoline, in a conventional vehicle under hot-start conditions. The gasoline consumption for the hot start is 10.1 L per 100 km over one UDDS cycle.

Table 2. Increase in conventional vehicle fuel consumption when E50 and E85 are used instead of gasoline

Fuel	% increase in fuel consumption with regard to gasoline in conventional vehicle, hot start
E50	18.4
E85	27

It can be seen that the increase in fuel consumption is similar to the energy density difference between gasoline and the two ethanol blends. Thus, the positive impact of increased engine efficiency at high loads is not observed for the conventional vehicle. This is because in the conventional vehicle, the engine does not operate in the more efficient high-load regions when the ethanol blends are used. Cold-start tests for the conventional vehicle also reveal that the engine

cold-start impact is the same (around 5%) for all three fuels (gasoline and the ethanol blends).

Impact of Ethanol Gasoline Blends on the Fuel Consumption of a Series PHEV

Figure 2 describes the series PHEV operation. The PHEV operates as an electric vehicle in the charge-depleting (CD) mode. The engine turns on when the battery's state of charge (SOC) approaches the charge-sustaining (CS) SOC, which is 30%. The engine goes through a low-load, constant-speed warm-up phase, to reduce cold-start emissions, before CS operation.

As stated earlier, the fuel consumption results for the series PHEV are calculated over consecutive UDDS cycles. Table 3 shows the increase in fuel consumption for E50 and E85 relative to gasoline, for the series PHEV in comparison to the conventional vehicle hot start.

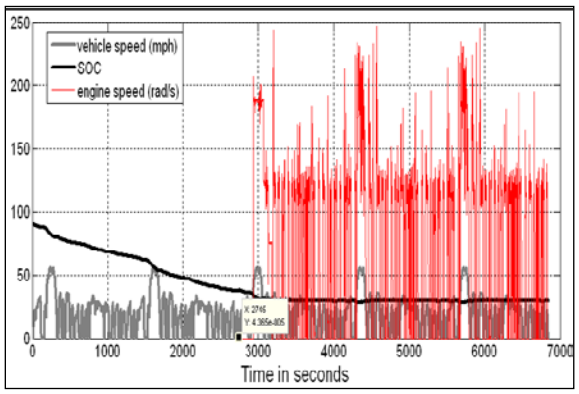

Figure 2. Series PHEV operation

Table 3. Comparison of increases in fuel consumption due to use of ethanol blends for conventional vehicle and series PHEV cases

Fuel	% increase in fuel consumption with regard to gasoline	
	Conventional vehicle, hot start	Series PHEV, CS mode
E50	18.4	15
E85	27	25

Table 3 shows that the impact of a lower energy density is lower for the series PHEV than the conventional vehicle (hot start). This is because the engine operates at a higher load for the series PHEV, so the improved efficiency of the ethanol blends (due to better knock properties) results in better fuel economy or a lower energy density impact. Figure 3 shows the engine operating points for the series PHEV on the efficiency gain map. Engine operation in the efficiency gain region can be easily seen. A close look at the map also suggests that there is potential to further reduce the energy density impact of E85 by operating the engine at higher speeds and load, as shown by the arrow in Figure 4. Performing proper system optimization (in the vehicle simulation), along with EIL tests to ensure low emissions, can be used to further reduce the energy density impact.

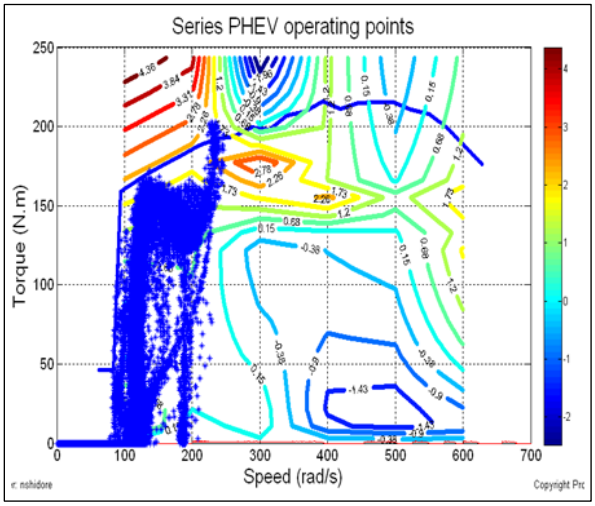

Figure 3. Series PHEV operating points on the efficiency gain map

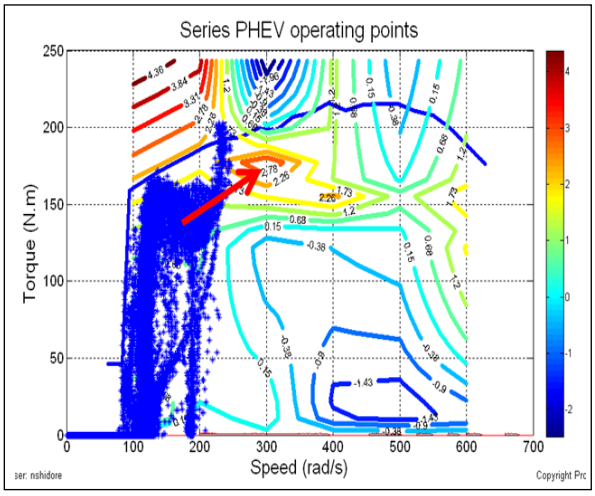

Figure 4. Further possible improvement in the fuel economy of an E85 series PHEV

Impact of Ethanol Gasoline Blends on the Fuel Consumption of a Power-Split PHEV

As stated earlier, the power-split PHEV operates in blended mode. Figure 5 describes the vehicle operation. It shows the battery SOC, engine speed in radians per second, and vehicle speed (scaled). The battery charge is allowed to deplete to 30% SOC (from an initial SOC of 90%), beyond which the battery maintains SOC in CS operation. In the blended mode, the vehicle control strategy turns the engine ON whenever the vehicle speed is faster than 20 mi per hour or the power demand at the engine is more than 32 kW. Because the first engine ON event is a cold start, the vehicle control strategy uses the engine in a controlled fashion so as to limit emissions.

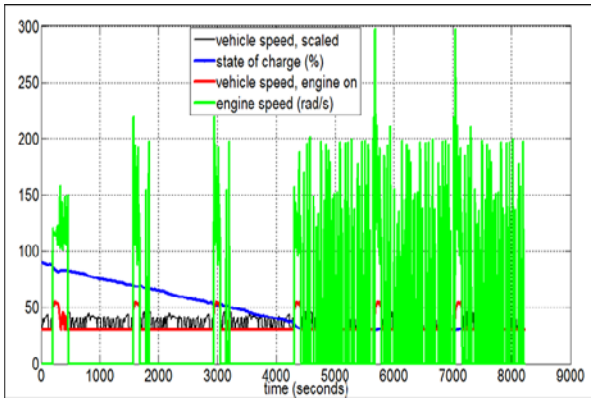

Figure 5. Blended mode PHEV operation

Table 4 shows the increase in fuel consumption for a power-split PHEV compared to a conventional vehicle (hot start) and a series PHEV, with E50 and E85 as the fuel. It shows that the power-split PHEV, unlike a series PHEV, does not have any efficiency gains.

Table 4. Comparison of the increase in fuel consumption due to the use of ethanol blends by a conventional series PHEV and a power-split PHEV

	% increase in fuel consumption with regard to gasoline		
Fuel	Conventional vehicle, hot start	Series PHEV,CS mode	Power-split PHEV, UF weighted
E50	18.4	15	18
E85	27	25	28

This is because even though the engine operates at high load for the blended-mode PHEV, it does not operate in the efficiency gain region for E50 or E85. Figure 6 shows the engine operating points and the efficiency gain map for E85. It shows that there are minimal excursions in the efficiency gain regions for power-split PHEV operation.

Note that while the power-split PHEV fuel consumption is utility-factor (UF)-weighted over consecutive UDDS cycles, the series PHEV fuel consumption is only for CS UDDS operation. Engine load is higher for CS operation than CD operation, since for CS operation, the engine is providing road load power as well as power to maintain the battery SOC. In addition, the series PHEV has a higher mass, which results in increased engine load when the engine is ON. As stated earlier, the series PHEV operates as an electric vehicle in the CD mode.

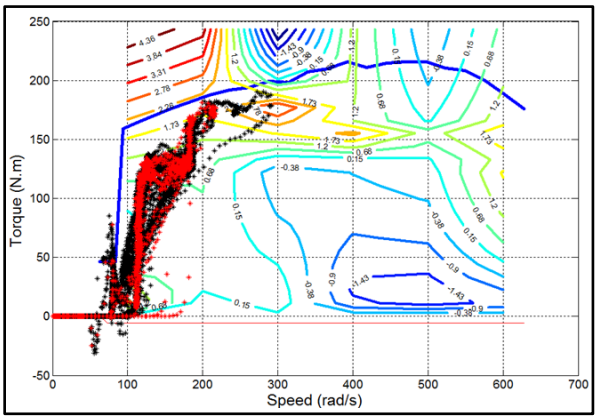

Figure 6. Power-split PHEV operating points on the efficiency gain map

To exploit the increased efficiency of the ethanol blends at high loads for the power-split PHEV, the vehicle control strategy for the this vehicle was modified, and the engine load was increased, as shown in Figure 7. Since the engine load is decoupled from the vehicle road load (hybrid operation), no vehicle-level impact is seen.

Table 5 shows a comparison of the increase in fuel consumption between conventional gasoline vehicle (hot start), series PHEV, and the two power-split PHEV scenarios.

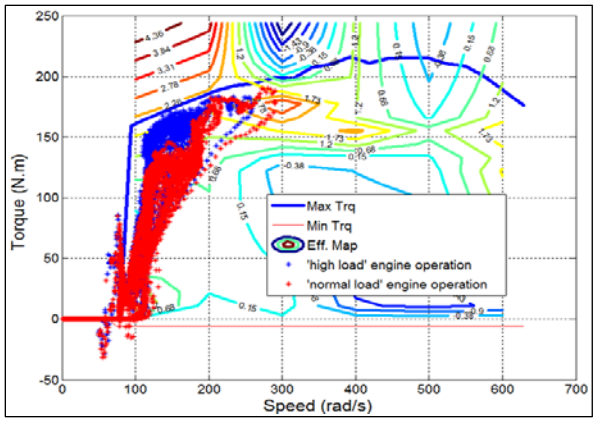

Figure 7. Increased engine load for the power-split PHEV

Table 5. Fuel consumption increase for a conventional vehicle (hot start), series PHEV, and power-split PHEV with a normal and increased engine load for E50 and E85

Fuel	% increase in fuel consumption with regard to gasoline			
	Conventional vehicle, hot start	Series PHEV, CS mode	Split PHEV, UF weighted	Split PHEV, increased engine load, UF weighted
E50	18.4	15	18	14.3
E85	27	25	28	25.8

It can be seen that with increased engine load, the energy density penalty for E50 and E85 is reduced, similar to the series PHEV case.

Conclusion

Several existing capabilities at Argonne National Laboratory (vehicle systems modeling in AUTONOMIE, expertise in flex fuel engine and emissions research, and EIL knowledge) have been leveraged to compare the fuel consumption of a power-split PHEV when gasoline (E0) and the ethanol-gasoline blends E50 and E85 are used. The fuel comparison was made possible by ensuring identical vehicle operation (engine utilization) and stoichiometric combustion for the three fuels. For conventional vehicles, the lower energy density of the ethanol-gasoline blends results in increasing fuel consumption with an increasing quantity of ethanol in the blend. For hybrid operation, there is potential to reduce the energy density impact by exploiting the higher efficiency of these engines at high loads (due to better knock properties). Results for the series PHEV demonstrate the impact from the higher efficiency of the ethanol blends. For the series PHEV, the engine turns ON only in the CS mode, and it provides road load demand while charging the battery at the same time. This generates sufficient engine load, so the efficiency improvements from using ethanol blends at high engine loads are realized.

In the CD (blended mode) operation of the power-split PHEV, the engine only provides road load demand. It appears that this mode of operation does not load the engine sufficiently to realize the better engine efficiency when the ethanol blends are used. Therefore, the vehicle control strategy was modified to increase the engine load (and reduce battery usage). The energy density penalty of the ethanol gasoline blends is reduced for the power-split PHEV with increased engine load (in comparison to that of a conventional vehicle).

V.K.3. Products

Publications/Presentations

1. Shidore, N., et al, "Evaluation of ethanol blends for PHEVs using simulation and engine in the loop," presented at the 2010 DOE Hydrogen Program and Vehicle Technologies Annual Merit Review, May 10, 2011.
2. Shidore, N., et al., "Evaluation of ethanol blends for power-split PHEV using engine in the loop," presented at U.S. Department of Energy, Sept. 28, 2011.
3. Shidore, N., et al., "Evaluation of ethanol blends for PHEVs using engine in the loop," presented at 2011 Vehicle Power and Propulsion Conference, Chicago, IL, Sept. 2011.
4. Shidore, N., et al., "Evaluation of ethanol blends for plug-in hybrid vehicles using engine in the loop," paper abstract submitted for SAE World Congress, 2012.

V.L. Integrated Vehicle Thermal Management – Combining Fluid Loops on Electric Drive Vehicles

Principal Investigator: John Rugh
National Renewable Energy Laboratory
Center for Transportation Technologies and Systems
1617 Cole Blvd. MS 1633
Golden, CO 80401
(303) 275-4413; john.rugh@nrel.gov
Fax: (303) 275-4415

DOE Program Manager: Lee Slezak and David Anderson
(202) 586-2335; Lee.Slezak@ee.doe.gov and (202) 287-5688; David.Anderson@ee.doe.gov

V.L.1. Abstract

Objective

- Work with industry partners to research the synergistic benefits of combining thermal management systems in vehicles with electric powertrains
  - Improve plug-in hybrid electric vehicles (PHEV) and electric vehicle (EV) performance (reduced weight, aerodynamic drag, and parasitic loads)
  - Reduce cost and volume
  - Improve battery life

Approach

- Develop a 1-D (lumped mass, uniform flow) thermal model using commercial software to assess the benefits of integrated vehicle thermal management and identify research opportunities
- Combine with vehicle performance/cost and battery life models
- Identify the synergistic benefits from combining cooling systems
- Assess vehicle performance and battery life impacts of combining fluid loops

Major Accomplishments

- Leveraged previous U.S. Department of Energy (DOE) development of a battery life model, vehicle cost/performance model, and lumped parameter motor thermal model
- High quality data provided by Visteon formed the basis of the detailed KULI component models
- Using KULI thermal software, built the A/C, cabin, power electronics cooling loop, and battery cooling loop models
  - Validated the models with test data when available
  - Simulated a full thermal management system in an EV
  - Results followed expected trends

Future Activities

- Work closely with industry partners to assess the most promising concepts through bench testing
- Refine and improve the 1-D thermal model as required
- Develop and assess new concepts for combining cooling loops

V.L.2. Technical Discussion

Background

Electric drive vehicles (EDVs) [e.g., hybrid electric vehicles (HEVs), PHEVs, fuel cell vehicles, and EVs] must provide cooling to protect powertrain-related subsystems, including the power electronics, electric motor, and energy storage system (ESS). In addition, climate control is required for passenger compartment comfort and safety (e.g., demisting and defrosting), and if there is an internal combustion engine, engine thermal management is necessary.

Advanced power electronics and electric machine (APEEM) components commonly use a dedicated cooling loop in today's HEVs. In the future, the cooling demands will only increase with the transition to more electrically dominant powertrains. Combining the APEEM cooling loop with other vehicle thermal management systems could reduce cost and complexity while providing the opportunity to manage the average and peak heat loads from multiple vehicle systems.

Lithium (Li)-ion batteries operate best at temperatures that are comfortable to the human body, around 10°C to 30°C. At lower temperatures, power output is reduced. At higher temperatures, battery life is reduced. In a hot thermal environment, the goals of battery thermal management are to lower the average and peak cell temperatures to within an acceptable range. In hot climates, active cooling of the battery is desirable during driving, charging, and even during standby while the vehicle is parked outdoors.

To reduce the total system cost of the vehicle, it is desirable to combine some of the multiple cooling loops while maintaining vehicle performance and reliability. In selecting approaches for combining thermal management systems, two high-level requirements were considered. The first is the need for a similar coolant temperature specification for different systems. The second requirement is the ability to manage the misalignment of peak component heat loads in an integrated system. The heat load for combined thermal management systems should be less than the sum of the peak heat loads from each of the individual systems. Different components experience peak heat loads at different times depending on their use, which leads to an overall decrease in the net heat exchanger weight and area.

Past efforts looking at combining cooling loops include work by Ap et al. [1], who proposed a low-temperature liquid water-ethylene glycol (WEG) coolant loop for the air conditioning (A/C) condenser, charge air cooler, and fuel cooler. They concluded that 60°C coolant to the liquid-to-refrigerant condenser ensured adequate A/C performance. This project intends to extend the work by Ap et al. [1] to investigate combined cooling systems for vehicles with electric drive systems.

The combined cooling loops research focuses on reducing vehicle cost and improving battery life. The pathways investigated in this analysis look at combining the cooling systems for the power electronics and electric motor with other vehicle cooling systems evaluated by Bennion and Thornton [2] and enabling technologies for vehicle cabin thermal preconditioning or standby ESS thermal management [3]. NREL's research focuses on the following combined thermal management approaches as applied to EDVs: a low-temperature WEG fluid loop that integrates the power electronics, electric motor, cabin heating ventilation and air conditioning (HVAC), and ESS where the ESS is cooled with:

- Air from the vehicle cabin
- A dedicated evaporator
- A secondary loop cooling system.

Approach

NREL developed a modeling process to assess integrated cooling loops in EDVs. The initial analysis focused on EVs. Once the EV analysis is completed, NREL will investigate PHEVs, which add engine cooling, oil cooling, variable engine control strategies, and the exhaust system.

There are three main parts to the modeling process: the vehicle cost/performance model, the thermal model, and the battery life model. The vehicle cost/performance model simulates an EV over a drive cycle. An output of the model is the time-dependent heat generated in the APEEM and ESS components. These data are used as an input to the thermal model. KULI software [4] was used to build a model of the thermal systems of an EV, including the passenger compartment, APEEM, and ESS. The thermal model calculates the temperatures of the components and the power required by the various cooling systems, including the fans, blowers, pumps, and A/C compressor. The power consumption profile is then used in the vehicle cost/performance model, and a new heat generation calculated. If the heat generation is significantly different from the initial run, it is input into the KULI thermal model again, and the cycle is repeated. An overview of the analysis flow is shown in Figure 1.

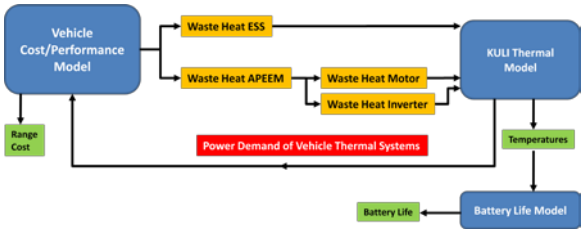

Figure 1. EV integrated vehicle thermal management analysis flow diagram.

The vehicle cost/performance model calculates the range at a fixed cost. For example, if combining thermal systems reduces cost, the vehicle model increases the battery size to maintain constant cost with an extended vehicle range. If combining cooling loops results in lower required power, then there is more electric power and energy for propulsion and the range is improved for the same cost.

The battery life model operates on a 10- to 15-year time scale while the KULI thermal model and vehicle cost/performance model operate on a 10- to 20-minute time scale. Therefore, in the battery life model, a composite 24-hour temperature profile for the battery is created based on assumptions about when during the day the vehicle is driven, parked + charging, or parked + standby. The composite battery temperature profile is then used to calculate average values for battery degradation rate constants. The resistance growth and remaining capacity of the battery, assuming 10 years of continuous exposure to this composite battery temperature profile, is calculated.

Air Conditioning Component Models

The components modeled in this effort represent a production A/C system for a model year 2008 mid-sized vehicle. Using actual dimensions, pressure drop, and heat transfer data, each component was built in the KULI model. The compressor used in the validation runs was a belt-driven, piston type, with a displacement of 213 cc. For the EV passenger compartment cooldown simulations, an electrically driven 33-cc scroll compressor was used. Heat was rejected to the air as the refrigerant phase changes from a vapor to a liquid in the condenser. The condenser was a two-pass design with 16-mm tubes and an external receiver-dryer (R/D). Liquid refrigerant exited the condenser and flowed into a 325-cc R/D where liquid and any remaining vapor were separated, allowing only liquid to exit. The R/D also removed any moisture. From the R/D, the liquid refrigerant continued to the Thermal eXpansion Valve (TXV), where it expanded and cooled significantly. Finally, refrigerant boiled as it absorbed heat in the evaporator, a 45-mm-deep plate-fin core with four end-tanks.

A/C System KULI Model

The KULI model of the A/C system was composed of a compressor, condenser, receiver/dryer, TXV, and evaporator. To ensure that each of the A/C components was modeled properly, a KULI model was written for each component, where the component of interest was the only element in an open cooling circuit. The model was given inputs from the component calorimeter data for various operating points with the intent of obtaining the corresponding outputs for each operating point. Once a satisfactory comparison was made between the calorimeter data and the model's results, the component was inserted into the A/C system model.

Passenger Compartment KULI Model

The advanced passenger compartment model that comes with KULI was used. The cabin dimensions, interior volume, and material properties were used to model a small U.S. sedan that the National Renewable Energy Laboratory (NREL) tested in Golden, Colorado. To tune the three critical KULI cabin heat transfer resistances, a simulation was run using the environmental conditions that occurred during the NREL thermal soak and cool-down test. The global horizontal solar irradiance (average 870 W/m^2) and ambient temperature (average 22.3°C) profiles were used for the simulated 2-hour soak and the 21-minute drive. The vent temperature was set to the measured profile, and the flow rate was determined by supplier data. The exterior velocity profile was set to approximate real vehicle speeds, and the HVAC blower setting was reduced from high to medium 13 minutes after the start of cooldown. The three KULI cabin heat transfer resistances were adjusted so the model temperatures approximated the test data. Figure 2 shows that the average cabin air temperature during the soak and cooldown matched the test data fairly well.

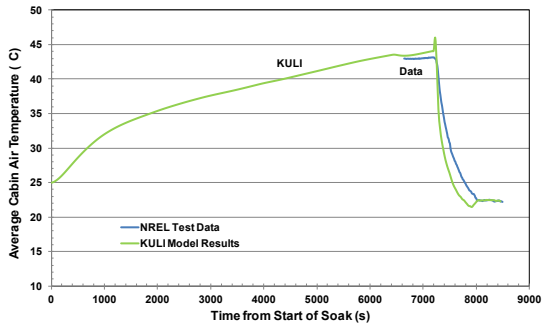

Figure 2. Comparison of passenger compartment average air temperature for the KULI model and test data.

The cabin model was then combined with the A/C system model described in the previous section. A proportional-integral-derivative (PID) controller was added to prevent evaporator icing early in the cooldown as well as passenger compartment overcooling later in the cooldown.

Power Electronics and Electric Machine KULI Model

As seen in Figure 1, the vehicle performance model outputs an overall heat load for the APEEM system. To properly model the cooling of the APEEM components, the heat load must be divided between the individual components that make up the APEEM system. For an EV, it was assumed that the APEEM system consisted of an inverter to convert the direct-current power that is supplied by the battery to three-phase alternating-current power to run an electric motor. A combined heat load for the inverter and motor was provided from the vehicle performance model, and the individual inverter and motor heat loads were estimated assuming that the heat loss within the inverter was always half of the heat loss in the motor. A more accurate heat loss model of the individual inverter and motor heat could be incorporated into the model. The heat loads for the inverter and motor were used in the KULI model to determine the temperatures of the cooling system, inverter, and motor.

The temperature constraints placed upon the model included a maximum allowable coolant temperature of 70°C [5,6] into the power electronics and the maximum motor end winding temperature. While class H insulation for motor windings is rated for 180°C [7], a lower limit of 130°C [8] for the motor windings was imposed on the model to be consistent with other published results.

The motor thermal characteristics were approximated by a first-order, lumped parameter, thermal spreadsheet model based on data for a motor cooled with a water jacket surrounding the stator [8]. The spreadsheet model approximated the transient thermal resistance between the end winding of the motor and the cooling fluid from the steady-state thermal resistance (R_{th}) and an overall effective thermal capacitance (C_{th}). The temperature response of the lumped model was determined according to equation 1 [9] for a first-order system where Q_m is the motor heat load, θ_0 is the initial winding temperature, $\theta(t)$ is the transient temperature response and t is time.

$$\theta(t) = R_{th}Q_m + (\theta_0 - R_{th}Q_m)e^{-t/R_{th}C_{th}} \quad (1)$$

The results were compared with data for the reference motor to determine R_{th} and C_{th}. The R_{th} and C_{th} values were finally converted into an effective heat transfer coefficient, effective cooling area, motor mass, and motor specific heat to supply the KULI model with the necessary input values.

The inverter temperature was not simulated in the KULI model because of the smaller thermal mass of the inverter as compared with the motor. Instead, all the heat loss of the inverter was assumed to go into the coolant fluid. As long as the coolant temperature into the inverter remained below the maximum allowable coolant temperature, it was assumed that the inverter could operate within its temperature limits.

A model of a baseline WEG cooling system was then built into KULI. Pump and engine cooling radiator data from Visteon were used to build the individual KULI components. The radiator was scaled to the size of the Japanese version of the Mitsubishi iMiEV. The heat added to the cooling loop from the inverter and motor APEEM components was rejected to the environment (air) by the radiator.

Energy Storage System KULI Thermal and Life Models

The KULI battery thermal model considered the cells in the pack to be a single, lumped thermal mass. Cell-internal heat generation rate, a function of drive cycle and vehicle design, was determined from separate vehicle simulations. Two additional mass nodes in the battery model represent the battery jacket and case. The jacket node was thermally connected to the WEG cooling loop, while the battery case node accounted for a passive cooling path for thermal conduction through the battery case and convection to the outside environment. In the initial simulations discussed in this report, we assumed a Nissan Leaf-sized 24-kWh Li-ion battery with a mass of 246 kg.

Two models of a baseline ESS WEG cooling system were then built in KULI. Pump and engine cooling radiator data from Visteon were used to build the individual KULI component models. One system model had a refrigerant to WEG heat exchanger (chiller) to remove energy from the WEG cooling system. This model was used in high ambient temperature simulations to quickly reduce the temperature of the battery cells. The second model used a low temperature radiator to remove heat energy from the WEG. This model was used in moderate environments. Software challenges prevented a single cooling loop model with the chiller and radiator in separate branches and the flow controlled with valves.

NREL's battery life model calculated performance fade due to battery temperature exposure and duty-cycle. For light-duty passenger vehicles under moderate duty cycles, calendar degradation (rather than cycling degradation) may control whether the battery will last for the 10- to 15-year life of the vehicle. Laboratory calendar aging tests typically show Li-ion battery performance falls off with the square root of time due to corrosion reactions that occur at electrode surfaces inside the cell. The battery calendar life model describes battery relative resistance growth, R, and relative capacity fade, Q, as:

$$R = 1 + a\,t^{1/2} \quad (2)$$

$$Q = 1 - b\,t^{1/2} \quad (3)$$

Rate constants a and b were made temperature-dependent using the Arrhenius equation:

$$n = n_{ref}\exp\left[\frac{-E_n}{R_{gc}}\left(\frac{1}{T} - \frac{1}{T_{ref}}\right)\right] \quad where\ n = a\ or\ b \quad (4)$$

In equation 4, R_{gc} is the universal gas constant, and the reference temperature is T_{ref}=293.15 K. Activation energies E_a and E_b and reference rate constants a_{ref} and b_{ref} were fit to calendar-life aging data for the nickel-cobalt-aluminum/graphite Li-ion chemistry [10].

Vehicle Performance Model

The vehicle performance model, used to predict range and fuel use, captured the critical parameters needed for this analysis. It calculated

the power to overcome drag, acceleration, ascent, rolling resistance, and inertia over specified drive cycles. The model included vehicle components such as the battery, electric motor, and engine. These components were modeled at a level that matched well with detailed component models included in vehicle simulation software such as Autonomie. The components were combined in the most common architectures, including conventional vehicles and EDVs. The model accounted for auxiliary loads, regenerative breaking, and energy management strategies.

To gain confidence in the model, component sizes and vehicle characteristics were entered into the model for a variety of vehicles. As seen in Figure 3, the model predicted the fuel economy within 10%. The electrical efficiency was defined as the electrical energy consumption per mile (Figure 4). While Nissan Leaf data were not available for constant speeds, the vehicle performance model prediction matched the U.S. Environmental Protection Agency's (EPA's) city/highway rating of 0.34 kWh/mi.

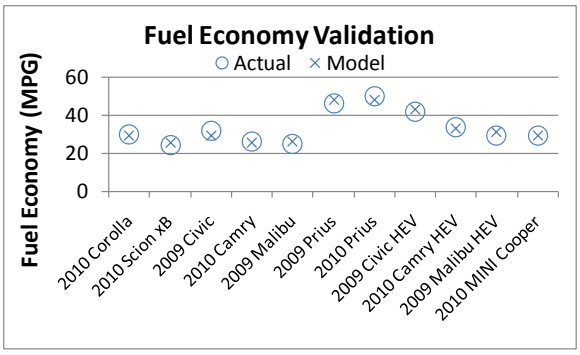

Figure 3. Vehicle validation data – fuel economy.

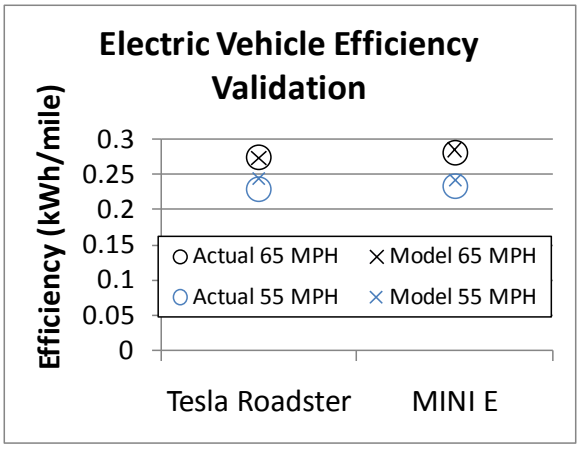

Figure 4. Vehicle validation data – electrical efficiency

A model of a Nissan Leaf was used to generate heat loss profiles for the APEEM components and ESS over the EPA FTP, Highway, and US06 drive cycles. Figure 5 shows the APEEM and battery heat loss over the US06. This heat load was used in the KULI model of the APEEM and ESS cooling loops.

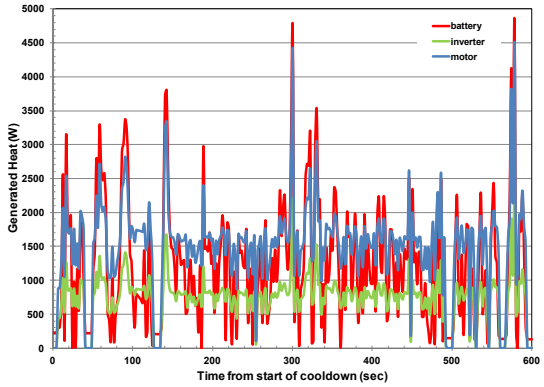

Figure 5. Heat generated in the APEEM and ESS components of a Nissan Leaf over the US06 drive cycle.

Results

The KULI A/C model system was run at three steady-state operating points. These steady-state bench data, obtained in Visteon environmental chambers, were used to validate the system model. For these validation runs, the 213-cc compressor was used. At the 35°C, high blower setting, and 48.3 km/hr (30 mph) vehicle speed, the pressure drops produced by the model for each of the components were within 24 kPa (3.5 psi) of the Visteon data. The temperatures of the components were also consistent with the Visteon data with some slight fluctuations at the

compressor outlet (Figure 6). Simulations with 45°C ambient, high HVAC blower speed and 35°C ambient, medium HVAC blower speed conditions were also run. The evaporator heat transfer for the non-cycling runs exceeded the Visteon data by approximately 480 W while the compressor work matched well. Overall, the A/C model matched the data to enable comparison of combined cooling loop configurations with a baseline configuration.

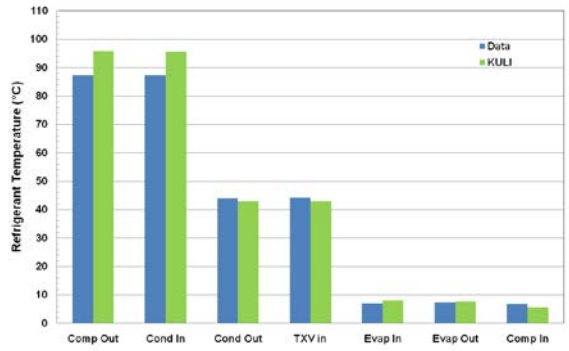

Figure 6. Refrigerant system temperatures for 35°C, high blower speed.

After the A/C system was validated with bench data, it was combined with the small sedan cabin model to approximate a small EV. A 33-cc scroll compressor was used with its rotational speed determined by a PID controller. The control parameters were set to obtain a 3°C evaporator air temperature and 20.6°C cabin air temperature. A solar load of 850 W/m^2 was applied, and the cabin interior temperatures were initialized to 20°C above ambient. The blower was set to high (0.136 kg/s) with only outside air (0% recirculation).

After separately testing the ESS and APEEM cooling loop models, they were combined with the A/C and cabin models. In this baseline vehicle simulation, the ESS cooling loop was connected to the A/C system through the chiller while the APEEM cooling loop remained standalone. On the air side, the low temperature radiator (blue in Figure 7) of the APEEM cooling loop impacted the A/C condenser (green in Figure 7) by virtue of its upstream location. A constant air mass flow of 0.796 kg/s was applied to the air side of a low temperature radiator and condenser.

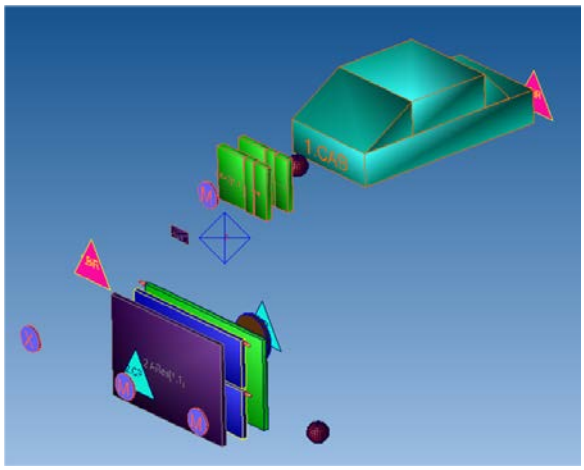

Figure 7. Air-side configuration of the baseline vehicle model.

A series of runs were conducted at 45°C, 35°C, and 25°C ambient temperatures to assess the performance of the thermal management systems in the baseline model. Figure 8 shows the evaporator exit air temperature did not reach the 3°C antifreeze control setpoint during the 10-minute drive cycle for the 45°C and 35°C ambient conditions. For the 25°C ambient condition, the evaporator air reached its 3°C control in 20 seconds. The cabin air temperature (Figure 9) did not reach its control setpoint of 20.6°C in any of the cases due to the short drive cycle and initial hot soak interior temperature.

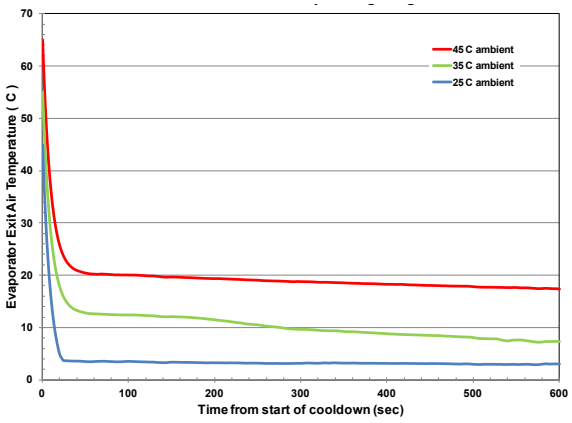

Figure 8. Evaporator exit air temperature over the US06 drive cycle for the chiller configuration.

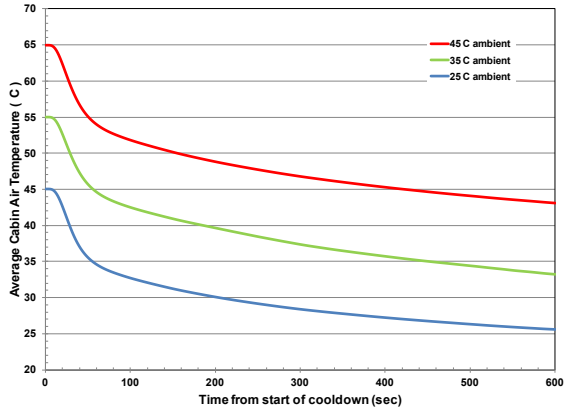

Figure 9. Cabin air temperature over the US06 drive cycle for the chiller configuration.

The APEEM cooling loop initial component temperatures were set to ambient temperature. A pump speed of 5,000 rpm resulted in a 50/50 WEG flow rate of 5 L/min. The heat generation for the motor and inverter over the US06 drive cycle was determined by the vehicle performance model. Figure 10 shows the motor temperature approached 65°C for the hottest environment. The inlet fluid temperature was 52°C for this case. Based on the author's experience, these temperatures were reasonable although the flow rate was slightly lower than typical.

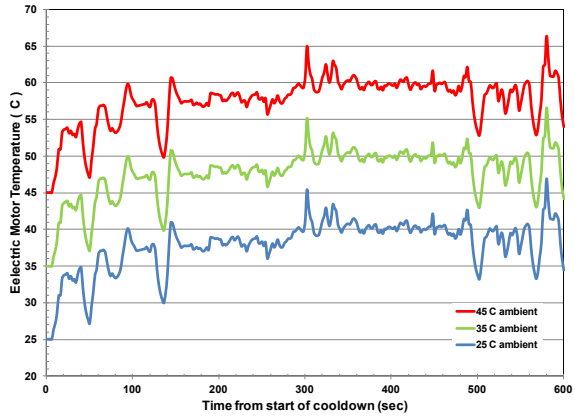

Figure 10. Electric motor temperature over the US06 drive cycle for the chiller configuration.

The ESS cooling loop initial component temperatures were set to 1.5°C above ambient temperature. The pump speed was controlled by a PID controller with setpoints designed to maintain the battery cell temperature at 26.5°C. Figure 11 shows the cell temperature for the 45°C ambient run never cooled to the setpoint while the cell temperatures for the 35°C ambient run attained the 26.5°C setpoint at the end of the run. A maximum 50/50 WEG flow rate of 4 L/min was attained at the beginning of the 45°C and 35°C runs. For the 25°C run, the battery did not require as much WEG flow because the cells started the drive cycle at the control temperature.

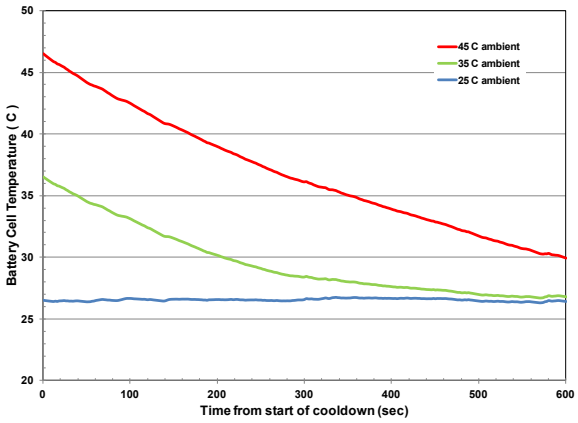

Figure 11. Battery cell temperature over the US06 drive cycle for the chiller configuration.

The combined thermal management power consumption included the A/C compressor, ESS pump, APEEM pump, A/C blower, and condenser fan. Figure 12 shows a 5-kW power consumption for the 45°C case while the 25°C case resulted in a 1.6-kW load. In the 25°C ambient case, the drop in power 20 seconds into the run was due to the A/C evaporator exit air temperature reaching its antifreeze control setpoint and the compressor rpm dropping.

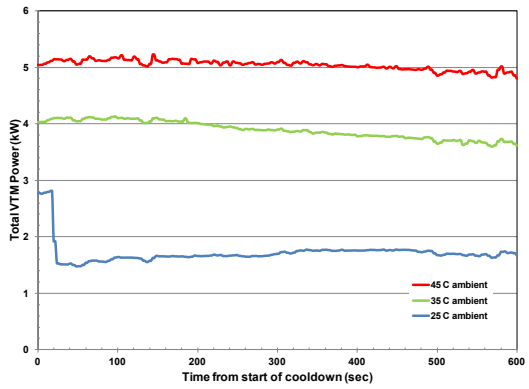

Figure 12. Total vehicle thermal management power over the US06 drive cycle for the chiller configuration.

For the 25°C ambient case, the second baseline vehicle thermal management configuration, which includes a low temperature radiator in the

ESS cooling loop, was run. Figure 13 shows the cell temperatures were higher for this case because the low temperature radiator was less efficient at removing heat than the chiller. The benefit of the low temperature radiator was less power consumption compared to the chiller as shown in Figure 14.

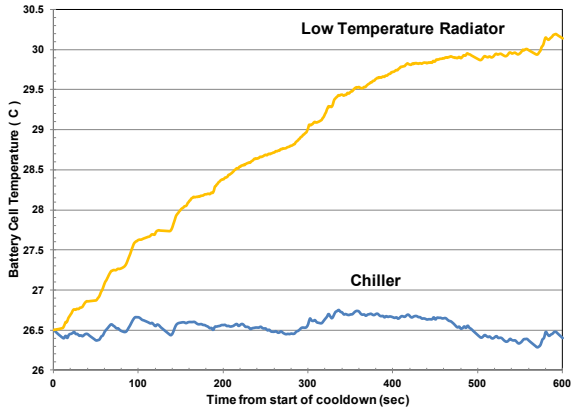

Figure 13. Battery cell temperature over the US06 drive cycle for 35°C ambient.

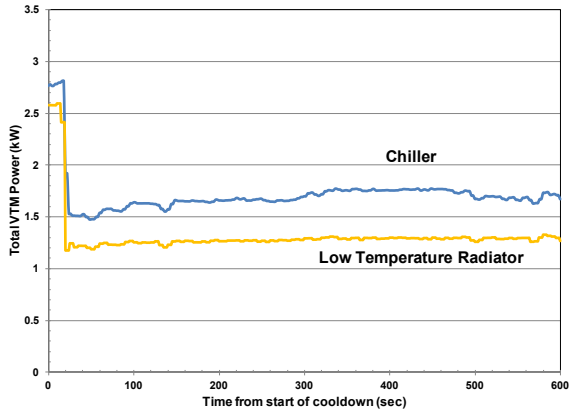

Figure 14. Total vehicle thermal management power over the US06 drive cycle for 35°C ambient.

Figure 15 illustrates the competing demands of battery cooling and occupant comfort. For the 35°C ambient temperature case, the chiller capacity used to cool the battery was initially 4 kW, while the evaporator capacity used to cool the passenger compartment was initially 3.2 kW. For this configuration, more of the cooling capacity initially went to cooling the battery. This is apparent in the resulting temperatures. Figure 11 shows the battery cells cooled to 26.5°C in 10 minutes while the passenger compartment was still above 33°C at the end of the run (Figure 9). This vehicle-level challenge will be critical for EDVs as automotive engineers trade battery temperature and life against occupant comfort in some operating conditions.

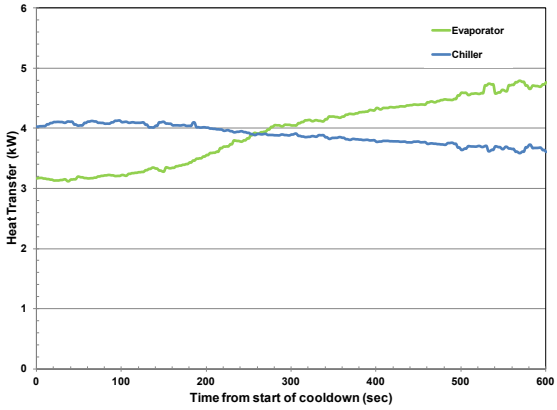

Figure 15. Evaporator and chiller capacity over the US06 drive cycle for 35°C ambient.

Conclusions

A modeling process was developed to assess the synergistic benefits of combining cooling loops in vehicles with electric powertrains. Visteon provided high-quality component data to form the basis of the models. Using KULI software, an A/C model was built and validated with test data. After a model of a small sedan cabin was built and tuned, it was combined with the A/C model and produced reasonable cool-down performance. APEEM and ESS cooling loops were built and produced typical temperatures and flow rates. These models were combined with the A/C and cabin models to form a baseline vehicle thermal model. The baseline vehicle model was run at three ambient conditions. As the ambient temperature dropped, the required thermal management power dropped as temperatures approached the desired values.

The next step is to link the KULI model and the vehicle cost/performance and battery life models and assess strategies for combining cooling loops. This type of vehicle-level analysis is critical for assessing potential cost reductions and performance improvements due to combined cooling systems in EDVs. The potential benefits

are unknown and need to be quantified. Reducing EDV cost and improving performance would increase consumer acceptance and incorporation of vehicles with electric powertrains.

V.L.3. Products

Publications

Rugh, J.P.; Bennion, K.; Brooker, A.; Langewisch, J.; Smith, K.; and Meyer, J. (2011) "PHEV/EV Integrated Vehicle Thermal Management - Development of a KULI Model to Assess Combined Cooling Loops," *Proceedings of the 10th Vehicle Thermal Management Systems Conference*, May 15-19, 2011, Gaydon Warwickshire, UK, Institution of Mechanical Engineers.

References

1. Ap, N-S., Guerrero, P., Jouanny, P., Potier, M., Genoist, J., Thuez, J., "UltimateCooling™ New Cooling System Concept Using the Same Coolant to Cool All Vehicle Fluids," 2003 Vehicle Thermal Management Systems Conference (VTMS6), IMechE C599/010/2003, May 2003.
2. Bennion, K., Thornton, M., "Integrated Vehicle Thermal Management for Advanced Vehicle Propulsion Technologies," SAE Paper 2010-01-0836, 2010.
3. Barnitt, R., Brooker, A., Ramroth, L., Rugh, J., Smith, K., "Analysis of Off-Board Powered Thermal Preconditioning in Electric Drive Vehicles," 25th World Battery, Hybrid and Fuel Cell Electric Vehicle Symposium & Exhibition, Shenzhen, China, November 2010.
4. KULI Energy Management Simulation Software, Version 8.0-1.02, Engineering Center Steyr GmbH & Co KG, http://www.kuli.at/, accessed November 16, 2010.
5. Hsu, J., Staunton, R., Starke, M., *Barriers to the Application of High-Temperature Coolants in Hybrid Electric Vehicles,* Oak Ridge National Laboratory Technical Report, ORNL/TM-2006/514, 2006.
6. Vehicle Technologies Program Plans and Roadmaps. "Electrical and Electronics Technical Team Roadmap," December 2010, http://www1.eere.energy.gov/vehicles andfuels/pdfs/program/eett_roadmap_12-7-10.pdf, accessed February 28, 2011.
7. Lipo, T., *Introduction to AC Machine Design*, 3rd Edition, Madison: University of Wisconsin. 2007.
8. Lindström, J., "Thermal Model of a Permanent-Magnet Motor for a Hybrid Electric Vehicle," Department of Electric Power Engineering, Chalmers University of Technology, Göteborg, Sweden, 1999.
9. Figliola, R., Beasley, D., *Theory and Design for Mechanical Measurements, 2nd Edition*, New York,: John Wiley and Sons. 1995.
10. Smith, K., Markel, T., Pesaran, A., "PHEV Battery Trade-off Study and Standby Thermal Control," 26th International Battery Seminar & Exhibit, Fort Lauderdale, FL, March, 2009.
11. Simpson, A., "Cost-Benefit Analysis of Plug-In Hybrid Electric Vehicle Technology," 22nd International Battery, Hybrid and Fuel Cell Electric Vehicle Symposium and Exhibition (EVS-22), Yokohama, Japan, October 23-28, 2006.

V.M. Real-World PHEV Fuel Economy Prediction

Jeffrey Gonder (Principal Investigator), Matthew Earleywine and Eric Wood
National Renewable Energy Laboratory (NREL)
1617 Cole Boulevard
Golden, CO 80401-3393
(303) 275-4462; Jeff.Gonder@nrel.gov

DOE Activity Manager: David Anderson
(202) 287-5688; David.Anderson@ee.doe.gov

V.M.1. Abstract

Objective

- Identify issues with real-world plug-in hybrid electric vehicle (PHEV) fuel economy prediction, and suggest which method(s) may most accurately predict a given PHEV's aggregate fuel saving potential.
- Help inform impartial assessment of specific PHEV powertrains (based on overall fuel savings).

Approach

- Examine factors affecting PHEV fuel economy prediction.
- Develop prospective methods to obtain real-world predictions from certification cycle test results.
- Evaluate each method by simulating multiple PHEV powertrain variants over 1,200 days of second-by-second real-world driving data.

Major Accomplishments

- The comparison between real-world cycle simulation results and the predictions from various adjustment methods highlights that common electricity adjustment assumptions may over-penalize large-scale PHEV electric consumption predictions.
- NREL determined that the adjustment approaches that seemed to best predict overall PHEV fuel and electricity consumption included a test for powertrain type as part of the adjustment process.
- The project identified and improved understanding of a number of PHEV fuel economy prediction issues. However, there are still a number of issues warranting further exploration.

Potential Future Activities

- Evaluate various adjustment methods against findings from initial real-world deployments of automaker PHEVs (as data become available).
- Further analyze fuel and electricity consumption impacts of ambient temperature and road grade.
- Examine additional powertrain designs as well as driver behavior considerations (e.g., characteristics of likely PHEV purchasers, potential for driver feedback, opportunity for mid-day charging, etc.).
- Develop alternate test cycles to better reflect real-world operation.

V.M.2. Technical Discussion

Introduction

While drive cycle variability between real-world and standard test cycles can lead to moderate fuel economy differences for conventional vehicles, it can create very large differences in plug-in hybrid electric vehicle (PHEV) fuel economy estimates. This analysis explores the factors that impact PHEV fuel economy, and how they can produce a wide range of results. The project also assesses various methods to adjust raw fuel and electricity usage from standard test cycles in order to most accurately predict the average fuel displacement

impact a given PHEV could achieve in the real world.

Approach

A key element of the project approach was to identify and document the multitude of issues impacting PHEV fuel economy prediction. To this end, NREL actively participated along with representatives from Argonne National Lab, multiple automakers and regulatory agencies in the SAE J1711/J2841 PHEV test procedures development process [1, 2]. This process addressed all of the various considerations for measuring PHEV fuel economy over a certification test cycle.

The well-known inability of raw certification cycle test results to represent real-world fuel economy necessitates a subsequent step of adjusting the laboratory results. To identify issues related to real-world adjustment for PHEVs, NREL examined the accepted adjustment process for conventional (CV) and hybrid electric vehicles (HEVs) and considered the complications presented by PHEV operation. Several prospective adjustment methods were then developed taking these issues into account.

To evaluate each adjustment method, NREL leveraged existing computer models for a variety of vehicle designs [3]. Table 1 summarizes the platform assumptions for each vehicle model. The adjustment methods were applied to simulation results for each vehicle over standard certification cycles to produce fuel and electricity consumption predictions. These predictions were then compared against the fuel and electricity consumption results from simulations over 1,200 full-day, second-by-second drive cycles obtained from a travel survey conducted in southern California. The travel survey utilized global positioning system (GPS) data collection devices to record the high-resolution driving data.

Table 1. Midsize vehicle platform assumptions.

				PHEV			
	Units	*CV*	*HEV*	*10*	*20*	*40*	*40s*
Engine Power	kW	123	77	77	78	80	85
Motor Power	kW	n/a	36	40	41	43	130
ESS Energy (total, DC)	kWh	n/a	1.7	4.5	8.2	16.4	16.4
Curb Mass	kg	1473	1552	1578	1614	1694	1789

Results

NREL highlighted a number of issues that complicate PHEV fuel economy prediction. For obtaining objective test results from a standard drive cycle, these include making sure to fully capture the vehicle's charge-depleting (CD) and charge-sustaining (CS) operation, separately measuring both fuel and electricity consumption, and combining the CD and CS consumption measurements with a utility factor (UF) based on national driving statistics and a once daily charging assumption [1, 2].

Further complications arise when applying adjustments to the standard cycle results in order to represent additional road loads that are not captured by the historic certification tests. In CS mode these additional loads will simply increase fuel use (just as occurs for a non-plug-in HEV). In CD mode the added loads could use more fuel, change the battery depletion rate, or both. This could variously impact fuel and electricity consumption, and the depletion distance used for the UF calculation (see Figure 1).

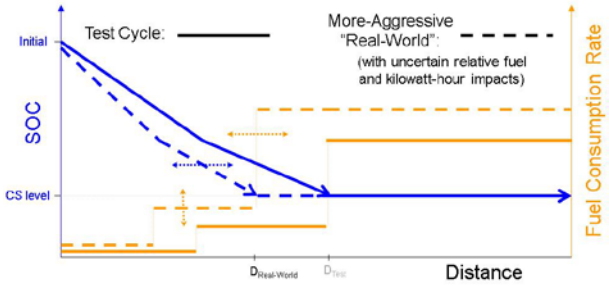

Figure 1. Multiple degrees of freedom for applying PHEV adjustments.

Various methods of simplification were examined to reduce the degrees of freedom in the adjustment process. One method, named the "Blended Method" based on its assumption of blended engine and electric operation during CD mode, assumed that the added road loads have no impact on electricity depletion and only cause fuel use to increase during CD mode at the same rate that it increases in CS mode. Another approach, called the "All-Electric Method" based on its presumption of electric-only operation during CD mode, assumes that no additional CD mode fuel consumption occurs to satisfy extra road loads and that instead the electric depletion rate increases (thereby decreasing the depletion

distance). One shortcoming for both of these methods is that they cannot be applied universally to all powertrain types.

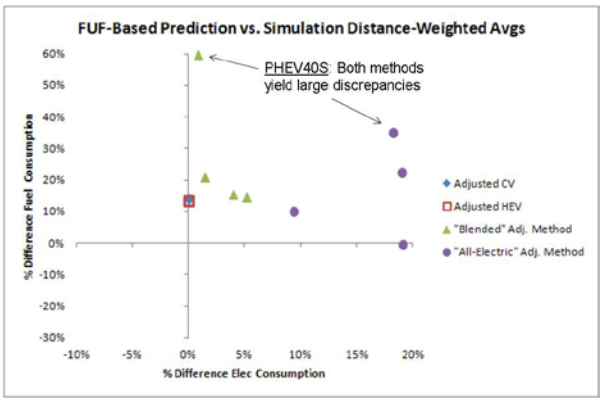

Figure 2. Difference between fleet UF (FUF)-based predictions from various adjustment methods and the average fuel/electricity consumption from the real-world simulations.

Figure 2 shows the results from applying both the Blended and All-Electric adjustment methods to each of the evaluated PHEV designs, and comparing the predictions to the distance-weighted average consumption results from the real-world simulations. The figure also shows the fuel economy predictions from established adjustment methods for the CV and HEV relative to their corresponding distance-weighted averages. Note that the established CV and HEV adjustment methods predict higher fuel consumption than the real-world simulations show. This could be because the established adjustment methods account for fuel consumption impacts from factors such as ambient temperature and road grade, which are not captured in the real-world simulations.

An accurate PHEV adjustment method might reasonably be expected to produce a similarly offset prediction relative to the simulated real-world consumption results. This does more or less occur for the Blended Method when applied to the PHEV10, 20 and 40 vehicles (which do operate in a blended CD mode over most drive cycles). However, the Blended Method does not work very well for the high electric power PHEV40S. It is also no surprise that the All-Electric Method does not work very well for the blended-type PHEV10, 20 and 40 (represented by the purple circles scattered on the right side of the figure), but it is less expected to see the large error for the All-Electric method with the PHEV40S.

The All-Electric Method adjustments shown in Figure 2 were made by applying the established adjustment equations (based on fuel consumption) after first converting the electricity use into a comparable amount of "fuel" using a 33.7 kWh of electricity per gallon of fuel equivalency factor. NREL found that this approach produced a large assumed increase in electric consumption between the test result and the adjusted prediction. Figure 3 shows that capping the assumed percent increase in electric consumption moves the method's predictions for the PHEV40S into the expected range.

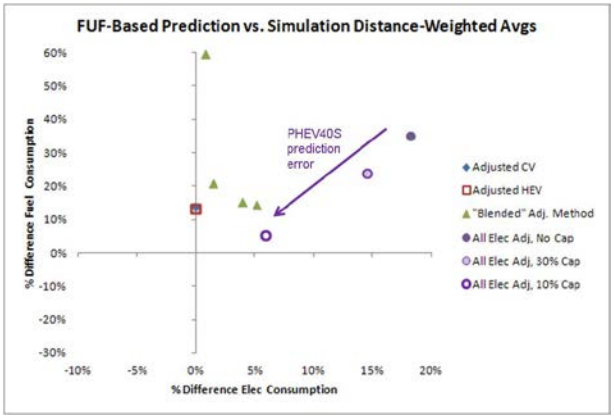

Figure 3. Improved All-Electric Method predictions by capping the adjustment in electric consumption (EC) relative to the rate measured on the standard city and highway test cycles.

NREL evaluated an additional adjustment approach, known as the "Variable Angle Method," which applied both fuel and electricity adjustments to the standard city and highway CD test results. The relative amount of the fuel vs. electricity adjustment was guided by the results of a more aggressive test cycle, such as the US06 profile. As Figure 4 shows, this method (combined with a similar cap on the electric consumption adjustment as described above), show reasonable universal applicability to both high electric power and blended-type PHEV powertrain designs.

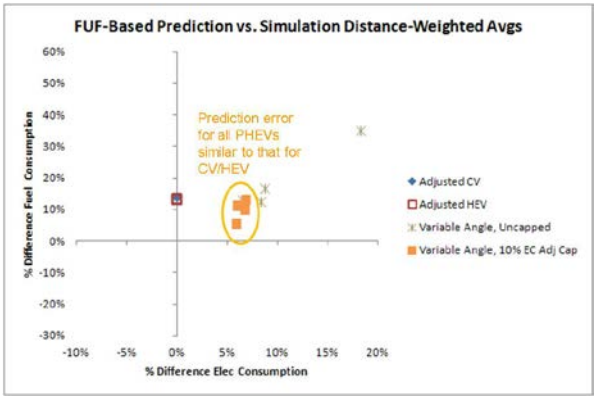

Figure 4. Reasonable predictions for the Variable Angle Method with capped electric consumption (EC) adjustment.

Conclusions

Real-world PHEV fuel economy prediction is a very complicated issue with many variables, but accurate prediction methods are important to help inform objective technology assessment. This project demonstrated the importance of limiting large electric consumption adjustments to avoid over-penalizing PHEVs. The project also showed promising results for either manually or automatically selecting an adjustment method based on some knowledge of the PHEV powertrain type (such as its relative electric power capability).

While accurate prediction of overall PHEV performance is certainly important, emphasis should also be placed on the substantial spread in fuel economy that a PHEV can achieve. By highlighting the spread as well as ways to move toward the higher end of the fuel economy range, PHEV drivers may be more inclined to adopt efficient driving behaviors and plug-in more frequently than once per day. Future work could consider such driver behavior impacts on real-world fuel economy predictions. Other topics warranting further research include analyzing ambient temperature and grade impacts in further detail, examining additional powertrain designs, and evaluating adjustment methods against field data from initial automaker PHEV deployments (as data become available).

References

1. SAE International, Surface Vehicle Recommended Practice SAE J1711—Recommended Practice for Measuring the Exhaust Emissions and Fuel Economy of Hybrid-Electric Vehicles, Including Plug-in Hybrid Vehicles; June 2010.
2. SAE International, Surface Vehicle Information Report SAE J2841—Utility Factor Definitions for Plug-In Hybrid Electric Vehicles Using Travel Survey Data; September 2010.
3. Earleywine, M., Gonder, J., Markel, T. and Thornton, M. "Simulated Fuel Economy and Performance of Advanced Hybrid Electric and Plug-in Hybrid Electric Vehicles Using In-Use Travel Profiles." *Proceedings of the 6th IEEE Vehicle Power and Propulsion Conference (VPPC); Sept.1-3, 2010, Lille, France.*

V.M.3. Products/Publications

Rask, E., Gonder, J. and Duoba, M. "Evaluation of Adjustment Methodologies for Estimating Real-World Plug-In Hybrid Electric Vehicle Fuel and Electricity Consumption." Submitted to The 26th International Battery, Hybrid and Fuel Cell Electric Vehicle Symposium and Exposition (EVS-26). May 6-9, 2012; Los Angeles, CA.

Tools & Data

Transportation Secure Data Center (TSDC) (Jeff.Gonder@nrel.gov)

V.N. Refinement of High-Level Vehicle Simulation and Analysis Tool

Principal Investigator: Aaron Brooker
National Renewable Energy Laboratory (NREL)
1617 Cole Boulevard
Golden, CO
(303) 275-4392; Aaron.Brooker@nrel.gov

DOE Activity Manager: David Anderson
(202) 287-5688; David.Anderson@ee.doe.gov

V.N.1. Abstract

Objective

- Refine and create documentation of the high-level vehicle simulation and analysis tool known as FAST (Future Automotive Systems Tool) in order to prepare it for distribution.

Approach

- Clean up and refine the organization of the tool
- Improve ease of use
- Add documentation to introduce the tool and expand on how to use it

Major Accomplishments

- Reorganized and cleaned up vehicle interface for easier use
  - Added buttons to help calculate input data based on vehicle spec sheets
  - Added buttons to display data such as efficiency map information
  - Developed interface to easily create new drive cycles
- Populated the model with data
- Added interfaces that include automated battery life and cost optimization
  - The Powertrain Comparison interface compares powertrain cost and efficiency
  - The Parametric Study interface is similar, but sweeps a variable such as mass or auxiliary load
- Added three forms of documentation
  - An outlined expandable traditional form of documentation
  - Context sensitive pop-ups for quick access to additional information
  - An automated tutorial that goes through the key aspects of the tool

Future Activities

- Distribute for beta testing and then a final public release
- Related activities
  - Apply the tool to medium duty truck analysis
  - Add option to optimize for consumer preference rather than cost

V.N.2. Technical Discussion

Background

The Future Automotive Systems Tool (FAST) was developed to easily and quickly compare technology improvement impacts on the efficiency, performance, and cost of the leading powertrains. This project was focused on refining and documenting it so it can be more widely leveraged.

The vehicle portion of the model includes all the key aspects. It has conventional, hybrid electric (HEV), plug-in hybrid electric (PHEV), and battery electric powertrains (EVs). FAST simulates a vehicle driving a speed vs. time profile calculating the drag, acceleration, ascent, and rolling resistance each second. It models the major powertrain components including the engine, electric motor, battery and the auxiliary loads. It captures the effects of regenerative braking and different energy management strategies.

It captures the major vehicles aspects, but still runs fast. Running a state of charge (SOC) balanced city and highway cycle takes about 2.5 seconds. Optimizing to compare the four powertrains takes roughly 2 minutes.

In addition to the vehicle side of the model, FAST integrates other key aspects of vehicle analysis. It includes the battery life, cost, and the distribution of driving distances. It also integrates a validation process to ensure all the key results, including efficiency, cost and battery life, match well with data.

Introduction

FAST is an easy to use model. In order to maximize user familiarity and comfort level, it was built in the widely-used Microsoft Excel analysis environment. FAST is designed to be as simplified as possible while still achieving useful results. As such, the inputs are high level, such as motor power or engine power, and can be easily found online rather than requiring detailed proprietary data. While it is easy to use, FAST still required refinement and documentation to make it suitable for distribution to a wider audience.

Approach

Four major steps were taken to prepare FAST for a wider distribution. One, it was cleaned up and refined. Two, buttons, interfaces, and feedback animations were developed to improve the ease of use. Three, data was added to provide a wide variety of vehicles to simulate. Four, several different forms of documentation were created to introduce the tool and improve the user experience.

Results

FAST is now an intuitively organized, fast, easy to use, data rich, low license cost tool. FAST takes a systems perspective by estimating battery life and cost along with simulating powertrain efficiency and performance.

Several steps were taken to improve the ease of use. Calculators were added to translate online data into FAST input format. For example, FAST now includes a calculator to estimate the frontal area in meters squared based on the online data of height and width in inches. Another calculator uses the tire side wall information to calculate the tire radius input, as seen in Figure 1.

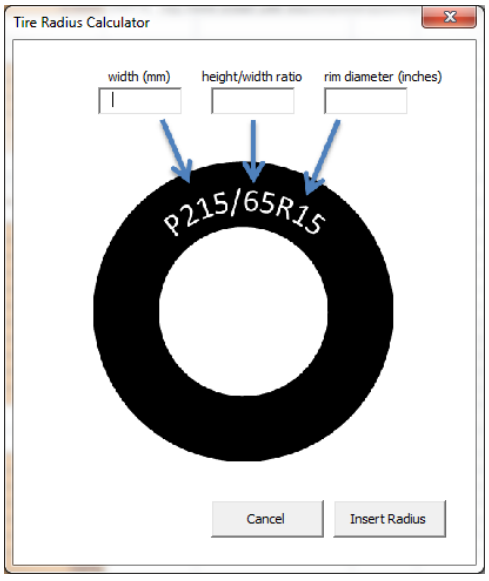

Figure 1. Tire radius calculator.

Buttons were added to show data. In the engine and motor sections, a button displays/hides the efficiency map. Another button displays the relationship between braking regeneration and

vehicle speed, as seen in Figure 2. Several interfaces were also added. One interface selects the extra drive cycles to be run. Another interface guides a user through adding a new drive cycle.

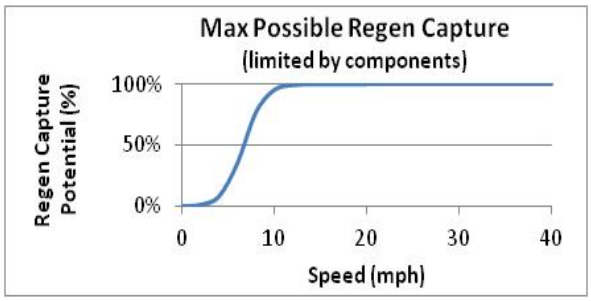

Figure 2. Maximum braking regeration curve.

Since it is easy to find and enter data into FAST, and it doesn't required detailed proprietary data, NREL populated it with a wide range of vehicles. Seven conventional gasoline vehicles ranging from compact to large truck were added. Similarly, six diesel vehicles were added. These were used to verify that the engine efficiency model was valid over a wide range of engine sizes, as seen in Figure 3. In addition, several HEVs, PHEVs, EVs, and a medium duty truck were included that were developed from previous studies.

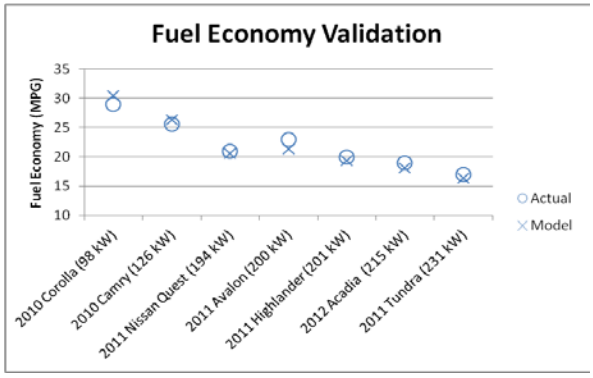

Figure 3. Engine model scaling validation.

Two interfaces were added to capture the systems perspective of FAST. One interface was developed in a worksheet named Powertrain Comparison. Key vehicle inputs, such as a base vehicle, HEV motor power, EV range, and fuel cost are entered. Then the model optimizes the four powertrains using the vehicle efficiency and performance model, cost model, battery life model, and distribution of driving distances to compare the petroleum use and cost, as seen in Figure 4.

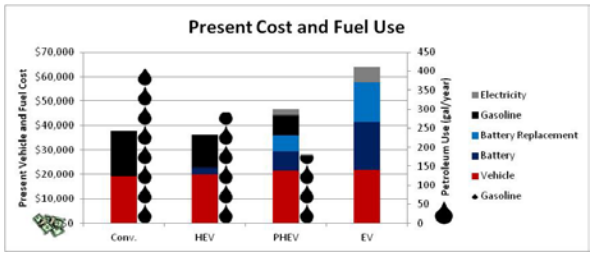

Figure 4. Powertrain Comparison example output chart.

Similarly, another interface was developed in a worksheet named Parametric Study. It has similar inputs and outputs, only it sweeps one selected variable, such as glider mass or auxiliary loads, to find the cost and efficiency trends as it improves.

While the tool is easy to use, documentation is still helpful. Three forms of documentation were developed. A traditional text documentation provides organization insight and model details. Embedded documentation provides additional information when hovering over inputs, descriptions, or outputs. This helps to quickly answer the most common questions. The third form of documentation is an automated tutorial. It steps through the different Excel worksheets, scrolling to different sections, and highlighting the key aspects and functions.

Conclusions

FAST easily and quickly compares technology improvement impacts on the efficiency, performance, and cost of the leading powertrains. Calculators have been added to help translate easily found data into FAST inputs. Buttons have been added to display additional model detail. Data was gathered to populate the model. Interfaces were added to compare powertrains and sensitivities. And finally, documentation was added to introduce and detail the tool.

V.N.3. Products

Publications

1. Brooker, A.; Thornton, M.; Rugh, J. P. (2010). Technology Improvement Pathways to Cost-Effective Vehicle Electrification. SAE Paper No. 2010-01-0824. Advanced Hybrid Vehicle Powertrains, 2010. SP-2275. Warrendale, PA: SAE International 13 pp.; NREL Report No. CP-540-48291. doi:10.4271/2010-01-0824
2. O'Keefe, M.; Brooker, A.; Johnson, C.; Mendelsohn, M.; Neubauer, J.; Pesaran, A. (2011). Battery Ownership Model: A Tool for Evaluating the Economics of Electrified Vehicles and Related Infrastructure; Preprint. 13 pp.; NREL Report No. CP-5400-49127.
3. Rugh, J. P.; Bennion, K.; Brooker, A.; Langewisch, J.; Smith, K.; Meyer, J. (2011). PHEV/EV Integrated Vehicle Thermal Management - Development of a KULI Model to Assess Combined Cooling Loops. [Proceedings of the] Vehicle Thermal Management Systems Conference and Exhibition, VTMS 10, 15-19 May 2011, Warwickshire, United Kingdom. Cambridge, UK: Woodhead Publishing Ltd. pp. 649-660; NREL Report No. CP-5400-50821.
4. Barnitt, R. A.; Brooker, A. D.; Ramroth, L. (2010). Model-Based Analysis of Electric Drive Options for Medium-Duty Parcel Delivery Vehicles: Preprint. 11 pp.; NREL Report No. CP-5400-49253.
5. Barnitt, R. A.; Brooker, A. D.; Ramroth, L.; Rugh , J.; Smith, K. A. (2010). Analysis of Off-Board Powered Thermal Preconditioning in Electric Drive Vehicles: Preprint. 10 pp.; NREL Report No. CP-5400-49252.

Tools & Data

Future Automotive Systems Tool (FAST)

The data included is all publicly available.

V.O. Medium-Duty Electric Drive Vehicle Simulation and Analysis

Laurie Ramroth (Principal Investigator), Jeff Gonder and Aaron Brooker
National Renewable Energy Laboratory
1617 Cole Boulevard
Golden, CO, 80401-3393
(303) 274-4407; Laurie.Ramroth@nrel.gov

DOE Activity Manager: David Anderson
(202) 287-5688; David.Anderson@ee.doe.gov

V.O.1. Abstract

Objective

- Evaluate petroleum reductions and cost implications of parcel delivery plug-in hybrid gasoline and diesel variants relative to a diesel conventional vehicle.

Approach

- Run plug-in hybrid variants on a field data-derived design matrix to analyze the effects of drive cycle, distance, battery replacements, battery capacity, and motor power on fuel consumption and lifetime cost.
- Evaluate lifetime cost under present-day assumptions of $700/kWh and $3/gal battery and fuel costs, respectively, and under a future cost scenario of $100/kWh and $5/gal fuel.

Major Accomplishments

- Demonstrated that PHEVs are cost effective under the future cost scenario of $100/kWh of battery energy and $5/gal fuel. Assuming a current cost treatment of $700/kWh and $3/gal fuel, however, PHEVs seldom recoup the additional motor and battery cost. In those instances where the additional cost is regained in fuel savings, the kinetic intensity and daily distance traveled does not coincide with the usage patterns observed in the field data. Alternate usage patterns could achieve cost effectiveness.
- Designing the battery to require replacement prior to the end of the assumed 15-year vehicle life is only cost effective if battery costs go down.
- A higher motor power was effective in those scenarios that included a battery replacement, or in those cases with no replacement where the drive cycle was kinetically intense and the vehicle traveled enough miles to recoup the extra cost through hybridization fuel savings (from regenerative braking, etc.).
- Drive cycles with higher kinetic intensity and longer daily travel distances produce the most favorable PHEV payback conditions.

Future Activities

- Evaluate the cost threshold at which plug-in hybrid parcel delivery vehicles become cost effective.
- Incorporate thermal and calendar battery wear into the model.
- Consider additional powertrain designs.
- Evaluate total cost of ownership, and analyze field data for potential midday charging opportunities.

V.O.2. Technical Discussion

Introduction

Medium-duty vehicles consume a significant amount of petroleum and emit a large amount of greenhouse-gas emissions. Fortunately, medium-duty vehicles in the parcel-delivery vocation are ideal candidates for electric drivetrains because they often share the following characteristics:

- Daily driving routes that return to a central depot, facilitating overnight charging
- Stop-and-go drive cycles that allow for energy capture from regenerative braking
- A buyer that values the bottom line over acceleration, performance, and style
- Fuel savings that can multiply across an entire for-hire/private fleet.

Approach

In this analysis, battery life and cost versus fuel consumption tradeoffs are compared for three different powertrain-configuration/fuel combinations: conventional (diesel), plug-in hybrid (diesel), and plug-in hybrid (gasoline).

This study includes several updates from a previous effort [1]. These improvements include battery replacements, all-electric controls, and a diesel conventional baseline parcel delivery model.

1. The minimum state-of-charge optimization algorithm includes battery replacement.

2. All-electric control changes in the gasoline hybrid parcel delivery vehicle model, which carry over into the plug-in hybrid vehicle models in this report:
   - Command engine on if the vehicle speed is ≥ 18 miles per hour (mph).
   - Command engine on if the power demand is ≥ 35 kilowatts (kW).
3. A validated diesel conventional model is used as a frame of reference in the cost analysis.

This section describes the approaches to model development and validation, to forecasting battery life, and to evaluating cost and fuel consumption tradeoffs.

Fuel Consumption Measurement and Model Validation

Two parcel delivery vehicles owned and operated by the United Parcel Service (UPS) were transported to the Renewable Fuels and Lubricants (ReFUEL) laboratory for fuel economy and emissions testing on the chassis dynamometer. Both the conventional and hybrid diesel vehicle used the same 149 kW engine. The hybrid-electric van was equipped with a parallel-hybrid system from Eaton. ReFUEL tested the vehicles on three cycles—the New York Composite Cycle (NYComp), the Heavy Heavy-Duty Diesel Truck (HHDDT), and the HTUF 4 (developed by the Hybrid Truck Users Forum).

Table 1. . Cycles Used for ReFUEL Testing

Configuration	Fuel	Cycles
Conventional/ Hybrid	Diesel	NYComp, HTUF 4, HHDDT

The models were developed using basic component specifications and engine-specific efficiency data when available.

Table 2. General Vehicle/Component Level Specifications

	Conventional Diesel	Diesel Hybrid
Test Weight **GVWR**[1]	6,813 kg 10,433 kg	7,303 kg 10,433 kg
Aerodynamics Drag Frontal Area[2]	 0.7 7.80 m^2	 0.7 7.80 m^2
Wheels 245/70R19.5 Rolling Resistance Coefficient	0.008	0.008
Battery—Lithium ion Capacity Power		1.8 kWh Matched to motor
Engine Maximum Power Maximum Torque	149 kW @ 240 rps 520 ft-lbs @ 1,600 RPM	149 kW @ 240 rps 520 ft-lbs @ 1,600 RPM
Motor Peak Continuous Power Peak Power		26 kW 44 kW
Accessories Power[3]	3 kW	1.22 kW

Figure 1 shows good agreement between the model's fuel consumption predictions and the measurements that were recorded at ReFUEL. The discrepancies between the modeled and the experimentally-measured values are slightly higher for the hybrid than for the conventional, but in all cases show less than 10% disagreement.

The engine efficiency map for the conventional model was created from ReFUEL test data and a maximum-torque curve from the engine manufacturer. The maximum-torque curve was not defined at low engine speeds so a linear trend was assumed. This could impact the accuracy of efficiency, thus impacting fuel consumption at low engine speeds.

The primary source of uncertainty in the hybrid model lies in the motor-efficiency map as component data for the motor was unavailable. The model uses a motor-efficiency map from another vehicle and assumes a peak efficiency of 93%.

It should be noted that the mechanical and electrical accessory loads were identified from the idle portion of the HHDDT cycle.

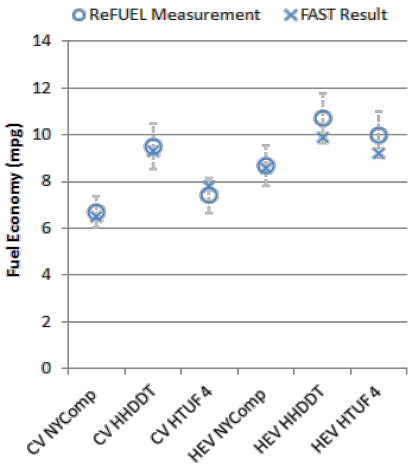

Figure 1. Validation of Conventional and Hybrid Vehicle Models

Plug-In Hybrid Model

The diesel conventional is intended as a point of reference for the other powertrain/fuel combinations in the cost and fuel-use analyses. The diesel hybrid had the same engine as the diesel conventional. A plug-in hybrid version of the model was developed based on the hybrid-diesel template.

To make the PHEV vehicles comparable, the Vehicle Systems Analysis team applied similar vehicle-specific parameters and matched the engine power to that of the diesel hybrid and conventional (150 kW). The engine power was held constant to ensure enough power for long hill climbs. Acceleration is typically used to identify two vehicles as comparable, however, for the parcel-delivery vocation we assume that fleet managers are primarily concerned with fuel economy and improving their bottom line.

The mass of both plug-in hybrids is based on the mass of the diesel hybrid with an appropriate adjustment for the additional battery capacity. No adjustment was made for the gasoline hybrid—the diesel hybrid and gasoline hybrid were assumed to be of the same mass. Battery power was matched to motor power through motor efficiency. To be consistent with the previous study, the Vehicle Systems Analysis team assumed a battery capacity of 2.5 kilowatt-hours (kWh). The accessory load used was drive train specific.

Battery-Life Model and Handling of Replacements

Battery life and replacements were estimated using cycle-wear data from Johnson Controls, as shown in Figure 2. The curve labeled "Original" represents data published by Johnson Controls. These data were obtained at the cell level and do not consider calendar-life, temperature, or power-level effects on life. To help account for those impacts, the "Today's Adjusted" curve was created by adjusting the "Original" case to match published data for the Nissan LEAF™ and the Chevy Volt battery life expectations [2].

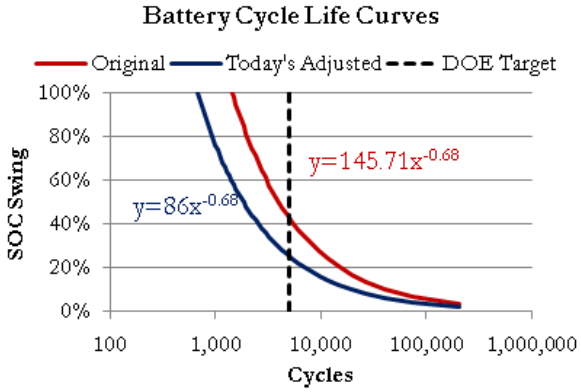

Figure 2. Battery cycle life curves

By solving for the number of cycles (x) and plugging in the state of charge (SOC) swing (y) the model can calculate the percent wear for every charge fluctuation.

$$x = \left(\frac{86}{y}\right)^{\frac{1}{0.68}}$$

End-of-life is assumed to be defined as a 20%–30% degradation of the battery's original

capacity. At this loss the battery is thought to be insufficient for automotive use. In the future, we hope to include calendar and temperature wear as well.

Cycle wear is broken down by mode—charge-depleting (CD) or charge-sustaining (CS). Charge-depleting is the mode of vehicle operation associated with the operation of an electric vehicle or the start up of a plug-in hybrid vehicle when fully charged. During this mode, power is primarily sourced from the battery with the engine providing supplemental power when necessary. When the battery of the plug-in hybrid depletes to its minimum state of charge, it enters charge-sustaining mode where regenerative braking and the power plant work to maintain that state of charge as necessary.

In plug-in hybrid vehicles, the charge-depleting mode can be all-electric or blended. In this study, all of the plug-in hybrid vehicles use a blend of electrical/mechanical power in charge-depleting mode—with the engine providing supplemental power when necessary. Specifically, the engine is commanded on if the vehicle speed or power demand exceeds a set limit. Charge-sustaining wear refers to the acceleration/regeneration cycles that occur during both the charge-depleting and charge-sustaining modes of a blended plug-in hybrid vehicle. Charge-depleting wear refers to the wear associated with deep cycling the battery to the CS level and recharging it to the initial SOC.

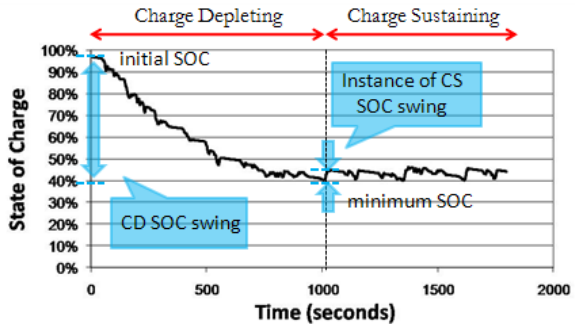

Figure 3. SOC swing wear associated with charge-depleting and charge-sustaining mode of a plug-in hybrid vehicle

The algorithm increases the minimum state of charge until the total cycle wear is at least 90% of the useable capacity. In the event of a battery replacement, the total lifetime wear is divided equally across all of the batteries.

Field Data Framing the Analysis

Leveraging concurrent U.S. Department of Energy-sponsored fleet evaluation activities with data from UPS and FedEx, the top two for-hire carriers, the NREL Fleet Test and Evaluation team is building a fleet data center of field drive cycle and performance data. A subset of this data was chosen because it was recorded using ISAAC loggers and appeared to have the best data quality of the group. It is also one of the most recent projects. For this subset, over a month of drive cycle data was collected for 11 vehicles instrumented with Global-Positioning System (GPS)-enabled data loggers. This field data framed the selection of the design matrix. Although several metrics including daily distance traveled and kinetic intensity were measured (e.g., average speed, stops/kilometer (km), and accelerations/decelerations) and evaluated for consistency, of particular importance was daily vehicle distance traveled and kinetic intensity.

The route predictability of parcel delivery fleet vehicles makes them ideal candidates for electrification. The electric drive train can be designed to optimize cost specific to the load and daily distance traveled. A kernel density plot of daily distance traveled illustrates where the design space (40–160 km) falls in relation to the field data collected (the blue curve in Figure 4). The design space envelops the daily distances traveled by these vehicles fairly well.

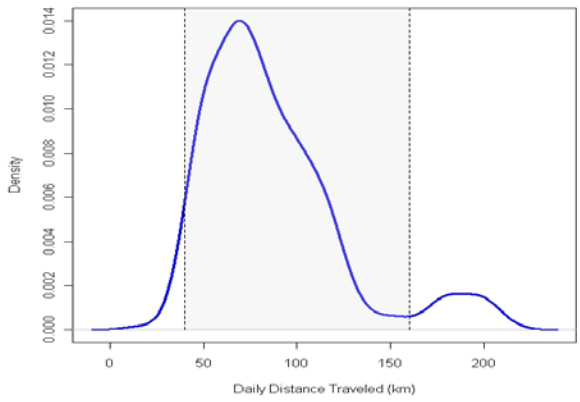

Figure 4. Comparison of daily distance traveled design space with field data

Kinetic intensity, a metric that is derived from the road-load equation for power, is linked to the magnitude and frequency of accelerations, and as such, offers insight into the cycle-specific benefits of adding an electric drive. A kernel density plot of kinetic intensity illustrates where the selected standard cycles fall in relation to the kinetic intensities measured in the field. The HTUF 4 drive cycle was selected as the standard drive cycle that best approximated the routes measured in the field, while the Orange County Bus (OC Bus) and Urban Dynamometer Driving Schedule Heavy-Duty (UDDS HD) cycles were selected as the upper and lower boundaries for vocational kinetic intensity. The density plot of the field data shows a bimodal distribution with the HTUF 4 cycle's kinetic intensity corresponding to the first mode/peak. The HTUF 4 cycle was developed by the Hybrid Truck Users Forum parcel delivery working group to be representative of a class four delivery truck predominantly in business delivery service.

Design and Cost Matrix

Figure 4 and Figure 5 lead to the development of the design matrix in Table 3. It should be noted that the additional battery capacity array is of varied step size. There is a finer resolution at lower battery capacities because it is expected that the battery capacity is a key cost driver in the total cost of ownership. The upper limit was set at 60 kWh since the Smith Newton all-electric vehicle has an 80-kWh battery pack. To ensure commercial availability of the battery, the power-to-energy ratio is set at a floor of 1.125.2 The battery power was held constant at 30 kW unless the power-to-energy ratio fell below the 1.125 limit. If the ratio fell below this limit, the battery power was increased to compensate. A set of simulations were run at a motor power matched to the 30-kW battery power. Another set of simulations were run matching the motor power to the varied battery power.

[2] Smith Newton P/E ratio. See appendix of full report for details on the Electric Vehicle Model.

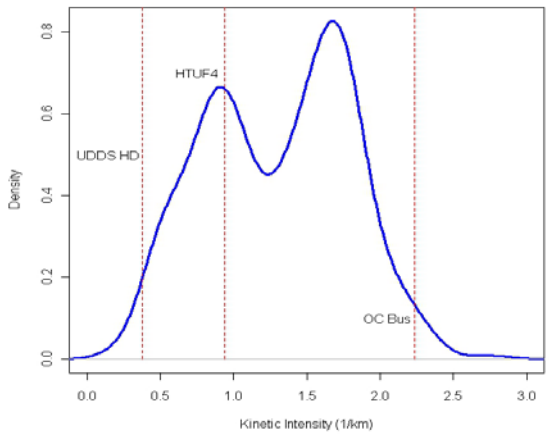

Figure 5. Comparison of kinetic intensities for field and stock drive cycles

Two cost scenarios were developed to represent a fair range of costs. Current and future fuel and electricity costs are yearly highs for 2011 and 2030, respectively[3]. Long term battery cost per kilowatt-hour is cited from the United States Advanced Battery Consortium (USABC) Goals for Advanced Batteries EVs[4]. FAST assumes a base packaging cost and then adds on a cost per kilowatt-hour as well as a cost per kilowatt.

Table 3. Design Matrix for PHEV's

Drive cycles	UDDS HD, HTUF 4, OC Bus
Control strategies	All-electric range (AER), CD-battery dominant
Daily distance traveled	40, 80, 120, 160 km
Additional battery capacity	10, 20, 40, 60 kWh
Battery power	MAX (30 kW, Capacity×P/E)
Battery power-to-energy ratio	1.125[3]

Table 4. Cost Matrix

Scenario	ESSuu Cost	Fuel Cost		Electricity Cost
		Gas	Diesel	
Current	$700/kWh	$0.81/L ($3.08/gal)	$0.85/L ($3.23/gal)	$0.11/kWh
Future	$100/kWh	$1.29/L ($4.90/gal)	$1.37/L ($5.19/gal)	$0.11/kWh

In addition to this cost matrix a diesel engine credit was applied to the gasoline plug-in hybrid in order to compare it with the diesel

[3] Smith Newton battery

conventional baseline. The diesel/gasoline cost difference was estimated using data from Ricardo. Battery replacement, lifetime electricity, and lifetime fuel use were discounted to make costs comparable in present day dollars.

Additional assumptions are listed in Table 5. The referenced battery targets were manipulated into a form compatible with FAST. This process is documented in the appendix of the full report.

Table 5. Additional Assumptions

Vehicle life (years)	15
Battery cost	\$22/kW × (kW) + scenario \$/kWh * (kWh) + \$680
Motor and controller cost	\$21.7/kW + \$425
Markup factor	1.75
Discount rate	8%
Charger efficiency	0.9

Results

This section presents analytical results for the specified range of vehicle configuration, usage, and economic scenarios.

Cumulative Fuel Consumption Versus Daily Vehicle Miles Traveled

The relationship between fuel consumption and daily distance traveled for the gasoline and diesel plug-in hybrids is illustrated in Figure 6–Figure 10. One set of simulations was run with a motor power matched to the 30-kW battery power. Another set of simulations was run matching the motor power to the varied battery power. Sets of simulations were also run with and without battery replacement. An expanded matrix of daily distances traveled is plotted in the cumulative fuel consumption plots. The shaded portions of the plot illustrate those areas that were not included in the cost design matrix.

Typically cumulative dependent variable plots are monotonic—i.e., have a strictly positive slope. With fuel consumption, however, the curve changes slope frequently and then levels out. A negative slope occurs in a situation where the engine turns on temporarily to provide excess power but the battery supplies the subsequent power until it reaches depletion. That initial liquid fuel use is averaged across a larger distance, resulting in lower cumulative fuel consumption.

It should be noted that the first iteration of the cycle is at a much finer resolution (second by second) than subsequent iterations. Subsequent iterations start at the drive cycle distance multiple that is greater than or equal to 8 km and continue at approximately 16-km increments (varies with cycle distance)4. See the appendix of the full report for drive cycle distances.

Several observations can be made from the fuel consumption vs. daily distance traveled plots. First, the charge-depleting and charge-sustaining mode of vehicle operation can be identified. The vehicle starts off in charge-depleting mode—only using the engine if the battery alone can't meet the power demand. Once the battery depletes, the upward slope indicates a transition into charge-sustaining, where it plateaus. The effect of fuel energy density, battery capacity, motor power, battery replacement and drive cycle on fuel consumption is illustrated in Figure 6–Figure 10.

- **Effect of decreasing energy density** (Figure 6). The gasoline plug-in vehicle has slightly higher fuel consumption in charge-depleting and significantly higher fuel consumption in charge-sustaining mode.
- **Effect of increasing battery capacity** (Figure 7). The 62.5-kWh battery consistently results in a lower fuel consumption when compared to the 22.5-kWh battery, independent of the daily vehicle miles traveled.
- **Effect of increasing motor power to match battery power** (Figure 8). A higher-power motor can provide the excess power that would have otherwise been supplied by the engine. Increasing the motor power on the 42.5-kWh (power 47.81 kW) and 62.5-kWh (power 70.31 kW) batteries—where the battery power-to-energy ratio is less than

[4] The daily distance traveled matrix for the cumulative fuel consumption plots covered a broader range of distances. [8 24 40 56 72 88 105 121 137 153 169] km. Note that the actual measurements were taken at drive cycle multiples that met or exceeded these values.

1.125—results in significantly lower fuel consumption in charge-depleting and slightly lower fuel consumption in charge-sustaining mode.

- **Effect of battery replacement** (Figure 9). Adding a battery replacement results in a larger useable capacity/state of charge window—illustrated in the plots by an extension of the charge-depleting operating mode.
- **Effect of drive cycle/kinetic intensity** (Figure 10). Kinetically intense drive cycles use electricity quickly, thereby reverting to charge-sustaining mode quicker than their less kinetically-intense counterparts.

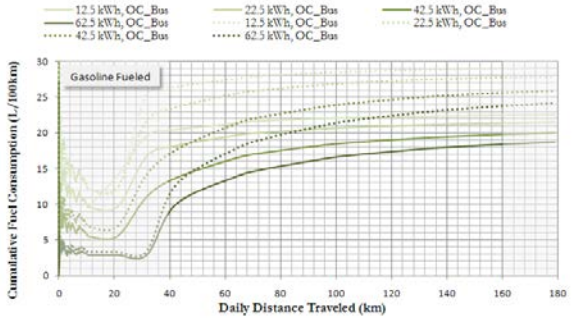

Figure 6. Effect of decreasing energy density

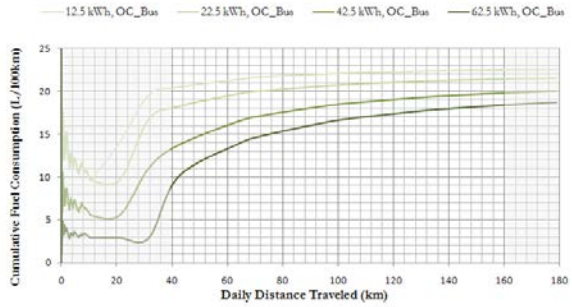

Figure 7. Effect of increasing battery capacity

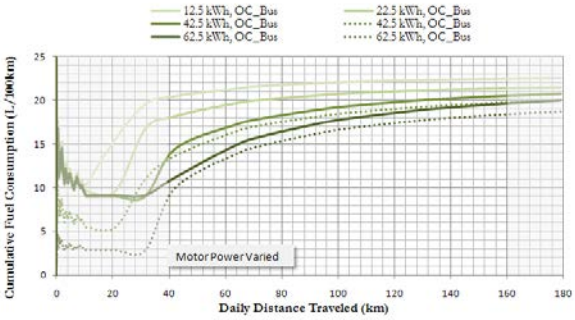

Figure 8. Effect of increasing motor power to match battery power

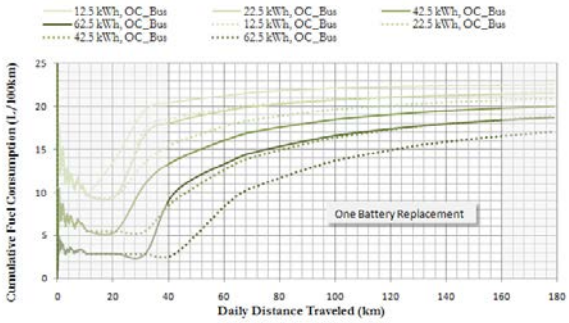

Figure 9. Effect of battery replacement

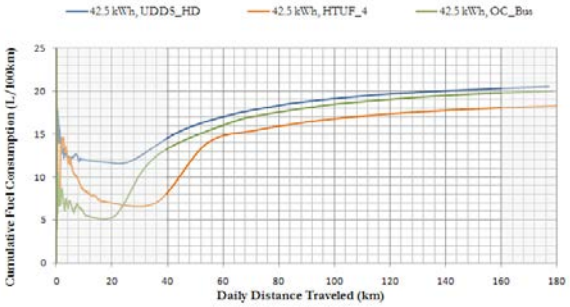

Figure 10. Effect of drive cycle/kinetic intensity

The mass penalty seen in the previous report was not realized here due to a modification to the battery mass equation. The initial equation did not account for a base packaging mass and instead split up the battery mass evenly according to its capacity. This resulted in an overestimation of battery mass in that paper.

Lifetime Cost Analysis

Three different methods compare costs: a relative comparison with the baseline diesel conventional, a component-level comparison, and a fuel savings comparison. The relative comparison subtracts the cost of the baseline diesel conventional (fuel) from the cost of the plug-in hybrid version (battery and motor, fuel, and electricity). The component-level comparison charts allow us to easily identify the cost makeup in terms of traction battery and motor, liquid fuel, electricity, and replacement battery. Lastly, the fuel savings comparison allows us to determine how many liters of diesel fuel were saved by the plug-in hybrid gasoline or diesel when compared to the diesel conventional and, furthermore how much was

spent or saved to save one liter of diesel fuel. In the following section a subset of the results is presented. For a complete presentation that is helpful in identifying trends, please see the appendix of the full report.

Vehicle Nomenclature

Column charts are organized by daily distance traveled, vehicle configuration and battery capacity, kinetic intensity of drive cycle, battery replacement, and motor power—in that order as applicable. The labels represent the configuration. The first set of labels—UDDS HD, HTUF 4, and OC Bus—show results for the conventional diesel vehicle. The subsequent sets of labels are in order of increasing battery capacity for the plug-in hybrid configurations; i.e. UDDS HD + 10, HTUF 4 + 10, OC Bus + 10, represent the plug-in hybrid configuration with a 12.5-kWh battery capacity. It should be noted that the +40 and +60 kWh scenarios resulted in a battery power-to-energy ratio of less than 1.125. For these cases the battery power was increased and two sets of motor power simulations were run: one with a motor power matched to the original 30-kW battery power and another with the motor power matched to the varied battery power. In the column charts this is shown in two instances of each cycle. The first instance corresponds to the constant-power scenario while the second corresponds to the varied motor power scenario. In the stacked column charts, battery replacements are treated in a similar manner but are easily identifiable by the battery replacement cost.

When Are Plug-In Hybrids Cost Effective?

Assuming $700/kWh battery costs and $3/gal fuel costs, there were very few usage patterns in which the plug-in hybrid paid off. The following column charts represent the difference between the plug-in hybrid lifetime cost and the diesel conventional lifetime cost where the plug-in hybrid lifetime cost is composed of upfront battery and motor costs, liquid fuel cost, electricity cost, and a battery replacement cost as applicable; and the diesel conventional lifetime cost is comprised of the cost of liquid fuel. A positive value indicates that the plug-in hybrid is more expensive.

Several observations can be made from these graphs. First, for each battery capacity the cycle with the highest kinetic intensity paid off first. Figure 11 and Figure 12 show the scenarios that paid off for the plug-in hybrid diesel—with and without replacements. For most battery sizes it doesn't make sense to buy a plug-in hybrid under the current-scenario cost assumptions. There were a few cases however, where the plug-in hybrid made sense. When a vehicle exceeded 160 km/day the 12.5-kWh battery paid back on all cycles. For those vehicles that travel distances greater than 160 km/day (Figure 4) on a cycle with high kinetic intensity, there is a potential for $10,000 in savings. In general the higher motor power was advantageous on those usage scenarios that exceeded 80 km daily distance traveled and ran on drive cycles of higher kinetic intensity (i.e. HTUF 4, and OC Bus). Battery replacements tended to be cost effective for the future scenario only.

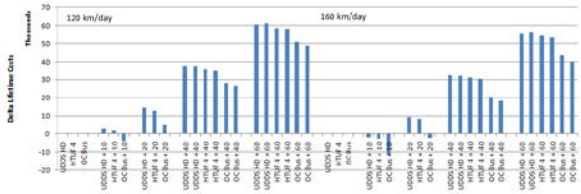

Figure 11. Current scenario, no replacement, diesel PHEV

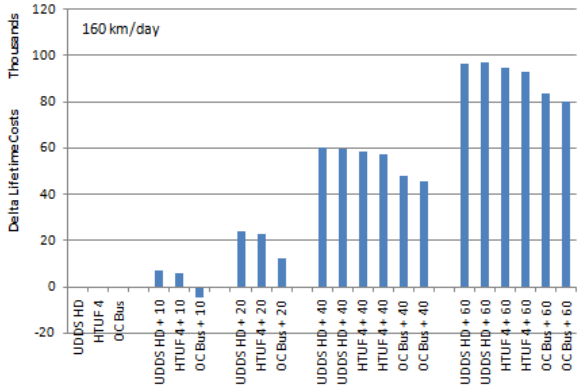

Figure 12. Current scenario, replacement, diesel PHEV

The gasoline plug-in hybrid vehicle did not pay off with or without battery replacements in the

current scenario therefore charts are included in the appendix of the full report.

In the future cost scenario, the plug-in hybrid vehicles were consistently less expensive than the diesel conventional. The results shown below—40 km and 160 km traveled per day—include the few scenarios that didn't pay off.

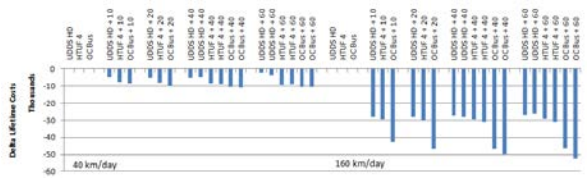

Figure 13. Diesel PHEV, future scenario, no replacement

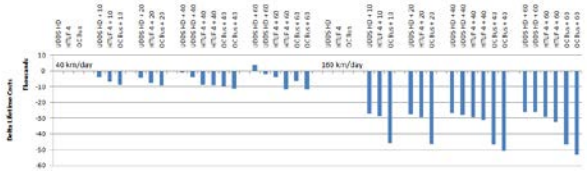

Figure 14. Diesel PHEV, future scenario, replacement

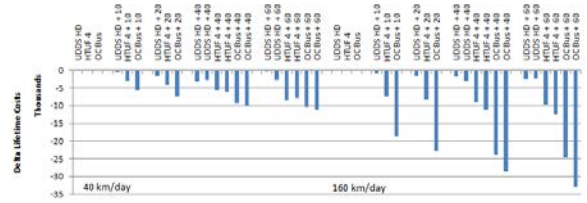

Figure 15. Gasoline PHEV, future scenario, no replacement

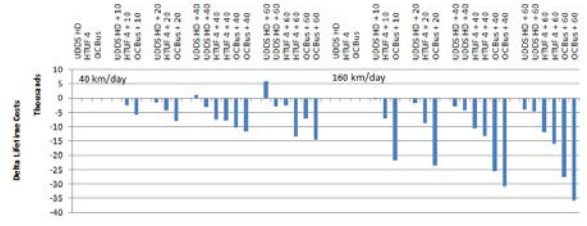

Figure 16. Gasoline PHEV, future scenario, replacements

Cost Breakdown

A stacked column chart aids in understanding how these costs add up.Figure 17 illustrates the cost breakdown for the diesel plug-in hybrid vehicle operated 160 km/day under the current scenario. It's in agreement with the results in Figure 11 and Figure 12. For the 12.5 kWh battery, all the scenarios without a battery replacement paid back while out of the scenarios with a battery replacement only the OC Bus paid back.

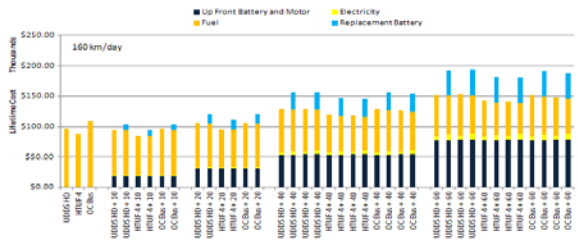

Figure 17. Diesel PHEV, current scenario

Cost Effectiveness

One of the benefits of adding an electric drive train is fuel savings. In Figure 18–Figure 21, fuel savings and cost effectiveness are plotted for the above scenarios. The scenarios where the PHEV was less expensive than the diesel conventional are identified by a negative investment per liter saved. As expected, the longer the distance traveled, the greater the fuel savings and the lower the cost/higher the savings per liter saved.

Figure 18. Diesel PHEV, no replacement

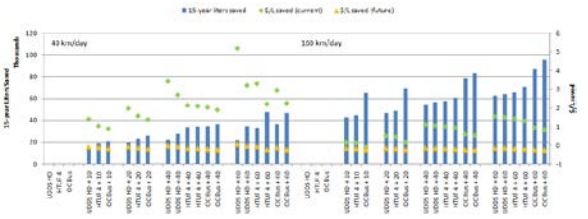

Figure 19. Diesel PHEV, replacement

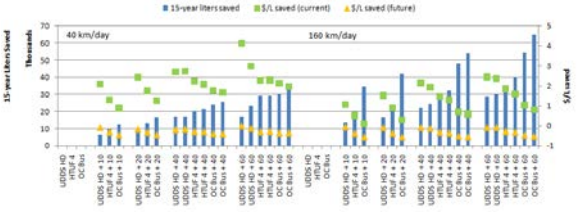

Figure 20. Gasoline PHEV, no replacement

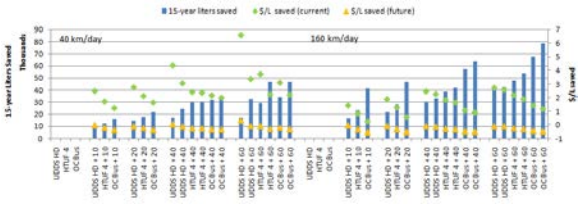

Figure 21. Gasoline PHEV, replacement

Conclusions

This study evaluated a gasoline and a diesel plug-in hybrid vehicle to determine when a plug-in is a good value in comparison to a conventional diesel parcel delivery vehicle. If battery costs meet USABC's long-term goals for advanced batteries for electric vehicles, plug-in hybrid vehicles could be cost effective. Under present-day cost assumptions of $700/kWh of battery energy and $3/gal fuel, PHEVs are generally not cost effective. With the future cost treatment of $100/kWh and $5/gal, plug-in hybrids are cost effective. It is also not cost effective to design the battery to be replaced during the life of the vehicle unless battery costs go down. A higher motor power was effective in those scenarios that included a battery replacement, or in those cases with no replacement where the drive cycle was kinetically intense and traveled enough miles to recoup the extra cost through hybridization fuel savings (from regenerative braking, etc.). The results show that kinetic intensity and distance traveled are important considerations when trying to evaluate if a plug-in hybrid vehicle is a good investment. Under the current scenario with no battery replacement, the plug-in hybrids that were cost effective traveled distances exceeding 160 km per day to pay off the additional 12.5 kWh battery cost on the UDDS HD, HTUF 4, and OC Bus cycles. For these simulations, the cost savings is greatest on the most kinetically intense cycle—the OC Bus cycle. This study does not include a hybrid discount for brake maintenance costs. The Fleet Testing and Evaluation Team observed roughly a doubling of brake life on most fleets. Future refinements could change the results of this study.

References

1. Robb A. Barnitt, Aaron D. Brooker, and Laurie Ramroth. Model-based analysis of electric drive options for medium-duty parcel delivery vehicles. Preprint. Conference Paper NREL/CP-5400-49253. December 2010. Available online at http://www.nrel.gov/docs/fy11osti/49253.pdf .
2. Michael O'Keefe, Aaron Brooker, Caley Johnson, Mike Mendelsohn, Jeremy Neubauer, and Ahmad Pesaran. Battery Ownership Model: A Tool for Evaluating the Economics of Electrified Vehicles and Related Infrastructure. Preprint. Conference Paper NREL/CP-5400-49127. January 2011. Available online at http://www.nrel.gov/docs/fy11osti/49127.pdf .
3. U.S. Energy Information Administration, Annual Energy Outlook 2011, Table 20, Energy Prices by Sector and Source, United States, Reference Case. Current 2011, Future 2030. http://www.eia.gov/forecasts/aeo/topic_prices.cfm. Direct Link http://www.eia.gov/oiaf/aeo/tablebrowser/aeo_query_server/?event=ehExcel.getFile&study=AEO2011&region=1-0&cases=ref2011-d020911a&table=3-AEO2011&yearFilter=0
4. United States Council for Automotive Research LLC. Electrochemical Energy Storage Tech Team. Energy Storage System Goals. USABC Goals for Advanced Batteries for EVs. http://www.uscar.org/guest/view_team.php?teams_id=11

V.O.3. Products

Publications

Ramroth, L., Gonder, J. and Brooker, A. "Medium-Duty Electric Drive Vehicle Simulation and Analysis." Submitted to The 26th International Battery, Hybrid and Fuel Cell Electric Vehicle Symposium and Exposition (EVS-26).

Tools & Data

Renewable Fuels and Lubricants Laboratory (ReFUEL) test data
(Matthew.Thornton@nrel.gov)

Future Automotive Systems Tool, FAST
(Aaron.Brooker@nrel.gov)

V.P. Analysis of Battery Wear Using Real-World Drive Cycles and Ambient Data

Jeff Gonder (Principle Investigator), Eric Wood, Jeremy Neubauer, Aaron Brooker, and Kandler Smith
National Renewable Energy Laboratory (NREL)
1617 Cole Boulevard
Golden, CO 80401-3393
(303) 275-4462; Jeff.Gonder@nrel.gov

DOE Activity Manager: David Anderson
(202) 287-5688; David.Anderson@ee.doe.gov

V.P.1. Abstract

Objective

- Model and interpret sensitivity of battery wear to variations in ambient conditions, consumer behavior, and vehicle design.

Approach

- Leverage existing strengths at NREL in both vehicle systems analysis and energy storage research including battery life modeling, thermal modeling of light-duty passenger vehicles, and modeling of advanced powertrains.
- Support modeling efforts with real-world data including drive cycles, distribution of travel patterns, and historical meteorological data.
- Focus analysis on markets where large hybrid electric vehicle populations indicate a tendency towards early adoption of advanced vehicle technology.

Major Accomplishments

- The wear characteristics of a battery electric vehicle and plug-in hybrid electric vehicle have been analyzed subject to ambient temperature profiles and solar loads in 100 markets identified as early adopters of advanced vehicle technology.
- The effect of depth-of-discharge control limits for a wide range of pack design scenarios has been quantified in terms of resistance growth and capacity loss after 8 years of simulated in-vehicle use.
- Contributions of calendar and cycling fade have been identified for vehicles subject to extreme usage conditions relative to vehicle miles traveled, charge pattern, and driving aggression.

Future Activities

- Further quantify ability of ambient conditions to impact both battery life and day-to-day utility to understand the ability of active thermal management to maximize petroleum displacement potential.
- Develop viable V2G usage scenarios that increase the value proposition of electric vehicle technology both to the consumer and to the electric grid.
- Incorporate additional longitudinal travel data to identify consumer attributes most favorable to electric vehicle utility and battery life.

V.P.2. Technical Discussion

Introduction

Plug-in electric vehicles (PEVs) are an advanced vehicle technology capable of reducing liquid petroleum consumption by storing and using energy from the electric grid in an on-board battery. Widespread adoption of PEVs hinges on the ability of OEMs to accurately predict battery life in order to produce durable vehicles at a

reasonable price. Unfortunately, battery life in PEVs is inherently variable with factors such as ambient temperature, vehicle miles traveled (VMT), and charging behavior all interacting to produce potentially disparate power and energy fade rates. In terms of vehicle design, battery wear is also sensitive to depth-of-discharge (DoD) and pack thermal management. The degree to which these design and usage conditions impact battery wear rates and the variability of wear rates is explored.

Approach

In order to explore the sensitivity and variability of battery wear rate in PEVs to various parameters, a predictive battery wear model developed by the National Renewable Energy Laboratory (NREL) was implemented [1]. The life model is informed by vehicle powertrain and battery pack thermal modeling capabilities developed internally at NREL. By leveraging these existing capabilities, it was possible to capture the effects of drive-cycle-based loading and ambient conditions on battery wear rates in a predictive and robust method. An overview of this integrated approach is provided, followed by an explanation of various design and usage scenarios examined.

Battery Life Model

Battery aging is caused by multiple phenomena related to both cycling and calendar age. Battery degradation is accelerated with the DoD of cycling, elevated temperature, and elevated voltage exposure, among other factors. At the battery terminals, the observable effects of degradation are an increase in resistance and a reduction in capacity. These two effects can be correlated with power and energy loss that cause battery end-of-life in an application.

In the present model, resistance growth and Li-capacity loss are assumed to be proportional to the square-root of time, $t^{1/2}$, typical of diffusion-limited film-growth processes [2]. Cycling-driven degradation is assumed to be proportional to the number of cycles, N. Cell resistance growth due to calendar- and cycling-driven mechanisms are assumed to be additive:

$$R = a_o + a_1 t^{1/2} + a_2 N \qquad (1)$$

Cell capacity is assumed to be controlled by either loss of cyclable Li or loss of electrode sites,

$$Q = \min(Q_{Li}, Q_{sites}) \qquad (2)$$

where

$$Q_{Li} = b_o + b_1 t^{1/2} \qquad (3)$$

$$Q_{sites} = c_o + c_1 N \qquad (4)$$

Models (1), (3), and (4) are readily fit to a resistance or capacity trajectory measured over time for one specific storage or cycling condition. Using multiple storage and cycling datasets, functional dependence can be built for rate constants $a_1(T, V, DoD)$, $a_2(T, V, DoD)$, $b_1(T, V, DoD)$, $c_1(T, V, DoD)$.

FAST Vehicle Model

Vehicle modeling was performed using a high-level tool developed by NREL known as FAST (Future Automotive Systems Tool). Analysis focuses on two midsize vehicle platforms: a battery electric vehicle with a nominal range of 75-mi (121-km) (BEV75) and a plug-in hybrid electric vehicle with 35-mi (56-km) of nominal charge depleting (CD) range followed by charge sustaining operation via a gasoline fueled internal combustion engine (PHEV35). Table 1 summarizes the platform and component parameters selected for the BEV75 and PHEV35 models, which are roughly similar to the configuration of the production Nissan Leaf and Chevrolet Volt, respectively[7] [8].

Table 1. FAST vehicle model inputs (baseline values).

	BEV75	PHEV35
Drag Coefficient (C_d)	0.29	0.28
Frontal Area (m^2)	2.27	2.13
Vehicle Mass (kg)	1663	1850
Engine Power (kW)	NA	53
Motor Power (kW)	80	45
Battery Capacity (kWh)	24	16
Battery Thermal Management System	No active cooling	Liquid cooling
Accessory Load (W)	300	300

Vehicle Thermal Model

In order to correlate ambient conditions to battery temperature, a detailed thermal vehicle model was implemented. Based on previous analysis done by NREL on a Toyota Prius [9], the thermal model captures both heating due to ambient temperature profiles and solar loading (see Figure 1). These inputs are merged with battery internal heat generation profiles during driving and charging to calculate average battery temperature over the course of a 24 hour period. In addition to passive-heat-transfer-to-ambient, the PHEV35 battery pack is equipped with an active thermal management system (TMS) capable of maintaining battery temperature within a desired band when driven or plugged-in. An active TMS was used to mitigate the effects of greater heat generation rates and smaller thermal mass in the PHEV35 pack whereas the modeled BEV75 employed passive thermal management. This methodology reflects current approaches of OEMs and provides a means for evaluating different TMS strategies.

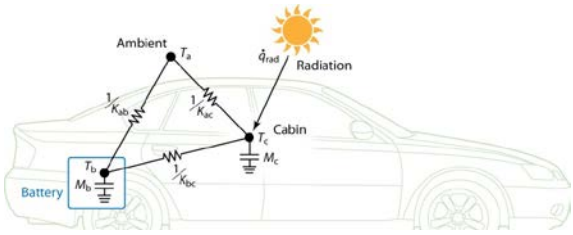

Figure 1. Vehicle thermal model employed to calculate battery temperature with respect to ambient temperature, solar loading, and thermal insulation.

Initial Sensitivity Analysis

Upon successful integration of the battery life model, vehicle model and thermal model the BEV75 and PHEV35 were run through an initial sensitivity analysis to determine the conditions under which battery wear rates exhibited the greatest variability. A matrix of location, vehicle design, and usage scenarios was implemented with the primary outputs being battery resistance growth and capacity fade at 8 years.

In terms of battery wear, the BEV75 was found to exhibit capacity fades greater than resistance growth while the PHEV35 was resistance growth dominated. Figure 2 and Figure 3 show the resulting variability of capacity loss for the BEV75 and resistance growth for the PHEV35.

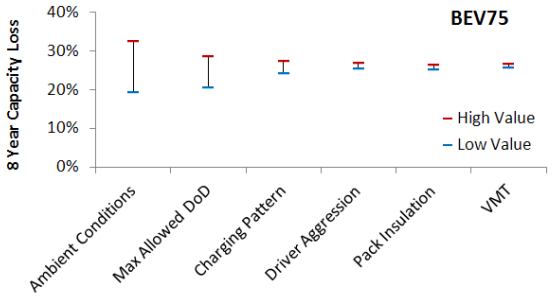

Figure 2. Battery wear sensitivity analysis for 8 year capacity loss on BEV75.

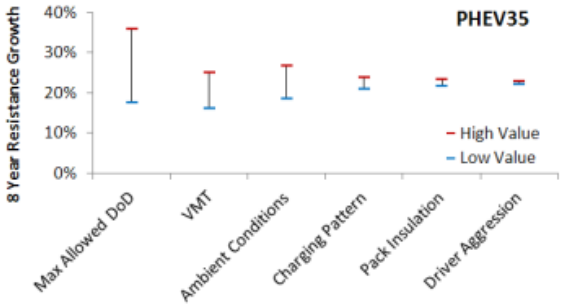

Figure 3. Battery wear sensitivity analysis for 8 year resistance growth on PHEV35.

Results

The BEV75 and PHEV35 were simulated in further detail to determine battery wear rates under the conditions outlined in Table 2.

Table 2. Tested conditions for the BEV75 and PHEV35.

BEV75	PHEV35
Distribution of US Ambient Conditions	Distribution of US Ambient Conditions
Range of DoD (80-94%)	Range of DoD (55-87%)

---	Range of VMT (5,000-20,000 mi)

BEV75 - US Ambient Conditions

Figure 4shows the capacity loss distribution after 8 years of wear for the BEV75 subject to US ambient temperatures and US average driving distributions. Capacity loss ranges from 20 to 32% subject to ambient conditions.

Wear rate variability is strongly linked to battery temperature variability. Figure 5 shows the distribution of yearly average battery temperatures experienced by the BEV75. Pack temperature in the BEV75 was found to be greater than or equal to ambient temperature in the absence of an active TMS. The BEV75 battery pack is heated above ambient due to solar loading and internal heat generation during driving and charging.

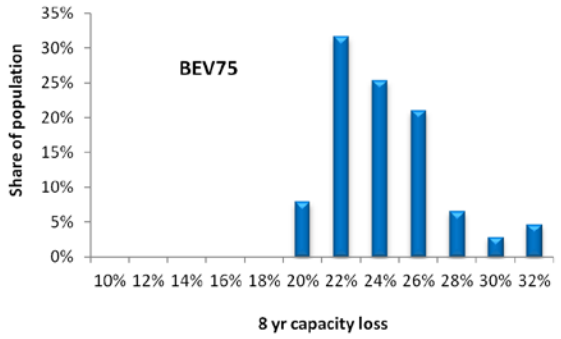

Figure 4. Distribution of 8 year capacity loss for BEV75 exposed to US ambient and national average driving distributions.

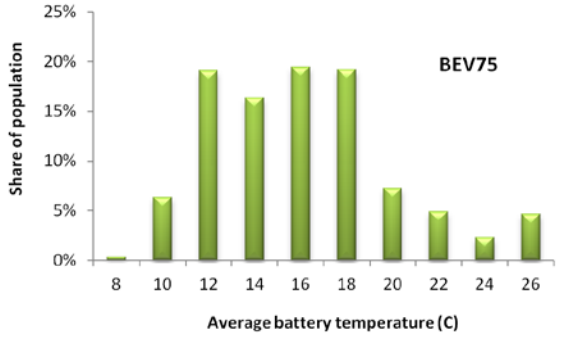

Figure 5. Distribution of average yearly battery temperatures for BEV75 exposed to US ambient conditions and national average driving distribution.

At the vehicle level, capacity fade causes the BEV75 range to decrease with age and use. On average the BEV75 is able to achieve just under 50,000 miles over its first 8 years of operation. VMT calculations for the BEV75 assume one charge per day and do not include driving days in the NHTS distribution where the total daily distance is greater than the vehicle range. These assumptions represent a conservative, near-term outlook. Alternate scenarios considering distributed charging, DC fast charging, or battery swapping would reflect greater utility for the BEV75.

BEV75 - Depth-of-discharge

Battery wear rate is sensitive to both DoD and maximum SOC allowed by the battery management system. This sensitivity was explored using the life model by simulating wear rates for a number of battery sizes in the BEV75 architecture. All battery sizes allowed the vehicle to discharge 21.6 kWh of energy from the battery and achieved consistent range, acceleration, and efficiency values to within ±1% of the nominal vehicle design. Figure 6 shows resistance growth and capacity loss at 8 years for multiple battery sizes subject to ambient conditions in Los Angeles, CA.

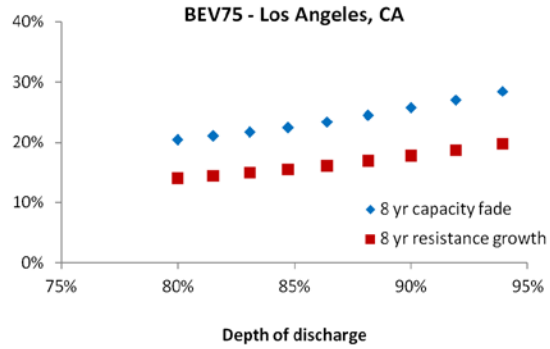

Figure 6. 8 year resistance growth and capacity fade for BEV75 exposed to ambient conditions in Los Angeles, CA.

As expected, wear can be seen to increase as the DoD window is expanded to maintain range for smaller battery packs. Increasing the maximum allowable DoD of the pack from 80 to 94% causes 8 year resistance growth and capacity fade to increase by 6 and 8% respectively.

Using a near term battery cost assumption ($700/kWh production cost [14]) the 94% DoD scenario represents a BOL pack cost savings of

$700 while the 80% DoD design increases cost by $2100 (both relative to the 90% DoD pack).

PHEV35 - US Ambient Conditions

The resistance growth distribution after 8 years of use for the PHEV35 subject to US ambient temperatures and average driving distributions can be seen in Figure 7. Resistance growth ranges from 18 to 26% over 8 years subject to variation in ambient temperature.

Figure 8 shows the distribution of battery temperatures experienced by the PHEV35 when exposed to US ambient conditions. By reducing average battery temperatures and minimizing the effect of ambient conditions on the battery, the active TMS in the PHEV35 allows for reduced wear rates with relatively low amounts of variability with respect to regional climate differences experienced in the US.

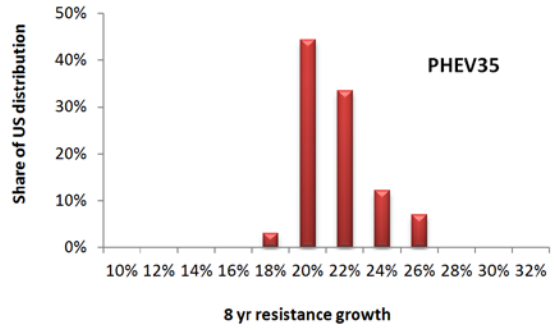

Figure 7. Distribution of 8 year resistance growth for PHEV35 exposed to US ambient and national driving distributions.

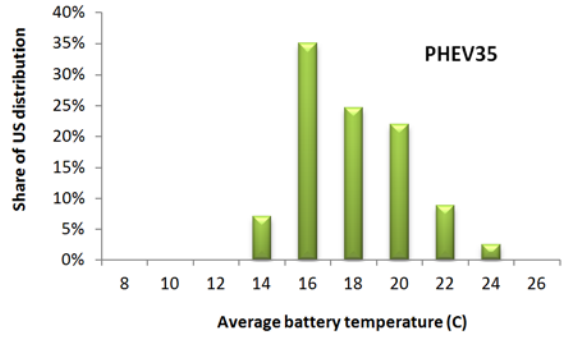

Figure 8. Distribution of average yearly battery temperatures for PHEV35 with US ambient and national driving distributions.

Additionally, the PHEV35 simulated in this analysis used a low enough DoD and experienced minimal capacity fade to allow for no loss of BOL CD range at 8 years of operation (for all US climates). This resulted in all PHEV35s achieving over 53,000 CD miles (85,600 CD km) of operation during their first 8 years.

PHEV35 - Depth-of-discharge

Battery wear sensitivity to DoD was explored for the PHEV35. All battery sizes allowed the vehicle to discharge 10.4 kWh of energy from the battery and achieve consistent CD range, acceleration, and efficiency values to within ±1% of the baseline case. Figure 9 shows resistance growth and capacity loss at 8 years for a range of battery sizes.

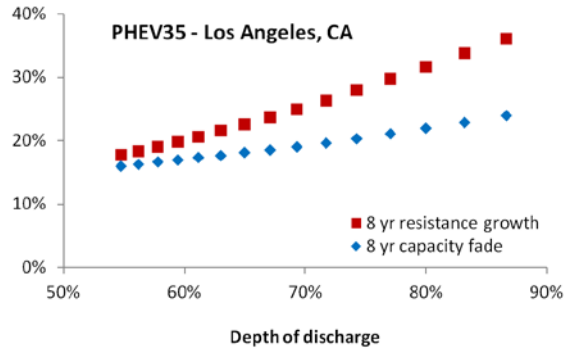

Figure 9. 8 year resistance growth and capacity loss for PHEV35 plotted against DoD.

Increasing the DoD window of the PHEV35 from 55 to 87% increased resistance growth by 18% while capacity loss increased by 8% over the same range. As the DoD window is expanded, increased resistance growth limits the power capability of the pack. Loss of pack power would be reflected at the vehicle level in an increased degree of blended electric/petroleum operation or reduced all-electric vehicle power.

The 87% DoD scenario represents a BOL pack cost savings of $2800 while the 55% DoD design increases cost by $2100 (both relative to the 65% DoD pack).

PHEV35 - Vehicle Miles Traveled

The PHEV35 was subjected to an array of annual VMT scenarios. Battery wear was calculated for annual VMTs from 5,000 to 20,000 miles (8,047 to 32,187 km*yr^{-1}). Figure 10 shows the results of this analysis in terms of resistance growth and capacity fade after 8 years subject to ambient conditions in Los Angeles, CA.

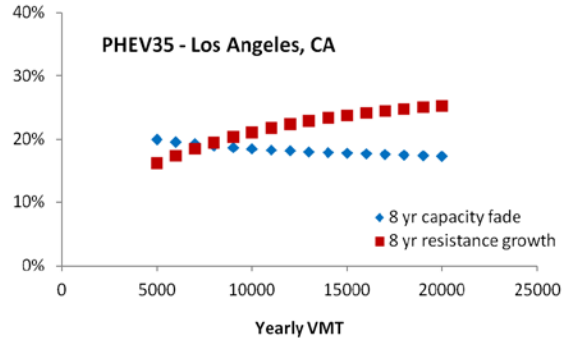

Figure 10. 8 year resistance growth and capacity loss as a function of annual VMT for PHEV35 subject to ambient conditions in Los Angeles, CA.

Increased VMT can be seen to have opposing effects on resistance growth and capacity loss in the PHEV35. 8 year resistance growth increases by 9% over the selected range of VMT while capacity fade actually decreases by 2% at high VMT.

In the life model, capacity loss is dictated by the greater of two fade mechanisms, calendar and cycling. In this case, calendar fade is the dominant mechanism driven by average daily voltage. By increasing VMT, the battery is allowed to spend greater amounts of time at lower voltages which extends calendar life and thus reduces capacity fade. While the simulated phenomena of reduced capacity fade at high VMT has not been directly validated via testing, the competing effects of calendar and cycling fade on capacity loss lead the authors to believe that the impact of PHEV VMT on capacity fade will be relatively muted.

Conclusions

Sensitivity of battery wear to ambient conditions, vehicle design, and usage patterns has been explored. Major results of this analysis include:

- The spectrum of climate and usage conditions PEVs are expected to face in the US market suggest that the assumption of a single average ambient condition for battery wear calculations may not be representative of observed behavior in the fleet.
- Ambient conditions have a large effect on battery wear for all variables considered in this study. The effects of ambient conditions on battery life can be mitigated by appropriate vehicle design. Thermal insulation and TMSs can be designed to improve fade rates for each vehicle platform.
- TMSs that employ active battery heating/cooling can significantly reduce the amount of temperature variability in the pack. The passively-cooled BEV75 experienced yearly average pack temperatures from 8 to 26 °C while the actively-heated/cooled PHEV35 battery pack ranged from 14 to 24 °C.
- DoD was found to significantly impact battery wear. Resistance growth and capacity fade were significantly reduced by designing a pack to operate with a relatively low DoD. However, pack design for low DoD can increase vehicle up-front costs by requiring additional total energy to achieve a desired CD range. For the modeled BEV75 the extra battery capacity required for a 80% vs. 94% DoD window represents a roughly $2800 increment in pack cost. For the modeled PHEV35 the extra battery capacity required for a 55% vs. 87% DoD window represents a roughly $4900 increment in pack cost. Increased battery energy may also require components such as the electric motor to be resized to maintain vehicle acceleration.
- Consumer usage behavior was found to have relatively low impact on battery wear. Both vehicle platforms saw minimal impact on battery wear due to charging pattern (end-of-day versus just-in-time) or driving aggression. Under the range-truncated NHTS national average driving distribution, the BEV75 saw negligible impact on capacity fade due to increased VMT.

Increasing VMT on the PHEV35 from 5,000 to 20,000 miles per year (8,047 to 32,187 km*yr-1) was found to decrease the percentage of CD range achievable at full power by 1%.

- It has been shown that the PHEV35 can achieve a comparable CD VMT to the BEV75 over 8 years despite the substantially longer CD range of the BEV75. This is a result of the assumption that driving trips longer than the range of the BEV75 will be accommodated by some other means of transportation. The effects of this assumption are magnified as the BEV75 experiences reduced range due to capacity loss.

Future work may focus on improving the comparison of 8 year VMT predictions for the BEV75 and PHEV35 vehicle platforms. Incorporating effects of temperature on pack internal resistance and capacity is expected to reduce the achievable VMT for BEVs in cold climates as vehicle range is compromised at low pack temperatures. Alternatively, utilizing longitudinal driving statistics (such as those developed using NREL's Transportation Secure Data Center) could allow analysis to focus on driving patterns well suited to potential BEV users and identify candidates most likely to utilize and benefit from opportunity charging. Daily distance distributions with low deviation and with averages below the range of the BEV could improve 8 year VMT projections. Additional analysis may also identify a range of potential near term V2G scenarios to investigate their impact on battery wear and achievable VMT.

References

1. National Renewable Energy Laboratory, Design of Electric Drive Vehicle Batteries for Long Life and Low Cost, Golden, CO, 2010, NREL/PR-540-48933.
2. Idaho National Laboratory, Technology Life Verification Testing, Idaho Falls, ID, 2010, INEEL-EXT-04-01986.
3. Broussely, M., "Aging of Li-ion batteries and life prediction, an update," 3rd Int. Symposium on Large Lithium-Ion Battery Technology and Application, Long Beach, California, May 2007.
4. Hall, J., Lin, T., Brown, G., Biensan, P., and Bonhomme, F., "Decay processes and life predictions for lithium ion satellite cells," 4th Int. Energy Conversion Engineering Conf., San Diego, California, June 2006.
5. Smart, M., Chin, K., Whitcanack, L., and Ratnakumar, B., "Storage characteristics of Li-ion batteries," NASA Battery Workshop, Huntsville, Alabama, Nov. 2006.
6. Broussely, M., Chap. 13 in: *Advances in Lithium-Ion Batteries,* van Schalkwijk, W., and Scrosati, B., editors. New York: Kluwer Academic / Plenum Publishers, 2002.
7. CarsDirect, Nissan Leaf Specifications, http://www.carsdirect.com/nissan/leaf/specs, retrieved on 8-25-2011.
8. GM Volt Specifications, http://gm-volt.com/full-specifications/, retrieved on 8-25-2011.
9. National Renewable Energy Laboratory Strategic Initiative Working Group Report: Thermal Model of Gen 2 Toyota Prius, Kandler Smith, Ahnvu Le, Larry Chaney.
10. National Renewable Energy Laboratory, Analysis of Off-Board Powered Thermal Preconditioning in Electric Drive Vehicles, Golden, CO, 2010, NREL/CP-5400-49252.
11. R.L. Polk & Co., https://polk.com.
12. National Renewable Energy Laboratory, National Solar Radiation Database, Typical Meteorological Year Database 3, Golden, CO.
13. 2001 National Household Travel Survey, http://nhts.ornl.gov/.
14. US Department of Energy, Office of Energy Efficiency and Renewable Energy, Vehicle Technologies Program, 2011 Annual Merit Review and Peer Evaluation Meeting, Energy Storage R&D, May 2011.

V.P.3. ProductsPublications

Wood, E., Neubauer, J., Brooker, A., Gonder, J., Smith, K., "Variability of Battery Wear in Light Duty Plug-In Electric Vehicles Subject to Ambient Temperature, Vehicle Design, and

Consumer Usage." Submitted to The 26th International Battery, Hybrid and Fuel Cell Electric Vehicle Symposium and Exposition (EVS-26).

Tools & Data

Battery Life Model
(Kandler.Smith@nrel.gov)

Vehicle Thermal Model
(Kandler.Smith@nrel.gov)

Battery Ownership Model
(Jeremy.Neubauer@nrel.gov)

Future Automotive Systems Tool, FAST
(Aaron.Brooker@nrel.gov)

Transportation Secure Data Center (TSDC)
(Jeff.Gonder@nrel.gov)

V.Q. LDV HVAC Model Development and Validation

Jason Lustbader (Principal Investigator)
National Renewable Energy Laboratory
1617 Cole Boulevard
Golden, CO 80401
(303) 275-4443; Jason.Lustbader@nrel.gov

DOE Program Managers: Lee Slezak and David Anderson
(202) 586-2335; Lee.Slezak@ee.doe.gov and 202-287-5688; David.Anderson@ee.doe.gov

V.Q.1. Abstract

Objective

- The objective of this project is to develop analysis tools to assess the impact of technologies that reduce the thermal load, improve the climate control efficiency, and reduce vehicle fuel consumption.
- To assist light-duty vehicle (LDV) modeling, the air conditioning (A/C) model framework developed in FY10 for heavy-duty vehicles will be modified to support light-duty vehicle simulations.
- This LDV A/C model will provide the basis for future development of a detailed, validated, heavy-duty vehicle A/C model.

Approach

- Develop a Matlab/Simulink-based simulation tool capable of modeling a transient vapor compression refrigeration cycle.
- Interface the A/C model with Autonomie for co-simulation of the A/C system and vehicle model.
- Model refrigerant lines and the heat exchangers as one-dimensional finite volumes, accounting for the lengthwise distribution of refrigerant and flow properties. Capture the effects of the complex flow, thermodynamics, and heat transfer on both refrigerant- and air-side. Approximate impact of oil on performance by modification of the heat transfer and pressure drop correlations during validation.
- Include all major components, such as the compressor, condenser, expansion device, evaporator, and accumulator/dryer (receiver/dryer).
- Develop a cabin thermal model to provide accurate evaporator loads and control feedback.

Major Accomplishments

- Developed a Matlab/Simulink model of a LDV HVAC system.
- A/C system components developed using one-dimensional finite volume basic line building block.
- A/C system and cabin model developed and demonstrated.
- Integration into Autonomie was demonstrated.

Future Activities

- Validate the LDV A/C model by working with industry partners.
- Add detail to the LDV A/C model as required.
- Evaluate the cabin model and determine if a simplified lumped thermal model is sufficient.
- Develop LDV A/C system simulations for several classes of vehicles (e.g., small, midsize, and SUV).

V.Q.2. Technical Discussion

Background

When operated, the A/C system is the largest auxiliary load on a vehicle. A/C loads account for more than 5% of the fuel used annually for light-duty vehicles in the United States [1]. A/C loads can have a significant impact on electric vehicle (EV), plug-in hybrid electric vehicle (PHEV), and hybrid electric vehicle (HEV) performance. Mitsubishi reports that the range of the i-MiEV can be reduced by as much as 50% on the Japan 10–15 cycle when the A/C is operating [2]. Hybrid vehicles have 22% lower fuel economy with the A/C on [3]. Increased cooling demands from the battery thermal management system in an EV may impact the A/C system. A flexible open source analysis tool is needed to assess the A/C system impact on advanced vehicles. Industry has expressed a need for both a standalone A/C system model as well as an A/C model that can co-simulate with a vehicle simulator such as Autonomie.

Introduction

The A/C system contains complex flow, thermodynamics, and heat transfer. On the refrigerant-side, the flow is transient and both compressible and two-phase. Calculating refrigerant properties near the phase transitions can also be computationally difficult.

Air flow through the condenser can vary widely depending on vehicle speed and condenser fan speed. In addition, re-entrainment of hot under-hood air is a common problem that affects heat-transfer performance. Heat is transferred from the refrigerant through the oil film and to the metal heat exchanger surface, then from the heat exchanger surface to the air.

Simulation of air flow through the evaporator must account for the condensation of water vapor from the humid air stream. The result is that the mass flow of air through the evaporator is constantly changing. The latent heat of water vapor condensation can account for a significant portion of the evaporator heat load. Heat is transferred from the air through the layer of condensed water on the heat exchanger surface to the metal of the heat exchanger, then through the oil film to the refrigerant.

A cabin model is also needed to provide a realistic load on the evaporator. The cabin model must consider all the major pathways of heat transfer into the cabin, including solar and convective loads from the environment, heat from the engine compartment, and sensible and latent heat loads in the air stream.

Approach

Matlab/Simulink was chosen as the platform to develop the model. Using this platform has several advantages. Autonomie is also built on Simulink, which will facilitate integration of the model into Autonomie. Matlab/Simulink is widely used in industry, so the standalone, open source version of the A/C model can be widely distributed.

The A/C system simulation uses control volume simulation blocks and line simulation blocks. Conservation of mass and energy is implemented in the zero-dimensional control volume blocks. Conservation of mass, momentum, and energy is implemented in the one-dimensional line simulation blocks. The mathematical description is shown in Figure 1. All refrigerant thermodynamic and material properties are determined from two-dimensional tables based on specific internal energy and density. The receiver/dryer and headers are modeled with the control volume blocks. The heat exchanger elements are modeled with the line simulation blocks. Condensation of water from air is accounted for in the evaporator model.

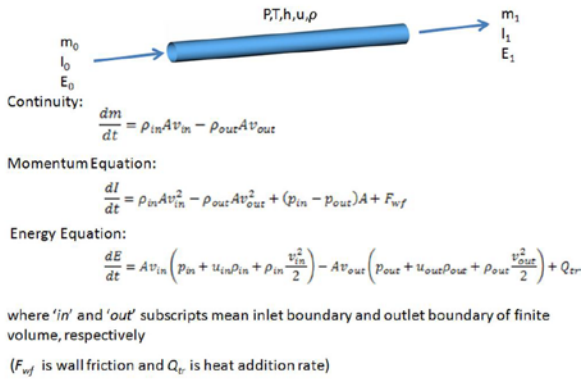

Figure 1. Conservation equations solved in refrigerant lines

A simplified cabin model was developed for incorporation with the A/C model. The model is a lumped thermal mass with inputs for the thermal loads (see Figure 2). The heat load on the cabin is based primarily on user input solar load and convective heat transfer. The evaporator load is based on ambient temperature and humidity, cabin fan speed, and cabin air recirculation rate. The cabin model includes some of the controls found in vehicles, such as fan speed and recirculation damper setting. Air properties in the cabin are re-calculated based on ambient temperature and humidity, cabin air temperature and humidity, and air recirculation rate (mix ratio). Outputs from the cabin model will determine the evaporator load in the main A/C model.

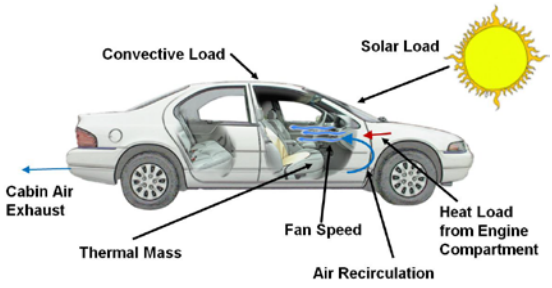

Figure 2. Vehicle cabin thermal parameters

A schematic illustrating the integration of the A/C and cabin model with Autonomie is shown in Figure 3. The blue and green lines indicate the information flow between the A/C model and the cabin model. The black lines show the information flow to and from Autonomie.

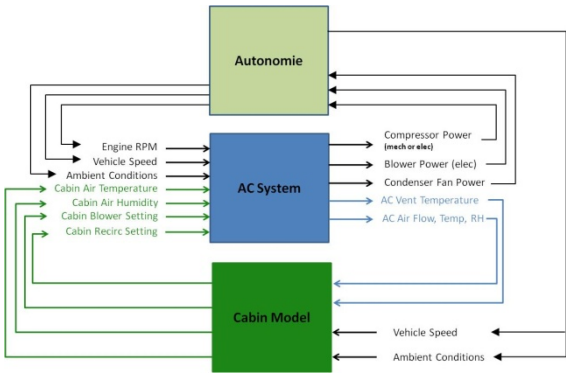

Figure 3. System integration schematic

A basic deadband temperature control and high- and low-limit pressure controls were implemented in the A/C model.

Results

The upper-level Simulink block diagram of the A/C model is shown in Figure 4, and the Simulink diagram of the A/C model and cabin model is shown in Figure 5.

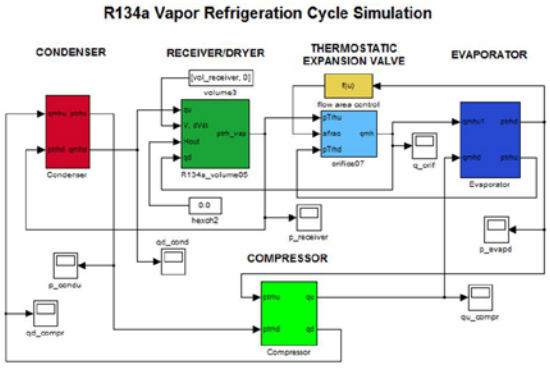

Figure 4. Top level of the Simulink A/C model

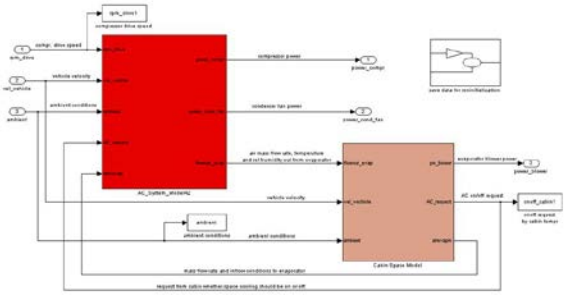

Figure 5. A/C and cabin Simulink model

The first step in evaluating any transient model is to run it in steady state mode. Without a transient boundary condition, the model can be

evaluated without the complication of dynamic effects.

Figure 6 shows a pressure-enthalpy thermodynamic diagram that was generated from the output of the steady state run. The two-phase region is the area under the black curve. As shown in the diagram, the magenta line (1-2) is the compression portion of the cycle. The compression is basically isentropic; however, an actual compressor map was used in the model. The red line (2-3) is the condensing portion of the cycle; the de-superheating region (right side, before the two-phase region) and sub-cooling regions (left side after the two-phase region) are included. The cyan-colored line (3-4) shows the expansion portion of the cycle (adiabatic expansion was assumed). The blue line (4-1) is the evaporation portion of the cycle, where the refrigerant changes from liquid to vapor while absorbing heat in the evaporator. There is a small region of superheat (right side) just before the vapor enters the compression part of the cycle. The values on the cycle diagram compare favorable to published data and diagrams for an automotive A/C system [4].

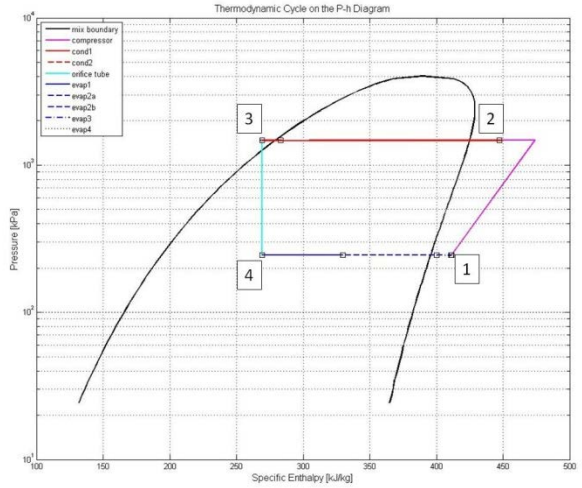

Figure 6. Thermodynamic cycle results from A/C model

After completing the steady state evaluation, the transient performance of the model was tested for various dynamic inputs. Among the inputs tested were step change and sinusoidal varying compressor speed. The model response to a step change in engine rpm is shown in Figure 7. The model response was stable and acceptable.

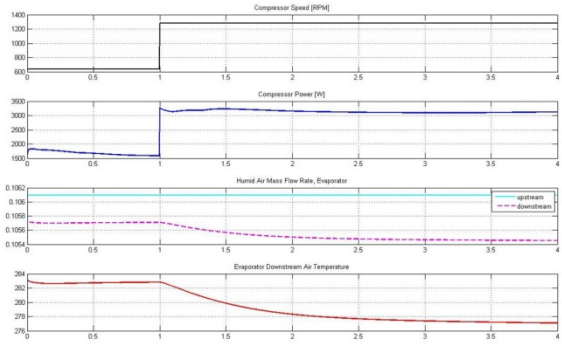

Figure 7. A/C model response to step change in rpm

The model was also tested with engine rpm and vehicle speed from a vehicle simulation of a SC03 drive cycle. The compressor power predicted by model response to the SC03 input is shown in Figure 8, and the predicted evaporator outlet air temperature is shown in Figure 9. The result of this simulation shows that the model can predict the mechanical power required to run the A/C system using a typical engine rpm as input.

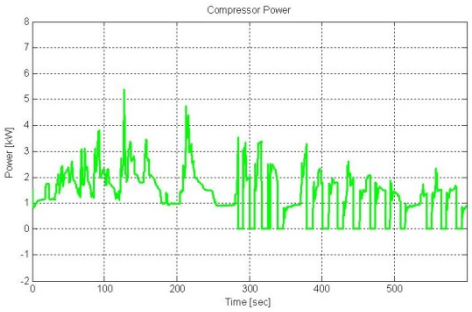

Figure 8. Compressor power during SC03 cycle.

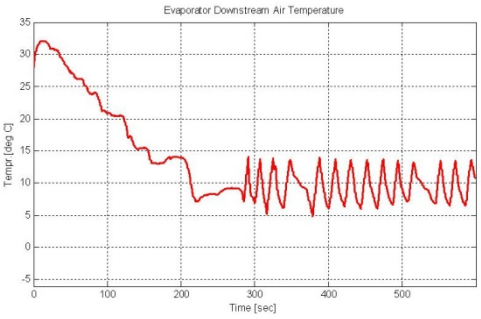

Figure 9. Evaporator air outlet temperature during SC03 cycle

The A/C model was then sent to Argonne National Laboratory for integration into Autonomie. Figure 10 shows a block diagram of

the NREL A/C model integrated into Automomie.

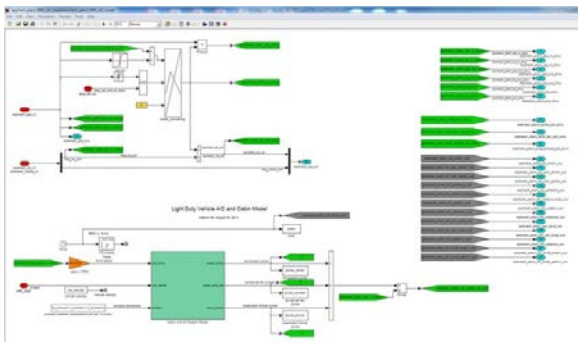

Figure 10. Integration of NREL A/C model into 'accmech block' in Autonomie

A vehicle simulation was run to test the A/C model integrated into Autonomie. The simulation used a conventional midsize vehicle on the Japan 10 mode cycle. Some of the output from the A/C model is shown in Figure 11. The first plot shows compressor rpm. The compressor rpm shows the effect of the compressor "clutching" or starting and stopping. The compressor cycles to maintain cabin temperature within a set-point band. The second plot contains the heat and work results from the simulation. The fourth plot shows the system pressure as well as the high- and low-limit setpoints. The last plot shows the evaporator air outlet temperature and the variation in the temperature due to variations in the engine rpm during the drive cycle. The A/C system was a generic mid-size automotive type not specific to any particular vehicle. However, the results of the co-simulation with Autonomie still produced realistic results. The coefficient of performance of the A/C system was approximately 2.0. For the Japan 10 cycle, A/C use resulted in a 11.4% increase in fuel consumption, and for the SC03 cycle, A/C use resulted in a 7.4 % increase in fuel consumption.

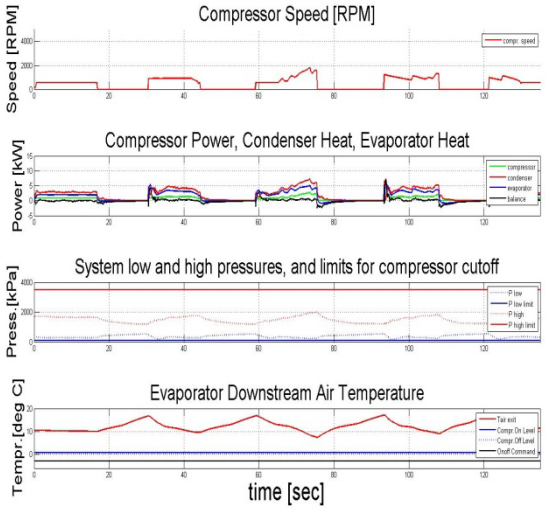

Figure 11. Result of A/C model co-simulated with Autonomie (mid-size auto, Japan 10 cycle)

Conclusions

A Matlab/Simulink model of a light-duty vehicle HVAC system was developed. The system was built up from components. The components were developed using a one-dimensional finite volume basic line building block. It is easy to change the system and components by changing the input parameters. A simplified cabin model was developed to give the A/C model realistic and dynamic boundary conditions for the evaporator. Basic system controls were implemented. A/C system performance was demonstrated over several test cases. Interface to and integration into Autonomie was demonstrated. An Autonomie vehicle and NREL A/C model co-simulation of the Japan 10 mode cycle showed realistic results with a COP of approximately 2.0 and an 11.4% increase in fuel consumption with A/C on.

References

1. Rugh et al., 2004, Earth Technologies Forum/Mobile Air Conditioning Summit.
2. Umezu et al., 2010, SAE Automotive Refrigerant & System Efficiency Symposium.
3. NREL, Vehicle Technologies Program 2007 annual report, p145.
4. Kargilis, A. Design and Development of Automotive Air Conditioning Systems.

V.Q.3. Products

Patents

Software Copyright CoolSim

Tools & Data

NREL's open source HVAC model, CoolSim, is planned for release in standalone and Autonomie software plug-in versions in FY12.

Acknowledgements

- Co-authors: Larry Chaney and Tibor Kiss (NREL)
- Additional thanks: John Rugh (NREL)

V.R. Advanced PHEV Engine Systems and Emissions Control Modeling and Analysis

Principal Investigator: Stuart Daw
Oak Ridge National Laboratory
National Transportation Research Center
2360 Cherahala Boulevard, Room L-04
Knoxville, TN 37932-6472
(865) 946-1341; dawcs@ornl.gov

DOE Program Manager: Lee Slezak
(202) 586-2335; Lee.Slezak@ee.doe.gov

V.R.1. Abstract

Objective

- Develop component models that accurately reflect the drive performance, cost, fuel savings, and environmental benefits of advanced combustion engines and aftertreatment components as they could potentially be used in leading-edge hybrid electric and plug-in hybrid electric vehicles (HEVs and PHEVs).
- Apply the above component models to help the Department of Energy (DOE) identify the highest HEV and PHEV R&D priorities for reducing U.S. dependence on imported fuels while attaining regulated pollutant emission levels.

Approach

- Develop, refine and validate low-order, physically consistent computational models for emissions control devices including three-way catalysts (TWCs), diesel oxidation catalysts (DOCs), lean NOx traps (LNTs), diesel particulate filters (DPFs), selective catalytic reduction reactors (SCRs), and other advanced catalyst technologies that accurately simulate HEV and PHEV performance under realistic steady-state and transient vehicle operation.
- Develop, refine and validate low-order, physically consistent computational models capable of simulating the power out and exhaust characteristics of advanced diesel and spark-ignition engines operating in both conventional and high efficiency clean combustion (HECC) modes.
- Develop and validate appropriate strategies for combined simulation of engine, aftertreatment, and exhaust heat recovery components in order to accurately account for and compare their integrated system performance in HEV and PHEV powertrains.
- Translate the above models and strategies into a form compatible with direct utilization in available vehicle systems simulation software.
- Leverage the above activities as much as possible through inclusion of experimental engine and aftertreatment data and models generated by other DOE activities.

Major Accomplishments

- Constructed and made preliminary parameter estimates for a computational model of a passive adsorber for exhaust hydrocarbons (HCs) and nitrogen oxides (NOx), and applied the adsorber model to simulations of HEVs and PHEVs with stoichiometric gasoline engines and TWC emissions controls.
- Enhanced a previously developed transient engine model to explicitly include thermal interactions among the engine block, coolant, and radiator, and applied the improved model to HEV and PHEV simulations.

- Evaluated the potential benefits of advanced engine combustion and aftertreatment technologies on fuel efficiency and emissions control of diesel-powered hybrid vehicles equipped with appropriate aftertreatment trains.
- Successfully translated ORNL's low-order TWC, DOC, LNT, catalyzed DPF, and transient engine models from Powertrain System Analysis Toolkit (PSAT) into the Autonomie software platform.
- Published comparisons of the simulated emissions and fuel efficiencies of diesel and gasoline hybrid electric vehicles (Proc. IMechE Part D: J. Automobile Engineering, 2011, 225(7), 944-959).
- Published a phenomenological computer model for rapidly estimating NOx and particulate emissions from advanced diesel engines operating in the partially premixed compression ignition (PCCI) mode (Fuel, 2011, 90(5), 1907-1918).

Future Activities

- This particular task is being phased out as of the end of FY 2011. In FY 2012, we anticipate continuing to utilize the aftertreatment and engine transient models developed under this task for new tasks associated with a CRADA between ORNL and Meritor and simulations of cold-start effects and control system optimization in collaboration with other national laboratories.

V.R.2. Technical Discussion

Background

Accurate predictions of the fuel efficiency and environmental impact of advanced vehicle propulsion and emissions control technologies are vital for making informed decisions about the optimal use of R&D resources and DOE programmatic priorities. Two key modeling tools available for making such simulations are the PSAT and Autonomie software platforms developed by Argonne National Laboratory (ANL) for DOE. However, the accuracy of PSAT and Autonomie simulations ultimately depends on the accuracy of the individual component sub-models or maps. In some cases of leading-edge technology, such as with engines utilizing high efficiency clean combustion (HECC) and lean exhaust particulate and NOx controls, the availability of appropriate component models or the data needed to construct them is very limited.

Oak Ridge National Laboratory (ORNL) is specifically tasked with providing data and models that enable hybrid vehicle systems simulations with advanced engines and emissions controls. ORNL has carried out many experimental measurements of emissions and fuel efficiency for advanced diesel and lean-burn gasoline engines and their associated emission control components. These data have been transformed into maps and low-order transient models that explicitly support vehicle performance simulations in vehicle simulation software such as PSAT and Autonomie.

Introduction

In FY2011, the ORNL team collaborated with ANL and Pacific Northwest National Laboratory (PNNL) to develop integrated transient engine and aftertreatment component models suitable for implementation in PSAT and Autonomie. These models were then used to generate improved simulations of emissions and fuel economy for HEVs and PHEVs powered by both stoichiometric and lean-burn engines. We concentrated our effort this year in the following specific areas:

- • Construction and testing of a preliminary adsorber model for simulating the performance of low-temperatue passive HC and NOx emissons control during cold-start and low-temperature transients;
- • Improvement of a transient engine heat transfer model for simulating engine-out temperature variations during cold-start and highly transient power demand conditions;
- • Generation of stoichiometric and lean gasoline engine maps from chassis

dynamometer measurements of a BMW direct-injection, spark-ignited (DISI) series 120i passenger car;

- Simulation of the potential fuel efficiency and emissions benefits of PCCI mode combustion enabled on diesel hybrid vehicles;
- Simulation of the potential emissions benefits of current commercial urea-SCR catalysts for NOx control in diesel-powered PHEVs; and
- Translation of computational models for TWC, DOC, LNT, catalyzed DPF, and engine thermal transients from the PSAT into the Autonomie simulation platform.

In addition, journal publications were issued documenting the ORNL TWC model and PCCI emissions model.

Approach

One of the greatest needs for improving simulations of advanced hybrid vehicles is to develop engine maps and models that accurately predict the varying exhaust species and temperatures emitted by engines under highly transient conditions. Such models are required to capture the effects of cold-start and/or start/stop transients on TWC devices in hybrid vehicles powered by conventional gasoline engines. In addition, to explore the potential benefits of using advanced lean burn engines in hybrid vehicles, it is necessary to have models that accurately represent the effects of both advanced combustion modes (e.g., HECC) and lean exhaust aftertreatment devices for removing NOx and particulate matter (PM).

One of the most prominent lean NOx control technologies, LNT, imposes a significant potential fuel penalty because of the need to periodically shift the engine exhaust from lean to rich to remove adsorbed nitrites/nitrates from the catalyst. The other major lean NOx control technology, urea-SCR, requires precise control of a urea dosing system to provide NH_3 for reduction. Too little urea addition allows NOx to be released at the tailpipe, while too much urea addition allows NH_3 release. DPFs trap and periodically oxidize the engine particulates. Like LNTs, DPFs can also require large transients in engine operation that consume additional fuel.

Thus, simulations of advanced hybrid vehicles require computationally efficient and physically accurate models for the various types of engines and aftertreatment devices that might be employed to maximize the overall vehicle energy efficiency. The ORNL team's approach for meeting this goal centers on the following:

- Low-order dynamic models for estimating time resolved temperature and species concentrations in the engine-out exhaust;
- Efficiently integrated 1-D differential, transient energy balances and balances of key reactant species in the aftertreatment devices;
- Current, publicly available kinetic and physical parameter values for the catalysts and associated materials in the aftertreatment components; and
- Utilization of well-defined, simple engine and aftertreatment control strategies (typically non-optimal but consistent) for comparing different advanced hybrid vehicle scenarios.

As much as possible, we simplify the complex internal processes in aftertreatment devices to account for the dominant physics while maintaining reasonable execution speeds. For example, there are no cross-flow (i.e., radial) spatial gradients accounted for, and kinetics are defined as global rather than elementary reactions. Nevertheless, this approach appears to do a good job of accounting for the strong coupling of after-treatment devices with both upstream and downstream components.

Due to the even greater complexity of engines, our approach for transient engine modeling relies on a very coarse representation of internal engine heat transfer and highly simplified assumptions about how engine-out species change as the engine heats up. The result is expressed in the form of an experimentally parameterized transient correction term that is

applied to steady-state or pseudo-steady-state engine-dynamometer data.

As mentioned above, our engine and device control strategies used to date are highly simplified and typically based on previously published studies or strategies used in public proof-of-principle demonstrations at national laboratories. These strategies are typically not optimal and frequently rely on sensor technology that may be ideal or at least not yet commercial. Thus our intention is to address general questions about trends rather than assess specific designs.

Results

Engine Mapping. One of the important recent developments in increasing passenger car fuel efficiency has been utilization of direct-injected lean burn gasoline engines. In order to provide a basis for simulating use of this type engine in hybrid vehicles, we generated fuel consumption and emissions maps based on chassis dynamometer measurements for a BMW series 120i vehicle equipped with TWC and LNT. The data used for generating the maps are publicly available from the CLEERS website (www.cleers.org). The resulting engine maps are partitioned into lean-stoichiometric operation and rich-stoichiometric operation sections. This particular engine operates lean at low speed and load and switches to rich combustion for LNT regeneration. At higher speed and load, the engine operates stoichiometrically and relies on the TWC for emissions control.

Component Models Development. Cold starting and intermittent operation are major concerns in meeting HEV and PHEV emissions and fuel consumption targets. To account for the associated engine thermal transients, we constructed a discretized engine heat transfer model to obtain better estimates of engine exhaust temperatures under arbitrary transient conditions. The model explicitly accounts for thermal interactions among the engine block, coolant, and radiator. The model has been calibrated with chassis dynamometer data supplied by ANL for a G2 Prius gasoline PHEV operating over a UDDS cycle beginning with a -7°C cold start. Figure 1(a) illustrates the agreement among the measured engine coolant temperatures and our calibrated heat-transfer simulation. Figure 1(b) compares the experimental and simulated exhaust temperature for the -7°C case. The experimental overall fuel economy was 33.4 mpg compared to 34.2 for our simulation. Using this same model, we made similar predictions of fuel consumption for the 20°C cold start data from ANL. In the latter case, our predicted fuel consumption is within 1% of that observed.

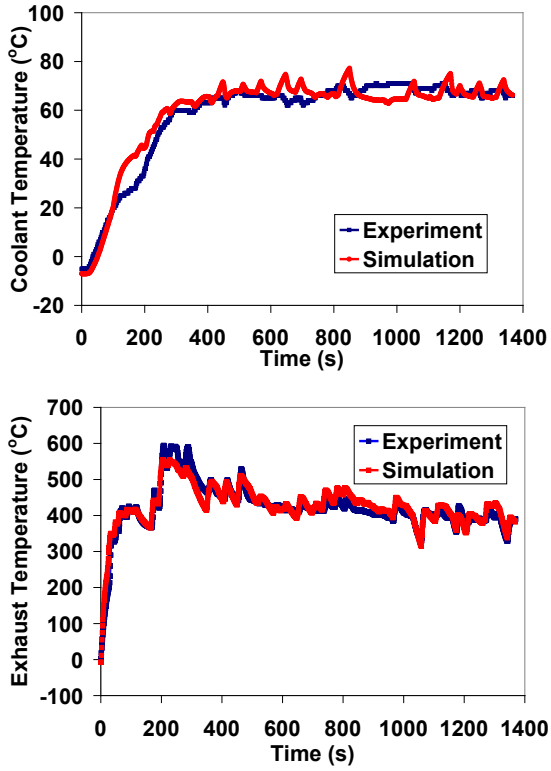

Figure 1. Comparison between predicted and measured coolant temperature and exhaust temperature for the PHEV Prius with a cold start at -7 °C.

We also developed a physically-based model for passive adsorber device to remove HC and NOx emissions during engine transients. Such passive adsorbers utilize low-cost adsorber materials (such as Ag-Beta-zeolite) to trap engine-out emissions temporarily at lower temperatures and then release them for removal by downstream catalytic devices after the aftertreatment train has become sufficiently heated. This type of trapping could become critical for HEVs and

PHEVs since the majority of their emissions are likely to occur during cold-starts and engine stop and restart. Preliminary estimates of the key kinetic parameters have been included in the current trap model based on data from ORNL and the open literature.

To illustrate how passive adsorbers might be combined with TWCs for emissions control in gasoline HEVs/PHEVs, we implemented PSAT simulations of a passenger HEV and PHEV operating over a UDDS drive cycle after a cold start. Because our sorbent parameter data are still quite limited, it is not appropriate to draw strong conclusions about the quantitative impact predicted by these simulations. But it is clear that HC emissions could be significantly reduced with the proper choice of sorbent materials as illustrated in Figure 2. We speculate that similar reductions of NOx might also be possible. Such emission controls are especially attractive because they do not involve any direct fuel penalty or require any change in engine operation. The sorbent materials currently available are also very inexpensive compared to conventional catalysts.

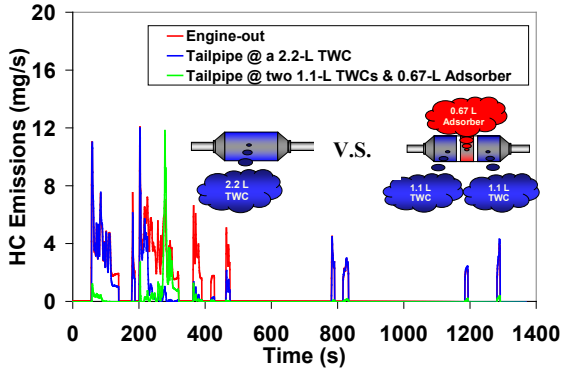

Figure 2. Comparison of simulated HC emissions from a hypothetical gasoline PHEV with a TWC operating over a UDDS cycle both with and without a passive adsorber.

Accurate predictions of the impact of advanced combustion modes on emissions are required in order to assess the potential for these modes to be effectively used in hybrid vehicles. To help facilitate such simulations, we developed a low-order combustion model for predicting NOx and PM engine-out emissions for simulations of diesel-powered HEVs and PHEVs with PCCI enabled. The combustion model was designed to estimate NOx and particulate emissions with minimal computational overhead, making it suitable for interpolating and extrapolating diesel engine emissions maps where experimental data for advanced combustion modes are limited or not available. As illustrated in Figure 3, the model estimated details about in-cylinder combustion trajectories to determine final NOx and particulate levels in the engine-out exhaust.

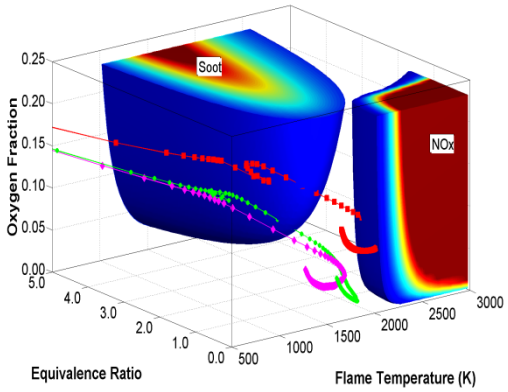

Figure 3. Predicted in-cylinder combustion trajectories from the low-order diesel combustion model. Red symbols track the progress of conventional diesel combustion, green symbols track high dilution diesel combustion (HDC), and pink symbols track to PCCI.

We further studied the potential effect of PCCI on a conventional passenger diesel vehicle and a diesel-powered HEV in terms of fuel economy and emissions. To account for emissions controls, we also included a complete aftertreatment train with a DOC, LNT, and catalyzed DPF. Based on current information, PCCI can only be utilized at low speeds and loads in a dual-mode strategy, as illustrated in Figure 4. At high speeds and loads, current engine technology still requires operation with conventional diesel combustion. Thus the PCCI mode can only be used intermittently during a typical drive cycle.

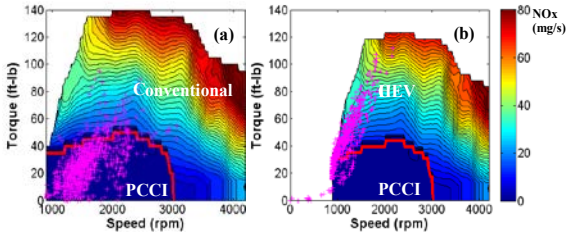

Figure 4. Engine speed-load map illustrating opportunities for PCCI utilization during a UDDS driving cycle for (a) a standard (non-hybrid) passenger vehicle and (b) an equivalent size HEV. Pink crosses correspond to engine operating points. Solid colors correspond to engine-out NOx levels.

The results indicate that PCCI can significantly improve fuel economy in the conventional vehicle by decreasing LNT and DPF regeneration frequencies. However, PCCI appears to provide less benefit for the HEV because PCCI is only rarely accessible over the drive cycle. These results illustrate the importance of extending the PCCI speed-load range and optimizing the engine size to maximize PCCI opportunities.

Recent developments in lean NOx control technology indicate increasing reliance on urea-based SCR. We simulated a diesel-powered PHEV equipped with a DOC and urea-SCR based on recent commercial Cu-zeolite SCR catalyst parameters from PNNL's analysis of bench reactor measurements made at ORNL with the CLEERS SCR transient protocol. Our simulations indicated that this particular SCR catalyst should be able to achieve 76%-85% NOx reduction for the baseline PHEV case. The upstream DOC was predicted to significantly improve SCR performance by converting exhaust NO to NO_2, but it also slowed the SCR catalyst light-off due to added thermal inertia. Addition of insulation to the SCR catalyst reduced its sensitivity to cold-start and improved NOx and NH_3 slip control (see Figure 5).

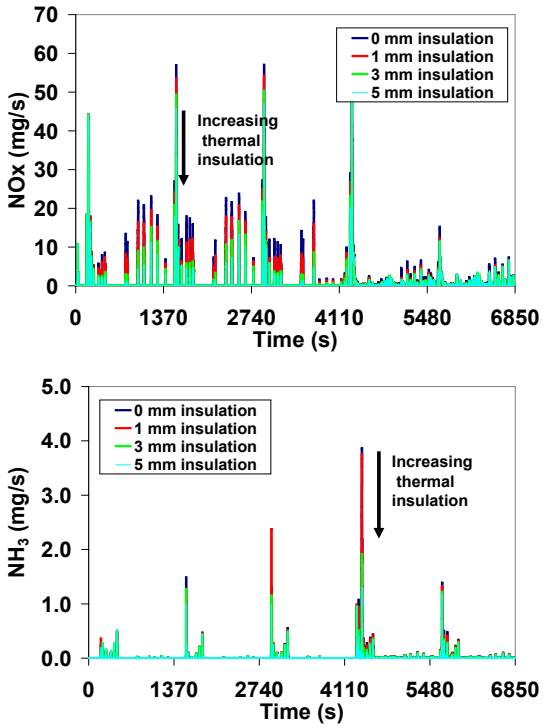

Figure 5. Illustration of the predicted impact of catalyst insulation on NOx and NH3 slip from a passenger PHEV equipped with DOC/SCR over five consecutive UDDS driving cycles beginning with a fully cold start.

Conclusions

- A preliminary device model for low-temperature passive emissions adsorption has been implemented for simulating cold-start and transient emissions control in gasoline-powered HEVs and PHEVs;
- Vehicle simulations based on the adsorber model indicate that such a device could significantly reduce HC and NOx tailpipe emissions with little or no modification to engine operation;
- A discretized engine heat transfer model has been developed to obtain improved estimates of engine exhaust temperature under cold and highly transient conditions;
- Lean and rich engine maps have been developed for the BMW direct-injected, spark-ignited series 120i engine based on vehicle chassis dynamometer measurements;
- Vehicle simulations indicate that extending the PCCI speed-load range is important for

maximizing PCCI opportunities in HEVs and PHEVs;

- Simulations of diesel-powered PHEVs with current commercial Cu-zeolite SCR catalysts indicate the catalysts can achieve 76%-85% NOx reduction;
- Addition of insulation to a PHEV SCR catalyst reduces sensitivity to cold-start and improves NOx and NH_3 slip control.
- With the completion of this project at the end of FY11, the transient engine and aftertreatment simulation tools developed to date will be transferred to newly initiated system simulations tasks associated with a CRADA between ORNL and Meritor and simulations of cold-start effects and control system optimization in collaboration with other national laboratories.

V.R.3. Products

Publications

1. Z. Gao, V.K. Chakravarthy, and C.S. Daw, "Comparisons of simulated emissions and fuel efficiency of diesel and gasoline hybrid electric vehicles," J. Auto. Eng., 2011, v225, 944-959.
2. Z. Gao, R.M. Wagner, C.S. Sluder, C.S. Daw, and J.B. Green Jr., "Using a phenomenological computer model to investigate advanced combustion trajectories in a CIDI engine," Fuel, 2011, v90, 1907–1918.
3. Z. Gao, C.S. Daw, R.M. Wagner, C.S. Sluder, and J.B. Green Jr., "Analysis of combustion trajectories of advanced combustion modes in a CIDI engine with a two-zone phenomenological model," 7th US National Technical Meeting of the Combustion Institute, Atlanta, GA, March 20-23, 2011.
4. Z. Gao, M.-Y. Kim, J.-S. Choi, C.S. Daw, J.E. Parks II, and D.E. Smith, "Cold-start emissions control in hybrid vehicles equipped with a passive hydrocarbon and NOx adsorber," Submitted to Journal of Automobile Engineering.
5. Z. Gao, C.S. Daw, and V.K. Chakravarthy, "Simulation of catalytic oxidation and selective catalytic NOx reduction in lean-exhaust hybrid vehicles," Submitted to SAE 2012 World Conference.
6. Z. Gao, C.S. Daw, K.D. Edwards, S. Sluder, and R.M. Wagner, "Effect of premixed charge compression ignition on vehicle fuel economy and emissions reduction over transient driving cycles," 2011 DOE-DEER Conference, October 3-6, 2011.
7. Z. Gao, C.S. Daw, J.A. Pihl, and M. Devarakonda, "Evaluation of 2010 urea-SCR technology for hybrid vehicles using PSAT system simulations," 2011 DOE-DEER Conference, October 3-6, 2011.
8. C.S. Daw, Z. Gao, V.K. and Chakravarthy, "Advanced PHEV engine systems and emissions control modeling and analysis," DOE Hydrogen and Vehicle Technologies Program Annual Merit Review and Peer Evaluation, May 9-13, 2011.
9. C.S. Daw, Z. Gao, V.K. Chakravarthy, and J.C. Conklin, "Development of models for advanced engines and emission control components," 2010 Annual Report to the DOE Office of Vehicle Technologies.

Patents

None

Tools & Data

Besides the models described above, an independent graphical input simulation tool for TWC has been developed for research use.

VI. COMPONENTS/SYSTEMS EVALUATION

VI.A. PHEV Powertrain Configuration and Control Strategies

Neeraj Shidore (Project Leader), Ram Vijayagopal, Aymeric Rousseau
Argonne National Laboratory
9700 South Cass Avenue
Argonne, IL 60439-4815
(630) 252-7416; nshidore@anl.gov

DOE Technology Manager: Lee Slezak

VI.A.1. Abstract

Objectives

- Investigate the effects of supervisory control strategy on plug-in hybrid electric vehicle (PHEV) fuel efficiency and tail-pipe emissions. For year 2 (2011), focus on the single-mode power-split PHEV.

Approach

- Use the Autonomie and engine-in-the-loop capabilities at Argonne National Laboratory.
- Reconfigure the supervisory control in Autonomie to integrate cold temperature operation (Oak Ridge National Laboratory [ORNL] lead) and hot temperature operation (Argonne lead) for the power-split PHEV.
- Maintain the same cold-start control strategy (developed by ORNL) throughout the study.
- With the power-split PHEV operating in the blended mode (the engine turns ON during charge-depleting [CD] operation), vary the engine ON threshold to evaluate the following under 'hot' engine conditions:
  - Impact of the engine ON threshold on trip and utility factor (UF) weighted fuel consumption,
  - Impact of the engine ON threshold on emissions, and
  - Impact on engine efficiency.
- Use the emissions-related control strategy adjustments made for the series PHEV study (year 1, 2010) for the power-split PHEV.

Accomplishments

- The key observations from the study are as follows:
  - A lower engine ON threshold (frequent engine ONs in the CD mode) results in higher engine efficiency in the CD mode of operation.
  - The impact of improved engine efficiency with lower engine ON thresholds does not translate to improved trip fuel consumption.
  - An improved engine efficiency impact can be seen in the UF weighted fuel and electrical energy consumption.
  - After the initial catalyst warm-up, the catalyst temperature remains above 'light off' for all engine ON thresholds.
  - Carbon monoxide (CO) and total hydrocarbon (THC) emissions rise with an increase in the number of engine ON events (tip-ins).
  - Nitrogen oxide (NOx) is high for the first (cold start) Urban Dynamometer Driving Schedule (UDDS) when the vehicle operates as an electric vehicle (EV) in CD mode.

Future Directions

- Incorporate the emissions-related vehicle control strategy adjustments into simulation studies.
- Combine engine-in-the-loop (impact of engine thermal effects and emissions) with the advanced thermal models in Autonomie for the rest of the powertrain, and perform studies on emissions and powertrain thermal effects.

VI.A.2. Technical Discussion

Introduction

The objective of this two-year project is to evaluate the impact of vehicle control strategy on fuel economy and emissions for a series PHEV (year 1) and a power-split PHEV (year 2). For the power-split PHEV, the thermal effects of variation in engine operation in the CD mode are evaluated, as well as the impact of these thermal effects on fuel consumption and emissions.

Power-split PHEV Specifications and Control Philosophy

The PHEV vehicle was sized by using the automated sizing routine in Autonomie. Table 1 lists the powertrain component specifications for the vehicle.

Table 1. Vehicle powertrain specifications

Parameter	Split PHEV
GVW	1859 kg
Engine	110 kW , 2.2 L SIDI engine
Electric Machine - 1 Power	70 kW peak
Electric Machine - 2 Power	45 kW peak
Battery	37 Ah
Cd	0.37
FA	2.64 m2
Tire	P225_75_R15 (0.359)
Fixed ratio	N.A
Final drive ratio	5.362

The engine size defined by the sizing algorithm is smaller than the engine actually used for the study. The actual engine is a 2.2-L, 110-kW spark-ignition direct-injection (SIDI) engine.

For the blended mode operation, the engine turns on whenever the wheel power demand at the engine is greater than a certain power threshold. In order to obtain different engine utilization scenarios for the study, this wheel power demand threshold is varied. In addition, as an additional threshold value, the vehicle is also run as an EV in the CD mode, followed by charge-sustaining (CS) operation. When the engine turns ON in the blended mode, it provides road load power demand. The battery state of charge (SOC) depletes from an initial SOC of 90% to a CS SOC of 30%. In the CS operation, the engine turns on at lower power thresholds and maintains battery SOC in addition to providing road load power.

The engine warm-up operation is ensured whenever the catalyst temperature is lower than 250 °C. The same warm-up control strategy is used throughout the experiment.

For the experiment, the vehicle is subjected to five consecutive urban (UDDS) cycles. A 10-minute soak time is allotted between each UDDS cycle, in order to emulate vehicle testing on a chassis dynamometer.

Design of the Experiment

The wheel power demand threshold for engine ON is varied in the following discrete steps: 22.5 kW, 26.25 kW, 30 kW, 33.75 kW, and 37.35 kW. In addition, as another engine ON parameter value, the vehicle is subjected to EV operation in the CD mode of operation, followed by the CS mode of operation, for the consecutive UDDS cycles.

By varying the engine ON threshold, the engine utilization varies. This impacts the engine temperature and causes differences in engine

efficiency and catalyst temperature behavior over the trip. Figure 1 details the key investigations for this study.

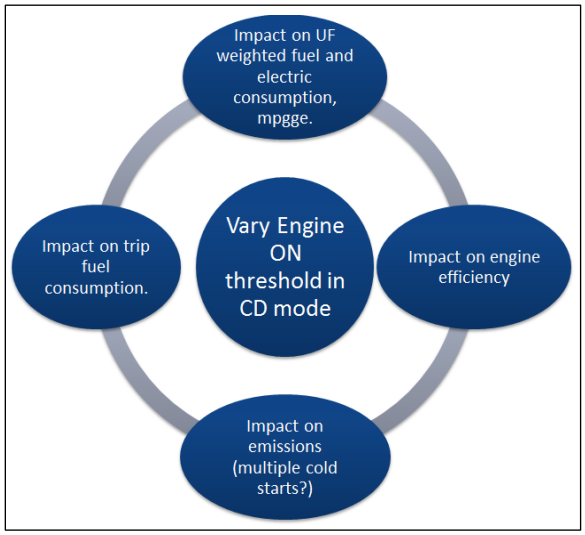

Figure 1. Design of experiment

Results and Analysis

Impact of varying engine ON thresholds on engine efficiency

With a higher engine ON threshold, the engine starts at a higher road load demand. Therefore, the higher the engine ON threshold, the more infrequent the engine ON event, and likewise, the engine temperature rise becomes slower. Low engine temperature results in lower engine efficiency as well. Figure 2 shows the engine coolant temperature for engine ON thresholds of 22.5 kW, 30 kW, and 37.5 kW. A higher engine temperature with increased engine utilization can be seen. The engine coolant temperature is around 80 °C in CS mode for all engine ON thresholds, resulting in comparable engine efficiencies.

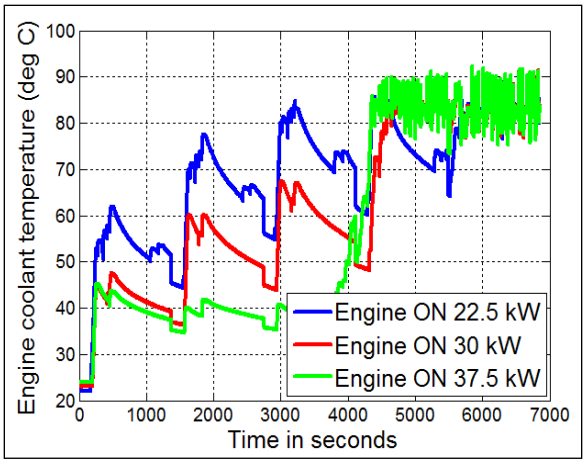

Figure 2. Engine coolant temperature for the engine ON thresholds of 22.5-kW, 30-kW, and 37.5-kW road load power

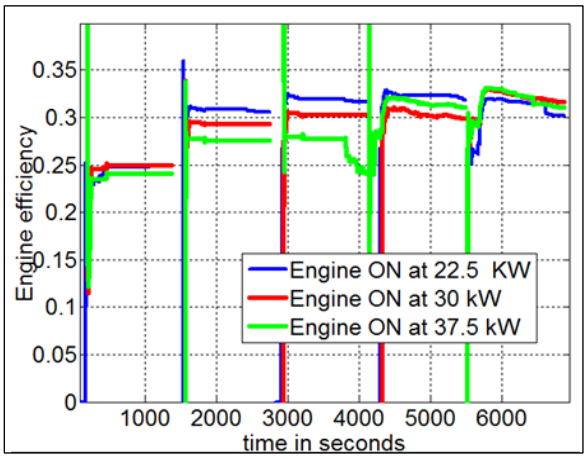

Figure 3. Instantaneous engine efficiency for the engine ON thresholds of 22.5-kW, 30-kW, and 37.5-kW road load power

Figure 3 shows the corresponding instantaneous engine efficiency for the three engine ON thresholds. The higher engine temperature indicates increased engine efficiency in the blended mode.

Impact of Varying Engine ON Thresholds on Emissions

For all the blended mode scenarios, the catalyst temperature remains above light off, resulting in no cold-start emissions beyond the first cycle. Figure 4 depicts the catalytic converter temperature for the different engine ON scenarios.

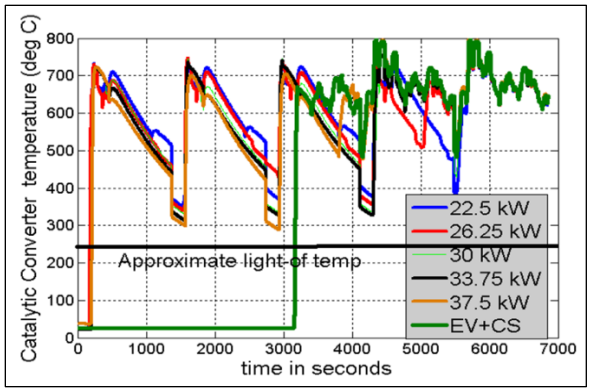

Figure 4. Catalytic converter temperature for the different engine ON thresholds

The catalytic converter temperature does not get below the approximate light-off temperature. Therefore, the cold-start control strategy, which also is used for engine re-warm-up, is not needed for any of the engine ON scenarios. Figures 5a and 5b show the CO and THC results for the cold start (first engine ON) for the different engine ON thresholds.

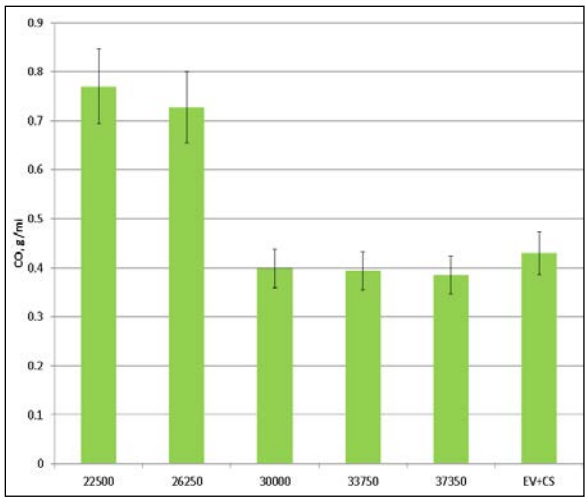

Figure 5. (a) CO emissions for the first (cold start) UDDS for the different engine ON thresholds

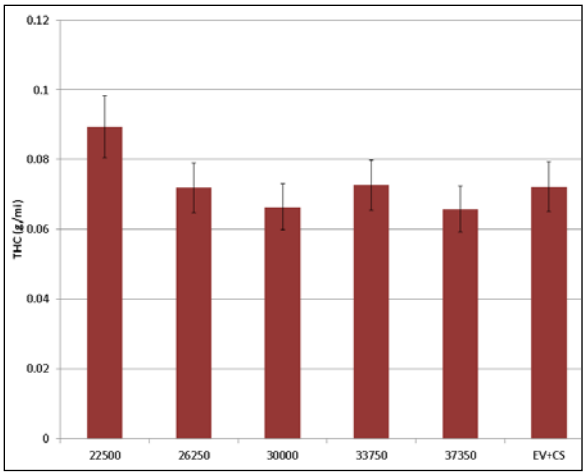

Figure 5. (b) THC emissions for the first (cold start) UDDS for the different engine ON thresholds

The CO emissions are observed at engine ON events (tip-ins). These emissions are high for the lower engine ON thresholds due to the higher number of engine ON events. The emissions for the cycles with the catalyst temperature beyond light off (second UDDS onwards) are comparable and independent of the control strategy.

Figure 6 shows the NOx emissions. The NOx emissions are high for the first engine ON for the EV+CS mode. The first engine ON for the EV+CS mode is at high engine power demand, since the engine not only supplies road load power, but also maintains battery SOC. This results in higher NOx as compared to the first engine ON for the other blended mode scenarios, where the vehicle controller has the freedom to warm-up the engine gradually with low engine power demand.

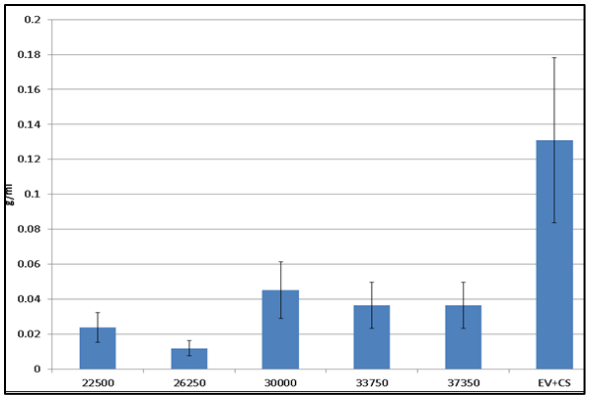

Figure 6. NOx emissions for first (cold start) UDDS for the different engine ON thresholds

Impact of Different Engine ON Thresholds on Trip Fuel Consumption

As seen previously, engine efficiency differs across engine ON thresholds due to differences in engine utilization. Figure 7 displays the trip fuel consumption for the different engine ON thresholds, where trip fuel consumption is the ratio of fuel consumed over the entire trip (five UDDS cycles) to the distance covered in the trip (five UDDS cycles). It can be seen that the trip fuel consumption for engine ON thresholds of 22.5 to 33.7 kW is within the test-to-test variation of the engine-in-the-loop set-up. Therefore, the efficiency gains shown with increased engine utilization (Figure 3) do not translate into fuel economy gains. Each cycle of the five UDDS cycles is weighted equally for the trip fuel economy consumption. Therefore, the high fuel economy consumption of the CS mode and the related higher test-to-test variation values 'wash away' any fuel efficiency improvement gained between 22.5 kW and 33.75 kW. Trip fuel consumption for the 37.3-kW and EV+CS case is much higher. For the 37.3-kW case, the engine hardly turns ON the CD mode, and it does not turn on for the EV mode. Therefore, most of the fuel consumption occurs in the CS mode, which is less efficient than the CD mode, thereby resulting in high fuel consumption for the 37.3-kW and EV+CS case.

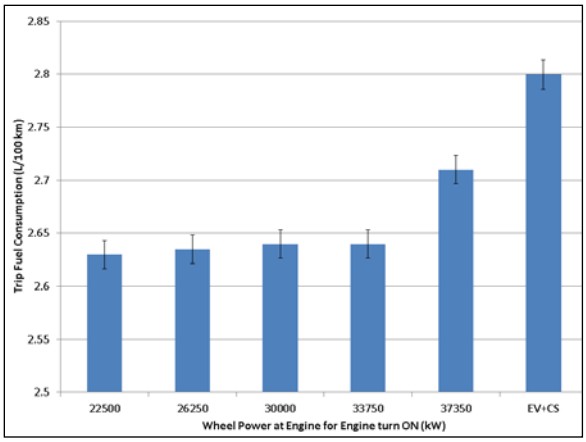

Figure 7. Trip fuel consumption for the different engine ON scenarios

Impact of Different Engine ON Thresholds on UF weighted Fuel and Electrical Consumption

A city specific, multi-day, individual UF was used for this study. Figure 8 shows UF weighted fuel consumption (L/100 km) on the Y axis and UF weighted electrical consumption (Wh/mi) on the X axis. In the figure, the solid red line connects an EV only Wh/mi (i.e., zero fuel consumption) on the X axis to a CS only (i.e., zero electrical consumption) on the Y axis. The two axes intercept points have been obtained from a simulation of the vehicle under 'hot' conditions. The blue line represents the fuel and electrical consumption for the different engine ON scenarios from the engine-in-the-loop tests. Because of the cold start, low engine efficiency operation with the real engine, the actual results are higher (for both electrical and fuel consumption) than the simulation values (red line).

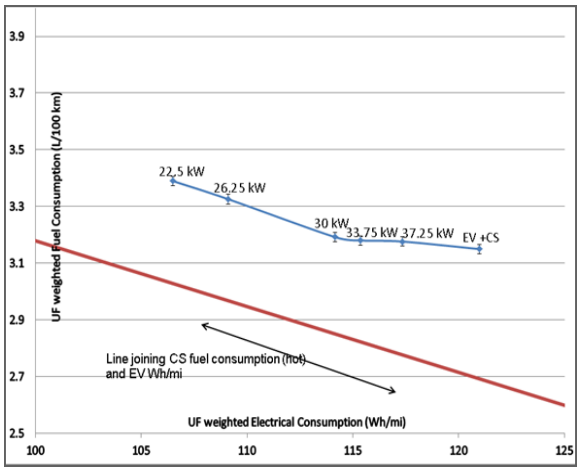

Figure 8. UF weighted fuel and electrical consumption for the different engine ON thresholds

It can be seen that the fuel and electrical consumption for the low engine ON thresholds (22.5 kW, 26.25 kW, and 30 kW) is closer to the theoretical red line, as compared to the higher engine ON thresholds — the 33.75-kW, 37.25-KW, and EV+CS scenarios. This indicates lower fuel and electrical consumption for the lower engine ON thresholds. (The red line indicates the best possible fuel and electrical consumption scenarios for different engine ON thresholds.) Since the fuel and electrical consumption is UF weighted, the initial cycles, which show the maximum difference in engine efficiency and hence fuel and electrical consumption, get the maximum weightage in the calculations.

Summary

Autonomie and engine-in-the-loop were used at Argonne National Laboratory to evaluate the impact of supervisory control strategy on a power-split PHEV. A 2.2-L SIDI engine was used as part of a small SUV. A default cold-start control strategy, developed by ORNL, was used for the study. The power-split PHEV was evaluated over consecutive UDDS cycles for different engine ON thresholds (based on wheel power demand) in the CD mode of operation. Engine efficiency, emissions, trip fuel consumption, and UF weighted fuel economy were calculated for the different engine ON thresholds.

Conclusions

1. For all engine utilization scenarios in the CD mode, the catalyst temperature remains above light off after the initial catalyst warm-up. Therefore, only cold-start emissions (first engine ON) vary between different engine ON scenarios.
2. Low engine ON thresholds, which result in frequent engine ON events in the CD mode, result in higher CO emissions due to frequent throttle tip-ins at each engine ON event.
3. The NOx is higher for the first engine ON event in the EV+CS case, since the first engine ON is at high engine load (as compared to an engine ON event in the CD mode).
4. The engine efficiency varies with engine utilization for the different CD modes of operation.
5. Improved engine efficiency for the CD mode for lower engine ON thresholds does not impact trip fuel consumption, since the difference in fuel consumption among different engine ON thresholds is insignificant (as compared to the test- to-test variation of the fuel consumption in the CS mode). The CS mode fuel consumption gets equal weightage as the CD mode for the trip fuel consumption calculation.
6. The UF weighted fuel and electrical consumption shows the impact of increased engine efficiency due to lower engine ON thresholds.

VI.A.3. Publications/Presentations

1. N. Shidore, et al., “Trade-off between Fuel Consumption and Emissions for PHEVs,” presentation at the 2010 DOE Hydrogen Program and Vehicle Technologies Annual Merit Review, June 8, 2010.
2. N. Shidore, et al., “Impact of Engine Temperature and Transient Behavior on Fuel Displacement Using Engine-in-the-Loop,” presentation to the U.S. Department of Energy, June 24, 2010.

3. N. Shidore, A. Rousseau, A. Ickes, and R. Vijayagopal, "Engine-in-the-Loop Analysis of Series and Power Split PHEV under 'Hot' Conditions," presentation to the U.S. Department of Energy, September 28, 2011.

VI.B. Investigation of Cold Thermal Modeling and Strategy Development

Principal Investigator: Forrest Jehlik, Eric Rask
Argonne National Laboratory
9700 South Cass Avenue
Argonne, IL 60439-4815
(630) 252-6403; fjehlik@anl.gov, erask@anl.gov

DOE Program Manager: Lee Slezak
(202)586-2335; lee.slezak@ee.doe.gov

VI.B.1. Abstract

Objective

- Research and quantify the effects that various ambient conditions have on the fuel consumption of advanced powertrain systems.
- Develop an ambient temperature-independent simplified methodology to predict the thermal effects on advanced powertrain fuel efficiency. The ultimate objective is to determine the amount of waste energy available under various ambient conditions that may be harnessed to increase system efficiency.

Approach

- Collect cold-weather vehicle testing data. Apply response surface methodologies to develop brake-specific fueling maps as a function of engine temperature.
- Develop a simplified, lump-capacitive thermal prediction model that does not require detailed and complex thermal modeling tools and techniques.
- Use the collected data to analyze and qualify the effects on modern advanced powertrains.

Major Accomplishments

- Collected preliminary cold weather data at the Environment Canada Cold Weather Testing Facility. (Issues with data did not allow for proper model development.)
- Sourced and procured a thermal conditioning testing cart. This cart independently controls the set point temperature of a vehicle's engine oil, as well as coolant.
- Procured a vehicle thermal testing mule, the MY11 Ford Fusion.
- Accomplished full instrumentation of the testing mule for in-depth thermal research.
- Completed the Advanced Powertrain Research Facility cold/hot facility testing upgrade.

Future Activities

- Complete baseline tests on the thermal mule testing vehicle (MY11 Ford Fusion)
  - EPA 5-cycle testing
- Conduct an in-depth thermal analysis of the powertrain system response to varied ambient conditions
- Develop a predictive model to be integrated into modeling efforts
- Investigate the ambient condition/drive-cycle coupled effects

VI.B.2. Technical Discussion

Background

Under real-world driving conditions, ambient temperature variations have a significant impact on fuel consumption (independent of drive cycle intensity). Research conducted at the Advanced Powertrain Research Facility at Argonne National Laboratory has shown variations in the fuel consumption of advanced powertrains on

the order of 40%, depending upon the ambient conditions. (This does not include creature-comfort effects.) Figure 1 displays an example of this dramatic fuel economy impact.

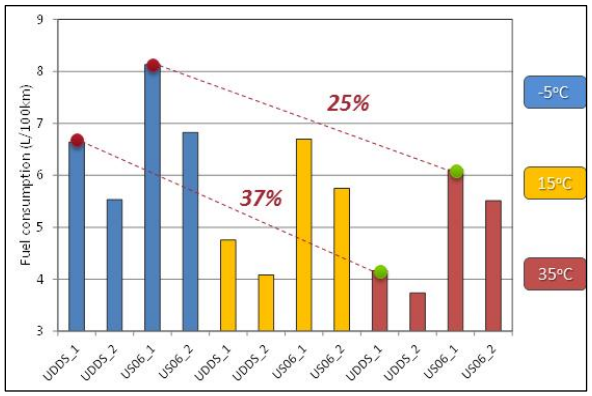

Figure 1. Gen-2 Toyota Prius: back-to-back Urban Dynamometer Driving Schedule cycle fuel consumption under various ambient temperatures

Although much effort is being applied to advancing powertrain hybridization and electrification, systems to minimize the efficiency losses of these powertrains from thermal effects are either not common or nonexistent. The first step in addressing this issue is the development of methodologies to understand the problem and to quantify the efficiency gain potential on a vehicle-systems level.

Introduction

A critical part of the DOE Office of *Energy Efficiency and Renewable Energy* plan is to develop and support technologies that displace petroleum usage. A portion of that work entails researching and benchmarking advanced powertrains, understanding their energy paths and usage, and researching methodologies to address inefficiency.

Even with the current rapid advancement of advanced powertrain technologies (i.e., hybrids, plug-in hybrids, and electric vehicles), market penetration remains very low, with the vast majority of transportation coming from fossil-fuel-powered, internal combustion (IC) engines. In order to meet the goals established by the DOE, significant benefits will be realized from addressing technologies that increase the efficiency of the IC engine (whether the configuration is standard or hybridized).

Prior to the EPA's adoption of the five-cycle testing procedure, all tests were conducted at 22 ^{o}C and above ambient temperatures. However, as shown in Figure 2, on an annual basis, most regions in the nation experience temperatures that are higher, or much lower, than these conditions.

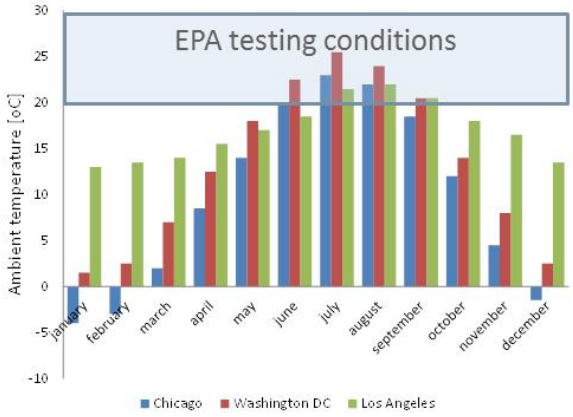

Figure 2. National seasonal temperature variations compared to traditional EPA Federal Test Procedure testing conditions.

Approach

The first step toward understanding the ambient effects of vehicle systems is to develop methodologies capable of predicting the fuel consumption of an IC engine as a function of operational temperature. Testing work was completed on a number of vehicles, and a methodology to do so was developed. The second step is to establish techniques to estimate powertrain temperature from its usage history. A first-step, lumped-capacitance technique was applied, and the results were published. However, for both steps, unresolved questions remained concerning the robustness of the technique due to a lack of available data.

To complete the first steps of developing a robust, predictive modeling capability, larger quantities of data over various drive cycles, as well as temperatures, had to be collected. Additionally, many more thermal signatures needed to be collected and analyzed to understand these effects.

To complete this work, a sufficient testing facility, a vehicle testing mule, and a fluid conditioning cart had to be designed and completed.

Mobile Thermal Testing Cart

A mobile fluid thermal conditioning cart was designed and procured that controls the engine coolant and the oil temperature by using a steady supply of facility cooling water. Additionally, heat may be added through the use of a 1.5 kW oil heater and a 3 kW coolant heater. Figure 3 and Figure 4 show the mobile thermal testing cart for this extended testing.

The engine coolant heat exchanger is a tube and shell construction sized to regulate the engine coolant temperature from 180 to 220 ºF. In series with the heat exchanger is an inline 3-kW oil heater that runs on 440 three-phase power. The heater has its own manually set thermostat. Included are a small pump and bypass loop to push coolant from the heater through the system while it is in a standby mode. The bypass loop and pump are controlled by an on/off switch from the control room.

The oil cooler also is a tube and shell heat exchanger. It is sized to remove 45 HP of heat and to control the oil temperature from 180 to 230 ºF. In series with the heat exchanger is an inline 1.5-kW oil heater that runs on 440 three-phase power. The heater has its own manually adjustable thermostat. This system has a separate oil pump to push the oil through the cooling system and back into the oil pans.

The engine coolant outlet temperature is monitored by thermocouples fitted to the expansion tank and the return coolant line. This provides the input signals to the self-contained temperature feedback controller. By controlling the exiting cooling water from the heat exchanger, the return engine coolant temperature is controlled. The oil system has a similar system.

Both controllers can supply output signals that can be monitored in the control room. The controllers can be set locally at the machine or via a signal from the control room. The systems are designed to be fail safe — cooling water will run through the system if the 110-VAC power is interrupted.

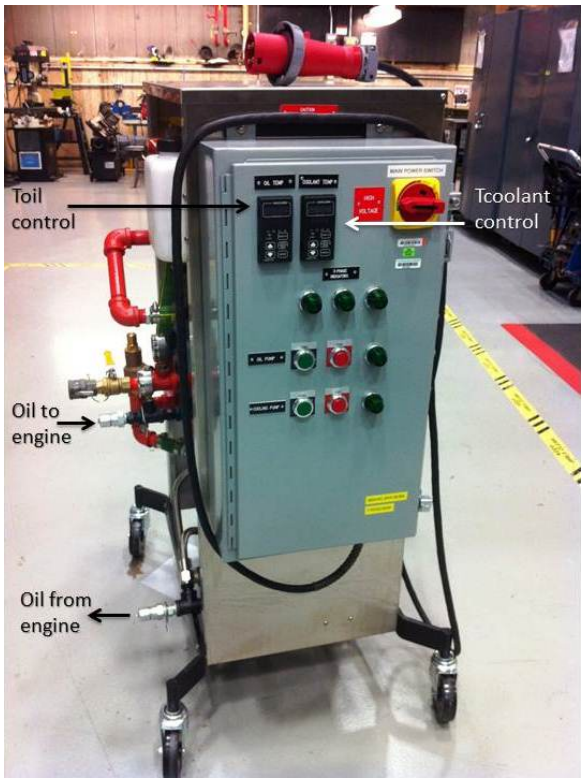

Figure 3. Thermal conditioning cart, control side.

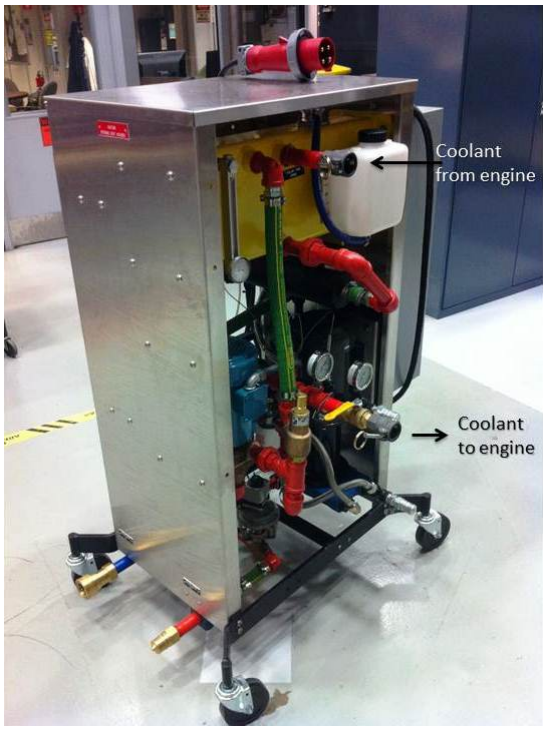

Figure 4. Thermal conditioning cart.

Ford Fusion Thermal Testing Mule

A standard four-cylinder, six-speed automatic 2011 Ford Fusion was purchased and instrumented to conduct detailed thermal research and analysis. Over 30 thermocouples were located on the vehicle to analyze energy flows at critical nodes along the powertrain. In addition, the vehicle was instrumented with flow measurement devices to enable the ability to calculate enthalpy calculations, where appropriate. Figure 5shows the test vehicle on the dynamometer at the Argonne facility.

Figure 5. 2011 Ford Fusion thermal testing mule. The vehicle is displayed in Argonne's Advanced Powertrain Research Laboratory 362 High Bay for baseline testing.

Results

Initial work was completed to develop brake-specific engine fueling maps as a function of engine operational temperature, as well as simplified oil/coolant predictive lumped-capacitance models. Two papers that outline the techniques were published (refer to the Publications section of this report). However, facilities and tools were not available to completely determine the potential to increase fuel efficiency through thermal optimization techniques over a broader range of temperatures and conditions. Additionally, best practices within the methodology were not determined.

After procuring and instrumenting the thermal test mule to further develop the methodology, baseline tests were conducted. Figure 6 and Figure 7 show signals that display several temperature profiles from a 50-mph steady state cruise, plus a 600-second cool down following the test.

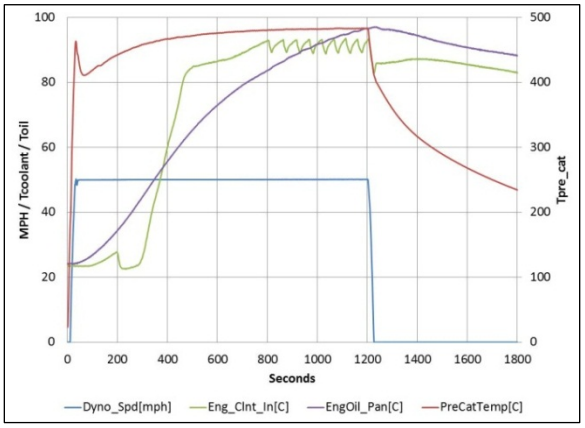

Figure 6. Steady state (50 mph) constant power thermal warm-up temperatures: coolant-in, engine oil pan, and pre-catalyst.

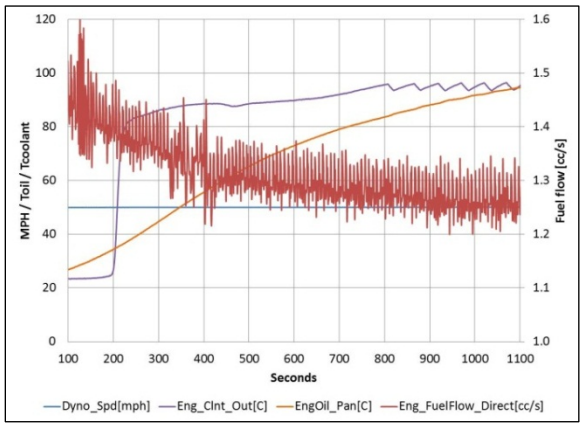

Figure 7. Steady state (50 mph) constant power thermal warm-up temperatures: coolant-out, engine oil pan, and fuel flow.

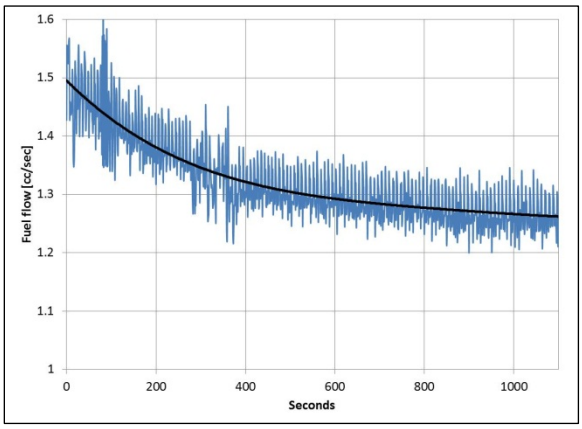

Figure 8. Average engine fuel flow: post catalytic converter warm-up. Note: as the engine warms (signified by the engine oil temperature in Figure 7), the mean fuel flow over the cycle is drastically reduced. 2011 Ford Fusion thermal testing mule: 50 mph steady state baseline data, 21 oC test cell conditions. Note: only selected temperature signals are shown out of 30 signals to demonstrate the system

From the data shown in Figure 8, it is apparent that the mean fueling rate over the cycle drastically reduces as the powertrain heat transfer reaches a steady state condition, and the fluids' viscosity decreases. This can be reviewed in Figure 6 and Figure 7. These figures highlight the potential for developing technologies and techniques to reduce real-world fuel economy over a myriad of ambient conditions. Conditioning both the oil and coolant of a vehicle occurs independent of the heat input from the engine itself. The vehicle testing mule is extensively instrumented with thermocouples, flow devices, and Controller Area Network communication in order to study the thermal effects and highlight technologies to address real-world fuel economy.

Two papers were published that detail the initial methodology of predicting the engine fueling rate as a function of its operating temperature, as well as a technique capable of predicting the temperature from the initial state. Additionally, a third paper was published that examines this technique in modeling to optimize control strategies relative to engine and battery operation. It was selected as an SAE Journal entry (refer to the Publications section of this report).

Conclusions

This project was focused on the development of an instrumented test vehicle and a means to study the effects of engine oil and coolant temperature, and control these in a manner independent of the engine's operation. The selected approach enables research methods to isolate and quantify the effects that various ambient conditions have on the fuel consumption of advanced powertrain systems. The application of a mobile fluid thermal conditioning cart has exhibited the ability to meet this need. The thermal testing cart is capable of developing an ambient temperature-independent methodology to predict the thermal effects on advanced powertrain fuel efficiency. These experiments will continue through the next year to strive for the ultimate objective to determine the amount of waste energy available under various ambient conditions that may be harnessed to increase system efficiency

VI.B.3. Products

Publications

1. "Development of Variable Temperature Brake-Specific Fuel Consumption Engine Maps," Jehlik, F., Rask, E., SAE Powertrain Fuels and Lube Conference, San Diego, CA, SAE 2010-01-218.
2. "Simplified Methodology for Modeling Cold Temperature Effects on Engine Efficiency for Hybrid and Plug-in Hybrid Vehicles," Jehlik, F., Rask, E., Christenson, M., SAE Powertrain Fuels and Lube Conference, San Diego, CA, SAE 2010-01-2213.
3. "PHEV Energy Management Strategies at Cold Temperatures with Battery Temperature Rise and Engine Efficiency Improvement Considerations," Shidore, N., Jehlik, F., Rask, E., SAE World Congress, Detroit, MI, SAE 2011-01-0872.

VI.C. Advanced HEV/PHEV Concepts Investigation

Jeffrey Gonder (Principal Investigator), Matthew Earleywine, Aaron Brooker, Joann Wang and Ahmad Pesaran
National Renewable Energy Laboratory (NREL)
1617 Cole Boulevard
Golden, CO 80401-3393
(303) 275-4462; Jeff.Gonder@nrel.gov

DOE Activity Manager: Lee Slezak
(202) 586-2335; Lee.Slezak@ee.doe.gov

VI.C.1. Abstract

Objective

- Refine three advanced concepts to increase the fuel savings and/or consumer value proposition for hybrid/plug-in hybrid electric vehicles (HEVs/PHEVs)
  - Lower-energy energy storage system (LEESS) to maintain high HEV fuel savings while reducing overall cost
  - Drive-on charging (DOC) for electrified vehicles to maximize total petroleum displacement with domestic electricity
  - Route-based control (RBC) to use information about upcoming driving to increase individual HEV/PHEV fuel economy

Approach

- Analysis
  - Investigate the HEV fuel economy impact of relaxed power targets for LEESS devices
  - Calculate fuel savings and evaluate infrastructure costs for various DOC scenarios and drivetrains
- Demonstration planning/partner coordination
  - Develop conversion plan for in-vehicle demonstration of LEESS operation in FY12
  - Initiate collaboration agreement to demonstrate RBC fuel savings in an automaker's plug-in vehicle platform in FY12

Major Accomplishments

- Demonstrated that HEVs with relaxed LEESS power requirements still achieve large fuel savings
- Quantified the fuel savings from an automatic DOC connection when parked, as well as the additional fuel savings and associated grid impacts when charging at stoplights or while vehicles are in motion
  - Identified multiple scenarios with fuel savings > 20%
  - Determined that installation costs would be significant for dynamic in-motion charging, but would be comparable to other complex road construction projects
- Secured partner support and initiated plans for in-vehicle LEESS and RBC demonstrations

Planned and Potential Future Activities

- In-vehicle demonstrations for LEESS and RBC operation
- Optimize DOC implementation strategies and consider potential automation synergies
- Conduct a detailed economic analysis of DOC scenarios

VI.C.2. Technical Discussion

Background

Hybrid and plug-in hybrid electric vehicle (HEV and PHEV) fuel savings depend on physical vehicle attributes, the size of the energy storage system (ESS) and other components, and drive cycle characteristics. PHEV fuel savings are also influenced by how often the vehicle is charged. By improving understanding of each of these attributes and better identifying and quantifying their impacts on fuel economy, it is possible to develop pathways to decrease fuel consumption on a per vehicle basis. However, if the overall goal is to decrease fuel consumption across the national fleet of vehicles, it is also essential to maximize the value of improved technologies to the consumer. In doing so, HEVs and PHEVs will achieve higher market penetration and therefore higher aggregate fuel savings. This study explores various advanced concepts for HEVs and PHEVs that could lead to increased fuel savings.

One advanced concept explored through this project was to refine HEV lower-energy energy storage system (LEESS) targets and demonstrate that large fuel savings can still be achieved with such devices. Lower-cost LEESS devices could help raise HEV market penetration and thereby increase overall fuel savings. LEESS operation will be demonstrated in vehicle hardware during FY12, as will another concept exploring the ability to improve HEV and PHEV fuel economy by using predictions about upcoming driving routes.

The final concept explored as part of this project was drive-on charging for electrified vehicles. This evaluation was motivated in part by studies of initial PHEV deployments showing that users fail to plug into an available outlet about 25% of the time [1]. A wireless or conductive charging mechanism that automatically connects to a parked PHEV could eliminate these missed charging opportunities. This project sought to begin quantifying the fuel savings from an automatic parked charging connection under various scenarios, as well as the potentially greater savings (and associated grid impacts) from using drive-on charging at stoplights or even while vehicles are in motion.

Introduction

General control strategies trading off engine and electric motor/battery operation in an HEV or PHEV will not be optimal over all drive cycles. A vehicle controller could make more optimal control decisions if it incorporates predictions about the upcoming driving route. NREL analysis has shown that such a route based control (RBC) strategy can yield fuel savings of 2% to 4% for HEVs. PHEVs could yield even higher savings, since PHEV fuel efficiency depends on driving distance as well as driving type.

While HEV technology presents a promising way to save fuel (which can be further increased with RBC), HEVs require consumers to pay a premium above the cost of a comparable conventional vehicle. To the extent that this premium can be reduced, more people may decide to purchase HEVs, which would increase their market penetration and overall fuel savings. A LEESS may present such an opportunity to reduce cost relative to traditional HEV energy storage while resulting in little or no increase in HEV fuel consumption.

One way to lower the required ESS size in a plug-in vehicle is to implement drive-on charging (DOC) systems. Such a system would increase driver convenience by automatically charging the vehicle without the driver having to plug it in. This could be done through some sort of automatic docking system or through wireless inductive charging.

In addition to potential use in drivers' garages, DOC systems could be used at stoplights or even on highways to continuously charge plug-in vehicles while they are in motion. Implementing such a system could allow smaller ESS vehicles to save as much fuel as larger ESS vehicles used without such a system. This could again help increase market penetration, and in the case of pure battery electric vehicles (BEVs) may help to eliminate range anxiety.

Approach

The remaining discussion will focus on the DOC concept evaluation since a more complete summary of the LEESS and RBC efforts will be made in FY12. To evaluate the fuel savings of different DOC scenarios, GPS travel survey data was used along with vehicle modeling and simulation software. The GPS travel survey data consisted of over 1,200 vehicle driving days collected by the Southern California Association of Governments (SCAG) [2]. Models for five different midsize vehicle powertrains were taken from a previous study [3]. The models included a conventional vehicle (CV), an HEV and three PHEVs. The PHEVs were designed to travel 10, 20 and 40 miles, respectively, on the Urban Dynamometer Driving Schedule (UDDS) before using any fuel, and were correspondingly labeled PHEV10, PHEV20 and PHEV40. Using these vehicles, three different DOC scenarios were evaluated: charging while parked, charging at stops, and charging while driving.

Results

To begin quantifying the potential fuel savings from automatic charging while parked, NREL considered the aforementioned statistic of vehicles failing to charge when they could have 25% of the time. Using the SCAG dataset, three charging scenarios were compared in which 25% of the vehicles were randomly selected to not charge as often as the rest. The different charge scenarios included: overnight charging in which the vehicle started the day with a full charge, but did not charge again the rest of the day; opportunity charging (opchg) in which the vehicles were plugged in every time they were parked; and charge sustaining (CS) in which the vehicles started the day at their CS state of charge (SOC) and never plugged in the entire day (operating simply as an HEV). Figure 1 shows three combinations of charging scenarios and their associated fuel savings for each type of PHEV. This analysis assumes a charge rate of 1.56 kW AC.

To evaluate the savings while charging at stops, new vehicle models were created to automatically charge when the vehicle was stopped. Figure 2 shows fuel savings for each vehicle at different charging rates.

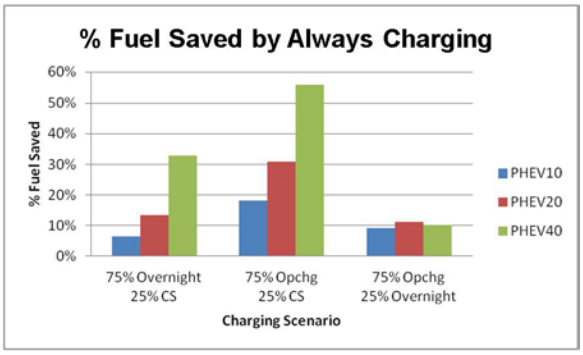

Figure 9. Percent fuel saved by getting the 25% of vehicles to charge like the other 75%.

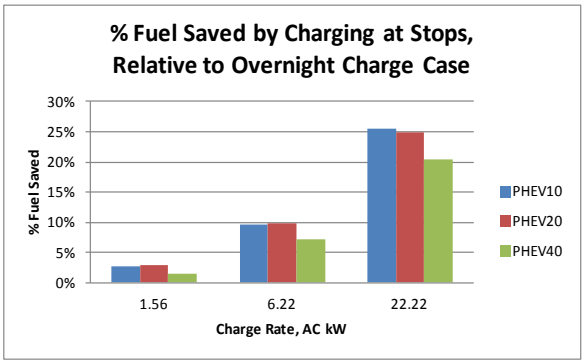

Figure 10. Percent fuel saved by charging at stops for different charging rates.

To approximate the fuel savings for charging while driving it was assumed that the vehicles could only charge dynamically on the highways. Since highways make up a small percentage of roadway but support a much larger percentage of vehicle miles travelled, they would presumably present the most cost-effective location to implement dynamic DOC. As a first pass, one could assume that the potential fuel savings equals the fuel used in highway driving without DOC. Figure 3 shows the average amount of fuel used per vehicle day during highway-type operation for each vehicle type. It should be noted that the CV is only displayed for reference as a CV would still use fuel on an electric roadway. However, it should also be noted that an electric roadway would make BEVs much more feasible and affordable as it would greatly reduce their required battery storage while also potentially eliminating electric range issues altogether. As an example, a consumer with a fairly efficient 30 mpg CV would save 400 gallons per year when switching to a BEV (assuming 12,000 miles of driving per year).

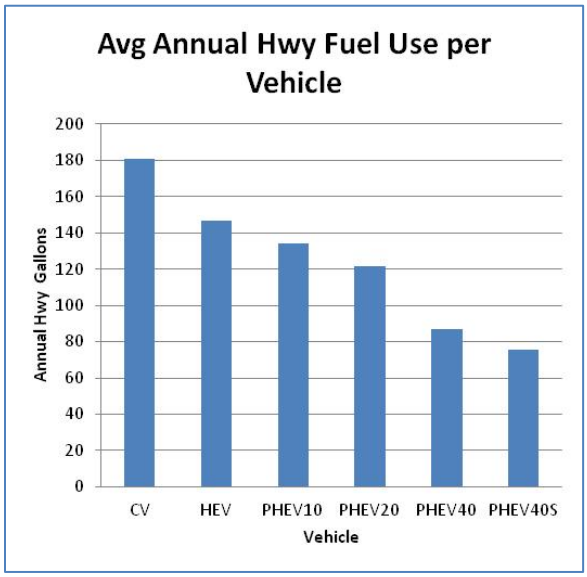

Figure 11. Average annual highway fuel use for different vehicle types, extrapolated from the real-world drive cycle simulations.

Conclusions

Avoiding missed charging opportunities and automatically charging PHEVs while parked can result in significant fuel savings (over 30% for one of the PHEV40 scenarios examined). Additional fuel could be saved by charging at stops during urban driving (one PHEV40 case showed over 20% fuel savings).

Switching from CVs to BEVs could save approximately 400 gal of fuel per vehicle per year. However, consumers are often unwilling to make this switch due to the high upfront costs and limited range of BEVs. DOC and electric highway systems can extend BEV and PHEV depleting range and allow for smaller energy storage systems which would decrease upfront vehicle costs. Even a vehicle with an HEV-sized ESS and dynamic charging capability could eliminate its fuel use on properly equipped sections of roadway.

Further analysis conducted as part of this study showed that considerable infrastructure costs would be required to install a dynamic roadway charging system, but that the costs would not be beyond the range of other complicated construction projects. While these initial findings are promising, further analysis is required to examine economic costs, benefits and feasibility in more detail.

References:

1. EERE/INL, http://avt.inel.gov/pdf/phev/HymPriusPersonal-useChAndDrSept08-Mar10.pdf.
2. Southern California Association of Governments, “Year 2000 Post-Census Regional Travel Survey: Final Report of Survey Results,” Fall 2003.
3. Earleywine, M., Gonder, J., Markel, T., and Thornton, M. “Simulated Fuel Economy and Performance of Advanced Hybrid Electric and Plug-in Hybrid Electric Vehicles Using In-Use Travel Profiles.” *Proceedings of the 6th IEEE Vehicle Power and Propulsion Conference (VPPC); Sept.1-3, 2010, Lille, France.*

VI.C.3. Products

Publications

Earleywine, M., Gonder, J. and Brooker, A. “Evaluation of the Costs, Benefits and Feasibility of Electric Roadway Technologies and Travel Scenarios.” To be published at the Conference on Electric Roads & Vehicles (CERV). Feb 16-17, 2012 in Park City, UT.

Tools & Data

Transportation Secure Data Center (TSDC) (Jeff.Gonder@nrel.gov)

VI.D. PHEV Emissions and Control Strategy

Principal Investigator: Andreas Malikopoulos
Oak Ridge National Laboratory
National Transportation Research Center (NTRC, Bld. II)
2370 Cherahala Boulevard
Knoxville, TN 37932-6472
(865) 946-1529; andreas@ornl.gov

DOE Program Manager: Lee Slezak
(202) 586-2335; Lee.Slezak@ee.doe.gov

VI.D.1. Abstract

Objective

- Optimize engine's cold-start events in plug-in hybrid electric vehicles (PHEVs) and establish conditions for proper use of engine by the power management controller.

Approach

- Develop a control function to provide the efficiency of the catalytic converter with respect to temperature.
- Implement a control function to realize the amount of energy required for the catalyst to increase its temperature with respect to its current temperature.
- Develop a control algorithm that aims to operate the engine on its highest efficiency while the engine is warming up.

Major Accomplishments

- Implemented a control algorithm that aims to warm up the engine optimally with the intention to reach the catalyst temperature corresponding to its highest efficiency in a small period of time.
- Integrated the algorithm within the state flow of the power management controller in Autonomie.
- Validated the efficiency of the effectiveness of the control algorithm over six consecutives UDDS driving cycles demonstrating a fuel consumption improvement, when the emphasis was on fuel consumption, and significant improvement in CO and HC, when emphasis was to rise catalyst temperature within a small amount of time during cold start events.

Future Activities

- This particular task is being phased out as of the end of FY 2011.

VI.D.2. Technical Discussion

Background

The necessity for environmentally conscious vehicle designs in conjunction with increasing concerns regarding U.S. dependency on foreign oil and climate change have induced significant investment towards enhancing the propulsion portfolio with new technologies. The automotive industry has recognized that widespread use of alternative hybrid powertrains is currently inevitable and many opportunities for substantial progress remain. Hybrid electric vehicles (HEVs) have been shown to have the potential to achieve greater fuel economy compared to vehicles powered only by internal combustion engines (conventional vehicles) [1-3]. This capability is mainly attributed to: a) the potential for downsizing the engine; b) the potential of

recovering energy during braking, and thus, recharging the energy storage unit; and c) the ability to minimize the operation of engine in inefficient brake specific fuel consumption (BSFC) regimes [4]. In addition, hybridization of conventional powertrain systems allows elimination of near idle engine operation, thus enabling in direct fuel economy enhancement [1, 2]. More recently, plug-in hybrid electric vehicles (PHEVs) have held great intuitive appeal and have attracted considerable attention [5]. PHEVs are hybrid vehicles with rechargeable batteries that can be restored to full charge by connecting a plug to an external electric wall socket. A PHEV shares the characteristics of both a HEV, having an electric motor and an internal combustion engine, and of an all-electric vehicle, also having a plug to connect to the electrical grid. It is especially appealing in situations where daily commuting distance is small [6]. Studies have shown that approximately 60% of U.S. passenger vehicles travel less than 30 miles each day [7]. PHEVs have the potential to reduce petroleum consumption and greenhouse gas (GHG) emissions by means of sophisticated control schemes [8, 9]. Under the average mix of electricity sources in the U.S., PHEVs can be driven with lower operation cost and fewer greenhouse gas (GHG) emissions per mile when powered by electricity rather than by gasoline [10]. Most PHEVs on the road today are passenger cars, but there are also versions of commercial vehicles, utility trucks, buses, and military vehicles.

PHEVs operate predominantly as electric vehicles (EVs) with intermittent assist from the engine during high power demands. As a consequence, the engine can be subjected to multiple cold start events. These cold start events may have a significant impact on the tailpipe emissions due to degraded catalyst performance and starting the engine under less than ideal conditions.

Introduction

A model corresponding to a pre-transmission series configuration PHEV was developed in Autonomie, which includes a vehicle system control module (VSCM) developed previously in [8, 9]. The VSCM is a supervisory controller that designates the operating point of each of the powertrain components and the interactions among the subsystems. The control system architecture is comprised of various control processes. The primary control processes of the VSCM are responsible for the status of the vehicle, the energy management and blending strategies, the regenerative braking functions, and energy storage control and status. Each of these control processes communicates with each other in order to facilitate the operation and interaction of the traction motor, energy storage system, and the engine. The supervisory control system of the PHEV powertrain allows both charge depleting (CD) and charge sustaining (CS) operations as appropriate over the entire usable state-of-charge (SOC) range of the energy storage system.

In the CD operation, the *maximum depletion* mode was selected that strives to discharge the battery pack as quickly as possible by operating the vehicle in all-electric model until the lower SOC bound is reached. In the CS operation, VSCM operates the engine much like a conventional vehicle where the commanded engine torque closely follows the demanded torque. Excess engine power can be used to charge the battery during instances of low power demand, e.g., cruising. The SOC is held tightly around a target SOC during CS operation.

Both the control functions that provides the efficiency of the catalytic converter with respect to temperature and realizes the amount of energy required for the catalyst to increase its temperature with respect to its current temperature were implemented into a Matlab embedded function and integrated into the state flow of the VSCM in Autonomie. The control algorithm that aims to operate the engine on its highest efficiency while the engine is warming up was also integrated within the aforementioned control functions.

Approach

In a typical oxidizing catalytic converter, there is a significant variation of the conversion

efficiency with respect to its operating temperature. At high temperatures the steady-state conversion efficiencies of a new oxidation catalyst are typically 98 to 99 percent for CO and 95 percent or above for HC [11]. However, the catalyst is ineffective until its temperature has risen above 250 to 300°C. The term *light-off temperature* is often used to describe the temperature at which the catalyst becomes more than 50 percent effective. Consequently, it is really important to reach the catalyst high temperature within a small time period, and thus operating the catalyst at the highest conversion efficiencies possible. In this context, a control function that provides the amount of energy required for the catalyst to increase its temperature with respect to its current temperature, illustrated in Figure 1, was implemented.

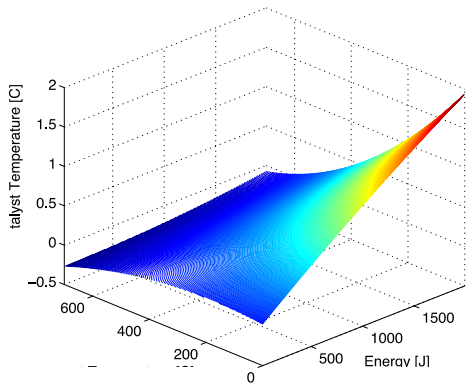

Figure 1. Energy required by the engine to increase catalyst's temperature with respect to the current catalyst's temperature.

The main objective of the control algorithm is to reach the catalyst temperature corresponding to high conversion efficiencies rapidly, to improve CO and HC in cold start events. However, we need to take into account fuel consumption as well. Therefore, an instantaneous optimization control problem was formulated founded on the Pontryagin minimum principle and the Hamilton-Jacobi equation [12]. The optimal control problem aims to determine the control which minimizes a given objective function . In this context, the control u is defined to be the engine power whereas the function is the sum of the inverse of the engine efficiency and the inverse of the catalyst conversion efficiencies. Namely, the objective of the control algorithm is to find the optimal engine power that operates the engine at its highest efficiency and also rises the catalyst temperature to the one corresponding to its highest conversion efficiencies. The highest engine efficiency with respect to engine speed is illustrated in Figure 2. The optimal power, i.e., the power corresponding to the highest engine efficiency, is shown in Figure 3.

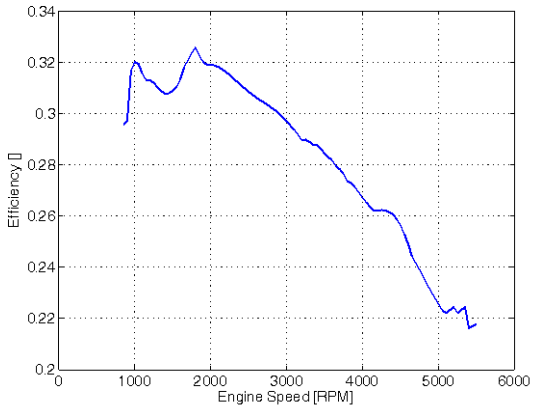

Figure 2. Engine's highest efficiency with respect to the engine speed.

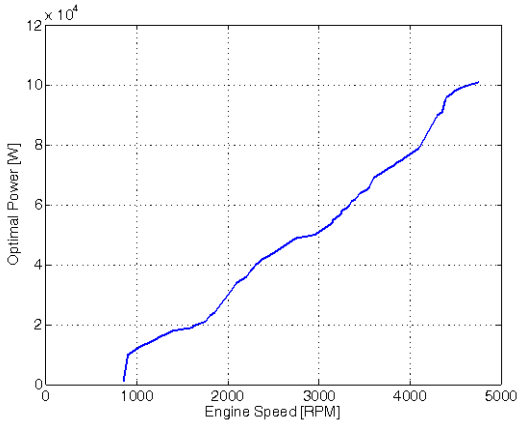

Figure 3. Optimal power with respect to the engine speed.

The control algorithm eventually computes the optimal control based on these functions. Namely, based on the highest engine efficiency from Figure 2 the algorithm identifies the engine speed. Then utilizing the function in Figure 3, the algorithm yields the optimal power. Thus the

optimal engine operating point, i.e., pair of engine torque and speed, can be specified in this fashion. However, there is a tradeoff between focusing on operating the engine optimally and rising the catalyst temperature within a small period of time. Therefore two different cases were considered: (a) the control algorithm with an emphasis on improving fuel economy at cold start events and (b) the control algorithm with an emphasis on rising the catalyst temperature within a small period of time.

The capability to operate the engine independently from the power demanded by the driver is mainly attributed to the series PHEV configuration that disengages the engine from the driver in CD mode. While the engine is running at its highest efficiency and the catalyst is warming up, the engine power is converted through the generator to electric power and charges the battery. Consequently, during the cold start events, the intention is for the engine to operate optimally resulting in fuel consumption improvement and for the catalyst to operate at the temperature corresponding to the highest conversion efficiencies.

Results

In the first case, the optimal control derived by the algorithm operates the engine on its highest efficiency during cold start events resulting in a 3% fuel economy improvement as depicted in Figure 4. The catalyst temperature is shown in Figure 5; it is noted that since the focus, in this particular case, was on fuel consumption, the catalyst temperature demonstrates a small variation in cold starting. At high temperatures the conversion efficiencies of the catalyst are typically almost 99 percent for CO and 95 percent or above for HC. Therefore a 10% improvement of CO was achieved. However, the conversion efficiency for HC at this temperature level is not as high as the one corresponding to CO resulting in a 13% percent increase of HC. Table 1 summarizes the results for fuel consumption, CO and HC. The SOC of the battery for the six consecutives UDDS driving cycles is shown in Figure 6.

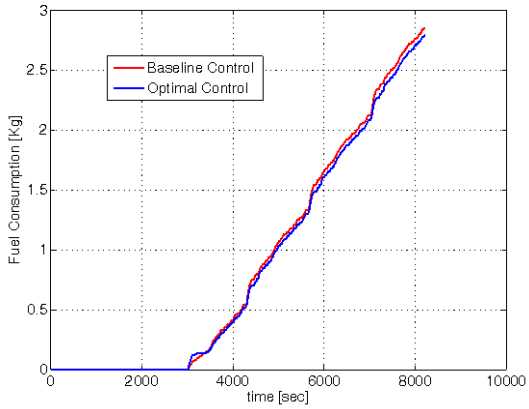

Figure 4. Cumulative fuel consumption.

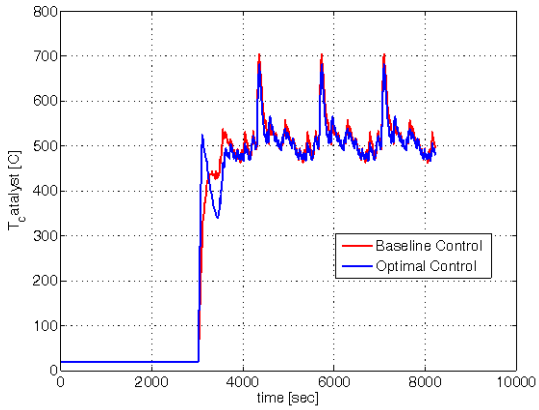

Figure 5. Catalyst temperature.

Table 1. Summary of Optimal Control Results

EMISSIONS	OPTIMAL CONTROL IMPROVEMENT [%]
FUEL CONSUMPTION	3
CO	10
HC	-13

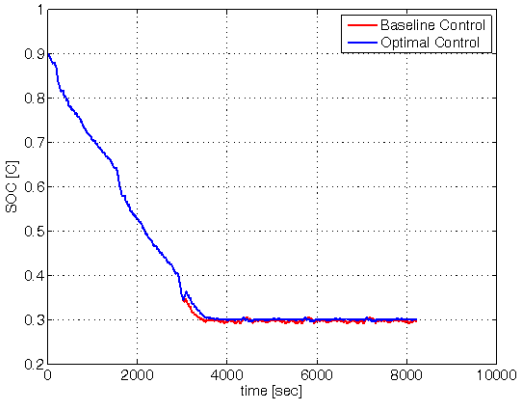

Figure 6. Battery SOC over six consecutives UDDS driving cycles.

In the second case, the emphasis of the optimal control derived by the algorithm was on increasing the catalyst temperature, and as a result there is an increase in fuel consumption as depicted in Figure7. The objective of the control algorithm in this case was to warm up the catalyst within a small period of time, which allows reaching the catalyst high temperature faster as shown in Figure 8. A significant improvement in both CO and HC was achieved since the catalyst was able to operate at temperatures where the conversion efficiencies for both CO and HC are high. Table 2 summarizes the results for fuel consumption, CO and HC. The SOC of the battery for the six consecutives UDDS driving cycles is shown in Figure 9. It is noted that the SOC of the optimal control is higher, which partly explains the increase of the resulting fuel consumption.

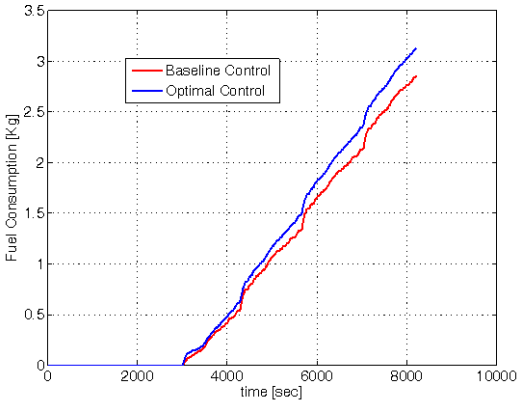

Figure 7. Cumulative fuel consumption.

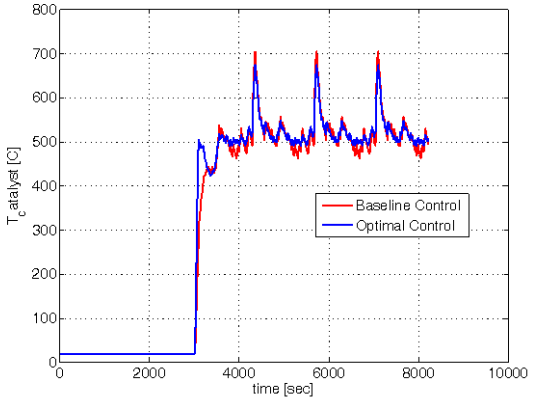

Figure 8. Catalyst temperature.

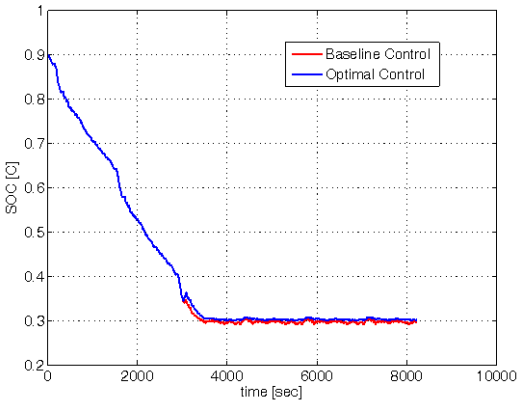

Figure 9. Battery SOC over six consecutives UDDS driving cycles.

Table 2. Summary of Optimal Control Results

EMISSIONS	OPTIMAL CONTROL IMPROVEMENT [%]
FUEL CONSUMPTION	-10
CO	47
HC	25

Conclusions

- A control algorithm has been developed for operating the engine optimally and reaching the catalyst temperature corresponding to its highest conversion efficiency.
- The algorithm has been integrated with the state flow of the power management

controller in a series PHEV configuration in Autonomie.

- When the objective is to minimize fuel consumption, vehicle simulations over six consecutives UDDS driving cycles demonstrate an improvement in fuel consumption at cold start events with a penalty in HC.
- When the objective is to increase catalyst temperature within a small period of time, vehicle simulations over six consecutives UDDS driving cycles demonstrate significant improvement in CO and HC with a penalty in fuel consumption.
- In both cases an increase in NOx was noticed during cold start events. Future research should incorporate NO_x into the objective function of the instantaneous optimization problem in conjunction with fuel economy to address the increase in NO_x at cold starting.

References

1. A. Sciarretta and L. Guzzella, "Control of Hybrid Electric Vehicles," *IEEE Control Systems Magazine,* vol. 27, pp. 60-70, 2007.
2. A. Sciarretta, M. Back, and L. Guzzella, "Optimal Control of Parallel Hybrid Electric Vehicles," *IEEE Transactions on Control Systems Technology,* vol. 12, pp. 352-363, 2004.
3. N. J. Schouten, M. A. Salman, and N. A. Kheir, "Energy Management Strategies for Parallel Hybrid Vehicles Using Fuzzy Logic," *Control Engineering Practice,* vol. 11, pp. 171-177, 2003.
4. A. A. Malikopoulos, Z. S. Filipi, and D. N. Assanis, "Simulation of an Integrated Starter Alternator (ISA) System for the HMMWV," in *Proceedings of the SAE 2006 World Congress and Exhibition, SAE 2006-01-0442*, Detroit, Michigan, 2006.
5. A. A. Malikopoulos and D. E. Smith, "An Optimization Model for Plug-In Hybrid Electric Vehicles," in *Proceedings of 2011 Fall Technical Conference of the ASME Internal Combustion Engine Division*, Morgantown, West Virginia, 2011.
6. Q. Gong, Y. Li, and Z.-R. Peng, "Trip-based Optimal Power Management of Plug-in Hybrid Electric Vehicles," *IEEE Transactions on Vehicular Technology,* vol. 57, pp. 3393-3401, 2008.
7. L. Johannesson, M. Asbogard, and B. Egardt, "Assessing the potential of predictive control for hybrid vehicle powertrains using stochastic dynamic programming," *IEEE Transactions on Intelligent Transportation Systems,* vol. 8, pp. 71-83, 2007.
8. D. E. Smith, "Plug-In Hybrid Electric Vehicle Emissions Impacts on Control Strategy and Fuel Economy," Ph.D. Dissertation, Department of Mechanical Engineering, University of Tennessee, Knoxville, TN, 2009.
9. D. E. Smith, H. Lohse-Busch, and D. K. Irick, "A Preliminary Investigation Into the Mitigation of Plug-in Hybrid Electric Vehicle Tailpipe Emissions Through Supervisory Control Methods," *SAE Intl. Journal of Engines,* vol. 3, pp. 996-1011, 2010.
10. C. Samaras and K. Meisterling, "Life Cycle Assessment of Greenhouse Gas Emissions from Plug-in Hybrid Vehicles: Implications for Policy," *Environmental Science and Technology,* vol. 42, pp. 3170-3176, 2008.
11. J. Heywood, *Internal Combustion Engine Fundamentals*, 1st ed.: McGraw-Hill, April 1988.
12. D. P. Bertsekas, *Dynamic Programming and Optimal Control (Volumes 1 and 2)*: Athena Scientific, September 2001.

VI.D.3. Products

Tools & Data

The controller has been implemented in a Matlab embedded function and integrated into the state flow of the vehicle system control module (VSCM) in Autonomie.

VI.E. PHEV Engine Control and Energy Management Strategy

Principal Investigator: Paul H. Chambon
Oak Ridge National Laboratory (ORNL)
National Transportation Research Center
2360 Cherahala Boulevard
Knoxville, TN 37932
(865) 946-1428; chambonph@ornl.gov

DOE Program Manager: Lee Slezak
(202) 586-2335; lee.slezak@ee.doe.gov

VI.E.1. Abstract

Objective

- Investigate novel engine control strategies targeted at rapid engine/catalyst warming for the purpose of mitigating tailpipe emissions from plug-in hybrid electric vehicles (PHEV) exposed to multiple engine cold start events.
- Validate and optimize hybrid supervisory control techniques developed during previous and on-going research projects by integrating them into the vehicle level control system and complementing them with the modified engine control strategies in order to further reduce emissions during both cold start and engine re-starts.

Approach

- Perform a literature search of engine control strategies used in conventional powertrains to reduce cold start emissions
- Develop an open source engine controller providing full access to engine control strategies in order to implement new engine/catalyst warm-up behaviors
- Modify engine cold start control algorithms and characterize impact on cold start behavior
- Develop an experimental Engine-In-the-Loop test stand in order to validate control methodologies and verify transient thermal behavior and emissions of the real engine when combined with a virtual hybrid powertrain

Major Accomplishments

- Commissioned a prototype engine controller on a GM Ecotec LAF 2.4l Gasoline Naturally aspirated Direct Injected engine on an engine test cell at the University of Tennessee.
- Obtained from Bosch (with GM's approval) an open calibration engine controller for a GM Ecotec LNF 2.0l Gasoline Turbocharged Direct Injection engine. Bosch will support the bypass of cold start strategies if calibration access proves insufficient. The LNF engine and its open controller were commissioned on an engine test cell at ORNL.
- Completed a literature search to identify key engine cold start control parameters and characterized their impact on the real engine using the Bosch engine controller to calibrate them.
- Ported virtual hybrid vehicle model from offline simulation environment to real-time Hardware-In-the-Loop platform.

Future Activities

- Validate cold start calibration on a stand-alone engine (decoupled from dynamometer for faster transients)
- Test re-calibrated engine when combined with virtual hybrid powertrain running on Hardware-In-the-Loop platform
- Integrate hybrid vehicle supervisory control strategies targeted at cold starts on Engine-In-the-Loop platform
- Jointly optimize engine controller and hybrid vehicle supervisory strategies to minimize cold start emissions.

VI.E.2. Technical Discussion

Background

Plug-in hybrid electric vehicle (PHEV) technologies have the potential for considerable petroleum consumption reductions, at the expense of increased tailpipe emissions due to multiple "cold" start events and improper use of the engine for PHEV specific operation. PHEVs operate predominantly as electric vehicles (EVs) with intermittent assist from the engine during high power demands. As a consequence, the engine can be subjected to multiple cold start events. These cold start events have a significant impact on the tailpipe emissions due to degraded catalyst performance and starting the engine under less than ideal conditions. On current conventional vehicles as well as hybrid electric vehicles (HEVs), the first cold start of the engine dictates whether or not the vehicle will pass federal emissions tests. PHEV operation compounds this problem due to infrequent, multiple engine cold starts.

Previous research focused on the design of a vehicle supervisory control system for a pre-transmission parallel PHEV powertrain architecture. Energy management strategies were evaluated and implemented in a virtual environment for preliminary assessment of petroleum displacement benefits before being implemented and tested on a powertrain test bed at the Argonne National Laboratories.

Engine cold start events were aggressively addressed by modifying vehicle supervisory strategies while retaining the base engine control strategies as they were developed for a conventional (non-hybrid) powertrain. This led to enhanced pre-warming and energy-based engine warming algorithms that provide substantial reductions in tailpipe emissions over the baseline supervisory control strategy.

Introduction

This project expands the work performed so far on hybrid vehicle supervisory strategies to include engine control strategies in order to proceed with a system approach of the powertrain control strategies optimization rather than independent component optimization.

Gasoline direct injection engines with variable valve timing, such as the one identified for this project, offer more degrees of freedom to optimize cold start emissions than port fuel injected engines. Furthermore their usage will vary in the case of a hybrid powertrain compared to a conventional powertrain. Therefore engine control strategies should be calibrated first to make the most of those added degrees of freedom and second to take advantage of the hybrid powertrain specific operating conditions.

This project will focus on adapting the conventional engine calibration to a hybrid powertrain application as well as optimizing cold start engine strategies. Then cold start emissions will be targeted by jointly optimizing both vehicle supervisory strategies and engine control strategies.

Approach

During FY10, a GM Ecotec LAF 2.4l Gasoline Naturally aspirated Direct Injected engine was selected as a test engine and a prototype engine controller was developed to replace the production module, whose strategies and calibration were not accessible and therefore did

not provide any opportunity to be optimized for our project.

During FY11, that controller and engine were commissioned at the University of Tennessee's Advanced Powertrain Controls and System Integration (APCSI) facility (see Figure 1). Steady-state closed-loop operation was verified over a restricted speed and load range (1500 to 4800rpm and 20 to 100% load).

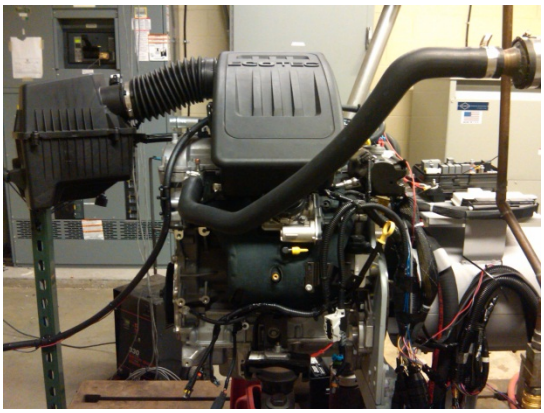

Figure 1. Ecotec LAF engine commissioned at the University of Tennessee's Advanced Powertrain Controls and System Integration (APCSI) facility

That approach consisting of developing of brand new prototype engine controller to replace the production module was selected during FY10 because no OEM was willing to support this project by providing an engine and its controller as well as access to its strategies.

During FY11, discussions with Robert Bosch LLC led the team to reconsider that approach: ORNL's Fuel Engine and Emissions Research Center agreed to share a GM Ecotec LNF 2.0l Gasoline Turbocharged Direct Injection engine, and Bosch offered to provide an open-calibration controller for that engine so that control strategies can be tuned differently from the production settings. Bosch will provide some support as well to bypass cold start strategies if calibration access is not sufficient to achieve our goals and strategies need to be further modified.

This approach consisting of using a modified production engine controller is preferable to the original prototype controller approach because it utilizes an existing proven set of production control strategies and modifies only cold start strategies which are the focus of this project. It therefore allows dedicating resources on cold start behavior without having to develop and refine the rest of the control strategies required to run an engine over all operating conditions.

So the project will proceed with the Ecotec LNF engine running a Bosch controller instead of the Ecotec LAF engine and its prototype controller.

The LNF engine and Bosch controller have been commissioned on an engine test cell at ORNL. Initial tests were performed without the three way catalytic converter and monitored fuel consumption, exhaust and post-turbo temperatures, as well as engine out emissions: hydrocarbons, nitrous oxides and carbon monoxide. The steady state performance and emissions of the LNF engine were characterized over a limited speed and load range (Figure 2 shows an example of the steady state mapping obtained during that phase)

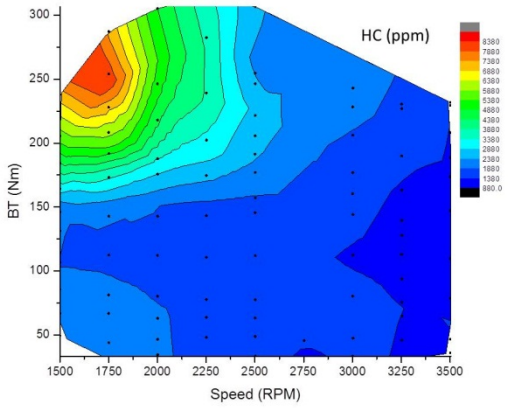

Figure 2. Ecotec LNF engine out hydrocarbon emissions

A literature search was completed to investigate control strategies used on gasoline direct injection engine to speed up catalyst warm-ups and reduce cold start emissions. Bosch and several OEMs published papers on that matter. There is a consensus on several operating modes: running dual injection strategies (early injection during the intake stroke and late injection during the compression stroke, referred to as HSP by Bosch), retarding spark timing, retarding the exhaust valve closing event, running leaner and operating at higher fuel rail pressure.

The various strategies identified during the literature phase were implemented in the open engine controller and tested on our engine test cell set-up. That testing platform proved acceptable for the post crank phase (or warm-up phase) when engine speed settles around 1400rpm. The same test set-up where the engine is coupled to a dynamometer was not suitable to reproduce the fast transient behavior of a cranking event because of the large dynamometer inertia. Therefore the calibration of the cranking phase of a cold start will be investigated on a stand-alone engine decoupled from the dynamometer.

By nature true cold starts happen only once a day; in order to complete testing in a reasonable amount of time, we performed pseudo cold starts where the engine coolant was cooled down to 25 degC between tests. This is deemed to be acceptable because this project focuses on PHEV applications where the engine experiences one cold start and several pseudo cold starts during a drive cycle. Therefore it does not have time to settle to a true stabilized cold temperature between multiple starts.

In parallel to the engine development activities, vehicle supervisory strategies were adapted from previous related projects to suit the series PHEV architecture that was selected for this project. An Autonomie vehicle model was developed and Simulink control strategies were modified to optimize cold starts on that vehicle platform.

Finally, a Hardware-In-the-Loop system was set-up to run the virtual vehicle model on a real-time computer while interacting with the actual engine on the test stand so that the hybrid powertrain and drive cycles can be emulated and yet, accurate measurements for fuel consumption and emissions can be obtained from a real engine (this configuration is therefore called Engine-In-the-Loop). National Instruments tools were selected. They allow running in real time and minimum effort the Autonomie vehicle models previously developed for offline simulation, while offering a wide variety of inputs and outputs to interface with the engine and dynamometer controller. Figure 3 shows a diagram of the Engine-In-the-Loop configuration.

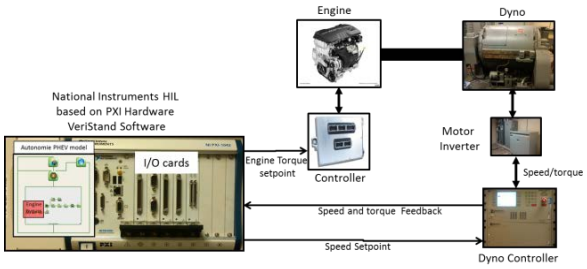

Figure 3. Engine-In-The-Loop diagram

Results

The simulation study refined vehicle supervisory strategies developed for a parallel hybrid application and adapted them to the series hybrid configuration considered in this project.

The focus was placed on pre-warming the engine independently from the vehicle traction requirements to optimize the warm-up phase. Some torque filtering was applied to remove fast transients and to wait for the engine to be fully warm before allowing large torque requests. Those key elements were calibrated on urban drive cycles.

Figure 4 shows the catalyst slow warm-up behavior when the engine is operating in load following mode without any warm-up conditioning (blue trace) whereas more or less aggressive pre-warm-up phases and as well as torque filtering (green and red traces) lead to faster temperature rises.

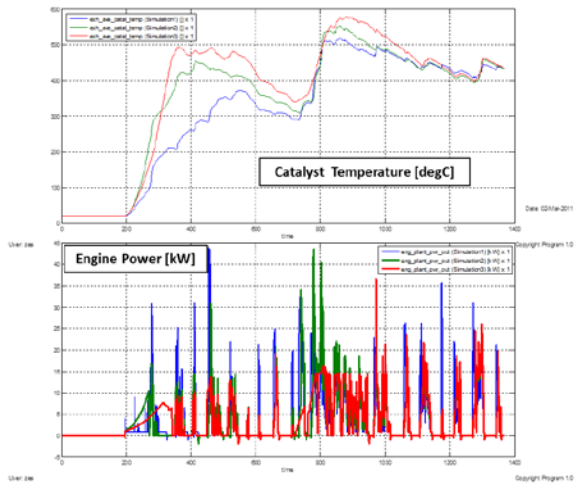

Figure 4. Series PHEV catalyst temperature behavior based on engine warm-up patterns

Figure 5 shows the emissions improvements associated with vehicle supervisory strategies that pre-warm the engine and filter out transient conditions while the engine is cold. Those results do highlight as well the fuel penalty associated with those strategies.

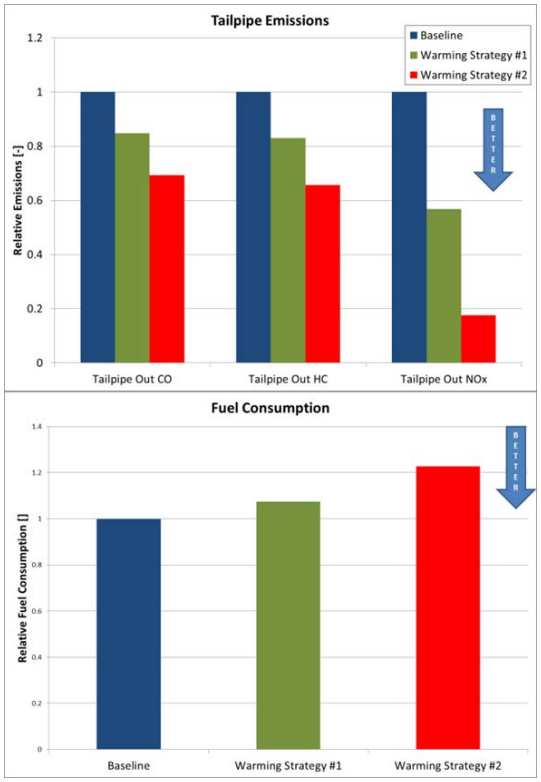

Figure 5. Tailpipe emissions improvement and fuel penalty associated with torque shaping strategies

Engine tests were performed to evaluate the effectiveness of several engine control parameters on exhaust temperature gradients and engine out emissions during the warm-up phase. Parameters selection was based on the literature search:

- Retarded spark timing
- Retarded injection timing
- Elevated fuel rail pressure
- Retarded exhaust valve closing
- Leaner mixture

As discussed earlier on, our dynamometer was not suitable to reproduce the fast transient behavior of a cranking event because of the large dynamometer inertia. Therefore the cranking phase lasts too long and leads to a larger hydrocarbon spike than expected. That spike should be ignored in the subsequent graphs and only the post crank behavior is deemed representative of an in-car cold start.

Figure 6 shows the effect of retarding spark timing on both hydrocarbons and exhaust temperature: it leads to an increase of about 200degC in post turbo temperature and decreases hydrocarbons by one to two thousand ppm.

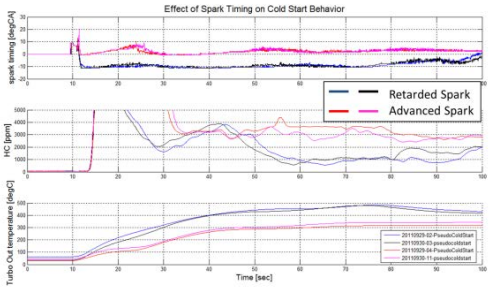

Figure 6. Effect of spark timing on LNF engine cold start behavior

Injection timing retard was shown to have a more modest influence but yet significant (see Figure 7).

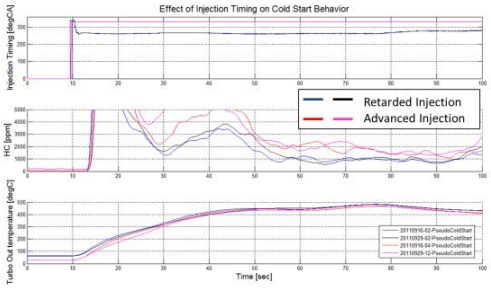

Figure 7. Effect of injection timing on LNF engine cold start behavior

Elevating fuel rail pressure from 15bar to around 60bar did provide some improvement with lower emissions and marginally higher temperatures (Figure 8) but taking it even higher (around 90bar) did not provide additional benefits.

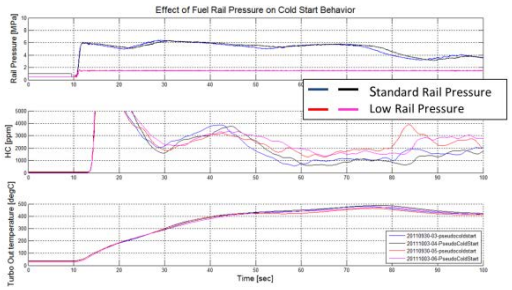

Figure 8. Effect of fuel rail pressure on LNF engine cold start behavior

Exhaust valve closing timing was investigated and demonstrated higher post turbo temperatures (Figure 9).

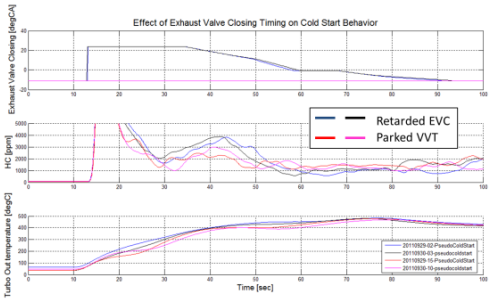

Figure 9. Effect of exhaust valve closing timing on LNF engine cold start behavior

Air Fuel ratio control during the post crank phase as well as the warm up phase showed promising hydrocarbons reduction results. By running less fuel enrichment during the post crank phase and running lean (lambda of 1.03) during the warm-up phase, engine out hydrocarbon can be further reduced and turbo out temperatures can be made higher (Figure 10).

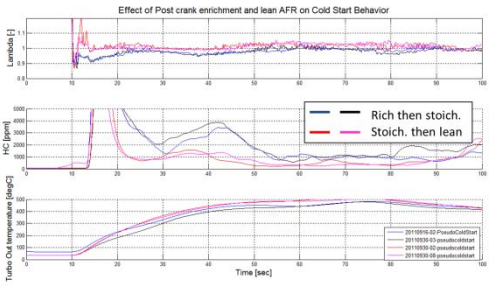

Figure 10. Effect of air fuel ratio on LNF engine cold start behavior

One of the main features that a direct injection gasoline engine is capable of is dual injection (HSP) during the warm-up phase. This creates a richer mixture concentrated around the spark plug and lean mixture elsewhere. This promotes an overall leaner mixture compared to homogenous port fuel injection, while stabilizing the combustion when retarding the spark timing, which in turn provides more heat to the after-treatment. Unfortunately, that feature could not be tested so far because of it is disabled in our engine controller and the team has not managed to enable it yet.

Conclusions

A control system for a gasoline turbocharged direct injection engine has been commissioned and tested to demonstrate the impact of various engine control parameters on cold starts emissions. This was made possible thanks to the support off Robert Bosch LLC who supplied the engine controller.

That set-up was used to demonstrate the potential for further emissions reduction and faster catalyst warm-up by modifying engine cold start calibration.

Previously, cold start emissions had been targeted using vehicle supervisory strategies instead of engine control strategies. This was achieved with Autonomie simulations of a series plug-in hybrid electric vehicle.

A Hardware-In-the-Loop system capable of running the Autonomie PHEV model and interfacing with the real engine on a dynamometer test stand was developed so that, during FY12, the project can proceed with a combined optimization of both engine and vehicle level strategies to achieve lower cold start emissions in the hybrid powertrain configuration.

VII. CODES AND STANDARDS

VII.A. Provide Technical Data Support and Leadership to SAE Advanced Vehicle Test Standards

Principal Investigator: Michael Duoba
Argonne National Laboratory
9700 South Cass Avenue
Argonne, IL 60439-4815
(630) 252-6398; mduoba@anl.gov

DOE Technology Manager: Lee Slezak
(202) 586-2335; lee.slezak@ee.doe.gov

VII.A.1. Abstract

Objectives

- Provide ideas and valuable test data critical to SAE J1634 (BEV Test Procedures) revision.
- Support the development of several procedures in the SAE Light Duty Vehicle Performance and Economy Measure Committee. These include procedures for dynamometer driving performance metrics (J2951) and coast-down and road-load derivation procedures (J2263 and J2264).
- Organize and run the task force to rewrite the medium- and heavy-duty dynamometer test procedures (J2711). A main focus is on tests for HEVs and PHEVs.
- Ensure that all stakeholders, including EPA, the California Air Resources Board, and ISO, are in consensus on the general direction and goals of the testing procedures. Provide expert insight to EPA during the development of new fuel economy labeling.

Approach

- Run chassis dynamometer tests on several battery electric vehicles (BEVs) to evaluate the robustness of the procedure concepts and calculation methods.
- Provide input and write the code that calculates the dynamometer driving metrics (J2951) for SAE and EPA.
- Organize and chair the J2711 Task Force. The initial effort was mostly to educate the members on generally accepted concepts from the light-duty procedure (J1711) and find areas where J2711 procedures require additional development.

Major Accomplishments

- Several test concepts were tested at Argonne, and the final-version procedure was validated using a Nissan Leaf BEV. Argonne staff invented several key calculation steps that make the new J1634 procedures robust for all stakeholders.
- Successfully balloted SAE J2951 in September 2011. Argonne provided the MATLAB™ code and a spreadsheet with intelligent macros that calculate the output parameters for J2951.
- Several specific comments and recommendations that Argonne provided to EPA became part of new labeling regulations for advanced vehicles.

Future Activities

- The dynamometer coast-down and road-load derivation procedures are still under rewrite, and this effort may ramp up to a point where Argonne's contribution would be providing special focus on advanced vehicles like BEVs and certain HEVs.
- The medium- and heavy-duty chassis dynamometer procedures will be a major effort next year. Whereas J1711 was indeed a technical challenge, the scope of J2711 is even wider and many more problems will need to have novel and robust solutions invented.

VII.A.2. Technical Discussion

Introduction

SAE has been involved in standards development for almost 100 years. Vehicle technology is currently undergoing many radical changes and these new technologies are pathways that the U.S. Department of Energy hopes will lead to meeting our current objectives in reducing petroleum usage in the transportation sector. In order to ensure that these new technologies do not stumble as they are introduced to the public, they need to be properly and accurately evaluated using robust analytical testing techniques. Argonne has been testing advanced vehicles for nearly two decades, and this expertise has been utilized to provide leadership and guidance for SAE committees involved in many vehicle testing areas.

In 2006, Argonne staff was recognized by industry to be the best choice to chair the HEV/PHEV test procedure. Argonne staff, acting as objective arbiters and impartial to specific technologies; and Argonne's state-of-the-art testing facility has been very successful in helping guide testing practices, especially for new and quickly advancing vehicle technology.

Since J1711 was completed, Argonne has continued its effort to invent and test out new testing approaches for battery electric vehicles (BEVs) and heavy-duty vehicles. Argonne has provided input and test data for several other task forces where critical advanced vehicle testing was involved.

Approach

Many of the existing testing programs at Argonne are heavily leveraged by the test-procedure development activity. The ongoing benchmarking effort through the Advanced Vehicle Testing Activity has allowed Argonne access to many advanced vehicles over the course of the last decade. Small-scale investigative experiments conducted with many vehicles have aimed at looking at the impact of various test-procedure decisions—in other words, asking such questions as "How important or sensitive is the outcome for each procedure or calculation option?"

Argonne has had activities and accomplishments in several SAE task force committees focusing on properly testing and evaluating advanced vehicles. This section highlights each of those accomplishments in greater detail.

SAE J1634: Battery Electric Vehicle Test Procedures

Led by Ford Motor Co. and Argonne, the task of updating the procedure included many meeting discussions and various rounds of testing.

The old J1634 test procedure takes a direct approach to finding the electric energy consumption and range of a BEV. In essence, the procedure entails running vehicle test schedules over and over from a full charge until the battery is fully depleted. This approach worked satisfactorily 20 years ago for BEVs whose expected range was about 30–50 miles. However for a vehicle like the Tesla, which can travel up to 245 miles on a single charge, this test becomes a two-shift, late-night, 16-hour endeavor. It was apparent that a new procedure (a "short-cut" test) was needed to test the next generation of advanced BEVs.

Much progress was made last year in validating the basic short-cut concept of testing multiple cycle types in a single discharge test and extrapolating the range for each cycle type.

However, this year, several remaining key issues were solved.

The main feature of the short-cut procedure was that battery energy would be quickly discharged by running steady-state speed cycles in place of slower discharging test schedules. There were questions regarding the best target speed: too slow and the test becomes longer than it needs to be; too fast and test accuracy can be compromised. Argonne had performed several BEV tests using 45-, 55-, and 65-mph speeds. Data from Argonne tests suggested that the 65 mph discharge speed choice was in fact too fast because the total capacity taken out of the pack would diminish beyond what was measured in the old range test. It was our recommendation to use 55 mph for the steady-speed portion of the test to avoid compromises in accuracy.

With many of the procedures and calculations fully defined, it was time to validate them using a reliable, production-intent vehicle. Argonne has many working-level relationships with suppliers. One such supplier had its hardware in an SUV package for development and evaluation. Argonne was able to borrow this vehicle for testing the most up-to-date short-cut test concepts at the time (see Figure 1).

Figure 1. Tier 1 BEV supplier vehicle undergoing methodology validation at Argonne.

The data were useful in understanding the impact of battery thermal management on the degree of test-to-test repeatability and how accurately one could expect to extrapolate range. The test procedure had been validated and nearly ready for ballot when it was suggested that test cycles needed to be run at the beginning and end of the battery state-of-charge (SOC) for best accuracy. This requirement added new complications because now the steady-state speed would need to be run in the middle SOC range of the discharge, at a length that would have to be known ahead of time.

The new approach is as follows:

1) Run two city cycles
2) Run one highway cycle
3) Run steady-speed cycle for *x* time or *y* miles
4) Run one highway cycle
5) Run two city cycles ending with less than 15% capacity (or range) left in the battery
6) Run steady-state cycle until vehicle can no longer maintain the steady-speed target

More validation testing was needed for this new version of the short-cut procedure. Once again, Argonne turned to its working-level contacts and found a willing battery supplier to lend Argonne a production Nissan Leaf vehicle that had been purchased for specific component testing (see Figure 2).

Figure 2. Nissan Leaf undergoing final test procedure validation testing at Argonne.

A focused test plan was developed in order to test out the single-cycle full-depletion test range and compare it to the new short-cut approach. The testing was a complete success, and because of the vehicle's lack of an active thermal management system (i.e., no consumption of additional energy), repeatability was well

beyond that of any other BEV tested or of any other vehicle tested at Argonne. For example, in Figure 3, all the highway cycles run in the test program are plotted on the same graph. Some of the test results are so nearly the same that the data points are not distinguishable from one another on the plot.

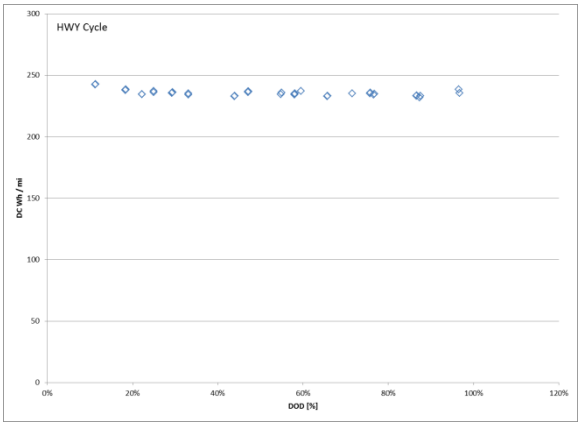

Figure 3. Highway-cycle results demonstrating high test-to-test repeatability.

During the Leaf testing, Argonne staff came up with a methodology to test the vehicle and measure enough information to be able to plan the middle steady-speed test even if the manufacturer provided no information about its expected range. The equations were put into a spreadsheet and were used for the last few Leaf tests in the test plan. The end-of-test was predicted and tested to within one mile. The extrapolated range, using weighting equations recommended by Argonne, predicted the city-cycle range to within one mile. The unweighted highway range was predicted to within 2 miles (see Table 1).

Table 1. Nissan Leaf test results and range extrapolation for city and highway cycles

	City Cycle		weighted	Highway Cycle	
	Short-Cut #1	104.36	105.45	Short-Cut #1	88.95
	Short-Cut #2	104.65	105.86	Short-Cut #2	89.75
	Full Test #1	105.80		Full Test #1	90.28
	Full Test #2	106.29		Full Test #2	90.72
Average	**RangeCITY**	**106.05**	Average	**RangeHWY**	**90.50**

Progress on standards development can be unpredictable. It appears that at the time of this writing the procedure has been frozen and no issues are unresolved. The document must be polished and then sent out for ballot. These actions are expected to take place in the fall.

SAE J2951: Dynamometer Drive Quality Metrics

Argonne has been using advanced driver performance metrics for about 10 years. However, in 2010, EPA approached SAE to develop a standard set of chassis dynamometer driver performance metrics. It is a fact of chassis dynamometer testing that test-to-test, driver-to-driver, and lab-to-lab variations exist and comparing test results among different labs and drivers can become problematic. It has been shown that fuel economy can and does change significantly, depending upon how the driver drives the test schedule. With a comprehensive set of driver performance metrics, these differences can be explained.

For example, the speeds and accelerations driven during a test cycle can be used to calculate the total energy driven by a vehicle and compared to other tests or the energy corresponding to the target speeds of the schedule. If driven energy is a small percentage higher than the target energy, then we may expect a similar increase in fuel consumption.

In addition to the cycle-energy metric, several other supplemental rating metrics were useful for analysis of chassis dynamometer results. The procedure contains Absolute Speed Change and Absolute Power Change metrics that are particularly well-suited to quantifying drive characteristics that might come about from accelerator pedal perturbations. This parameter is especially useful when analyzing hybrid electric vehicle results. In some cases, if the driver is trying too hard to maintain the speed according to the drive schedule, over-corrections can start the engine more frequently and thus consume more fuel.

Other parameters include a root mean squared error, a contribution from Argonne. This parameter was installed in Argonne's dynamometer host computer over 10 years ago to quantify a driver's speed-matching performance immediately after run-time.

Argonne made a number of technical contributions to this standard. The committee decided to provide line-by-line MATLAB™ code that will calculate all the parameters in the document so there are no questions about the interpretation of the equations in the document. Argonne wrote this code and also created an Excel™ spreadsheet with macros that calculate the results and populate a results table. The results of these two tools were compared to validate their accuracy. The spreadsheet will be freely available to any vehicle testing laboratory for use in calculating the results.

SAE J2711: Medium and Heavy-Duty Chassis Dynamometer Test Procedures

Just as J1711 (light-duty HEV and PHEV test procedures) was originally developed in the absence of actual production-intent vehicles, so too was J2711. Many important developments were made in J1711 that can carry over to J2711.

Argonne is taking a leading role in the committee by chairing the task force and organizing regular meetings. Much of the time has been spent on defining the new challenges for trucks and finding which components of J1711 readily apply and which parts will need further development and validation for the particular scope of this procedure.

Conclusions

Argonne's decades of experience in fuel-economy and emissions testing of HEVs and PHEVs are an important resource in the DOE system. Because of this expertise, the industry regularly turns to Argonne and the DOE to help lead test procedure efforts. As new vehicles undergo a radical change in advanced powertrain technology, it is critical that testing procedures properly characterize the efficiency gains and do not bias one technology over another. Argonne, in its role as a research/test lab that is always developing and improving new test procedures, is a key part of DOE's vehicle systems program.

A key objective of the year was wrapping up the BEV test procedure. Many stakeholders in industry, EPA, DOE, and the California Air Resources Board are in need of efficient, accurate and up-to-date procedures to test a growing number of production BEVs announced for sale in the U.S. Because of the diversity and large size of the task force, there were many requirements that had to be met with everyone in agreement. Argonne provided many novel components that were key to the success of the procedure. The final document write-up of J1634 was validated with two major procedure-validation test programs. The importance of Argonne's contribution is that our staff members are world experts at BEV testing and the generated data are not normalized or obfuscated (as industry has done with their test data offerings). Argonne's contribution has ensured that the procedure is valid, accurate, and easily administered. It will be the basis for many BEV tests for years to come.

Argonne's involvement in other SAE activities is also focused on providing expert input to vehicle testing procedures and standards that address the new challenges with new advanced-technology vehicles. With our partners, this program will continue to help accelerate the deployment of new technology and reduce the risks of that deployment in order to achieve DOE goals in petroleum consumption and emissions reductions.

VII.A.3. Products

Publications

1. Duoba, M., "Update on Test Standards for Green Car," Korea-USA Workshop for Green Car Collaboration, Chungnam, Korea, September 28, 2011.
2. Duoba, M., "Opportunity to Standardize Vehicle Testing Procedures," Electric Vehicle and Battery Technology Workshop, Argonne National Laboratory, August 4, 2011
3. Duoba, M., "Design of an On-Road PHEV Fuel Economy Testing Methodology with Built-In Utility Factor Distance Weighting," 2011 SAE Congress, Detroit, MI, April 24–26, 2011.

4. Duoba, M., "Beyond MPG: Characterizing and Conveying the Efficiency of Advanced Plug-In Vehicles," SAE 2011 Hybrid Vehicle Technologies Symposium, February 9–10, 2011, Anaheim, CA.
5. SAE J2951, "Drive Quality Evaluation for Chassis Dynamometer Testing," Light Duty Vehicle Performance and Economy Measurement Committee, WIP (work in progress as of November 2011).
6. Duoba, M., "Development and Investigation of Practical (Shortened) Standard Test Procedures for Battery Electric Vehicles," The 25th World Battery, Hybrid and Fuel Cell Electric Vehicle Symposium and Exhibition (EVS25), Shenzhen, China, November 5–9, 2010.

Tools & Data

J2951 MATLAB™ code to calculate all drive quality metrics, July 14, 2011.

J2951 Excel spreadsheet to calculate all drive quality metrics. Available by contacting Chris Nevers, nevers.chris@epamail.epa.gov, at the U.S. Environmental Protection Agency in Ann Arbor, Michigan.

Nissan Leaf J1634 Procedure Validation Data. One hundred and seven (107) dynamometer test cycle and recharge data files (501 MB). Tests performed from 8/31/11 to 9/12/11.

VII.B. Codes and Standards Support for Vehicle Electrification

Principal Investigator: Theodore Bohn
Argonne National Lab – Energy Systems Division
9700 S. Cass Avenue
Argonne, IL 60439
(630) 252-6982; tbohn@anl.gov

DOE Program Manager: Lee Slezak
(202) 586-2335; Lee.Slezak@ee.doe.gov

VII.B.1. Abstract

Objectives

- Provide world-class support and information dissemination of the issues and practices that are used to define and create standards within the standards-defining organizations (SDOs), such as the Society of Automotive Engineers (SAE), the *Institute of Electrical and Electronics Engineers* (IEEE), the International Organization for Standardization (ISO), the *International Electrotechnical Commission* (IEC), and the *National Electrical Manufacturers Association (NEMA)*.

Approach

- Participate in monthly and semi-monthly Standards Working Group meetings, through in-person attendances as well as via WebEx remote access to save on travel overhead.
- Develop literal standards verbiage and host meetings as the chair of the SAE J2907 Motor Rating Standards.
- Design and develop a test bench and methodology to perform benchmark validation of parameters and to gain insight into gaps of knowledge required to craft useful, high-quality standards related to plug-in electric vehicles (PEVs).
- Create software and test fixtures to evaluate the attributes described in the standards, such as data throughput in communication or efficiency/max power for electric machines.
- Interact with industry experts in an effort to harmonize standards for vehicle charging issues among the various SDOs and industry segments, such as the Grid Interaction Tech Team, bridging utilities, and automotive original equipment manufacturers.

Major Accomplishments

- Created an initial working draft of the SAE J2907 Motor Rating Standards document.
- Commissioned the creation of the Autorem module, based on the Texas Instruments pre-production Octave universal baseband chip set and G3 PLC communication method. Thirty copies of the automotive-oriented information were produced and shared openly with vehicle industry representatives. These are the first power-line communication (physical layer) over pilot-wire validation results upon which the standards community representatives will vote for the single standard PEV communication method.
- Developed a working prototype of a 10-MHz, coreless, low-cost, high-efficiency wireless charging emitter and receiver based on near-field magnetic resonance coupling in a copper-plated 3-D rapid prototyping form factor that contains actual permittivity and leakage inductance parameters, which can be used to validate the Solidworks and finite element analysis (FEA) software models of the emitter design.
- Produced a lightweight, highly interactive Smart Grid demo/display for exhibit at the Electric Vehicle Symposium (EVS-25) in Shenzhen, China.

- Created three iterations of a validated working prototype end-use monitoring device (EUMD) submeter. The device has a low materials cost ($10 in high volume), is compact (smaller than a business card), and complies with standard communication protocols over an IEEE 802.15.4 Zigbee physical layer to a standard gateway device. It also communicates directly with an AMI meter.
- Addressed the (relatively) high installation labor costs for EUMDs on a Level 1 AC charging circuit (120vac, 15A) by creating a low-cost EUMD on a standard 60A high-volume socket, which can be installed without special tools by the premises owner. This is especially valuable for multi-family dwellings with shared parking areas and a single utility service connection.
- Produced a low-cost option for electric-vehicle support equipment (EVSE) installations on a residential/industrial circuit panel that is full and normally would require an upgrade and replacement of the entire panel. This method adds EUMD sub-metering functionality to a standard 60A fused disconnect device, downstream of the main premises meter.
- Created a low-cost transformer monitoring system, with meshed network communication, that can be installed without special tools.
- Developed SAE J2931/J2953 Communication and Interoperability Test Fixtures.
- Provided support to the California Public Utilities Commission. Consulting efforts regarding sub-meter implementation will continue.
- Verified connectivity, communication, and interoperability between vehicles, EVSE, communication networks, and grids (i.e., service providers/grid operators/utilities).

Future Activities

- Incorporate cyber security initiatives into a solar-fed DC fast-charging station with local grid storage, including bi-directional power flow for utility-level (100-kW) bidding in the utility ancillary services market.
- Investigate and support the wireless communication methods required for secure controls of wireless PEV charging, based on IEEE 802.11p Direct Short Range Communication (DSCR) protocols. This work will leverage previous IEEE 802.15.4g Software Defined Radio accomplishments.
- Evaluate and validate the performance claims of the first production bi-directional on-board PEV charger, EETREX Inverger, and work with the parent company, Methode Electronics in Rolling Meadows, Illinois, to incorporate SAE J2847/3 reverse power flow control messages.
- Implement and validate an SAE J1772-DC Level 2 combination coupler with an SAE J2931/1 PLC over pilot-wire robust communication by using an SAE J2847 message set to control the Supply Equipment Communications Controller (SECC).
- Continue to host standards meetings for SAE J2907 Motor Ratings Standards, and participate in other monthly standards creation meetings.
- With input from the SAE J2954 wireless charging standards community, design, develop, and deploy a standardized testing fixture with three-axis magnetic field probes and coil positioning systems to allow system-level performance on safety, alignment, and communication to be uniformly evaluated.

VII.B.2. Technical Discussion

Background

Standards enable lower risk innovative solutions to charging PEVs.

Introduction

Electric drive vehicles, including battery electric vehicles (EVs), and PHEVs have the potential to dramatically improve fuel economy and reduce greenhouse gas emissions compared with conventional technologies. These technologies require new infrastructure to become a significant part of the vehicle fleet. In the case of EVs and PHEVs, an electric charging infrastructure is needed in the form of charging stations, most often at home or at the workplace, but also in public parking locations. At present, few charging points are available. However, projects are under way to deploy new electric-drive vehicle charging infrastructure and to collect data to facilitate analyses of future needs.

While gasoline and diesel-fuel vehicles refill at a gas station, electric-drive vehicles recharge at a charging station. Three charging levels are currently under consideration. Level 1 charging uses a standard 120-volt (V), 15–20 amps (A) rated (12–16 A usable) circuit and is available in standard residential and commercial buildings. Level 2 charging uses a single-phase, 240-V, 20–80 A circuit and allows much shorter charge times. Level 3 charging — sometimes colloquially called "quick" or "fast" charging — uses a 480-V, three-phase circuit. Level 3 charging is available mainly in industrial areas, and it typically provides 60–150 kW of off-board charging power.

This report summarizes current activities to demonstrate and deploy the electric recharging infrastructure, the communications challenges associated with EVSE, the potential impacts on the electric grid and distribution network, and government cooperation in developing industry-recognized EVSE standards.

Approach

The Argonne Center for Transportation Research Engineers provides world-class, independent third-party benchmark comparisons of power line communication candidate technologies for use in PEV-EVSE smart-charging communication over existing connections. Unlike the dedicated pins and conductors required for other DC charging controls standards, the SAE-ISO/IEC standard for modulating over the existing pilot wire simplifies the connector design, thereby leading to reduced complexity by eliminating the insertion force assist mechanism.

Argonne engineers are leading the standards community in creating bona fide proof-of-concept systems for validating standards that complement previous electrical circuit simulations. Each of the SAE standards listed below relies, in a sequential manner (i.e., all are held up until the communication system is validated), on quality results in a real-world context, such as that provided in the Argonne Advanced Powertrain Embedded Control Systems (APECS) laboratory located in Building 362. The SAE standards are as follows:

- SAE J1772-DC (specification of the combination AC/DC single coupler solution point of contention; see Figure 1);
- SAE J2847/1-5 (five-part communication messages — utility messages, DC charging messages, V2G messages, etc.);
- SAE J2931/1-4 (physical layer definitions, G3 PLC, HomePlug GreenPhy);
- SAE J2953 (interoperability of EV charging systems from utility communications, gateways, EVSEs, and PEVs);
- SAE J2954 (wireless charging safety, performance, and interoperability); and
- IEEE 802.11p (direct short-range communication for wireless charging).

Figure 1. Example of an SAE J1772 charge coupler connector for vehicle battery charging.

Defining Voluntary Standards

"Voluntary" standards (i.e., those not required by regulation[5]) address essentially all aspects of automobiles and are issued by several organizations around the world, such as the SAE in the United States, the ISO or IEC in Europe, and the Japan Automobile Research Institute (JARI) in Asia. The electrical content of automobiles adheres to standards developed by the IEEE. As plug-in vehicles and EVSE utilize the electric power grid, they are subject to standards established by Underwriters Laboratories and the fire and building safety

[5] Although voluntary in some regions of the United States, SAE J1772 is essentially a regulatory requirement in California and in many other states that have adopted the CA ZEV Regulation, because California requires vehicles to comply with J1772 in order to earn ZEV credit.

standards set by the National Fire Protection Association (NFPA), including the National Electrical Code (NEC).

Codes and Standards Activities

Starting from the vehicle and moving upstream to the utility, the first requirement for standards development involves the charge coupler — the physical connector — and vehicle receptacle for hybrid and electric-vehicle charging. This provides the means by which the vehicle interacts with the EVSE.

Development of the End-Use Monitoring Device

A needed breakthrough in technology occurred with the delivery of the EUMD to address the need for compact metrology. The EUMD is a small device that the EVSE uses to measure energy consumption. In addition, it provides the method of communicating that information back to the Smart Grid — in terms of both hardware (wired and wireless universal communication technologies) and software/protocols (grid-operator home-vehicle communication).

Argonne has developed an EUMD, as shown in Figure 2, with the capabilities of a smart meter (i.e., revenue-grade power measurement and communication) in a compact package that is less intrusive and has a much lower cost than a standard meter. Three versions/generations have been developed this year to assess the relative merits of different current sensors and communication technologies. Ultimately, these communicated data are transmitted to the utility provider, where software can be standardized to facilitate grid-wide smart management with targeted goals, such as balancing electricity supply and demand and sequencing vehicle charging to avoid local transformer overloads.

In addition, the design is adaptable for various installation locations. It is capable of being installed in the vehicle, EVSE, power distribution panel, secondary panel, plug receptacle, and even the distribution transformer (as a smart monitor to enable local grid optimization).

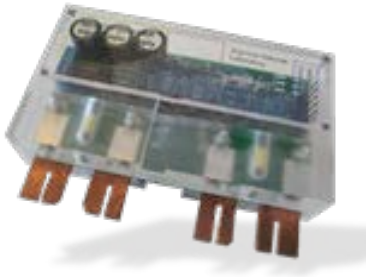

Figure 2. Prototype EUMD with FGM current sensor.

SAE J2953/J2931Communication Test Fixture

Figure 3 shows a version of a test bench that was constructed to illustrate various options for vehicle-grid connectivity and practical choices for integrating the EUMD. The set-up includes essential elements of a vehicle-grid connection using various standard enclosures. It has demonstrated that two-way messaging consistent with proposed data rates can be accomplished for compliance with SAE J2931/J2953.

Figure 3. Table-top display to demonstrate Smart Grid interoperability, developed by Argonne.

EV Charging Pilot Exercise

Argonne's campus has been selected for running some real-world trials of hardware and communications software to validate the EV codes and standards. To date, there are 25 EUMDs installed campus-wide, tied to a selection of EVSE examples from various suppliers (Figure 4). Four more combinations will be evaluated in the near-term when delivered.

Figure 4. View of the EV charge stations of several different suppliers, installed by the Advanced Powertrain Test Facility.

A solar cell array also has been installed to capture solar energy (Figure 5), and a wind turbine has been erected on campus (Figure 6) to provide a source of renewable electrical energy for charging vehicles. The amount of renewable energy captured is measured and the data are transmitted through a local Universal Metropolitan Area Network (UMAN) with a 4G router on the mesh. Vehicle charge station usage can be tracked through a User ID by use of an employee RFID badge.

Figure 5. Argonne's solar energy array as a node for providing renewable solar energy for the pilot Smart Grid experiment to supply two vehicle charge stations.

Figure 6. Installation of a wind turbine to provide another source of renewable energy connected to Argonne's pilot Smart Grid/EV Charging exercise.

Wireless EV Charging, SAE J2954

The objective is to validate various designs of wireless charging approaches to assess their performance, overall efficiency, interoperability with other devices (EVSE), and safety. As part of this task, Argonne researchers are exploring new emitter and receiver coil topologies based on near-field magnetic resonance coupling. The emitter shown in Figure 7 depicts a ~10-kW hollow (air core) seven-turn foil-based primary coil designed to operate at 8 MHz. This coil can be manufactured very cost competitively by rotational-molding and by applying thin copper plating. Figure 8 shows both plated and foil wrapped. The vehicle-side receiver (upper coil) is a single-turn copper tube with a SiC rectifier (passive) with voltage regulation off-board. The resonant-mode power electronics with DSRC controls (not shown) use coil natural resonance for tuning.

Figure 7. Hollow core primary resonance coil antenna design for low-cost manufacture.

Figure 8. View of the wireless charging system showing the resonant antenna components. The top coil is the receiver that would be mounted to the vehicle, while the lower coil is the transmitter embedded in the floor or road bed.

Conclusions

The creation of standards is accomplished by the groups of standards-defining organizations. Argonne engineers have provided extensive technical support and contributed to the collection of independent and balanced validation data for the creation of codes and standards that enable vehicle electrification.

The EUMD and communication modules will directly support laboratory and field testing to refine standards, promote harmonization, and evaluate hardware interoperability assessment.

The SAE standards committees have requested support to obtain sufficient data prior to voting on the critical communications and connectivity standards. Argonne has developed test fixtures and related resources to facilitate this activity.

VII.B.3. Products

Publications/Presentations

1. T. Bohn, "EVSE Interoperability; Verifying Compatibility and Compliance," presentation at the EVS-25 Plug-in Hybrid Electric Vehicle Workshop, Shenzhen, China, November 2010.
2. T. Bohn, "Vehicle Standards Update — Hybrid Vehicles," presentation at the NFPA Electric Vehicle Safety Summit, Detroit, MI, October 2010.
3. T. Bohn, "NIST Smart Grid Interoperability Priority Action Plan 11 — Plug-in Electric Vehicles DC Charging Coupler White Paper," White Paper: NIST PAP-11, January 2010.
4. T. Bohn, "EV Charging 101," presentation at Clean Cities: Plug-in Vehicle and Infrastructure Community Readiness Workshop, Indianapolis, IN, June 2011.

Patents

No patents have been created from this work, since standards are by definition open and not protected.

Tools and Data

Tools:

- Tools include the Python script-based software that controls the SAE J2953 interoperability evaluation test fixture.
- Argonne has developed an EUMD, as shown in Figure 9. This EUMD has the capabilities of a smart meter (i.e., revenue-grade power measurement and communication) in a compact package that is less intrusive, and it has a much lower cost than a standard meter. Three versions/generations have been developed this year to assess the relative merits of different current sensors and communication technologies.

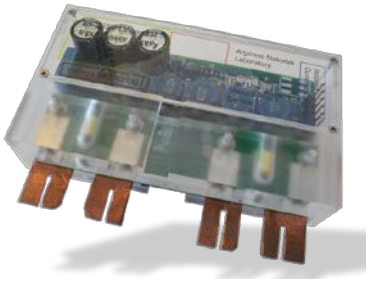

Figure 9. Prototype EUMD with FGM current sensor.

Other tools include:

- Freescale Kinetis K60 processor tower system connected to three similar, but different, physical layer solutions for a side-by-side comparison of performance and reliability attributes;
- Autorem T.I. Octave G3 Narrow Band Orthogonal Frequency Division Multiplexing (N-OFDM) to Controller Area Network (CAN) module for evaluating cross-talk effects, maximum throughput, and worst-case latency;
- Maxim MAX2992 module for evaluating similar criteria as Autorem; and
- Qualcomm-Atheros wide-band Homeplug GreenPhy solution (Figure 10).

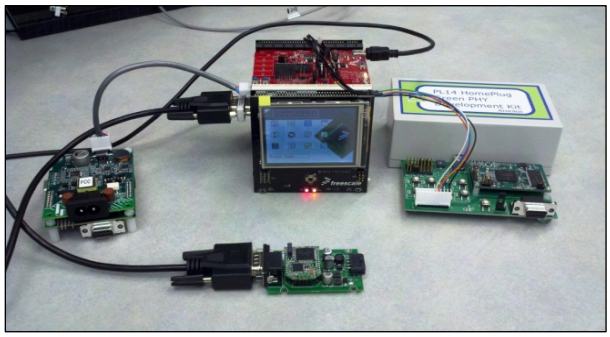

Figure 10. Qualcomm-Atheros wide-band Homeplug Green Phy, shown being tested.

Test Data:

- T.I. Octave G3 test results: 45 bytes of payload in ~12.5 ms time on wire (TOW), ~28.8 kbps actual data.

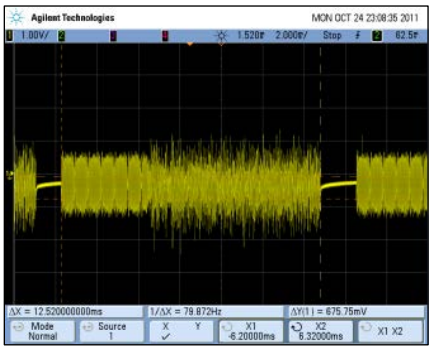

- Bit error rate test (QPSK, Cenelec ABC, 62 carriers, PWM signal State B):
  - Signal Output: ~300mV$_{pp}$ -> high BER, and
  - Signal Output: ~2 V$_{pp}$ -> low BER.

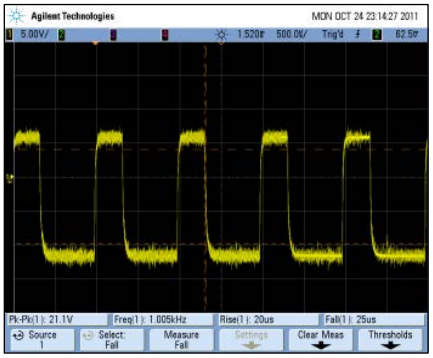

VII.C. Vehicle to Grid Interconnectivity Technical Team Support

Principal Investigator: Keith Hardy
ANL-East
Energy Systems Division
955 L'Enfant Plaza SW, Suite 6000
Washington, DC
(202) 488-2431; khardy@anl.gov

DOE Program Manager: Lee Slezak
(202) 586-2335; Lee.Slezak@ee.doe.gov

VII.C.1. Abstract

Objective

- Co-chair the US DRIVE Grid Interaction Technical Team (GITT), whose membership* includes automotive manufacturers, electric utilities, government agencies and national laboratories, to identify, prioritize and set objectives for DOE-sponsored activities at the labs to address R&D needs in support of standards development associated with the electric vehicle-electric infrastructure interface. This interface encompasses elements of the vehicle and charging infrastructure that are directly involved in connecting and communicating between vehicles, Electric Vehicle Supply Equipment (EVSEs), communication networks and utilities to transmit and receive necessary and sufficient information to provide recharge power consistent with the constraints, control parameters and business systems of service providers, grid operators and utilities. The time frame of interest is the next two years; to support government and industry decision-making consistent with the 2015 goal of 1 million plug-in vehicles on U.S. roads.
  * Industry: Chrysler, Ford, GM, DTE Energy, SCE and, more recently, Tesla and EPRI (when US DRIVE replaced the FreedomCAR partnership)
    Government: DOE (VT and OE), DOC and DOT
    National Laboratories: ANL, INL, ORNL and PNNL

Approach

Owing to the expected introduction of plug-in vehicles in volume in the U.S. (targeting 1 million by 2015), GITT activities focus on near-term implementation of projects with potential long-term impact including:

- Reduce the cost of the vehicle-grid interface
  - Low-cost, compact sub-meter with wired/wireless communication
  - Universal communication to meet global requirements
- Enhance the viability of faster/more convenient charging
  - Wireless charging; benchmarking and enabling technology development
  - Impact of fast charging (with grid storage and demand response)
- Implement smart charging (consistent with smart-grid load management)
  - Pilot sub-meter and communication in ORNL/ANL EV charging stations
  - Smart monitor for local distribution transformers (i.e., for locally managed charge scheduling)

- Support harmonization of global connectivity and communications standards (requirements, test equipment, verification, etc.)
  - Charge coupler, communication, interoperability and wireless charging committees
  - State-level activities with national impact (e.g., sub-metering in CA)
  - Cooperative projects to promote SAE (U.S.), IEC (Europe) and GB (China) harmonization

Major Accomplishments

- EVSE Installation Permitting Template
  - Completed and transferred to Clean Cities for deployment
- End Use Measurement Device (EUMD)
  - Developed a low-cost, revenue-grade meter with wired/wireless communication to utility, smart meter or Home Area Network
- Auto-rem module (based on TI Octave chip; Power Line Communication)
  - Vehicle-to-EVSE communication; designed for automotive application
- SAE J2931/J2953 Communication and Interoperability Test Fixture
  - Verify connectivity, communication and interoperability between vehicles, EVSEs, communication networks and grids (i.e., service providers/grid operators/utilities)

Future Activities

- SAE J2931 committee support – Communication testing to collect data for SAE balloting process
- SAE J2954 committee support – Benchmarking wireless charging products; specifications for wireless charging test apparatus
- Enabling-technology development for wireless charging at ANL, ORNL and U. of Wisconsin-Madison
- Integration of EUMD in solar EV charging stations (ANL/ORNL)
- Characterization of synergy of, and issues with, integrating fast charging and grid storage
- California Public Utilities Commission (CPUC) support – Continue consulting regarding sub-meter implementation
- EV-Smart Grid Interoperability Center support – Work with EC Joint Research Center to assess potential establishment of a comparable laboratory in Europe to assess interoperability; consult regarding requirements and lab setup at the EC Joint Research Center-Institute for Energy & Transport (JRC-IET)

VII.C.2. Technical Discussion

Background

The drivers for Grid Interaction Technical Team (GITT) activities are 1) interoperability of vehicles and the charging infrastructure, 2) reduction of the cost of the vehicle-grid interface and associated installation, 3) mitigation of the impact of plug-in vehicles on the electric infrastructure, i.e., local grid optimization and smart grid integration, and 4) harmonization of vehicle-grid connectivity and communication standards to facilitate global product proliferation, cost reduction and increased consumer confidence.

The time frame of interest is within the next two years, to support decision-making associated with pending production and introduction of plug-in vehicles. In addition to automotive manufacturers, suppliers are investing in component production facilities while states, municipalities and electric-service providers are attempting to prepare the infrastructure. For example, the California Public Utilities Commission is currently considering a requirement for a separate circuit and sub-meter for an EV charge station, to allow separate energy monitoring and potentially differential pricing as an incentive for EVs. However, the installation cost for this additional capability at a residence is reported to be well over $1000,

which could be a deterrent since it exceeds the cost of a Level 2 home charge station. Hence the GITT initiated activities in FY 2010 to reduce both sub-meter and installation costs, resulting in a prototype low-cost current sensor and adaptable communication technology, which are enablers for a compact revenue-grade power meter that could potentially be integrated in the EVSE or power panel, eliminating separate installation costs.

Introduction

The GITT was launched in late FY 2009 to include utilities in the FreedomCAR partnership, in recognition of the increasing emphasis on plug-in vehicles and the need to work together on the vehicle-grid interface. Projects were launched in mid-FY 2010, addressing practical matters such as streamlining the permitting process for installing charge stations and supporting SAE standards committees as well as R&D to address sub-metering and vehicle-grid communication technology.

Approach

Despite their research content, GITT projects are heavily oriented toward application engineering because of the urgency of addressing the vehicle-grid interface barriers prior to vehicle introduction. Hence, the automotive OEM partners and suppliers were directly involved, resulting in a focused, relevant and efficient activity with a pathway to prototype products.

Results

Technical details can be found in reports of individual national laboratories (ANL, NREL, ORNL and PNNL). This section summarizes the team's results.

EVSE Installation Permitting Template:

NREL completed the generic document for consideration by local jurisdictions as they attempt to become "EV ready." The template utilizes familiar language and references elements of building codes used in essentially all municipalities. Following review by key stakeholders, the template was transferred for deployment through the Clean Cities network.

End Use Measurement Device (EUMD):

Argonne developed the EUMD that has the capabilities of a smart meter, i.e., revenue-grade power measurement and communication, in a compact package that is less intrusive than a standard meter. Three versions/generations were developed this year to assess the relative merits of different current sensors and communication technologies. In addition, the design was adapted for various installation locations, including a vehicle, EVSE, power distribution panel, secondary panel, plug receptacle and even the distribution transformer (as a smart monitor to enable local grid optimization).

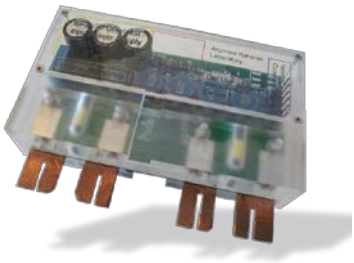

Figure 1. Prototype EUMD with FGM current sensor.

Auto-Rem Module:

Designed for automotive application, this module enables messaging between the vehicle and EVSE using Power Line Communication.

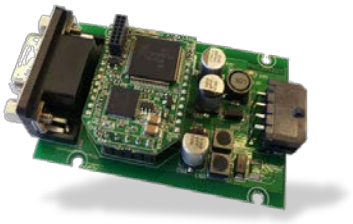

Figure 2. Auto-rem module with CAN interface.

SAE J2953/J2931Comunication Test Fixture:

Argonne developed a demonstration version of a test bench constructed to illustrate various options for vehicle-grid connectivity and practical choices for integrating the EUMD. Figure 3 shows the setup displayed at the GITT Annual Review in October. The setup included essential elements of a vehicle-grid connection using various standard enclosures and demonstrated that two-way messaging consistent

with proposed data rates (i.e., SAE J2931/J2953) can be accomplished.

Figure 3. Smart grid interoperability demonstration bench.

Conclusions

Members of the GITT, with the support of vendors, OEMs and suppliers, produced realistic working hardware for the vehicle-grid interface.

The EUMD and communication modules will directly support lab and field testing to refine standards, promote harmonization and assess hardware interoperability.

SAE standards committees have requested support to obtain sufficient data prior to voting on the critical communications and connectivity standards. The GITT has developed testing resources to facilitate this activity.

VII.C.3. Products

Tools & Data

Work is continuing to finalize the text fixture and test procedures to validate that two-way messaging between the vehicle and EVSE/ utility grid interface are consistent with proposed data rates and accuracy required by SAE J2931/J2953.

VII.D. Support for the Green Racing Initiative

Robert Larsen and Forrest Jehlik (Project Leaders)
Argonne National Laboratory
9700 South Cass Avenue
Argonne, IL 60439-4815
(630) 816-5464; blarsen@anl.gov
(630) 252-6403; fjehlik@anl.gov

DOE Technology Manager: Lee Slezak
(202) 586-2335; Lee.Slezak@ee.doe.gov

VII.D.1. Abstract

Objective

- Incentivize vehicle manufacturers to develop, validate, and promote advanced technology relevant to production vehicles through racing
- Increase the use of renewable fuels in racing
- Increase the use of electric drive technologies in racing
- Use racing as a platform to educate the public on the acceptability of renewable fuels and the capabilities of advanced vehicle technologies through highly visible demonstrations of their performance
- Increase the acceptance of "green racing" in the United States and internationally
- Diversify the success of the Green Racing Initiative beyond sports cars to include other racing series with even greater potential for wider participation and visibility
- Maintain collaborative partnership with the U.S. Environmental Protection Agency (EPA) and Society of Automotive Engineers (SAE) International.

Approach

- Work with the American Le Mans Series (ALMS) to strengthen its green racing program
- Refine scoring system; make it easier to understand
- Increase outreach to teams to encourage renewable fuel use
- Recommend hybrid electric vehicle (HEV) rules that create incentives for use, emphasizing safety
- Move toward a scoring system based on energy allocation
- Improve visibility and understanding of Green Challenge scores with media and race fans
- Increase U.S. Department of Energy (DOE) visibility at ALMS events
- Increase availability of second-generation biofuels
- Provide technical support for Project GREEN, sponsored by Circle Track Magazine
- Demonstrate the feasibility of accurate fuel control and aftertreatment for racing applications
- Promote the adoption of renewable fuels for grassroots racing across the United States

Major Accomplishments

- Dramatically increased the number of teams using advanced fuels with significant renewable percentages in ALMS racing to include all but two Grand Touring category cars and two Le Mans Prototype cars.
- Displaced a 2011 season high of 51.8% of petroleum at the inaugural ALMS Baltimore race. For the entire season on a distance-weighted basis, renewable fuels displaced 43.5% of the petroleum typically used in racing.
- Refined the Green Challenge scoring system to make it more transparent by showing the results as the sum of three scoring elements: Clean, Fast, and Efficient.
- Increased Green Challenge visibility on national and international television coverage, and with teams and media.
- Increased DOE visibility at every ALMS race; produced Green Challenge scoring summary after each race to assist media explanation of race results.
- Developed a more robust two-seat E85 HEV race car simulator in a specially designed trailer, and used it for public education at five ALMS races and several supporting events around the country.
- Raced the second-generation Porsche 911 GT3 R Hybrid at Mazda Raceway Laguna Seca with significantly improved hybrid components and controls, obtaining energy consumption data from this advanced vehicle.
- ALMS announced the content of Green Racing 2.0 based on input from the Green Racing Initiative that includes the use of energy allocations, electric drive technologies, and additional advanced fuel options including compressed natural gas (CNG).
- Successfully demonstrated a renewable fueled circle track car that exhibited drastically reduced well-to-wheel greenhouse gas and petroleum use.

Future Activities

- Support and incentivize the use of energy recovery technology in race cars. We expect several new-technology HEV race cars to compete in the 2012 season.
- Revise SAE J2880, the Green Racing Protocols, to reflect a new emphasis on electric drive technology; update definitions and lifecycle analysis approaches to keep it current with evolving technology and the needs of racing.
- Work with a wider range of sanctioning bodies to recommend ways to incorporate renewable fuels and advanced technology into racing.
- Develop technical and safety recommendations to enable the successful introduction of electric vehicle racing.
- Support and advance the use of renewable fuels at the grassroots level in American short track racing.
- Continue the development of more optimized production-based race engines tuned to renewable fuels and emissions controls.
- Apply vehicle electrification technology to short track racing cars and demonstrate its effectiveness.
- Provide technical support and recommendations to sanctioning bodies and rulemakers concerning Green Racing content.
- Support the development of more accurate on-vehicle fuel use measurement and a practical energy allocation system for racing.
- Develop and demonstrate renewable fueled, hybrid system in stock car application.
- Demonstrate enormous reduction of both petroleum use and greenhouse gases.

VII.D.2. Technical Discussion

Introduction

The Green Racing Initiative is a collaborative effort led by DOE in partnership with the U.S. Environmental Protection Agency. SAE International, a silent partner in this initiative, is lending its support. FY 2011 was the third year of activity in this program, signified by the second full season of the Green Challenge award in the American Le Mans Series. The short track stock car initiative developed last year in collaboration with *Circle Track Magazine*'s Project GREEN, continued to develop the technical basis to prove cost-effective engine and propulsion technology based on renewable fuels with emissions control was feasible. Through Argonne National Laboratory, DOE provides technical assistance, instrumentation, and analysis for this paradigm-shifting project. In FY11, the Green Racing Initiative made major strides in taking advantage of racing's huge potential for rapid technical development and the equally large potential to achieve DOE's objectives for public outreach.

Approach

Motor sports are the only professional sports that can help attain critical national energy and environmental objectives. Such racing-based events can help achieve these objectives by directing the vast creativity and engineering talent, significant spending, and rapid developmental cycles in racing toward the use of technology and fuels that reduce our dependence on petroleum and lower the carbon footprint of vehicles – while still providing the entertainment and drama that has made racing one of the largest and most followed sports around the world. Because of these unique attributes, racing is one of the biggest and best platforms for reaching a large audience with the message that, through advanced vehicle technologies and renewable fuels, we can maintain the personal mobility we want while moving toward energy security and sustainability we need.

Racing uses the crucible of competition to bring out the best in automotive technology, and the people who are willing to push the limits in using it touch a core cultural value that resonates with the public. Living on the edge with technology and danger adds to racing's interest, drama, and entertainment. Racing also inherently values efficiency, an attribute that underpins our national energy and environmental objectives. We have developed the Green Racing Initiative with our partners by building on this core value in racing, using its need for cutting-edge high-technology machinery and adding renewable fuels and advanced technology as ways to achieve it.

Results from the 2011 American Le Mans Series Season

The Green Racing Initiative has become an integral part of the ALMS, which claims to be the global leader in green racing. The 2011 season continued the growth and acceptance of green racing activities in the series. This fact is illustrated by the announcement in August of ALMS's intention of implementing Green Racing 2.0 in coming years.

The 2011 ALMS season saw the use of non-petroleum and renewable fuels become dominant. Every Green Challenge victory in the Grand Touring (GT) category and five out of nine victories in the Le Mans Prototype (LMP) were won by a car using advanced fuels. The LMP category winners shown in Figure 1 predominately used isobutanol/gasoline (the Dyson Mazda, a turbocharged 2-liter, four-cylinder engine) or E85 (the Pickett Racing Aston Martin naturally aspirated V12). More than half of the vehicles in the Prototype field used fuels with significant non-petroleum content. All but five of the LMP category competitors used advanced fuels; two cars only competed in three of nine races and three competed in only one race.

Figure 1. Five of nine LMP Green Challenge winners used advanced fuels. Photo of the Season and Green Racing Champion Dyson Mazda turbocharged 2-liter fuel with isobutanol (top) and the Pickett Aston Martin naturally aspirated V12 fueled with E85 (bottom).

In the ultra-competitive GT category, E85 dominated as the fuel of choice. All three of the top finishers in all the races used E85 fuel, and in seven of the nine races all top five finishers were on E85. Only two cars that raced the full season used E10 fuel. The GT class is based on cars that are on the road today and pits the largest and most sophisticated auto manufacturers from around the world in door-to-door competition that may be the most competitive class in racing anywhere in the world. All BMW, Corvette, Ferrari, and Porsche factory and most privately entered cars used this renewable fuel with great success (these cars are pictured in Figure 2). The wholesale movement to E85 was motivated both by the performance potential of this excellent fuel and its energy security and environmental advantages.

Figure 2. The top three finishers in all nine ALMS races used E85 fuel, including the factory cars from BMW (Overall and Green Challenge Season Champions), Ferrari, GM's Corvette, and Porsche. Top photo: RLL BMW M3 GT; second photo: Risi Competizione Ferrari 458 Italia; third photo: Corvette Racing's ZR1R; and bottom photo: Flying Lizard Porsche 911GT3 RSR.

Underlining the significance of this movement to advanced renewable fuels, teams and engineers from all over the world made the switch to these fuels because of their performance advantages alone. There were no incentives for switching in the form of funding or extra points. ALMS goes to great lengths to balance the performance of all the cars, so the switch to these fuels was made solely because they offered better efficiency and, in some cases, more power. The Green Challenge scoring system accurately reflects the fuel's characteristics in terms of its greenhouse gas and oil replacement attributes without rewarding their selection of these over conventional fuels. That is what makes this switch to renewable replacements for conventional oil-based fuels in

this elite form of motorsports even more impressive and significant.

In terms of the percentage of oil replaced by the Green Racing Initiative in the ALMS in 2011, the peak performance was at the inaugural Baltimore Grand Prix where there was a record-setting 51.8% reduction of the oil consumed on a well-to-wheel basis throughout the race in the LMP and GT categories. For the entire season, taking into account the total number of miles raced, 43.5% of the oil that would have been used before the Green Racing Initiative began was replaced by renewable and non-petroleum fuels. This noteworthy accomplishment demonstrates that these fuels are capable of outstanding performance and reliability, and capable of widespread use in street vehicles.

This year brought more visibility for DOE's involvement in the ALMS Green Challenge awards through a concerted effort of DOE, Argonne National Laboratory (ANL), and EPA staff in cooperation with ALMS media relations representatives. More television and radio time was devoted to Green Challenge scoring and explanations. Broadcast interviews with DOE sponsors grew, including radio and television segments with Deputy Assistant Secretary Kathleen Hogan at the inaugural Baltimore Grand Prix (Figure 3).

Figure 3. DOE Assistant Deputy Kathleen Hogan provides interviews explaining the benefits of the Green Racing Program to the media during the ALMS Baltimore Grand Prix event.

Following the success of the first year deploying the Green Racing simulator, a second-generation mobile trailer outreach simulator was developed for the Green Racing program. This two-seat simulator models a renewable-fueled, hybrid-powertrain, race car, allowing the participants to drive a simulated renewably fueled, hybrid race car, while recording both their Green Racing score as well as lap time. The fuel usage is calculated, and the savings compared using the regenerative system versus systems that did not use it. Included was a simulation of petroleum displaced using E85 versus racing fuel, the message of which is displayed at the conclusion of the race. In addition, a second monitor displays pertinent DOE program information, as well as tips and facts that may be used to reduce petroleum consumption.

Prior to being allowed to drive the simulator, contact information (e-mail) data is collected from the participants. These data will be made available to the program sponsors. Figure 4 shows the improved mobile Green Racing simulator. From Figure 4 it can be seen that graphics surrounding the simulator highlight DOE pertinent technologies and programs, further serving as an outreach tool as it is transported.

Figure 4. Green Racing mobile simulator at Clean Cities Summit, Indianapolis Motor Speedway, Indianapolis Indiana, June 29, 2011.

Following the completion of the simulation, a plastic card is printed out with the participants name, event, Green Racing score, time, and a highlight for the Green Racing Web site. The

cards were presented to each participant along with a Green Racing lanyard for additional promotion of the program.

Figure 5. Lyn St. James, former Indy car driver, competing in the Green Racing simulator. The Green Racing simulator developed by Argonne incorporates a program that calculates the amount of regenerative braking energy captured and fuel used during two laps of simulated racing. This simulator was set up at five ALMS races in 2011. It served as a notable means of disseminating the DOE Green Racing's key message that the use of renewable fuels and hybrids can displace a substantial amount of imported petroleum.

Another round of improvements were made to the Green Challenge scoring system for the 2011 season that completely repackaged the results into a more easily understood format. The scores were grouped into three major categories – Clean, Fast, and Efficient – each with equal impact on the overall scores. This change was very well accepted by the media and the teams, because it provided a simple way to understand the elements that go into the score. The changes also improved the correlation between on-track performance and Green Challenge scores. At the end of every race, a summary of the results of the Green Challenge scores were produced, highlighting the comparative energy efficiency and average speeds of the competitors in MJ/km and km/hour, respectively. Updates to the well-to-wheel petroleum and greenhouse gas calculations using the latest GREET model release were made again this season. The energy efficiency element of the Green Challenge scoring system has gained international credibility and is being considered for implementation in the newly formed FIA World Endurance Cup spanning Europe, the United States, and Asia in 2012, further validating the quality of this system developed for the Green Racing Initiative.

An important element of the Green Racing Initiative is to promote the use of energy recovery systems in racing. Major steps toward this goal were achieved this year when the Automobile Club de l'Ouest (ACO), the sanctioning body for international sport car racing, approved rules for the incorporation of hybrid electric technology into the Prototype class after significant input provided by the Green Racing Initiative. Several HEV LMP cars are expected to compete next year (Toyota, Peugeot, and Oak Racing). Our focus remains encouraging future rules packages for both GT and Prototype cars to allow energy recovery from braking and waste heat sources. The prospects for allowing HEV technology for the GT category remains the most positive in the ALMS after a general update in rules for the 2014 season. Visible progress in the accelerating development of hybrid electric technology was demonstrated when the second-generation Porsche 911 GT3 R Hybrid shown in Figure 6 debuted at Mazda Raceway Laguna Seca in September.

Figure 6. The Porsche 911 GT3 R Hybrid V2.0 goes through technical inspection before the ALMS race in Monterrey, CA. In the background, Bob Larsen (ANL) discusses the changes to the car with a Porsche race engineer.

This improved version of Porsche's rolling HEV test bed used lightweight electric drives and a more compact and powerful electromechanical

flywheel energy storage. Impressive integration of controls was a major development this year, going from simple paddle actuation to full integration with the car's braking and traction control systems (see steering wheel with various map functions in Figure 7 below).

Figure 7. The steering wheel from the Porsche 911 GT3 R Hybrid. Note the extra dials to fine-tune the maps for hybrid components such as energy recovery, electric propulsion, and traction control close to the Porsche crest.

The 911 GT3 R Hybrid had up to an extra 140 hp for about 6 seconds when the flywheel was fully charged from braking and had noticeably better acceleration out of the corners in spite of its 65 kg extra weight. The objective of the car is to reduce fuel consumption while maintaining the performance of the current race car. Fuel consumption data will be supplied by Porsche during the off season for analysis by DOE technical staff. During the race, the 911 GT3 R Hybrid finished at the front of the GT field but was officially unclassified as it was racing as an experimental vehicle.

Figure 8. The Porsche 911 GT3R Hybrid in action.

The growing interest in electric vehicle racing led to considerable work in the last half of FY11 to lay the technical and safety groundwork for incorporating electric-drive-only vehicles into future racing activities. Although there have been many announcements of electric racing series and individual races, further work on developing the technical foundations for the success of this new form of racing remains to be done in coming years. Everything from proper battery containment and cooling to recharging protocols needs technical review and development. Facilitating this form of racing over the next few years will make an important contribution to accelerating the development of this important advanced vehicle technology and its acceptance by the public.

ALMS Green Challenge Championships Awarded for the Third Year

The DOE/EPA/SAE International's season-long Green Challenge awards were given to the vehicle manufacturer that consistently placed the best – week in and week out – in Green Challenge scoring. For 2011, the winner in the Prototype category was Mazda for its championship-winning P1 Lola B09/86 Mazda, run by Dyson Racing (Figure 9). This car, powered by an isobutanol/gasoline blend in its turbocharged 2-liter, four-cylinder engine, foreshadows the direction of top-level sports car racing in the future. The Dyson Lola/Mazda also won the overall Championship in the Le Mans Prototype (LMP) category. In an interview after the ceremony, John Doonan stated that winning the Green Challenge award was more important to Mazda than winning the racing championship.

Figure 9. Scott Atherton (left), ALMS CEO, congratulates John Doonan (second from left), Motorsports Director, Mazda, as Lee Slezak (DOE) presents Mazda with the Green Challenge Championship trophy for the LMP category along with Rick Klein (President of SAE International) and Karl Simon (EPA).

In the GT category, BMW won for its M3 GT cars that used E85 all season and were fast and efficient all season (Figure 10). Although Corvette Racing won twice as many Green Challenge trophies at individual races compared with the BMW (four vs. two), the consistently high finishes of the BMW team brought them their first Green Challenge Championship. These cars won more races than all other cars in the category combined. It is worthwhile to note that Ferrari won its first Green Challenge race award late in the season as the new 458 Italia steadily improved. Porsche and Ford each also won one Green Challenge race victory.

Figure 10. Ludwig Willisch, President of BMW North America, accepts the Green Challenge Championship trophy for the GT category from Lee Slezak (DOE), Rick Klien (President, SAE International), and Karl Simon (EPA).

Results from the Stock Car Program and Project GREEN

Continuing the push to integrate renewable fuels and advanced technologies in American stock car racing, Project GREEN successfully demonstrated the viability of the approach during the first quarter of FY11 by entering the car in a highly competitive, nationally ranked race. Running unclassified as an experimental vehicle, data on the car's performance was collected from a purpose-built data acquisition system and its petroleum and greenhouse gas reduction potential were characterized. A series of articles was published in Circle Track Magazine to disseminate this information to the circle track racing community.

Racing Demonstration

In October, 2010, the Project GREEN Camaro was raced at the half-mile LaCrosse Speedway in LaCrosse, Wisconsin, at the annual end-of season Oktoberfest national invitational event. The car competed in three race stints composed of 33 laps each. Competing against a field of 64 cars, the Project GREEN Camaro placed 14th overall. The production-based, renewable-fueled engine used in the car cost about one-quarter of the engines it raced against. In addition, during the time of the race, E85 was available locally for $2.37/gallon compared to the race fuel used by the other competitors at $10.75/gallon. Figure 11 shows the vehicle on the track at the event.

Figure 11. Zehr Racing Project GREEN Chevrolet Camaro, 2010 LaCrosse Oktoberfest race weekend.

Analysis of the data collected showed a nearly 80% reduction of petroleum utilizing renewable E85 compared to conventional racing gasoline. During a 33-lap stint, the car would have consumed nearly 4.4 gallons of petroleum-based race fuel. Using E85, the car consumed over 5.6 gallons with 85% of that fuel displaced by renewable ethanol; only 0.84 gallons of

petroleum were used for the renewable fueled configuration. This can be seen in Figure 12.

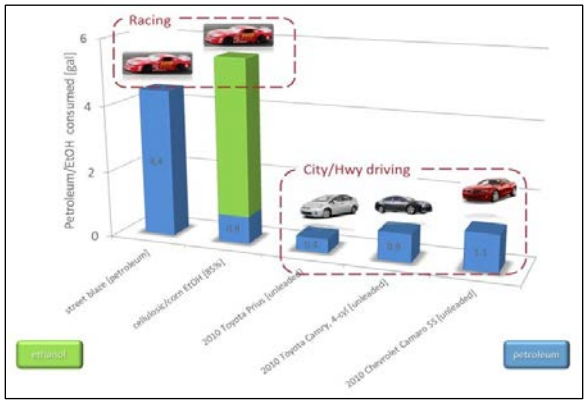

Figure 12. Petroleum-displacement, renewable-fueled ethanol powered stock car vs. production-based, gasoline-fueled counterparts. Data for stock car collected over 33 laps of racing. Data for production vehicles averaged from FTP (city + highway) cycle, EPA estimates.

In addition, well-to-wheels analysis on the greenhouse gas contribution was completed using Argonne's GREET model. The fuel supplied came from the Green Racing Initiative's collaboration with the American Le Mans Series, and used second-generation (cellulosic) ethanol in its formulation. Calculations were completed to determine the well-to-wheels impact of the Project GREEN car compared to production-based petroleum-fueled vehicles. Fuel consumption rates for these vehicles were calculated using the EPA-certified numbers. Results are shown in Figure 13.

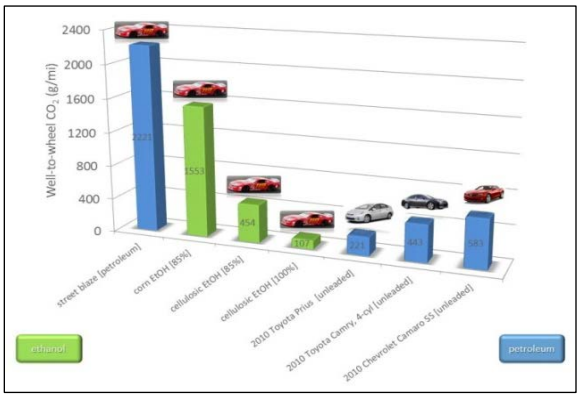

Figure 13. Well-to-wheel greenhouse gas estimates from renewable-fueled ethanol-powered stock car vs. production-based gasoline-fueled counterparts. Data for stock car collected over 33 laps of racing. Data for production vehicles averaged from FTP (city + highway) cycle, EPA estimates. Calculations completed using ANL GREET model.

In Figure 13, it can be seen that, due to integrating advanced cellulosic E85 in the Project GREEN race car, the well-to-wheels greenhouse gas impact from the fuel usage is on par with a small, four-cylinder, production sedan. In addition, over 80% of the fuel would come from domestic production, keeping more money inside the U.S. economy. It is important to note that these results were obtained using a state-of-the-art, production-based OEM engine in conjunction with renewable fuel. Using these readily available technologies, the total cost savings to a racer exceeds $30,000 (compared to the cost of a custom-built race engine burning petroleum-based race fuel that costs ~$10/gallon). Since there are over 440,000 race teams/drivers within the United States and over 1,100 circle tracks where they race, adoption of these technologies into the grassroots racing community would have a significant impact and save billions of dollars. In addition, reaching the grassroots circle track racing community with E85 would build the backbone of a national E85 refueling infrastructure. Moreover, showing the advantage of these fuels to racers and audiences around the country would be a major outreach and educational opportunity regarding the benefits of advanced technologies and renewable fuels in domestic energy security and reducing the environmental impact of the entire transportation system.

Conclusions

FY 2011 saw significant results from and developments in the Green Racing Initiative. Great advances were recorded in the ALMS program with 44% displacement of oil achieved, the complete domination of cars powered by advanced and renewable fuels, and the near-complete conversion of the GT class to renewable fuels. Important accomplishments in incorporating energy recovery into world-class sports car racing were achieved with the first factory-backed LMP HEVs announced for the next racing season and a second-generation prototype GT HEV car raced in the United States. The stock car program built on its success of a year ago in partnership with *Circle Track Magazine* and is poised to add electric-drive technologies to the menu of low-cost advance technologies for the circle track grassroots racing community. The relationship between our partners at the EPA and SAE International is strong and the future holds many opportunities for building acceptance of Green Racing principals in other forms of racing. The Green Racing Initiative continues to deliver high returns and value for DOE's modest investment.

VII.E. International Cooperation to Promote Plug-In Electric Vehicles

Principal Investigator: Keith Hardy
ANL-East
Energy Systems Division
955 L'Enfant Plaza SW, Suite 6000
Washington, D.C.
202-488-2431; khardy@anl.gov

DOE Program Manager: Lee Slezak
202-586-2335; Lee.Slezak@ee.doe.gov

VII.E.1. Abstract

Objective

- Facilitate international cooperation to support harmonization of vehicle-grid interface standards and U.S. Government (USG) policy initiatives related to e-mobility by identifying and initiating mutually beneficial activities with government agencies in Europe and Asia.

Approach

- Leverage projects of the DOE Vehicle Technologies Program (VT) to establish cooperative activities with the European Commission, select European Union (EU) Member States, and China; specific VT projects include:
  - Vehicle/Infrastructure Learning Demonstration Program (American Recovery and Reinvestment Act of 2009 [ARRA] -funded "EV Project")
  - Vehicle-grid interface technology development (e.g., compact metrology, universal communication) under the auspices of the Grid Interaction Technical Team
  - SAE codes & standards committee support; specifically, vehicle-grid connectivity and communication under the auspices of VT Codes & Standards
- Coordinate with DOE Policy & International Affairs (PI), the United States-EU Energy Council working group(s), the Transatlantic Economic Council (TEC), and the Transatlantic Business Dialogue (TABD)
- Coordinate with the U.S. Mission to the EU; ensure compatibility with USG e-mobility/trade policy and support related programmatic/diplomatic initiatives
- Coordinate with European Commission (EC) Directorates (DG Move, DG Energy, and DG Trade); ensure EC programmatic support for direct project interactions
- Coordinate with Federal Republic of Germany (FRG) Ministries (Economics & Technology, Environment, Transport) and the Joint Unit for Electric Mobility (GGEMO); identify activities to support the agreement in principle between the German Chancellor and the President of the United States to cooperate on e-mobility
- Support U.S.-China EV Initiative; facilitate data sharing between vehicle demonstration programs and promote harmonization of standards related to the vehicle-grid interface
- Promote global cooperation and harmonization of standards through participation in and organization of technical conferences and workshops

Major Accomplishments

- Co-organized (with Belgium, the European Commission, and Sweden) the "Transatlantic Workshop on EVs and Grid Connectivity," Brussels, November 17, 2010; prepared presentation and remarks for Deputy Cabinet Ministers, facilitated vehicle-grid connectivity session, and delivered two

presentations; as a result, invited by the EC (DG Move) to join external shareholders' board of the Green eMotion (GeM) program, a four-year, EU-wide e-mobility and vehicle demonstration program.

- Facilitated agreement in principle with DG Move and Siemens (GeM program manager) to share data between GeM and DOE VT's Vehicle/Infrastructure Learning Demonstration Program; mechanism for data sharing and management in discussion between Idaho National Laboratory (INL) and Siemens.
- Selected as featured speaker at the US-EU Electric Vehicle Roundtable organized by the U.S. Mission to the EU; participants included representatives of the EC Directorates (Move, Energy and Transport), the Transatlantic Business Dialogue (TABD), and European/US standards development organizations (SDOs); established communication links between DOE and EU SDOs and identified priorities for standards development/harmonization, which resulted in contribution to the proposed EU-US E-Mobility Plan.
- Organized and chaired the Plug-in Vehicle Workshop at the International Electric Vehicle Symposium (EVS 25), Shenzhen, December 2010; Presented "Global Harmonization of Coupler Standards" and third-generation, interactive EV-Smart Grid display. Established communication links to government agencies, automotive community, and SDOs in China; received direct input on common near-term needs to support vehicle-grid interface development. As a result, invited to organize and chair the Plug-in Vehicle Workshop at EVS-26 in Los Angeles, May 2012.
- Developed concept for joint EU-US EV-Smart Grid Interoperability Centers sponsored by DOE and the European Commission; concept proposed by the White House coordinator of the Transatlantic Economic Council (TEC) to the EU Trade Commission; adopted as a joint DOE-EC e-mobility "deliverable" of the TEC. Planning and technical coordination between Argonne and Joint Research Centre (JRC) in process, targeting an agreement between DOE and the JRC by the end of November 2011.
- Facilitated the vehicle roundtable of the U.S.-China Bilateral Meeting held at Argonne, August 2011; resulted in an action to map U.S. (SAE) and Chinese national (GB) standards as a basis for a joint SAE-International Electrotechnical Commission (IEC)-GB standards harmonization plan; mapping by National Institute of Standards and Technology (NIST) in process.
- Presented "Advanced Vehicle Technologies Development" at the U.S.-Japan Technology Forum, Nashville, TN; resulted in request to pursue cooperation between the United States and Japan on the development of EV-grid interface technologies/methodologies as DOE has in the EU; made specific request to meet with major Tokyo rail operator regarding integrating e-mobility.

Future Activities

- United States-China cooperation: *Harmonization of Vehicle-Grid Standards, Data Sharing*
  - Hold discussions with Chinese SDOs regarding harmonization of vehicle-grid connectivity; facilitate coordination meeting between SAE, IEC, CATARC and other organizations and agencies involved in developing EV standards
  - Facilitate DOE/INL and MOST/subcontractor discussions to agree on scope and data management process of data sharing between EV Project (Los Angeles sites) and Shanghai (sites to be determined)
- United States-European (EC) cooperation: *EV-Smart Grid Interoperability, Data sharing, Twin Cities*
  - Refine technical content of DOE-JRC agreement regarding EV-SG Interoperability Centers
  - Develop EV-Smart Grid technical display and literature to support the TEC and EU-U.S. Energy Council Meetings in Washington, D.C. (Q1, FY 2012); the U.S.-EU Roundtable in Brussels (Q2, FY 2012); and EVS-26 in Los Angeles (Q3, FY 2012)
  - Initiate EV-grid connectivity pilot projects to establish scope and requirements of interoperability labs; develop joint U.S.-EU implementation plan (Q2/3, FY 2012)
  - Facilitate coordination between the EV Project (INL) and the GeM project (Siemens) to agree on scope, data exchange mechanism, and data management process
  - Facilitate coordination between candidate U.S. cities and DOE/EC to clarify objectives and discuss potential benefits of Twin Cities program in the EU and United States, identify specific

requirements for participation (e.g., ongoing ARRA-funded activities), and answer questions of candidate sites

- U.S.-FRG cooperation
  - Initiate EV-grid connectivity pilot projects to define the scope of the EV-grid "system" and identify control parameters/requirements at nodes in the U.S. and German charging infrastructures
  - Facilitate agreement between Twin Cities on wireless charging implematation

VII.E.2. Technical Discussion

Background

The international cooperation task was initiated in 2009 to promote the introduction of plug-in vehicles and the supporting infrastructure. The European focus has evolved from a bi-lateral activity with Sweden to the European Commission directorates and sponsored programs, the Joint Research Center, the Transatlantic Business Dialogue (TABD), and multinational companies. In addition, bi-lateral activities with Germany are being established pursuant to the agreement by the U.S. President and German Chancellor to cooperate on e-mobility. The Asian focus is on China, and activities are being pursued to support harmonization of standards and sharing of data between vehicle/infrastructure demonstration programs.

The expansion of activities has resulted in the need to coordinate with additional USG organizations, including the Departments of State and Commerce, the U.S. Mission to the EU, various U.S. consulates in Europe, and the German Federal Ministries.

Approach

Direct support to the VT Program is provided through partial support of the M&O assignment of Keith Hardy to DOE Headquarters in Washington, D.C. The activity leverages ongoing ARRA-funded programs and technology development within VT to minimize the use of additional technical resources. The most obvious dependency is the Argonne Codes & Standards activity (Ted Bohn, Principal Investigator), which is the critical resource for the vehicle-grid communication technology.

VII.E.3. Products

Papers/Presentations

1. "US-China Electric Vehicle Initiative – Overview and Progress to Date," EVS-25 Plug-in Vehicle Workshop, Shenzhen, 6 November 2010.
2. "The Role of Electromobility in US Energy Policy" (presentation and speech), prepared for Deputy Chief of Mission Thomas White for the Transatlantic EV Workshop, 17 November 2010.
3. "Opportunities for Cooperation on Technology Development to Support a Robust Vehicle-Grid Interface," Transatlantic EV Workshop, 17 November 2010.
4. "US Vehicle/Infrastructure Learning Demonstration Program," Transatlantic EV Workshop, 17 November 2010.
5. "PEV Connectivity Standards … Global Perspective," ANSI PEV Standards Workshop, 5–6 March 2011.
6. "PEV Operation, Fuel Economy, Connectivity and Cooperation," Transatlantic Electric Vehicle Roundtable, Brussels, 17 March 2011.
7. "Electric Drive Vehicle Infrastructure … the Smart Grid Connection," EFI Emerging Technology Forum, San Francisco, 30 March–1 April 2011.
8. DOE/ANL E-Vehicle Activities and Opportunities for Cooperation, Featured in (2) YouTube Videos produced by the Media Hub at the U.S. Embassy in Brussels, April 2011.
9. "Advanced Vehicle Research Programs," 22nd United States-Japan Technology Forum, 17–18 May 2011.

10. "Vehicle-Grid Connectivity … Potential for Global Cooperation?," RWE Deutschland AG, New Technologies, 30 May 2011.
11. "Collaboration to Accelerate Vehicle-Grid Connectivity Standards Development," EV Infrastructure World Congress, Berlin, 21 June 2011.
12. White Paper: "DOE Proposal to the Transatlantic Economic Council (TEC); Establish Electric Vehicle-Smart Grid Interoperability Centers in Europe and the US," 19 July 2011; Presented to the White House TEC Coordinator.
13. "Accelerating PEV Production and Market Penetration … Manufacturing, Infrastructure & Cooperation," Batteries2011, Cannes-Mandelieu, 28–30 September 2011.

VII.F. SAE Dynamical Modeling and Simulation (DM&S) Technical Committee

Chuck Folkerts (Project Leader), Larry Michaels, Aymeric Rousseau
Argonne National Laboratory
9700 South Cass Avenue
Argonne, IL 60439-4815
(630) 252-7261; cfolkerts@anl.gov

DOE Technology Managers: David Anderson, Lee Slezak

VII.F.1. Abstract

Objectives

- Establish modeling and simulation standards to facilitate dynamical modeling and simulation of automotive systems

Approach

- Define committee overall charter
- Define tasks allowing for models plug ability and playability
- Propose recommendations to the entire community for each of the tasks considered

Accomplishments

- Developed overall committee charter
- Completed Task 2 focused on model documentation

Future Directions

- Address the following tasks, starting with model architecture
- Provide document describing best practices

VII.F.2. Technical Discussion

Introduction

Complexity of automotive systems (as used in passenger cars, heavy duty trucks, military vehicles, and agricultural and construction equipment) is increasing at a rapid rate along with competitive pressures to reduce product development cycle times. These modern automotive systems require highly coordinated collaboration between disciplines of engineering and physics within organizations, and between a network of OEM's, suppliers, research laboratories and universities across the industry and around the globe. To keep up with technology change and competitive pressures, these global teams need virtual engineering methods for responsive, cost effective and efficient collaborative development. In order to make global enterprise and cross-enterprise virtual engineering methods cost effective, efficient and robust, automotive industry wide-standards for virtual engineering of dynamical modeling and simulation are required.

The future development of automotive systems will continue to be driven by the same forces and trends that they experience today. These factors will require continual improvements in

terms of higher fuel efficiency, higher quality and reliability, lower emissions, and improved safety, while providing more value to the customer at a lower cost. To minimize costs and time, systems will be developed by global teams collaborating across an industry network using virtual engineering processes and methods with minimal physical builds required only to confirm designs and performance. Virtual engineering of automotive systems will require dynamical modeling and simulation using the integration of models from different companies and disciplines with varying levels of abstraction (fidelity and complexity) to engineer and develop them rapidly, efficiently, and effectively and to facilitate an integrated development process that seamlessly flows between all processes from research to production.

A committee formed from experts from the industry, academia and National Laboratories was formed to address these issues.

Objective

The objective of the committee is to establish modeling and simulation standards to facilitate dynamical modeling and simulation of automotive systems. These standards will facilitate integrated and multidisciplinary virtual engineering processes for highly coordinated and collaborative engineering work. SAE Standards, Recommended Practices and Information Reports (standards) will be established and published to facilitate and promote cost effective, efficient and robust:

1) Model and data sharing and reuse,
2) Seamless modeling, simulation and analysis workflows,
3) Virtual engineering processes,
4) Modeling and simulation tool interoperability, and
5) Model portability across simulation tools.

Scope

The committee's activities will develop standards for dynamical models and simulations that mathematically describe an automotive system's time varying response, behavior and interactions of subsystems and components. These standards will include processes, methods, performance metrics and analyses related to dynamical modeling and simulation of automotive systems. The focus is on standards to make models reusable and simulation results predictable and repeatable across engineering and physics disciplines, application tools, and the automotive industry.

Benefits

The established standards will improve overall efficiency of development processes by providing a "common language" and a means for sharing and reusing data and mathematical simulation models of dynamical systems across engineering disciplines within companies and across the industry network. Hence, these standards will facilitate virtual engineering of automotive systems, resulting in optimized performance, improved process efficiency, and reduced development time and costs for the automotive industry and companies, which will accelerate the rate of development and adoption of new technologies.

Accomplishments

Tasks Definition

After defining the charter for the committee, four main tasks were defined.

1. Model Architecture and Interfaces Definition Document Project Task:
   - Define model organizations for vehicle system and subsystems (input, outputs), including location of controls models in the architecture
   - Define conventions for naming, data types, units…
   - Define MIL, SIL, RCP and HIL interfaces to controls models
   - Define how model parameters are set and its impact on interfaces (parameterization)
2. Model Description Document Project Task:
   - Define content of document necessary to decide if a model is appropriate for a given task
   - Define model uses or applications it is appropriate for

- Define what the model does, what principles, theories and/or equations is it based on, what approximations or assumptions were made
- Provide any validation work (i.e., test data, reports)

3. Model Data Dictionary Document Project Task:
   - Define metadata required to support reuse of models between software application tools by interoperability (such as co-simulation or wrapped-code) or porting of models between tools with repeatable results.
   - The Metadata includes
     i. model classification type, version, creator, fidelity, accuracy, computational workload, tool version compatibility, and other model classification characteristics etcetera
     ii. model interfaces (inputs, outputs and buses), variables, parameters and names and meaning of interfaces, variables and parameters
4. Model Compatibility and Playability Requirements Document Project Task:
   - Define model simulation requirements needed to make it function in the simulation of a system with repeatable results
   - Define precision of arithmetic, integration interval, integration type (fixed or variable), sampling interval required, ODE solvers required
   - Define metrics for computer resources requirements such as ROM, RAM, disk space, computation time using standard benchmark tests
   - Define task scheduling for controls models of algorithms
   - Define model simulation initialization process or method for establishing initial conditions

The committee then decided to address the Model Description Document Project Task first.

Model Project Description Document

The goal of this task is to define standards for the documentation of finished (or production ready) dynamical models, which make models reusable by providing a clear, concise and complete description of their capabilities, requirements, applications and assumptions.

Dynamical modeling as part of enterprise-wide and/or industry-wide engineering processes requires different types of documentation to support different engineering functions for model management, production, and application. These functions require both unique and common information about a model. In addition, to protect the exposure of intellectual property, different levels of documentation are required for engineering collaboration functions internally within a company, externally between companies, and globally for internal and external work across national borders. Specifically, Model Description Documents (MDD's) are needed for the following 4 categories of work functions:

1. Model users and simulation analysts from different disciplines apply models for various engineering tasks. For sharing and reusing existing models, they require a high level overview description document to select an application appropriate model with the capabilities, features, and performance required for their specific analysis purposes.

2. Model developers or producers (Simulation Modelers/Developers/Providers/Suppliers) create new models or maintain, integrate and modify existing models. To develop new models, they need to receive a document that specifies the requirements for the model to enable an intended analysis application to be performed.

3. Simulation model requestors are model users and simulation analysts, who require new or improved models to perform specific engineering analysis functions for which models don't exist or are inadequate.

4. Modeling and simulation process managers control the introduction, update and removal

of models from libraries of models available for standard engineering analysis.

A list of the main document content and the different views was then developed. The main content includes but is not limited to the following sections:

- Model Title and High Level Description
- Model Administrative Information
- Purpose/Usage/Applications
- Features & Capabilities
- External Interface Variables (or Inputs and Outputs)
- Internal Variables
- Parameters and Calibration Procedures
- Model's Architectural Structure
- Functional Description (Detailed)
- Applicability
- Implementation Requirements/Dependencies
- Performance
- Operating Instructions
- Verification & Validation
- Access Availability & Restrictions
- Miscellaneous (not sure this section is necessary)
- Model Classification (not sure that this section is necessary)
- Glossary

Conclusion

During the first year, the committee has developed a charter as well as four separate tasks. The first task that was addressed focused on model documentation content and how it would be adapted based on the audience. Next step will focus on the architecture organization.

VII.G. Vehicle to Grid Communication Standards Development, SAE J2847/1 Testing and Validation

Principal Investigator: Krishnan Gowri
Pacific Northwest National Laboratory
P.O.Box 999, MS K5-16
Richland, WA 99352
(425) 273-0190; Krishnan.gowri@pnnl.gov

DOE Program Manager: Lee Slezak
(202) 586-2335; Lee.Slezak@ee.doe.gov

VII.G.1. Abstract

Objective

- Contribute to SAE J2931, SAE J2836/3 and SAE J2836/5 standards development for vehicle to grid communication.
- Develop laboratory infrastructure and test methods to evaluate narrow-band and broad-band power line communication technologies.
- Provide laboratory testing and document development support to SAE for accelerating the development of communication standards.

Approach

- PNNL in collaboration with Electric Power Research Institute (EPRI), Argonne National Laboratory (ANL) and Grid Interaction Tech Team (GITT) members will identify the communication testing requirements for the application layer implementing J2847/1 messages.
- Participate in SAE Hybrid committee meetings, American National Standards Institute (ANSI) and National Institute of Standards and Technology (NIST)

Major Accomplishments

- Completed testing two narrow-band PLC technologies over the mains and provided results to the SAE J2931 committee and the EPRI testing team.
- Prepared architectural scenarios and use cases for J2836/5 development of customer to vehicle communication requirements.
- Participated in the ANSI Electric Vehicle Standard Panel and identified gaps in standards for vehicle telematics.

Future Activities

- PNNL will continue the application layer level testing of communication over control pilot for point-to-point communication of DC messages and SEP 2.0 messages.
- PNNL will develop a laboratory test setup for end-to-end communication using a utility AMI network, consumer home area network (HAN) in the manufactured house test facility. PNNL will identify industry partners to develop communication module prototypes and perform field testing of demand response and optimized charging using J2847/1 messages.

VII.G.2. Technical Discussion

Background
In the US, more than 10,000 electric vehicles (EV) have been delivered to consumers during the first three quarters of 2011. A large majority of these vehicles are battery electric, often requiring 220 volt charging. Though the vehicle manufacturers and charging station manufacturers have provided consumers options for charging preferences, there are no existing communications between consumers and the utilities to manage the charging demand. There is also wide variation between manufacturers in their approach to support vehicle charging. There are in-vehicle networks, charging station networks, utility networks each using either cellular, Wi-Fi, ZigBee or other proprietary communication technology with no standards currently available for interoperability. The current situation of ad-hoc solutions is a major barrier to the wide adoption of electric vehicles. SAE, the International Standards Organization/International Electrotechnical Commission (ISO/IEC), ANSI, National Institute of Standards and Technology (NIST) and several industrial organizations are working towards the development of interoperability standards. PNNL has participated in the development and testing of these standards in an effort to accelerate the adoption and development of communication modules.

Introduction

SAE began the development of electric vehicle communication standards in 2009 with the initial focus on use-case development and communication messages for vehicle to utility communication. The first set of documents, SAE J2836/1 and J2847/1, were balloted and initially published in 2010, with revisions and adoption by the NIST Smart Grid Interoperability Panel in 2011 into their catalog of smart grid standards. In parallel, SAE has been developing several additional standards to define the communication protocol implementation requirements, DC charging, reverse energy power flow, telematics, customer to EV communications and wireless charging. Originally, SAE planned ten documents for communication standards, but this now has evolved into a four distinct categories totaling 21 standards. The significant progress of SAE standards development in 2011 includes the finalization of J2836/2, J2847/2, and J2931/1 documents for balloting and the beginning of work in J2836/3, J2836/4, J2836/5, and the addition of security, telematics and wireless charging communication standards.

The most critical standard for communication module development is J2931/1 which specifies the performance requirements and evaluation of power line communication technologies. EPRI has developed a requirements document, test plan and schedule, and coordinated this effort working with automobile manufacturers, utility partners and SAE hybrid committee participants. The current agreement is to test communication over control pilot (inband) using HomePlus GreenPHY and G3 to harmonize the requirements between SAE and ISO/IEC. In addition, G3 over mains will be tested as well. EPRI is coordinating the testing with ANL, PNNL and EPRI for all three communication options and based on the test plan for association, data rate, co-existence, latency and DC charging tests.

Approach

During FY11, PNNL primarily participated in the J2931 document review, and J2836/3 and J2836/5 document development activities.

1. The SAE document J2931 defines requirements for digital communications interface between EV and off-board device for energy transfer. These were reviewed and used in PNNL internal testing of power line communication modules. The smart charging implementation design in J2931 was implemented in the PNNL tests and validated for sequence of operation. Further testing of the communication modules will be coordinated with EPRI in FY12.

2. The primary focus of J2836/3 committee is to insure that the architecture of the Reverse Energy flow standard will meet IEEE 1547, NEC, UL 1741 and will be consistent with other standards. This standard has four

primary use cases: V2G – Vehicle to Grid, V2H – Vehicle to Home, V2L – Vehicle to Load, and V2V – Vehicle to Vehicle. The major issues being addressed include: V2L – output voltage and frequency need to be controlled in vehicle, output power limiting circuitry needed; V2H – requires digital communication and transfer switches in the home are needed; V2G – no digital communication needed; etc. PNNL has been actively providing input and design review of the communication architecture, wiring and messages. This work has only recently begun and more active participation and support will be provided in FY12.

3. The J2836/5 document is aimed at defining the use cases for communication between the customer and vehicle using the home area network or neighborhood area network. PNNL prepared an initial discussion document of three possible architectures based on OpenHAN to focus the use case development. Two use cases of vehicle to utility though either telematics or home area networks are identified for further development. PNNL will continue to work on the use case development in FY12.

In addition, PNNL continued the FY10 testing tasks and developed a test plan and lab test bench (Figure 1) for verification of J2847/1 standard. This test plan includes test cases, validation criteria, and certification requirements to verify reliability, robustness, repeatability, maximum communication distance, authentication, and security features of communication modules at the application layer level. The communications signals were subjected to varying conditions on the power line, similar to those expected in an actual vehicle battery charging application. These conditions included using a representative commercial vehicle battery charger (A123/Hymotion L5), a commercial charging station (Coulomb Technologies CT2100) with J1772 connector and cable, changing the length of 240VAC cable for power line communications, charging at different charge rates, and observing the immunity of the communications to in-band signal sources. Over 37 million messages were transmitted and 3.2 million messages were transmitted while charging. Following each charging cycle, the Hymotion battery was discharged using a 4.2kW Aurora Inverter to the grid.

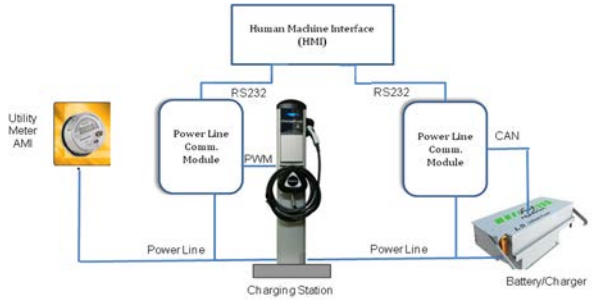

Figure 1. Laboratory test bench setup

The highest communication data rate necessary to implement SAE J2836 / J2847 vehicle to grid communications takes place when the vehicle connects to the charging station. The PEV ID, customer preferences, energy request, and energy schedule are communicated. Since the longest message (PEV ID) might be up to 20 characters, variable 5-character and variable 20-character messages were used to test the communication speed.

For initial testing, two power line communication technologies from Echelon and Maxim were used based on availability of hardware and development support. Both the Echelon PL3170 and the MAXIM2990 Power Line Carrier modules provided reliable communications between the EVSE and PEV Charger. Both modules require a hardware interface between the PLC physical layer and the proposed SEP2.0 application layer.

Results

The results of testing are summarized below:

1. The Maxim's MAX2990 data rate varies from 2Kbps for very short messages to nearly 100Kbps for long messages. When operating the correct mode, the MAX2990 had less than 1 x 10-6 bit error rate.

2. The Echelon PL3170 data rate was consistently 1.9Kbps. The PL3170 was not affected by interfering signals and its bit error rate was typically less than 28 x 10-6.

3. A key finding is that only eight SAE J2847 messages need to be communicated between the PEV and EVSE during the highest data rate period.

4. Since both technologies need a hardware interface between the SEP2.0 application layer and the Power Line Carrier physical layer, the long SEP2.0 messages could be given aliases and communicated within 2 seconds.

Conclusions

Significant progress has been made in SAE standards development for defining the requirements for digital communications and in developing the test plan. However, there is a significant amount of development and testing that remains to be done in order to help the vehicle manufacturers and charging station manufacturers to develop communication modules critical for charge management by utilities.

During FY11, The test plan and laboratory test setup provide all the required components for interoperability testing of communication over the mains. Further development is underway to test communications over control pilot and DC charging, in collaboration with SAE and EPRI.

In FY12, PNNL will continue to work with EPRI in testing the application layer implementation of J2847/1 messages using the SEP 2.0 protocol and provide reference designs for industry adoption. Further work will also continue to support the SAE standards development for reverse energy power flow messages and customer to EV communication use cases.

VII.G.3. Products

Publications

1. Scholer, R.A., D. Mepham, S. Girimonte, D. oliver, K. Gowri, N. Tenney, J. Lawlis, E. Taha, J. Halliwell, "*Communication Requirements for Plug-in Electric Vehicle",* SAE 2011 World Congress, Detroit, MI. April 2011.
2. Pratt, R., F. Tuffner and K. Gowri, "*Electric Vehicle Communication Standards Testing and Validation – Phase I: SAE J2847/1",* PNNL Report No. 20913, Richland, WA. September 2011.

VIII. VEHICLE SYSTEMS OPTIMIZATION

VIII.A. DOE Project on Heavy Vehicle Aerodynamics

Principal Investigator: K. Salari
Lawrence Livermore National Laboratory
P.O. Box 808
Livermore, CA 94551-0808
(925) 424-4635; salari1@llnl.gov

DOE Program Manager: Lee Slezak
Lee.Slezak@ee.doe.gov

VIII.A.1. Abstract

Objective

Class 8 tractor-trailers consume 11-12% of the total US petroleum use. At highway speeds, approximately 65% of the energy expenditure for a Class 8 truck is used to overcome aerodynamic drag. The project objective is to improve fuel economy of Class 8 tractor-trailers by providing guidance on methods for reducing drag by at least 25%. This 25% reduction in drag would present a 12% improvement in fuel economy at highway speeds, equivalent to about 130 midsize tanker ships per year. The specific goals of this project include:

- Provide guidance to industry in improving the aerodynamics of tractor-trailers
- Explore the aerodynamic benefits of tractor-trailer integration for drag reduction (geometry, flow, and thermal)
- Develop innovative drag reducing concepts that are operationally and economically viable
- Establish a database of experimental, computational, and conceptual design information for improving the aerodynamics of heavy vehicles
- Demonstrate the potential of new drag-reduction concepts including tractor-trailer integration

Approach

- Simulate and analyze the aerodynamic flow around heavy vehicles using advanced computational fluid dynamics (CFD) tools
- Generate an experimental and computational database to improve our understanding of the flow physics and to perform code validation
- Provide industry with aerodynamic design guidance and insight into the flow physics
- Investigate and improve the aerodynamic drag reduction potential of devices (e.g., base flaps, tractor-trailer gap stabilizers, underbody skirts, wedges and fairings, and blowing and acoustic devices, etc.)
- Provide industry with conceptual designs of drag reducing devices for tractor-trailers and tanker-trailers
- Demonstrate the full-scale fuel economic potential of the aerodynamic improvements through the use of the track and on the road tests
- Investigate the aerodynamics of tanker trailers for the purpose of drag reduction
- Develop and test various aerodynamic treatments for tanker trailers

Major Accomplishments

For the fiscal year (FY) 2011, the Heavy Vehicle Aerodynamic Drag Project achieved three major accomplishments. The first is the publication of a design document entitled "Aerodynamic Design Criteria for Class 8 Heavy Vehicles Trailer Base Devices to Attain Optimum Performance," by K. Salari and J. Ortega, LLNL-TR-464265. The objective of this report is to provide design guidance for trailer base devices to improve their aerodynamic performance. These devices are commonly referred to as boattails, base flaps, tail devices, and etc. The report is presented in the Appendix.

The second is the analysis of the full-scale 80'×120' wind tunnel test results acquired at NASA Ames National Full-Scale Aerodynamics Complex (NFAC) facility in FY10 in collaboration with Navistar and the completion of a report entitled "Fuel economy improvement of class 8 heavy vehicles through aerodynamic drag reduction: a full-scale wind tunnel study," by J. Ortega, K. Salari, A. Brown, and R. Schoon, which is ready for submission to a peer-reviewed journal (and presented in the Appendix). The full-scale test was completed over the period of three months in which 23 aerodynamic drag reduction devices/concepts were tested from LLNL, Navistar, Freight Wing, ATDynamics, Aerofficient, Laydon, Windyne, and AeroIndustrie with four different combinations of tractors and trailers: a long-sleeper tractor with a 53' straight-frame trailer, a long-sleeper tractor with a 28' straight-frame trailer, a day-cab tractor with a 53' straight-frame trailer, and a day-cab tractor with a 53' drop-frame trailer. Approximately 140 wind tunnel runs were completed throughout this study. Lawrence Livermore National Laboratory would like to thank Navistar for its significant contribution toward the successful execution of this full-scale wind tunnel test by providing a number of in kind contributions. Navistar provided both tractors and two of the trailers as well as significant part of the tunnel installation and mounting hardware. Navistar provided resources for interaction with industry to participate and to host series of device installation. This ensured proper device fitting ahead of the wind tunnel test. Navistar also dedicated test engineers and mechanics to support model changes over the course of the three month test, as well as contracted external engineering support.

The third major accomplishment is the improvement of a selected number of drag reduction add-on devices. Number of computational fluid dynamics simulations were conducted based, in part, upon heavy vehicle configurations that were track tested (Figure 1 and 2) under the support of a Dept. of Energy grant, "Fleet Evaluation and Factory Installation of Aerodynamic Heavy Duty Truck Trailers" (DE-PS26-08NT01045-03). The simulations are run on a full-scale heavy vehicle geometry in a 6 degree crosswind (7 mph) at highway speed (65 mph) using a finite-volume code (STAR-CCM+) with polyhedral meshes up to approximately 700 million cell faces. The Reynolds-averaged Navier-Stokes equations are solved for the turbulent flow over the vehicle with various drag reduction devices installed in the tractor-trailer gap, trailer underbody, and trailer base (Figure 3). The results of the simulations demonstrate a number of important trends. First, extending the 3-sided boattail length from 24" to 48" produces only a marginal change in the aerodynamic drag reduction (ΔCD = -0.169 (25.2%) for the 24" boattail; ΔCD = -0.168 (25.1%) for the 32" boattail; ΔCD = -0.175 (26.0%) for the 48" boattail).

Figure 1. Track test vehicle equipped with a gap fairing, trailer skirts, and a trailer boattail.

Figure 2. Trailer tail devices

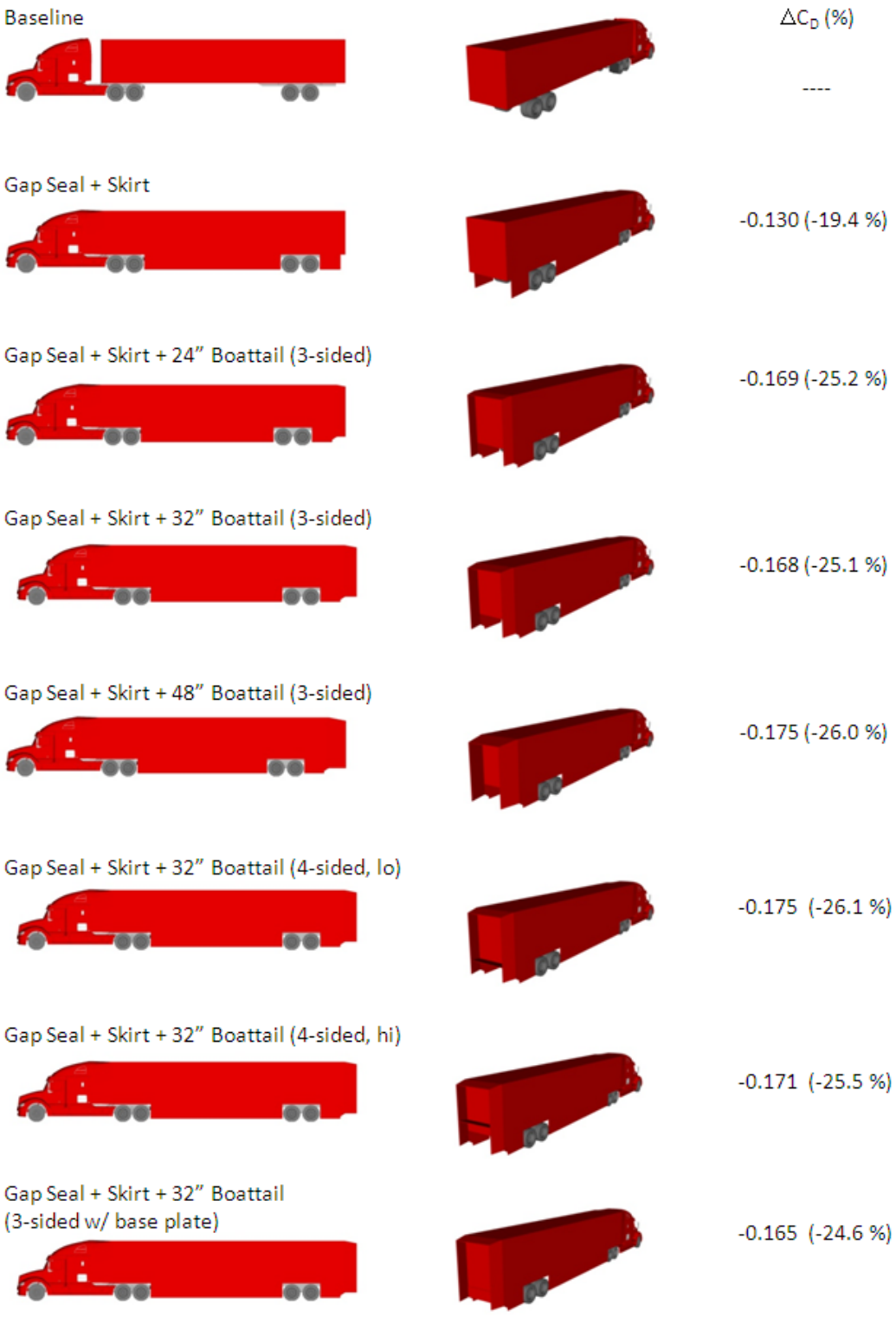

Figure 3. Heavy vehicle configurations modeled using computational fluid dynamics simulations. The trailer skirt and boattail devices are representative of those evaluated in a track test.

Second, there is very little difference between the two 32" 4-sided boattail configurations in which the fourth bottom plate is placed at a vertical location either below or above the trailer door handles (ΔC_D = -0.175 (-26.1%) for the lower location; ΔC_D = -0.171 (-25.5%) for the higher location). Third, the most effective combination of drag reduction devices is the tractor-trailer gap seal, trailer skirt, and the 4-sided 32" boattail with the fourth plate at the lower location. This set of devices is followed very closely by the combination of the tractor-trailer gap seal, trailer skirt, and the 3-sided 48" boattail (ΔC_D = -0.175 (-26.0%)). In addition to the drag coefficient, the simulations reveal details of the flow physics about the heavy vehicle, such as regions of reversed velocity where drag-producing low pressures exist and vortical structures that contribute to flow unsteadiness and induced drag (Figure 4).

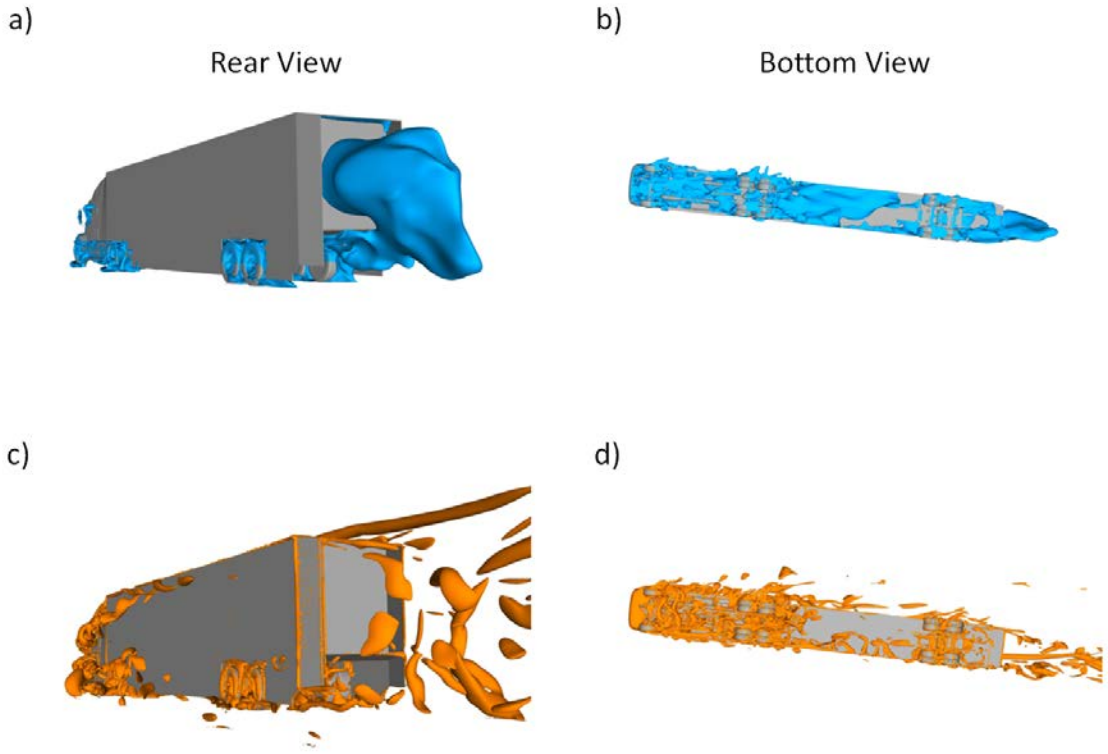

Figure 4. Iso-surfaces of a-b) reversed velocity and c-d) vortical structures about the heavy vehicle configuration with a tractor-trailer gap seal, trailer skirts, and a 4-sided 32" boattail with the fourth plate at the lower location.

Future Activities

- Evaluate the performance of aerodynamic fairings for tanker trailers in a 1/8th scale wind tunnel test at the University of Maryland
- Acquire aerodynamic force data and high-resolution velocimetry data of the flow about a heavy vehicle to obtain further insight into the massively separated regions and the shear layer/wake interactions. The measurements will be made at the NASA Ames 7’ x 10’ wind tunnel facility using a 1/8th scale model.
- Continue to investigate the benefits of tractor-trailer integration for drag reduction (geometry, flow, and thermal)
- Continue to work with Praxair to design aerodynamic drag reduction devices for tanker trailers to improve the fuel economy

- Submit the full-scale wind tunnel test report for publication
- On behalf of DOE, continue to coordinate industry participation and achieve industry-accepted drag reduction devices

Acknowledgments

This work performed under the auspices of the U.S. Department of Energy by Lawrence Livermore National Laboratory under Contract DE-AC52-07NA27344.

VIII.A.2. Technical Discussion

The Appendix presents detailed technical discussion as provided in the project's publications.

VIII.A.3. Products

Publications

1. Salari, K. and Ortega J. "Aerodynamic Design Criteria for Class 8 Heavy Vehicles Trailer Base Devices to Attain Optimum Performance", LLNL-TR-464265, 2011. (see Appendix)
2. Ortega J., Salari K., Brown A., and Schoon R., "Fuel economy improvement of class 8 heavy vehicles through aerodynamic drag reduction: a full-scale wind tunnel study.",(see Appendix)

VIII.B. Experimental Investigation of Coolant Boiling in a Half-Heated Circular Tube – CRADA with PACCAR

Principal Investigators: Wenhua Yu and Jules L. Routbort, co-workers: David M. France and Roger K. Smith
Organization: Argonne National Laboratory
Address: South Cass Avenue, Argonne, IL 60439
Voice; E-mail: 630 252 7361; wyu@anl.gov
DOE Program Manager: Lee Slezak
Voice; email: 202 586 2335; Lee.Slezak@ee.doe.gov

VIII.B.1. Abstract

Objective

- Understand and quantify subcooled engine coolant boiling heat transfer in heavy duty trucks.
- Experimentally determine subcooled flow boiling heat transfer rates and limits in the head region of heavy duty truck engines.
- Develop predictive mathematical models for subcooled boiling heat transfer results.
- Provide measurements and models for development/validation of heavy duty truck engine computer codes.

Approach

- Design and fabricate an experimental test facility with the test section sized to the specification of a cooling channel in the head region of a heavy truck engine.
- Experimentally determine subcooled boiling heat transfer rates and critical heat fluxes with water.
- Experimentally determine subcooled boiling heat transfer rates and critical heat fluxes with 50/50 and 25/75 ethylene glycol/water mixtures.

Major Accomplishments

- Completed the concept design, the technical design, and the fabrication of the experimental test facility and support systems.
- Completed the LabVIEW-based data acquisition and test control hardware and software.
- Completed the heat loss calibrations of the experimental test facility.
- Completed single-phase convective heat transfer experiments and data reduction with water.
- Prepared system for subcooled boiling experiments with water.

Future Activities

- Perform subcooled boiling experiments and data analysis with water.
- Conduct single-phase convective heat transfer and subcooled boiling experiments and data reduction with 50/50 and 25/75 ethylene glycol/water mixtures.

VIII.B.2. Technical Discussion

Background

Started in FY 10 as a CRADA between Argonne National Laboratory and PACCAR Inc./DAF Trucks (PACCAR/DAF), this project aims to provide heat transfer and critical heat flux measurements and models of subcooled coolant boiling in the head region of heavy duty truck engines for development and validation of heavy duty truck engine computer codes.

Introduction

Subcooled boiling is an important phenomenon that must be understood in order to design efficient diesel engine cooling systems. If the system fluid is at or below the critical heat flux (CHF), the cooling can be very efficient. However, if the system is allowed to go above the CHF, the system can become unstable. PACCAR/DAF is designing engines to take advantage of subcooled boiling heat transfer below the CHF, but the CHF and heat transfer rates have not been determined under realistic conditions. These experiments address this situation using a design specified by DAF. The data will be used in computational fluid dynamics models and designs by PACCAR/DAF, and could result in more efficient engines for heavy trucks. The objective of this project is to measure heat transfer rates during subcooled boiling of engine coolants in a geometry typical of valve bridge areas in heavy truck engines under various operating conditions.

Experimental Test Facility

The test facility used in this investigation was designed and fabricated to study subcooled boiling heat transfer of flowing water and ethylene glycol/water mixtures at temperatures <200 ˚C at pressures just above atmospheric. The experimental test facility shown schematically in Figure 1 is a closed-loop system with major components consisting of a pump, a flowmeter, two preheaters, an experimental test section, a heat exchanger (cooler), three power supplies, and a data acquisition system. The selected extreme-head compact bronze turbine-style centrifugal pump (Marathon Electric, Model 5K42FN2048) has the capability of pumping the testing fluids at the required liquid velocity range of <1.5 m/s (corresponding to the liquid volume flow rate range of $<1.4\times10^{-4}$ m^3/s) with enough head to accommodate the entire experimental facility including the test section, balance of piping, and throttling. The flowmeter (Endress + Hauser, Model Promag 10) was chosen to cover the required flow rate range with an uncertainty of <2%. The preheaters provide a means to set the inlet temperature of the test section at various desired levels. The preheaters and the test section are resistance-heated with controllable direct current power supplies (Sorensen Company, Model DCR 16-625T for the preheaters and Electronic Measurements, Inc., Model EMHP 40-450-D-11111-0933 for the test section). As shown in Figure 1, provisions are made to measure temperatures along the test section for calculating heat transfer coefficients. The outlet pressure, the inlet fluid temperature and the outlet fluid temperature of the test section are also measured. The estimated uncertainties in the measurements of pressure and temperature are ±3% and ±0.2˚C, respectively. As a safety precaution, the preheaters and the test section are provided with high-temperature limit interlocks to prevent them from overheating. After leaving the test section, the fluid is cooled in the heat exchanger (cooler) and returns to the pump to close the system loop.

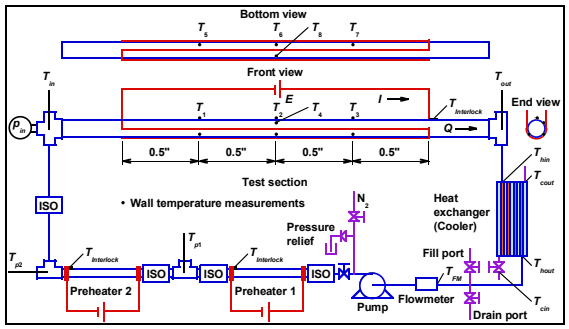

Figure 1. Schematic of PACCAR heat transfer test facility.

A data acquisition system consisting of a Dell computer (Model Optiplex GX270) and a Hewlett-Packard multiplexer (Model HP 75000)

was assembled to record outputs from all sensors. A LabVIEW data acquisition program, which includes all calibration equations and conversions to desired engineering units, was written. Shown in Figure 2, the data acquisition system provides not only an on-screen display, of analog signals from all sensors and graphs of representative in-stream and wall-temperature measurements, but also a means of recording temperature measurements and pertinent information such as input power, mass flux, and inlet pressure for further data reduction.

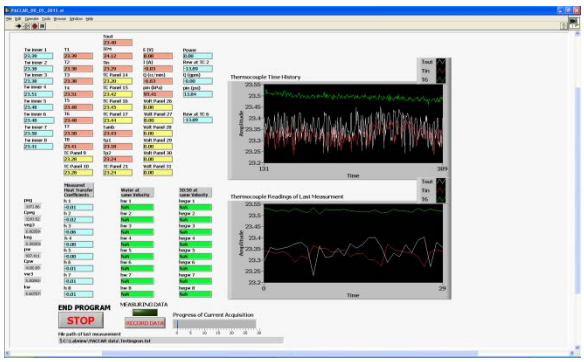

Figure 2. LabVIEW data acquisition program.

An overview of the completely-fabricated PACCAR heat transfer test facility is shown graphically in Figure 3 before it was insulated.

Figure 3. Overview of PACCAR heat transfer test facility.

Results

Heat Loss. Although the experimental test section is well insulated thermally from the atmosphere to minimize heat loss to the environment, the heat loss is not negligible during flow boiling heat transfer experiments because of the relatively high driving temperatures. Therefore, heat loss experiments were performed for the experimental test section wall temperatures up to the boiling heat transfer conditions, and the heat loss will subsequently be incorporated into the data reduction procedures for single-phase convective and two-phase boiling heat transfer data. The heat loss was characterized through a special series of experiments with no fluid in the experimental test section. Power was applied to the experimental test section to bring its wall temperature to a selected level. The heat loss rate q_{loss}, the input power required for maintaining the wall temperature at the selected value and calculated by the product of the voltage drop across the heating wire and the current through the heating wire ($q_{loss}=EI$), is related to the difference between the experimental test section wall temperature T_w and the ambient temperature $T_{ambient}$. Experimental results confirmed a linear dependence on this driving temperature difference. Then the heat loss rate can be expressed approximately as $q_{loss}=c(T_w-T_{ambient})$ where the proportional constant c, which depends on the heat transfer coefficient and the heat transfer surface area between the experimental test section and ambient for this particular experimental apparatus, was determined from the heat loss experiments. Figure 4 shows the heat loss rate as a function of the driving temperature difference for the experimental test section. The test section heat loss is expected to be <1% of the applied input power to the experimental test section in all subsequent heat transfer tests.

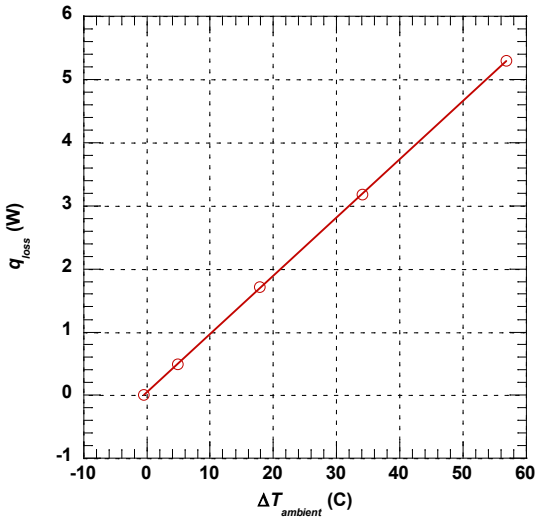

Figure 4. Heat loss calibration.

Single-Phase Experiments with Water. To validate the experimental apparatus, data acquisition, and data reduction, a series of single-phase heat transfer experiments was carried out prior to two-phase flow boiling experiments. During the single-phase heat transfer experiments, the water flowrates were chosen to cover the whole boiling flow velocity range. The velocity range was 0.22–1.46 m/s which corresponds to turbulent flow conditions with Reynolds numbers in the range of 2400–16500. The experimental single-phase heat transfer coefficients for the Reynolds numbers in the range of Re=2400–16500 and the Prandtl number of approximately Pr=1.8 were compared with the modified Sieder-Tate equation

$$h=0.273\mathrm{Re}^{1/2}\mathrm{Pr}^{1/3}(\mu_{fluid}/\mu_{wall})^{0.14}(k/d)$$

where d is the test section inside diameter, k is the thermal conductivity, μ_{fluid} is the fluid viscosity calculated at the average fluid temperature, μ_{wall} is the fluid viscosity calculated at the wall temperature. In the above equation, the term $(\mu_{fluid}/\mu_{wall})^{0.14}$ and the modifications to the leading constant and the Reynolds number exponent in the equation account for thermal developing conditions. As shown in Figure 5 where the heat transfer coefficients are plotted, the experimental data are in very good agreement with the predicted values from this modified Sieder-Tate equation.

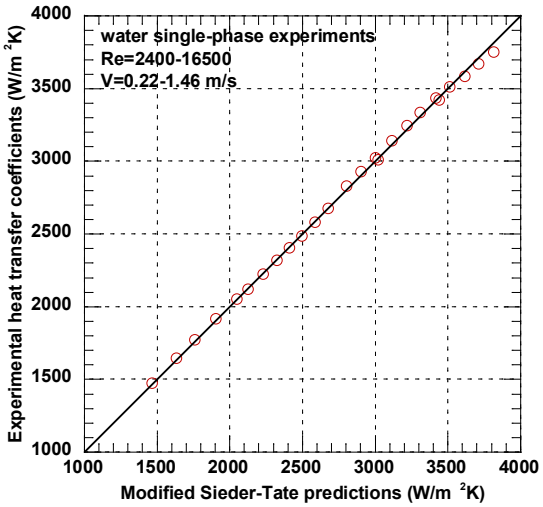

Figure 5. Heat transfer coefficient comparison.

Two-Phase Boiling with Water. In preparation for subcooled boiling heat transfer testing from the half-heated tube, the single-phase data were analyzed to establish a division between the top and bottom areas of the test section tube, which had different temperature distributions due to the half-heated test section wall. The area division along with the modified Sieder-Tate equation will be used for single-phase heat transfer portions of the test section during experiments where subcooled boiling occurs at the bottom.

Conclusions

In summary, the design and fabrication of the PACCAR heat transfer test facility have been completed; the LabVIEW-based data acquisition and test control hardware and software have been established; the experiments and data reduction for single-phase convective heat transfer with water have been performed, and experiments for two-phase boiling with water have been prepared. The project is on schedule and the future work will be focused on experiments and data reduction of two-phase subcooled boiling with water and ethylene glycol/water mixtures.

VIII.C. Thermal Control Through Air-Side Heat Transfer

Principal Investigator: Jules Routbort, co-workers Wen Yu, David France, and Tanju Sofu
Argonne National Laboratory
9700 S. Cass Avenue
Argonne, IL 60439
(630) 252 5065; Routbort@anl.gov

DOE Program Manager: Lee Slezak
(202) 586 2335; Lee.Slezak@ee.doe.gov

VIII.C.1. Abstract

Objective

- Explore possibilities of repositioning the class 8 tractor radiator and modifying the frontal area of the tractor to reduce aerodynamic drag
- Explore possibilities of using evaporative cooling under extreme conditions of temperature and engine load

Approach

- Perform CFD on the Generic Conventional Model Tractor ($1/8^{th}$ scale) at an air speed equivalent to 65 mph at 0° yaw with various radiator configurations. The model was modified to allow airflow through the radiator.
- Calculate how much water would be required to use evaporative cooling under extreme conditions
- Calculate the best way to modify the radiator to minimize the amount of water required and to maximize the cooling effect.

Major Accomplishments

- CFD indicates that repositioning the radiator with suitable modifications of the frontal area of the truck will reduce aerodynamic drag by 11% for the condition investigated. This would result in a 5.5% increase in fuel economy.
- Calculations indicate that the radiator can be easily modified and that 76 liters of water is sufficient to account for driving under the most extreme conditions (fully loaded climbing the Baker Grade when the temperature is 47°C). This would allow downsizing the radiator by 21% for all other driving conditions or allow 19% more heat removal with the same size radiator.

Future Activities

- Detailed CFD will be performed on a more complete model of a class 8 tractor/trailer supplied by an OEM. The calculations will include various yaw angles
- Theoretical calculations of evaporative cooling will have to be experimentally verified using a small radiator.
- Working with an OEM, the engineering feasibility and the cost-effectiveness of the two technologies will be assessed.

VIII.C.2. Technical Discussion

Background

This project started in FY 11 with 150K in seed funding to explore the possibilities of 1. Reducing aerodynamic drag on class 8 trucks by repositioning the radiator and modification of the frontal area to reduce aerodynamic drag, and 2. To explore the possibility of using evaporative cooling under extreme temperature, load, and grade conditions that would be encountered in the US. ANL reports and invention disclosures have been written for both technologies.

Introduction

Aerodynamic drag is a major contributor to fuel consumption in class 8 trucks, especially at highway speeds. Aerodynamic drag, i.e. the resistance to truck's movement through the air, consists of two main components, pressure drag and shear drag. The shear drag for trucks is small compared to the pressure drag, and the basic shape of the truck imposes the pressure drag on the vehicle. Typically, a high-pressure zone is created in the front of the tractor due to the stagnation effect, and a low-pressure zone is created in the rear of the truck both resulting in pressure drag. The frontal shape of the tractor is dictated in a large part by the radiator and its placement resulting in a large stagnation area. The method for reducing aerodynamic drag on trucks proposed in this study is to modify the frontal shape of the tractor by relocating the radiator to a different location.

A hybrid radiator-cooling system was investigated for reducing the size or increasing the cooling capacity of vehicle coolant radiators. The hybrid system is a combination of conventional airside finned surface cooling and active evaporative water cooling. The airside-finned surface is sized to transfer required heat under all driving conditions except for the most severe. In the later case, evaporative cooling is used in addition to the conventional airside finned surface cooling. Together the two systems transfer the required heat under all driving conditions. However, under most driving conditions, only the airside finned surface cooling is required. Consequently, the finned surface may be smaller than in conventional radiators that utilize airside-finned surface cooling exclusively. This study presents details of the hybrid system and calculations of the radiator size and evaporative cooling loads at various evaporation rates.

Approach

Both the relocation of the radiator and the evaporative cooling components of this work were computational in nature. The scoping study of placement of the radiator was performed using with a commercial CFD code (Star-CCM+) to solve mass and momentum equations of airflow past a numerical simulation model of the physical GCM. Using a porous medium to simulate airflow through the radiator modified the ANL computational model of the GCM truck. Drag coefficient was calculated for the base model and compared to the base model with the radiator moved behind the air deflector on the top of the cab. To smooth out the flow, a hemispherical deflector was mounted on the front of the trailer. Furthermore, the front of the tractor was modified and its drag coefficient was compared to the base GCM model. Hence there were three cases to compare the drag coefficient. All calculations were performed on the GCM at an equivalent speed of 65 mph at 0° yaw.

Figure 1 shows schematically a top view of a section of the radiator in the example hybrid radiator-cooling system with vertical coolant channels and fins between them (shaded area) on the airside. The channels have been extended beyond the fins on the downstream airside of the radiator as shown. These extended channel surfaces are to be cooled by evaporating water flowing downwards by gravity into the plane of Figure 1. The combination of the conventional cooling from the finned surfaces and the evaporative cooling from the extended channel surfaces is the total heat transfer from the radiator to the atmosphere. Under the thermal design condition, both cooling mechanisms would be functioning. However, at most thermal loads below the design condition, only the conventional airside finned surface cooling would be required. Thus, the active cooling of

the water evaporation would be used only at or very near the thermal design condition.

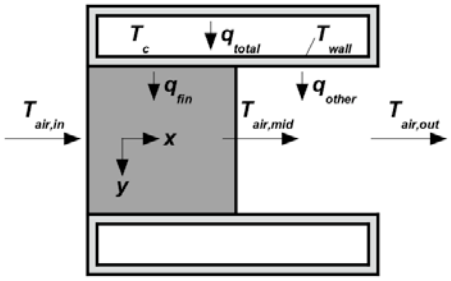

Figure 1. Top view of a section of the hybrid radiator (z direction is into the picture).

Having modified the tubes to allow for the flow of water, it is necessary to minimize the amount of water required to reduce the size of the radiator while removing the required amount of heat under the most severe driving conditions. There are also options on the form of water droplets and the contact angles to consider. This calculation used radiator/engine data kindly provided by Cummins Engine, Inc.

Results-Repositioning the radiator

Figure 2 shows the pressure distribution on the frontal surface of the tractor with the radiator behind the deflector without modification of the frontal area of the tractor.

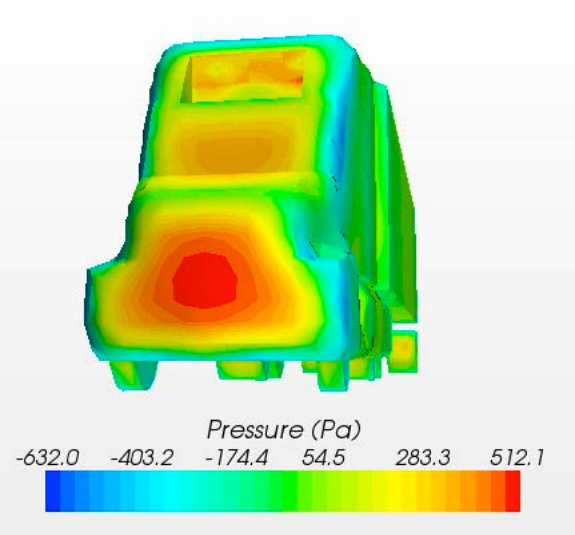

Figure 2. Front view of the pressure distribution along the front of the tractor.

Figure 3. Shows the proposed modification to the front of the tractor

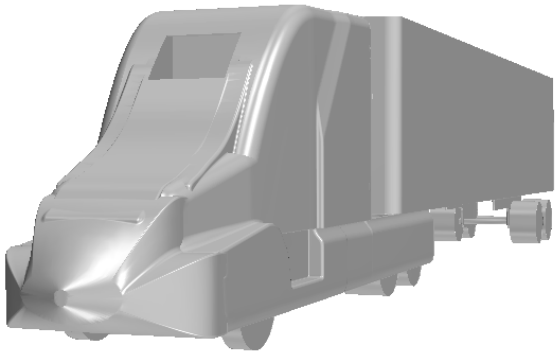

Figure 3. Side view of the modified tractor-trailer.

Results are shown in Table 1.

Table 2. Comparison of drag coefficients for the three cases considered.

Model	C_d
GMC with conventional radiator	0.43
GMC with radiator behind deflector	0.43
GMC with Radiator behind deflector and modified front	0.38

It is clear that modification of the frontal area has a large effect on the aerodynamic drag. The 11% decrease in drag computes to a 5.5 % increase in fuel efficiency, and a more pleasing shape. It is admitted that the GMC truck is simplistic and continued funding will allow calculations on a more detailed model. Furthermore, this was a modeling study and if results are confirmed using a more detailed model, engineering details will have to be addressed.

Results-Hybrid Radiator Cooling System

For heat transfer increases, three cases were studied for the geometry of Figure 1 and the dimensions obtained from Cummins Engine Inc. The first case analyzed the increased heat transfer benefits of utilizing evaporating water in the form of a continuous falling film on the extended coolant channel surfaces of the radiator by comparing it to the radiator without evaporative cooling. The second and third cases involved discrete water droplets falling by gravity on the extended channel surfaces in the form of semispherical and elongated droplets, respectively, which focused on the percentage of

evaporation from the given dimensions and contact angles of the droplets. The final part of this study analyzed the potential of the decrease in radiator size with the addition of evaporative cooling.

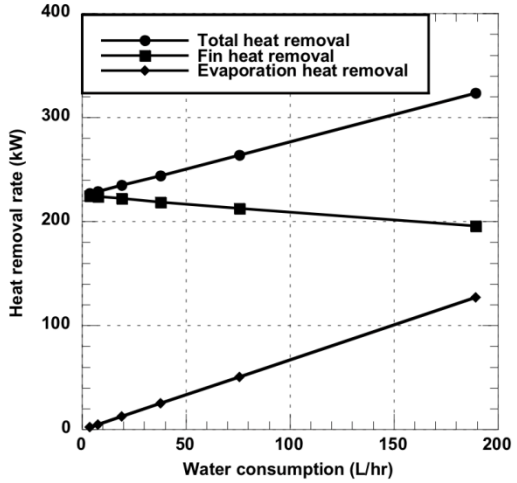

Figure 4. Increased radiator heat transfer with an evaporating liquid film.

Figure 4 shows the effect of the evaporating liquid film on the heat transfer. Obviously the evaporative cooling increases the amount of heat transfer as the water consumption increases and decreases the fin heat removal. The questions are what are the minimum consumption required for optimal results and how best can the thin liquid film be formed?? The latter question concerns the size of the hole in the manifold and the contact angle between the vertical surface and the water droplet.

Figure 5 shows the calculated value of droplet evaporation rate as a function of contact angle for various sizes of holes. Obviously the smallest hole results in more evaporation for a given contact angle. It should be mentioned that there is a literature base for inexpensive modifications of the contact angles (down to 3°) for aluminum, a typical radiator material.

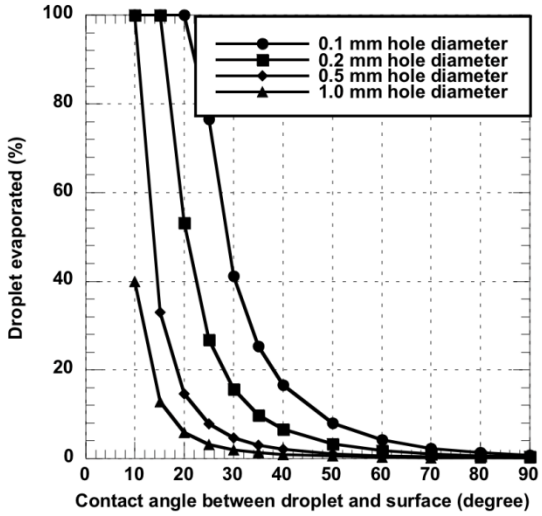

Figure 5. Droplet evaporation traveling downwards along a vertical surface for various source hole diameters.

Figure 6. Illustrates the reduction of radiator width that can be achieved using a fixed heat transfer rate. It is noted that 76 l/hr will result in a 21% decrease in radiator width (and area). It should be mentioned that the increase in weight of water, tank, pump and control will be partially compensated by the decreased size/weight of the radiator. Furthermore, the water will only be necessary when the truck is run under the extreme conditions of temperature, grade and load.

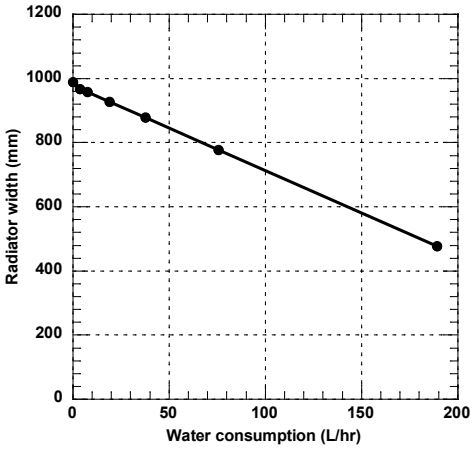

Figure 6. Reduced radiator size with liquid film evaporation at fixed heat transfer rate.

Conclusions

Using the CFD tool, drag coefficients were found for a 1/8th scale, class-8, GCM truck and its variants by repositioning the radiator and steam lining the front end. Firstly, a radiator and engine compartment was added to the GCM truck and airflow was simulated for a speed of 65mph at 0° yaw for normal US highway operating conditions. However, moving the radiator to the top of the cab and redesigning the frontal shape of the truck gives 11 % reduction in drag coefficient. Despite engineering involved in repositioning the radiator, the increase in energy efficiency is substantial (≈5.5%).

Coolant radiators in trucks and automobiles were shown to be amenable to evaporative cooling. Using a hybrid truck radiator, 19% and 46% heat transfer increases were obtained with 76-L/hr (20-gal/hr) and 189-L/hr (50-gal/hr) water flow rates, respectively. These results were dependent on the establishment of water flow with small thickness from the radiator surfaces. It was found that such thickness could readily be obtained by using droplet flow with contact angle management.

An alternative to the heat transfer increase from an existing radiator with the addition of evaporative cooling is the radiator size reduction. It was shown that, at the design heat load, the 76-L/hr water flow rate yielded radiator area reduction of 21%.

VIII.C.3. Products

Publications

1. "Aerodynamics of Class – 8 Trucks with Radiator Repositioning", S. Mitra, J. Routbort, D. France, T. Sofu, and D. Pointer ANL internal report
2. "Hybrid Radiator-Cooling System", D. Smith, D. France, W. Yu, and J. Routbort.

   ANL internal report

Patents

Two invention reports filed September 2011.

VIII.D. Efficiency Improvements through Parasitic Loss Reduction

Principal Investigator: George Fenske
Co-PIs: Nicholaos Demas, Robert Erck
Argonne National Laboratory
9700 S. Cass Avenue
Argonne, IL 60439
(630) 252-5190; gfenske@anl.gov

DOE Program Manager: Lee Slezak
(202) 586-2335; lee.slezak@ee.doe.gov

VIII.D.1. Abstract

Progress on a Department of Energy (DOE) project to improve fuel efficiency of advanced vehicles by reducing parasitic engine friction is discussed. The project focuses on the integration of existing engine component codes to predict changes in the friction mean effective pressure of small-, medium-, and heavy-duty diesel engines. A major task of the project is to develop realistic databases on boundary friction properties for use in pedictive models and to validate the codes using tests with fired engines.

Objective

- Develop and integrate mechanistic models of engine friction and wear to identify key sources of parasitic losses as functions of engine load, speed, and driving cycle.
- Develop advanced tribological systems (lubricants, surface metrology, and component materials/coatings) and model their impact on fuel efficiency with a goal to improve vehicle efficiency by 2% in FY 2015.
- Develop engine component maps to model the impact of friction and wear on fuel efficiency for use in analytical system toolkits.
- Develop database required for models of mechanistic friction and wear of coatings, lubricant additives, and engineered surface textures.
- Validate mechanistic models by performing instrumented, fired-engine tests with single-cylinder engines to confirm system approaches to reduce friction and wear of key components.
- Identify common issues associated with commercial and military ground vehicles on the impact of low-friction lubricant technologies to reduce parasitic friction losses and vehicle efficiency.

Approach

- Predict fuel economy improvements over a wide range of oil viscosities by using physics-based models of asperity and viscous losses.
- Model changes in contact severity loads on critical components that occur with low-viscosity lubricants.
- Evaluate the potential of advanced low-friction surface treatments (e.g., coatings, surface texturing, and additives) to reduce parasitic losses and predict potential fuel economy improvements.
- Measure friction and wear improvements on advanced laboratory rigs and fired engines to validate model calculations.
- Develop component maps of parasitic energy losses for heavy-vehicle system models.

Major Accomplishments

- Examined applicability of traditional drive cycles developed for on-road vehicles to replicate military drive cycles.
- Defined statement of goals for a Cooperative Research and Development Agreement (CRADA) to develop predictive tools to model parasitic friction losses in engines.
- Examined the impact of advanced carbon-based additives on friction.
- Continued efforts with the U.S. Army Tank Automotive Research, Development and Engineering Center (TARDEC) to identify mutual areas of collaboration for lubricant development.
- Examined protocols to extract boundary friction data from bench-top rigs using Stribek analysis.

Future Activities

- Establish CRADA and initiate studies to predict the impact of tribological system properties of fuel economy and potential trade-offs for future vehicles.
- Evaluate engine friction measurement techniques to validate predictive models and identify site for future engine validations.
- Develop database on critical boundary layer friction.

VIII.D.2. Technical Discussion

Background

Friction, wear, and lubrication affect energy efficiency, durability, and environmental performance of critical transportation systems, including diesel engines. Total frictional losses in a typical diesel engine may alone account for more than 10% of the total fuel energy (depending on the engine size, driving condition, etc.). The amount of emissions produced by these engines is related to the fuel economy of that engine. In general, the higher the fuel economy, the lower the emissions. Higher fuel economy and lower emissions in future diesel engines may be achieved by the development and widespread use of novel materials, lubricants, and coatings. For example, with increased use of lower viscosity oils (that also contain lower amounts of sulfur- and phosphorus-bearing additives), the fuel economy and environmental performance of future engine systems can be dramatically improved. Furthermore, with the development and increased use of smart surface engineering and coating technologies, even higher fuel economy and better environmental soundness are feasible.

Integration of advanced lubricant chemistries, textured/superfinished surfaces, and advanced component materials and coatings necessitates pursuing a systems approach. Changes in one system component can readily change the performance of other components. For example, application of a hard coating on a liner to improve its durability may decrease the durability of the mating rings. Also, lowering the viscous drag will cause certain components (e.g., bearings) to operate under boundary lubrication regimes not previously encountered, resulting in accelerated degradation. A systems approach is required to not only identify the critical components that need to be addressed in terms of energy savings, but also to identify potential pitfalls and find solutions.

The main goal of this project is to utilize advanced models of engine component friction and contact loading to predict the impact of smart surface engineering technologies (e.g., laser dimpling, near frictionless carbon, and superhard coatings) and energy-conserving lubricant additives on parasitic energy losses from diesel engine components. The project also aims to develop more realistic databases on the boundary or asperity friction that are used in advanced codes to predict total (asperity and hydrodynamic) friction losses and, in the future, to validate the predictions using fired engines. Such information will help identify critical engine components that can benefit the most from the use of novel surface technologies, especially when low-viscosity engine oils are used to maximize the fuel economy of these

engines by reducing churning and/or hydrodynamic losses. The long-term objective of the project is to develop a database that provides a "look-up" capability to predict the impact of lubricant viscosity, asperity friction, and surface finish on friction mean effective pressure (FMEP) and contact severity at different engine operating modes.

Introduction

Starting in 2003, Argonne and Ricardo, Inc., collaborated to identify heavy-duty diesel engine components that can benefit from low-friction coatings and/or surface treatments. The specific components included rings, piston skirts, piston pin bearings, crankshaft main and connecting rod bearings, and cam bearings. Using computer codes, Ricardo quantified the impact of low-viscosity engine oils on fuel economy. Ricardo also identified conditions that can result in direct metal-to-metal contacts, which, in turn, can accelerate engine wear and asperity friction. Efforts were also initiated to identify approaches that can validate the predictions under fired conditions.

Argonne focused on the development and testing of low-friction coatings under a wide range of sliding conditions with low- and high-viscosity engine oils. These coatings (such as near frictionless carbon) as well as laser-textured surfaces were subjected to extensive friction tests using bench-top rigs. The test conditions (i.e., speeds, loads, and temperatures) were selected to create conditions where direct metal-to-metal contacts will prevail, as well as situations where mixed or hydrodynamic regimes will dominate. Using frictional data generated by Argonne, Ricardo estimated the extent of potential energy savings in diesel engines and identified those components that can benefit the most from such low-friction coatings and/or surface treatments. Argonne developed a test rig to simulate engine conditions for piston rings sliding against cylinder liners – one of the major sources of parasitic energy losses identified in Ricardo's studies. The test rig is being used to identify candidate technologies (e.g., coatings and additives) that can provide not only the level of friction reduction assumed in the Ricardo models, but also information on the impact of the technologies on material and component wear/durability.

During FY 2009 Argonne analyzed earlier Ricardo simulation studies to determine the impact of (1) low-friction surfaces and low-viscosity fluids on the overall FMEP and (2) low-viscosity fluids on component durability. Argonne also initiated piston skirt/liner tests to determine the effect of several low-friction additives on skirt/liner friction.

During FY 2010 Argonne's activities on parasitic energy losses were modified to establish a collaborative effort between the DOE and Department of Defense (DOD) on the subject of parasitic losses and their impact on fuel economy. As part of these activities, discussions were initiated with TARDEC and DOD to identify areas of mutual interest related to mitigation of parasitic losses. Work also continued to investigate the potential of several advanced additives to improve scuffing resistance under severe tribological conditions.

In FY 2011, Argonne's activities continued to examine the role of tribological variables on fuel consumption, examining the distribution of asperity and hydrodynamic losses on fuel economy. Efforts also continued on establishing a collaborative project with TARDEC on low-viscosity lubricants and additives. Finally, activities continued to explore the potential of several nanoadditives and their impact on asperity friction.

Approach

The approach used in this project to model the impact of tribological parameters on fuel economy involves modeling and laboratory testing of additives.

- Modeling of parasitic friction losses (FMEP) is performed with codes for piston skirts (PISDYN), rings (RINGPAK), valve trains (VALDYN), and bearings (ORBIT/ ENGDYN). Results were tabulated for different lubricant viscosities, asperity friction, and engine modes (Ricardo "8-mode") to predict the impact on fuel

consumption using a fuel consumption scaling factor (FCSF) defined as:

where ΔFMEP is the change in the FMEP relative to the base case (40 weight oil with baseline asperity friction coefficients) and IMEP is the indicated mean effective pressure. Results of the modeling approach have been presented elsewhere [1-4].

- The experimental activities are aimed at identifying more realistic asperity friction coefficients. The current models assume the boundary friction coefficient is a fixed constant independent of temperature and interfacial composition/structure. The early models used in Refs. 1-4 assumed friction coefficients ranging from 0.005 to 0.12, depending on the component (0.005 for camshaft follower, 0.02 for cam bearing and rocker bushing, 0.05 for pushrod and rocker tip, 0.08 for piston skirt/liner, 0.12 for piston ring/liner, and 0.08 for the piston pin). In reality, the boundary friction is a function of temperature, additive package, and component material/coating. The laboratory-scale testing performed in this project utilizes bench-top rigs to simulate engine conditions and provide meaningful data on boundary friction coefficients that can be used in the models. In the meantime, the model predictions are performed by using a "what-if" or sensitivity basis, where the predictions are based on the assumption that the boundary friction is reduced by 25 to 90% to gauge the impact of asperity friction on fuel economy.
- Validation studies are planned as part of the project. Early tests used a "fixed-liner" method to measure skirt and ring friction in-situ under compression conditions (no combustion). Future plans will identify alternative techniques and sites for fired engine validation.

Results

During FY 2010 and 2011, efforts were initiated to identify common tribological pathways to improve the fuel economy of on-road civilian vehicles as well as ground vehicles used by the military. This requires information on the typical drive cycle for a military ground vehicle, which is difficult to define. Initial studies identified four drive cycles/missions for a traditional Humvee vehicle – tactical idle, convoy escort, urban assault, and cross-road. An overlay of engine points (engine speed and load) for a typical military proving-ground simulation course suggests that the traditional driving modes developed for on-road civilian vehicles (such as those shown in Figure 1) do not adequately represent a military drive cycle, and thus, use of a Ricardo or AVL 8-mode cycle or ISO 11-mode cycle to simulate FCSF will not be sufficient.

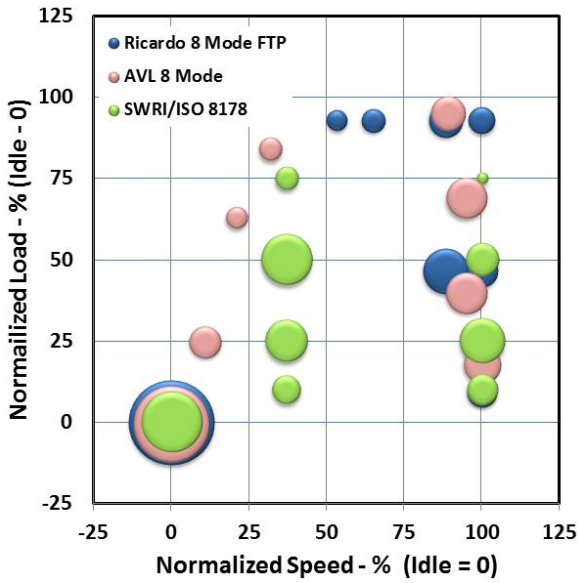

Figure 1. Engine map (engine load vs. speed) for commercial/civilian drive cycles.

A more inclusive set of engine points may be required to build a database from which FCSF can be extracted once a drive cycle (engine speed, load, and frequency) is specified.

Figure 2 shows an example of the information available through this type of analysis. Here, the relative contact severity is shown as a function of lubricant viscosity, and one can see that as viscosity decreases, the relative contact severity (a measure of reliability and durability) increases. Such information can be used to

evaluate trade-offs of different tribological paths and help identify which components may require additional improvements in terms of wear resistance.

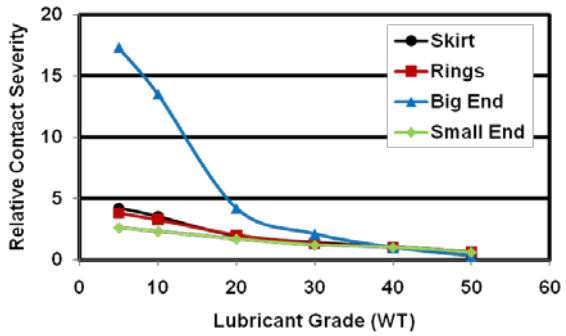

Figure 2. Relative contact severity (normalized to 40 weight oil) for different engine components.

Early studies [1-4] using this approach have been successful in modeling parasitic losses; however, they were limited to heavy-duty diesel engines. More comprehensive modeling of parasitic losses will be performed to include small- and medium-size engines and surface finish under a CRADA that is under negotiation with an engine engineering firm.

The codes used to model parasitic energy losses for different components separate losses into hydrodynamic and asperity contributions. Asperity friction is modeled as a fixed constant independent of temperature. The hydrodynamic friction is modeled using a mass-conserving solution to the Reynolds equations, where elasticity of the components is considered. The experimental portion of this project utilizes laboratory-scale rigs to quantify the friction (and wear) of lubricants at temperatures ranging from room temperature to 100°C. Photos of the laboratory-scale rigs are shown in Figures. 3 and 4 for a pin-on-disc (POD) and high-frequency reciprocating rig (HFRR), respectively.

Figure 3. Pin-on-disc rig used to quantify friction and wear.

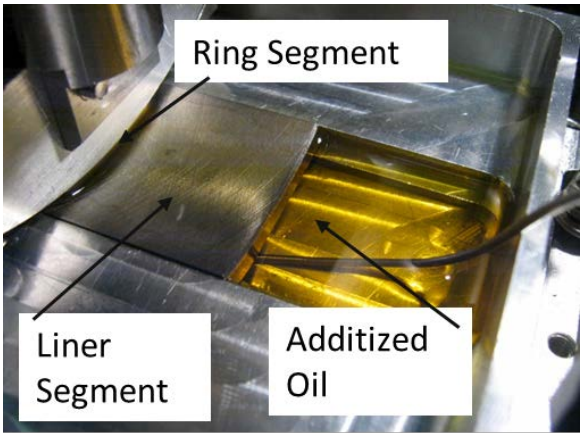

Figure 4. High-frequency reciprocating rig.

Both rigs provide high-fidelity data on the friction and wear properties. The POD rig operates in unidirectional sliding with spherical (or cylindrical) samples sliding against flat discs. The HFRR can use spherical or cylindrical samples sliding against flat counterparts or, as shown in Figure 4, prototypical ring segments that reciprocate against liner segments.

An example of the information that can be obtained from the HFRR is given in Figure 5, which shows a Stribek curve for a formulated synthetic lubricant Mobil 1 10W/30 and an unformulated synthetic base fluid, PAO10 (poly alpha olefin), that has the same viscosity (10 cSt) at 100°C. Figure 5 is a compilation of many tests performed at different temperatures and reciprocating speeds and demonstrates that the impact of reciprocating speed and viscosity can

be compensated by using an analysis in which the friction is plotted as a function of the Stribek parameter (ηV/L), where η is the dynamic viscosity, V is the local speed, and L is the load (N per unit contact length). This technique is being further refined to generate experimental data on the boundary friction coefficient, i.e., the friction coefficient in Figure 5 at Stribek numbers near zero. The data in Figure 5 show that the boundary friction at zero Stribek number for the 100°C tests is higher than those at room temperature. The reason for this difference is not readily apparent – the Stribek analysis should have compensated for differences in the viscosity at the two different temperatures, yet a significant difference in boundary friction is noticeable. Further analysis is required to determine if the observed differences are due to the accelerated formation of tribo-films at elevated temperatures, or to differences in the shear strength of the tribo-films at the two temperatures.

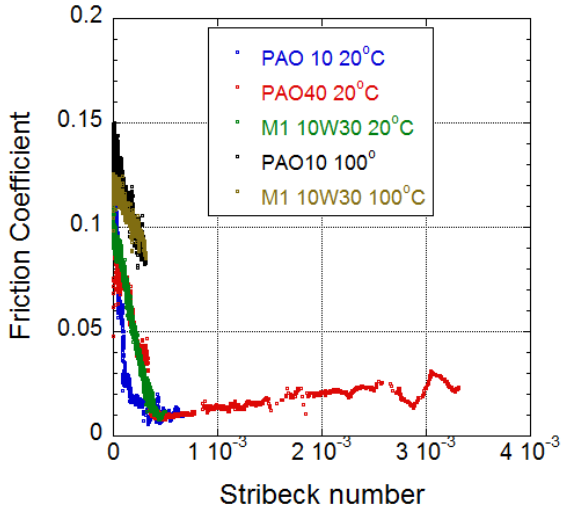

Figure 5. Stribek curve for unformulated and formulated synthetic lubricants.

Another example of a Stribek curve is shown in Figure 6, which demonstrates the ability of the POD rig to accurately measure the friction as a function of sliding speed. In this case the friction response of Mobil 1 10W/30 is shown as a function of speed, where the red data points show real-time friction, and the blue points show a running average – all at room temperature.

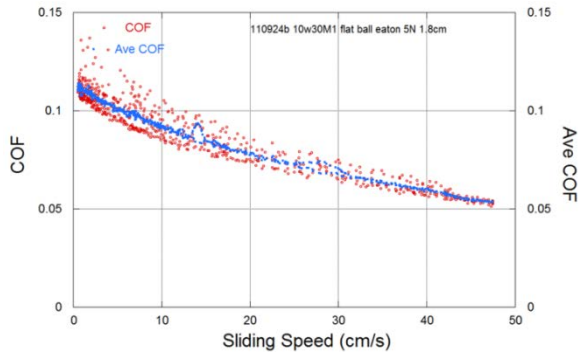

Figure 6. POD coefficient of friction (COF) as a function of sliding speed at room temperature.

Figures 5 and 6 show examples on the use of the POD and HFRR rigs to obtain boundary friction data for unformulated or formulated oils. The formulated oil in this case is a conventional oil with a commercial additive package. The POD and HFRR rigs can also provide information on non-conventional additives. An example is given in Figure 7, which shows HFRR data at different temperatures for unformulated oil (PAO10) that had been treated with a nano-additive (MoS_2). At room temperature and 40°C the friction response is similar (close to 0.1) – comparable to the performance for untreated PAO10. At 100°C, however, the friction decreases significantly – down to near 0.06 – thus demonstrating the strong impact that friction can have on the boundary friction behavior.

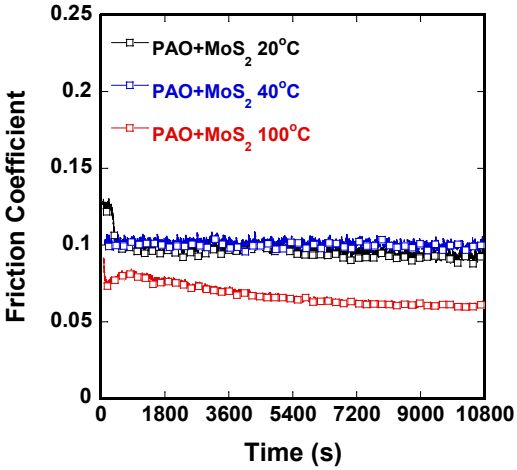

Figure 7. HFRR friction data for PAO10 treated with nano-MoS2 powders.

Conclusions

The Parasitic Energy Loss Reduction project examines the effects that tribological variables such as viscosity, boundary friction, and surface finish have on the friction losses in an engine and the overall vehicle fuel economy. Negotiations are in progress to establish a CRADA with an engineering firm to extend the heavy-duty diesel modeling to small- and medium-size engines and to include surface finish effects. Studies based on prior heavy-duty diesel engine models suggest that fuel economy of military ground vehicles can be significantly improved. Furthermore, due to military policies to perform periodic "resets" of vehicles, it may be feasible to retrofit military vehicles with improved materials and coatings on critical components and thus achieve even greater fuel economy improvements than achievable with advanced lubricants/additives alone.

Studies on HFRR and POD rigs indicate that more realistic information on boundary friction coefficients can be achieved as functions of temperature and composition.

Future activities will focus on CRADA activities to develop realistic boundary friction databases for non-ferrous friction couples (materials, coatings, and additives) at temperatures prototypic of internal combustion engines. Also, code predictions will be validated using fired engines. Efforts to further define a cohesive collaboration with TARDEC are in progress under a formal memorandum of understanding developed between DOE and DOD to pursue advanced vehicle power technologies.

References

1. I. Fox, "Numerical Evaluation of the Potential for Fuel Economy Improvement due to Boundary Friction Reduction within Heavy-Duty Diesel Engines," ECI International Conf. on Boundary Layer Lubrication, Copper Mountain, CO, Aug. 2003.
2. George Fenske, "Parasitic Energy Loss Mechanisms," *FY 2006 Progress Report for Heavy Vehicle Systems Optimization* (2006).
3. George Fenske, "Parasitic Energy Loss Mechanisms: Impact on Vehicle System Efficiency," U.S. Department of Energy Heavy Vehicle Systems Review, Argonne National Laboratory, Argonne, IL, April 18-20, 2006.
4. G. Fenske, O. Ajayi, R Erck, C. Lorenzo-Martin, A Masoner, and A. Comfort, "Reliability of Powertrain Components Exposed to Extreme Tribological Environments," Proceedings of the 2010 Ground Vehicle Systems Engineering and Technology Symposium, Dearborn, MI, 2010.

VIII.D.3. Products

Publications

1. Demas, N. G., Erck, R. A., and Fenske, G. R., "Tribological Evaluation of Piston Skirt/Cylinder Liner Contact Interfaces under Boundary Lubrication Conditions," Lubrication Science, March 2010.
2. Fenske, G. R., Erck, R. A., Ajayi, O. O., Masoner, A., and Comfort, A. S., "Impact of Friction Reduction Technologies on Fuel Economy for Ground Vehicles," Proceedings of the 2009 Ground Vehicle Systems Engineering and Technology Symposium, Warren, MI, August 2009.
3. Demas, N., Ajayi, O. O., Lorenzo-Martin, C., Fenske, G. R., "Correlation between Tribological Performance and Tribochemical Film Nanomechanical Properties," Presentation at 2010 ASME/STLE International Joint Tribology Conference, San Francisco, CA, October 2010.
4. Fenske, G, "Lubricants – Pathway to Improving Fuel Efficiency of Legacy Fleet," Presentation at Transportation Technologies and Fuels Forum, Arlington, VA, June 2011.
5. Fenske, G. R., Ajayi, O. O., Erck, R. A., Lorenzo-Martin, C., Masoner, A., Comfort, A. S., "Reliability of Powertrain Components Exposed to Extreme Tribological Environments," Proc. 2010 Ground Vehicle Systems Engineering and Technology Symposium (GVSETS), Dearborn, MI, August 2010.

VIII.E. Boundary Layer Lubrication Mechanisms

Principal Investigator: O. O. Ajayi, C. Lorenzo-Martin, R.A. Erck, N. Demas, and G. R. Fenske
Argonne National Laboratory
9700 South Cass Avenue
Argonne, IL 60439
(630) 252-9021; ajayi@anl.gov
fax: (630) 252-4798

DOE Program Manager: Lee Slezak
202-586-2335, Lee.Slezak@hq.doe.gov

VIII.E.1. Abstract

Objective

Develop a better understanding of the mechanisms and reactions that occur on component surfaces under boundary lubrication regimes with the ultimate goal of friction and wear reduction in oil-lubricated components and systems to meet the demands of advanced transportation vehicles. Specific objectives are the following:

- Determine the basic mechanisms of catastrophic failure in lubricated surfaces in terms of materials behavior. This knowledge will facilitate the design of higher power density components and systems.
- Determine the basic mechanisms of chemical boundary lubrication. This knowledge will facilitate lubricant and surface design for minimum frictional properties.
- Establish and validate methodologies for predicting the performance and failure of lubricated components and systems.
- Integrate coating and lubrication technologies for maximum enhancement of lubricated-surface performance.
- Transfer the technology developed to original equipment manufacturers (OEMs) for transportation vehicle components and systems.

Approach

- Characterize the dynamic changes in the near-surface material during scuffing. Formulate a model of the material-behavior-based scuffing mechanism with prediction capability.
- Determine the chemical kinetics of boundary film formation and loss rate by in-situ X-ray characterization of tribological interfaces at the Advanced Photon Source (APS) of Argonne National Laboratory.
- Characterize the structural, mechanical, and tribological properties of tribo-chemical films.
- Integrate the performance of all the structural elements of a lubricated interface to formulate a method for predicting performance and/or failure.
- Maintain continuous collaboration with vehicle component and system OEMs to facilitate effective technology transfer.

Major Accomplishments

- Developed and validated a model for scuffing failure of metallic materials based on an adiabatic shear instability mechanism for initiation for scuffing and thermally driven plastic instability for its propagation as determined by a balance between heat generation and heat dissipation rates.

- Developed a method to increase scuffing resistance by the creation of a graded nanocrystalline surface layer produced by severe plastic deformation. A U.S. patent was granted for the process (Patent #7,682,650).
- Extended scuffing mechanism study into ceramics and metals contact pairs as well as cast iron, which is typically used as a cylinder liner in internal combustion engines.
- Demonstrated the ability to characterize tribo-chemical films generated from model oil additives using X-ray fluorescence, reflectivity, and diffraction at the APS.
- Developed unique techniques to characterize the structure of tribochemical boundary films with different frictional behavior by combining focused ion beam (FIB) milling, transmission electron microscopy (TEM), and grazing incidence X-ray diffraction (GIXRD) at APS.
- Initiated the measurement of nano-mechanical properties of tribo-chemical boundary films.
- Formulated the framework for friction prediction and control at lubricated contact interfaces, taking into account the contribution of the fluid film, boundary film, and near-surface material.

Future Activities

- Develop and evaluate methods and technologies to prevent scuffing in oil-lubricated components and systems of high power density vehicles.
- Characterize the physical, mechanical, and failure mechanisms of tribochemical films with nano-contact probe devices. Formulate all constitutive equations for friction prediction and control.
- Evaluate the impact of various surface technologies, such as coating and laser texturing, on boundary lubrication mechanisms.

VIII.E.2. Technical Discussion

Introduction

Many critical components in diesel engines and transportation vehicle systems such as gears and bearings are lubricated by oil. Satisfactory performance of these components and systems in terms of efficiency and durability is achieved through the integration of materials, surface finish, and oil lubricant formulations. Material selection is often based on an Edisonian trial-and-error approach. Indeed, experience is likely the sole basis for new designs and methods to solve failure problems in lubricated components. Because of the technology drive to more efficient and smaller systems, more severe operating conditions are invariably expected for component surfaces in advanced engines and vehicle systems. The trial-and-error approach to effective lubrication is inadequate and certainly inefficient. Departure from this approach will require a better understanding of the fundamental mechanisms of both boundary lubrication and surface failure in severely loaded lubricated components.

Emission reduction is another major technical thrust for the Department of Energy in the development of diesel engine technology for heavy vehicles. Indeed with the higher efficiency of diesel engines compared to gasoline engines, significant reduction in emissions will facilitate wider adoption of diesel engines for automotive applications. Unfortunately, some essential components in oil lubricants and diesel-fuel additives (such as sulfur, phosphorus, and chlorine) are known to poison the catalysts in emission-reducing after-treatment devices for diesel engines. Reduction or elimination of these additives will make emission after-treatment devices more effective and durable; it will, however, make the surfaces of many lubricated components more vulnerable to catastrophic failure. Therefore, an effective replacement for these essential lubricant additives is needed. To that end, a better understanding of the mechanisms of boundary lubrication and the failures therein is also needed.

Increases in vehicle efficiency will require friction reduction and increase in power density

in the engine and powertrain systems. Higher power density translates to increased severity of contact among many tribological components. This contact will compromise the reliability of various critical components, unless they are effectively lubricated. The efficacy of oil additives in reducing friction and in protecting component surfaces depends on the nature and extent of the chemical interactions between the component surface and the oil additives.

In addition to reliability issues, the durability of lubricated components also depends on the effectiveness of oil lubrication mechanisms, especially under boundary conditions. Components will eventually fail or wear out by various mechanisms, including contact fatigue. Wear is the gradual removal of material from contacting surfaces, and it can occur in many ways, such as abrasion, adhesion, and corrosion. The repeated contact stress cycles to which component contact surfaces are subjected can initiate and propagate fatigue cracks and, ultimately, lead to the loss of a chunk of material from the surface. This damage mode by contact fatigue is often referred to as "pitting." Wear and contact fatigue are both closely related to boundary lubrication mechanisms. Antiwear additives in lubricants are designed to form a wear-resistant protective layer on the surface. The role of lubricant additives on contact fatigue failure is not fully understood, although it is clear that the lubricant chemistry significantly affects contact fatigue. Again, lack of a comprehensive understanding of the basic mechanisms of boundary lubrication is a major obstacle to a reasonable prediction of the durability of lubricated components and systems.

Significant oil conservation benefits would accrue by extending the drain interval for diesel engine oil, with an ultimate goal of a fill-for-life system. Successful implementation of the fill-for-life concept for the various lubricated systems in heavy vehicles requires optimization of surface lubrication through the integration of materials, lubricant, and, perhaps, coating technologies. Such an effort will require an adequate fundamental understanding of surface material behavior, chemical interactions between the material surface and the lubricant, and the behavior of material and lubricant over time.

Some common threads run through all of the challenges and problems in the area of effective and durable surface lubrication of components and systems for efficient and high power density engines, briefly described above. The two key ones are lack of adequate basic and quantitative understanding of the failure mechanisms of component surfaces and lack of understanding of the basic mechanisms of boundary lubrication, i.e., how lubricant chemistry and additives interact with rubbing surfaces, and how this interaction affects performance in terms of friction and wear.

To progress beyond the empirical trial-and-error approach for predicting lubricated component performance, a better understanding is required of the basic mechanisms regarding the events that occur on lubricated surfaces. Consequently, the primary objective of the present project is to determine the fundamental mechanisms of boundary lubrication and failure processes of lubricated surfaces.

Approach

The technical approach taken in this study differs from the usual one of empirical friction and wear testing combined with post-test characterization of lubricated surfaces in that it includes development of unique characterization techniques for the analysis of near surface materials and tribochemical surface films. This capability will enable better understanding of the basic mechanisms of lubrication and performance in the boundary regime. Ultimately, in-situ characterization techniques will be developed for lubricated interfaces that will use the X-ray beam at the APS. Using a combination of different X-ray-based surface analytical techniques, we will determine, in real time, the interactions between oil lubricants and their additives and the surfaces they lubricate. Such study will provide the basic mechanisms of boundary lubrication. In addition to surface chemical changes, the materials aspects of various tribological failure mechanisms (starting with scuffing) will be studied.

Results and Discussions

In FY 2010, we presented a new characterization technique for the analysis of the structure of boundary layer films. During FY 2011, efforts were devoted to the application of the new characterization technique to numerous boundary layer films, formed from both commercially available and model lubricants. More than 15 types of boundary films were analyzed. The films analyzed showed a variety of frictional behavior during tribological testing. Based on this extensive analysis of the structure and frictional behavior we succeeded in establishing a firm and consistent correlation between the structure and friction of boundary layer films.

All the films with crystalline structure exhibited consistently higher and, for the most part, nearly constant friction coefficient, as shown in Figure 1a. This behavior can be attributed to the existence of a fixed or constant shear strength for a crystalline tribochemical film. It is well known that crystalline solids exhibit a fixed shear strength. For crystalline tribochemical boundary films, the magnitude of the friction coefficient will most likely depend on the film shear strength. Incidentally, a crystalline film with high shear strength is also likely to exhibit good wear resistance.

For tribochemical boundary layer films that are amorphous or a mixture of crystalline and amorphous, significantly lower friction was observed under the boundary lubrication regime. Friction coefficients were as low as 0.03, typical for full fluid film lubrication. Based on this observation, we were able to produce boundary films with both amorphous and mixed phases, both of which showed a sustainable friction reduction in the boundary lubrication regime, as shown in Figures 1b and 1c. Note that the λ ratio, defined as the ratio of lubricant fluid film thickness to the composite surface roughness, is much lower at the end of the tests than at the beginning. This finding indicates that the contacts in Figures 1b and 1c were under the boundary lubrication regime for the duration of the test with increasing severity of contact. The friction coefficient of 0.03 shown in Figures 1b and 1c, being lower than the typical 0.1-0.13 values under the severe boundary lubrication regime contact, represents a significant advance in our understanding and control of friction.

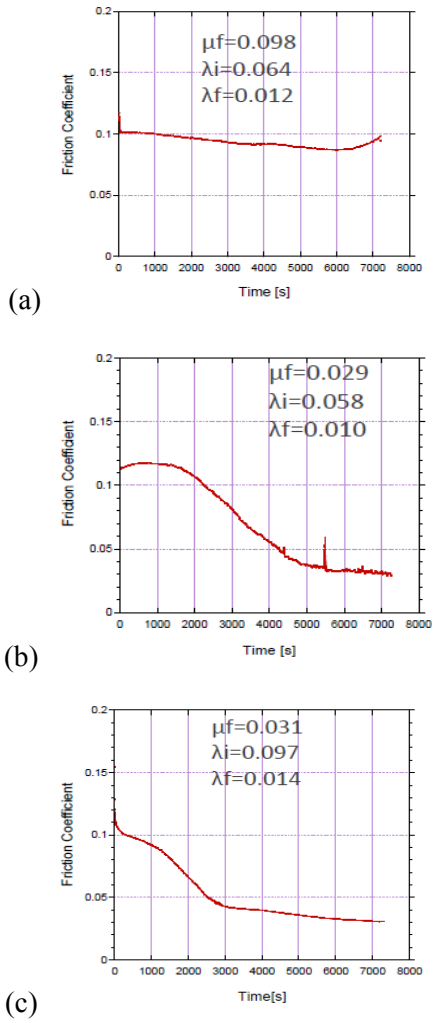

Figure 1. Friction coefficient variation with time for tribochemical boundary films with (a) crystalline structure, (b) mixture of amorphous and crystalline, and (c) amorphous structure.

A major sustainable friction reduction was achieved under the boundary lubrication regime through modification of the tribochemical boundary layer. Through boundary layer structural design, the "Stribeck" curve representing the frictional behavior in the various lubrication regimes can be modified, as shown in Figure 2.

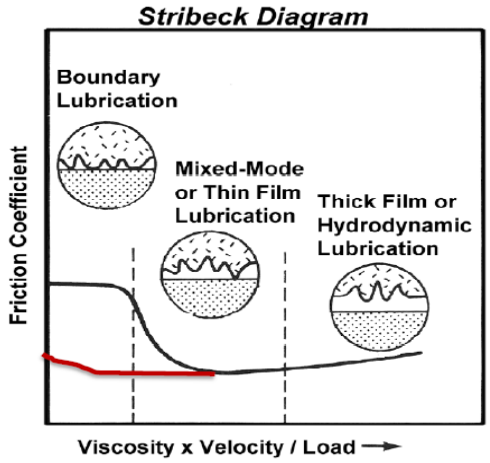

Figure 2. Possible modification of the Stribeck curve (red) through boundary film engineering to achieve low friction under boundary regime.

In addition to sustainable friction reduction, the present findings on the connection between structure and friction also have implication for applications requiring high, constant friction. such as the relatively new continuously variable transmission (CVT), for which high traction/friction is desirable. Tribochemical boundary films with crystalline structure and high sheer strength would be highly desirable for such application.

Finally, during FY 2011, we attempted to formulate a methodology for the comprehensive friction modeling of lubricated contacts, taking into account all the contributions to friction. Most current approaches to friction prediction and modeling are based on fluid film calculation, usually with the assumption that the asperity contacts under boundary regime are dry. Based on our work in this project, we are including shearing of the fluid, boundary film, and the near surface materials in the friction calculation. Thus, the friction coefficient can be written as:

$$\mu = \frac{F_{sf} + F_{sb} + F_{sa}}{F_N}$$

F_{sf} = Fluid film shear force
F_{sb} = Boundary film shear force
F_{sa} = asperity shear force

The experimentally measured can be related to a calculated total friction by integrating the shear forces of the three contributions over the entire contact area as a function of time, taking into account their changes over time. We still must formulate constitutive equations for the shear behavior of the boundary film and the near surface material.

Conclusions

Through detailed analysis of the structure of several tribochemical boundary films, and the measurement of the friction behavior of the film, a firm and consistent correlation was established between the structure and friction behavior of the boundary film. From this relationship, tribochemical boundary films were produced with a sustainable 70% reduction in friction under the boundary lubrication regime. This friction reduction has a potential for significant fuel savings in transportation vehicles.

An approach to comprehensive friction prediction was also developed. It incorporates the contribution of boundary films and the near surface material in addition to the usual lubricant fluid films.

VIII.E.3. Products

Publications

1. O. O. Ajayi, C. Lorenzo-Martin, R. A. Erck, and G. R. Fenske, “Scuffing mechanism of near-surface material during lubricated severe sliding contact,” Wear, 271 (2011), 1750-1753.
2. J. Han, R. Zhang, O. Ajayi, G. Barber, Q. Zou, L. Guessous, D. Schall, and S. Alnabulsi, “Scuffing behavior of gray cast iron and 1080 steel in reciprocating and rotational sliding,” *Wear*, 271 (2011), 1854-1861.
3. A. Kovalchenko, O. Ajayi, A. Erdemir, and G. Fenske, “Friction and wear behavior of laser textured surface under lubricated initial point contact,” *Wear*, 271 (2011), 1719-1725.

4. R. A. Erck, O. O. Ajayi, C. Lorenzo-Martin, G. R. Fenske, "Frictional anisotropy in boundary lubrication regime: Effect of surface texture," Presented at Society of Tribologists and Lubrication Engineers (STLE) 66th Annual Meeting, Atlanta, GA.
5. O. O. Ajayi, C. Lorenzo-Martin, R. A. Erck, N. Demas, and G. R. Fenske, "Boundary lubrication mechanisms," FY 2010 Annual Progress Report for DOE Vehicle Technologies Office.

Patents

O. O. Ajayi and J. G. Hershberger, "Method for producing functionally graded nanocrystalline layer on metal surfaces," **US Patent # 7,682,650** (March 2010).

VIII.F. Development of High Power Density Driveline for Vehicles

Principal Investigator: O. O. Ajayi, C. Lorenzo-Martin, A. C Greco, and G. R. Fenske
Argonne National Laboratory
9700 South Cass Avenue
Argonne, IL 60439
(630) 252-9021; fax: (630) 252-4798; e-mail: ajayi@anl.gov

DOE Program Manager: Lee Slezak
(202) 586-2335, Lee.Slezak@hq.doe.gov

VIII.F.1. Abstract

Objective

- Achieve significant reduction in transportation vehicle weight and the consequent fuel savings through size and weight reduction of driveline systems, such as transmission and axles.
- Develop a durable, reliable high power density (HPD) driveline system that is smaller and lighter than current systems.

Approach

- Conduct analysis of planetary gear systems to establish materials, surface finishes, and lubricants that meet tribological performance requirements for a specific gearbox size reduction.
- Develop, integrate, and evaluate appropriate materials, surface finishes, and lubricants to reduce wear, scuffing, and contact fatigue of gears and bearings.

Major Accomplishments

- Completed preliminary analysis of the contact kinematics for specific size reduction in a simple planetary gearbox.
- Assessed the effect of new contact kinematics in terms of Hertzian contact stresses, surface velocities of meshing gear teeth on wear, and scuffing and contact fatigue lives.

Future Activities

- Develop bench-top test methodologies to evaluate wear, scuffing, and contact fatigue lives of new materials, surface finishes, and lubricants for HPD drivelines.
- Evaluate the baseline wear, scuffing, and contact fatigue performance of current materials, surface finishes, and lubricants.
- Develop new materials, surface finishes, and lubricants and evaluate their ability to meet new requirements for HPD drivelines.
- In collaboration with transportation vehicle OEM and/or suppliers, optimize the design for a smaller and lighter HPD gearbox.

VIII.F.2. Technical Discussion

Introduction

One of the main goals, perhaps the ultimate goal, of the U.S. Department of Energy's Vehicle Technologies Program (DOE-VTP) is the dramatic reduction of the amount of petroleum oil used in transportation vehicles. This would reduce the nation's dependence on foreign oil, thereby enabling greater energy independence and homeland security. In addition, consumption of

less oil in vehicles would reduce environment-degrading emissions, such as greenhouse gases and particulates. Such emissions have been associated with climate change and detrimental effects on human health.

Significant fuel savings can be achieved in all classes of transportation vehicle through weight reduction. Numerous analyses have shown that 2-5% reduction in fuel consumption is possible by a 10% reduction in automobile weight. Table 1 shows such a calculation for three classes of vehicles based on the new European drive cycle (NEX) for both gasoline- and diesel-fueled internal combustion engines (ICEV-G and ICEV-D). Consequently, all vehicle OEMs are adapting vehicle weight reduction as a prime approach to reduce fuel consumption.

Table 1. Calculated fuel saving in different classes of automotive vehicles

	NEDC ICEV-G	NEDC ICEV-D
Compact Class	-2.6 %	-3.5 %
Mid-Size Class	-1.9 %	-2.7 %
SUV	-2.4 %	-2.6 %

Weight reduction must be accomplished without sacrificing safety, reliability, and durability for a vehicle to gain public acceptance and market share. Figure 1 shows the weight distribution for a typical automobile, highlighting the systems and components that present an opportunity for weight reduction. The DOE-VTP currently has programs and projects devoted to weight reduction in vehicle structures and engines (light-weight materials). The driveline system constitutes about 20% of a vehicle's weight, making it an excellent target for weight reduction. One route to reducing the size and weight of the driveline system without sacrificing performance, nor compromising reliability and durability, is by increasing its power density.

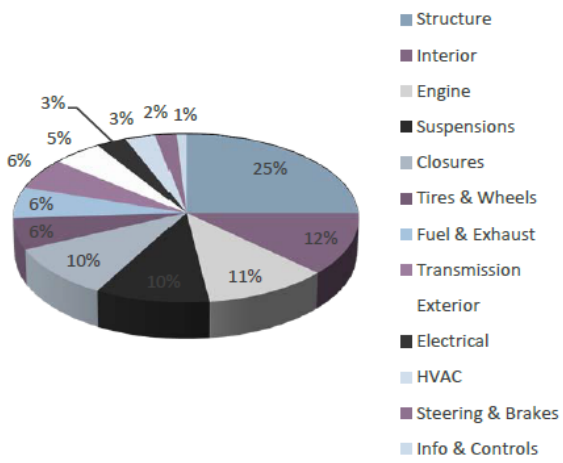

Figure 1. Typical vehicle weight distribution.

The ultimate objective of this project is the development of a smaller, lighter, and more efficient driveline system for transportation vehicles by increasing the power density without sacrificing reliability and durability. Such a system will result in significant vehicle weight reduction and concomitant increase in fuel savings. Furthermore, an HPD driveline may enable the downsizing of the powertrain system, resulting in further improvement in fuel savings.

Approach

Vehicle driveline systems such as transmission and axles consist of planetary gear systems and bearings to form a gearbox, as exemplified in Figure 2. Development of HPD gears and bearing would enable a size and weight reduction of the gearbox. Size reduction of the gears and bearings would increase the contact severity of the gear teeth and bearings, leading to reduction in wear, scuffing, and contact fatigue lives. To mitigate the tribologically induced reliability and durability issues expected in an HPD gearbox, materials, surface finishes, and lubricants have to be developed and integrated into the system – the focus of the present project.

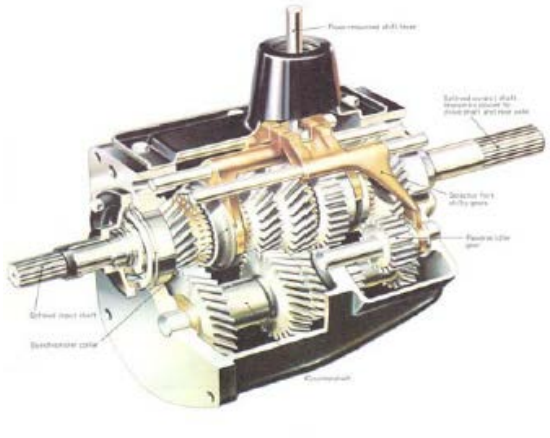

Figure 2. Example of an automotive transmission gearbox.

To begin, we are conducting gear contact kinematic analyses for different size reductions to establish material, surface finish, and lubricant requirements in terms of wear scuffing and contact fatigue lives. Performance evaluation/testing methodologies are being developed to determine wear, scuffing, and contact fatigue life. The test methodologies will be used to evaluate state-of-the-art and newly developed materials, surface finishes, and lubricants for the gearbox. Then, select materials, surface finishes, and lubricants will be integrated to create a high-fidelity HPD gearbox system. Finally, in collaboration with OEM partners, design optimization and implementation of the new integrated technologies will be undertaken to build and evaluate a prototype HPD gearbox for transportation vehicles.

Results and Discussions

Gearbox contact kinematics analysis and calculation are very complicated. Transportation vehicle gearbox designers normally use proprietary are often expensive software for that purpose. However, simplified analytical gear contact equations can be used to assess the effect of size reduction on gear contact kinematics, assuming there is no other design change or modification.

During FY 2011, efforts on this project were devoted to gear contact kinematics analyses for a simple planetary gear system, as shown in Figure 3. The size of the gear system was assumed to be reduced by 5, 10, 15, … 50% without reduction in the power transmission. Gear tooth bending stress, Hertzian contact stress, and surface velocities (rolling and sliding) were calculated for meshing gear teeth at the different percent reductions in gear size. Results of this simple preliminary calculation showed that decreased gear size substantially increases the severity of contact at gear meshing teeth. The Hertzian contact increase was about 5.2% to 30% for 5% and 25% size reduction, respectively.

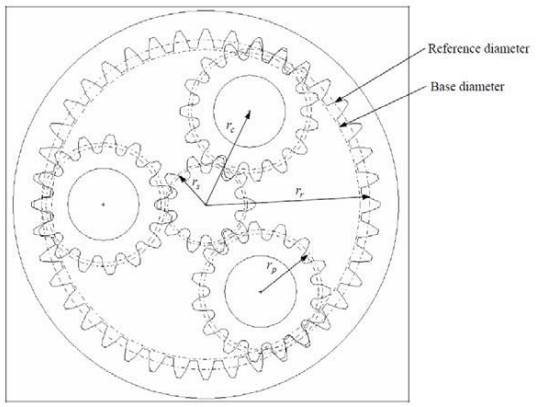

(a)

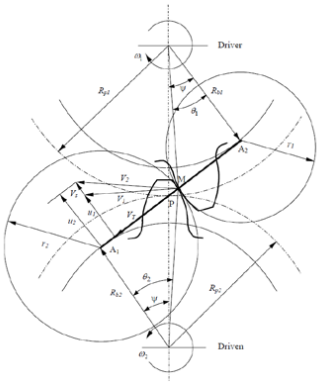

(b)

Figure 3. Schematics of (a) planetary gear system and (b) contact of gear teeth meshing

We used the following relationships to determine the impact of the severity of contact increase on wear, scuffing, and contact fatigue life for the 5% to 50% size reduction. For a Hertzian contact stress (S_H), the scuffing resistance (life) is estimated by the contact severity index (CSI), defined as

CSI = μ S_H.S, where μ is the friction coefficient, and S is the surface sliding velocity. The wear life

can be estimated from the Archard wear rate (W) model,

$$W = (K. S_H. S)/ H$$

where K is the wear factor, S is sliding velocity, and H is hardness. Finally, the change in contact fatigue life (CF) at two Hertzian contact stresses, S_{H1} and S_{H2}, can be estimated as

$$CF = (S_{H1}/S_{H2})^{6.67}$$

On the basis of these analyses, the percent reduction in scuffing, wear, and fatigue lives for the different reductions in gear size is given in Table 2. The data clearly show that substantial enhancements of scuffing, wear, and especially contact fatigue lives are required to achieve significant reduction in gearbox size. Design changes and optimization may reduce the tribological performance requirements.

Table 2. Reduction in scuffing, wear, and contact fatigue life for various levels of gear size reduction.

Size reduction (%)	Scuffing life reduction (%)	Contact fatigue life reduction (%)	Wear life reduction (%)
5	5.2	28.9	5.2
10	11.1	50.4	11.1
15	17.6	66.1	17.6
20	25.0	77.4	25.0
25	33.3	85.3	33.3
30	42.9	90.7	42.9
35	53.8	94.3	53.8
40	66.7	96.7	66.7
45	81.8	98.1	81.8
50	100	99.0	100

Conclusions

Significant fuel savings can be achieved in all transportation vehicle platforms through weight reduction brought about by size reduction of the gearbox in a HPD driveline system. Initial gearbox contact kinematics analyses showed that gearbox size reduction will significantly increase gear teeth contact severity in terms of Hertzian stress. Analyses also showed that this increase in contact severity is expected to lead to substantial reduction in reliability and durability from significant reduction in wear, scuffing, and contact fatigue life. There is thus a critical need for the development and integration of materials, surface finishes, and lubricants to produce a reliable HPD driveline system for transportation vehicles.

VIII.F.3. Products

Publications

1. A. Greco, O. Ajayi, and R. Erck, “Micro-Scale Surface Texture Design for Improved Scuffing Resistance in Gear Applications,” Proc. 11th International Power Transmission and Gear Conference, Aug. 2011, Washington, DC.

VIII.G. Wireless PEV Charging Development/Demonstration

Principal Investigator: John M. Miller
Oak Ridge National Laboratory,
National Transportation Research Center
2360 Cherahala Blvd.
Knoxville, TN 37932-1563
(865)946 1469; millerjm@ornl.gov

DOE Program Manager: Lee Slezak

VIII.G.1. Abstract

Wireless charging has the potential to eclipse plug and cable methods because it is a safe, convenient and flexible way to transfer large amounts of power to electric vehicles in both stationary and eventually, on-road dynamic situations. Wireless charging technology for stationary applications has significant potential and is being pursued vigorously by industry as the most convenient and autonomous means to replenish PEV energy storage packs. Wireless charging is now seen by DOE and many in the automotive field as the enabling technology if wide spread implementation of electric vehicles is to occur. Convenience and ease of use are seen as the technology advance that will facilitate broader acceptance of battery or plug in vehicles. Wireless power transfer (WPT) from a utility connection to the energy storage system on a plug-in or battery electric vehicle is commercially feasible only if the efficiency of power delivery across this cascade of charger components is >90%. Current wireless power transfer systems operating at high power typically have efficiencies in the high 70% to high 80% range. The ORNL wireless concept has achieved efficiencies in the low 90% range in our laboratory experimental system. A summary of ORNL's development and demonstration activities are given in this report.

Objective

- Develop full analytical, computational and experimental understanding of the physics of wireless power charging of PEV's so that implementation designs will meet industry requirements for efficiency, safety, cost, and vehicle packaging criteria.
- Develop wireless power transfer stationary charging sufficiently for integration into a demonstration vehicle.

Approach

- The WPT program incorporates the findings of ORNL's earlier seed LDRD project and advances that laboratory design to vehicle concept readiness in terms of suitable package, compliance with international standards for emissions, and push for industry interoperability standardization.
- ORNL's work on WPT will follow the recommendations of the SAE J2954 Wireless Charging Task Force in general, and will focus on topics of interoperability, coupling coil compatibility, alignment tolerance and positioning control, and DOT recommended wireless communications.
- Technically, the program will be guided by theory and analysis, validated through laboratory experiment, with an end goal of a stationary WPT charging system that:
  - Minimizes additional complexity to the target vehicle,
  - Maximizes the utility of the grid-tied power converter by placing the major burden of regulation in this common location,

- Initially relies on a modified on-board-charger (OBC) at SAE Level 2 for both final regulation and interface to the vehicle on-board energy storage system,
- Incorporates DOT recommended V2I communications in the form of dedicated short range communications (DSRC) protocol to close the loop on grid-side power converter regulation.

Major Accomplishments

- ORNL's "evanescent wave" LDRD experimental hardware was used to show the flexibility of WPT in accommodating arbitrary receiver side voltage levels (120Vdc, 240Vdc and moving to 270Vdc). This is a requirement for WPT in future vehicle applications because there is no standardized PEV battery pack voltage level.
- Initiated design modification specifications with an OBC supplier to provide a unit having mutually exclusive J1772 ac port (240Vac, 7kW) and a dc port (390 +/-15Vdc) as the WPT input.
- Completed accuracy tests on laboratory sensors needed for experimental and vehicle work.
- Completed investigation into electromagnetic performance of copper tube and printed circuit "ribbon" coupling coil conductors.
- Completed builds of alternative coupling coils and evaluated two designs on the WPT experimental apparatus (see photo below).
- Commenced procurement activities for coupling coil materials that will be utilized in early FY12 for the demo vehicle build.

Future Activities

- Optimize the coupling coil designs for industry acceptable vehicle packaging at SAE level 2 power.
- Fabricate and test suitably packaged transmit and receiver pads based on the optimized coupling coil designs (ferrite backplane, Litz conductor, aluminum shield plate).
- Evaluate the effects of concrete, asphalt, plastic and plywood on coupling coil transfer efficiency and system tuning. Issue: present WPT frequency limited to available 20kHz IGBT's.
- Bench validate the modified OBC for both ac and dc port power input over full output power load range. This will be done in the WPT laboratory using recently procured test equipment.
- Obtain suitable DSRC communications hardware and validate interface to OBC CAN port and to the grid-tied converter control port. Set-up and validate on WPT laboratory bench.
- Fabricate a power converter suitable to deliver SAE level 2 power of 7kW via the WPT coupling coils to the OBC for 6.6kW to a battery load. Perform laboratory validation using newly constructed 15kW light tree. All DSP control board programming will be accomplished in-house.
- Validate the full WPT system performance on the bench in the WPT laboratory with DSRC feedback of mock-up vehicle battery (laboratory battery eliminator) then integrate into demo vehicle.

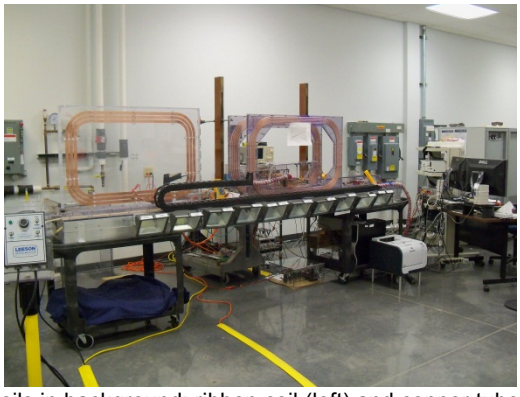

Transmit coils in background: ribbon coil (left) and copper tube coil (right)
WPT Laboratory Apparatus with 3.3kW lamp load in foreground

VIII.G.2. Technical Discussion

Background

WPT development for stationary charging initially relied on the laboratory apparatus constructed during the seed LDRD funded work shown in Figure 1. The experimental hardware consisted of a borrowed power inverter, copper tube coupling coils and a DSP regulated lamp load.

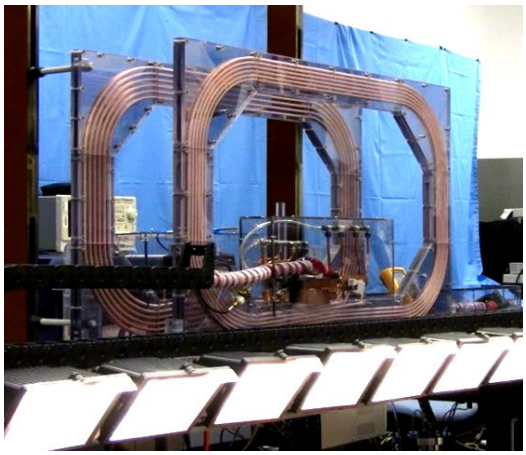

Figure 1. WPT coupling coil and lamp load

A notable outcome of the experimental hardware was validation of coupling coefficient, k, and alignment tolerance. Figure 2 depicts the coupling coefficient variation with coil spacing, or transmit pad to vehicle receiver coil gap and its variation with misalignment. Figure 3 summarizes the experimental results showing the transfer power as a function of longitudinal position of the receiver coil relative to the transmit coil (background in Figure 1).

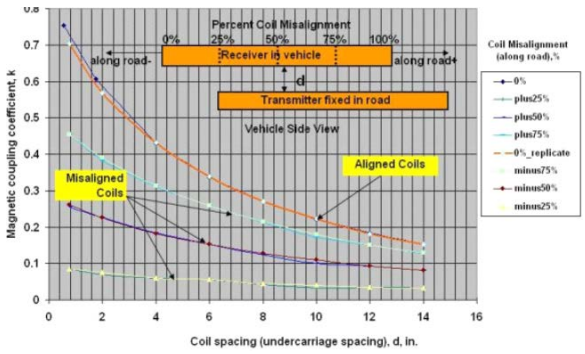

Figure 2. WPT coupling coefficient and sensitivity to misalignment of coils all versus spacing/gap

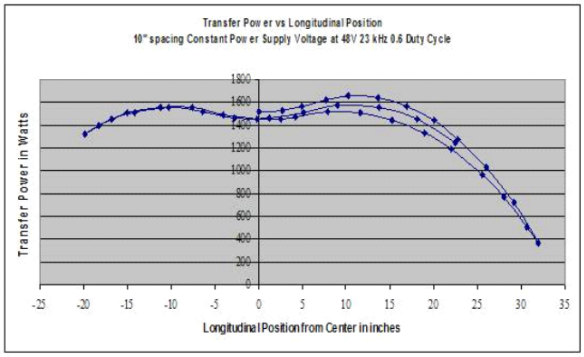

Figure 3. WPT transfer power as function of longitudinal misalignment

Experimental results obtained from the large format, air core, coupling coil work provided assurance that substantial power could be transferred across gaps ranging from 150mm to 250mm. This spacing range is sufficient for passenger vehicle stationary charging and has been explored in detail over the course of the past year

Introduction

During the closing months of FY11 a laboratory area in L101 of the NTRC was dedicated to WPT work (Figure 1). This lab space has available 240Vac for level 2 charger work, a 480Vac, 3 phase supply for power equipment and separate 600Vdc up to 300A regulated supply all located on the wall to the right of the 2 coil WPT demonstration rig shown in Figure 1. Stationary WPT charging work and vehicle integration will proceed in this laboratory space since it also has a large overhead door access from the parking lot.

A schematic for the experimental WPT hardware is shown in Figure 4. A laboratory power supply provides dc power to the high frequency power converter's dc link with voltage measurement V_{dc_link}.

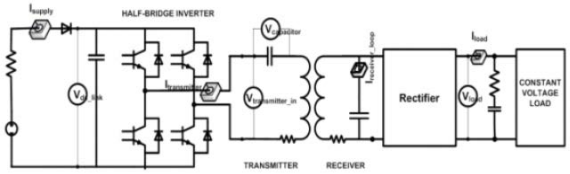

Figure 4. WPT circuit schematic showing IBGT based power converter, coupling coils, rectifier and load

The essentials of WPT operation are briefly explained here as an introduction to the topic and will be elaborated on later, and in depth, in a dedicated tutorial on the topic. The 2 phase leg power converter (H-bridge) receives gating signals to diagonal IGBT switch pairs according to the desired duty cycle, d, so that a quasi-square wave of voltage is impressed on the primary coupling coil. The transmit and receiver (capture) coil pair are series-parallel (S-P) tuned with capacitor values selected for a resonance frequency of approximately 24kHz. A half wave-rectifier was used in early work for economy and efficiency followed by a filter bank that mimics a vehicle battery. Lastly, and not shown in the figure, is a DSP and IGBT steering switches that select a lamp load and PWM each in turn depending on power level. The PWM control action effectively regulates the dc output voltage. In a vehicle application only the receiver coil, rectifier and small filter will be integrated on-board. Control and regulation will be done by the grid-tied power converter using messaging obtained from the vehicle battery management system (BMS). Functionally, and as shown in Figure 5, the high frequency power converter supplies a quasi-square excitation source to the coupling coils and the induced current is rectified and provided to the filter.

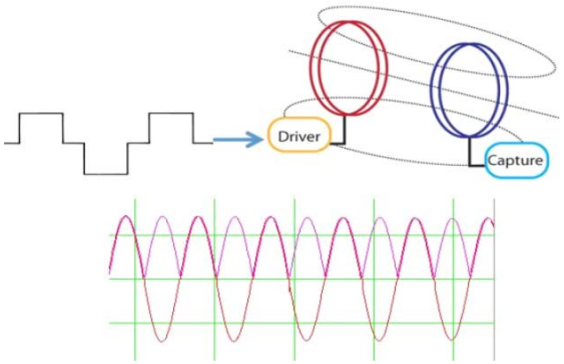

Figure 5. Functional representation of WPT

A small filter will be sufficient to smoothen the high frequency current pulsations shown graphically in Figure 5. Note, that for approximately 25kHz operating frequency that the current pulsations will be at 50kHz and readily filtered using metalized film capacitors.

Approach

Project technical approach selected is based on analytical understanding followed by modeling, simulation and laboratory experimentation. Models are validated through experiment. For WPT this means viewing the full system from the primary and analytically reflecting the secondary into the primary for evaluation. This is most directly done by starting with a WPT having only a load resistance connected across the tuned secondary or capture coil. In this case, the general impedance at the secondary appears in the primary as a coupled element where the coupling is realized via the wide gap resonant transformer mutual inductance, M. At arbitrary angular frequency, ω, the input impedance of this resulting network is:

——— — (1)

To illustrate this fundamental approach more clearly, Figure 4 is recast in modeling format to show all the essential elements and then reduced to a functional equivalent of (1).

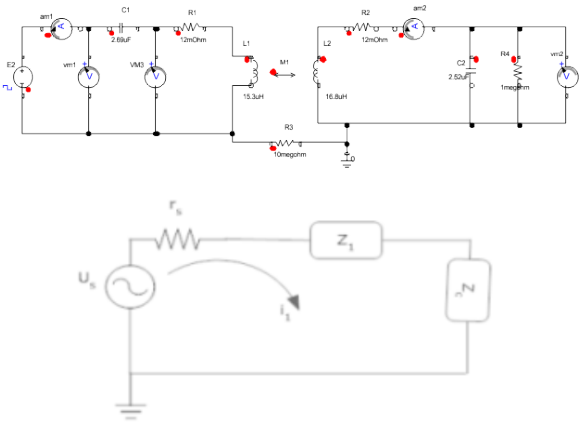

Figure 6. Model and primary referenced representation of WPT

It can be shown that the WPT primary current, I_1, will bifurcate in response to the mutual coupling and applied load variation. For control purposes this means the optimal operating frequency is dependent on spacing between the transmit and receiver coils (k and M influence) and on reflected battery charging load via $R_L=U_{bat}/I_{chg}$. Define the secondary side time constant of this load resistance and secondary

tuning capacitance, C_2, as τ_L. The load portion of the secondary impedance can therefore be represented as Z_L having real and imaginary parts as given by (2):

(2)

(3)

Using (3) in (1) and solving for the coupled impedance, Z_C, and reducing results (1) at the onset of bifurcation when $Im\{Z_{in}\}=0$. The primary current to the WPT is then given by (4) for this transitional case.

(4)

The trend can be shown more clearly from frequency response function (FRF) simulation of the laboratory experimental hardware. Note the onset of bifurcation with the low frequency peak just beginning to emerge near 23kHz.

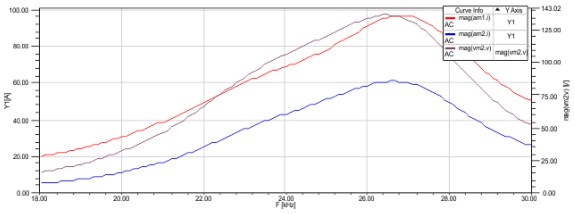

Figure 7. FRF of experimental WPT at limit of single frequency peak

Note that input current peaks at approximately 27kHz when U_s=30Vrms, k=0.236 and R_L=7Ohm. This is consistent with (4) for the parameters given. When the load resistance is changed to R_L=100Ohm, the input current response is distinctly bifurcated with one peak at f_{01}=22.1kHz and a second, higher peak at f_{02}=28.2kHz. Note that the tuning elements set the WPT resonant frequency to 24.8kHz primary and 24.4kHz secondary, when unloaded.

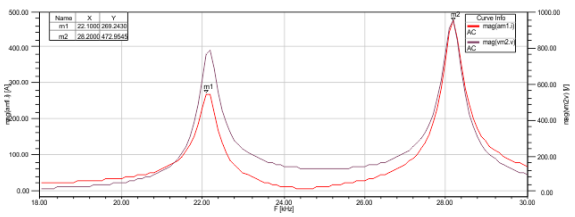

Figure 8. FRF of experimental WPT showing bifurcated response with output power of 4.59kW at the second peak

The experimental hardware is not loaded with only a resistor, but a diode rectifier and filter combination. The next section presents results found under transient simulation and for experimental testing.

Results

Experimental hardware is closely modeled using the schematic shown in Figure 9 and by application of the frequency selected for WPT laboratory demonstrations, f=21kHz (because these are 20kHz rated IGBT's it was necessary to restrict higher frequency operation).

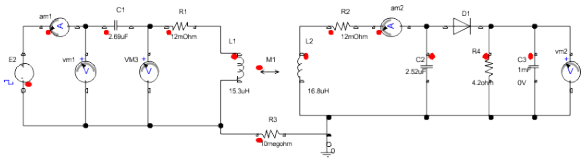

Figure 9. Simulation circuit that corresponds to the laboratory set-up with half-wave rectifier and filter

In Figure 10 the output voltage is specified as $120V_{dc}$ and this is being held with approximately $0.95V_{pk\text{-}pk}$ ripple (dark center trace). The characteristics box states that I_l=125.3A_{rms}, U_L= 119.45V_{dc} average and output power is 3.43kW represented by all the experiment lamps being illuminated (i.e., R_L=4.2 Ohm).

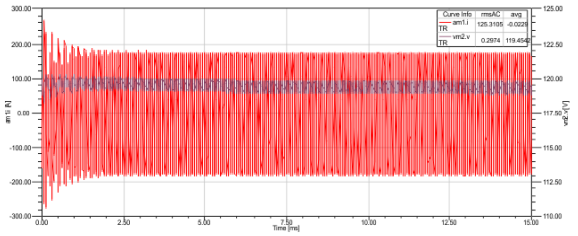

Figure 10. Transient response of half-wave rectifier design, P_0=3.43kW at $120V_{dc}$ and U_s=$125V_{rms}$ f=21kHz

Figure 11 illustrates operation above resonance (near 2nd peak shown in Figure 8) which requires only 20% of the driving voltage for the same output power.

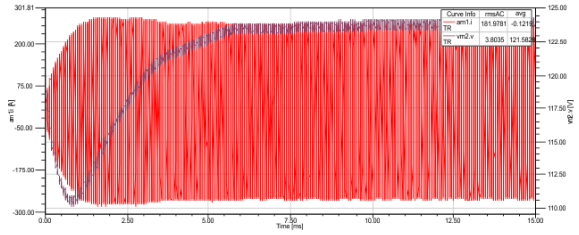

Figure 11. Transient response of half-wave rectifier design, P_0=3.43kW at 120V_{dc} and U_s=25V_{rms} when f=26.2kHz

The experimental results corresponding to Figure 10 are summarized in the tables below for both the copper tube and the ribbon coils. Note that the copper tube coil (4 each 0.25" diameter tubes in parallel,) have a cross sectional copper area of 63.892mm^2 whereas the single ribbon coil has a copper cross sectional area of 62.58mm^2, a ratio of 1.02, or the copper content is within 2% of being identical in both designs. At the test frequency of 21kHz and 145A_{rms} the ac resistance of the copper tube coil is 12.26mΩ and that of the ribbon coil is 11.9mΩ, 4.6 times the dc resistance of 2.58mΩ.

Table 1. WPT experimental data taken with 2 transmit coils connected in series with d=60% and f=21kHz

Utility input power				Transmit coil			Load side		
	U_{dc}	I_{dc}	P_{dc}	I_{ac}	P	S	U_L	I_L	P_o
Unit	V_{dc}	A_{dc}	kW	A_{rms}	kW	kVA	V	A	kW
Tube	232.4	24.8	5.76	149.4	4.03	24.5	120.8	25.9	3.14
Flat	231.6	26.2	6.06	142	4.28	22	120	28.7	3.44

The data summarized in Table 1 shows this to be a relatively inefficient operating point. For example, the efficiency from the power inverter output to the load bank is only 80% and from the utility input to the load bank its only 60%. Refer to Figures 8 and 10 and note that the location of the 21 kHz operating point on the FRF plot is well to the left of the lower frequency peak response and from the transient response plot it's clear that excessive power inverter drive is required to deliver the output power. This shows up in Table 1 as the high apparent power, S, and the reason the inverter has low efficiency. Operation at the higher frequency response peak would require only 20% of the power inverter drive effort to deliver the same power, and this would be at much higher efficiency.

Follow on work will focus on procurement of higher frequency IGBT's for the power inverter. During 2011 International Rectifier announced the development of "warp" IGBT's capable of high current switching up to 200kHz. The WPT project will work with the Advanced Power Electronics and Electric Machines group packaging laboratory to fabricate high frequency power modules if packaged IGBT's cannot be obtained.

Conclusions

Work to date has established a firm foundation in the fundamentals of WPT operation from both analytical and experimental investigations. Primary activity has focused on coupling coil electromagnetic performance, magnetic field strength, emissions levels and closest approach boundary for compliance with international standards. Coupling coils constructed of copper tube and flat designs were compared in experimental test with the finding that both exhibited comparable efficiency with ac resistance of each being within 2%. The more fundamental finding, based on analytical work, was that current technology IGBT's are limiting the operation to sub-optimal conditions.

VIII.G.3. Products

Currently, there are no products as a result of this program work.

Publications

1. John M. Miller, *Wireless Power Transmission*, ORNL Power Electronics Industry Symposium, ORNL Conference Center, 22 July 2011
2. John M. Miller, "*Demonstration of Electric Vehicle Dynamic on-Road Wireless Power Charging*," LDRD presentation, ORNL Conference Center, 20 June 2011
3. John M. Miller, *Wireless Charging Project*, Electrical & Electronics Technical Team, USCAR Office, Southfield, MI, 26 May 2011
4. John M. Miller, *Wireless Plug-in Electric Vehicle (PEV) Charging*, DOE Annual

Merit Review, project ID#VSS061 oral, 10 May 2011

5. Matthew Scudiere, John McKeever, John M. Miller, "*Wireless Power Transfer for Electric Vehicles*," SAE World Congress, paper #2011-01-0354, Cobo Center, Detroit, MI, 11 April 2011

Patents

6. John M. Miller, *Coupling Coil ac Resistance Minimization Using Graphene Coatings,* U.S. Patent Application 61/510,206, filed July 21, 2011.
7. John M. Miller, *Regulation Control and Energy Management Strategy for Wireless Power Transfer*, U.S. Patent Application 61/510,210, filed July 21, 2011.
8. John M. Miller and Perry Todd Jones, *WPT EVSE Installation and Validation Tool,* U.S. Patent Application 61/510,231, filed July 21, 2011.
9. John M. Miller, Cliff White, P.T. Jones, Paul Chambon, *Vehicle to Wireless Power Transfer Coupling Coil Alignment Sensor*, U.S. Patent Application disclosure #201102667 approved Aug. 17, 2011

Tools & Data

This project will benefit from the purchase of ANSYS Q3D software for more detailed analysis of coupling coil design and compatibility.

VIII.H. APPENDIX

LLNL-TR-464265

Aerodynamic Design Criteria for Class 8 Heavy Vehicles Trailer Base Devices to Attain Optimum Performance

K. Salari, J. Ortega

December 20, 2010

This work performed under the auspices of the U.S. Department of Energy by Lawrence Livermore National Laboratory under Contract DE-AC52-07NA27344.

Aerodynamic Design Criteria for Class 8 Heavy Vehicles Trailer Base Devices to Attain Optimum Performance

Kambiz Salari and Jason Ortega
salari1@llnl.gov
Lawrence Livermore National Laboratory, Livermore CA

Lawrence Livermore National Laboratory (LLNL) as part of its Department of Energy (DOE), Energy Efficiency and Renewable Energy (EERE), and Vehicle Technologies Program (VTP) effort has investigated class 8 tractor-trailer aerodynamics for many years. This effort has identified many drag producing flow structures around the heavy vehicles and also has designed and tested many new active and passive drag reduction techniques and concepts for significant on the road fuel economy improvements. As part of this effort a database of experimental, computational, and conceptual design for aerodynamic drag reduction devices has been established.

The objective of this report is to provide design guidance for trailer base devices to improve their aerodynamic performance. These devices are commonly referred to as boattails, base flaps, tail devices, and etc. The information provided here is based on past research and our most recent full-scale experimental investigations in collaboration with Navistar Inc. Additional supporting data from LLNL/Navistar wind tunnel, track test, and on the road test will be published soon.

The trailer base devices can be identified by 4 flat panels that are attached to the rear edges of the trailer base to form a closed cavity. These devices have been engineered in many different forms such as, inflatable and non-inflatable, 3 and 4-sided, closed and open cavity, and etc. The following is an in-depth discussion with some recommendations, based on existing data and current research activities, of changes that could be made to these devices to improve their aerodynamic performance.

There are 6 primary factors that could influence the aerodynamic performance of trailer base devices:

1. Deflection angle
2. Boattail length
3. Sealing of edges and corners
4. 3 versus 4-sided
   - Position of the 4th plate
5. Boattail vertical extension
   - Skirt – boattail transition
6. Closed versus open cavity

1. **Recommended deflection angle: 11-15 degrees, depending on the upstream flow quality**

   a. Many different researchers have found the following optimum deflection angles:

      i. Cooper (1985, 2003): 15 ±? degrees, 3-sided boattail, full and scale wind tunnel test and road test, not clear if this optimum angle was determined with other devices installed
      ii. Browand, et al. (2005): 13 ±? degrees, 3-sided boattail, full scale track test, no tractor roof fairing, no gap fairing, no trailer skirts
      iii. Grover & Visser (2006): 15 ±? degrees sides and top, 7 degrees bottom, full scale road test, no gap fairing, no trailer skirts
      iv. Schoon & Pan (2007): ~12.5 ±? degrees, 4-sided boattail, scale wind tunnel test
      v. LLNL/Navistar NASA NFAC Full Scale Test (2010): 11 ±2 degrees, full scale wind tunnel test, reduced tractor-trailer gap size, trailer skirts

   It should be noted that none of these studies have measured the impact of the boattail length upon the optimum deflection angle. Experiments should be conducted to obtain such a correlation. The observed variation in the angle can potentially be attributed to the upstream flow quality, which depends upon the aerodynamic treatment of the tractor, tractor-trailer gap, and trailer underbody. This effect was observed in the studies of DOE/LLNL/NASA/Storms, et al. (2006) and LLNL/Navistar NASA NFAC Full Scale Test (2010). In DOE/LLNL/NASA/Storms, et al. (2006), the optimum angle increased to 20 degrees which we speculate was due to both the GCM being a more aerodynamic tractor and also, the 12 foot pressure wind tunnel having a very clean flow.

   References

Cooper, K.R., The Effect of Front-Edge Rounding and Rear-Edge Shaping on the Aerodynamic Drag of Bluff Bodies in Ground Proximity, SAE Paper 850288, 1985.

Cooper, K.R., Truck Aerodynamics Reborn-Lessons from the Past, SAE Paper 2003-01-3376, 2003.

Browand, F., Radovich, C., Boivin, M., Fuel Savings by Means of Flaps Attached to the Base of a Trailer: Field Test Results, SAE Paper 2005-01-1016, 2005.

Grover, K. and Visser, K.D., Over-the-Road Tests of Sealed Aft Cavities on Tractor Trailers, SAE Paper 2006-01-3529, 2006.

Storms, B.L., et al., A Summary of the Experimental Results for a Generic Tractor-Trailer in the Ames Research Center 7- by 10-Foot and 12-Foot Wind Tunnels, NASA/TM-2006-213489, 2006.

Schoon, R., Pan, F.P., Practical Devices for Heavy Truck Aerodynamic Drag Reduction, SAE Paper 2007-01-1781, 2007.

2. **Recommended boattail length: 24"-32"**

In our recent research, we have not observed measureable improvement in performance when the boattail length is increased from 32" to 48". Cooper (2003) has tested shorter length boattails and found the optimum length to be about 24". Croll, et al. (1996) has shown that there is an aerodynamic benefit to extending the boattail length up to 96". However, due to DOT regulations and operational constraints, this long of a boattail is not recommended. In addition, the boattail performance can be impacted by the upstream flow quality, which depends upon the presence of gap devices and the tractor-trailer gap size, tractor aerodynamic treatments, and trailer underbody devices.

References

Cooper, K.R., Truck Aerodynamics Reborn-Lessons from the Past, SAE Paper 2003-01-3376, 2003.

Croll, R.H., et al., Experimental Investigation of the Ground Transportation System (GTS) Project for Heavy Vehicle Drag Reduction, SAE Paper 960907, 1996.

3. **Recommendation of sealing of edges and corners**

The aerodynamic performance of the boattail is dependent upon proper sealing of the corner edges of the vertical and horizontal plates. In addition, the edges of the boattail that join to the trailer must be sealed and not protrude out into the freestream flow.

4. **Recommendation on the number of boattail plates: 3 versus 4-sided boattail, position of the fourth plate**

We have inconclusive data from both the full-scale wind tunnel and track tests on the aerodynamic benefits of the fourth boattail plate. In the full-scale wind tunnel test, we observed a slight improvement in the boattail performance when the fourth plate was removed, but this change was within the experimental uncertainty. In the track test, removal of the fourth plate produced a change in the performance that was also within the experimental uncertainty. The same result was observed when the vertical position of the fourth plate was changed between two positions. In summary, the boattail performance was not sensitive to the presence of the fourth plate, which is in contrast to the findings of Cooper (2003), who showed that the fourth plate made a contribution to the overall performance of the boattail. We propose that additional research be conducted to address this question of the fourth boattail plate and its location. Hence, no recommendation can be made at the present time.

References

Cooper, K.R., Truck Aerodynamics Reborn-Lessons from the Past, SAE Paper 2003-01-3376, 2003.

5. Recommendation of the boattail vertical extension and the transition to the rear trailer skirt

Lanser, et al. (1991) and Cooper (2003) included rear trailer skirts in their wind tunnel study, but only Cooper explored the benefits of these skirts and their transition to the trailer boattail device and showed that they provided additional drag reduction. In our recent experiment, we observed improvements in drag reduction when the rear trailer skirts were installed and blended into the boattail. We propose that the rear trailer skirts be further investigated with a boattail that has vertical extensions.

References

Cooper, K.R., Truck Aerodynamics Reborn-Lessons from the Past, SAE Paper 2003-01-3376, 2003.

Lanser, W.R., Ross, J.C., Kaufman, A.E., Aerodynamic Performance of a Drag Reduction Device on a Full-Scale Tractor/Trailer, SAE Paper 912125, 1991.

6. **Recommendation of closed versus open cavity**

Based on low-Reynolds number experimental testing, the open cavity provides a benefit by positioning the trailer base at a distance from the large vortices that roll up from the edges of the boattail plates. This allows the low pressure region of the vortex core to be shifted away from the trailer base. However, at higher Reynolds number, the flow structures are much smaller and the same trend may not hold. Currently at full-scale Reynolds number, there is not enough conclusive data for heavy vehicle geometries to suggest whether there are benefits to opening or closing the trailer base cavity.

Recommendation for boattail application of drop-frame versus straight-frame trailer

A typical straight-frame trailer boattail device is designed to increase the pressure on the trailer base area and hence reduce the aerodynamic drag. For the drop-frame trailers this area is larger and the boattail side panels should be extended to cover this additional area. The aerodynamic benefit is apparent since the elevated pressure is now applied on a larger surface area which translates to enhanced drag reduction. Such a boattail device for a drop-frame trailer is shown here.

End of Aerodynamic Design Criteria for Class 8 Heavy Vehicles

Fuel economy improvement of class 8 heavy vehicles through aerodynamic drag reduction: a full-scale wind tunnel study

J. Ortega*, K. Salari†,

A. Brown‡, R. Schoon§

10/7/2011

Abstract

A wind tunnel investigation is conducted to evaluate the performance of both commercially-available and prototype drag reduction devices for modern class 8 heavy vehicles. Drag force measurements are made on three full-scale, heavy vehicle configurations at a nominal Reynolds number of 4.6×10^6 based upon the vehicle width. To compare the performance of the devices, the wind-averaged drag coefficient is calculated from the drag force data for a vehicle speed of 29.1 m/s (65 mph) and a crosswind of 3.1 m/s (7 mph). The wind-averaged drag coefficient is also used to estimate the fuel savings afforded by individual and combinations of devices. For the tractor-trailer gap, the most effective modification is found to be reducing the gap size from 1.1 m to 0.61 m. Numerous trailer skirts are installed on the three heavy vehicle configurations and the resulting change in the wind-averaged drag coefficient is shown to have a nominally linear dependence upon the change in the trailer skirt area, with the largest reductions in drag typically occurring for skirts with large surface area and low ground clearance. The trailer base drag is alleviated through the installation of boattail devices. For two prototype boattails, which have variable deflection angles, the optimum angle for reducing drag is found to be approximately 11° for both a straight-frame and a drop-frame trailer with a day-cab tractor. When used in combination, the devices often provide a reduction in drag that is greater than the individual contribution from each device, an effect which is especially evident when a trailer underbody fairing is used in conjunction with a boattail, trailer wheel fairings, and a tractor-trailer gap fairing. The largest reductions in drag arise when the devices are simultaneously installed in the tractor-trailer gap and on the trailer underbody and base. For the best cases of the three vehicle configurations, the wind-averaged drag coefficient and the resulting estimated fuel use decrease by 0.097 to 0.150 and approximately 10000 to 15000 L per 2.012×10^8 m of highway mileage driven, respectively.

1 Introduction

Combination heavy vehicles in the United States consume approximately 30 billion gallons of fuel each year [17]. By 2035, this number is expected to increase to approximately 40 billion gallons per year as a result of the continued growth of the highway transportation sector [1]. The majority of the shaft power derived from this fuel is used to overcome aerodynamic drag at highway speeds, while the remaining portion is dissipated through tire rolling resistance and drive train friction [5, 46].

These aerodynamic losses were first given considerable attention following the 1970's oil crisis. Prior to that time, heavy vehicles were primarily designed for functionality and ease of manufacturing and, therefore, little thought was given to aerodynamics, which resulted in box-shaped tractors and trailers. To improve the fuel economy of these vehicles, several conference workshops and numerous research programs and studies were conducted on heavy vehicle aerodynamics [5, 6, 8, 9, 10, 11, 12, 16, 21, 28, 29, 33, 36, 37, 38, 39, 47, 48, 50, 53, 56, 57, 58, 64]. Although the entire vehicle was investigated for various avenues of reducing drag, the primary focus of these efforts was the aerodynamics of the tractor and the front of the trailer. From wind tunnel, track, and road test data, it was shown that considerable reductions in aerodynamic drag could be achieved through tractor roof fairings, skirts, aerodynamic visors, rounding of the tractor and trailer front edges, and through the installation of trailer nose cones. Since these modifications did not significantly hamper the operational performance of the heavy vehicles, the trucking industry generally accepted them, which led to a definitive transition to the modern aerodynamic tractor and the rounded, front-corner trailer. These aerodynamic changes, along with improvements in tire, engine, and component designs, resulted in an increase in the fuel economy of heavy vehicles from 99000 L/2.012×10^8 m driven (4.8 mpg) in 1970 to 88000 L/2.012×10^8 m driven (5.4 mpg) in 2008, where 2.012×10^8 m (125000 mi) is a nominal distance traveled by a heavy vehicle each year [17]. For more thorough reviews of the early aerodynamic developments of heavy vehicles, the reader is directed to [13, 14, 38, 48, 49].

With the present day rise of fuel costs and the uncertainty of foreign oil supplies, there is a continued demand in the United States for increased fuel economy of heavy vehicles. Therefore, a number of the drag reduction devices and concepts that were not originally implemented in the design of modern day heavy vehicles have become potential candidates for further fuel economy improvements. Some of these second generation devices include boattails and trailer skirts, as well as tractor-trailer gap devices [2, 3, 7, 9, 12, 13, 14, 15, 22, 23, 31, 32, 35, 38, 42, 44, 45, 54, 55, 59, 60, 61, 62]. A number of studies, a sampling of which are shown in Tables 1-4, have either measured or estimated that these devices can produce fuel economy improvements when they are used both individually and in combination with one another. (It should be noted that the fuel savings data summarized in each of these tables are for various tractor-trailer geometries, Reynolds numbers, and drag reduction device designs.) From these studies, the average fuel savings of the gap, skirt, and boattail devices are about 3000, 5000, and 4000 L/2.012×10^8 m driven of highway mileage, respectively, while that of their combinations is on average approximately 12000 L/2.012×10^8 m driven of

highway mileage. Other research concepts that have been recently investigated include tractor and trailer base blowing systems [18, 19, 43], fluidic actuators [26, 41, 51, 52, 63] and trailer wheel and bogie fairings [15, 42, 55].

Despite the fuel economy benefits of these second generation devices, they have not been widely accepted by the trucking industry due to both operational issues and the nature of heavy vehicle manufacturing in the United States. Unlike the first generation devices, a number of the second generation devices are more susceptible to damage, restrict access to portions of the vehicle, or must be continually deployed and stowed during routine operations. For example, the trailer skirts reduce the ground clearance of the vehicle, causing them to scrape against the ground at railroad crossings and sunken loading docks. In addition, the skirts can limit access to the trailer underbody for tire and brake inspections. The gap devices, especially those constructed from aluminum sheet metal, are prone to damage during maneuvers that require the vehicle to articulate to extreme angles. Boattails are the least accepted of these devices since the trailer base upon which they are installed receives the most interaction during fleet operations. As a result, the boattail must be stowed before backing the trailer into the loading dock, thus requiring the driver or dock worker to manually perform this additional task. Some manufacturers attempt to circumvent this step by designing the boattail to self-retract when the vehicle comes to a stop. However, freezing and snowy conditions can potentially hamper this self-actuation motion. As a result of these many shortcomings, the majority of fleet operators have purposely decided not to adopt these devices in their current forms [30].

Clearly, there is a need to improve the design of second generation devices so that the trucking industry will welcome them and thereby benefit from the fuel economy gains that can be had through their implementation. This can only be accomplished through a coordinated effort of the trucking industry, aerodynamic researchers, and government regulators [13]. Therefore, we have formed a multi-disciplinary team comprised of trucking industry manufacturers (tractor, trailer, tire, and drag reduction devices), a commercial fleet, and a national laboratory. The ultimate goal of this team is to develop a trailer with factory-installed devices that are not only effective in reducing aerodynamic drag, but are also robust and operationally-minded.

The purpose of the present study is to take the first step towards accomplishing this goal by evaluating the performance of a number of drag reduction devices, the majority of which are currently on the market. A full-scale wind tunnel investigation is employed to measure the changes in the drag coefficient that arise from the installation of these devices and to obtain a better understanding of how different devices affect the performance of other devices installed simultaneously. The utility of this experimental approach is that it provides a controlled environment for investigating the devices under varying wind speeds and vehicle yaw angles, as well as eliminating any Reynolds number effects. In addition, the full-scale model obviously has all of the details of a modern heavy vehicle along with those specific to the various drag reduction devices. Similar full-scale wind tunnel studies of heavy vehicles and devices have been conducted in the past, though these were restricted to either a limited number of devices or to a shortened trailer with a high

tunnel blockage due to size restrictions of the wind tunnel test section [15, 31, 32]. Before discussing the wind tunnel setup, we first describe in the following section the theory of the wind-averaged drag coefficient, which is employed as a metric for comparing the performance of the various devices.

2 Wind-Averaged Drag Coefficient

When a vehicle is in motion, the body-axis drag coefficient is given by the expression, $C_A = D_A/(\frac{1}{2}\rho V_r^2 A)$, where D_A is the drag force in the direction along the axis of the vehicle, V_r is the wind speed relative the vehicle, ρ is the air density, and A is the vehicle cross-sectional area. While the information obtained from C_A at multiple yaw angles, ψ, is useful, it is somewhat cumbersome since this quantity does not summarize the performance of a drag reduction device into a single quantity that can be easily compared to that of other devices. In addition, the mean value of C_A over a range of yaw angles is insufficient since it does not account for the fact that crosswind velocities cause a vehicle traveling at a particular speed to experience certain yaw angles more than others. A quantity that resolves both of these issues is the wind-averaged drag coefficient, $C_{A_{wavg}}$, which is derived as follows [5, 8, 27].

Assume that a vehicle is traveling at a velocity V_t with respect to the roadway and there is a crosswind that has a velocity V_w at the mid-height of the vehicle acting at an angle ϕ with respect to V_t (Fig. 1). The total speed of the wind relative to the vehicle is given by

$$V_r = V_t\sqrt{1 + 2(V_w/V_t)\cos\phi + (V_w/V_t)^2} \tag{1}$$

and the yaw angle by

$$\tan(\psi) = \frac{(V_w/V_t)\sin\phi}{1 + (V_w/V_t)\cos\phi} \tag{2}$$

The wind-averaged drag force is found from

$$D_{A_{wavg}} = \int_0^{2\pi}\int_0^{V_{w_{max}}} D_A p(V_w,\phi)dV_w d\phi \tag{3}$$

$$D_{A_{wavg}} = \int_0^{2\pi}\int_0^{V_{w_{max}}} C_A(\psi)\frac{1}{2}\rho V_r^2 A \;\; p(V_w,\phi)dV_w d\phi \tag{4}$$

$$D_{A_{wavg}} = \int_0^{2\pi}\int_0^{V_{w_{max}}} C_A(\psi)\frac{1}{2}\rho V_t^2(1 + 2(V_w/V_t)\cos\phi + (V_w/V_t)^2)A \;\; p(V_w,\phi)dV_w d\phi \tag{5}$$

where $p(V_w,\phi)$ is the probability of a wind speed V_w blowing at an angle ϕ with respect to the vehicle and $V_{w_{max}}$ is the maximum wind speed. Dividing Eq. 5 by $\frac{1}{2}\rho V_t^2 A$ gives the wind-averaged drag coefficient. Assuming that the wind speed, V_w, is determined from a national average and that it has an equal probability of occurring in any direction, such that $p(V_w,\phi) = 1/2\pi$, and that the vehicle is symmetric about its longitudinal body axis, gives a wind-averaged drag coefficient of

$$C_{A_{wavg}} = \frac{1}{\pi}\int_0^{\pi} C_A(\psi)(1 + 2(V_w/V_t)\cos\phi + (V_w/V_t)^2)d\phi \tag{6}$$

Equation 6 can be numerically integrated from

$$C_{A_{wavg}} = \frac{1}{6}\sum_{j=1}^{6} M(j)C_A(\psi(j)) \tag{7}$$

where

$$M(j) = 1 + 2(V_w/V_t)\cos\phi(j) + (V_w/V_t)^2 \tag{8}$$

$$\phi(j) = \frac{\pi}{6}j - \frac{\pi}{12} \tag{9}$$

$$\psi(j) = \tan^{-1}\frac{(V_w/V_t)\sin\phi(j)}{1 + (V_w/V_t)\cos\phi(j)} \tag{10}$$

The power needed to overcome this aerodynamic drag force is given by

$$P = \frac{D_{A_{wavg}}V_t}{\eta} = \frac{\frac{1}{2}\rho V_t^2 A C_{A_{wavg}} V_t}{\eta} \tag{11}$$

where η is the driveline efficiency of the heavy vehicle. The amount of fuel, μ, used by the engine to produce this power can be estimated from

$$\mu = \frac{\gamma}{V_t}P = \frac{\gamma}{V_t}\frac{\frac{1}{2}\rho V_t^2 A C_{A_{wavg}} V_t}{\eta} \tag{12}$$

$$\mu = \frac{\gamma}{\eta}\frac{1}{2}\rho V_t^2 A C_{A_{wavg}} \tag{13}$$

where γ is the specific fuel consumption rate of the engine. The change in fuel usage due to the installation of a drag reduction device is thus given by

$$\Delta\mu = \frac{\gamma}{\eta}\frac{1}{2}\rho V_t^2 A \Delta C_{A_{wavg}} \tag{14}$$

where $\Delta C_{A_{wavg}}$ is the corresponding reduction in the wind-averaged drag coefficient.

3 Wind Tunnel Setup

The body-axis drag coefficient data is acquired by making drag force measurements on three full-scale tractor-trailer vehicles: a 2008 Navistar ProStar long sleeper (LS) tractor with a Wabash 16.2 m straight-frame (SF), dry freight trailer; a 2008 Navistar ProStar day-cab (DC) tractor with the SF trailer; and the DC tractor with a Kentucky Trailer 16.2 m drop-frame (DF), dry freight trailer (Fig. 2a-c). These vehicles have overall lengths ranging from 20 to 22 m and cross-sectional areas of 10.5 m^2, 10.5 m^2, and 10.6 m^2, respectively. The gap between the tractor and trailer is set to 1.1 m for each baseline vehicle configuration and the trailer bogie on the SF trailer is positioned such that the midpoint between the trailer wheels is 3.7 m from the trailer base. The measurements are made within the NASA Ames 80×120 wind tunnel, which has a contraction ratio of 5:1 and a test section cross-section of 24.4 m × 36.6 m. Aside from a few select runs at speeds as low as 8.9 m/s (20 mph) and as high as 35.8 m/s (80 mph), the nominal tunnel speed is set to $U_\infty = 25.9$ m/s (58 mph, dynamic pressure of 420 Pa) with a free-stream turbulence intensity of $\approx 1\%$ [67]. The resulting Reynolds number, $Re_w = U_\infty w/\nu$, based upon the trailer width, $w = 2.6$ m, is 4.6×10^6, where ν is the kinematic viscosity of air. Although this tunnel speed is slightly less than the typical highway speed in the United States (29.1 m/s or 65 mph), a series of runs at various tunnel speeds shows that the wind-averaged drag coefficient is relatively independent of Reynolds number by $Re_w = 4.6 \times 10^6$ (Fig. 2d). The front of each tractor is positioned approximately one vehicle length downstream of the test section inlet. From the measurements of Zell [67], the boundary layer displacement thickness is 0.11 m approximately 1.1 m and 3.0 m upstream of the LS and DC tractors, respectively, within the empty tunnel. When the vehicles are yawed about the z-axis to the maximum extent of 15° relative to the free-stream velocity, the blockage within the test section is only $\approx 3\%$ and, therefore, no blockage corrections are applied to the drag measurements.

The heavy vehicle is supported by a system similar to that of Cooper & Leuschen [15] and Leuschen & Cooper [32], which permits the vehicle to partially rest upon the tunnel and turntable floor, while still transmitting the drag force to the balance (Fig. 2c). This is accomplished by placing aluminum plates beneath the tractor steering wheels and trailer wheels and resting these wheels upon air bearings, which receive a continuous air supply from the wind tunnel facility. When the air bearings are inflated, the bottom of the tires is about 0.15 m above the tunnel floor, placing them at the approximate height of the boundary layer displacement thickness at the front of the vehicle. The tractor drive wheels are chocked and strapped to a steel plate that is fixed to the balance. The low friction coefficient provided by the air bearings thus makes it possible to transmit not only the drag force, but also the side force and the yawing moment to the balance through the tractor drive wheels. Since the steering wheels of the LS tractor extend beyond the edge of the turntable onto the tunnel floor, the aluminum plate beneath these wheels must be large enough to allow the air bearings to remain on the plate as the vehicle is yawed. For the shorter DC tractor, the steering wheels remain on turntable and, as a result, much smaller aluminum plates are employed beneath these wheels.

The same approach is used for the trailer wheels that are located on the turntable. Although the tractor and trailer remain rigid relative to one another through the use of turnbuckles and chains, flexure of the entire vehicle does occur relative to the steel plate supporting the tractor wheels as a result of the compliant the tractor tires. Depending on the location of the center of pressure on the vehicle, rotation about the steel plate can alter the vehicle yaw angle by as much as 1°. To account for this non-negligible amount of rotation, a photo-electric proximity sensor (SICK DT 10-P10B5 accurate to ±0.006 m) and optical target are placed on the aluminum trailer wheel plate and trailer wheel air bearing, respectively. Using the proximity sensor and turntable yaw angle data, the actual yaw angle of the vehicle is then calculated.

The external balance system used to measure the drag force has a range of $\pm 2.224 \times 10^5$ N with an accuracy of ±53 N over this entire range. However, only a small fraction (≈2%) of this range is utilized for the vehicle drag. To determine the balance accuracy over this much smaller range, check loads are applied to the installed vehicle by hanging known weights on a pulley system with a load cell (Dillon ED Xtreme, 11120 N capacity) accurate to within ±2.2 N. The resulting drag force measurement accuracy is found to be ±44N, which is the same as that of a previous heavy vehicle study using this same balance [31]. Thus for the present study, we take the drag force accuracy of the balance to be ±44 N. Due to the fact that the vehicles span both the metric and non-metric portions of the balance system through the air bearings, it is also necessary to assess the drag force measurement error incurred by this aspect of the setup. This is accomplished by recording the drag force on the vehicle when it is rotated through a yaw sweep during a wind-off condition. For a perfectly rigid vehicle, balance system, air bearings, and tunnel floor and for completely frictionless air bearings, the resulting drag force should equal zero for all yaw angles. However, the results of this exercise demonstrate drag force errors of ±58 N, ±19 N, and ±23 N for the LS/SF, DC/SF, and DC/DF configurations, respectively. Note that the LS/SF configuration has the largest error as a result of the steering wheel air bearings having to sweep across the surface of the aluminum plate, while those of the DC/SF and DC/DF configurations remain stationary relative to the smaller aluminum plates beneath the steering wheels.

During each experimental run, the vehicle is yawed on the turntable through a range of angles to simulate varying cross-winds from which the wind-averaged drag coefficient can be calculated. For the majority of the runs, the yaw sweep ranges from -9° to +9° in 3° increments with an accuracy of ±0.1°, though for a select number of runs, data is acquired from -15° to +15° in 3° increments. Once the vehicle is at a desired yaw angle, the balance shaker and a shaker (Vibco Inc., SCR-1000) installed on the tractor chassis are activated for several seconds in order to settle both the balance and the air bearings beneath the vehicle wheels. Three data points are collected at 1024 Hz for 10 seconds per data point, which corresponds to about 12 to 13 vehicle length flow passes per data point for $U_o = 25.9$ m/s. The wind-averaged drag coefficient is obtained by first averaging the measured $C_A(\psi)$ data at each value of $\pm\psi$ and then linearly interpolating this data to $\psi(\phi(j))$. The values of $C_{A_{wavg}}$ are calculated using $V_t = 29.1$ m/s (65 mph) and $V_w = 3.1$ m/s (7 mph),

where 3.1 m/s is the national-average wind speed in the United States at 2.1 m above the ground [5], and the resulting savings in the estimated fuel usage (Eq. 14) using $\rho = 1.23$ kg/m^3, $\eta = 0.85$, and $\gamma = 7.639 \times 10^{-8}$ L/W·s [5, 8, 9, 32]. Performing an uncertainty analysis [20] that takes into account the accuracy of the measurement systems, the drag force errors due to the air bearing setup, and the repeatability of the force measurements shows that the resulting errors in $C_{A_{wavg}}$ are ± 0.006, ± 0.005, and ± 0.004 for the LS/SF, DC/SF, and DC/DF configurations, respectively. The 10 second sample time is shown to be adequate since increasing it to 20 seconds produces a change in the computed wind-averaged drag coefficient that is smaller than the measurement error. In addition, the effects of flow hysteresis are shown to be negligible on $C_{A_{wavg}}$ when the direction of the yaw sweep is reversed. Since the steel plate and supporting hardware immediately beneath the tractor drive wheels protrude approximately 0.1 m into the boundary layer flow above the tunnel floor, they contribute an additional drag force to the balance system during a wind-on condition, resulting in a larger value of $C_{A_{wavg}}$. Measurements made without a vehicle installed on the balance reveal that this force is on the order of 160 N. Due to the non-linear interactions of the boundary layer flow between the vehicle underside and the steel plate and supporting hardware, this force is not necessarily the same when the vehicle is installed on the balance and therefore it cannot simply be subtracted from the measured drag force. It is assumed that this force does not change significantly as drag reduction devices are installed since the devices typically reside rather far from the steel plate and supporting hardware. Therefore, no attempt is made to correct for this additional force in the present study.

Using this experimental procedure, the drag reduction characteristics are evaluated for devices that are installed in the tractor-trailer gap, trailer underbody, and trailer base. The three gap fairings (GP1, GP2, GP3), which attach to the front of the trailer, are comprised of curved plastic or aluminum plates that increase the radii of curvature of the front edge of the trailer sides and top (Figs. 2c, 3a-c). Other modifications to the tractor-trailer gap include reducing the distance between the back of the tractor to the front of the trailer from 1.1 m to 0.61 m (0.61m_gap), installing revised side extenders (REV_SE) that flare slightly outboard in order to accommodate the smaller tractor-trailer gap on the LS tractor, and filling the gap between the DC side extenders and the trailer front with aluminum sheets (full_SE)(Fig. 3d). The devices installed on the trailer underbody are various trailer skirts (SK#), a prototype fairing (UBF1), and trailer wheel fairings (TWF1), the last of which are qualitatively similar to those in [5] (Figs. 4-5). For one trailer skirt design (SK5), adjustments are made to both the trailer skirt area and the angle of the skirt relative to the trailer side (Fig. 4e-g). Lastly, four boattails are installed on the trailer bases of various vehicle configurations (Fig. 6). While the boattails BT1 and BT2 have fixed angles, θ, relative to the trailer, boattails BT3 and BT4 are designed to have variable deflection angles on the top and side boattail plates in order to determine an optimum angle setting. Since the plates used in the construction of these boattails are not perfectly flat, the measurement of the deflection angle is accurate to within only $\pm 2°$.

4 Results

To establish a baseline for assessing the drag reduction performance of the various add-on devices, the body-axis drag coefficient, C_A, is first measured for vehicle configurations in which no devices are installed. The resulting drag curves for the three baseline configurations (DC/SF, DC/DF, LS/SF) with a 1.1 m tractor-trailer gap exhibit the behavior typical of that for heavy vehicles, wherein C_A increases with increasing ψ (Fig. 7a), as seen in [5, 8, 9, 12, 13, 14, 15, 33, 34, 37, 38, 39, 40, 60] and others. This increase in C_A is due to several phenomena that occur as the vehicle is yawed, such as flow entrainment into the tractor-trailer gap, exposure of the trailer bogie to the free-stream flow, production of large, stream-wise vortices on the top and leeward side of the vehicle, and flow separation from the leeward side of the vehicle [5, 24, 25, 34, 37, 59, 60, 66]. The DC/SF vehicle is the least aerodynamic of these configurations due to a combination of the steeper angle of the roof aero-shield and the exposed trailer bogie on the straight-frame trailer. However, pairing the DC tractor with the DF trailer significantly reduces the trailer underbody flow, producing a vehicle that has the least aerodynamic drag of the three baseline configurations.

The drag reduction devices are installed on these baseline configurations both individually and in combination with other devices or vehicle modifications. An example of this is the installation of trailer skirts (SK1) and a boattail (BT2) to the LS/SF configuration with a reduced tractor-trailer gap size of 0.61 m and revised tractor side extenders (Fig. 7b). The combination the reduced gap size and revised side extenders result in a nearly constant offset from the baseline drag curve, while both the trailer skirts and boattail exhibit larger reductions at larger yaw angles. When applied individually, the reduced gap size/revised side extenders, trailer skirts, and boattail decrease $C_{A_{wavg}}$ by 0.016, 0.062, and 0.056, respectively. However, when these modifications are applied in combination, the net reduction in $C_{A_{wavg}}$ is measured to be 0.142, which is slightly greater than the sum (0.134) of their individual contributions (Fig. 7c). This effect is likely due to the fact that the reduced tractor-trailer gap size and trailer skirts decrease the amount of flow separation arising from the tractor-trailer gap and trailer underbody, respectively, resulting in a thinner boundary layer on the surface of the trailer. When this thinner boundary layer approaches the boattail, the flow carries additional momentum near the surface of the trailer and is therefore better able to remain attached to the angled boattail plates, thereby producing more positive trailer base pressres. A similar observation is made by Cooper [13], who measured an increase in the performance of a boattail when it is placed downstream of a more aerodynamic forebody. The enhanced performance of a combination of devices is even more pronounced when the underbody fairing and trailer wheel fairings (UBF1 + TWF1), boattail (BT1), and gap fairing (GP1) are installed on the LS/SF configuration. In this case, the sum of the individual wind-averaged drag reductions of the devices is 0.067, whereas their combined reduction is 0.098. The majority of this non-linear behavior is due to a favorable interaction between the boattail and the trailer underbody fairing and trailer wheel fairings (Fig. 7c).

The incremental reductions in both $C_{A_{wavg}}$ and the estimated fuel usage are plotted in Figs. 8-10 for

the individual gap, trailer underbody, and trailer base devices. Note that the estimated fuel savings in these figures are *only for highway mileage traveled* since the associated wind-averaged drag coefficient would change at slower vehicle speeds. To identify the two vehicle configurations, c_0 and c_1, that are being compared in the calculation of $\Delta C_{A_{wavg}}$ in these figures, we define the following plotting notation, where c_0 and c_1 are the configurations before and after the installation of the device in question, respectively. Each of the symbols in Figs. 8-10 is divided into four quadrants representing the tractor-trailer gap (upper-left quadrant), trailer base (upper-right quadrant), trailer underbody that is upstream of the trailer bogie (lower-left quadrant), and trailer underbody that is downstream of the trailer bogie (lower-right quadrant). If one or more devices or modifications are present on the c_0 vehicle, one or more of the corresponding quadrants are shaded solid. The quadrant location of the device that is being installed and assessed is identified with hatch marks. For example in Fig. 8, consider the top-most circle symbol (107, bsln) in the GP1 column, corresponding to the installation of the GP1 device on the DC/SF configuration. In this case, there is no solid shading in any of the quadrants, indicating that the c_0 configuration is a baseline configuration with a 1.1 m tractor-trailer gap. The hatch marks in the upper-left quadrant denote the fact that the c_1 vehicle now has the GP1 device installed in the tractor-trailer gap. The corresponding value of $\Delta C_{A_{wavg}}$ (-0.013) is therefore the difference in drag between the c_1 vehicle (DC/SF with the GP1 device) and the c_0 vehicle (DC/SF with no devices) due to the effect of the GP1 device only. The annotation "107, bsln" next to the circle symbol indicates the run numbers of the c_1 and c_0 configurations, respectively. A table listing the specific devices and vehicle configurations for each of these run numbers is provided in each figure.

The reductions in $C_{A_{wavg}}$ and the estimated fuel usage for the gap devices and modifications are plotted in Fig. 8. The best performing gap device/modification occurs when the tractor-trailer gap of the baseline DC/SF configuration is decreased from 1.1 m to 0.61 m. This leads to a reduction in $C_{A_{wavg}}$ of 0.021 and an estimated fuel savings of about 2100 L/2.012×10^8 m hwy, which is comparable to the scaled wind tunnel results of Cooper [11] for a reduced tractor-trailer gap size (see Table 1). Performing the same modification to the LS/SF configuration (93, bsln) along with the installation of the revised side extenders yields a smaller (0.016) reduction in $C_{A_{wavg}}$, which is likely due to the fact that the more streamlined LS/SF has less cross-stream flow to begin with in the tractor-trailer gap than that of the DC/SF.

Figure 9 shows a plot of the reductions in $C_{A_{wavg}}$ and the estimated fuel usage as a function of the incremental skirt area, ΔA_{skirt}, for the various trailer skirt devices. Although the plot contains data from the three different vehicle configurations (DC/SF, DC/DF, LS/SF), the collective values of $\Delta C_{A_{wavg}}$ all increase in a nominally linear fashion with ΔA_{skirt}. Cooper [13], Cooper & Leuschen [15], and Schoon & Pan [55] also measure an increase in $-\Delta C_{A_{wavg}}$ with increasing skirt area, though the increase in area is accomplished by independently increasing either the skirt height or length. A linear curve fit to the data in Fig. 9 yields the expression

$$-\Delta C_{A_{wavg}} = 9.31 \times 10^{-3} \Delta A_{skirt} - 8.39 \times 10^{-3} \quad (15)$$

where A_{skirt} is in the units of m^2.

In addition, a number of noteworthy trends can be identified from the plot in Fig. 9. First, it is evident that while the baseline DC/DF configuration has a reduced ground clearance due to the drop-deck design of the trailer (0.65 m from the ground to the trailer underside compared to 1.1 m for the SF trailer), the installation of skirts (134, 136) both upstream (SK8) and downstream (TWSK3) of the bogie nevertheless leads to a reduction in $C_{A_{wavg}}$ (-0.024) and the estimated fuel usage (-2400 L/2.012×10^8 m hwy). Next, although the trailer wheel skirts (TWSK1 + TWSK2—67, bsln) leave a sizeable portion of the underbody open on SF trailer, this skirt design reduces $C_{A_{wavg}}$ by an amount comparable to that of skirts that span nearly the entire distance between the trailer landing gear and wheels (SK5A—71, bsln; SK3—78, bsln). Such a design may provide the advantage of allowing easier access to the trailer underbody for the inspection of brakes and tires or for the storage of tire snow chains, while still producing an estimated fuel savings of about 3500 L/2.012×10^8 m hwy. The series of runs for the SK5A (71, bsln), SK5B (72, bsln), SK5C_0.4m (73, bsln), and SK5C_0.2m (74, bsln) skirts identify the changes in $-\Delta C_{A_{wavg}}$ that result when a single trailer skirt is sequentially modified by first extending its height from 0.9 m (71, bsln) to 1.0 m (72, bsln), then increasing the upstream area of the skirt by 1.0 m^2 (73, bsln), and finally reducing the distance from the front edge of the skirt to the trailer side from 0.4 to 0.2 m (74, bsln). Each of these changes yields an improvement in the skirt performance, though the largest incremental changes in $-\Delta C_{A_{wavg}}$ during this sequence correspond to the first and third modifications. Applying this final skirt design (SK5C_0.2m) to the DC/SF configuration (105, bsln) yields an even larger value of $-\Delta C_{A_{wavg}}$, highlighting the sensitivity of skirt performance to the tractor geometry. The resulting reductions in both $C_{A_{wavg}}$ (-0.076) and the estimated fuel usage (-7500 L/2.012×10 m hwy) for this configuration (105, bsln) are the largest of any individual device evaluated in the present study. In addition, this estimated fuel savings is slightly larger than the average value (≈5000 L/2.012×10^8 m hwy) of the previously tested skirts shown in Table 2. Lastly, it is interesting to note that even though the trailer skirt SK2 has a value of A_{skirt} nearly equal to that of skirt SK5C_0.2m (6.8 m^2 versus 6.9 m^2), the SK2 skirt yields a significantly smaller reduction in $C_{A_{wavg}}$ when a performance comparison is made on the DC/SF configuration (105, bsln versus 119, bsln). The primary differences between these two skirts is that the SK5C_0.2m skirt is angled relative to the trailer side and has a height of 1.0 m, while the SK2 skirt is parallel to the trailer side and has a height of 0.8 m. This once again demonstrates that slight variations in design can yield substantial changes to the skirt performance, which in this case lead to a difference in the estimated fuel savings of approximately 3000 L/2.012×10^8 m hwy between the two skirts.

The values of -$\Delta C_{A_{wavg}}$ for three of the boattail devices are plotted as a function of the boattail angle, θ, in Fig. 10. As θ is increased from 0° to 20° on the BT4 boattail (DC/DF configuration), which has

plates on the top and sides of the trailer base, $-\Delta C_{A_{wavg}}$ increases to a maximum value before steadily decreasing. Fitting a second-order polynomial to the BT4 boattail data demonstrates that the maximum occurs at θ about equal to $11 \pm 2°$. This angle is comparable to a number of the optimum boattail angles found within previous studies, despite the differences in the Reynolds number, vehicle geometry, boattail length, or number of boattail plates [3, 12, 13, 22, 26, 42, 55]. The two other boattails, BT1 and BT2, have fixed angles of approximately 12° and 9°, respectively. A comparison of runs 84, bsln and runs 95, 94 shows the enhanced performance of the BT2 boattail when additional drag reduction devices or modifications are made upstream of the trailer base. A similar result is observed for the BT1 boattail (54, bsln or 80, bsln vs. 79, 78). By removing the bottom, horizontal boattail plate from this boattail, it is possible to assess the influence of the plate on the drag reduction performance of the BT1 boattail (54, bsln or 80, bsln vs. 81, bsln). This modification subsequently leads to a larger value of $-\Delta C_{A_{wavg}}$, though it should be noted that the change in $-\Delta C_{A_{wavg}}$ between the three and four-sided configurations is comparable to the measurement error. This possible trend is the opposite to that in the study of Cooper [13], who showed that a four-sided boattail yields a slightly larger reduction in the wind-averaged drag coefficient than a three-sided one. A variable-angle boattail, BT3, is also installed on the DC/SF configuration along with several other drag reduction devices (0.61m_gap + SK1 + TWSK1 + TWSK2) (Fig. 11). Since no measurements are made for this specific configuration less the BT3 boattail, the values of $-\Delta C_{A_{wavg}}$ are calculated relative to a baseline DC/SF configuration with a 1.1 m tractor-trailer gap. Most notably, the optimum boattail deflection angle is about equal to that shown previously for the BT4 boattail, in spite of the fact that the trailer geometry and boattail height differ. Combined with the contributions from the gap modification and the trailer skirt devices, the resulting optimum value of $-\Delta C_{A_{wavg}}$ is approximately 0.14, which is equivalent to a savings in the estimated fuel usage of nearly 14000 L/2.012×10^8 m hwy.

The changes in $-\Delta C_{A_{wavg}}$ for all of the drag reduction devices, installed either individually or in combination with other devices, are plotted in Figs. 12-14 relative to the corresponding baseline DC/SF, LS/SF, or DC/DF configurations, respectively. For the LS/SF configuration, the top performing individual devices are both trailer skirts (SK1—run 82; SK5C_0.2m—run74), each of which yields a value of $-\Delta C_{A_{wavg}}$ equal to 0.062 or an estimated fuel savings of approximately 6000 L/2.012×10^8 m hwy. The largest drag reduction ($-\Delta C_{A_{wavg}}$= 0.144) for the LS/SF configuration occurs for the simultaneous installation of the SK1 and TWSK1 skirts and the BT2 boattail along with a reduced tractor-trailer gap size of 0.61 m and the revised tractor side extenders. The resulting estimated fuel savings is approximately 14000 L/2.012×10^8 m hwy. An even larger reduction in drag ($-\Delta C_{A_{wavg}} = 0.150$) occurs when the same skirts and boattail are installed on the DC/SF configuration with a 0.61 m tractor-trailer gap, which is completely covered on both the driver and passenger sides. In this case, the estimated fuel savings is calculated to be nearly 15000 L/2.012×10^8 m hwy, which is the largest of the entire study and comparable to the scaled wind tunnel data of Cooper [13] for a similar combination of devices.

5 Discussion

While it is apparent that there is a great potential for fuel savings through the use of aerodynamic drag reduction devices, the commercial fleet operators responsible for purchasing them take into account a number of additional factors before they consider these devices to be a truly viable means for cost savings. Therefore, in addition to the wind tunnel investigation, we conducted a survey from August to September 2010 of 256 small and large fleet companies and owner/operater companies that operate class 8 heavy vehicles in the United States (we define a small fleet as one in which there are at most 25 tractor-trailers and a large fleet as one in which there are more than 26 tractor-trailers). A number of questions are asked of these fleets to better understand their past experiences with drag reduction devices, to determine the criteria and requirements the devices would have to meet in order to have them installed throughout the majority of their fleets, and to further improve the design of the devices. The feedback from this survey along with device performance data will be essential as we move towards our goal of designing a trailer with factory-installed devices that are both effective in reducing aerodynamic drag and acceptable by the fleet operators who purchase them.

From the results of the survey, only 5% of the companies are currently using tractor-trailer gap devices and trailer base devices, while 4% are using trailer skirts. However, 2-7% of the companies are planning to use these various devices in their operations and another 27-30% would consider using them within the next 12 months to increase their fleet fuel economy and reduce fuel costs. Most notably, the majority of the companies currently using drag reduction devices observe an increase in vehicle fuel economy comparable to that which was expected when the devices were purchased. Additional benefits that result from the installation of these devices are reported to be improved vehicle handling under windy conditions and a reduction in the amount of debris and water spray ejected by the vehicle, the latter of which is similar to the findings of Weir, *et al.* [66].

In spite of these benefits, a number of shortcomings and challenges are identified with the current drag reduction devices on the market. The purchase price is found to be the primary barrier that prevents the adoption of these devices. About half of the companies are willing to spend only $1000 or less on aerodynamic devices for each tractor-trailer combination, while 29% will spend only $500 or less. At the time of this survey, the former cost requirement prevents all of the commercially available trailer skirts and base devices evaluated in the 80×120 wind tunnel from being viable options for nearly half of the companies surveyed. In addition, the payback time for the devices is required to be 1 to 2 years for about half of the companies and 3 years for another third of the companies. Second, the durability of the devices is another shortcoming that must be met given that two-thirds of the companies expect to spend only 5 hours or less per trailer each year for aerodynamic device maintenance. And it is a lack of device durability, increased maintenance costs, vehicle downtime, and a lack of device service stations for long-haul fleets that have often caused a number of companies to discontinue the use of certain devices. Third, since a number of

fleets operate their vehicles up to a maximum load capacity, the weight of the devices can also prohibit the fleets from employing them. In fact, about one-half of the surveyed companies are willing to add only 68 kg (149 lb) or less to their vehicles. Except for the gap devices, this requirement eliminates nearly all of the commercially available trailer skirt and base devices evaluated in this study. Lastly, the design of the device and its manner of deployment presents a challenge to the fleets from both operational and cost standpoints. More than two-thirds of the companies prefer that the aerodynamic devices deploy in a fully automatic fashion in order to eliminate driver errors and to decrease the possibility of accidents or injuries. However, the convenience of automatic deployment comes with additional device complexity, which reduces reliability and increases the purchase price and maintenance time of the device. For about one-quarter of the companies, this disadvantage is too costly and they would rather have their drivers manually deploy devices that are simpler in construction and much easier to repair.

These concerns and issues must first be addressed before aerodynamic drag reduction devices can be accepted on a widespread basis throughout the United States. Both mass production of devices and government tax breaks for fleets utilizing them can reduce the purchase price barrier, making the devices affordable for a greater number of companies. To provide device maintenance for long-haul trailers that are traveling cross-country, nationwide service centers that presently repair tires or tractors can be trained and equipped to also repair aerodynamic devices. Furthermore, improved designs can minimize the weight penalty of the devices and increase their durability. An example of the latter can be seen in the evolution of trailer skirts, which originally had designs that were often constructed from aluminum sheet metal. While aluminum is corrosion resistant and lightweight, it is unforgiving when flexed beyond a certain point. To remedy this shortcoming, a number of trailer skirt manufacturers have started to use deformable, plastic panels that are attached to the trailer underside in a manner that allows the skirt to flex without permanent deformation when it contacts the ground.

The question of whether or not the devices should be manually or automatically deployed remains to be answered. Perhaps, one solution is to integrate the device completely into the trailer design, such that deployment is not even necessary. An example of this is seen in the work of Schoon [54], wherein a prototype trailer is designed with an integrated boattail shape along the last 0.61 m of the trailer. With the boattail constructed in a structural manner similar to that of a standard trailer, it is robust enough to withstand operational mishaps, such as accidental backing into a loading dock. The aerodynamic drag due to the tractor-trailer gap can also be reduced with an automated fifth-wheel that is integrated into the tractor. At highway speeds, where vehicle maneuvering is minimal, the fifth-wheel would automatically decrease the distance between the tractor and trailer, while, below a certain speed, the fifth wheel would increase this distance to allow for pivotal motion between the tractor and trailer. Such a system would require no driver intervention, though it would need to be designed for both safe and reliable operation without significantly increasing the cost of the tractor.

6 Conclusions

Through this experimental study, we have investigated the performance of drag reduction devices for modern class 8 heavy vehicles. Wind tunnel measurements are made on three full-scale heavy vehicle configurations, which are comprised of a long sleeper tractor with a straight-frame trailer, a day-cab tractor with a straight-frame trailer, and a day-cab tractor with a drop-frame trailer. The devices are installed in the tractor-trailer gap and trailer underbody and base in order to alleviate the drag sources arising from these portions of the vehicle. While the gap fairings provide a reduction in the vehicle drag, the most effective gap modification for the two straight-frame trailer configurations is found to be a reduced tractor-trailer gap size of 0.61 m. For these two cases, the wind-averaged drag coefficient is reduced by 0.016 and 0.021, yielding an estimated fuel savings of about 1600 and 2100 L/2.012$\times 10^8$ m of highway mileage driven. Larger reductions in drag are achieved through the installation of a boattail on the trailer base. For the two fixed angle boattails, the wind-averaged drag coefficient is reduced by 0.047 to 0.056 when the boattails are installed without any other devices. The corresponding fuel savings is about 4600 to 5500 L/2.012$\times 10^8$ m of highway mileage driven. The boattail performance is enhanced when drag reduction devices are installed upstream of the trailer base. The largest reduction in drag for a single device arises from one of the trailer skirts, which yields a decrease in the wind-averaged drag coefficient and the estimated fuel use of 0.076 and about 7500 L/2.012$\times 10^8$ m of highway mileage driven, respectively, for the day-cab tractor with a straight-frame trailer. When the devices are simultaneously installed on the tractor-trailer gap and trailer underbody and base, the drag reduction is even greater, resulting in estimated fuel savings of about 15000, 14000, and 10000 L/2.012$\times 10^8$ m of highway mileage driven for the day-cab tractor with the straight-frame trailer, the long sleeper tractor with the straight-frame trailer, and the day-cab tractor with the drop-frame trailer, respectively.

While this study has successfully highlighted the aerodynamic performance of a wide range of drag reduction devices, there are two important matters that remain to be determined at the present time. The first is the actual fuel savings provided by these devices during normal operations. Since the data from this study has been acquired in a very controlled environment, *it may not be entirely representative of the flow fields that heavy vehicles encounter when travelling on the road.* For example, the wind tunnel does not produce the freestream unsteadiness and turbulent length scales that arise from an environmental flow and its interactions with roadside objects and nearby vehicles. In addition, the non-moving ground plane beneath the vehicle produces a thick boundary layer that may underestimate the performance of the trailer underbody devices. As has been observed in previous studies, these types of effects can lead to differences between the estimated fuel savings from wind tunnel data and that actually observed on the road [4, 5, 6, 16, 29, 50, 65]. To remedy this potential shortcoming, future studies will include fuel economy data from both track testing and subsequent fleet evaluations of select devices. The second matter that remains to be determined is properly addressing the concerns raised by fleets regarding the drag reduction devices. From the results of

the fleet survey, it is clearly evident that a number of the devices evaluated within this study are simply unacceptable to the fleets due to numerous economic, weight, and durability issues. As we move forward on this project, we will work closely with our fleet and third-party device manufacturer team members to develop robust, operationally-minded, and cost-effective solutions to these concerns. This process will provide a definitive path to implementing the drag reduction devices into future trailers, thereby providing viable options for fleets seeking to improve the fuel economy of their heavy vehicle operations.

7 Acknowledgments

The authors would like to thank M. Betzina, C. Hartley, S. Lee, J. Sacco, and the entire National Full-Scale Aerodynamics Complex team for their support during the wind tunnel testing, J. Martinez and R. Flach of Texas A&M University for their wind tunnel testing guidance and expertise, S. Baker, B. Hirschy, A. Spieth, and V. Swager of Navistar for their mechanic support, E. Buckholtz, J. King, and S. LaMunyon of LLNL for their support in device fabrication, the device manufacturers for loaning their gap fairings, trailer skirts, and boattails, and F. Browand of the University of Southern California and P. Urbanczyk of LLNL for their helpful feedback in the manuscript preparation. Lastly, the authors would like to thank Lee Slezak of the Department of Energy Office of Heavy Vehicle Technologies for his programmatic support of this research effort. This work was performed under the auspices of the US DOE by LLNL under contract DE-AC52-07NA27344. LLNL-JRNL-473454-DRAFT.

References

[1] *Annual Energy Outlook 2010 with Projections to 2035*, DOE/EIA-0383(2010), 2010.

[2] Bachman, L.J., Erb, A., Bynum, C.L., Effect of single wide tires and trailer aerodynamics on fuel economy and NOx emissions of class 8 line-haul tractor-trailers, SAE Paper 05CV-45, 2005.

[3] Browand, F., Radovich, C., Boivin, M., Fuel savings by means of flaps attached to the base of a trailer: field test results, SAE Paper 2005-01-1016, 2005.

[4] Buckley, F.T., Jr., Marks, C.H., Walston, W.H., Jr., Analysis of coast down data to assess aerodynamic drag reduction on full-scale tractor-trailer trucks in windy environments, *SAE Trans.*, **85**:2756-2769, 1976.

[5] Buckley, F.T., Jr., Marks, C.H., Walston, W.H., Jr., A study of aerodynamic methods for improving truck fuel economy, Final Report on National Science Foundation, Grant No. SIA-74-14843, Mechanical Engineering Department, University of Maryland, College Park, MD, 1978.

[6] Buckley, F.T., Jr., Walston, W.H., Jr., Marks, C.H., Fuel savings from truck aerodynamic drag reducers and correlation with wind-tunnel data, *J. Energy*, **2**(6):321-329, 1978.

[20] FIGLIOLA, R.S., BEASLEY, D.E., *Theory and Design for Mechanical Measurements*, 2nd Edition, John Wiley & Sons, Inc., New York, 1995.

[21] FLYNN, H., KYROPOULOS, P., Truck aerodynamics, SAE Paper 620531, 1962.

[22] GROVER, K., VISSER, K.D., Over-the-road tests of sealed aft cavities on tractor trailers, SAE Paper 2006-01-3529, 2006.

[23] GUTIERREZ, W.T., HASSAN, B., CROLL, R.H., RUTLEDGE, W.H., Aerodynamics overview of the ground transportation systems (GTS) project for heavy vehicle drag reduction, SAE Paper 960906, 1996.

[24] HAMMACHE, M., BROWAND, F., On the aerodynamics of tractor-trailers, in McCallen, R., Browand, F., Ross, J., Eds., *The Aerodynamics of Heavy Vehicles: Trucks, Buses, and Trains*, Lecture Notes in Applied and Computational Mechanics, **19**, Springer, Heidelberg, 185-205, 2004.

[25] HEINECK, J.T., WALKER, S.M., SATRAN, D., The measurement of wake and gap flows of the generic conventional truck model (GCM) using three-component PIV, in McCallen, R., Browand, F., Ross, J., Eds., *The Aerodynamics of Heavy Vehicles: Trucks, Buses, and Trains*, Lecture Notes in Applied and Computational Mechanics, **19**, Springer, Heidelberg,173-184, 2004.

[26] HSU, T.-Y., HAMMACHE, M., BROWAND, F., Base flaps and oscillatory perturbations to decrease base drag, *The Aerodynamics of Heavy Vehicles: Trucks, Buses, and Trains*, McCallen, R., Browand, F., Ross, J., Eds., Lecture Notes in Applied and Computational Mechanics, **19**, Springer, Heidelberg 303-316, 2004.

[27] INGRAM, K.C., The wind-averaged drag coefficient applied to heavy goods vehicles, Transportation and Road Research Laboratory, TRRL Supplementary Report 392, 1978.

[28] KELTON-FOGG, G., Aerodynamic Drag Reduction Devices in the Trucking Industry: A Market Study, SRI Project 7171, Contract NAS 2-9846, 1979.

[29] KETTINGER, J.N., Tractor-trailer fuel savings with an aerodynamic device–a comparison of wind tunnel and on-road tests, SAE Paper 820376, 1982.

[30] LAFLAMME, R., A fleet operator's perspective on commercial vehicle drag reduction, in McCallen, R.C., Browand, F., Ross, J., Eds., *The Aerodynamics of Heavy Vehicles II: Trucks, Buses, and Trains*, Lecture Notes in Applied and Computational Mechanics, **41**, Springer, Heidelberg, 463, 2009.

[31] LANSER, W.R., ROSS, J.C., KAUFMAN, A.E., Aerodynamic performance of a drag reduction device on a full-scale tractor/trailer, SAE Paper 912125, 1991.

[32] LEUSCHEN, J., COOPER, K.R., Full-scale wind tunnel tests of production and prototype, second-generation aerodynamic drag-reducing devices for tractor-trailers, SAE Paper 06CV-222, 2006.

[33] LISSAMAN, P.B.S., Ed., *Reduction of the Aerodynamic Drag of Trucks*, Conference/Workshop Proceedings, California Institute of Technology, Pasadena, CA, October 10-11, 1974.

[34] MASON, W.T., BEEBE, P.S., The drag related flow field characteristics of trucks and buses, in Sovran, G., Morel, T., Mason, W.T., Jr., *Aerodynamic Drag Mechanisms of Bluff Bodies and Road Vehicles*, Plenum Press, 45-90, 1978.

[35] MCCALLEN, *et al.*, Aerodynamic drag of heavy vehicles (class 7–8): simulation and benchmarking, SAE Paper 2000-01-2209, 2000.

[36] MONTOYA, L.C., STEERS, L.L., Aerodynamic drag reduction tests on a full-scale tractor-trailer combination with several add-on devices, NASA TM X-56028, 1974.

[37] MUIRHEAD, V.U., An investigation of drag reduction for tractor trailer vehicles, NASA Contractor Report 144877, 1978.

[38] MUIRHEAD, V.U., SALTZMAN, E.J., Reduction of aerodynamic drag and fuel consumption for tractor-trailer Vehicles, *J. Energy*, **3**(5):279-284, 1979.

[39] MUIRHEAD, V.U., An investigation of drag reduction for tractor trailer vehicles with air deflector and boattail, NASA Contractor Report 163104, 1981.

[40] NAKAGUCHI, H., Recent Japanese research on three-dimensional bluff-body flows relevant to road-vehicle aerodynamics, in Sovran, G., Morel, T., Mason, W.T., Jr., *Aerodynamic Drag Mechanisms of Bluff Bodies and Road Vehicles*, Plenum Press, 227-246, 1978.

[41] NAYERI, C.N., *et al.*, Drag reduction on a generic tractor-trailer using active flow control in combination with solid flaps, in McCallen, R.C., Browand, F., Ross, J., Eds., *The Aerodynamics of Heavy Vehicles II: Trucks, Buses, and Trains*, Lecture Notes in Applied and Computational Mechanics, **41**, Springer, Heidelberg, 179-191, 2009.

[42] ORTEGA, J.M., SALARI, K., An experimental study of drag reduction devices for a trailer underbody and base, Paper AIAA-2004-2252, 2004.

[43] ORTEGA, J., SALARI, K., STORMS, B., Investigation of tractor base bleeding for heavy vehicle aerodynamic drag reduction, in McCallen, R.C., Browand, F., Ross, J., Eds., *The Aerodynamics of Heavy Vehicles II: Trucks, Buses, and Trains*, Lecture Notes in Applied and Computational Mechanics, **41**, Springer, Heidelberg, 161-178, 2009.

[44] PETERSON, R.L., Drag reduction obtained by the addition of a boattail to a box shaped vehicle, NASA Contractor Report 163113, 1981.

[45] RADOVICH, C.A., Wind tunnel test of cab extender incidence on heavy truck aerodynamics, SAE Paper 2005-01-3527, 2005.

[46] RITCHIE, D., Beat the built-in headwind, *Commercial Car Journal*, September, 1973.

[47] SALTZMAN, E.J., MEYER, R.R., JR., Drag reduction obtained by rounding vertical corners on a box-shaped vehicle, NASA TM X-56023, 1974.

[48] SALTZMAN, E.J., A summary of NASA Dryden's truck aerodynamic research, SAE Paper 821284, 1982.

[49] SALTZMAN, E.J., MEYER, R.R., JR., A Reassessment of heavy-duty truck aerodynamic design features and priorities, NASA/TP-1999-206574, 1999.

[50] SAUNDERS, J.W., WATKINS, S., HOFFMANN, P.H., BUCKLEY, F.T., JR., Comparison of on-road and wind-tunnel tests for tractor-trailer aerodynamic devices, and fuel savings predictions, SAE Paper 850286, 1985.

[51] SEIFERT, A., *et al.*, Large trucks drag reduction using active flow control, in McCallen, R.C., Browand, F., Ross, J., Eds., *The Aerodynamics of Heavy Vehicles II: Trucks, Buses, and Trains*, Lecture Notes in Applied and Computational Mechanics, **41**, Springer, Heidelberg, 115-133, 2009.

[52] SEIFERT, A., HORRELL, C., GROSSMANN, J., SMITH, A., Heavy Trucks Fuel Savings Using the SaOB Actuator (abstract), The Aerodynamics of Heavy Vehicles: Trucks, Buses, and Trains III, Potsdam, Germany, Septmeber 12-17, 2010.

[53] SERVAIS, R.A., BAUER, P.T., Aerodynamic devices can significantly reduce the fuel consumption of trucks: experience with CECA designs, SAE Paper 750707, 1975.

[54] SCHOON, R.E., On-road evaluation of devices to reduce heavy truck aerodynamic drag, SAE Paper 2007-01-4294, 2007.

[55] SCHOON, R., PAN, F.P., Practical devices for heavy truck aerodynamic drag reduction, SAE Paper 2007-01-1781, 2007.

[56] SOVRAN, G., MOREL, T., MASON, W.T., JR., *Aerodynamic Drag Mechanisms of Bluff Bodies and Road Vehicles*, Plenum Press, New York-London, 1978.

[57] STEERS, L.L., MONTOYA, L.C., SALTZMAN, E.J., Aerodynamic drag reduction tests on a full-scale tractor-trailer combination and a representative box-shaped ground vehicle, SAE Paper 750703, 1975.

[58] STEERS, L.L., SALTZMAN, E.J., Reduced truck fuel consumption through aerodynamic design, *J. Energy*, **1**(5):312-318, 1977.

[59] STORMS, B.L., ROSS, J.C., HEINECK, J.T., WALKER, S.M., DRIVER, D.M., ZILLIAC, G.G., An experimental study of the ground transportation system (GTS) model in the NASA Ames 7- by 10-ft wind tunnel, NASA/TM-2001-209621, 2001.

[60] STORMS, B.L., SATRAN, D.R., HEINECK, J.T., WALKER, S.M., A study of Reynolds number effects and drag-reduction concepts on a generic tractor-trailer, Paper AIAA-2004-2251, 2004.

[61] STORMS, B.L., SATRAN, D.R., HEINECK, J.T., WALKER, S.M., Detailed experimental results of drag-reduction concepts on a generic tractor-trailer, SAE Paper 2005-01-3525.

[62] SURCEL, M.-D., MICHAELSEN, J., PROVENCHER, Y., Track-test evaluation of aerodynamic drag reducing measures for class 8 tractor-trailers, SAE Paper 2008-01-2600, 2008.

[63] TAUBERT, L., WYGNANSKI, I., Preliminary experiments applying active flow control to a $1/24^{th}$ scale model of a semi-trailer truck, in McCallen, R.C., Browand, F., Ross, J., Eds., *The Aerodynamics of Heavy Vehicles II: Trucks, Buses, and Trains*, Lecture Notes in Applied and Computational Mechanics, **41**, Springer, Heidelberg, 105-113, 2009.

[64] WALSTON, W.H., JR., BUCKLEY, F.T., JR., MARKS, C.H., Test procedures for the evaluation of aerodynamic drag on full-scale vehicles in windy environments, SAE Paper 760106, 1976.

[65] WATKINS, S., COOPER, K.R., The unsteady wind environment of road vehicles, part two: effects on vehicle development and simulation of turbulence, SAE Paper 2007-01-1237, 2007.

[66] WEIR, D.H., STRANGE, J.F., HEFFLEY, R.K., Reduction of adverse aerodynamic effects of large trucks, Federal Highway Administration Report FHWA-RD-79-84, 1978.

[67] ZELL, P.T., Performance and test section flow characteristics of the National Full-Scale Aerodynamics Complex 80- by 120-foot wind tunnel, NASA TM 103920, 1993.

Investigators	Ref. #	Test method	Fuel savings ($L/2.012 \times 10^8$ m hwy)	Remarks
Cooper	[9]	SWT	3978	Full GS
Cooper	[11]	SWT	2253	Reduced gap (1.5 m to 1.0 m)
Cooper	[11]	SWT	3219	GS
Cooper	[11]	SWT	5151	Filled gap, sides & top
Cooper	[11]	SWT	3863	SE
Cooper	[13]	SWT	2556	Full GS
Cooper, *et al.*	[15]	SWT	2082	0.25 m SE
Cooper, *et al.*	[15]	SWT	3029	0.51 m SE
Cooper, *et al.*	[15]	SWT	3644	0.76 m SE
Cooper, *et al.*	[15]	SWT	2130	0.53 m "vortex stabilizer"
Cooper, *et al.*	[15]	SWT	2272	0.64 m "vortex stabilizer"
Cooper, *et al.*	[15]	SWT	2556	1.1 m GS
Cooper, *et al.*	[15]	FSWT	5679	"Vortex stabilizer"
Cooper, *et al.*	[15]	FSWT	7335	SE
Leuschen, *et al.*	[32]	FSWT	1258	Trailer nose fairing, 8.5 m trailer
Leuschen, *et al.*	[32]	FSWT	167	Labryrinthine plates, 8.5 m trailer

Table 1: Summary of highway fuel savings for tractor-trailer gap devices. FSWT–full scale wind tunnel test, GS–gap seal, SE–tractor side extenders, SWT–scale wind tunnel test. Note: some studies refer to the gap seal as a "vortex stabilizer," gap splitter plate, or trailer nose fairing.

Investigators	Ref. #	Test method	Fuel savings ($L/2.012 \times 10^8$ m hwy)	Remarks
Cooper	[8]	SWT	4865	SK
Cooper	[9]	SWT	3296 to 5286	SK & arched SK
Cooper	[11]	SWT	3541	SK
Cooper	[13]	SWT	6909	SK
Cooper	[13]	SWT	4592	SK
Cooper	[13]	SWT	9465	SK & TWSK
Cooper	[13]	FSWT	3691	SK, 8.5 m trailer
Cooper, *et al.*	[15]	SWT	2224	Short-length SK
Cooper, *et al.*	[15]	SWT	3502	Mid-length SK
Cooper, *et al.*	[15]	SWT	4401	SK
Cooper, *et al.*	[15]	FSWT	5206	SK
Leuschen, *et al.*	[32]	FSWT	4456	SK, 8.5 m trailer
Leuschen, *et al.*	[32]	FSWT	3645	SK & TWSK, 8.5 m trailer
Leuschen, *et al.*	[32]	FSWT	3504	SK, 8.5 m trailer
Leuschen, *et al.*	[32]	FSWT	3420	SK, 8.5 m trailer
Muirhead, *et al.*	[38]	SWT	9792	SK
Surcel, *et al.*	[62]	Track	7827	SK & TWSK
Surcel, *et al.*	[62]	Track	7384	SK & TWSK

Table 2: Summary of highway fuel savings for trailer skirts. FSWT–full-scale wind tunnel test, SK–trailer skirt, SWT–scale wind tunnel test, TWSK–trailer wheel skirt located behind the trailer bogie.

Investigators	Ref. #	Test method	Fuel savings ($L/2.012 \times 10^8$ m hwy)	Remarks
Browand, *et al.*	[3]	Track	3320	3-sided BT
Coon, *et al.*	[7]	Road	5914	4-sided inset BT
Cooper	[9]	SWT	0 to 1307	Trailer rear corner rounding
Cooper	[13]	FSWT	2983	3-sided BT
Cooper	[13]	FSWT	3313	4-sided BT
Cooper	[13]	Road	2605	3-sided BT
Cooper	[13]	SWT	3597	3-sided BT
Cooper	[13]	SWT	4119	4-sided BT
Cooper	[13]	SWT	3786	3-sided BT
Cooper, *et al.*	[15]	SWT	4401	3-sided BT
Cooper, *et al.*	[15]	FSWT	5206	3-sided BT
Grover, *et al.*	[22]	Road	4338	4-sided BT
Leuschen, *et al.*	[32]	FSWT	4716	3-sided BT, 8.5 m trailer
Leuschen, *et al.*	[32]	FSWT	4083	Inflatable BT, 8.5 m trailer
Muirhead, *et al.*	[38]	SWT	4459	Rounded BT
Surcel, *et al.*	[62]	Track	2817	3-sided BT

Table 3: Summary of highway fuel savings for trailer base devices. BT–boattail, FSWT–full-scale wind tunnel test, SWT–scale wind tunnel test.

Investigators	Ref. #	Test method	Fuel savings ($L/2.012 \times 10^8$ m hwy)	Remarks
Cooper	[9]	SWT	8923	GS & SK
Cooper	[13]	SWT	15996	SK, TWSK, full GS, & 3-sided BT
Cooper *et al.*	[15]	SWT	9512	SK, TWSK, & 3-sided BT
Cooper *et al.*	[15]	SWT	10175	Mid-length SK, 0.76 m SE, & 3-sided BT
Cooper *et al.*	[15]	SWT	13156	SK, TWSK, 0.76 m SE, & 3-sided BT
Cooper *et al.*	[15]	FSWT	12825	Mid-length SK, 0.76 m SE, & 3-sided BT

Table 4: Summary of highway fuel savings for combinations of devices. BT–boattail, GS-gap seal, FSWT–full-scale wind tunnel test, SK–trailer skirt, SWT–scale wind tunnel test, TWSK–trailer wheel skirt located behind the trailer bogie.

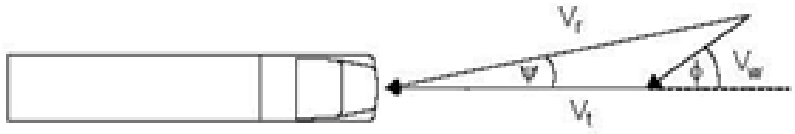

Figure 1: Wind vectors relative to the heavy vehicle.

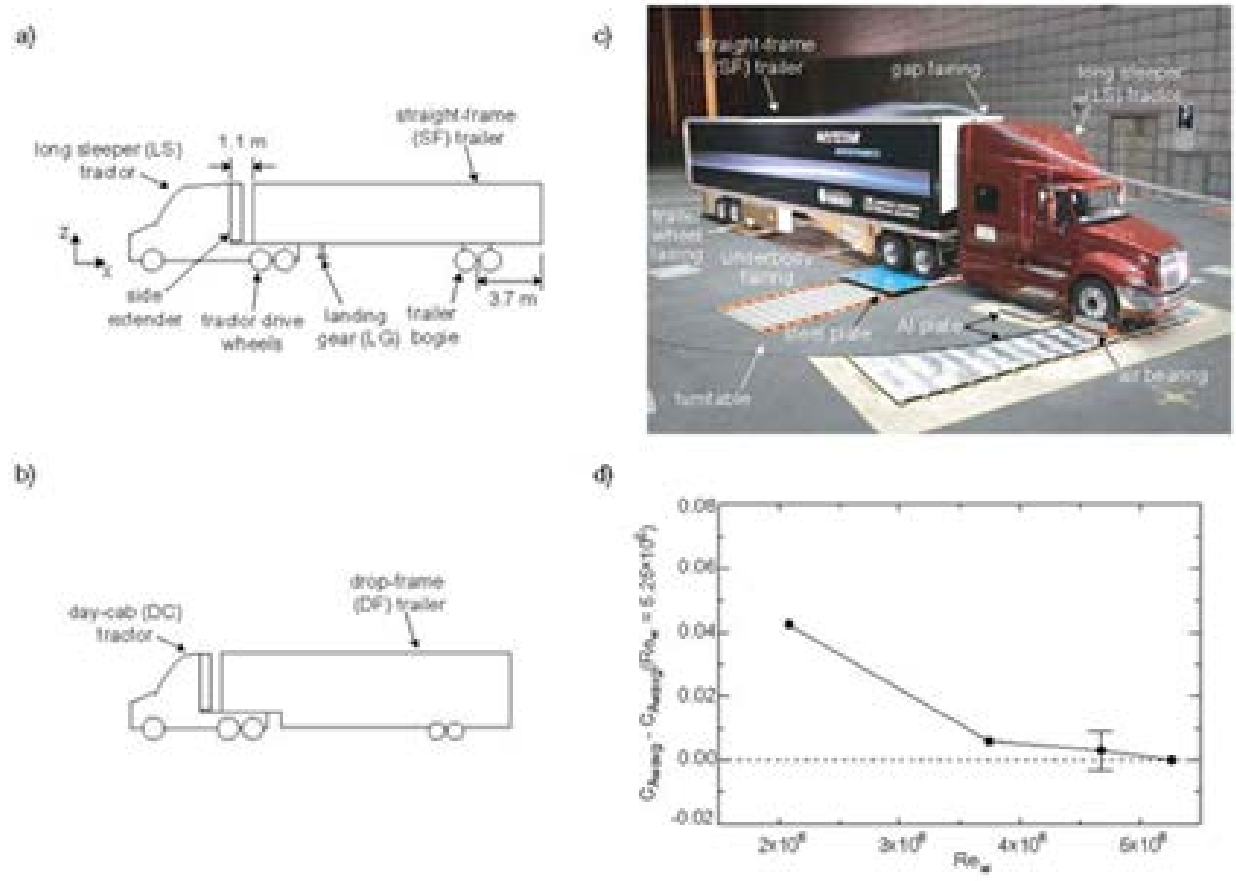

Figure 2. Ortega, Salari, Brown, & Schoon.

Figure 2: a) Long sleeper (LS) tractor and straight-frame (SF) trailer and b) day-cab (DC) tractor and drop-frame (DF) trailer configurations. c) LS/SF configuration mounted on the wind tunnel force balance. d) Wind-averaged drag coefficient, C_{Aavg}, relative to C_{Aavg} at $Re_w = 5.25 \times 10^6$ as a function of Re_w.

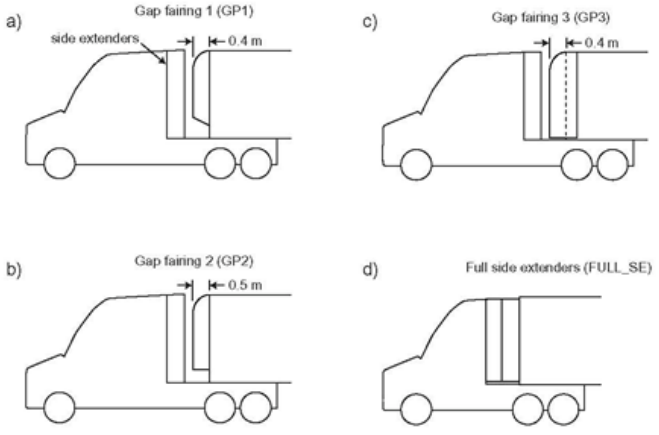

Figure 3. Ortega, Salari, Brown, & Schoon.

Figure 3: a-c) Fairings and d) full side extenders (FULLSE) for the tractor-trailer gap.

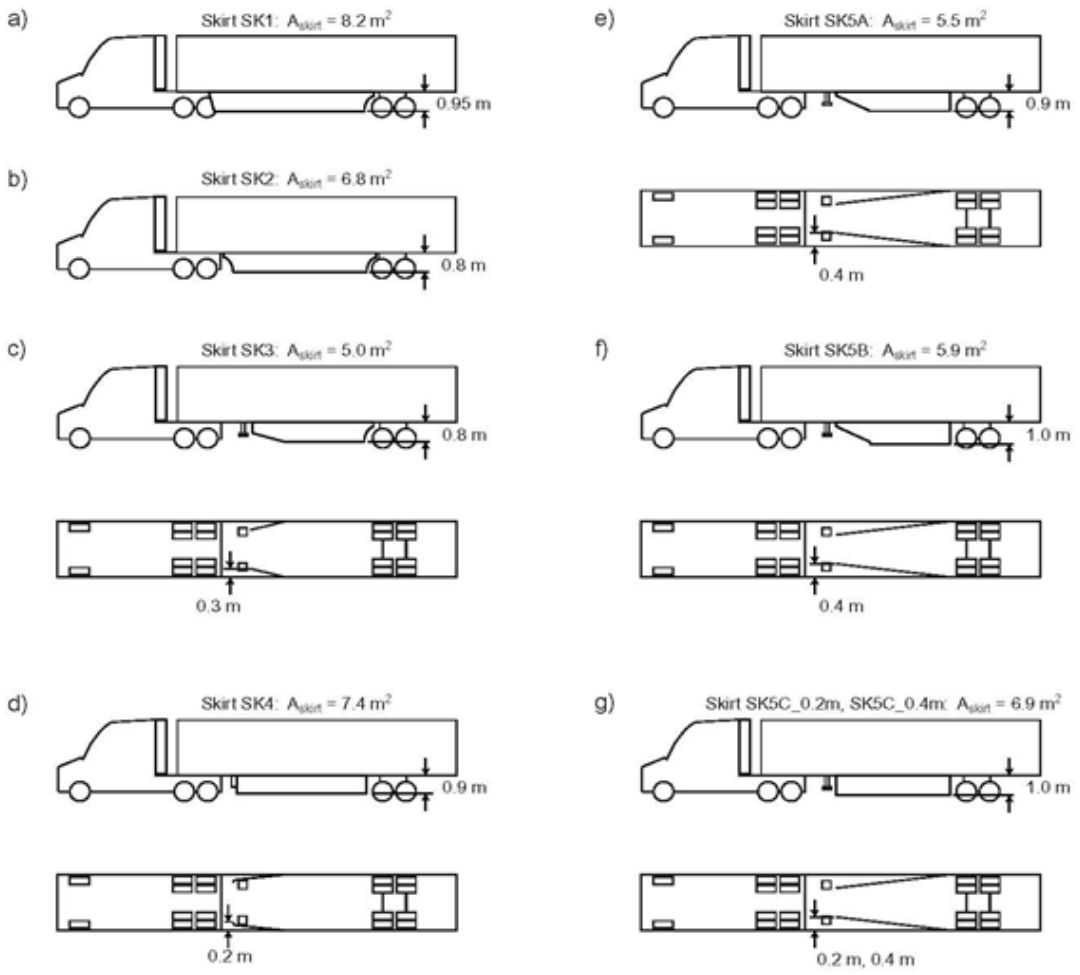

Figure 4. Ortega, Salari, Brown, & Schoon.

Figure 4: Trailer side skirts (SK). A_{skirt} denotes the surface area of the trailer skirt.

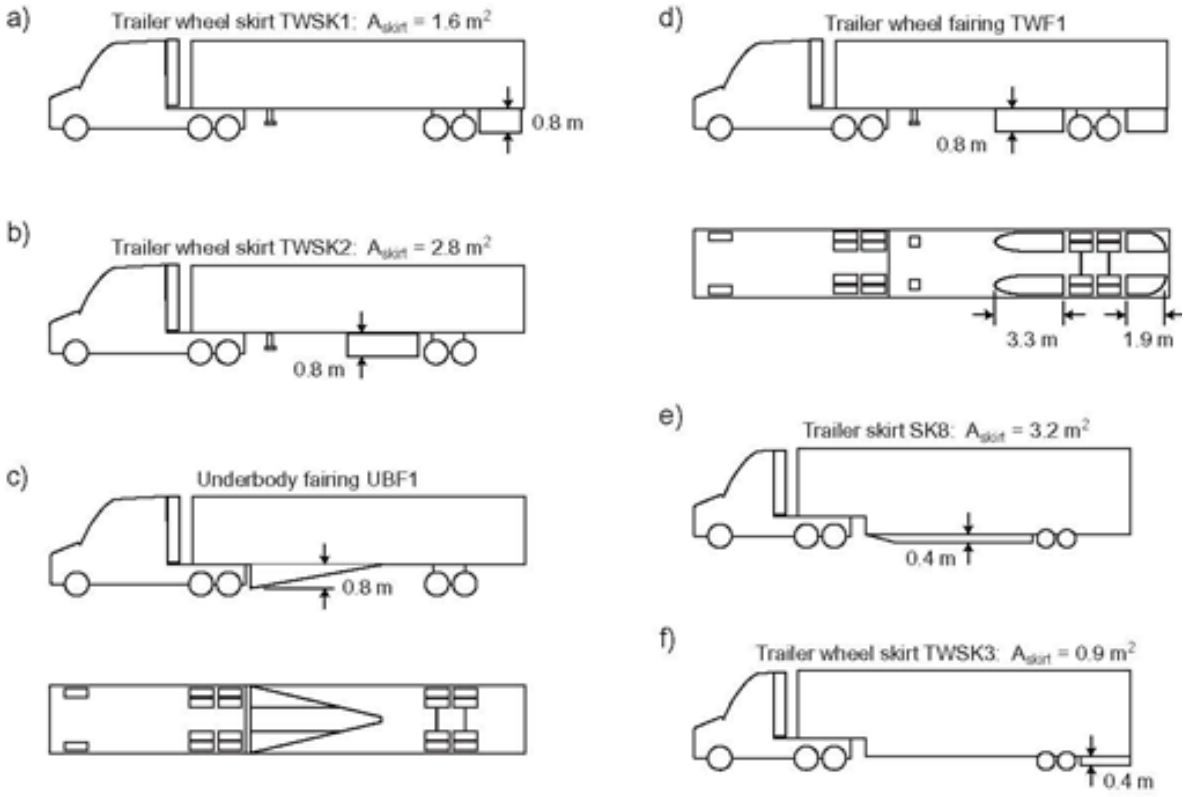

Figure 5. Ortega, Salari, Brown, & Schoon.

Figure 5: a-b, e-f) Trailer side skirts (SK) and c-d) underbody devices. A_{skirt} denotes the surface area of the trailer skirt.

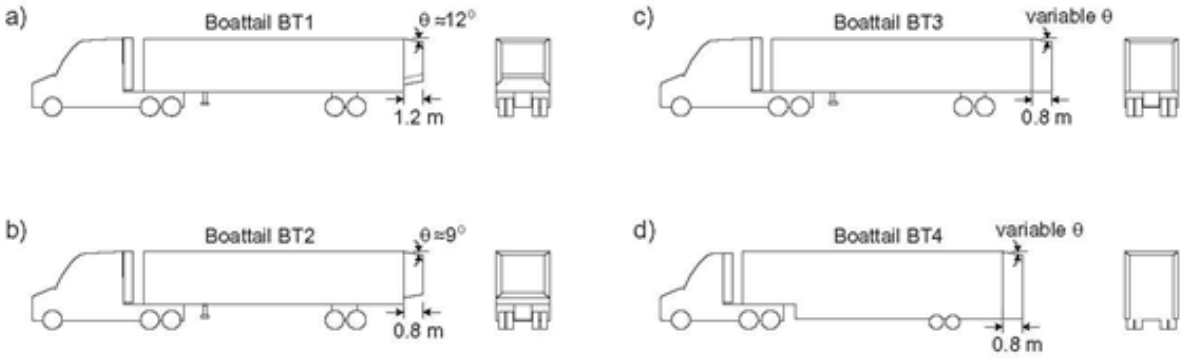

Figure 6. Ortega, Salari, Brown, & Schoon.

Figure 6: Trailer boattails (BT) for the a-c) straight-frame (SF) trailer and the d) drop-frame (DF) trailer. Boattails a-b) are 4-sided and c-d) are 3-sided.

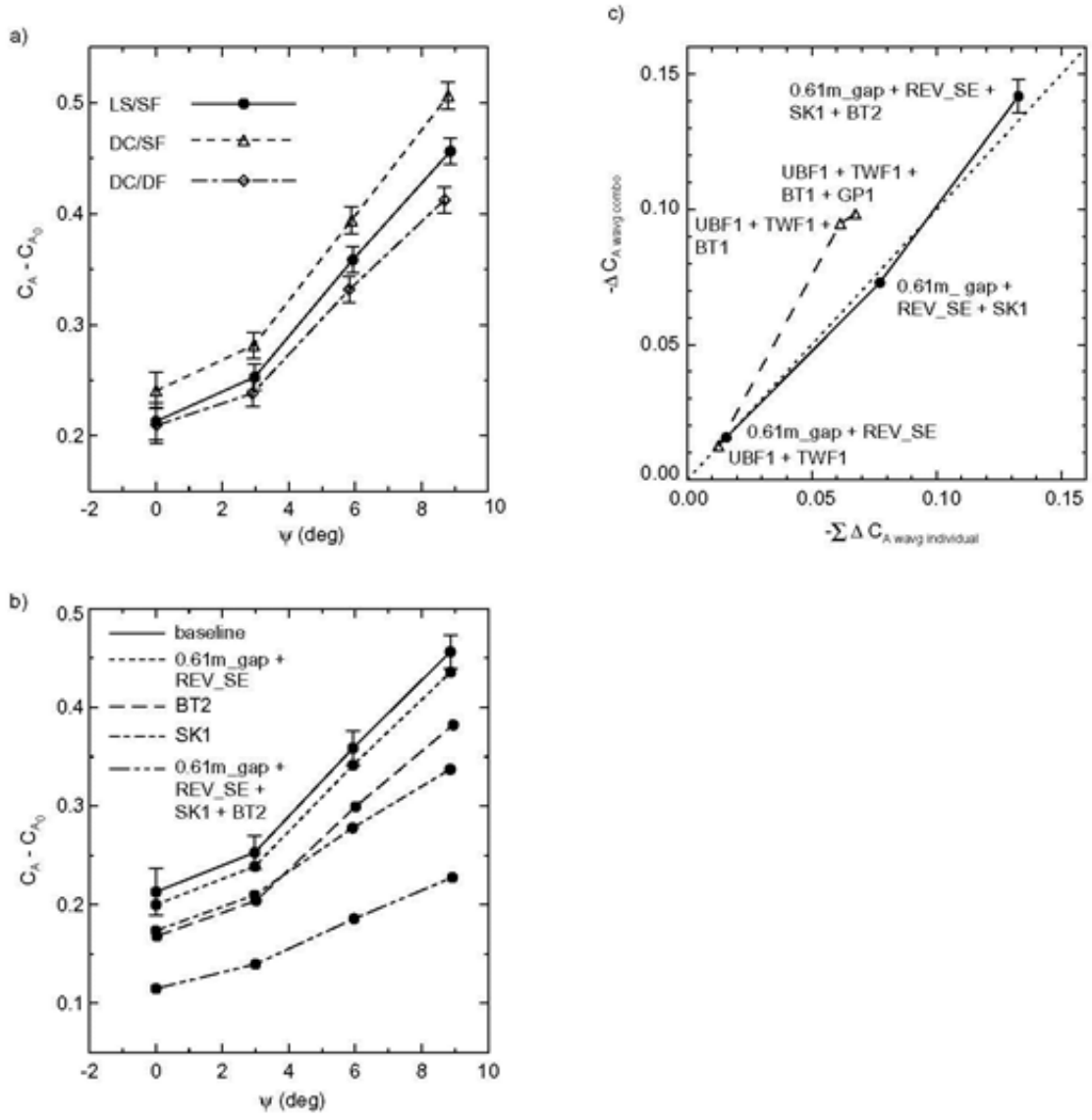

Figure 7. Ortega, Salari, Brown, & Schoon.

Figure 7: a) Body-axis drag coefficients as a function of the vehicle yaw angle for the three baseline configurations (LS–long-sleeper tractor, DC–day-cab tractor, SF–straight-frame trailer, DF–drop-frame trailer) and b) for the LS/SF configuration with drag reduction devices and modifications on the tractor-trailer gap (0.61m_gap + REV_SE–0.61 m tractor-trailer gap with revised side extenders), underbody (SK1–trailer skirt 1), and base (BT2–boattail 2). Note that the body-axis drag coefficients are relative to an arbitrary value, C_{A_0}. The 0.61m_gap + REV_SE + SK1 + BT2 data in b) is the drag curve resulting from the simultaneous installation of the three drag reduction devices and modifications. c) Reduction of the wind-averaged drag coefficient for multiple device installations on the LS/SF configuration. The horizontal axis is the linear summation of the drag reduction values when the devices are installed individually, while the vertical axis is the drag reduction that results when the devices are installed simultaneously with one another. The drag reduction values from multiple devices that combine in a perfectly linear fashion fall upon the 45° dashed line.

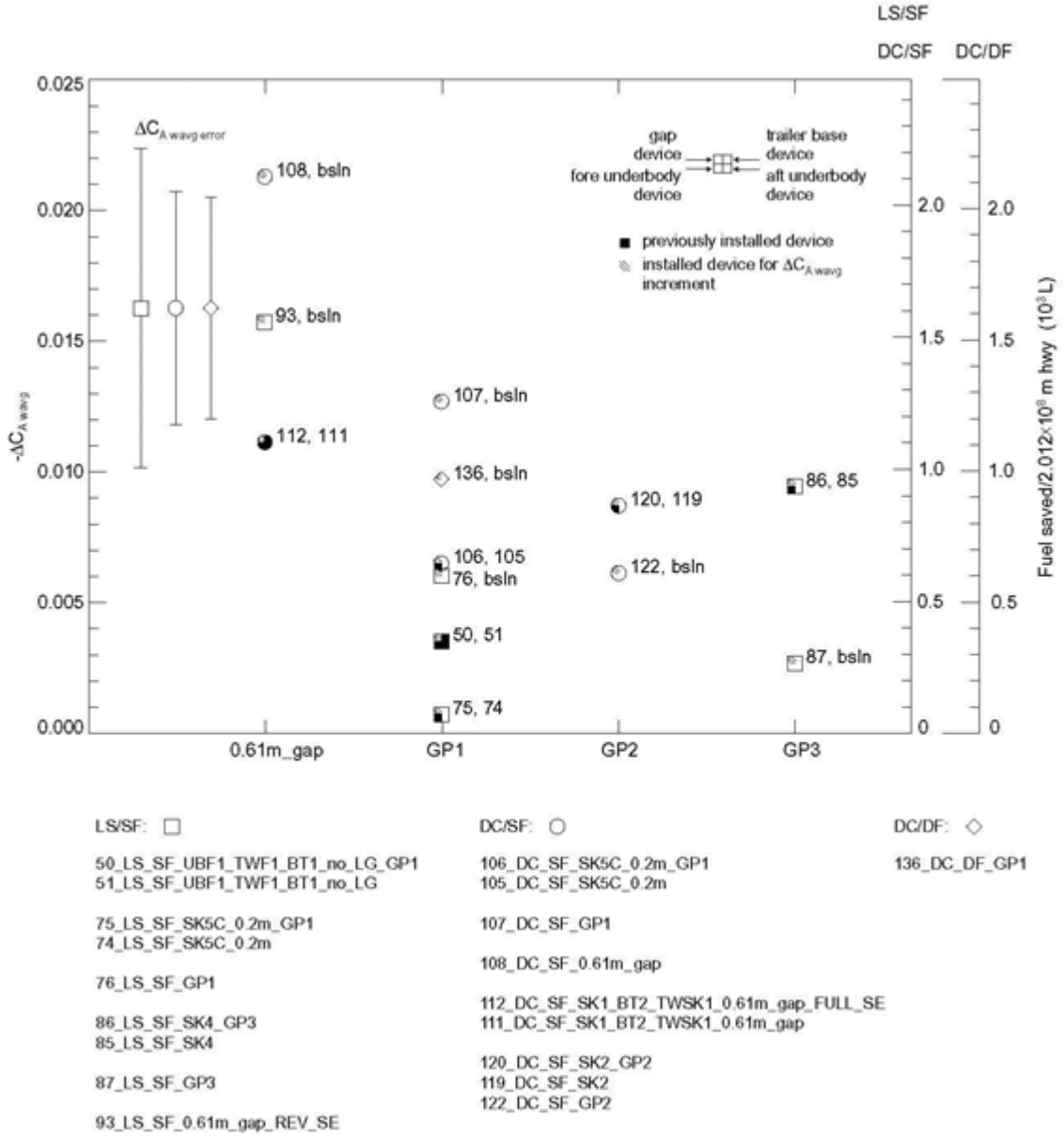

Figure 8. Ortega, Salari, Brown, & Schoon.

Figure 8: Incremental reduction in the wind-averaged drag coefficient and estimated highway fuel usage for the various tractor-trailer gap devices and modifications. LS–long-sleeper tractor, DC–day-cab tractor, SF–straight-frame trailer, DF–drop-frame trailer, GP–gap device, FULL_SE–full side extenders, REV_SE–revised side extenders, 0.61m_gap–0.61 m tractor-trailer gap, SK–trailer skirt, TWSK–trailer wheel skirt, TWF–trailer wheel fairing, UBF–trailer underbody fairing, BT–boattail, LG–trailer landing gear. See Figures 2-6 for schematics of the vehicle configurations and devices.

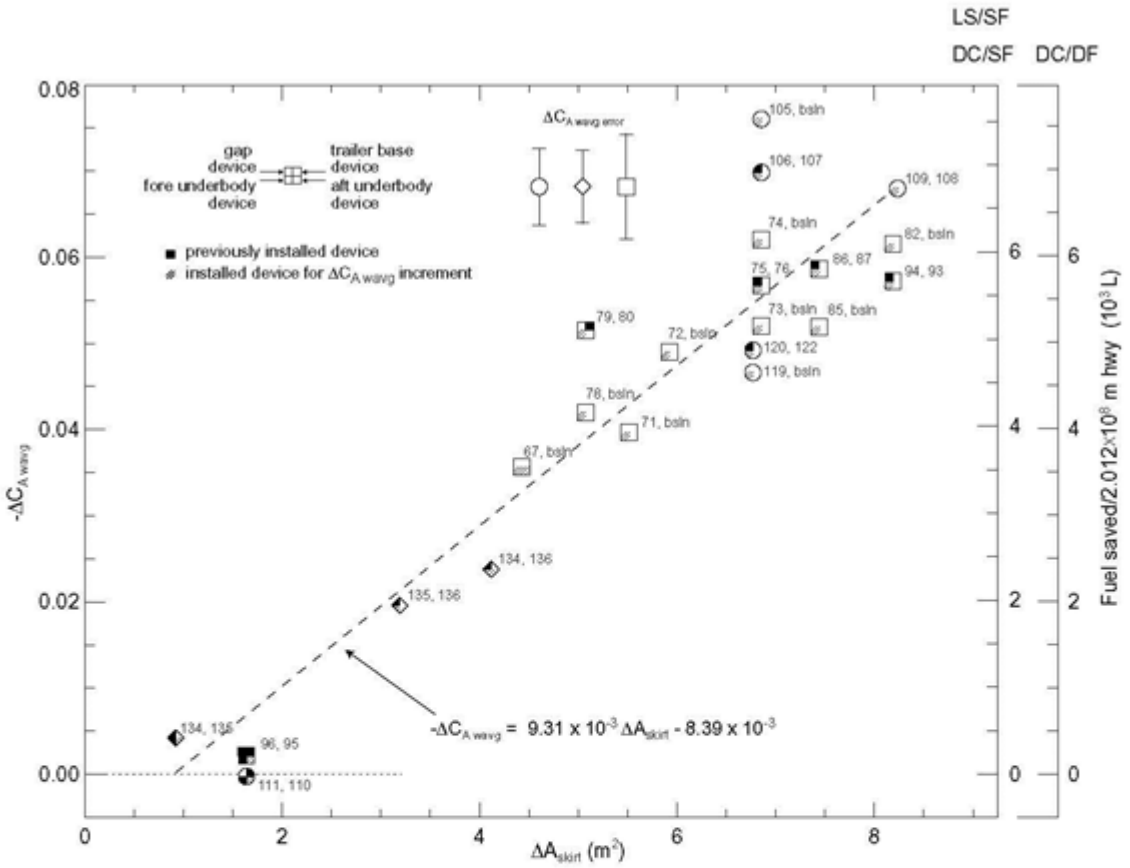

LS/SF: □

67_LS_SF_TWSK1_TWSK2
71_LS_SF_SK5A
72_LS_SF_SK5B
73_LS_SF_SK5C_0.4m
74_LS_SF_SK5C_0.2m
75_LS_SF_GP1_SK5C_0.2m
76_LS_SF_GP1
78_LS_SF_SK3

LS/SF: □

79_LS_SF_BT1_SK3
80_LS_SF_BT1
82_LS_SF_SK1
85_LS_SF_SK4
86_LS_SF_GP3_SK4
87_LS_SF_GP3
94_LS_SF_0.61m_gap_REV_SE_SK1
93_LS_SF_0.61m_gap_REV_SE
96_LS_SF_0.61m_gap_REV_SE_SK1_BT2_TWSK1
95_LS_SF_0.61m_gap_REV_SE_SK1_BT2

DC/SF: ○

105_DC_SF_SK5C_0.2m
106_DC_SF_GP1_SK5C_0.2m
107_DC_SF_GP1
109_DC_SF_0.61m_gap_SK1
108_DC_SF_0.61m_gap
111_DC_SF_0.61m_gap_BT2_SK1_TWSK1
110_DC_SF_0.61m_gap_BT2_SK1
119_DC_SF_SK2
120_DC_SF_GP2_SK2
122_DC_SF_GP2

DC/DF: ◇

134_DC_DF_SK8_GP1_TWSK3
135_DC_DF_SK8_GP1

DC/DF: ◇

135_DC_DF_GP1_SK8
136_DC_DF_GP1

DC/DF: ◇

134_DC_DF_GP1_SK8_TWSK3
136_DC_DF_GP1

Figure 9: Incremental reduction in the wind-averaged drag coefficient and estimated highway fuel usage as a function of the incremental skirt area for the various trailer skirt devices. See the caption in Figure 8 for the configuration definitions.

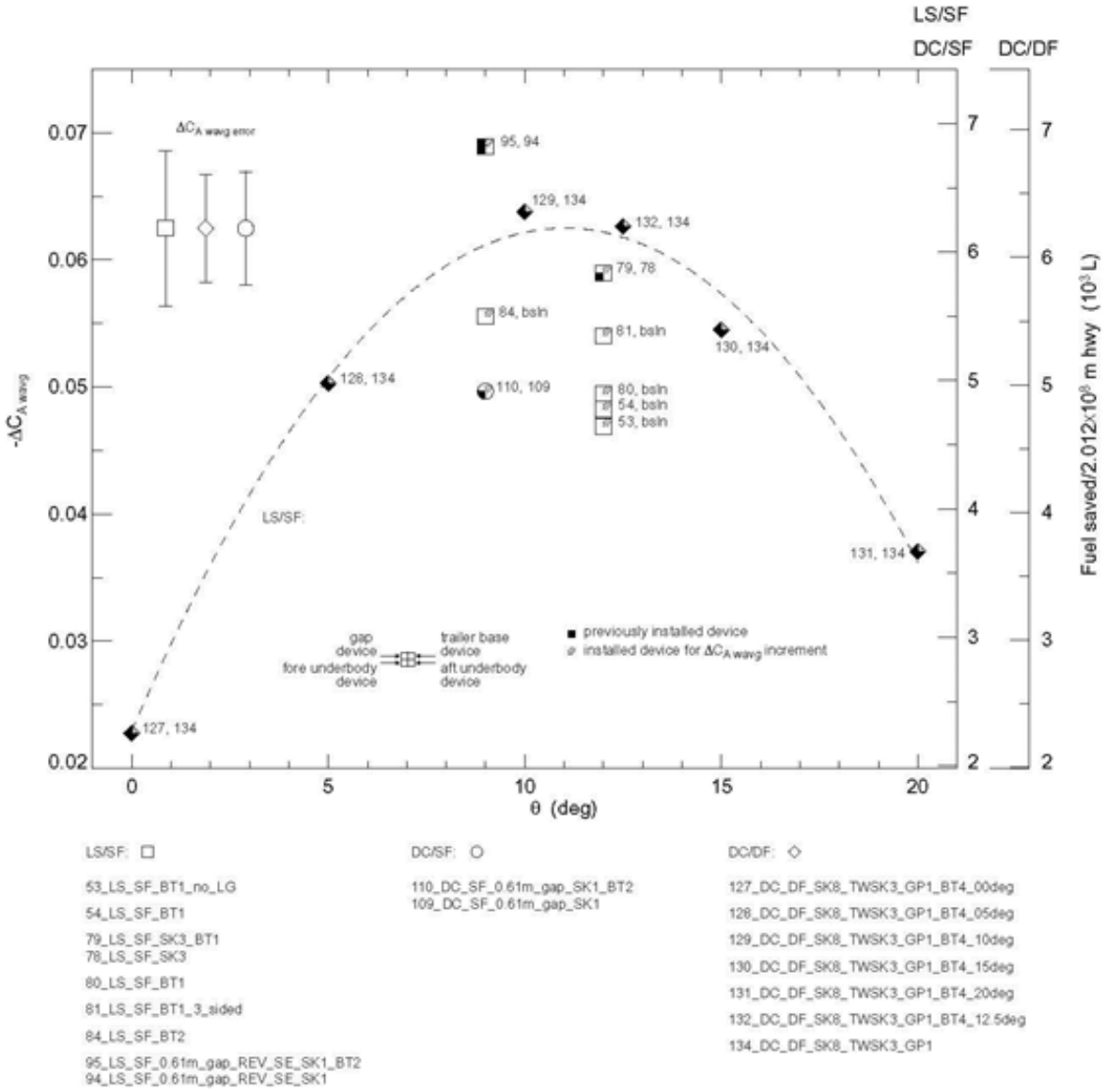

Figure 10. Ortega, Salari, Brown, & Schoon.

Figure 10: Incremental reduction in the wind-averaged drag coefficient and estimated highway fuel usage as a function of the boattail deflection angle for the various trailer boattail devices. The dashed curve is a second-order polynomial fit to the day-cab/drop-frame trailer (DC/DF) data for boattail 4 (BT4). The maximum $-\Delta C_{A_{wavg}}$ of this curve fit is at $11 \pm 2°$. See the caption in Figure 8 for the configuration definitions.

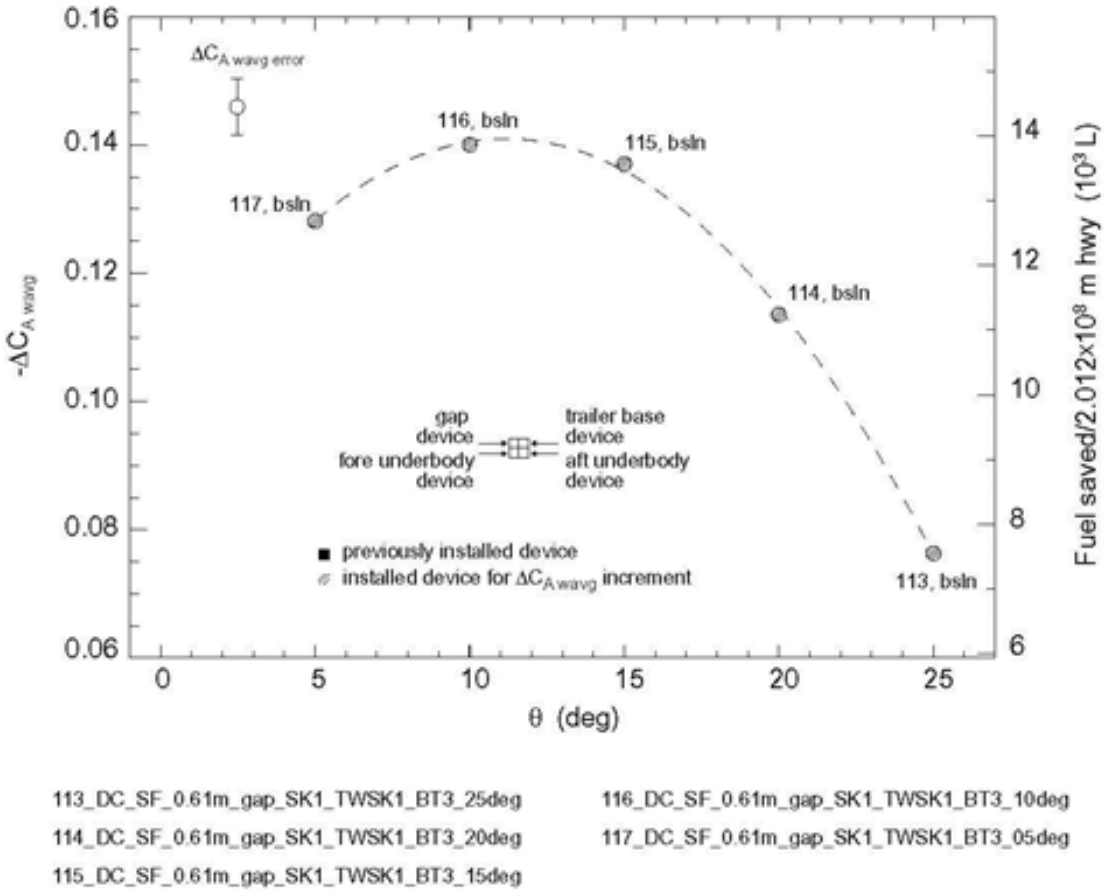

Figure 11. Ortega, Salari, Brown, & Schoon.

Figure 11: Reduction in the wind-averaged drag coefficient and estimated highway fuel usage relative to the baseline day-cab/straight-frame trailer (DC/SF) configuration as a function of the boattail 3 (BT3) deflection angle. The maximum $-\Delta C_{A_{wavg}}$ of the second-order polynomial curve fit is at $11 \pm 2°$. See the caption in Figure 8 for the configuration definitions.

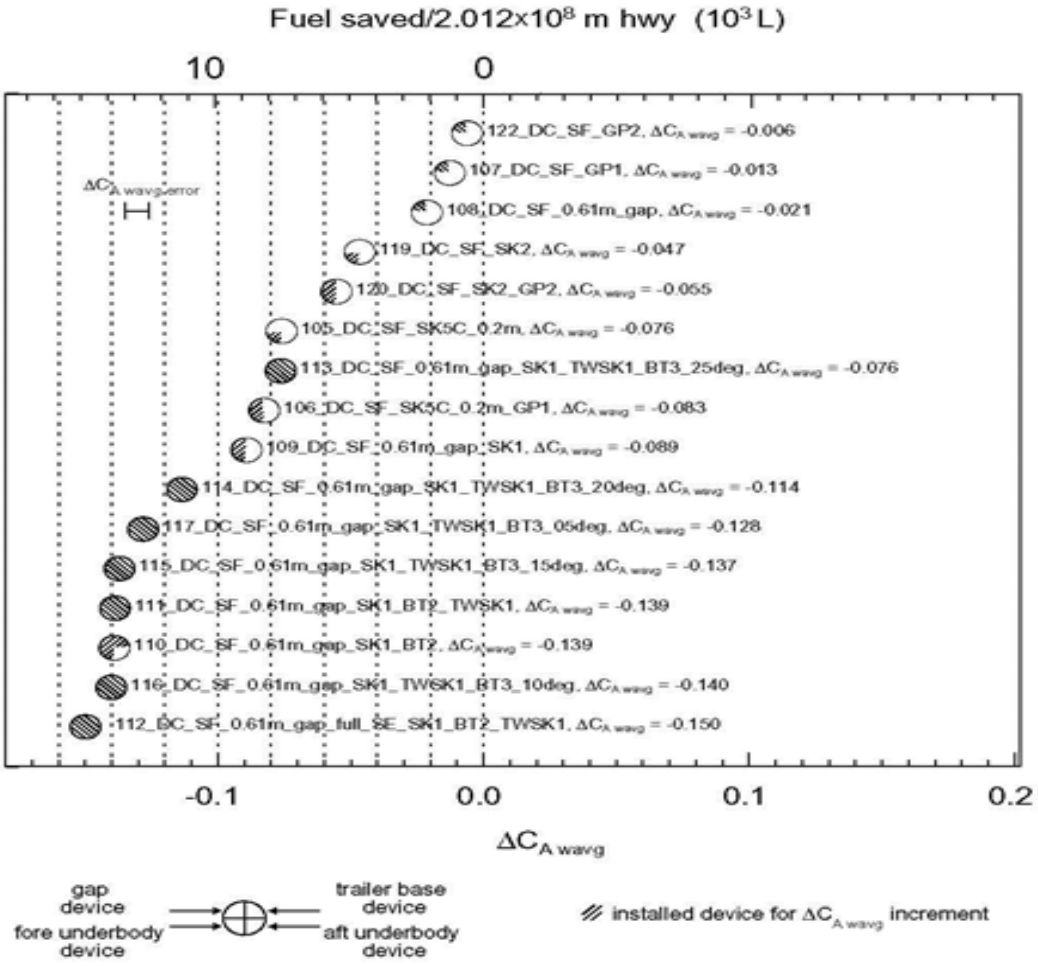

Figure 12. Ortega, Salari, Brown, & Schoon.

Figure 12: Reduction in the wind-averaged drag coefficient and estimated highway fuel usage for the day-cab/straight-frame trailer (DC/SF) configuration. See the caption in Figure 8 for the configuration definitions.

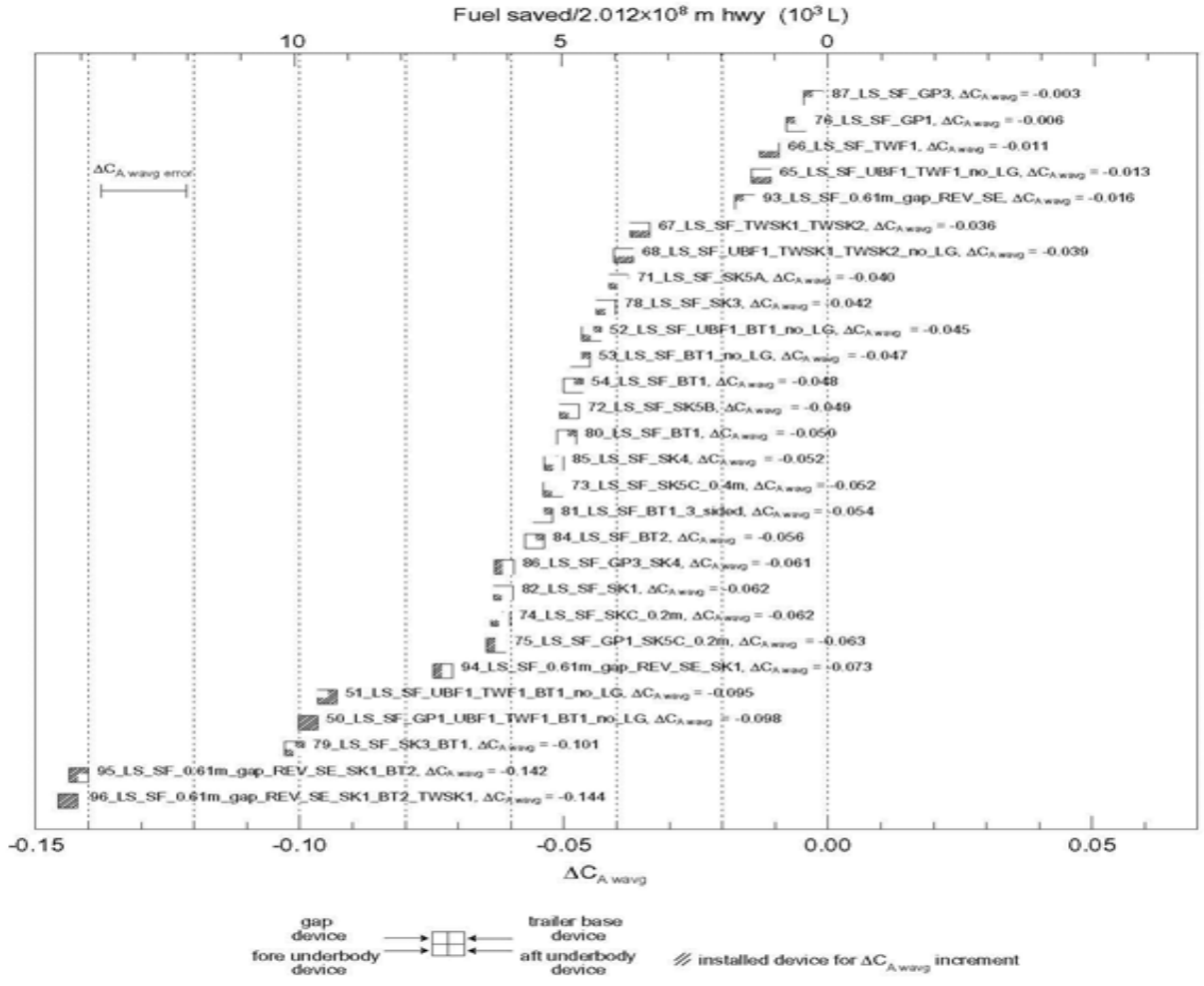

Figure 13. Ortega, Salari, Brown, & Schoon.

Figure 13: Reduction in the wind-averaged drag coefficient and estimated highway fuel usage for the long-sleeper/straight-frame trailer (LS/SF) configuration. See the caption in Figure 8 for the configuration definitions.

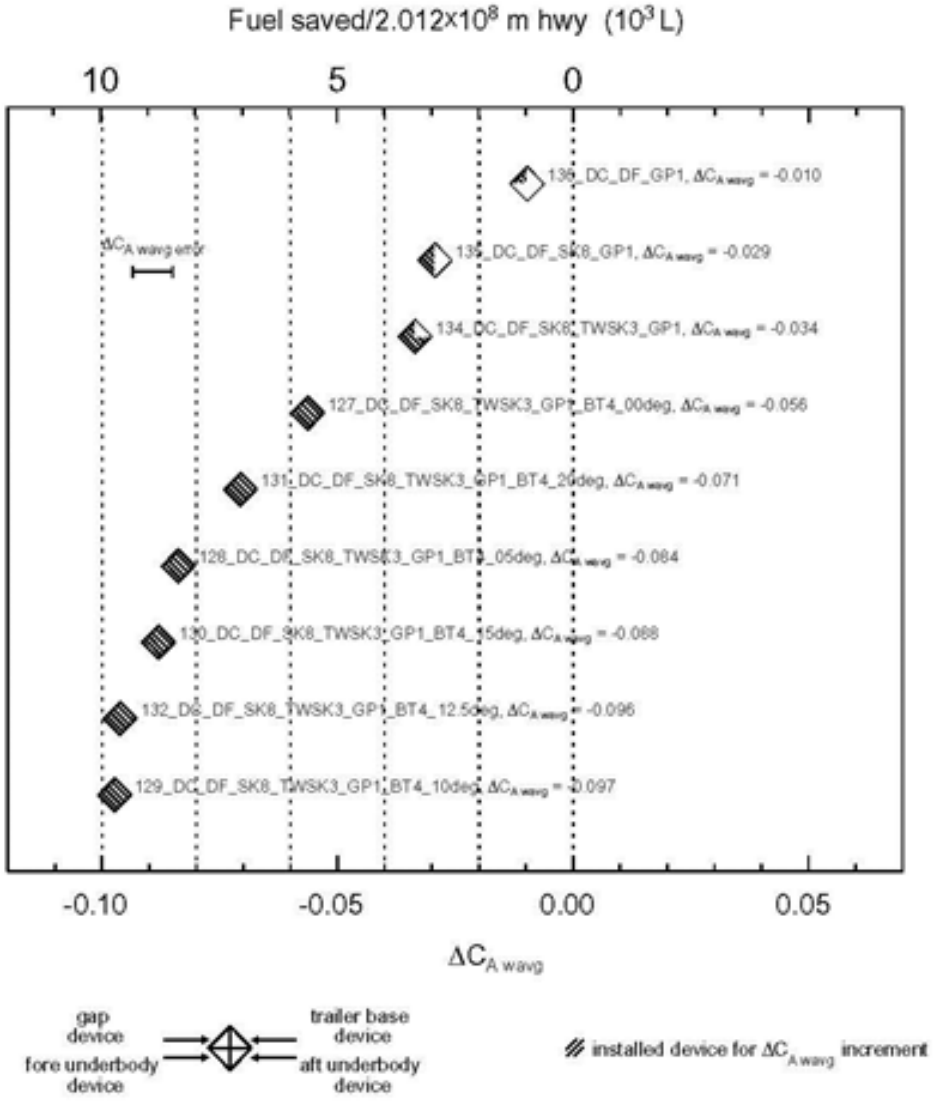

Figure 14. Ortega, Salari, Brown, & Schoon.

Figure 14: Reduction in the wind-averaged drag coefficient and estimated highway fuel usage for the day-cab/drop-frame trailer (DC/DF) configuration. See the caption in Figure 8 for the configuration definitions.

End of Fuel Economy Improvement of Class 8 Heavy Vehicles, Ortega, Salari, Brown, & Schoon

End of Appendix

U.S. DEPARTMENT OF ENERGY | Energy Efficiency & Renewable Energy

For more information
eere.energy.gov

DOE/EE-0703 January 2012
Printed with a renewable-source ink on paper containing
at least 50% wastepaper, including 10% post consumer waste.